METHODS IN MOLECULAR BIOLOGY™

Volume 277

Trinucleotide Repeat Protocols

Edited by

Yoshinori Kohwi

HUMANA PRESS

Trinucleotide Repeat Protocols

METHODS IN MOLECULAR BIOLOGY™

John M. Walker, SERIES EDITOR

300 **Protein Nanotechnology:** *Protocols, Instrumentation, and Applications,* edited by *Tuan Vo-Dinh, 2005*

299 **Amyloid Proteins:** *Methods and Protocols,* edited by *Einar M. Sigurdsson, 2005*

298 **Peptide Synthesis and Application,** edited by *John Howl, 2005*

297 **Forensic DNA Typing Protocols,** edited by *Angel Carracedo, 2005*

296 **Cell Cycle Protocols,** edited by *Tim Humphrey and Gavin Brooks, 2005*

295 **Immunochemical Protocols, Third Edition, edited by Robert Burns, 2005**

294 **Cell Migration:** *Developmental Methods and Protocols,* edited by *Jun-Lin Guan, 2005*

293 **Laser Capture Microdissection:** *Methods and Protocols,* edited by *Graeme I. Murray and Stephanie Curran, 2005*

292 **DNA Viruses:** *Methods and Protocols,* edited by *Paul M. Lieberman, 2005*

291 **Molecular Toxicology Protocols**, edited by *Phouthone Keohavong and Stephen G. Grant, 2005*

290 **Basic Cell Culture**, *Third Edition,* edited by *Cheryl D. Helgason and Cindy Miller, 2005*

289 **Epidermal Cells**, *Methods and Applications,* edited by *Kursad Turksen, 2004*

288 **Oligonucleotide Synthesis**, *Methods and Applications,* edited by *Piet Herdewijn, 2004*

287 **Epigenetics Protocols**, edited by *Trygve O. Tollefsbol, 2004*

286 **Transgenic Plants:** *Methods and Protocols,* edited by *Leandro Peña, 2004*

285 **Cell Cycle Control and Dysregulation Protocols:** *Cyclins, Cyclin-Dependent Kinases, and Other Factors,* edited by *Antonio Giordano and Gaetano Romano, 2004*

284 **Signal Transduction Protocols,** *Second Edition,* edited by *Robert C. Dickson and Michael D. Mendenhall, 2004*

283 **Bioconjugation Protocols,** edited by *Christof M. Niemeyer, 2004*

282 **Apoptosis Methods and Protocols,** edited by *Hugh J. M. Brady, 2004*

281 **Checkpoint Controls and Cancer, Volume 2:** *Activation and Regulation Protocols,* edited by *Axel H. Schönthal, 2004*

280 **Checkpoint Controls and Cancer, Volume 1:** *Reviews and Model Systems,* edited by *Axel H. Schönthal, 2004*

279 **Nitric Oxide Protocols,** *Second Edition,* edited by *Aviv Hassid, 2004*

278 **Protein NMR Techniques,** *Second Edition,* edited by *A. Kristina Downing, 2004*

277 **Trinucleotide Repeat Protocols,** edited by *Yoshinori Kohwi, 2004*

276 **Capillary Electrophoresis of Proteins and Peptides,** edited by *Mark A. Strege and Avinash L. Lagu, 2004*

275 **Chemoinformatics,** edited by *Jürgen Bajorath, 2004*

274 **Photosynthesis Research Protocols,** edited by *Robert Carpentier, 2004*

273 **Platelets and Megakaryocytes, Volume 2:** *Perspectives and Techniques,* edited by *Jonathan M. Gibbins and Martyn P. Mahaut-Smith, 2004*

272 **Platelets and Megakaryocytes, Volume 1:** *Functional Assays,* edited by *Jonathan M. Gibbins and Martyn P. Mahaut-Smith, 2004*

271 **B Cell Protocols,** edited by *Hua Gu and Klaus Rajewsky, 2004*

270 **Parasite Genomics Protocols,** edited by *Sara E. Melville, 2004*

269 **Vaccina Virus and Poxvirology:** *Methods and Protocols,*edited by *Stuart N. Isaacs, 2004*

268 **Public Health Microbiology:** *Methods and Protocols,* edited by *John F. T. Spencer and Alicia L. Ragout de Spencer, 2004*

267 **Recombinant Gene Expression:** *Reviews and Protocols, Second Edition,* edited by *Paulina Balbas and Argelia Johnson, 2004*

266 **Genomics, Proteomics, and Clinical Bacteriology:** *Methods and Reviews,* edited by *Neil Woodford and Alan Johnson, 2004*

265 **RNA Interference, Editing, and Modification:** *Methods and Protocols,* edited by *Jonatha M. Gott, 2004*

264 **Protein Arrays:** *Methods and Protocols,* edited by *Eric Fung, 2004*

263 **Flow Cytometry,** *Second Edition,* edited by *Teresa S. Hawley and Robert G. Hawley, 2004*

262 **Genetic Recombination Protocols,** edited by *Alan S. Waldman, 2004*

261 **Protein–Protein Interactions:** *Methods and Applications,* edited by *Haian Fu, 2004*

260 **Mobile Genetic Elements:** *Protocols and Genomic Applications,* edited by *Wolfgang J. Miller and Pierre Capy, 2004*

259 **Receptor Signal Transduction Protocols,** *Second Edition,* edited by *Gary B. Willars and R. A. John Challiss, 2004*

258 **Gene Expression Profiling:** *Methods and Protocols,* edited by *Richard A. Shimkets, 2004*

257 **mRNA Processing and Metabolism:** *Methods and Protocols,* edited by *Daniel R. Schoenberg, 2004*

METHODS IN MOLECULAR BIOLOGY™

Trinucleotide Repeat Protocols

Edited by

Yoshinori Kohwi

Life Science Division,
Lawrence Berkeley Laboratory,
Berkeley, CA

HUMANA PRESS TOTOWA, NEW JERSEY

999 Riverview Drive, Suite 208
Totowa, New Jersey 07512

www.humanapress.com

This publication is printed on acid-free paper. ∞
ANSI Z39.48-1984 (American Standards Institute)

Permanence of Paper for Printed Library Materials.

Cover Illustration: Fig. 2 from Chapter 18, "Techniques for Thick-Section Golgi Impregnation of Formalin-Fixed Brain Tissue," by Tracie L. Moss and William O. Whetsell, Jr.

Production Editor: Angela L. Burkey.
Cover design by Patricia F. Cleary.

For additional copies, pricing for bulk purchases, and/or information about other Humana titles, contact Humana at the above address or at any of the following numbers: Tel.: 973-256-1699; Fax: 973-256-8341; E-mail: humana@humanapr.com; or visit our Website: www.humanapress.com

Printed in the United States of America. 10 9 8 7 6 5 4 3 2 1
e-ISBN: 1-59259-804-8
ISSN: 1064-3745

Library of Congress Cataloging-in-Publication Data

Trinucleotide repeat protocols / edited by Yoshinori Kohwi.

p. ; cm. -- (Methods in molecular biology ; 277)

Includes bibliographical references and index.

ISBN 1-58829-243-6 (alk. paper)

1. Trinucleotide repeats--Laboratory manuals.

[DNLM: 1. Trinucleotide Repeats. QU 58 T833 2004] I. Kohwi, Yoshinori. II. Series: Methods in molecular biology (Clifton, N.J.) ; v. 277.

QP625.N89T74 2004

616.8'0442--dc22

2003025446

Preface

Trinucleotide repeats are relatively common in the human genome. These simple repeats have received much attention since epoch-making discoveries were made that particular trinucleotide repeats are expanded in the causal genes of human hereditary neurological disorders. For example, the CGG repeat is expanded in fragile X syndrome at the 5' untranslated region (UTR) of its causal gene. In myotonic dystrophy, it is the CTG repeat that is expanded at the 3' UTR of its causal gene. The CAG repeat was also found expanded in coding regions of the genes responsible for X-linked spinal and bulbar muscular atrophy, Huntington's disease, spinocerebellar ataxia, and other disorders.

On the other hand, expansion of the GAA repeat was identified in the intron of the gene responsible for the Friedreich's ataxia. For these trinucleotide repeat diseases, the longer the trinucleotide expansion, the earlier the age of onset and the more severe the syndrome. Thus, these findings that showed the intriguing link between a particular trinucleotide expansion and its associated neurological disorders have led to a new field of intensive study. Active research addressing the underlying mechanisms for trinucleotide repeat diseases has employed various approaches ranging from DNA biochemistry to animal models for the diseases. In particular, animal models for the triplet repeat diseases have provided excellent resources not only for understanding the mechanisms but also for exploring therapeutic interventions.

Dr. Bates and Dr. Hay have introduced an overview of trinucleotide repeat diseases in Chapter 1, using mouse models. Our book, *Trinucleotide Repeat Protocols*, covers a broad range of biochemical, histochemical, and molecular biological methods, as well as animal model systems. In the protocols, one will find how each of these techniques has been used effectively to address the unique questions relevant to trinucleotide repeat diseases. Most methods described in *Trinucleotide Repeat Protocols* are also essential and widely applicable in modern biology, not necessarily related to trinucleotide repeat diseases. All protocols are written in a self-sufficient manner so that one can repeat the entire course of the experiment without needing to refer to other texts.

Trinucleotide Repeat Protocols is divided into five sections: a review chapter, analysis of trinucleotide repeat DNA and RNA, analysis of polyglutamine-containing proteins, establishment of animal and culture models of trinucleotide repeat diseases, and their applications. All authors in *Trinucleotide Repeat Protocols* have made important milestone discoveries toward a better under-

standing of the mysterious characteristics of trinucleotide repeat sequences at the levels of DNA, RNA, and proteins to elucidate the mechanisms of hereditary neurological diseases and develop effective therapeutic interventions. *Trinucleotide Repeat Protocols*, which covers a wide range of modern molecular-biology techniques, should be of high utility not only to scientists interested in neuronal genetic diseases, but also postgraduate students and established investigators in related fields.

I wish to take this opportunity to express my great appreciation for the efforts of all authors in preparing the protocols.

Yoshinori Kohwi

Contents

Contributors

Patrick Aebischer • *Institute of Neurosciences, School of Life Sciences, Swiss Federal Institute of Technology Lausanne (EPFL), Lausanne, Switzerland*

Montserrat Arrasate • *Gladstone Institute of Neurological Disease, and Departments of Neurology and Physiology, University of California, San Francisco, CA*

Gillian P. Bates • *Department of Medical and Molecular Genetics, GKT School of Medicine, King's College, Guy's Hospital, London, UK*

Caroline L. Benn • *Mass General Institute for Neurodegenerative Disease and Department of Neurology, Massachusetts General Hospital, Charlestown, MA*

Saumitri Bhattacharyya • *Eppley Institute for Research in Cancer and Allied Diseases, University of Nebraska Medical Center, Omaha, NE*

Sanjay I. Bidichandani • *Departments of Biochemistry & Molecular Biology and Pediatrics, University of Oklahoma Health Sciences Center, Oklahoma City, OK*

Melissa W. Braveman • *Mass General Institute for Neurodegenerative Disease and Department of Neurology, Massachusetts General Hospital, Charlestown, MA*

Elizabeth Brooks • *Gladstone Institute of Neurological Disease, and Departments of Neurology and Physiology, University of California, San Francisco, CA*

Jang-Ho J. Cha • *Mass General Institute for Neurodegenerative Disease and Department of Neurology, Massachusetts General Hospital, Charlestown, MA*

Alice S. Chen-Plotkin • *Mass General Institute for Neurodegenerative Disease and Department of Neurology, Massachusetts General Hospital, Charlestown, MA*

Kenneth Cheung • *Gladstone Institute of Neurological Disease, and Departments of Neurology and Physiology, University of California, San Francisco, CA*

Nicole Déglon • *Institute of Neurosciences, School of Life Sciences, Swiss Federal Institute of Technology Lausanne, Lausanne, Switzerland*

Michael J. Dixon • *Eppley Institute for Research in Cancer and Allied Diseases, and Department of Pathology and Microbiology, University of Nebraska Medical Center, Omaha, NE*

Maria Eriksson • *Department of Medical Nutrition, Karolinska Institutet, Huddinge, Sweden*
Laurie A. Farrell • *Mass General Institute for Neurodegenerative Disease and Department of Neurology, Massachusetts General Hospital, Charlestown, MA*
Steven M. Finkbeiner • *Gladstone Institute of Neurological Disease, and Departments of Neurology and Physiology, University of California, San Francisco, CA*
Mário Gomes-Pereira • *Division of Molecular Genetics, Institute of Biomedical and Life Sciences, Anderson College Complex, University of Glasgow, Glasgow, UK*
Geneviève Gourdon • *INSERM UR383, Hospital Necker-Enfants Malades, Université René Descartes Paris V, Paris, France*
Anne C. Hart • *Department of Pathology, Harvard Medical School, and Cancer Center, Massachusetts General Hospital East, Charlestown, MA*
David G. Hay • *Department of Medical and Molecular Genetics, GKT School of Medicine, King's College London, Guy's Hospital, London, UK*
Noriko Hazeki • *Division of Neuroscience, Department of Neurology, CREST, Japan Science and Technology Corporation, Graduate School of Medicine, University of Tokyo, Tokyo, Japan*
Nihar Ranjan Jana • *Department of Cellular and Molecular Neuroscience, National Brain Research Centre, Gurgaon, India*
Claudine Junien • *INSERM UR383, Hospital Necker-Enfants Malades, Université René Descartes Paris V, Paris, France*
Ichiro Kanazawa • *National Institute of Neuroscience, National Center of Neurology and Psychiatry, and Department of Neurology, CREST, University of Tokyo, Tokyo, Japan*
Ali Khoshnan • *Biology Division, California Institute of Technology, Pasadena, CA*
Jan Ko • *Biology Division, California Institute of Technology, Pasadena, CA*
Yoshinori Kohwi • *Life Science Division, Lawrence Berkeley Laboratory, University of California, Berkeley, CA*
Irina V. Kovtun • *Department of Pharmacology, Mayo Clinic, Rochester, MN*
Maria M. Krasilnikova • *Department of Molecular Genetics, University of Illinois at Chicago, IL*
Robert S. Lahue • *Eppley Institute for Research in Cancer and Applied Diseases, University of Nebraska Medical Center, Omaha, NE*

Raffaele Lodi • *Dipartimento di Medicina Clinica, E Biotecnologia Applicata "D. Campanacci," Universita di Bologna, Policlinico S. Orsola, Bologna, Italy*
Cynthia T. McMurray • *Department of Pharmacology, Mayo Clinic, Rochester, MN*
Sergei M. Mirkin • *Department of Molecular Genetics, University of Illinois at Chicago, IL*
Darren G. Monckton • *Division of Molecular Genetics, Institute of Biomedical and Life Sciences, University of Glasgow, Anderson College Complex, Glasgow, UK*
Tracie L. Moss • *Division of Neuropathology, Department of Pathology, Vanderbilt University School of Medicine, Nashville, TN*
Nobuyuki Nukina • *Laboratory of Structural Neuropathology, RIKEN Brain Science Institute, Saitama, Japan*
Ben A. Oostra • *Department of Clinical Genetics, Erasmus University, Rotterdam, The Netherlands*
Susan Ou • *Biology Division, California Institute of Technology, Pasadena, CA*
Paul H. Patterson • *Biology Division, California Institute of Technology, Pasadena, CA*
Francisca Pérez-Severiano • *Departamento de Neuroquímica, Instituto Nacional de Neurología y Neurocirugía, Manuel Velasco Suárez, México*
Etienne Régulier • *Institute of Neuroscience, School of Life Sciences, Swiss Federal Institute of Technology Lausanne (EPFL), Lausanne, Switzerland*
Cédric Savouret • *INSERM UR383, Hospital Necker-Enfants Malades, Université René Descartes Paris V, Paris, France*
Martin Schalling • *Department of Molecular Medicine, Karolinska Hospital, Stockholm, Sweden*
Anthony Schapira • *University Department of Clinical Neurosciences, Royal Free and University College Medical School, University College, UK*
José Segovia • *Departamento de Fisiología, Biofísica y Neurociencias, Centro de Investigación y de Estudios Avanzados del IPN, Mexico City, Mexico*
Donna L. Smith • *Department of Medical and Molecular Genetics, GKT Schoolof Medicine, King's College, Guy's Hospital, London, UK*
Craig Spiro • *Department of Pharmacology, Mayo Clinic, Rochester, MN*
Violeta Stoyanova • *Department of Clinical Genetics, Erasmus MC, Rotterdam, The Netherlands*

Cindy Voisine • *Department of Pathology, Harvard Medical School, and Cancer Center, Massachusetts General Hospital East, Charlestown, MA*
William O. Whetsell, Jr. • *Division of Neuropathology, Department of Pathology, Vanderbilt University School of Medicine, Nashville, TN*
George J. Yohrling • *Mass General Institute for Neurodegenerative Disease and Department of Neurology, Massachusetts General Hospital, Charlestown, MA*
Qiu-Ping Yuan • *Division of Hematology, University of Wisconsin, Medical Science Center, Madison, WI*
Diana Zala • *Institute of Neuroscience, School of Life Sciences, Swiss Federal Institute of Technology Lausanne (EPFL), Lausanne, Switzerland*

I

Introduction

1

Mouse Models of Triplet Repeat Diseases

Gillian P. Bates and David G. Hay

Summary Title

Since their discovery in 1991, triplet repeat mutations have been found to be the cause of genomic fragile sites, two of which are linked to mental retardation, myotonic dystrophy, and several late-onset neurodegenerative diseases. In all cases, these mutations exhibit gametic and/or somatic instability once they have expanded into the mutant range. The mutations are located in coding and noncoding gene regions and have been found to act by dominant and recessive mechanisms. A wide range of mouse models has been generated to understand both of the mechanisms that underlie repeat instability and the molecular pathogenesis of the diseases. Mouse models have proved extremely useful in these goals and are now also being used for the preclinical testing of therapeutic compounds. This chapter reviews the successes and limitations of the approaches that have been developed.

Key Words: Triplet repeat; polyglutamine disease; fragile X syndrome; myotonic dystrophy; Friedreich's ataxia; mouse models; repeat instability; Huntingtin's disease.

1. The Triplet Repeat Diseases

The first triplet repeat expansion mutations were described in 1991 and demonstrated that Fragile X syndrome involves a CGG repeat ***(1)*** and spinal and bulbar muscular atrophy (SBMA), a CAG repeat ***(2)***. Since that time, a further 14 triplet repeat disorders have been described. They essentially fall into three categories. In Fragile X syndrome, the CGG repeat lies in the promoter of the *FMR1* gene, and in Friedreich's ataxia, the GAA repeat is located in intron 1 of the gene encoding frataxin ***(3)***, and both are loss-of-function mutations. The second category comprises nine neurodegenerative disorders that are predominantly gain-of-function mutations caused by a CAG repeat expansion in the coding region of the gene in question and resulting

From: *Methods in Molecular Biology, vol. 277: Trinucleotide Repeat Protocols*
Edited by: Y. Kohwi © Humana Press Inc., Totowa, NJ

in a polyglutamine (polyQ) expansion in the disease protein ***(4)***. These include Huntington's disease (HD), dentatorubral pallidoluysian atrophy (DRPLA), spinal and bulbar muscular atrophy (SBMA), and the spinocerebellar ataxias 1, 2, 3, 6, 7, and 17. The third category is exemplified by the autosomal dominant disorders myotonic dystrophy (DM) ***(5)*** and spinocerebellar ataxia type 8 (SCA8) ***(6)*** caused by noncoding CTG expansions. This review summarizes progress in generating mouse models of these disorders and the subsequent insights into disease pathogenesis.

2. Models of Pathology

2.1. Loss-of-Function Mutations

2.1.1. Fragile X

Fragile X syndrome is the most common form of inherited mental retardation causing cognitive impairment, macro-orchidism (large testis), and behavioral abnormalities. The predominant Fragile X syndrome mutation is a CGG repeat, which resides in the 5' untranslated region of the *FMR-1* gene ***(7,8)***. The product of this gene, FMRP, is a ubiquitously expressed RNA-binding protein that contains nuclear localization (NLS) and nuclear export (NES) signals. FMRP associates with numerous other proteins and multiple RNAs to form a messenger ribonuclear protein complex that is predominantly found to be associated with the actively translating ribosomes in the cell. Upon expansion to a full mutation (>200 repeat units), the repeat becomes hypermethylated, preventing *FMR-1* transcription, thereby acting as a null mutation, which has been modeled by a conventional knockout strategy ***(9)***. An excellent evaluation of this mouse as a model of the human disease has recently been published ***(10)***.

Numerous cognitive tests have been applied to the FMR-1 knockout mice to determine whether they exhibit a cognitive impairment that might be compared to the mental retardation observed in the patients. The mice develop a mild learning impairment in the Morris water maze, a plus-shaped water maze test, and a terrestrial radial arm maze (*see* **ref. *10***). Although they also showed evidence of alterations in sensorimotor integration, there was no indication of the increased anxiety or hyperactivity seen in patients. Morphologically, the mice model the macro-orchidism seen in patients very accurately, arising as the consequence of increased Sertoli cell proliferation in early life ***(11)***. There are no gross anatomical changes in either patient or mouse brains. However, both do show an excess of dendritic spines, suggesting a role for FMRP in synaptic maturation ***(12,13)***. Finally, seizures occur in 22% of Fragile X patients, and although spontaneous seizures were not observed in the FMR-1 knockout mice, they were more prone to seizures than their control littermates ***(14)***.

The FMR-1 knockout mouse provides a very useful model of Fragile X syndrome, which has led to a greater understanding of the molecular pathology of this disease and will also be valuable in testing therapeutic strategies. However, it can neither be used to uncover molecular processes related to the CGG expansion nor to test therapeutic approaches that might act directly on the mutation. A knock-in model has been described in which the $(CGG)_8$ endogenous repeat in the promoter of the mouse FMR-1 gene was replaced with $(CGG)_{98}$ ***(15)***. The article describes the moderate instability

of the $(CCG)_{98}$ with the majority of changes occurring as expansion but does not present a phenotypic analysis. This repeat will continue to expand with further generations but whether it might expand to a size by which it could cause disease in the mouse is currently uncertain.

2.1.2. Friedreich's Ataxia

Friedreich's ataxia (FRDA) is a neurodegenerative disease that is characterized by the degeneration of the large sensory neurons of the spinocerebellar tracts, cardiomyopathy, and increased incidence of diabetes. GAA repeat expansions (ranging from 100 to 1100 repeats) in intron 1 of the gene encoding frataxin have been shown to inhibit transcription and result in a severe reduction in frataxin levels. Frataxin is a ubiquitously expressed mitochondrial protein for which proposed functions include mitochondrial iron transport, iron–sulfur (Fe-S) cluster biogenesis, iron binding/sequestration, and the response to oxidative stress. The accumulation of iron, a decrease in the activity Fe-S proteins, and the generation of reactive oxygen species are all features of the human disease (for reviews, *see* **refs. *16*** and ***17***).

The first approach to generating a mouse model of FRDA used a classical knockout strategy to delete the frataxin gene by homologous recombination ***(18)***. This showed that homozygous deletion of frataxin in the mouse causes embryonic lethality a few days after implantation, demonstrating that frataxin plays an important role in early development. An absence of iron accumulation during embryonic resorption indicated that cell death might be caused by an independent mechanism. However, this model was likely to have limited use, and the milder phenotype in humans most likely arises as a result of the residual frataxin activity associated with the expansion mutations. To circumvent the embryonic lethality, the Koenig group employed a strategy to create two independent conditional knockout models ***(19)***. Through the use of mice expressing Cre recombinase under the control of the muscle creatine kinase promoter or the neuron-specific enolase promoter, they generated a striated-muscle frataxin-deficient line and a neuron/cardiac-muscle frataxin-deficient line. Together, these reproduce important progressive pathophysiological and biochemical features of the human disease, including cardiac hypertrophy without skeletal muscle involvement, large sensory neuron dysfunction without alteration of the small sensory and motor neurons, and impaired activities of complexes I–III of the electron transport chain and of the aconitases. In these models, inactivation of the iron–sulfur-dependent enzymes and the onset of pathology occurred before intramitochondrial iron accumulation. These models are likely to be extremely useful in testing therapeutic options and a beneficial strategy has already been suggested ***(17)***.

It still remains important to produce a mouse model that molecularly reproduces the human disease. A knock-in mouse was recently generated through the introduction of a $(GAA)_{230}$ repeat into the mouse frataxin gene ***(20)***. These were crossed to frataxin knockout mice to generate mice expressing 25–36% of wild-type frataxin levels. Unfortunately, these mice did not develop anomalies of motor coordination, iron metabolism, or response to iron loading. As an alternative approach, the recent demonstration that the embryonic lethality in frataxin null mice can be rescued by crossing to

transgenic mice expressing the human frataxin gene as a yeast artificial chromosome (YAC) clone ***(21)*** raises the possibility that a mouse model could be generated by the introduction of a YAC derived from a patient who expresses frataxin at sufficiently reduced levels to induce pathology.

2.2. Myotonic Dystrophy

Myotonic dystrophy is an autosomal dominant disorder characterized by skeletal muscle wasting, myotonia, cardiac arrhythmia, hyperinsulinemia, mental retardation, and ocular cataracts. The mutation is a CTG repeat expansion in the 3' untranslated region of the DM protein kinase gene (*DMPK*) and 5' to a homeodomain-encoding gene (*SIX5*). The disease exhibits pronounced anticipation, and, in general, mildly affected individuals have 50–150 repeats, classic adult onset cases have 100–1000 repeats, and congenital cases can range from 500 to more than 2000 repeats. There are three potential mechanisms by which the CTG expansion might act in a dominant manner and cause DM. First, the expansion might reduce DMPK levels by perturbing the processing or transport of the mutant *DMPK* mRNA. Second, the repeated motif might exert its toxic effects at either the level of DNA or, more likely, the RNA. Third, the CTG expansion might modify the chromatin surrounding the CTG expansion, thereby altering the expression level of one or more neighboring genes, thereby resulting in a contiguous gene syndrome ***(5,22,23)***. Mouse models have been generated to address the likely contribution of each of these potential mechanisms to the pathogenesis of DM.

To test the hypothesis that decreased expression of *DMPK* contributes to DM, two research groups independently generated mice nullizygous for *Dm15* (the mouse *DMPK* homolog) ***(24,25)***. Homozygous nulls were found to have a reduced force generation in skeletal muscle ***(24)***, a deficiency in skeletal muscle sodium channel gating ***(26)***, and abnormal cardiac conduction ***(27)***, suggesting that loss of *DMPK* function might contribute to the muscle weakness and cardiac disease in myotonic dystrophy, although these mice did not develop the myotonia and progressive myopathy seen in DM. Similarly, a strain of mice in which the *six5* gene (located 3' to *Dm15*) has been deleted developed ocular cataracts ***(28,29)*** and cardiac conduction system abnormalities ***(30)***. The progressive rate and severity of cataract formation was inversely related to *six5* dosage, suggesting that *SIX5* transcription might be important in the etiology of DM1 and supporting the contiguous gene syndrome hypothesis. However, more recently, the mutation causing DM2 has been identified as a CCTG repeat located in intron 1 of the gene encoding the zinc-finger protein 9 (*ZNF9*) ***(31)***. The demonstration that a second repeat expansion mutation in an entirely different genomic context can cause all DM symptoms questions the requirement for the involvement of other genes ***(23)***.

Two mouse models have successfully tested the toxic mRNA hypothesis. The first derived a transgenic mouse model in which a $(CUG)_{250}$ repeat was inserted into the 3' untranslated region of the human skeletal actin gene and expressed at high levels in muscle. The mutant mRNA was retained in the nucleus, as in DM, and the mice developed myotonia and myopathy ***(32)***. Further analysis of these mice showed that aber-

rant splicing of the pre-mRNA for CIC-1, the main chloride channel in muscle, resulted in a loss of CIC-1 protein from the surface of the membrane, resulting in a reduction of transmembrane, chloride conductance below that expected to cause myotonia ***(33)***. A second model in which a $(CUG)_{300}$ repeat is expressed in the context of human DMPK mRNA displayed clinical, histological, molecular, and electrophysiological abnormalities in skeletal muscle consistent with those observed in DM patients. Also as in DM patients, they showed abnormal tau expression in the brain, thereby demonstrating that the toxic gain of function by mutant RNA can at least occur in muscle and brain ***(34)***.

2.3. Polyglutamine Repeat Diseases

The predominant mechanism underlying the molecular pathogenesis of polyQ disease is a toxic gain of function and the generation of mouse models for these diseases has been extremely successful. A total of nine mouse models of HD have been published that include those transgenic for a mutated version of an N-terminal fragment of the human HD gene ***(35–37)***, a full-length human cDNA ***(38)***, human genomic YAC clones ***(39)***, and knock-in models in which CAG expansions of varying lengths have been inserted into the mouse *hdh* gene ***(40–43)***. Mouse models for the spinocerebellar ataxias include those transgenic for human versions of an SCA1 cDNA ***(44)***, SCA2 cDNA ***(45)***, SCA3 YAC genomic clone ***(46)***, and SCA7 cDNAs ***(47–49)***. Knock-in models have also been generated for SCA1 ***(50)*** and SCA7 ***(51)***. Transgenic models for DRPLA include mutated human versions of a cDNA ***(52)*** and a genomic cosmid clone ***(53)***, and for SBMA, they include mice transgenic for a fragment of the human androgen receptor (AR) gene ***(54,55)*** and the human AR cDNA ***(56,57)***.

The analysis of mouse models of polyQ disease has led to major insights into the pathogenesis of these disorders; however, because of space constraints, it is only possible to highlight a few of these investigations. Mouse models were instrumental in the discovery of polyQ aggregation as a neuropathological hallmark of polyQ disease ***(58–60)*** and have highlighted that nuclear inclusions are preceded by a nuclear accumulation of the mutant protein ***(42)***. Both nuclear and neuropil aggregates are found in HD postmortem brains ***(61,62)***, whereas they are restricted to the nucleus in most of the other polyQ disorders. Schilling et al. have generated models of HD and of DRPLA by the expression of an N-terminal fragment of the human *HD* gene and the full-length *DRPLA* gene under the control of the prion promoter ***(63)***. The detection of nuclear inclusions in both models and neuropil aggregates only in the HD model indicates that this distribution is not governed by expression pattern and that the protein context of the repeat must play an important role. The overexpression of the inducible form of hsp70 was found to slow the disease progression in an SCA1 ***(64)*** and SBMA model ***(65)***, suggesting that the misfolding of the polyQ protein and its nuclear accumulation is important for pathogenesis. The analysis of gene expression changes in mouse models of HD ***(66,67)*** and SCA1 ***(68)*** were instrumental in pinpointing transcriptional dysregulation as an early event in polyQ disease. Without exception, neuronal cell death is not a prominent feature in the mouse models, and when it does occur, it is a late-stage event, indicating that the phenotypes arise as a result of neuronal dysfunc-

tion. The expression of mutant ataxin 7 in either photoreceptors or Purkinje cells indicated that neurodegeneration is not limited to the neurons in which the transgene is expressed but also causes secondary alterations in the postsynaptic neurons *(47)*.

Mouse models of HD are now being used extensively for the preclinical assessment of pharmacological approaches to treat HD. Positive outcomes have been achieved for the following neuroprotective compounds targeted at free-radical damage, excitotoxicity, and loss of membrane integrity: creatine *(69,70)*, coenzyme Q *(71,72)* remacemide *(71,72)*, riluzole *(73)*, α-lipoic acid *(74)*, and essential fatty acids *(75)*. Although, the rationale for using these agents predates the cloning of the HD gene, recent data continue to support a contribution of these mechanisms to the disease process, and although these strategies are unlikely to be curative, there is every reason to believe that they might be beneficial. Therapeutic interventions targeted against specific molecular events include cystamine *(76,77)*, an inhibitor of tissue transglutaminase, Congo red *(78)*, an inhibitor of polyglutamine aggregation, and suberoylanilide hydroxamic acid (SAHA), a histone deacetylase inhibitor *(79)*. The possible beneficial effects of minocycline *(80)* were not repeated in a second study *(81)*. In all cases, it is currently unknown if the compounds are acting at the target for which they were selected; for example, riluzole *(82)* and minocycline *(81)* have both been found to be polyQ aggregation inhibitors and cystamine also acts as an antioxidant *(77)*. The most promising therapeutic intervention strategy to date has been the demonstration that leuprorelin, a lutenizing hormone-releasing hormone (LHRH) agonist that reduces testosterone release from the testes, dramatically rescued motor dysfunction and nuclear accumulation of mutant ARs in male SBMA transgenic mice *(56,83)*.

An HD mouse model expressing exon 1 huntingtin under the control of an inducible promoter has shown that the behavioral and neuropathological phenotypes can be reversed *(84)*. The inducible expression in the forebrain of an exon 1 HD construct with $(CAG)_{94}$ resulted in a progressive movement disorder accompanied by neuropathological changes, including an aggregate pathology, striatal atrophy, enlarged lateral ventricles, astrocyte proliferation, and a reduction in D1 dopamine receptor binding. The transgene was switched off at time after the phenotype had developed and, remarkably, the aggregates pathology and nuclear accumulation of the mutant protein; had mostly disappeared, the movement disorder was reversed, and the progression of the other neuropathological characteristics was halted. Therefore, the progression of the disease depends on the continuous expression of the mutant protein; neurons are capable of degrading the aggregated form of huntingtin and neuronal recovery is possible if irreversible changes that commit the cell to neurodysfunction or cell death have not occurred. This was the first indication that it might be possible to treat HD after the onset of symptoms and that the disease may not be irreversible.

3. Models of Repeat Instability

All of the triplet repeat disorders exhibit gametic and somatic repeat instability. The mechanisms that underlie this instability are little understood and attempts to model repeat instability in the mouse have met with mixed success. In the case of

models of Fragile X syndrome, no intergenerational instability was detected in mice transgenic for a maximum of 97 uninterrupted CGG repeats in the *FMRI* promoter, despite the fact that permutations of this size are invariably unstable in human transmission ***(10)***. When introduced in the context of the *FMR1* gene either as $(CGG)_{90}$ in a human YAC clone ***(85)*** or after the recombination of $(CGG)_{98}$ into the mouse *Fmr1* gene ***(15)***, the repeat showed mild instability, but the large expansions that are seen upon inheritance of alleles of this size from a permutation female to a full mutation in humans were never observed. In contrast, a $(GAA)_{230}$ repeat that had been introduced into the mouse frataxin gene and, therefore, also in its appropriate genomic context showed no meiotic or mitotic instability ***(20)***.

By comparison, CAG and CTG repeat instability has been relatively straightforward to model in the mouse. $(CAG)_{78}$–$(CAG)_{>150}$ repeat expansions in both transgenic and knock-in models have consistently shown a tendency to expand on male transmission and contract on female transmission; for example, in the context of a fragment of the human HD gene ***(86)***, the mouse homolog of the HD gene (*hdh*) ***(87)***, a human *SCA1* cDNA ***(88)***, the mouse *sca1* locus ***(89)***, and the human *DRPLA* gene ***(53)***. However, the large repeat expansions that would be observed in humans upon the male transmission of repeats of this size are rare events in the mouse. Pronounced somatic instability has also been observed in selective brain regions and peripheral tissues ***(53,86,87)*** and the use of small-pool polymerase chain reaction (PCR) techniques showed that expansions from 72 repeats up to more than 250 repeats can occur in the striatum of an HD knock-in mouse ***(90)***. Somatic instability has been detected in human HD cases ***(91)***, although repeat expansions of this size have yet to be reported. $(CTG)_{160}$ repeats in the context of the 3' untranslated region of the *DMPK* gene also show a tendency to expand on male transmission and contract on female transmission ***(92)***. In contrast, a $(CTG)_{320}$ repeat that lies within the context 45-kb of human DNA containing the *DMPK* gene recapitulates the instability that occurs in DM patients more closely and shows expansions and contracts on both male and female transmission with a strong bias toward expansion ***(93)***, indicating that flanking sequences contribute to the pattern of instability. Pronounced somatic instability has also been reported in the mouse lines carrying these large CTG expansions ***(93,94)***.

Investigations into the mechanism underlying repeat instability in the mouse have focused on manipulation of the mismatch repair system. The mismatch repair enzyme MSH2 had been shown to bind to slipped strand structures generated from CTG·CAG repeats in a structure-specific manner ***(95)***. The affinity increased with the length of the repeat sequence and preferentially bound to looped-out CAG repeats, suggesting that MSH2 might participate in triplet repeat expansion. Consistent with this, an absence of the *Msh2* gene product was found to stabilize the somatic instability of repeats of approx $(CAG)_{120}$ in the R6/1 Huntington's disease mouse model ***(96)***. Subsequently, Wheeler et al. have shown that an absence of *Msh2* also stabilizes the striatal instability of the CAG repeat in the Hdh^{Q111} knock-in mouse model of HD leading to a 5-mo delay in the nuclear accumulation of the mutant protein ***(97)***. In addition, an *Msh2–/–* background led to a switch from predominance of expansions on paternal

transmission to only contractions, whereas both expansions and contractions were still observed on maternal transmission ***(97)***. Similar experiments have been conducted to examine the effects of *Msh3* and *Msh6* deficiency on the stability of a $(CTG)_{84}$ repeat that had been introduced into the mouse *DM* locus ***(98)***. This repeat is relatively stable during intergenerational segregation, but somatic tissue showed substantial repeat expansion. Introduction of the alleles onto an *Msh3*-deficient background completely blocked somatic instability, whereas *Msh6* deficiency resulted in a significant increase in the frequency of somatic expansions ***(98)***. The authors suggested that these contrasting effects might be explained by competition of *Msh3* and *Msh6* for binding to *Msh2* in functional complexes with different DNA mismatch-recognition specificity ***(98)***.

Acknowledgments

The work in the author's laboratory is funded by the Wellcome Trust, Hereditary Disease Foundation, Huntington's Disease Society of America, the Human Frontiers Science Program, and Medical Research Council.

References

1 Verkerk, A. J., Pieretti, M., Sutcliffe, J. S., et al. (1991) Identification of a gene (FMR-1) containing a CGG repeat coincident with a breakpoint cluster region exhibiting length variation in fragile X syndrome. *Cell* **65,** 905–914.

2 La Spada, A. R., Wilson, E. M., Lubahn, D. B., et al. (1991) Androgen receptor gene mutations in X-linked spinal and bulbar muscular atrophy. *Nature* **352,** 77–79.

3 Campuzano, V., Montermini, L., Molto, M. D., et al. (1996) Friedreich's ataxia: autosomal recessive disease caused by an intronic GAA triplet repeat expansion. *Science* **271,** 1423–1427.

4 Gusella, J. F. and MacDonald, M. E. (2000) Molecular genetics: unmasking polyglutamine triggers in neurodegenerative disease. *Nature Rev. Neurosci.* **1,** 109–115.

5 Mankodi, A. and Thornton, C. A. (2002) Myotonic syndromes. *Curr. Opin. Neurol.* **15,** 545–552.

6 Koob, M. D., Moseley, M. L., Schut, L. J., et al. (1999) An untranslated CTG expansion causes a novel form of spinocerebellar ataxia (SCA8). *Nature Genet.* **21,** 379–384.

7. O'Donnell, W. T. and Warren, S. T. (2002) A decade of molecular studies of fragile X syndrome. *Annu. Rev. Neurosci.* **25,** 315–338.

8 Jin, P. and Warren, S. T. (2003) New insights into fragile X syndrome: from molecules to neurobehaviors. *Trends Biochem. Sci.* **28,** 152–158.

9. The Dutch–Belgian Fragile X Consortium (1994) Fmr1 knockout mice: a model to study fragile X mental retardation. *Cell* **78,** 23–33.

10 Frank Kooy, R. (2003) Of mice and the fragile X syndrome. *Trends Genet.* **19,** 148–154.

11 Slegtenhorst-Eegdeman, K. E., de Rooij, D. G., Verhoef-Post, M., et al. (1998) Macroorchidism in FMR1 knockout mice is caused by increased Sertoli cell proliferation during testicular development. *Endocrinology* **139,** 156–162.

12 Comery, T. A., Harris, J. B., Willems, P. J., et al. (1997) Abnormal dendritic spines in fragile X knockout mice: maturation and pruning deficits. *Proc. Natl. Acad. Sci. USA* **94,** 5401–5404.

13 Irwin, S. A., Idupulapati, M., Gilbert, M. E., et al. (2002) Dendritic spine and dendritic

field characteristics of layer V pyramidal neurons in the visual cortex of fragile-X knockout mice. *Am. J. Med. Genet.* **111,** 140–146.
14 Chen, L. and Toth, M. (2001) Fragile X mice develop sensory hyperreactivity to auditory stimuli. *Neuroscience* **103,** 1043–1050.
15 Bontekoe, C. J., Bakker, C. E., Nieuwenhuizen, I. M., et al. (2001) Instability of a $(CGG)_{98}$ repeat in the Fmr1 promoter. *Hum. Mol. Genet.* **10,** 1693–1699.
16 Patel, P. I. and Isaya, G. (2001) Friedreich ataxia: from GAA triplet-repeat expansion to frataxin deficiency. *Am. J. Hum. Genet.* **69,** 15–24.
17 Puccio, H. and Koenig, M. (2002) Friedreich ataxia: a paradigm for mitochondrial diseases. *Curr. Opin. Genet. Dev.* **12,** 272–277.
18 Cossee, M., Puccio, H., Gansmuller, A., et al. (2000) Inactivation of the Friedreich ataxia mouse gene leads to early embryonic lethality without iron accumulation. *Hum. Mol. Genet.* **9,** 1219–1226.
19 Puccio, H., Simon, D., Cossee, M., et al. (2001) Mouse models for Friedreich ataxia exhibit cardiomyopathy, sensory nerve defect and Fe-S enzyme deficiency followed by intramitochondrial iron deposits. *Nature Genet.* **27,** 181–186.
20 Miranda, C. J., Santos, M. M., Ohshima, K., et al. (2002) Frataxin knockin mouse. *FEBS Lett.* **512,** 291–297.
21 Pook, M. A., Al-Mahdawi, S., Carroll, C. J., et al. (2001) Rescue of the Friedreich's ataxia knockout mouse by human YAC transgenesis. *Neurogenetics* **3,** 185–193.
22 Meola, G. (2000) Myotonic dystrophies. *Curr. Opin. Neurol.* **13,** 519–525.
23 Ranum, L. P. and Day, J. W. (2002) Dominantly inherited, non-coding microsatellite expansion disorders. *Curr. Opin. Genet. Dev.* **12,** 266–271.
24 Reddy, S., Smith, D. B., Rich, M. M., et al. (1996) Mice lacking the myotonic dystrophy protein kinase develop a late onset progressive myopathy. *Nature Genet.* **13,** 325–335.
25 Jansen, G., Groenen, P. J., Bachner, D., et al. (1996) Abnormal myotonic dystrophy protein kinase levels produce only mild myopathy in mice. *Nature Genet.* **13,** 316–324.
26 Mounsey, J. P., Mistry, D. J., Ai, C. W., et al. (2000) Skeletal muscle sodium channel gating in mice deficient in myotonic dystrophy protein kinase. *Hum. Mol. Genet.* **9,** 2313–2320.
27 Berul, C. I., Maguire, C. T., Aronovitz, M. J., et al. (1999) DMPK dosage alterations result in atrioventricular conduction abnormalities in a mouse myotonic dystrophy model. *J. Clin. Invest.* **103,** R1–R7.
28 Sarkar, P. S., Appukuttan, B., Han, J., et al. (2000) Heterozygous loss of Six5 in mice is sufficient to cause ocular cataracts. *Nature Genet.* **25,** 110–114.
29 Klesert, T. R., Cho, D. H., Clark, J. I., et al. (2000) Mice deficient in Six5 develop cataracts: implications for myotonic dystrophy. *Nature Genet.* **25,** 105–109.
30 Wakimoto, H., Maguire, C. T., Sherwood, M. C., et al. (2002) Characterization of cardiac conduction system abnormalities in mice with targeted disruption of Six5 gene. *J. Interv. Cardiol. Electrophysiol.* **7,** 127–135.
31 Liquori, C. L., Ricker, K., Moseley, M. L., et al. (2001) Myotonic dystrophy type 2 caused by a CCTG expansion in intron 1 of ZNF9. *Science* **293,** 864–867.
32 Mankodi, A., Logigian, E., Callahan, L., et al. (2000) Myotonic dystrophy in transgenic mice expressing an expanded CUG repeat. *Science* **289,** 1769–1773.
33 Mankodi, A., Takahashi, M. P., Jiang, H., et al. (2002) Expanded CUG repeats trigger aberrant splicing of ClC-1 chloride channel pre-mRNA and hyperexcitability of skeletal muscle in myotonic dystrophy. *Mol. Cell* **10,** 35–44.
34 Seznec, H., Agbulut, O., Sergeant, N., et al. (2001) Mice transgenic for the human myo-

tonic dystrophy region with expanded CTG repeats display muscular and brain abnormalities. *Hum. Mol. Genet.* **10,** 2717–2726.

35 Mangiarini, L., Sathasivam, K., Seller, M., et al. (1996) Exon 1 of the HD gene with an expanded CAG repeat is sufficient to cause a progressive neurological phenotype in transgenic mice. *Cell* **87,** 493–506.

36 Schilling, G., Becher, M. W., Sharp, A. H., et al. (1999) Intranuclear inclusions and neuritic aggregates in transgenic mice expressing a mutant N-terminal fragment of huntingtin. *Hum. Mol. Genet.* **8,** 397–407.

37 Laforet, G. A., Sapp, E., Chase, K., et al. (2001) Changes in cortical and striatal neurons predict behavioral and electrophysiological abnormalities in a transgenic murine model of Huntington's disease. *J. Neurosci.* **21,** 9112–9123.

38 Reddy, P. H., Williams, M., Charles, V., et al. (1998) Behavioural abnormalities and selective neuronal loss in HD transgenic mice expressing mutated full-length HD cDNA. *Nature Genet.* **20,** 198–202.

39 Hodgson, J. G., Agopyan, N., Gutekunst, C. A., et al. (1999) A YAC mouse model for Huntington's disease with full-length mutant huntingtin, cytoplasmic toxicity, and selective striatal neurodegeneration. *Neuron* **23,** 181–192.

40 Shelbourne, P. F., Killeen, N., Hevner, R. F., et al. (1999) A Huntington's disease CAG expansion at the murine Hdh locus is unstable and associated with behavioural abnormalities in mice. *Hum. Mol. Genet.* **8,** 763–774.

41 Levine, M. S., Klapstein, G. J., Koppel, A., et al. (1999) Enhanced sensitivity to *N*-methyl-D-aspartate receptor activation in transgenic and knockin mouse models of Huntington's disease. *J. Neurosci. Res.* **58,** 515–532.

42 Wheeler, V. C., White, J. K., Gutekunst, C. A., et al. (2000) Long glutamine tracts cause nuclear localization of a novel form of Huntington in medium spiny striatal neurons in HdhQ92 and HdhQ111 knock-in mice. *Hum. Mol. Genet.* **9,** 503–513.

43 Lin, C. H., Tallaksen-Greene, S., Chien, W. M., et al. (2001) Neurological abnormalities in a knock-in mouse model of Huntington's disease. *Hum. Mol. Genet.* **10,** 137–144.

44 Burright, E. N., Clark, H. B., Servadio, A., et al. (1995) SCA1 transgenic mice: a model for neurodegeneration caused by an expanded CAG trinucleotide repeat. *Cell* **82,** 937–948.

45 Huynh, D. P., Figueroa, K., Hoang, N., et al. (2000) Nuclear localization or inclusion body formation of ataxin-2 are not necessary for SCA2 pathogenesis in mouse or human. *Nature Genet.* **26,** 44–50.

46 Cemal, C. K., Carroll, C. J., Lawrence, L., et al. (2002) YAC transgenic mice carrying pathological alleles of the MJD1 locus exhibit a mild and slowly progressive cerebellar deficit. *Hum. Mol. Genet.* **11,** 1075–1094.

47 Yvert, G., Lindenberg, K. S., Picaud, S., et al. (2000) Expanded polyglutamines induce neurodegeneration and trans-neuronal alterations in cerebellum and retina of SCA7 transgenic mice. *Hum. Mol. Genet.* **9,** 2491–2506.

48 Yvert, G., Lindenberg, K. S., Devys, D., et al. (2001) SCA7 mouse models show selective stabilization of mutant ataxin-7 and similar cellular responses in different neuronal cell types. *Hum. Mol. Genet.* **10,** 1679–1692.

49 La Spada, A. R., Fu, Y., Sopher, B. L., et al. (2001) Polyglutamine-expanded ataxin-7 antagonizes crx function and induces cone-rod dystrophy in a mouse model of sca7. *Neuron* **31,** 913–927.

50 Watase, K., Weeber, E. J., Xu, B., et al. (2002) A long CAG repeat in the mouse Sca1 locus replicates SCA1 features and reveals the impact of protein solubility on selective neurodegeneration. *Neuron* **34,** 905–919.

51 Yoo, S. Y., Pennesi, M. E., Weeber, E. J., et al. (2003) SCA7 knockin mice model human SCA7 and reveal gradual accumulation of mutant ataxin-7 in neurons and abnormalities in short-term plasticity. *Neuron* **37,** 383–401.
52 Schilling, G., Wood, J. D., Duan, K., et al. (1999) Nuclear accumulation of truncated atrophin-1 fragments in a transgenic mouse model of DRPLA. *Neuron* **24,** 275–286.
53 Sato, T., Oyake, M., Nakamura, K., et al. (1999) Transgenic mice harboring a full-length human mutant DRPLA gene exhibit age-dependent intergenerational and somatic instabilities of CAG repeats comparable with those in DRPLA patients. *Hum. Mol. Genet.* **8,** 99–106.
54 Abel, A., Walcott, J., Woods, J., et al. (2001) Expression of expanded repeat androgen receptor produces neurologic disease in transgenic mice. *Hum. Mol. Genet.* **10,** 107–116.
55 Adachi, H., Kume, A., Li, M., et al. (2001) Transgenic mice with an expanded CAG repeat controlled by the human AR promoter show polyglutamine nuclear inclusions and neuronal dysfunction without neuronal cell death. *Hum. Mol. Genet.* **10,** 1039–1048.
56 Katsuno, M., Adachi, H., Kume, A., et al. (2002) Testosterone reduction prevents phenotypic expression in a transgenic mouse model of spinal and bulbar muscular atrophy. *Neuron* **35,** 843–854.
57 McManamny, P., Chy, H. S., Finkelstein, D. I., et al. (2002) A mouse model of spinal and bulbar muscular atrophy. *Hum. Mol. Genet.* **11,** 2103–2111.
58 Davies, S. W., Turmaine, M., Cozens, B. A., et al. (1997) Formation of neuronal intranuclear inclusions underlies the neurological dysfunction in mice transgenic for the HD mutation. *Cell* **90,** 537–548.
59 Li, H., Li, S. H., Cheng, A. L., et al. (1999) Ultrastructural localization and progressive formation of neuropil aggregates in Huntington's disease transgenic mice. *Hum. Mol. Genet.* **8,** 1227–1236.
60 Skinner, P. J., Koshy, B. T., Cummings, C. J., et al. (1997) Ataxin-1 with an expanded glutamine tract alters nuclear matrix-associated structures. *Nature* **389,** 971–974.
61 DiFiglia, M., Sapp, E., Chase, K. O., et al. (1997) Aggregation of Huntington in neuronal intranuclear inclusions and dystrophic neurites in brain. *Science* **277,** 1990–1993.
62 Gutekunst, C. A., Li, S. H., Yi, H., et al. (1999) Nuclear and neuropil aggregates in Huntington's disease: relationship to neuropathology. *J. Neurosci.* **19,** 2522–2534.
63 Schilling, G., Jinnah, H. A., Gonzales, V., et al. (2001) Distinct behavioral and neuropathological abnormalities in transgenic mouse models of HD and DRPLA. *Neurobiol. Dis.* **8,** 405–418.
64 Cummings, C. J., Sun, Y., Opal, P., et al. (2001) Over-expression of inducible HSP70 chaperone suppresses neuropathology and improves motor function in SCA1 mice. *Hum. Mol. Genet.* **10,** 1511–1518.
65 Adachi, H., Katsuno, M., Minamiyama, M., et al. (2003) Heat shock protein 70 chaperone overexpression ameliorates phenotypes of the spinal and bulbar muscular atrophy transgenic mouse model by reducing nuclear-localized mutant androgen receptor protein. *J. Neurosci.* **23,** 2203–2211.
66 Cha, J. H., Kosinski, C. M., Kerner, J. A., et al. (1998) Altered brain neurotransmitter receptors in transgenic mice expressing a portion of an abnormal human huntington disease gene. *Proc. Natl. Acad. Sci. USA* **95,** 6480–6485.
67 Luthi-Carter, R., Strand, A., Peters, N. L., et al. (2000) Decreased expression of striatal signaling genes in a mouse model of Huntington's disease. *Hum. Mol. Genet.* **9,** 1259–1271.
68 Lin, X., Antalffy, B., Kang, D., et al. (2000) Polyglutamine expansion down-regulates

specific neuronal genes before pathologic changes in SCA1. *Nature Neurosci.* **3,** 157–163.

69 Ferrante, R. J., Andreassen, O. A., Jenkins, B. G., et al. (2000) Neuroprotective effects of creatine in a transgenic mouse model of Huntington's disease. *J. Neurosci.* **20,** 4389–4397.

70 Andreassen, O. A., Dedeoglu, A., Ferrante, R. J., et al. (2001) Creatine increase survival and delays motor symptoms in a transgenic animal model of Huntington's disease. *Neurobiol. Dis.* **8,** 479–491.

71 Ferrante, R. J., Andreassen, O. A., Dedeoglu, A., et al. (2002) Therapeutic effects of coenzyme Q10 and remacemide in transgenic mouse models of Huntington's disease. *J. Neurosci.* **22,** 1592–1599.

72 Schilling, G., Coonfield, M. L., Ross, C. A., et al. (2001) Coenzyme Q10 and remacemide hydrochloride ameliorate motor deficits in a Huntington's disease transgenic mouse model. *Neurosci. Lett.* **315,** 149–153.

73 Schiefer, J., Landwehrmeyer, G. B., Luesse, H. G., et al. (2002) Riluzole prolongs survival time and alters nuclear inclusion formation in a transgenic mouse model of Huntington's disease. *Mov. Disord.* **17,** 748–757.

74 Andreassen, O. A., Ferrante, R. J., Dedeoglu, A., et al. (2001) Lipoic acid improves survival in transgenic mouse models of Huntington's disease. *Neuroreport* **12,** 3371–3373.

75 Clifford, J. J., Drago, J., Natoli, A. L., et al. (2002) Essential fatty acids given from conception prevent topographies of motor deficit in a transgenic model of Huntington's disease. *Neuroscience* **109,** 81–88.

76 Karpuj, M. V., Becher, M. W., Springer, J. E., et al. (2002) Prolonged survival and decreased abnormal movements in transgenic model of Huntington disease, with administration of the transglutaminase inhibitor cystamine. *Nature Med.* **8,** 143–149.

77 Dedeoglu, A., Kubilus, J. K., Jeitner, T. M., et al. (2002) Therapeutic effects of cystamine in a murine model of Huntington's disease. *J. Neurosci.* **22,** 8942–8950.

78 Sanchez, I., Mahlke, C., and Yuan, J. (2003) Pivotal role of oligomerization in expanded polyglutamine neurodegenerative disorders. *Nature* **421,** 373–379.

79 Hockly, E., Richon, V. M., Woodman, B., et al. (2003) Suberoylanilide hydroxamic acid, a histone deacetylase inhibitor, ameliorates motor deficits in a mouse model of Huntington's disease. *Proc. Natl. Acad. Sci. USA* **100,** 2041–2046.

80 Chen, M., Ona, V. O., Li, M., et al. (2000) Minocycline inhibits caspase-1 and caspase-3 expression and delays mortality in a transgenic mouse model of Huntington disease. *Nature Med.* **6,** 797–801.

81 Smith, D. L., Woodman, B., Mahal, A., et al. (2003) Minocycline and doxycylcine do not improve phenotype in the R6/2 model of HD. *Ann. Neurol.*, **54,** 186–196.

82 Heiser, V., Engemann, S., Brocker, W., et al. (2002) Identification of benzothiazoles as potential polyglutamine aggregation inhibitors of Huntington's disease by using an automated filter retardation assay. *Proc. Natl. Acad. Sci. USA* **99(Suppl. 4),** 16,400–16,406.

83 Katsuno, M., Adachi, H., Doyu, M., et al. (2003) Leuprorelin rescues polyglutamine-dependent phenotypes in a transgenic mouse model of spinal and bulbar muscular atrophy. *Nature Med.* **9,** 768–773.

84 Yamamoto, A., Lucas, J. J., and Hen, R. (2000) Reversal of neuropathology and motor dysfunction in a conditional model of Huntington's disease. *Cell* **101,** 57–66.

85 Peier, A. M. and Nelson, D. L. (2002) Instability of a premutation-sized CGG repeat in FMR1 YAC transgenic mice. *Genomics* **80,** 423–432.

86 Mangiarini, L., Sathasivam, K., Mahal, A., et al. (1997) Instability of highly expanded CAG repeats in mice transgenic for the Huntington's disease mutation. *Nature Genet.* **15,** 197–200.

87 Wheeler, V. C., Auerbach, W., White, J. K., et al. (1999) Length-dependent gametic CAG repeat instability in the Huntington's disease knock-in mouse. *Hum. Mol. Genet.* **8,** 115–122.

88 Kaytor, M. D., Burright, E. N., Duvick, L. A., et al. (1997) Increased trinucleotide repeat instability with advanced maternal age. *Hum. Mol. Genet.* **6,** 2135–2139.

89 Lorenzetti, D., Watase, K., Xu, B., et al. (2000) Repeat instability and motor incoordination in mice with a targeted expanded CAG repeat in the Sca1 locus. *Hum. Mol. Genet.* **9,** 779–785.

90 Kennedy, L. and Shelbourne, P. F. (2000) Dramatic mutation instability in HD mouse striatum: does polyglutamine load contribute to cell-specific vulnerability in Huntington's disease? *Hum. Mol. Genet.* **9,** 2539–2544.

91 Telenius, H., Kremer, B., Goldberg, Y. P., et al. (1994) Somatic and gonadal mosaicism of the Huntington disease gene CAG repeat in brain and sperm. *Nature Genet.* **6,** 409–414.

92 Monckton, D. G., Coolbaugh, M. I., Ashizawa, K. T., et al. (1997) Hypermutable myotonic dystrophy CTG repeats in transgenic mice. *Nature Genet.* **15,** 193–196.

93 Seznec, H., Lia-Baldini, A. S., Duros, C., et al. (2000) Transgenic mice carrying large human genomic sequences with expanded CTG repeat mimic closely the DM CTG repeat intergenerational and somatic instability. *Hum. Mol. Genet.* **9,** 1185–1194.

94 Fortune, M. T., Vassilopoulos, C., Coolbaugh, M. I., et al. (2000) Dramatic, expansion-biased, age-dependent, tissue-specific somatic mosaicism in a transgenic mouse model of triplet repeat instability. *Hum. Mol. Genet.* **9,** 439–445.

95 Pearson, C. E., Ewel, A., Acharya, S., et al. (1997) Human MSH2 binds to trinucleotide repeat DNA structures associated with neurodegenerative diseases. *Hum. Mol. Genet.* **6,** 1117–1123.

96 Manley, K., Shirley, T. L., Flaherty, L., et al (1999) Msh2 deficiency prevents in vivo somatic instability of the CAG repeat in Huntington disease transgenic mice. *Nature Genet.* **23,** 471–473.

97 Wheeler, V. C., Lebel, L. A., Vrbanac, V., et al. (2003) Mismatch repair gene Msh2 modifies the timing of early disease in Hdh(Q111) striatum. *Hum. Mol. Genet.* **12,** 273–281.

98. van den Broek, W. J., Nelen, M. R., Wansink, D. G., et al. (2002) Somatic expansion behaviour of the $(CTG)_n$ repeat in myotonic dystrophy knock-in mice is differentially affected by Msh3 and Msh6 mismatch-repair proteins. *Hum. Mol. Genet.* **11,** 191–198.

II

Analysis of Triplet Repeat DNAs and RNAs

2

Analysis of Triplet Repeat Replication by Two-Dimensional Gel Electrophoresis

Maria M. Krasilnikova and Sergei M. Mirkin

Summary

Expansions of triplet repeats are responsible for more than 15 hereditary neurological disorders in humans ***(1,2)***. Triplet repeats are fairly stable when the number of elementary units is under approx 30, but become polymorphic in length with a clear bias for expansions when this threshold is exceeded. This results in the rapid addition of hundreds or even thousands of extra repeats and, ultimately, disease. The mechanisms of triplet repeat expansions are not yet understood. The role of several genetic processes, including replication ***(3)***, recombination ***(4,5)***, and repair ***(6)***, was suggested. However, given the swift accumulation of extra DNA material, DNA replication seems to be an intuitive candidate for generating expansions. Numerous data point to the aberrant replication of triplet repeats as a cause of triplet repeat expansions ***(3,7–16)***. Direct experimental proof of aberrant replication through triplet repeats was lacking. This encouraged us to study the mode of replication fork progression through triplet repeats in vivo. We analyzed the effects of triplet repeats on replication of bacterial or yeast plasmids using an approach called two-dimensional neutral/neutral gel electrophoresis of replication intermediates. This technique, originally developed for mapping replication origins ***(17,18)***, is also instrumental in defining replication pause sites ***(19)***. Using this technique, we were able to unambiguously demonstrate that expandable triplet repeats attenuate replication fork progression in vivo and get some insights into the mechanisms of repeat expansions ***(20,21)***.

Key Words: Triplet repeats; 2-D gel electrophoresis; replication fork; replication attenuation; bacterial plasmid; yeast plasmid.

1. Introduction

In our studies, we used two model systems based on cloning triplet repeats into standard *Escherichia coli* and *Saccharomyces cerevisiae* vectors ***(20,21)***. These multicopy plasmids replicate very efficiently, which allowed us to isolate and analyze

From: *Methods in Molecular Biology, vol. 277: Trinucleotide Repeat Protocols*
Edited by: Y. Kohwi © Humana Press Inc., Totowa, NJ

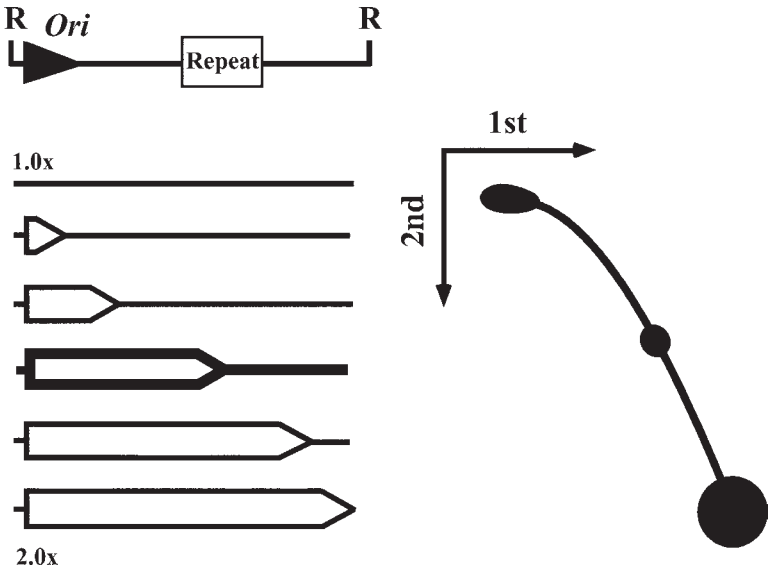

Fig. 1. Schematic representation of electrophoretic separation of replication products of bacterial plasmid containing repeats. Upper left panel shows the structure of the plasmid. The restriction enzyme R cleaves the plasmid upstream of the replication origin. The lower left panel shows the set of intermediates generated during replication. Stalling of the replication fork at a repeat results in the accumulation of a specific bubble intermediate (shown in bold). The right panel diagrams the separation of bubblelike intermediates by two-dimensional neutral/neutral gel electrophoresis. They are resolved by mass in the first dimension and by mass and shape in the second dimension. Stalling of the replication fork at a repeat leads to the appearance of a bulge on the bubble arc.

replication intermediates with a relative ease. The important difference between these two systems from the replication point of view is that replication origins are unidirectional in bacterial vectors and bidirectional in yeast. Consequently, only one replication fork replicates the whole bacterial plasmid, whereas the yeast plasmid is replicated by two forks moving in opposite directions.

The principles of electrophoretic analysis of replication intermediates were first applied to unidirectional replication in **ref. *22***. Intermediate products of plasmid replication are Θ shaped. Upon cleaving these intermediates with a restriction enzyme upstream of the replication origin, they convert into bubble-shaped molecules, where the size of the bubble correlates with the duration of replication (*see* **Fig. 1**). Bubble intermediates differ in their molecular mass (ranging from one to two plasmid masses) and shape. They are separated in two dimensions: first by mass (low-percentage agarose) and second by mass and shape (high-percentage agarose with ethidium bromide). Southern blotting hybridization with the radioactive plasmid probe reveals a so-called bubble arc (*see* **Fig. 1**).

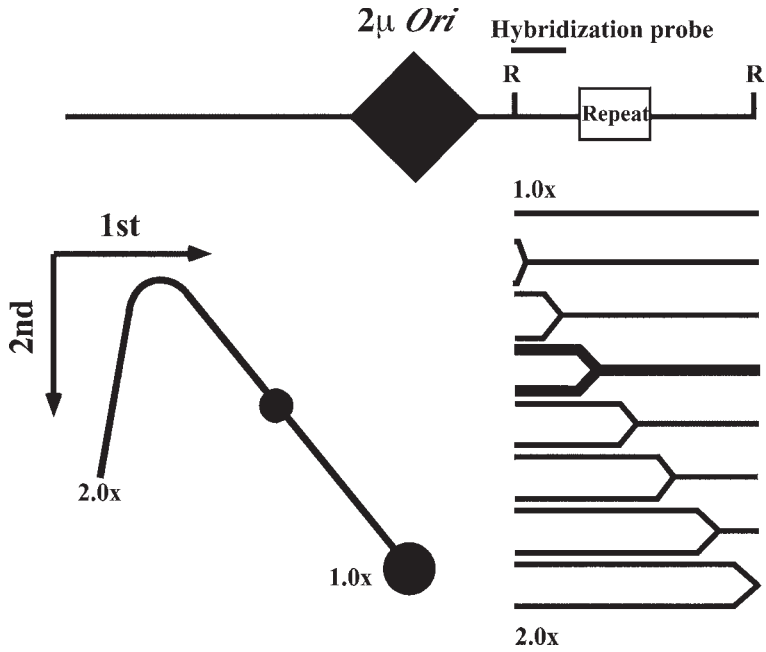

Fig. 2. Electrophoretic analysis of replication intermediates in yeast. Cleavage of replication intermediates with restriction enzyme R generates Y-shaped DNA molecules differing in size and shape that can be resolved by two-dimensional gel electrophoresis. Replication stalling at a repeat leads to the accumulation of a replication intermediate of a given size and shape (right panel), resulting in the appearance of a bulge on the Y arc.

Analysis of replication intermediates in the case of bidirectional replication ***(17,18)*** is schematically presented in **Fig. 2**. Because of the bidirectionality, the plasmid is separated into two domains replicated by different forks. In this diagram, triplet repeats are positioned in the path of the left-to-right replication fork. Replication intermediates generated by this fork convert into Y-shaped structures upon restriction digest downstream of *ori* and in the middle of the plasmid. These Y-shaped intermediates can be resolved in two-dimensional agarose gel and detected by hybridization with the corresponding restriction fragment (*see* **Fig. 2**).

For both unidirectional and bidirectional replication, stalling of the replication fork by a triplet repeat should result in the appearance of a bulge on the otherwise smooth bubble or Y arc, respectively, as a result of the preferential accumulation of replication intermediates of a specific size and shape.

Using this approach, we found that all expandable triplet repeats—d(CGG)$_n$•d(CCG)$_n$, d(CTG)$_n$•d(CAG)$_n$, and d(GAA)$_n$•d(TTC)$_n$—attenuate replication fork progression in both bacteria and yeast ***(20,21)***. Characteristic results for (CGG)$_n$-caused replication blockage in bacteria and yeast are shown in **Fig. 3**. One can clearly see a bulge on either bubble or Y arcs in replication intermediates isolated from bacteria and yeast, respectively.

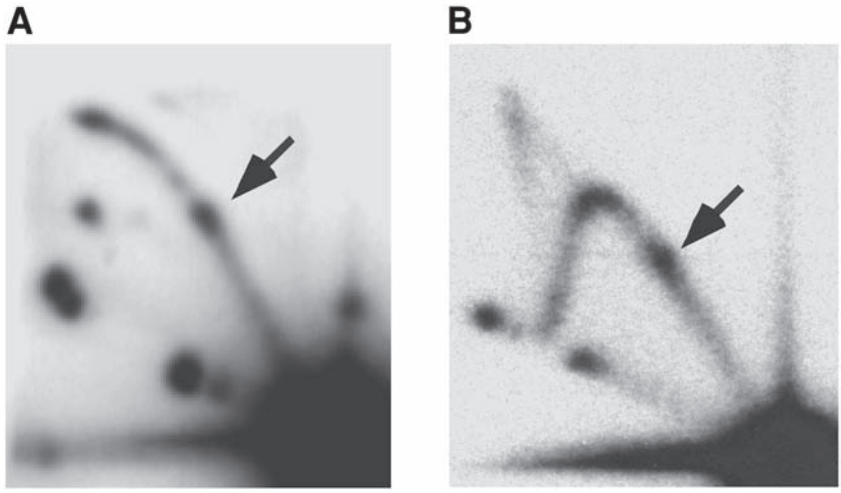

Fig. 3. Experimental data demonstrating replication stalling at the GGC_{70} repeat in *E. coli* **(A)** and GGC_{40} repeat in *S. cerevisiae* **(B)**. Arrows show replication stall sites.

The ratio of the radioactive signal of this bulge to that of the corresponding area of a smooth arc reflects the efficiency of replication fork stalling by a repeat. **Figure 4** shows an example of the quantitative analysis of the data for a $(CGG)_{40}$ repeat in yeast using a phosphoimager. The ratio of radioactivity in the peak area (areas 1+2) to that in the corresponding area of a smooth replication arc (area 2) represents the extent of replication slowing. In this particular case, it corresponds to 1.8-fold; that is progression of the replication through the repetitive is slowed down about 2-fold.

In both bacteria and yeast, the inhibitory effects of triplet repeats on replication increased with their length. The strength of inhibition in both systems depended on the repeat's base composition in the following order: $(CGG)_n$•$(CCG)_n$ > $(GAA)_n$•$(TTC)_n$ > $(CAG)_n$•$(CTG)_n$. However, even in the strongest cases, replication was only moderately (several-fold) slowed down. Thus, it is exceptionally high resolution of the electrophoretic analysis of replication intermediates that allowed us to detect these effects.

The question still remains: Is there a link between the replication attenuation at triplet repeats and their propensity to expand? It is plausible to speculate that extra repeats are added while the replication fork is trying to bypass the stall site. Although this hypothesis could not be verified by electrophoretic analysis of replication intermediates alone, the approach has already provided important clues to the mysteries of triplet repeat expansions.

2. Materials

2.1. Isolation of Replication Intermediates From E. coli

1. Resuspension solution: 25% (w/v) sucrose, 0.25 *M* Tris-HCl, pH 8.0, store at 4°C.
2. Lysozyme stock solution: 50 mg/mL in water. Store in small aliquots at –20°C.

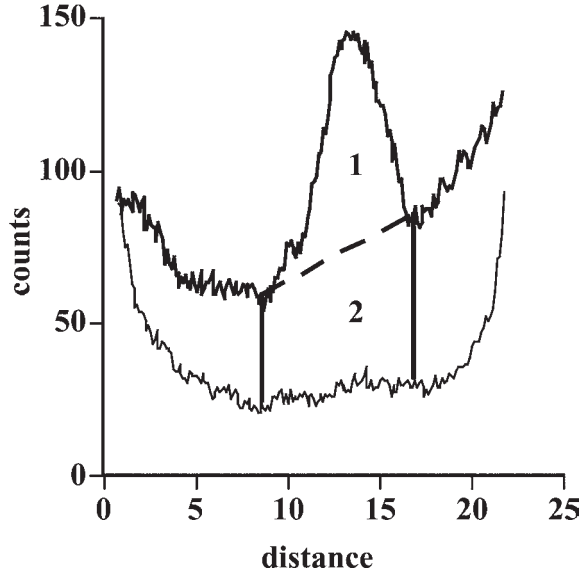

Fig. 4. Densitogram showing a quantitative analysis of the data presented in **Fig. 3B**. One can see a peak on the portion of the Y arc containing the GGC_{40} repeat. Thick line = Y arc; thin line = background noise.

3. RNase A stock solution: 10 mg/mL in 10 m*M* Tris-HCl, pH 7.5, 15 m*M* NaCl. Incubate in boiling water bath for 5 min to destroy DNase. Store in small aliquots at –20°C.
4. Lysis buffer: 1% (v/v) Brij-58, 0.4% (w/v) sodium deoxycholate, 0.063 *M* EDTA, pH 8.0, 50 m*M* Tris-HCl, pH 8.0, store at 4°C.
5. PEG+NaCl: 25% (w/v) PEG 6000–8000, 1.5 *M* NaCl. Store at 4°C.
6. Deproteinization solution: 1 *M* NaCl, 10 m*M* Tris-HCl (pH 9.0), 1 m*M* EDTA, 0.1% (w/v) sodium dodecyl sulfate (SDS). Store at room temperature.
7. Proteinase K stock solution: 20 mg/mL in H_2O. Store in small aliquots at –20°C.
8. Tris-buffered phenol, pH 8.0; store at 4°C.
9. Chloroform.
10. TE: 10 m*M* Tris-HCl, pH 8.0, 1 m*M* EDTA.

2.2. Isolation of Replication Intermediates From S. cerevisiae

1. NIB buffer: 17% glycerol, 50 m*M* MOPS, 150 m*M* NaOAc, 2 m*M* $MgCl_2$, 0.5 m*M* spermidine, 0.15 m*M* spermine, pH 7.2; store at 4°C.
2. YSTE buffer: 100 m*M* NaCl, 50 m*M* Tris-HCl, pH 8.0, 20 m*M* EDTA; store at 4°C.
3. Sarkosyl stock solution: 10% (w/v) solution; store at room temperature.
4. Proteinase K stock solution: 20 mg/mL in water. Store in small aliquots at –20°C.
5. Hoechst 33258 trihydrochloride stock solution: 2 mg/mL in water. Store in a dark bottle at 4°C.
6. TE: 10 m*M* Tris-HCl, pH 8.0, 1 m*M* EDTA; store at 4°C.

2.3. Electrophoretic Separation of Replication Intermediates

1. 10X TBE: 450 m*M* Tris-borate, 10 m*M* EDTA; store at room temperature.
2. Ethidium bromide stock solution: 10 mg/mL in water; store in a dark bottle at 4°C.

3. Methods

3.1. Isolation of Replication Intermediates From E. coli

1. Grow an overnight culture in 2 mL of selective media.
2. Inoculate 2 mL of an overnight culture into 200 mL of fresh selective media.
3. Grow cells until OD_{600} = 0.6 (about 3.5 h).
4. While the cells are growing, make sure that the centrifuge and rotor for pelleting the cells are cold.
5. Mix 100 g of ice with 3 mL NaCl in a 500-mL centrifuge tube, shake intensively.
6. When the culture reaches OD_{600} = 0.6, transfer it into a centrifuge tube with ice, mix, centrifuge for 7 min at 2500*g* at 0°C, decant the supernatant, and put the tubes on ice (*see* **Note 1**).
7. Resuspend cells in 2.5 mL of ice-cold resuspension solution and transfer suspension into a cold 50-mL centrifuge tube. Add 400 µL of lysozyme stock solution and 25 µL of RNase A stock solution, mix gently, and incubate on ice for 5 min.
8. Add 1 mL of 0.25 *M* EDTA, mix gently, and incubate for 5 min on ice.
9. Add 4 mL of lysis buffer, mix by inverting the tube gently, and incubate on ice for 10–20 min, inverting the tube every 5 min.
10. Centrifuge at 14,000*g* for 1 h at 4°C (*see* **Note 2**).
11. Transfer supernatant into a 50-mL centrifuge tube, add 5 mL of cold PEG+NaCl solution, vortex, and incubate on ice for about 1–2 h (*see* **Note 3**).
12. Centrifuge for 20 min at 14,000*g* at 4°C; decant the supernatant.
13. Dissolve the pellet in 400 µL of deproteinization solution, add 2 µL of Proteinase K stock solution, and incubate for 20 min at 65°C (*see* **Note 4**).
14. Extract DNA two times with an equal volume of tris-buffered phenol, pH 8.0.
15. Extract DNA one time with an equal volume of chloroform.
16. Add 2.5 vol of 100% ethanol, cool at –70°C for 20 min, centrifuge at 14,000*g* for 15 min, and decant the supernatant.
17. Wash the pellet with 70% ethanol.
18. Dry the pellet in a SpeedVac centrifuge.
19. Dissolve in 30–50 µL of TE, depending on the pellet size.
20. Check the amount of isolated plasmid DNA using 0.8% agarose gel electrophoresis (*see* **Note 5**).

3.2. Isolation of Replication Intermediates From S.cerevisiae

1. Grow an overnight culture in 10 mL of selective media.
2. Inoculate an overnight culture into 400 mL of fresh selective media to reach OD_{600} = 0.1. Grow cells until OD_{600} = 2.0.
3. Put 80 mL of 0.2 *M* EDTA into a 500-mL centrifuge tube and freeze at –20°C.
4. Stop cell growth by adding 4 mL of 10% NaN_3.
5. Pour the culture into the centrifuge tube with 0.2 *M* frozen EDTA; mix until the ice comes off the wall.
6. Pellet cells in a cold centrifuge for 5 min at 2500*g*.
7. Resuspend the pellet in 50 mL of ice-cold water and transfer into a 50-mL centrifuge tube. Centrifuge for 5 min at 2500*g*.
8. Resuspend the pellet in 4 mL of NIB buffer. Add an equal volume of glass beads and disrupt cells by vortexing for 10 min; chill on ice for 30 s after every 30 s of vortexing.
9. Allow beads to settle out and collect the supernatant. Add another 4 mL of NIB buffer to the beads, vortex, and collect the supernatant again.

10. Combine all the supernatant and centrifuge at 13,000*g* for 25 min.
11. Resuspend the pellet in 1.5 mL of the YSTE buffer by spreading it along the wall with the pipet. Add 0.225 mL of 10% sarkosyl and 30 μL of 20 mg/mL proteinase K stock solution, mix gently, and incubate for 1 h at 37°C.
12. Centrifuge at 12,000*g* for 5 min. Transfer the supernatant into a 15-mL tube.
13. Add 4.5 g of CsCl and 125 μL of Hoechst 33258 trihydrochloride stock solution and adjust the volume to 5.4 mL with distilled H_2O. Transfer into a Beckman Quick-Seal tube for a VTi65 rotor; seal the tube.
14. Centrifuge the density gradient in a Beckman ultracentrifuge (rotor VTi65) overnight at 55,000 rpm, 25°C.
15. Collect the lower DNA band under ultraviolet (UV) light (*see* **Note 6**). Adjust the volume to 1 mL with TE.
16. Purify DNA from Hoechst 33258 by four consequent butanol extractions (*see* **Note 7**).
17. Add 2 vol of 80% ethanol. Invert the tube until chromosomal DNA forms a visible coil. Centrifuge for 1 min at 13,000*g*; wash the pellet with 70% ethanol. Remove ethanol without drying the pellet.
18. Dissolve the pellet in 30–50 μL of TE.

3.3. Gel Electrophoretic Separation of Replication Intermediates

3.3.1. Restriction Digestion

1. Digest 2–5 μL of a replication intermediates sample (approx 0.5–1 μg of plasmid DNA isolated from bacterial cells, or approx 7–15 μg of DNA isolated from yeast) with a restriction endonuclease(s) in 50 μL for 1–3 h (*see* **Note 8**).
2. Add 50 μL of TE, extract DNA with 100 μL of phenol, followed by 100 μL of chloroform.
3. Add 15 μL of 3 *M* NaOAc, pH 7.0, and 300 μL of ethanol, cool for 10 min at –70°C and centrifuge for 6 min at 13,000*g*. Remove supernatant with a pipet, spin for 20 s, and remove the rest of supernatant.
4. Add 300 μL of 70% ethanol, vortex for 3 min, and remove the supernatant completely as after precipitation. Dry the pellets for about 3 min in a SpeedVac.
5. Dissolve in 12 μL of TE. Add 2 μL of glycerol dye.

3.3.2. First Dimension of Electrophoresis

1. Prepare 0.4% agarose gel with 1X TBE (*see* **Note 9**).
2. Load the sample on the gel.
3. Load a 1-kb ladder into the last two wells. Load 10 μL of concentrated bromophenol blue in one of the wells.
4. Run electrophoresis at 1 V/cm for about 15 h, until bromophenol blue, which runs approximately as a 2-kb-length fragment, reaches the end of the gel.
5. After electrophoresis is completed, cut one of the ladders from the gel and stain it with ethidium bromide to assure that a nonreplicated DNA fragment is at the very end of the gel. If not, continue electrophoresis until the nonreplicated fragment reaches the end of the gel (12 cm from the start).

3.3.3. Second Dimension of Electrophoresis

1. Prepare 1X TBE with 0.3 μg/mL of ethidium bromide for the second dimension and cool it to 4°C.
2. Stain the first-dimension gel in 400 mL of 1X TBE with 0.3 μg/mL of ethidium bromide for 20 min (*see* **Note 10**).

3. Set the second-dimension electrophoresis apparatus at 4–10°C (*see* **Note 11**).
4. Cut the lane with intermediates from the first-dimension gel under UV light using a razor blade (*see* **Note 12**). Cut out a portion of the lane corresponding to 1X to 2X sizes of intermediates, according to the ladder; add an extra 5 mm from each end.
5. Place the resultant piece of the gel onto the second-dimension tray on its side in a perpendicular direction. The bottom surface of the gel fragment should be positioned in the direction of electrophoresis.
6. Prepare 1% agarose in 1X TBE with 0.3 μg/mL of ethidium bromide stock solution.
7. Slowly pour the agarose onto the second-dimension tray to cover a piece of the gel from the first dimension.
8. Run electrophoresis with buffer circulation at 5 V/cm at 4–10°C until nonreplicated DNA migrates 7–8 cm from the start (*see* **Note 13**).
9. Blot-transfer the gel to the positively charged Nylon membrane.
10. Hybridize the blot to radiolabeled probe using a standard protocol.
11. Analyze the radiolabeled membrane on phosphoimager or expose it with an X-ray film (*see* **Note 14**).

4. Notes

1. All of the steps prior to cell lysis should be performed rapidly without delays. Once chilled, cells should stay cold.
2. The longer the centrifugation step is, the cleaner are the replication intermediates from chromosomal DNA.
3. If a low yield of plasmid is expected (low-copy plasmid, insufficient amount of cells), then overnight incubation is recommended.
4. The pellet will dissolve better if its not overdried. Warming deproteinization solution at 65°C before dissolving the pellet also helps to dissolve it better.
5. Replication intermediates samples are also going to contain variable amount of chromosomal DNA. Equal amounts of plasmid DNA should be taken for electrophoretic analysis.
6. The lower band containing chromosomal and plasmid DNA, along with the thin ribosomal DNA band just below it, should be pooled out with a 1-mL syringe. It usually comes out in a 0.25- to 0.5-mL volume.
7. If CsCl starts to precipitate at any step, add several drops of TE and mix until it dissolves.
8. Choosing restriction enzymes, it is important to remember that to achieve the best electrophoretic resolution, a triplet repeat should be positioned around the center (for the bubble arc) or first third (for the Y arc) of a 2- to 4-kb restriction fragment relative to the direction of replication.
9. The electrophoretic device should be free of ethidium bromide. If it was ever used for ethidium bromide-containing gels, it is necessary to wash it carefully with butanol. Use the tray and electrophoretic apparatus suitable for a 12- to 15-cm tray.
10. The 0.4% agarose gels are very easy to break; thus, staining on the tray helps to keep them intact. Slide the first-dimension gel onto another 12- to 15-cm tray that is specifically reserved for ethidium bromide staining. Staining on the same tray that was used for electrophoresis in the first dimension is not recommended to avoid ethidium bromide contamination. The 1X TBE buffer that was used for the first-dimension electrophoresis can be reused for staining the gel.
11. The second dimension requires an electrophoretic apparatus with a buffer circulation system. It should be different from the first-dimension device to avoid subsequent ethidium

bromide contamination of the first-dimension apparatus. A large device suitable for a 20 × 25-cm tray allows one to process up to nine samples simultaneously.

12. Make cuts as close to the lane as possible.
13. Chromosomal arcs (for yeast) or nonreplicated DNA spots (for bacteria) are easy to visualize under UV light.
14. Exposure times may vary. The usual exposure time for a blue-based film is overnight. For low-copy plasmids, a supersensitive film (Kodak Biomax MS) may be helpful.

Acknowledgments

We thank Randal Cox for proofreading the manuscript. This work was supported by grant GM60987 from NIH to S. M. Mirkin.

References

1 Bowater, R. P. and Wells, R. D. (2001) The intrinsically unstable life of DNA triplet repeats associated with human hereditary disorders. *Prog. Nucleic Acid Res. Mol. Biol.* **66,** 159–202.

2. Siyanova, E. Y. and Mirkin, S. M. (2001) Expansion of trinucleotide repeats. *Mol. Biol. (Mosc.)* **35,** 168–182.

3 Kang, S., Jaworski, A., Ohshima, K., et al. (1995) Expansion and deletion of CTG repeats from human disease genes are determined by the direction of replication in *E. coli*. *Nature Genet.* **10,** 213–218.

4 Jakupciak, J. P. and Wells, R. D. (2000) Gene conversion (recombination) mediates expansions of CTG.CAG repeats. *J. Biol. Chem.* **275,** 40,003–40,013.

5 Richard, G.-F., Goellner, G. M., McMurray, C. T., et al. (2000) Recombination-induced CAG trinucleotide repeat expansions in yeast involve the MRE11–RAD50–XRS2 complex. *EMBO J.* **19,** 2381–2390.

6 Kovtun, I. V. and McMurray, C. T. (2001) Trinucleotide expansion in haploid germ cells by gap repair. *Nature Genet.* **27,** 407–411.

7 Balakumaran, B. S., Freudenreich, C. H., and Zakian, V. A. (2000) CGG/CCG repeats exhibit orientation-dependent instability and orientation-independent fragility in *Saccharomyces cerevisiae*. *Hum. Mol. Genet.* **9,** 93–100.

8 Cleary, J. D., Nichol, K., Wang, Y. H., et al. (2002) Evidence of cis-acting factors in replication-mediated trinucleotide repeat instability in primate cells. *Nature Genet.* **31,** 37–46.

9 Freudenreich, C. H., Kantrow, S. M., and Zakian, V. A. (1998) Expansion and length-dependent fragility of CTG repeats in yeast. *Science* **279,** 853–856.

10 Ireland, M. J., Reinke, S. S., and Livingston, D. M. (2000) The impact of lagging strand replication mutations on the stability of CAG repeat tracts in yeast. *Genetics* **155,** 1657–1665.

11 Iyer, R. R., Pluciennik, A., Rosche, W. A., et al. (2000) DNA polymerase III proofreading mutants enhance the expansion and deletion of triplet repeat sequences in *Escherichia coli*. *J. Biol. Chem.* **275,** 2174–2184.

12 Miret, J. J., Pessoa-Brandao, L., and Lahue, R. S. (1998) Orientation-dependent and sequence-specific expansions of CTG/CAG trinucleotide repeats in *Saccharomyces cerevisiae*. *Proc. Natl. Acad. Sci. USA* **95,** 12,438–12,443.

13 Schweitzer, J. K. and Livingston, D. M. (1999) The effect of DNA replication mutations on CAG tract stability in yeast. *Genetics* **152,** 953–963.

14 Schweitzer, J. K. and Livingston, D. M. (1998) Expansions of CAG repeat tracts are frequent in a yeast mutant defective in Okazaki fragment maturation. *Hum. Mol. Genet.* **7,** 69–74.
15 Spiro, C., Pelletier, R., Rolfsmeier, M. L., et al. (1999) Inhibition of FEN-1 processing by DNA secondary structure at trinucleotide repeats. *Mol. Cell* **4,** 1079–1085.
16 White, P. J., Borts, R. H., and Hirst, M. C. (1999) Stability of the human fragile X (CGG)n triplet repeat array in *Saccharomyces cerevisiae* deficient in aspects of DNA metabolism. *Mol. Cell. Biol.* **19,** 5675–5684.
17 Brewer, B. J. and Fangman, W. L. (1987) The localization of replication origins on ARS plasmids in *S. cerevisiae*. *Cell* **51,** 463–471.
18 Huberman, J. A., Spotila, L. D., Nawotka, K. A., et al. (1987) The in vivo replication origin of the yeast 2 microns plasmid. *Cell* **51,** 473–481.
19 Deshpande, A. M. and Newlon, C. S. (1996) DNA replication fork pause sites dependent on transcription. *Science* **272,** 1030–1033.
20 Pelletier, R., Krasilnikova, M. M., Samadashwily, G. M., et al. (2002) Replication and expansion of trinucleotide repeats in yeast. *Mol. Cell. Biol.* **23,** 1349–1357.
21 Samadashwily, G. M., Raca, G., and Mirkin, S. M. (1997) Trinucleotide repeats affect DNA replication in vivo. *Nature Genet.* **17,** 298–304.
22. Martin-Parras, L., Hernandez, P., Martinez-Robles, M., et al. (1991) Unidirectional replication as visualised by two-dimensional agarose gel electrophoresis. *J. Mol. Biol.* **220,** 843–855.

3

Genetic Assays for Triplet Repeat Instability in Yeast

Michael J. Dixon*, Saumitri Bhattacharyya*, and Robert S. Lahue

Summary

The unusual genetic features of trinucleotide repeat (TNR) diseases have stimulated a substantial body of research into the underlying molecular mechanisms of repeat instability. As one useful tool to study TNR instability, selectable genetic assays for expansions and contractions were developed in the yeast *Saccharomyces cerevisiae*. These assays are sensitive, quantitative, easy to manipulate, and reproducible. Once colonies are identified through genetic selection, follow-up experiments with PCR help detail the precise molecular changes that occurred at the TNR tract. This chapter describes these yeast assays and provides useful technical insights into creating and testing triplet repeat instability in a classic model system.

Key Words: Trinucleotide repeat; expansion; contraction; yeast; genetic selection; Reporter construct; targeted chromosomal integration; mutant allele; polymerase chain reaction; genetic variability.

1. Introduction

The unusual genetic features of trinucleotide repeat (TNR) diseases ***(1–3)*** have stimulated a substantial body of research into the underlying molecular mechanisms of repeat instability ***(4–6)***. In many systems, including humans, mice, yeast, and bacteria, both small and large allele changes have been observed. Although there is no strict definition that separates the two classes, small events typically yield alterations ± one to three repeats. These TNR mutations almost certainly arise from DNA polymerase slippage events. In some disease genes, small expansions are important. For example, expansion of $(CAG)_{35}$ to $(CAG)_{36}$ at the HD locus might mean a life of disease to a Huntington's family member. More frequently, however, it is the larger

* These authors contributed equally to this chapter.

From: *Methods in Molecular Biology, vol. 277: Trinucleotide Repeat Protocols*
Edited by: Y. Kohwi © Humana Press Inc., Totowa, NJ

size changes of ± 4 to approx 1000 repeats that are relevant to disease ***(1–4,6)***. Also, large changes involve more intricate mutagenesis pathways that are unique to triplet repeats and therefore of inherent mechanistic interest.

One of the key technical challenges for studying TNR instability has been development of suitable assays. Most laboratories use physical techniques such as polymerase chain reaction (PCR) or Southern blotting to detect TNR instability. These physical approaches are appropriate when the mutation frequency is high, as in affected human families (e.g., *see* **ref. *7***). For other experimental situations, however, where the frequency of instability is lower, physical analysis may not provide suitable sensitivity. Therefore, some laboratories have developed genetic assays to evaluate TNR instability ***(8–10)***. Unfortunately, there is no good precedent to work with from the microsatellite instability literature. Other, nontriplet microsatellites contain runs of 1, 2, 4, or 5 basepairs, which can be readily assayed for mutation through genetic frameshift assays (i.e., restoration of a reporter gene function by an expansion or deletion in the repeat run [for an example, *see* **ref. *11***]). These types of frameshift assay are not possible with TNRs, which alter the tract length in multiples of three basepairs and, therefore, do not change the translational reading frame.

Our laboratory developed a genetic selection scheme whereby TNR expansions or contractions can be identified in *Saccharomyces cerevisiae* based on changes in expression of a selectable reporter gene ***(9,12)***. The basis for this assay is shown in **Fig. 1A** and a detailed description is provided in the figure legend. This assay was specifically designed to score for changes in tract length of ± five repeats or more and, therefore, measures TNR mutations that fall into the large size class mentioned earlier. In wild-type cells, we have observed expansions up to +28 repeats ***(9)*** and contractions of as many as –42 repeats ***(12)***. In certain mutant strains, expansions up to +100 repeats have been observed ***(13)***. The advantages to this assay are as follows:

1. There is sensitivity down to 10^{-7} mutations per cell generation or lower.
2. The assay is quantitative and yields absolute mutation rates. Reproducibility is also very good, with rate values typically falling within twofold of the average.
3. The assay is reversible, as seen in **Fig. 1A**, meaning that either expansions or contractions can be assayed by simple manipulations of the system.
4. With this assay, the length and sequence of the tract is easily controlled (*see* **Fig. 1B**; plasmid structure) by cloning synthetic oligonucleotides into the reporter construct.
5. The reporter can be integrated into yeast genome at three different loci (*see* **Fig. 1B**). This feature maximizes the likelihood that the TNR tract will be metabolized like chromosomal material. Also, integration occurs at positions where the direction of DNA replication is known, an important facet for examining replication-based instability. The integration properties also provide experimental controls for position effects, although typically the reporter behaves very similarly at all sites of integration that have been examined.
6. Once colonies are identified by genetic selection, it is easy to follow up with PCR to identify exact changes in tract length among genetically independent events, even when the mutation rate is low.
7. It is easy to test mutant strains, either by incorporating the reporter into a candidate mutant strain ***(13–15)*** or by screening disruption libraries ***(16)***.

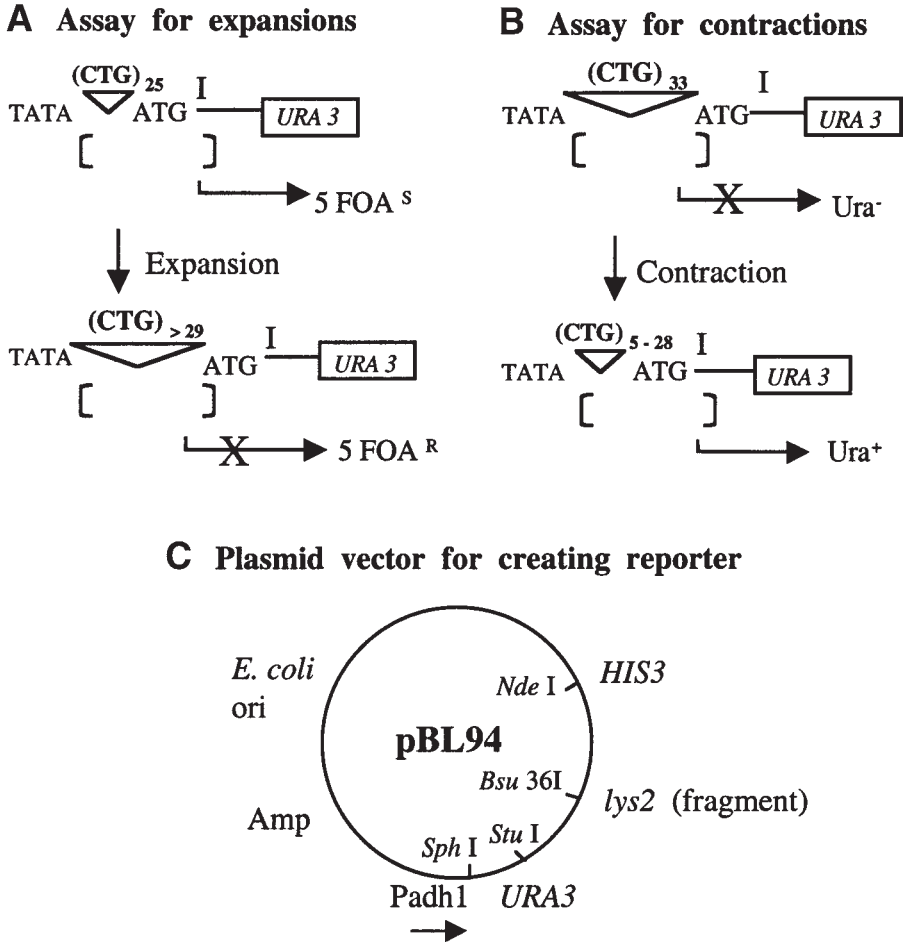

Fig. 1. Diagram illustrating the genetic selection of triplet repeat mutations and the important vector. **(A)** shows how expansions are identified genetically ***(9)***. The regulatory region controlling expression of the reporter gene *URA3* includes these important features: the TATA box; the triplet repeat region, marked with an inverted triangle; an out-of-frame ATG initiator codon; the preferred transcription initiation site I (CCACA sequence); and the start of the *URA3* structural gene. The top diagram illustrates the starting construct, with anticipated transcription (right-angle arrow) initiating within 55–125 bp (square brackets) from TATA. Initiation at I results in functional expression of *URA3* and sensitivity to 5FOA. If the TNR expands to >29 repeats (bottom diagram), the window of allowed transcription no longer includes I. Transcription initiating upstream of I will include the out-of-frame ATG, resulting in translational

(*continued*)

The main limitation to the assay is that it does not allow one to examine expansions for tracts longer than about 28 repeats. Alleles above this size range turn off the *URA3* reporter gene, so there is no opportunity to look for further expansions because there is no selection for them.

Creation of the reporter construct is straightforward and is outlined here and in **Fig. 1D**. More specific methodology is provided in **Subheading 3.** Candidate clones are identified by DNA sequencing of plasmids recovered from *Escherichia coli* transformants. Sequencing provides several important quality controls. First, it identifies the orientation of the TNR relative to the vector. Because the oligonucleotide cassette has identical cohesive ends, ligation can occur in two ways. Sequencing discriminates, for example, CAG repeats from CTG repeats on the *URA3* coding strand. Sequencing also ensures that no basepairs were added or deleted during the cloning process. Because TNR alleles of interest usually contain perfect triplet repeats, it is important to validate the integrity of the cloned product. Finally, sequencing will distinguish single cassette insertions from multiply-inserted clones. A useful primer for DNA sequencing is described in **Subheading 3.1.** Once verified, the appropriate cloned DNA is isolated on a large scale (such as Qiagen maxiprep) and resequenced as final verification.

Creation of the proper strain is the most important step in the assay. The process involves several steps, detailed in **Subheading 3.3.**, and includes both the basic protocols and the essential quality controls. Quality control is important because triplet repeats are inherently unstable. To work with them successfully, the investigator must be assured of the accuracy of the starting reagents. The TNR-containing reporter plasmid is cleaved with a restriction enzyme to facilitate targeting by homologous recombination and then introduced into yeast by transformation. Southern analysis is then performed to assure a single integration event at the desired chromosomal locus. **Fig-**

Fig. 1. (*continued*) incompetence (indicated by X) and resistance to 5FOA. **(B)** illustrates the assay for contractions ***(12)***. The only differences from the expansion assay are the following: (1) The starting tract for contractions is longer, typically 33 repeats, and (2) selection for contractions occurs by activation of expression of the *URA3* gene. In cells containing an inactive chromosomal *ura3* allele, such as *ura3-52*, the reactivation of the *URA3* reporter gene permits growth on media lacking uracil (SC-Ura). **(C)** shows the 7.5-kb plasmid vector used to create the various reporters ***(12)***. *HIS3* is used as a selectable marker to identify cells that have taken up the vector. The unique *Sph*I site permits cloning of oligonucleotide cassettes with 3' CATG overhangs into the promoter region, as detailed in **(D)**. Other relevant restriction sites are the *Bsu*36I site in the *lys2* fragment, which targets genomic integration to the *LYS2* locus, and the *Stu*I site in *URA3*, which targets integration to the genomic *ura3* locus. The reporter can also be targeted to genomic *his3* locus by cleavage of the vector with *Nde*I, but this site has not been used as extensively as targeting to *LYS2* or *ura3*. **(D)** shows a closeup of the oligonucleotide cassette insertion into the *Sph*I site. The lines represent the *Sph*I-cleaved, dephosphorylated pBL94 vector. The oligonucleotide duplex, with nonradioactive 5' phosphoryl groups denoted by asterisks, is shown inserting into the CAG orientation; the opposite orientation, with CTG repeats on the top strand is equally likely. The 3' CATG single-strand ends of each oligonucleotide provide complementarity to the termini generated by *Sph*I cleavage of the vector.

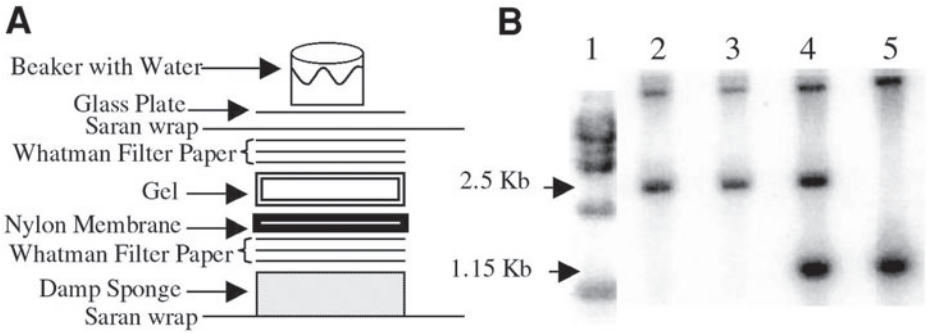

Fig. 2. Experimental setup and example of Southern analysis of yeast integrants. **(A)** shows a simple method for transferring restriction digests from an agarose gel to a Nylon membrane. See **Subheading 3.5.3.** for details. **(B)** provides an example of different types of integrant possible at the *LYS2* locus. Lane 1 contains 1- to 6-kb molecular-weight markers. Lanes 2 and 3 are digests that contain the proper single integration of the promoter/reporter construct. Lane 4 shows the results of a double integration, and lane 5 shows no integration.

ure 2A shows a simple but effective method for transferring the DNA from the gel to the membrane, and **Fig. 2B** provides a useful example of single integrants, a double integrant, or no integration. A final quality control step is a nonradioactive PCR reaction to confirm that the starting number of repeats has been maintained. Spontaneous expansions or deletions sometimes occur during preparation or workup of the strain. These must be excluded from the subsequent analysis because the TNR length has changed from the desired length. **Figure 3B** shows an example of this analysis.

Once the starting tract length is confirmed, the mutation rate can be determined by fluctuation analysis. A schematic of this assay can be seen in **Fig. 3A**. Cells are allowed to grow on nonselective media (**Fig. 3A2**) where there is no selective pressure for or against expansions or contractions. Cells containing any length of repeat can propagate on this media. Colonies from these yeast extract-peptone-dextrose (YPD) plates are then resuspended (*see* **Fig. 3A3**) in water and plated on nonselective and selective media to determine the mutation rate (*see* **Fig. 3A4**). The small dilution plated on the nonselective plate is used to determine the original colony size. The rest of the colony is allowed to grow on a selective plate, which specifically selects for yeast cells that have undergone a mutation within the triplet repeat tract. To measure contraction rates, SC-His-Ura plates are used. To measure expansions, SC-His plates (*see* **Note 2**) containing the drug 5-fluoroorotic acid (5FOA) are used ***(18)***. If the Ura3p is expressed, it converts 5FOA to a cytotoxic metabolite. If the *URA3* gene is shut off first because of an expansion in the promoter, 5FOA is not metabolized to the toxic form. The overall mutation rate is ascertained by determining the mean number of yeast cells that are able to grow on the selective media in comparison with the total number of cells in the original colony ***(19)***.

The final step of this assay is to ensure that the colonies growing on the selective plate contain actual triplet repeat mutations. For expansions, the reporter may be turned off by either an expansion within the promoter or another mutational event inactivat-

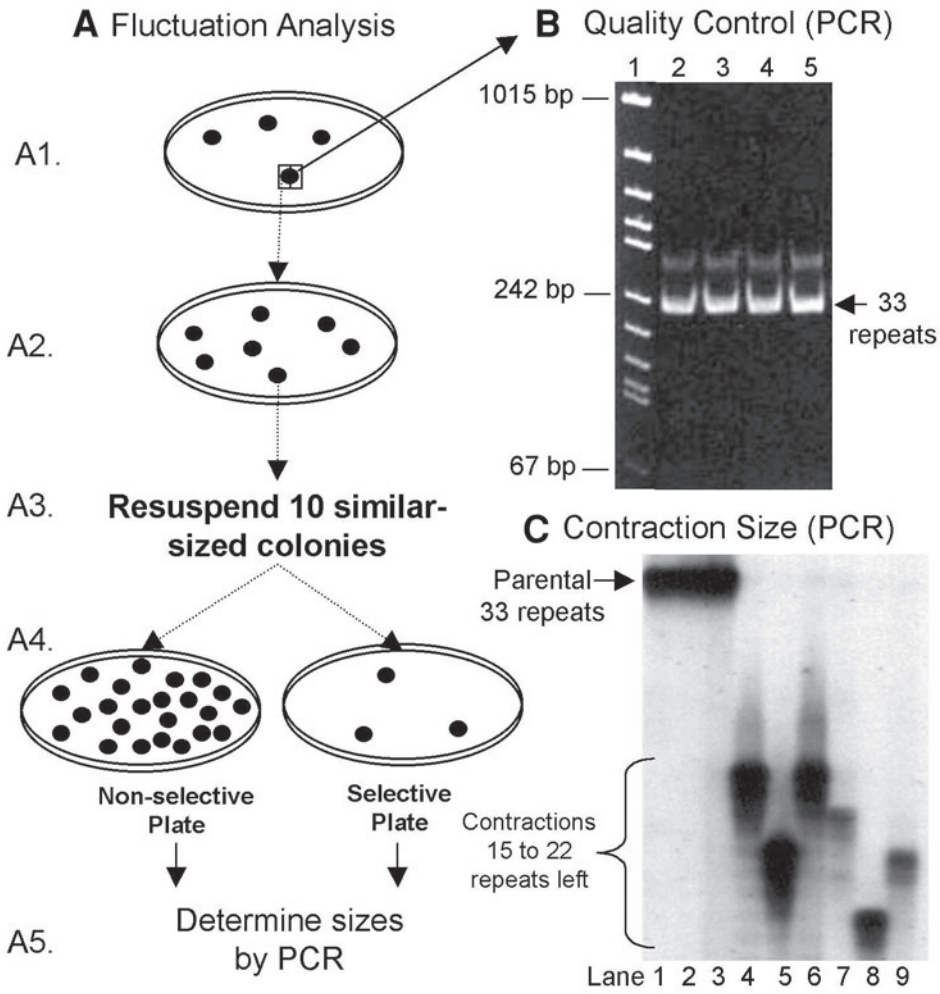

Fig. 3. Schematic chart showing steps in a fluctuation assay: **(3A1)**. From single colonies on YPD, confirm repeat tract size by PCR **(B)** analysis of about one-half the colony. Once confirmed, resuspend the remaining half colony and plate 100–300 cells onto a fresh YPD plate. Choose three independent isolates to ensure reproducible results. For the purposes of this diagram, only one isolate is shown. **(3A2)** Allow colonies to grow until the colonies are a predetermined size (from 40,000 to over 25 million; *see* **Note 5**). **(3A3)** Resuspend 10 independent isolates in sterile water (once again, for this diagram, only one isolate is shown). **(3A4)** From the suspension, plate a small aliquot onto another YPD plate to determine the total number of cells in that colony. Plate the rest of the cells onto a selective plate (SC-His+5FOA to test expansions and SC-His-Ura to test contractions). **(B)** Quality control by nonradioactive PCR verifies the proper starting size of the TNR tract. Lane 1 contains molecular-weight markers [the plasmid pRS313 ***(17)*** digested with *Hpa*II]. This provides molecular-weight markers from 67 to 1015 basepairs. Lanes 2–5 contain the PCR products (217 bp) of yeast strains containing 33 CTG repeats. Without the repeat tract (99 bp), the PCR product would be 118 bp. The more slowly migrating band in lanes 2–5 is a common artifact, probably the result of TNR DNA with

(*continued*)

ing the reporter gene. The latter of these two events is a false positive. To distinguish real events from false positives, single-colony PCR analysis is used (*see* **Fig. 3C**). For this, colonies from both the YPD and selective plates are chosen and amplified in the presence of radiolabeled dCTP. This labeled nucleotide is used because of the C richness of most TNR sequences from human disease genes. Repeat tract sizes (± two repeats) are then visualized on a 6% denaturing polyacrylamide gel ***(9)***. An example of contractions is shown in **Fig. 3C**.

A useful qualitative test can determine the general stability of a triplet repeat tract (*see* **Fig. 4**). This optional step is helpful in estimating relative mutation rates and therefore expedites proper performance of the more arduous fluctuation assay. For these assays, yeast cells are grown to an approx 1- to 2-cm^2 patch on YPD plates. Using sterile replica-plating techniques, the patches are transferred to selective media (either SC-His+5FOA for expansions or SC-His-Ura for contractions). Because some of these cells on the original YPD plate spontaneously expand or contract the TNR tract, they will be able to grow on the selective plate as small outgrowth colonies called papillae. The number of papillae in each patch is proportional to the mutation rate of the TNR. Papillae, like other yeast colonies, are white, but when photographed on a lightbox, they appear as dark spots. **Figure 4** shows an example where the number of papillae reflects the relative mutation rate in wild-type yeast strains compared to several mutants. These mutants raise the CTG expansion rate and therefore increase the number of papillae.

2. Materials

2.1. General Reagents

1. Sheared calf thymus DNA (≥ 4 mg/mL): Add 20 mg calf thymus DNA (Sigma) to 10 mL TE, pH 8.0. Dissolve the DNA at 50°C overnight. Shear the DNA by pipetting up and down four to five times, using a 5-mL pipet. Add 0.5% sodium dodecyl sulfate (SDS) and 100 μg/mL proteinase K. Incubate overnight at 50°C. Extract the DNA once with 1:1 phenol/chloroform and once with chloroform. Precipitate the DNA with sodium acetate and ethanol. Wash with 70% ethanol. Drain off the excess ethanol and resuspend the DNA in 1500 μL TE overnight at 60°C. Determine the final DNA concentration by measuring absorbance at 280 nm. Boil the DNA for 5 min, cool down, and freeze at –20°C.
2. 44% Polyethylene glycol (PEG; 200 mL): Add 88 g PEG (Sigma; molecular weight [MW] 3350) to 100 mL double-distilled H_2O (ddH_2O). Apply low heat to dissolve PEG. Bring up the volume to 200 mL with ddH_2O. Filter-sterilize and store at room temperature.
3. RNaseA (10 mL): Dissolve 100 mg RNaseA (Sigma) in 7 mL TE, pH 7.5. Bring the volume up to 10 mL with TE, pH 7.5. Aliquot 1 mL into Eppendorf tubes and boil for 10 min. Store at –20°C.

Fig. 3. (*continued*) aberrant secondary structure. (**C**): Examples of radioactive PCR analysis of contracted TNR alleles. Lanes 1–3 contain colonies from a nonselective plate. The major product corresponds to the length of the parental tract (33 repeats). PCR products from the selective plates are shown in lanes 4–9. These triplet repeat alleles have undergone contractions such that 15–22 repeats remain, judged by comparison to an M13 sequencing ladder. The shadow bands in lanes 4–9 are PCR artifacts that commonly arise when TNR sequences are amplified.

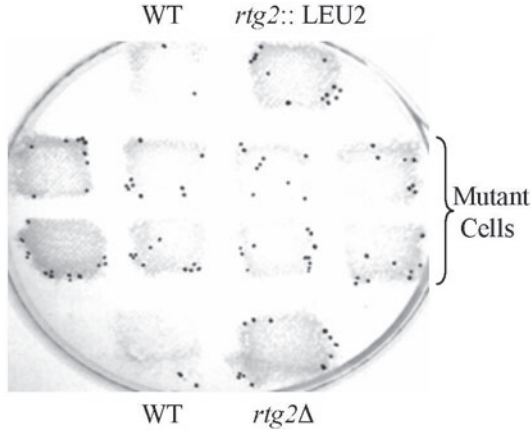

Fig. 4. Expansions of the $(CTG)_{13} + (C,T,G)_{12}$ repeat construct in yeast. Cells containing the expansion reporter were grown as patches on nonselective media, then replica plated onto media containing 5FOA. Control wild-type (WT) and several different mutant strains were also patched and replica plated. Papillae representing $5FOA^R$ outgrowths were recorded by photography with underlighting. Thus, the papillae appear as dark spots. For the eight patches from the mutants, the mutant phenotype is clearly elevated compared to the stable wild-type strain (one to two papillae) harboring the same reporter. The mutants give more than five papillae in each patch. Results with an isogenic mutant control (*rtg2::LEU2)* strain are also included. Based on known expansion rates in wild-type and *rtg2::LEU2* strains ***(16)***, this patch test distinguishes changes in rate of as little as twofold to threefold above wild type.

4. Agarose gel-loading buffer (loading dye): 1% SDS, 50 m*M* EDTA, 50% glycerol, 0.1% bromophenol blue, 0.1% xylene cyanol.
5. TE buffer: 10 m*M* Tris-HCl, pH 8.0, 1 m*M* EDTA.
6. 5X Tris-borate–EDTA buffer (TBE; 4L): In a 4-L beaker, add 14.9 g disodium EDTA (20 m*M*), 216 g Tris-HCl (445 m*M*), and 110 g boric acid (445 m*M*). Bring to volume (4 L) and stir to dissolve.

2.2. Southern Blotting

1. Prehybridization solution (100 mL): 50 mL 100% formamide, 10 mL 100X Denhardt's (0.2 g/mL each of Ficoll 40, polyvinyl pyrrolidone, and bovine serum albumin [BSA] [Miles Laboratories]), 25 mL of 20X SSPE (3 *M* NaCl, 0.2 *M* NaH_2PO_4, 20 m*M* EDTA), 10 mL of 10% SDS, 5 mL water.

2.3. Fluctuation Analysis

1. 20% Glucose: Add 200 g glucose and bring to volume (1000 mL) with water. Autoclave to sterilize.
2. Dropout mix: 4 g each of aspartic acid, isoleucine, phenylalanine, serine, threonine, tyrosine, and valine. Homogenize components in a coffee grinder and place in a storage bottle with six to eight marbles. Mix overnight on an end-over-end shaker to allow complete homogenization.
3. 10X AA: 2.6 g dropout mix dissolved in 1000 mL water. Sterilize with an 0.22-μm filter.

4. 10X B: Allow 17 g yeast nitrogen base without AA and ammonium sulfate and 10 g ammonium sulfate to dissolve in 1000 mL water. Sterilize by autoclave.
5. YPD plates: Add 20 g peptone, 10 g yeast extract, and 18 g agar to a 2-L flask. Add 900 mL water and autoclave (make sure there is a stir bar in this solution so it can be stirred later). After cooling to 55°C, add 100 mL of 20% glucose and stir. Pour approx 25 mL per 100-mm plate. Allow plates to dry and store at room temperature for 1–2 d to prevent moisture buildup on lids. Long-term storage should be at 4°C.
6. Synthetic complete (SC) dropout plates (1 L): The following amino acid (AA) volumes are necessary: 20 mL of 0.93 mg/mL adenine; 10 mL of 1.85 mg/mL uracil; 5 mL of the rest of the amino acids, each at 7.4 mg/mL (histidine, leucine, lysine, tryptophan, arginine, and methionine). From this list, determine which AA solution is going to be "dropped out" to make the desired set of plates (i.e., for SC-His plates, leave histidine out of solution). It is important to add additional water to the mix to make up the volume lost when components are dropped out, so that different types of plate are consistent with each other. For example, SC-His plates need an additional 5 mL water (5 + 640 = 645 mL total). Add correct amount of water to 17.5 g agar in a 2-L flask (with a stir bar). Autoclave media and put in a dry 250-mL bottle. Add the desired amino acids to the 250-mL bottle (from the above list; only leave one of these AAs out if the plate is supposed to be deficient for that particular AA). Allow media to cool to 55°C in a water bath. Once it has cooled, add to the bottle of AAs from **step 6**, 100 mL of 10X AA, 100 mL of 10X B, and 100 mL of 20% glucose. Use the stir bar to mix and pour 25 mL per plate. Allow plates to dry as previously described.
7. 5FOA plates: Use the same protocol as in **Subheading 2.3.6.** except for the following: In a 500-mL beaker, add 100 mL of 10X AA and all desired amino acid solutions except uracil. For uracil, add only 6.5 mL (of 1.85 mg/mL) and an extra 3.5 mL water (to compensate for volume). Heat while stirring (do not exceed 65°C) and add 1 g of 5FOA (US Biological, Swampscott, MA) and allow to fully dissolve. Filter-sterilize and add to media (which has cooled to 55°C). Also, add 100 mL of 10X B and 100 mL of 20% glucose. Mix well and pour 25 mL per plate.

2.4. PCR

1. Colony PCR premix composition (7.5 µL): There are two types of PCR listed in this protocol. Nonradioactive PCR is quicker to analyze, has less sensitivity, and does not use radioactivity; radioactive PCR is more sensitive and provides precise allele sizes. The composition listed here is for cold PCR. The premix composition for hot PCR is identical, except for the radioactivity (add 0.125 µL of 20 µCi/µL [α-P^{32}]dCTP) and only 20 µ*M* dCTP is present in the dNTP mixture. To analyze the cold-PCR products, we use a 7.5% polyacrylamide gel. To analyze the hot-PCR products we use a 6% denaturing polyacrylamide gel.
2. Single-colony PCR premix composition (7.5 µL): 1.25 µL of 10X *Taq* polymerase buffer (Invitrogen), 0.25 µL of 50 m*M* $MgCl_2$, 0.75 µL of 50% glycerol, 0.25 µL of all four dNTPs at 10 m*M* each, 0.25 µL primer oBL91 at 50 µ*M*, 0.25 µL primer oBL157 at 50 µ*M*, 4.435 µL water, and 0.065 µL *Taq* polymerase (5 U/µL; Invitrogen). The sequences of the two primers are specified in **Subheading 3.6.3.**
3. 7.5% Polyacrylamide gel (30 mL): 7.5 mL polyacrylamide (30% stock); 3.0 mL of 5X TBE; 19.2 mL water; 0.3 mL ammonium persulfate (10%); 0.02 mL TEMED.
4. 6% Denaturing polyacrylamide gel (70 mL): 16.8 mL Sequagel (National Diagnostics); 45.8 mL Sequagel diluent; 7.0 mL of 10X Sequagel buffer; 0.4 mL of 10% ammonium

persulfate; 0.04 mL TEMED. Pour gel using plates that are 38 cm wide and approx 45 cm long.

5. Formamide stop solution dye: Mix 50 mL of good quality formamide with 0.05% (w/v) bromophenol blue, 0.05% (w/v) xylene cyanol, and 20 m*M* EDTA.
6. M13 ladder: M13 DNA (1 μg) is sequenced using the Amersham Biosciences (Piscataway, NJ) T7 DNA Polymerase protocol. The –40 primer for M13 (GTTTTCCCAGTCACGAC) is used (1 pmol). Load 1 μL of the M13 ladder onto denaturing polyacrylamide gel as a marker.

3. Methods

3.1. Creation of Reporter Plasmid

All steps are routine molecular biology procedures. The pBL94 vector without the TNR but containing all other DNA elements is available on request. To add a triplet repeat of interest, complementary oligonucleotides are annealed to each other. It is necessary that each end of the duplex molecule contain a 3' CATG sequence for cloning purposes. Oligonucleotides synthesized with a 5' phosphoryl group improve ligation of the cassette into the vector. Cleave pBL94 with *Sph*I and dephosphorylate the vector 5' ends with calf intestinal phosphatase or an equivalent enzyme. After inactivation of the enzymes by heat or phenol extraction, add the oligonucleotide cassette in an approx 10-fold molar excess over the vector and ligate the DNAs together by standard techniques. Transformation into any standard *E. coli* strain (we typically use DH5α) yields ampicillin-resistant colonies. DNA is isolated from the colony by standard techniques such as Qiagen minipreps and submitted for DNA sequence analysis of the TNR region. A useful sequencing primer is 5' ACTTGGGGAGAGGTGCG, whose 3' end anneals approx 52 bp upstream of the *Sph*I cloning site.

3.2. Creation and Verification of Strain

1. After the TNR portion of the plasmid is verified by sequencing, it can be transformed into the appropriate yeast strain at the *LYS2* site because of the presence of appropriate targeting sequence in the vector. We typically use yeast strain MW3317-21A ***(9)***. The standard lithium acetate transformation procedure is suitable for this purpose ***(20)***. Transformation is followed by two important quality control steps (Southern blotting and PCR confirmation of the starting tract size). Then fluctuation analysis and PCR sizing of the TNR mutations can be performed. Alternatively, a qualitative patch test can be done to provide estimated mutation rates, relative to a standard strain.
2. Digest TNR-containing plasmid with the restriction enzyme *Bsu*36I for targeting the construct to the chromosomal *LYS2* locus. The digestion is verified by running the product in an agarose gel and looking for a clean, full-length linear band of about 7.5 kb on the gel. Next, the digested plasmid is transformed into the yeast strain using the standard lithium acetate protocol for transformation (*see* **Subheading 3.3.**). The digested plasmid will undergo homologous recombination at the chromosomal *LYS2* site. Some of the transformants will possess the correct single integrants and others may not. For the subsequent assays, one must make sure that the starting strain has the correct integrant. Perform Southern hybridization at this step to check for proper chromosomal integration (*see* **Fig. 2**) of the reporter construct. The probe is the 1.2-kb *lys2* fragment of pBL94 (*see* **Subheading 3.5.5.**). The starting TNR tract size is verified by nonradioactive single-

colony PCR (*see* **Fig. 3C**). Before determining the rates of contraction or expansion, it is very important to ensure that the starting tract contained the desired number of repeats. By performing PCR on the repeat tract, we can determine whether the repeat tract length is properly maintained or if it has undergone some mutation. Sometimes, the reporter may even be deleted, leading to no PCR signal at all.

3.3. Yeast Transformation by Lithium Acetate

1. Grow a single yeast colony in 5 mL YPD liquid overnight at 30°C. The following morning, use a small volume of the overnight culture to inoculate fresh YPD liquid. Ten milliliters of cell culture is needed for each plasmid to be transformed. Grow the cells to A_{600} of 0.5–1.0 (approx 2×10^7 cells/mL). This cell density helps ensure optimal transformation efficiency. Most yeast strains double their cell number every 1.5–2 h.
2. Centrifuge the cells for 5 min in a clinical centrifuge. Discard the supernatant and wash the cells in 0.5 vol of 0.1 *M* lithium acetate, 10 m*M* Tris-HCl, pH 7.5, 1 m*M* Na_2EDTA (LTE). Spin the cells once again and resuspend in 0.01 vol LTE.
3. Aliquot 0.1 mL of the cell suspension into a fresh 1.5-mL Eppendorf tube or a 15-mL snap-cap tube. To it, add 10 μL sheared calf thymus DNA (≥ 4 mg/mL), 150–175 ng linear plasmid DNA, and 700 μL of 40% PEG 3300 in LTE. This solution is prepared by mixing 9 vol of 44% PEG with 1 vol of 10X LTE.
4. Mix the solution gently, either by inverting or pipetting. Incubate the mixture at 30°C for 30 min. Heat shock in a waterbath at 42°C for 15 min.
5. Spin down the cells for 20 s, decant off supernatant, and wash them with 1 mL TE or water. Make sure the cells are well suspended in the liquid. Repeat the spin and wash step once. Spin a final time and resuspend in 100 μL water. Plate the entire cell suspension on a selective plate (usually SC-His, to select for uptake of the plasmid) and incubate at 30°C for 2–3 d, or until colonies appear. For 150–175 ng linear plasmid, one would expect approx 100 transformants.
6. Make a master plate of the transformants by patching or streaking them over a small area on selective media.

3.4. Genomic DNA Preparation

1. This step checks integration of the TNR-containing plasmid at the *LYS2* site on the chromosome and also confirms the presence of correct single integrants. This is achieved by Southern hybridization. Southern transfer to a Nylon membrane is far more convenient than trying to hybridize in a gel.
2. Grow a small portion of cells from the master plate (*see* **Subheading 3.3.6.**) in 5 mL YPD for 2 d. Centrifuge the cells for 5 min in a tabletop centrifuge. Discard the supernatant and resuspend the pellet in 500 μL water. Transfer the mixture to an Eppendorf tube and spin the tube for 5 s. Pour off the supernatant and briefly (approx 10 s) vortex the tube to resuspend the cells in the residual liquid.
3. Add 200 μL of 2% Triton X-100, 1% SDS, 100 m*M* NaCl, 10 m*M* Tris-HCl, pH 8.0, 1 m*M* EDTA. Then, add 200 μL acid washed glass beads (Sigma; *see* **Note 3**) and 200 μL phenol/chloroform (1:1). Vortex the tubes vigorously for 4 min. Phenol is toxic to the skin, so wear gloves during vortexing to avoid accidental exposure.
4. Add 200 μL TE and spin the tubes for 5 min in a microcentrifuge. Transfer the aqueous (top) layer to a new tube (*see* **Note 4**). Add 1.0 mL of 100% ethanol to the aqueous solution, and mix by inversion. Wait for 5 min and then spin the tubes for 2 min in a microcentrifuge.

5. Discard the supernatant and resuspend the pellet well in 400 μL TE. Add 3 μL of 10 mg/mL RNaseA. Incubate the mixture for 5 min at 37°C. Add 10 μL of 4 *M* ammonium acetate and 1.0 mL of 100% ethanol. Mix the solution by inversion and wait 5 min. Spin the tubes for 2 min in a microcentrifuge. Decant the supernatant and dry the pellet for 10 min under vacuum. Once the pellet is dried, resuspend it in 50 μL TE. Use 10 μL for Southern blot.

3.5. Southern Blot

1. Digest 10 μL of the genomic DNA (*see* **Subheading 3.4.**) in a 15-μL reaction to completion with *Bam*HI to visualize proper integration at the *LYS2* site. Load the entire sample onto a 0.8% agarose gel using 0.5X TBE buffer. Electrophorese at approx 100 V until the dye front is approx 75% of the way down the gel (about 3 h for a 15-cm gel). Ethidium stain and photograph the gel. A smear of cleaved genomic DNA fragments should be visible between approx 1 and 8 kb.
2. Place the stained gel in a glass cake dish and shake gently in the following series of solutions at room temperature for the specified times: denaturing solution (300 mL of 0.5 *M* NaOH, 1.5 *M* NaCl) one time for 60 min; neutralizing solution (300 mL of 1 *M* Tris-Cl, pH 8.0, 1.5 *M* NaCl) twice for 30 min each.
3. Set up overnight transfer as shown in **Fig. 2A**. Have ready a clean plastic or Pyrex dish containing 10X SSC (1.5 *M* NaCl, 0.15 *M* sodium citrate dihydrate). Soak Whatman filter papers and the Nylon membrane in 10X SSC. Label the side of the Nylon membrane that will face the gel with a soft lead pencil, to distinguish orientation of the lanes following transfer. The filters and the membrane must be handled with forceps or gloved hands. Place the blotting stack together as shown in **Fig. 2A**. Be sure to eliminate any air bubbles between the gel and the Nylon membrane. Transfer overnight at room temperature.
4. Disassemble the blotter stack. Discard blotting papers in the regular trash and the gel in an ethidium waste container. Put the membrane inside a UV-crosslinking device (Stratagene Stratalinker model 2400 or equivalent) on a clean paper towel (*see* **Note 1**). Crosslink according to the manufacturer's specifications. When the crosslinking is complete, allow the blot to air-dry on the bench for about 1 h prior to prehybridization.
5. While the genomic DNA is being digested, separated on the gel, and transferred, obtain the DNA probe for radiolabeling by digesting plasmid pBL94 with *Bam*H1. This digestion will release the 1.2-kb *lys2* fragment. Gel purify this fragment using the QIAquick gel extraction kit from Qiagen. Radiolabel the DNA using the Random Primers DNA Labeling System from Invitrogen. Purify the labeled probe using Probe Quant G-50 Microcolumns from Amersham Pharmacia Biotech. These columns remove unincorporated labeled nucleotides from the DNA labeling reaction mix.
6. Prehybridize the membrane in 10–25 mL of prehybridization buffer in a sealed plastic bag. Use the minimum volume of buffer that covers the membrane. Incubate for 2 h at 42°C.
7. Boil the probe for 5 min and cool on ice for 5 min before adding it to the blot. Add the radiolabeled DNA probe to a final concentration of (1–5) × 10^6 cpm/mL. Hybridize the membrane overnight at 42°C. Wash the membrane 3X 30 min at 65°C in 500 mL of 0.1X SSC, 1% SDS. Wrap the membrane in plastic wrap and expose it overnight or longer at –70°C to X-ray film with an intensifier screen. You can also expose the membrane to a phosphorimager screen overnight. An example of a Southern blot is shown in **Fig. 2B**.

3.6. Quality Control Using Nonradioactive Single-Colony PCR

1. Once the integration of the digested plasmid is confirmed by Southern blotting, streak the cells on YPD media for single colonies. To ensure that the starting tract size in the yeast cells contained the proper number of repeats, a portion of each colony on the YPD plate is examined by PCR.
2. Resuspend a small amount of the colony in 100 µL of 50 m*M* dithiothreitol, 0.5% Triton X-100 using a sterile toothpick. The amount of cells taken in this step is important—too many or too few cells will not produce an adequate signal. Between 100,000 and 3,000,000 cells (colony size 0.1–1.2 mm) is a sufficient number. Incubate the suspension at 37°C for 30 min, heat to 95°C for 5 min, and chill on ice for 5 min. Vortex the tube after each incubation step.
3. Use 5 µL of the cell lysate from **step 2** as a template for PCR analysis. Add 7.5 µL of master mix solution containing all the other reagents needed for PCR, including primers oBL91 (AAACTCGGTTTGACGCCTCCCATG, coordinates –54 to –31 of pBL24) and oBL157 (AGCAACAGGACTAGGATGAGTAGC, complementary to coordinates 53–30 of *URA3*). Perform PCR as follows: 35 cycles of 1 min at 95°C; 1 min at 55°C; 1 min at 72°C. End with a 10-min incubation at 72°C.
4. After amplification, analyze the products on a 7.5% polyacrylamide gel. An example gel is shown in **Fig. 3B**.

3.7. Fluctuation Analysis

1. After PCR confirms the tract length, fluctuation analysis can begin. The first step in this assay is to plate between 100 (on smaller—100-mm plates) and 300 (on larger—150-mm plates) yeast cells on nonselective media (YPD). This usually is done with at least three genetically independent clones to produce statistically significant results. Cell dilutions can be quantified by counting yeast cells with a hemocytometer.
2. Let the yeast cells grow at 30°C until visible colonies appear on the YPD. It is at this step that expansions and contractions are permitted to occur. At this point, it is very helpful to have some idea of the general mutation rate of your test sequence, either by patch test (*see* **Subheading 3.9.**) or from literature values. Using this information, let the yeast colony grow to a predetermined size (*see* **Note 5**).
3. Pick 10 similar-sized colonies per plate and resuspend each in 200 µL sterile H_2O (*see* **Note 6**). Plate a small aliquot on nonselective media (YPD) to determine the total number of cells in the original colony (*see* **Note 7**). Plate the rest of the resuspension on the selective media to look for cells that have undergone a TNR mutation. If the number of yeast cells is higher than required (which would give an uncountable number on the selective plate), it is possible to plate only a portion of the cells. However, this dilution must be accounted for when determining the number of mutations.
4. After plating, allow the cells to grow for 3 d at 30°C. The mutation rate is determined by counting the number of colonies on the selective and nonselective plates. The yeast cells will grow quicker on the nonselective (YPD) media, so these colonies will be large and easy to count. The yeast will grow more slowly when required to provide their own amino acids, so the colonies growing on the selective plates will be somewhat smaller. When counting these colonies, it is most important to be consistent. A general rule is if the colony can be collected by a flat toothpick and yield a PCR signal, it should be counted.
5. The expansion/contraction rate per cell generation is derived by using the method of the median ***(19)***. To accomplish this, first calculate the average number of colonies on the

YPD plates. This number is multiplied by the dilution factor to produce the average size of the 10 colonies tested. Next, the median number of colonies on the selective plates is determined. With 10 plates (an even number), the median number of colonies is the average between the fifth and sixth largest plates. This number is also corrected for any dilutions from the original 200-µL suspension. The mean is then determined by dividing the corrected median by the r_o/m number provided on the Method of the Median chart (*see* **Note 8** and **Table 3** from **ref. *19***). The number derived from this is then divided by the average number of cells per colony (obtained from the YPD average). This quotient is the overall mutation (either expansion or contraction) rate per cell generation for the repeat tract tested.

3.8. Radiolabeled Single-Colony PCR to Determine Expansion and Contraction Sizes

1. To determine the size of the expanded or contracted triplet repeat, single-colony PCR analysis is used. After a fluctuation assay, this analysis will determine the size (± two repeats) of the mutational events and also identifies any false positives. It is important to perform single-colony PCR on at least one colony from each of the 10 selective plates to make sure that a TNR mutation actually took place. It may be necessary to correct the expansion rate by multiplying the initial rate by the percentage of "real events." For example, if only 7 out of 10 events were "real," then the initial mutation rate would be multiplied by 70% to produce the corrected expansion rate. This analysis usually is done with both the colonies on the nonselective plate (which should show the parental length) and a colony off each selective plate (to show the expansion or contraction size) (*see* **Note 9**). The necessary components for radiolabeled PCR are the same as nonradiolabeled PCR, except the nucleotide mixture contains 10 times less dCTP (20 µ*M*) and 2.5 µCi of [α-P^{32}]dCTP.
2. The same thermocycler program is used as in **step 3** of **Subheading 3.6**. After radioactive PCR, add 0.5 vol formamide dye to the samples, denature by boiling for 5 min at 95°C, and put on ice. Samples and sequenced M13 sequence ladder are then loaded onto a 6% denaturing polyacrylamide gel (prewarmed for 30 min). Run the gel at a constant 100 W (milliamps and volts may vary) for approx 3 h with 1X TBE as the buffer (*see* **Note 10**). Afterward, fix the gel with 10% glacial acetic acid, 12% methanol for 15 min. To dry the gel, attach it to a piece of Whatman 3M paper, cover it with plastic wrap, and place on a heated vacuum (80°C) for 1–2 h. After drying, expose gel to film (or phosphorimager) overnight and expose to visualize the PCR products. Direct comparison with the M13 ladder allows PCR products sizes (± two repeat units) to be determined. An example of contracted TNR alleles is shown in **Fig. 3C** (*see* **Note 11**).

3.9. Qualitative Patch Tests to Estimate TNR Instability

1. Patch transformant colonies carrying the TNR tract of interest from the selective plate (SC-His) to a nonselective media like YPD. The patches should be approx 1–2 cm^2. Allow the cells to grow for 48 h.
2. Replica plate these patches to appropriate media to identify either expansions (SC-His+5FOA) or contractions (SC-His-Ura). Allow the selective plates to incubate 3 d. The number of papillae (outgrowth colonies) on the selective plate is proportional to the TNR instability rate. An example of this technique is shown in **Fig. 4**, where expansions have been selected from wild-type and several mutant yeast backgrounds. Clearly, the occurrence of resistant papillae is elevated in the mutants, relative to control wild-type cells.

3. For extra accuracy, the papillae on the selective plate can be checked by single-colony PCR to look for *bona fide* expansions or contractions.

4. Notes

1. As an alternative to UV crosslinking, the membrane can be baked for 1–2 h at 80°C under vacuum.
2. Histidine is omitted from both of these plates because it is used as a marker for the promoter/reporter construct. As a result, only yeast cells that contain this construct will be able to produce histidine and grow on the selective media. The lack of histidine in the selective plates is especially important for measuring expansions because it eliminates an undesirable side reaction—spontaneous deletion ("popout") of the entire reporter construct from the chromosome. Because popouts delete the *URA3* gene, these events show up as 5FOA resistant. Popouts occur at roughly the same rate as many TNR expansions, so it is important to eliminate popouts by selection on media lacking histidine. The *HIS3* marker gene is also deleted in popouts, so these events do not show up on media lacking histidine, whereas expansions can grow without histidine because the *HIS3* gene is retained.
3. Beads are most easily pipetted with by snipping off the end of a 1-mL pipettor tip.
4. The volume of the aqueous layer should be approx 600 µL; avoid transferring the white precipitate.
5. A highly unstable tract (mutation rate of approx 10^{-3} per cell generation; typically, contractions of starting tracts containing 33 repeats or more) should only be allowed to grow to approx 40,000 cells before being assayed. A yeast colony with 40,000 cells is barely visible to the naked eye (approx 0.1 mm) and usually takes approx 24 h of growth. A moderately unstable tract [approx 10^{-5} per cell generation; expansions of $(CTG)_{25}$, for example] should be grown to a colony of about 2 million cells (approx 1 mm). This typically takes approx 32–36 h for wild-type cells. A stable tract ($<10^{-7}$, such as a control sequence of nonrepeating DNA) can be grown for 48 h or longer to achieve a colony size of 20 million or greater.
6. For this step, stab the colony with a 20- to 1000-µL sterile capillary tube and transfer colony and media to make certain the entire colony gets into the water resuspension. Once again, a hemocytometer may be used at this step to count a portion of the resuspension to make certain the proper-sized colony is chosen.
7. If the original colony contained 1 million cells, then plating 10 µL of a 1:1000 dilution of the original suspension should yield 50 colonies on the nonselective plate.
8. The chart accurately allows for rate determination when the median number of colonies is between 1.4 and 4395 ***(19)***.
9. There are several factors that may influence the percentage of *bona fide* expansions or contractions. (1) Length of the repeat tract. As the repeat tract gets shorter, the rate goes down, and the chance for more false positives goes up. For example, expansions of $(CTG)_{25}$ are 95% authentic; for $(CTG)_{15}$, 82%; for $(CTG)_{13}$, 50%; and for $(CTG)_{10}$, 0% ***(12)***. (2) Another factor that may influence the percentage of false positives is the yeast background. If the yeasts are deficient for a specific repair protein (such as *msh2, pms1,* or *rad27*), an inability to repair mutations within the *URA3* gene would cause more false positives. For example, in a *rad27* background, only 17% of $(CTG)_{13}$ expansions are authentic, compared to 50% for wild type ***(12)***.
10. Be careful when handling the buffer in the bottom reservoir of the gel. It likely contains the unincorporated [α-P^{32}]dCTP.

11. Controls for the PCR include the plasmid constructs containing 25, 33, or 50 repeats. These plasmids are available on request. As a negative control, the parental yeast strain without the plasmid can be amplified to show that the primers are plasmid-specific.

Acknowledgments

This work was supported by a graduate fellowship from the University of Nebraska Medical Center and by NCI Training Grant T32 CA09476 (both to M. J. Dixon), by a postdoctoral fellowship from the Huntington's Disease Society of America (to S. Bhattacharyya), by NIH grant GM61961 (to R. S. Lahue), and by NCI Cancer Center Support Grant P30 CA36727 (to the Eppley Institute).

References

1 Paulson, H. L. and Fischbeck, K. H. (1996) Trinucleotide repeats in neurogenetic disorders. *Annu. Rev. Neurosci.* **19,** 79–107.
2 Cummings, C. J. and Zoghbi, H. Y. (2000) Fourteen and counting: unraveling trinucleotide repeat diseases. *Hum. Mol. Genet.* **9,** 909–916.
3 Usdin, K. and Grabczyk, E. (2000) DNA repeat expansions and human disease. *Cell. Mol. Life Sci.* **57,** 914–931.
4 Richards, R. I. (2001) Dynamic mutations: a decade of unstable expanded repeats in human genetic disease. *Hum. Mol. Genet.* **10,** 2187–2194.
5 Kovtun, I., Goellner, G., and McMurray, C. T. (2001) Structural features of trinucleotide repeats associated with DNA expansion. *Biochem. Cell Biol.* **79,** 325–336.
6 Sinden, R. R., Potaman, V. N., Oussatcheva, E. A., et al. (2002) Triplet repeat DNA structures and human genetic disease: dynamic mutations from dynamic DNA. *J. Biosci.* **27,** 53–65.
7 Nolin, S. L., et al. (2003) Expansion of the fragile X CGG repeat in females with premutation or intermediate alleles. *Am. J. Hum. Genet.* **72,** 454–464.
8 Freudenreich, C. H., Kantrow, S. M., and Zakian, V. A. (1998) Expansion and length-dependent fragility of CTG repeats in yeast. *Science* **279,** 853–856.
9 Miret, J. J., Pessoa-Brandao, L., and Lahue, R. S. (1998) Orientation-dependent and sequence-specific expansions of CTG/CAG trinucleotide repeats in *Saccharomyces cerevisiae*. *Proc. Natl. Acad. Sci. USA* **95,** 12,438–12,443.
10 Hashem, V. I., Rosche, W. A., and Sinden, R. R. (2002) Genetic assays for measuring rates of (CAG)•(CTG) repeat instability in *Escherichia coli*. *Mutat. Res.* **502,** 25–37.
11 Sia, E. A., Kokoska, R. J., Dominska, M., et al. (1997) Microsatellite instability in yeast: dependence on repeat unit size and DNA mismatch repair genes. *Mol. Cell. Biol.* **17,** 2851–2858.
12 Rolfsmeier, M. L., Dixon, M. J., Pessoa-Brandao, L., et al. (2001) Cis-elements governing trinucleotide repeat instability in *Saccharomyces cerevisiae*. *Genetics* **157,** 1569–1579.
13 Spiro, C., Pelletier, R., Rolfsmeier, M. L., et al. (1999) Inhibition of FEN-1 processing by DNA secondary structure at trinucleotide repeats. *Mol. Cell* **4,** 1079–1085.
14 Dixon, M. J. and Lahue, R. S. (2002) Examining the potential role of DNA polymerases h and z in triplet repeat instability in yeast. *DNA Repair* **1,** 763–770.
15 Pelletier, R., Krasilnikova, A. S., Samadishwily, G. M., et al. (2003) Replication and expansion of trinucleotide repeats in yeast. *Mol. Cell. Biol.* **23,** 1349–1357.
16 Bhattacharyya, S., Rolfsmeier, M. L., Dixon, M. J., et al. (2002) Identification of *RTG2* as a modifier gene for CAG•CTG repeat instability in *Saccharomyces cerevisiae*. *Genetics* **162,** 579–589.

17 Sikorski, R. S. and Hieter, P. (1989) A system of shuttle vectors and yeast host strains designed for efficient manipulation of DNA in *Saccharomyces cerevisiae*. *Genetics* **122,** 19–27.
18 Boeke, J. D., Lacroute, F., and Fink, G. R. (1984) A positive selection for mutants lacking orotidine-5'-phosphate decarboxylase activity in yeast: 5-fluoro-orotic acid resistance. *Mol. Gen. Genet.* **197,** 345–346.
19. Lea, D. E. and Coulson, C. A. (1948) The distribution of the number of mutants in bacterial populations. *J. Genet.* **49,** 264–284.
20. Schiestl, R. H. and Gietz, D. (1989) High efficency transformation of intact yeast cells by single stranded nucleic acids as carrier. *Curr. Genet.* **16,** 339–346.

4

Detection and Isolation of Trinucleotide Repeat Expansions Using the RED Method

Qiu-Ping Yuan and Martin Schalling

Summary

To facilitate identification of disease genes containing an expanded trinucleotide repeat, a repeat expansion detection (RED) and gene cloning system was established. The RED method was developed to enable detection of expanded trinucleotide repeat sequences in any DNA sample from any species without prior knowledge of the DNA sequences flanking the repeat. The DNA to be tested is used as a template for a repeat oligonucleotide to anneal and ligate in a two-step cycling procedure. After hundreds of annealing/ligation cycles, a large amount of oligonucleotide multimers is accumulated. The longest multimer represents the largest repeat expansion in the genome tested. The gene isolation strategy is based on size separation of genomic fragments, followed by subcloning and library hybridization with an oligonucleotide probe. The expanded trinucleotide repeat is identified throughout the procedure using the RED method. Using this approach, two disease genes, the Huntington's disease gene and the MJD/SCA3 gene, were cloned. This cloning strategy should be applicable to isolation of any DNA fragment containing large trinucleotide repeat expansions in any species.

Key Words: Trinucleotide; trinucleotide repeat expansion; gene; the repeat expansion detection (RED).

1. Introduction

Microsatellites, the simplest and most common tandem repeats, are widely dispersed throughout the genome ***(1)***. Their instability during transmission creates polymorphisms in repeat copy number (usually below 35 copies) in the human population, making them useful markers for population genetics, medicine, and forensic analysis. One class of microsatellites, trinucleotide repeats, has become a subject of particular

From: *Methods in Molecular Biology, vol. 277: Trinucleotide Repeat Protocols*
Edited by: Y. Kohwi © Humana Press Inc., Totowa, NJ

interest to the scientific community since the 1990s. A growing number of neurodegenerative repeat disorders, including eight forms of spinocerebellar ataxia, have been shown to result from an intergenerational increase in the size (in most cases, above 35 copies) of triplet repeats within genes (reviewed in **refs. *2–6***). The increased size leads to an alteration either of gene function or gene expression, which results in various clinical manifestations. Anticipation, defined as a more severe form of the disease or earlier age of onset in successive family generations, is seen in the vast majority of triplet disorders. In addition, using the repeat expansion detection (RED) method ***(7,8)***, several other neuropsychiatric disorders that display anticipation, including bipolar disorder and schizophrenia, have been associated with trinucleotide repeat expansions ***(9–12)***. In particular, 20–40% of patients with a diagnosis of spinocerebellar ataxia (SCA) have mutations at unknown genetic loci, and the disease may be caused by trinucleotide repeat expansions ***(13–15)***. To meet the need for rapid repeat expansion isolation, several methods have been developed for the direct detection of repeat containing genes, including the RED cloning strategy ***(16,17)***, the direct identification of repeat expansion and cloning technique (DIRECT) ***(18)***, and the repeat analysis, pooled isolation, and detection of individual clones containing expanded trinucleotide repeats (RAPID cloning) ***(19)***. The DIRECT and RAPID techniques have been applied to the identification of the genes for spinocerebellar ataxia type 2 (SCA2) ***(18)*** and type 8 ***(20)***. The RED cloning strategy utilizes the RED method to follow the repeat expansion through a series of physical enrichment steps until a single, isolated clone is obtained. This method allows identification of a repeat-containing gene within a couple of months. Using this approach, two disease genes containing large repeats have been cloned, the Huntington's disease gene and the MJD/SCA3 gene ***(15,16)***. The detailed RED cloning procedures are presented here.

The RED method was developed to enable detection of expanded trinucleotide repeat sequences in any DNA sample from any species without prior knowledge of the DNA sequences flanking the repeat ***(7–12,16,19–23)***. In RED, repeat oligonucleotides, such as $(CTG)_{10}$, are used to generate RED products. After denaturation, single-stranded genomic DNA serves as a template, allowing annealing of a repeat oligonucleotide to loci containing repeat sequences complementary to the oligonucleotide used—in this case, the $(CAG)_n$ repeats. When two or more $(CTG)_{10}$ molecules anneal at adjacent positions in the presence of a thermostable DNA ligase, ligation of two or more molecules occurs to form dimers $(CTG)_{20}$, trimers $(CTG)_{30}$, or multimers. Following 500 cycles of denaturation and annealing/ligation, RED products that consist of large amounts of multimers in different sizes accumulate (*see* **Fig. 1A**). Following size separation through denaturing polyacrylamide gel electrophoresis, the RED products are transferred onto a Hybond-N+ membrane by blotting and are visualized by hybridization with an isotope-labeled repeat probe and autoradiography. The maximum product size observed corresponds to the longest repeat sequence existing in the genome tested (*see* **Fig. 1B**).

The RED cloning strategy is designed to identify the chromosomal location of the expanded triplet repeat through a combination of several classical techniques. The RED method was used to identify genomic DNA fractions as well as cloned DNA

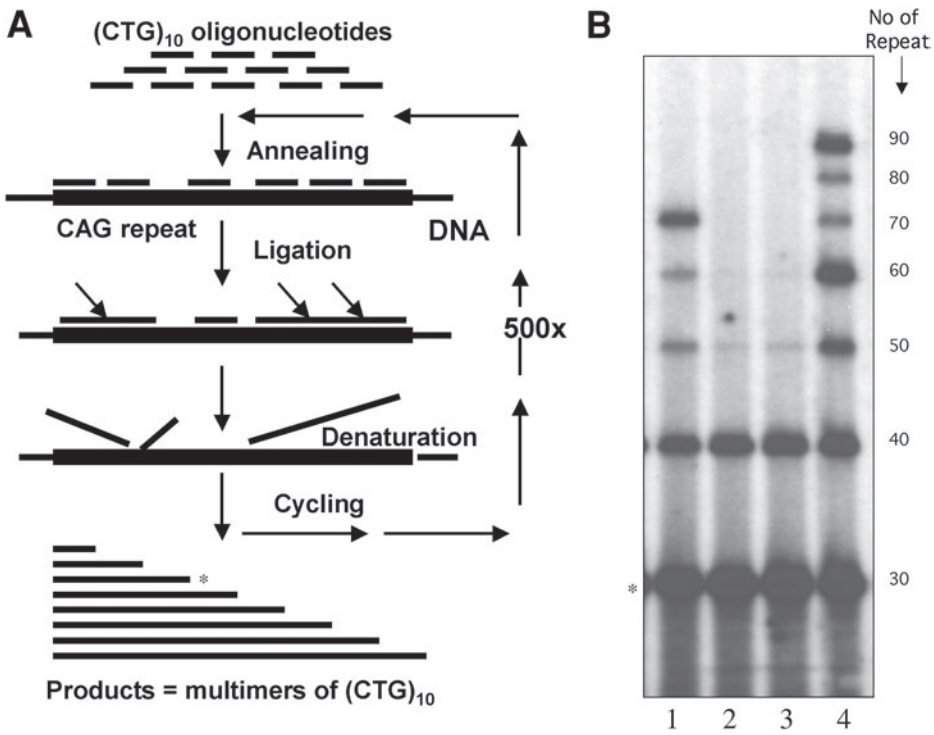

Fig. 1. **(A)** A schematic presentation of the principle of the repeat expansion detection (RED) method. **(B)** Autoradiograph showing RED products from individuals with spinocerebellar ataxias using a $(CTG)_{10}$ oligonucleotide. The "baseline" ligation products of trimers are at the bottom. The top band represents the longest repeat expansion in the genome tested. Note that lane 4 shows two expansions with 90 repeats and 60 repeats, respectively.

fragments containing an expanded repeat at different cloning stages. In general, genomic DNA from patients with candidate diseases was screened by the RED method for the presence of repeat expansion. Polymerase chain reaction (PCR) amplification was used to exclude the possibility of repeat expansion of any of the known disease-causing repeat loci. The remaining DNA samples were then subjected to several cloning steps until a single clone containing an expanded repeat was obtained (*see* **Fig. 2**).

2. Materials

2.1. The RED Method

1. DNA template: A standard phenol/chloroform extraction method or QIAmp Blood Kit (Qiagen Inc., Chatsworth, CA) can be used for DNA preparation. Dissolve DNA in 5 m*M* Tris buffer (pH 9.0) with final concentration of 0.2 μg/μL.
2. Oligonucleotides: Oligonucleotides must be 5' phosphorylated. The denaturation/ligation cycling conditions described in this chapter are optimized for use with a $(CTG)_{10}$ oligonucleotide. Please *see* **Note 1** if a different oligonucleotide is used.

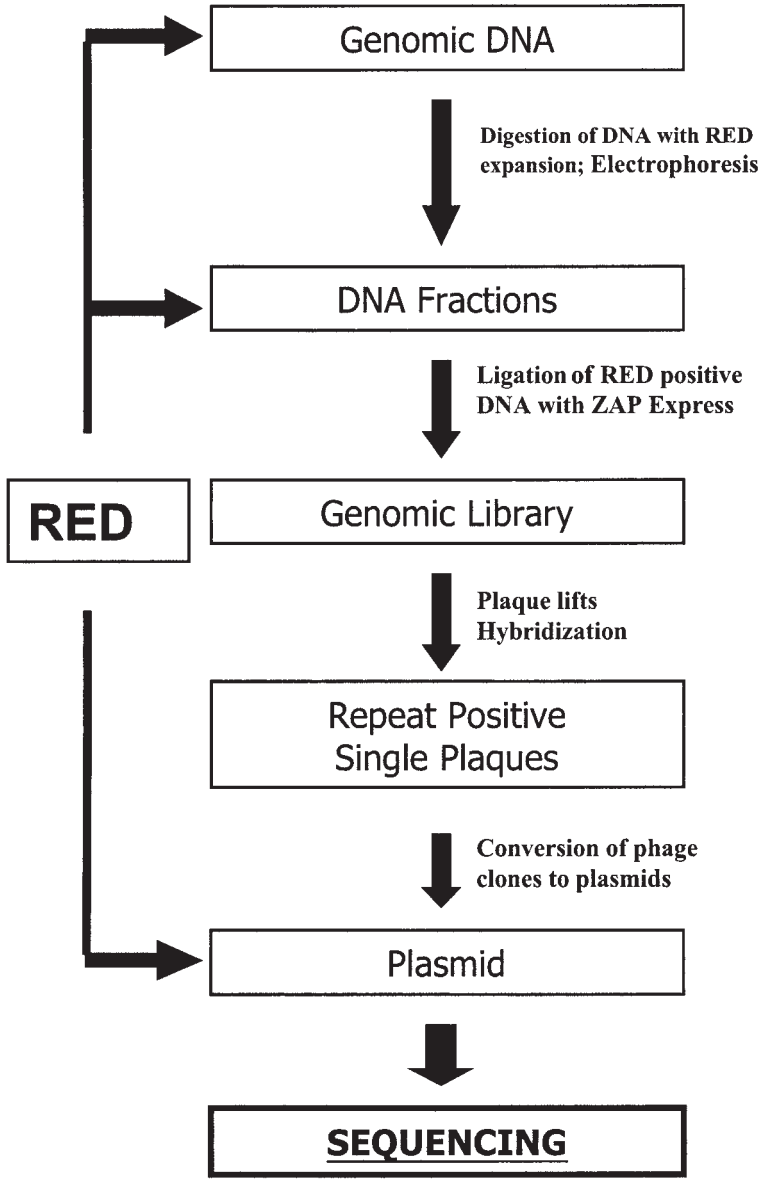

Fig. 2. Diagram illustrating the major steps of the RED cloning procedure. The RED method was used at three different stages to identify the target repeat expansion.

3. Ampligase (100 U/μL) (Epicentre Technologies) with supplied buffer.
4. Terminal deoxynucleotide transferase (TdT) (Amersham) with supplied buffer for end-labeling of hybridization probes.
5. Isotope α^{32}P-dATPs (6000 Ci/mmol) (NEG 012Z, NEN DuPont Medical).
6. Rapid Hybe buffer (Amersham).
7. 6% Denaturing polyacrylamide/6 *M* urea gel solution and supplied buffer (National Diagnostics).
8. 10X TBE: 0.89 *M* Tris-boric acid, 20 m*M* Na_2EDTA, pH 8.0.
9. 20X SSC (175.3 g NaCl, 88.2 g sodium citrate/L, pH 7.0 with NaOH).
10. 20% Sodium dodecyl sulfate (SDS) stock solution.
11. Formamide gel-loading dye: 100% formamide, 0.1% xylene cyanol, 0.1% bromophenol blue.
12. GeneAmp PCR System 9600 (Perkin-Elmer Cetus) and the PTC-225 Peltier Thermal Cycler (MJ Research). Any thermocycler with a heated lid should work.
13. Whatman 3-mm filter paper and Hybond-N+ membrane (Amersham). Any similar membrane.
14. DuPont reflection, NEF 495 X-ray film, and intensifying screen or a similar product is needed.
15. 0.2-mL Microtube strips and caps are used for the RED reactions (Continental Lab Products—CLP).

2.2. The RED Cloning Strategy

1. Phage and competent cells (XL-1 Blue cells and XLOLR cells).
2. Maltose medium and XLOLR in NZY broth.
3. Luria–Bertani (LB) medium: 10 g of tryptone, 5 g of yeast extract, 10 g of NaCl, per liter; pH 7.5.
4. LB–maltose media: LB media, 0.2% maltose, 10 m*M* $MgSO_4$.
5. NZY broth: 5 g NaCl, 2 g $MgSO_4$, 5 g yeast extract, 10 g NZ amine, per liter; pH 7.5.
6. NZY–top agarose: NZY broth + 0.7% (w/v) agarose.
7. NZY–agar dishes: NZY broth + 15 g Bacto-agar, per liter.
8. LB–tetracycline dishes: LB medium + 12.5 mg tetracycline per liter.
9. LB–kanamycin dishes: LB medium + 50 mg of kanamycin per liter.
10. SM buffer: 5.8 g NaCl, 2 g $MgSO_4 \cdot 7H_2O$, 50 mL of 1 *M* Tris-HCl, 5 mL of 2% gelatin, pH 7.5.
11. 0.5 *M* isopropylthio-β-D-galactoside (IPTG) in water and X-gal (250 mg/mL in dimethyl sulfoxide [DMSO]) from Sigma.

2.3. Common Enzymes, Buffers, and Reagents

1. Enzymes: T4 ligase (10 U/μL), restriction enzyme (*Mbo*I), and supplied buffer, Agarose-Digesting Enzyme AgarACE (Promega).
2. SeaPlaque CTG low-melting temperature agarose (FMC BioProducts).
3. 6X Gel-loading dye: 4.0 mL of 0.5 *M* EDTA, 2 mL of 10 *M* Tris-acetate, 50 mg bromphenol blue, 2.0 g Ficoll.
4. Size standard: 1-kb ladder and 100-bp ladder (Gibco-BRL, Life Technologies, and Täby, Sweden).
5. Reagents for DNA precipitation: 99.5% and 95% ethanol; 3 *M* NaOAc, pH 5.2; TE buffer.
6. Denaturation solution: 67.6 g NaCl, 20 g NaOH, per liter.
7. Renaturation solution: 67.6 g NaCl, 121.1 g Trizma base, per liter; pH 7.0.

8. SNAP kit for phagemid DNA preparation (Invitrogen).
9. DNA sequencing kit: BigDye™ Terminator Cycle Sequencing Ready Reaction (ABI PRISM).

3. Methods

3.1. The RED Method

The principle of RED is presented in **Fig 1**.

3.1.1. RED Reaction

1. The RED reaction mixture contains the following: 1 0.5–2 μg genomic DNA, 1.0 μL $(CTG)_{10}$ oligonucleotide (50 ng/μL), 1.0 μL TE-4, 0.15 μL Ampligase (100 U/μL), 0.5–1.0 μL co-buffer and add H_2O to a final volume of 10 μL. Make sure tubes are tightly capped.
2. Amplification in a thermal cycling machine with the following conditions: a primary denaturation at 95°C for 5 min, followed by 500 cycles of annealing/ligation at 80°C for 20 s and denaturation at 95°C for 10 s. This step needs approx 10 h.

3.1.2. Electrophoresis and Blotting

1. Electrophoresis: Use a 6% polyacrilamide/6 *M* urea gel with a wide-tooth comb. Pre-electrophorese at 90 W for 20 min. Heat denature RED products in 0.5X formamide gel-loading dye for 5 min at 95°C and load all content onto gel. Electrophorese at 90 W until xylene cyanol (xc) has migrated 12 cm into gel. Separate plates and discard gel below 16 cm to avoid probe hybridization to excess oligonucleotides.
2. Blotting: Place a wet (with 1X TBE) sheet of a Hybond-N+ membrane on the gel and overlay with three dry 3-mm Whatman papers cut to fit the top glass plate and a weight. Let gels sit for 2 h to permit capillary blotting. Thereafter, immobilize the DNA on the membrane by crosslinking in an ultraviolet (UV) light box.

3.1.3. Hybridization

1. Labeling probe: 3'-end-labeling using TdT is preferred because it effectively permits addition of multiple ^{32}P-dATPs to each molecule, yielding a high specific activity. Mix 8.7 μL H_2O, 5 μL of 5X Cobuffer and 2.5 μL $(CAG)_{10}$ oligonucleotide (50 ng/μL) on ice. Add 7 μL of α^{32}P-dATP and 1.8 μL TdT enzyme. Incubate for 1 h at 37°C. Add 500 μL of 0.1 *M* Tris•Cl, pH 8.0, to stop the reaction. Probe should be labeled to a specific activity of (2–9) × 10^9 cpm/μg.
2. Hybridization: Prehybridize membrane in Rapid Hybe (Amersham) solution for 20 min; add labeled probe and hybridize for 1 h at 60°C. Wash the membrane for 20 min at room temperature and 30 min at 60°C in 1X SSC + 0.1% SDS with at least one change of wash solution.

3.1.4. Autoradiography

Expose membranes overnight (or up to 7 d) to X-ray film at –70°C using intensifying screens.

3.1.5. Results

Products are revealed as a ladder of bands (*see* **Fig. 1B**) with a 30-nucleotide interval between neighboring bands. The band with the highest molecular weight represents

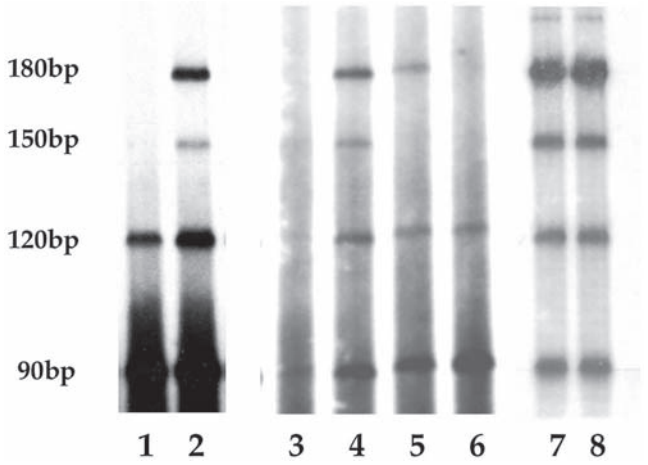

Fig. 3. Autoradiographs showing a series of RED products detected from DNA samples from a patient at different cloning stages. A consistent 180-bp RED product was seen in genomic DNA (lane 2) and in two *Mbo*I–DNA fractions (lanes 4 and 5), but not in the flanking fractions (lanes 3 and 6), nor in two representative cloned DNA fragments (lanes 7 and 8). RED was performed using a $(CTG)_{10}$, generating multimers at 30-nt intervals, represented as bands after size separation, blotting, hybridization, and autoradiography. The bottom band corresponds to 90 bp.

the largest repeat expansion in that particular genome. A "baseline" ligation product formed by trimers of the oligonucleotide should be seen in all lanes because the human genome contains many short repeat sequences. Absence of such a product should be regarded as a reaction failure. A sample with a known repeat expansion should be included as a positive control to deduce RED product expansion sizes in the samples analyzed. Individuals carrying two or more expansions in different sizes are shown as a terminal band (the largest expansion) on the top and a distinct band of a smaller size (*see* **Fig. 1B**, lane 4). See also **Notes 1–5** for troubleshooting guidelines.

3.2. The RED Cloning Strategy

An overview of the cloning procedure is presented in **Fig. 2**, detailing the major steps involved. **Figure 3** shows an example of RED products detected at different cloning stages.

3.2.1. Physical Enrichment of DNA Fragments Containing Long Trinucleotide Repeats

1. Digestion of genomic DNA: Select genomic DNA from an individual with an expanded trinucleotide repeats that you wish to clone. Set up digestion reaction containing 10 μg of DNA, 20–40 U of the restriction enzyme (*Mbo*I), 6 μL supplied buffer for the restriction enzyme, and add water to a total volume of 60 μL. After incubation in a 37°C water bath for 4–5 h, DNA should be fully digested (*see* **Note 6**).
2. Precipitation of digested DNA: Add 1/10 vol of 3 *M* NaOAc and 2X volume of 99.5%

ethanol. Mix thoroughly by inverting the tube. Place the tube on ice for 30 min or at –20°C for 15 min. Centrifuge at 8000*g* at 4°C for 15 min. Discard supernatant. Dry DNA pellet in a vacuum oven.

3. Electrophoresis: Resuspend DNA in 20 μL TE buffer and mix with 4 μL of 6X loading dye. Load all contents to a 0.8% low-melting temperature agarose gel. Load the 1-kb and 100-bp ladders as size standards in separate lanes. Electrophorese at 20 V for 17–18 h. The100-bp DNA fragments should then have migrated approx 11 cm into the gel.
4. Dissection of agarose lane containing DNA separated by size: Cut the agarose lane, dissect it into uniform 2-mm pieces, and place each piece in a clean Eppendorf tube.
5. Digestion of agarose using AgarACE: Melt agarose pieces at 70°C for 10 min and then transfer tubes to a water bath or heating block at 42°C. Add 2–3 U AgarACE to each tube and mix by vortexing. Incubate at 42°C for 15 min. Inactivate AgarACE at 70°C for 10 min.
6. Precipitation of DNA: Add 1/10 vol of 3 *M* NaOAc and 2X volume of 99.5% ethanol. Mix thoroughly by inverting the tube. Leave the tubes at room temperature for 1.5–2.0 h. Centrifuge at 8000*g* at room temperature for 15 min and dry the pellet as in **step 2**. Resuspend the DNA pellet in 10 μL H_2O.
7. RED analysis: Perform the RED analysis (as described in **Subheading 3.1.**) on each DNA fraction to identify the fractions enriched for DNA fragments containing the expanded repeat. Use 3 μL DNA to set up RED reaction (*see* **Note 7**).
8. Select the one or two fractions containing the expanded repeat of interest.

3.2.2. Cloning of the DNA Fragments Containing an Expanded Repeat

Every step in the cloning procedure is performed following the instructions supplied with the vector kit, with some modifications. Please read the original protocol for details if necessary.

1. Generation of genomic library using the RED positive DNA fraction: Set up ligation reaction mixture containing the following: 1.0 μL of the ZAP Express Vector (1 μg/μL, Stratagene), 1.0 μL of the repeat-containing DNA fraction, 0.5 μL of 10X ligase buffer, 0.5 μL of 10 m*M* ATP, 0.2 μL of T4 ligase (10 U/μL), and 1.8 μL H_2O. Incubate at 4°C for 48 h.
2. Packaging ligation: Take one tube of GigaPack Golden III (Stratagene) from –70°C. Thaw the content by holding the tube. Add 5 μL ligation into packaging content. Mix by moving the tip gently. Incubate at room temperature for 1.5–2 h. Add 500 μL SM buffer and 20 μL chloroform. Invert the tube and spin briefly.

3.2.3. Titering

1. Dilute packaged ligation at 1:10.
2. Prepare XL-1 Blue cell at OD_{600} = 0.5 in 10 m*M* $MgSO_4$.
3. Mix 200 μL XL-1 Blue cell with 1 μL of original ligation package and 1:10 serial dilution ligation followed by incubation at 37°C for 15 min.
4. Meanwhile, melt top agarose and cool to 48°C.
5. Add 3 mL top agarose with the content in the tube and with 15 μL of 0.5 *M* IPTG, 40 μL X-gal.
6. Pour quickly onto big NZY plates. Incubate at 37°C overnight.
7. Count white plaques (recombinants). The titer of the white plaques should reach 10^5–10^6 PFUs/mL. Titer lower than this number can lead to a failure in cloning the long repeat-

containing fragment. (*See* **Note 8**.)

3.2.4. Plating Library

1. 600 µL XL-1 Blue cells prepared at OD_{600} = 0.5 in 10 m*M* $MgSO_4$.
2. Mix with the calculated amount of packaged ligation, so that each plate contains 200,000–400,000 recombinants.
3. Incubate at 37°C for 10–11 h. Wrap plates with plastic film and store them at 4°C for 2 h. (Plates are now ready for plaque lifts.)

3.2.5. Plaque Lifts

1. Make duplicate Hybond-N+ filters for each plate. Place filter A on the plate for 2 min, remove it, and place filter B on the plate for 4 min before removing it.
2. Directly after removing each filter from the plate, slowly place the filter on the surface of denaturation solution, with the plaque-containing side upward for 5 min.
3. Transfer filters into renaturation solution for 5 min.
4. Dip filters in 2X SSC solution for 2 min.
5. Immobilize DNA to the filter by UV light autocrosslink (Stratagene).
6. Prewash filters at 65°C in wash solution (2X SSC + 0.1% SDS) for 2 h.

3.2.6. Hybridization

A $(CTG)_{17}$ repeat-oligonucleotide probe is used for the selection of long-repeat-containing plaques from the library. Conditions for probe-labeling and library hybridization are the same as for the RED hybridization step (*see* **Subheading 3.1.3.**), except that the temperature should be 65°C for hybridization and 72°C for wash with wash solution (0.2X SSC + 0.1% SDS). **Figure 4** shows the positive spots after autoradiography, using probes of different lengths.

3.2.7. Picking Positive Plaques

Pick positive plaques according to their position on the film and place them separately in 1 mL SM buffer. Add 20 µL chloroform. Vortex and store them at 4°C at least overnight.

3.2.8. Isolate Single Positive Plaques

Repeat steps from **Subheadings 3.2.4.–3.2.7.**, using positive phage stock in different dilution (10 µL, 1 µL, 0.1 µL, and 0.01 µL) until single positive plaques are obtained. Pick these single plaques and place them in 200 µL SM buffer and 5 µL chloroform. Incubate at 4°C overnight.

3.2.9. Conversion of Phage DNA to Phagemid DNA

1. Prepare XL-1 Blue cells at OD_{600} = 1.0 in 10 m*M* $MgSO_4$.
2. Mix 100 µL XL-1 Blue cells with 50 µL of concentrated phage and 0.5 µL of assistant helper phage (ZAP cloning kit).
3. Incubate at 37°C for 15 min.
4. Add 1.5 mL NZY broth and incubate with shaking at 225 rpm at 37°C for 2.5 h.
5. Heat tubes at 70°C for 20 min. Spin down cells at 1500*g* for 15 min.
6. Take 100 µL supernatant and mix with 200 µL XLOLR cells at OD_{600} = 1.0 in 10 m*M* $MgSO_4$.

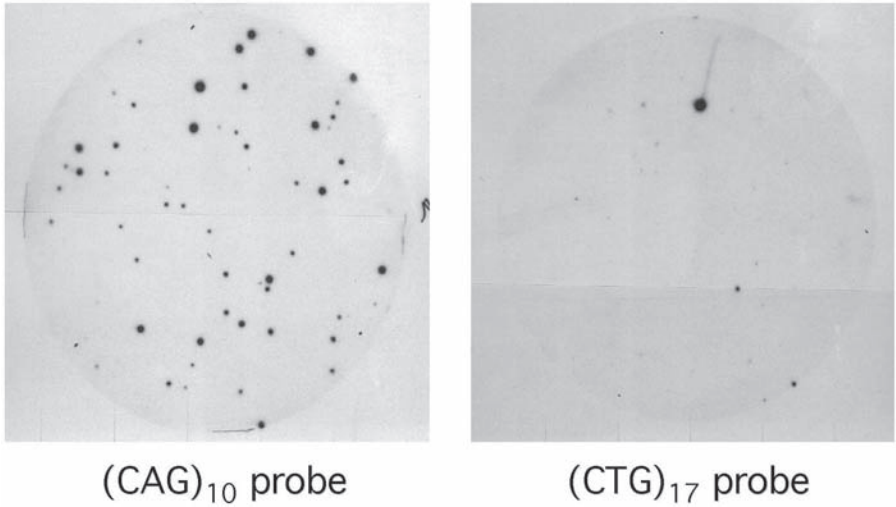

Fig. 4. Autoradiograph of library screening of repeat-containing plaques using a $(CAG)_{10}$ repeat probe or a $(CTG)_{17}$ probe. The number of positive spots was reduced when the $(CTG)_{17}$ probe was used. Hybridization stringency used for $(CAG)_{10}$: hybridization at 60°C and washed at 65°C with 1X SSC + 0.1% SDS; for $(CTG)_{17}$: 65°C and washed at 72°C with 0.2X SSC + 0.1% SDS.

7. Incubate at 37°C for 15 min.
8. Add 300 µL NZY broth and incubate at 37°C for 45 min.
9. Plate out 200 µL onto kanamysin–LB plates. Incubate overnight at 37°C.

3.2.10. Preparation of Phagemid DNA

Collect bacteria from each plate and prepare DNA using the SNAP-kit (Invitrogen). Finally, dissolve the DNA in 60 µL TE buffer.

3.2.11. Sequencing Using 377 ABI DNA Sequencer

1. Sequencing primers: T3 and T7 promoter sequences located on the vector flanking the insert DNA are used to sequence the insert from both ends.
2. Set up the sequencing reaction containing 2 µL phagemid DNA (0.3 µg/µL), 3.2 pmol of T3 or T7 primer and 2 µL BigDye Terminator Cycle Sequencing Ready Reaction. Conditions for cycling: 35 cycles of 96°C for 10 s, 50°C for 5 s, and 60°C for 4 min.
3. Sequence on a denaturing 6% gel on ABI 377.

4. Notes

1. The RED method can be used to detect expansions of 8 out of the 10 triplet repeat permutations (*see* **Table 1**). However, optimization of conditions for the CGG/CCG and AAT/ATT repeats has been unsuccessful, probably the result of the extremely high and low GC content. In general, if the GC content of the repeat motif to be analyzed is low, then the oligonucleotide length may need to be increased and an optimization of the cycling conditions is needed. Oligonucleotides of different sizes may be used when screening for

Table 1
Optimized RED Conditions for the 10 Possible Triplet Permutations

Repeat motif	Oligonucleotide	Cycling condition (annealing + ligation)	Probe	Hybridization temperature	Frequency of RED product >120
CTG/CAG	$p(CTG)_{10}$	80°C/30 s + 94°/10 s	$(CAG)_{10}$	60°C	approx 30%
CCT/AGG	$p(CCT)_{13}$	80°C/30 s + 94°/10 s	$(AGG)_{10}$	60°C	approx 5%
TGG/CCA	$p(TGG)_{12}$	80°C/30 s + 94°/10 s	$(CCA)_{10}$	60°C	approx 100%
CGT/ACG	$p(CGT)_{11}$	80°C/30 s + 94°/10 s	$(ACG)_{10}$	60°C	0%
ATG/CAT	$p(ATG)_{15}$	70°C/30 s + 94°/10 s	$(CAT)_{10}$	55°C	approx 100%
AGT/CTA	$p(AGT)_{16}$	70°C/30 s + 94°/10 s	$(CTA)_{10}$	55°C	0%
GTT/CCA	$p(GTT)_{13}$	65°C/40 s + 94°/10 s	$(CCA)_{10}$	55°C	approx 5%
CTT/AAG	$p(CTT)_{14}$	70°C/30 s + 94°/10 s	$(AAG)_{10}$	55°C	approx 100%

several motifs simultaneously *(7)*. It is important that oligonucleotides are phosphorylated and purified in order for the RED reaction to work. Any residue of shorter molecule from the synthesis will reduce the signal markedly.

2. Empty tubes resulting from evaporation following the long RED cycling procedure can be a problem. Select PCR tubes carefully. We have found that CLP tubes work well.
3. Light areas on autoradiograph can be caused by poor contact during blotting. Too much buffer may obscure part of the ladder present in a given lane.
4. Dark autorad without visible lanes can sometimes be produced. The probe has randomly hybridized to the whole filter. This can be caused by a spill of RED reaction sample with a large excess of oligonucleotide into the upper buffer tank during gel loading.
5. Dark sample lanes and lack of products may be the result of reaction failure, possibly secondary to the quality of the DNA. Check the level of degradation and the actual concentration of high-molecular-weight DNA on an agarose gel. High salt concentration may reduce the efficiency of the Ampligase. Try to lower the Ampligase buffer concentration to 0.5X. A low pH also lowers the reaction yield and may cause reaction failure. Include 1 μL buffered TE-4, pH 8.0, in the RED reaction if the DNA is in an unbuffered solution. Weak bands could also be the result of poor handling of the reagents. We have noticed that the ampligase buffer is sensitive to repeated thawing.
6. Complete DNA digestion is important, as enrichment of repeat-containing DNA fragments is dependent on the size.
7. Pure DNA is essential for the RED reaction. Therefore, the fractionation and extraction steps of the cloning procedure must work well. Too much agarase or agarose residues may inhibit the RED reaction. This problem can be avoided by repeating the DNA extraction step using a standard DNA extraction protocol using phenol/chloroform/isoamyl alchohol.
8. A titer of recombinants lower than 10^5 PFUs/mL may lead to a failure of cloning the long repeat-containing fragments, as a result of preferential selection against DNA fragments containing a long repeat during the cloning procedure. Low ligation efficiency again may be caused by poor DNA quality.

References

1 Lander, E. S., Linton, L. M., Birren, B., et al. (2001) Initial sequencing and analysis of the human genome. *Nature* **409,** 860–921.

2. Warren and Wells, R. D. (1998) *Genetic Instabilities and Hereditary Neurological Diseases*, Academic, San Diego, CA.
3. Lindblad, K. and Schalling, M. (1999) Expanded repeat sequences and disease. *Semin. Neurol.* **3,** 289–299.
4 Zoghbi, H. Y. and Orr, H. T. (2000) Glutamine repeats and neurodegeneration. *Annu. Rev. Neurosci.* **23,** 217–247.
5 Bowater, R. P. and Wells, R. D. (2000) The intrinsically unstable life of DNA triplet repeats associated with human hereditary disorders. *Prog. Nucleic. Acid. Res. Mol. Biol.* **66,** 159–202.
6. Margolis, R. L. (2002) The spinocerebellar ataxias: order emerges from chaos. *Curr. Neurol. Neurosci. Rep.* **5,** 447–456.
7 Schalling, M., Hudson, T. J., Buetow, K. H., et al. (1993) Direct detection of novel expanded trinucleotide repeats in the human genome. *Nature Genet.* **4,** 135–139.
8 Zander, C., Thelaus, J., Lindblad, K., et al. (1998) Multivariate analysis of factors influencing repeat expansion detection. *Genome Res.* **8,** 1085–1094.
9 Lindblad, K., Nylander, P. O., De Bruyn, A., et al. (1995) Detection of expanded CAG repeats in bipolar affective disorder using the repeat expansion detection (RED) method. *Neurobiol. Dis.* **2,** 55–62.
10. O'Donovan, M. C., Guy, C., Craddock, N., et al. (1995) Expanded CAG repeats in schizophrenia and bipolar disorder. *Nature Genet*. **10,** 380–381.
11. O'Donovan, M. C., Guy, C., Craddock, N., et al. (1996) Confirmation of association between expanded CAG/CTG repeats and both schizophrenia and bipolar disorder. *Psychol. Med.* **26,** 1145–1153.
12 Oruc, L., Lindblad, K., Verheyen, G. R., et al. (1997) CAG repeat expansions in bipolar and unipolar disorders. *Am. J. Hum. Genet.* **60,** 730–732.
13 Stevanin, G., Durr, A., and Brice, A. (2000) Clinical and molecular advances in autosomal dominant cerebellar ataxias: from genotype to phenotype and physiopathology. *Eur. J. Hum. Genet.* **8,** 4–18.
14 Tang, B., Liu, C., Shen, L., et al. (2000) Frequency of SCA1, SCA2, SCA3/MJD, SCA6, SCA7, and DRPLA CAG trinucleotide repeat expansion in patients with hereditary spinocerebellar ataxia from Chinese kindreds. *Arch. Neurol.* **57,** 540–544.
15 Basu, P., Chattopadhyay, B., Gangopadhaya, P. K., et al. (2000) Analysis of CAG repeats in SCA1, SCA2, SCA3, SCA6, SCA7 and DRPLA loci in spinocerebellar ataxia patients and distribution of CAG repeats at the SCA1, SCA2 and SCA6 loci in nine ethnic populations of eastern India. *Hum. Genet*. **106,** 597–604.
16 Yuan, Q. P., Lindblad, K., Zander, C., et al. (2001) A cloning strategy for the identification of novel genes containing trinucleotide repeat expansion. *Int. J. Med. Genet*. **8,** 427–431.
17. Yuan, Q. P., Lindblad, K., and Schalling, M. (2003) Repeat expansion detection (RED) and the RED cloning strategy. *Methods Mol. Biol.* **217,** 51–60.
18 Sanpei, K., Takano, H., Igarashi, S., et al. (1996) Identification of the spinocerebellar ataxia type 2 gene using a direct identification of repeat expansion and cloning technique, DIRECT. *Nature Genet.* **14,** 277–284.
19 Koob, M. D., Benzow, K. A., Bird T. D., et al. (1998) Rapid cloning of expanded trinucleotide repeat sequences from genomic DNA. *Nature Genet.* **18,** 72–75.
20 Koob, M. D., Moseley, M. L., Schut, L. J., et al. (1999) An untranslated CTG expansion causes a novel form of spinocerebellar ataxia (SCA8). *Nature Genet.* **21,** 379–384.

21 Lindblad, K., Savontaus, M. L., Schalling, M., et al. (1996) An expanded CAG repeat sequence in spinocerebellar ataxia type 7. *Genome Res.* **6,** 965–971.
22 Lindblad, K., Lunkes, A., Schalling, M., et al. (1996) Mutation detection in Machado–Joseph disease using repeat expansion detection. *Mol. Med.* **2,** 77–85.
23. Holmes, S. E., O'Hearn, E. E., McInnis, M. G., et al. (1999) Expansion of a novel CAG trinucleotide repeat in the 5' region of PPP2R2B is associated with SCA12. *Nature Genet.* **23,** 391–392.

5

Analysis of Unstable Triplet Repeats Using Small-Pool Polymerase Chain Reaction

Mário Gomes-Pereira, Sanjay I. Bidichandani, and Darren G. Monckton

Summary

Small-pool polymerase chain reaction (PCR) constitutes the PCR amplification of a trinucleotide repeat in multiple small pools of input DNA containing in the order of from 0.5 to 200 genome equivalents. Products are resolved by agarose gel electrophoresis and detected by Southern blot hybridization under conditions that allow the identification of products derived from single-input molecules. The method allows the detailed quantification of the degree of repeat-length variation in a given sample, including the detection of common variants and those alleles present only in a small subset of cells. Detailed analysis of repeat dynamics is essential for a complete understanding of the molecular mechanisms that generate diversity and lead to disease in the unstable trinucleotide DNA repeat disorders.

Key Words: Mutation; polymerase chain reaction; trinucleotide repeat; myotonic dystrophy; Huntington's disease; Friedreich ataxia; spinocerebellar ataxia; small-pool PCR; unstable DNA; expansion; repeat dynamics; Southern blot; triplet repeat; sperm; microsatellite.

1. Introduction

Expanded trinucleotide disease-associated alleles are genetically highly unstable and can undergo repeat-length mutations in both the germline and soma ***(1)***. Understanding the mutational mechanism(s) that lead to the continuous accumulation of repeat size variability over time and the contribution of different factors to repeat instability must be grounded on extensive analysis of mutation profiles in humans and animal models.

From: *Methods in Molecular Biology, vol. 277: Trinucleotide Repeat Protocols*
Edited by: Y. Kohwi © Humana Press Inc., Totowa, NJ

Standard methods for assessing trinucleotide repeat-length variability in a given sample are based on Southern blot analysis of restriction digested genomic DNA (typically 5–20 μg DNA) or polymerase chain reaction (PCR) (typically using 100–500 ng DNA). Both of these approaches analyze simultaneously the expansion size in thousands of cells (at least 10^4 cells). Therefore, samples that contain a high proportion of mutant alleles present as broad smears, consisting of multiple unresolved mutant DNA molecules, and rarer mutant molecules comprising <10% of the total population are not detected.

However, the heterogeneous smears can be dissected into discrete alleles, derived from single cells, by more sensitive techniques. There are two main approaches to detect mutant alleles in single cells. Conceptually, the simplest would be to physically isolate single cells, recover the alleles present by PCR amplification, and determine the allele lengths present by gel electrophoresis. This approach is at the least technically challenging and most frequently unmanageable for large numbers of cells/samples. Nonetheless, it has been successfully applied to the analysis of triplet repeat loci, with particular utility in analyzing the variation present in single sperm ***(2,3)***. A more efficient method comprises the serial dilution of bulk genomic DNA into multiple PCR amplifications, such that each reaction contains no more than a few DNA templates, and the resolution and detection of amplification products derived from single-input molecules in a process termed small-pool PCR (SP-PCR) ***(4,5)*** (*see* **Figs. 1** and **2**).

Input DNAs vary from an average of less than one up to a few hundred molecules, the exact number depending on the degree of variability within the sample and the biological question being asked. The amplification of a low number of template molecules per reaction allows the detailed examination of the mutational spectrum present in a sample, revealing biases and subtle, yet important events not observed using standard bulk DNA procedures. Higher-input DNA, as high as 50–100 amplifiable molecules per reaction, is useful to quickly determine the overall degree of variation within a given sample and to identify rarer events not commonly observed using smaller amounts of template DNA. Electrophoretic profiles generated by bulk PCR analysis (more than 1000 template molecules per reaction) using fluorescently labeled oligonucleotide primers and detection on automated DNA-sequencing-type apparatus have failed to reveal such mutants. In fact, Genescan®-based methodologies greatly underestimate the true level of length heterogeneity, in particular the presence of large expanded alleles ***(6–8)***.

When performed as we describe, amplification artifacts in SP-PCR are rare. Several lines of evidence confirm that the products observed are faithful representations of the alleles present in the original cells rather than experimental artifacts. First, variant-length alleles are associated with only the expanded allele and reflect the variation observed on Southern blot analysis of restriction digested genomic DNA (accepting the inability of the bulk DNA analysis approach to reveal rarer mutants). Second, the intensity of PCR signals from variant alleles amplified in a single reaction are very similar, consistent with the signal being derived from a single-input molecule. Third, the frequency of mutant products detected in individual amplifications is proportional

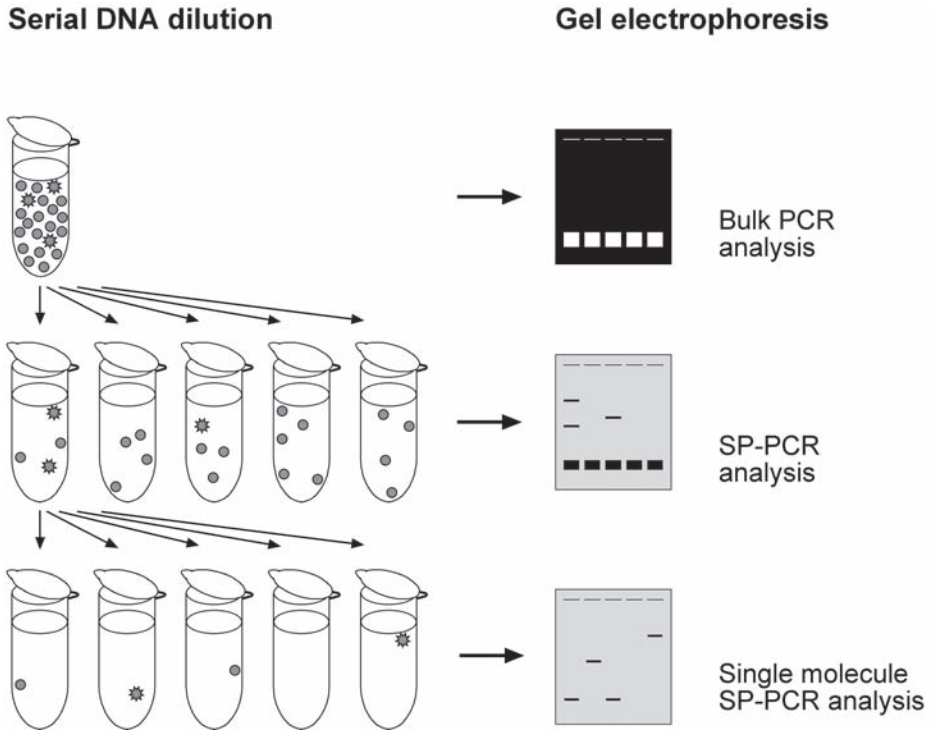

Fig. 1. Schematic representation of SP-PCR analysis. The DNA sample of interest contains both progenitor alleles (circles) and a low number of derived mutant alleles (stars). Standard bulk PCR techniques fail to reveal any amplified mutant alleles in ethidium bromide-stained agarose gels. Serial dilution of the original DNA sample, such that only a few molecules are input into each SP-PCR amplification, allows detection of individual mutant alleles, upon Southern blot and hybridization. Further dilution of template DNA to the single-molecule level per reaction results in the detection of single alleles per lane, generated by the amplification of a single template molecule.

to the template DNA input. Fourth, prolonged autoradiography exposure fails to reveal any additional bands as predicted for PCR artifacts that could arise at any stage of amplification. Fifth, deliberate attempts to induce PCR artifacts by increasing DNA degradation (by extending the denaturation time during PCR) only created relatively faint additional bands much shorter than the progenitor allele. Finally, the distributions derived are highly sample- and cell-type-specific and not merely a reflection of allele repeat length ***(4,5,9)***.

In summary, SP-PCR is a robust, highly sensitive, and efficient approach, remarkably free of artifacts, for the accurate assessment of the level of repeat-length variation, providing both quantitative and qualitative data, as well as important clues to the dissection of fundamental aspects in trinucleotide repeat biology.

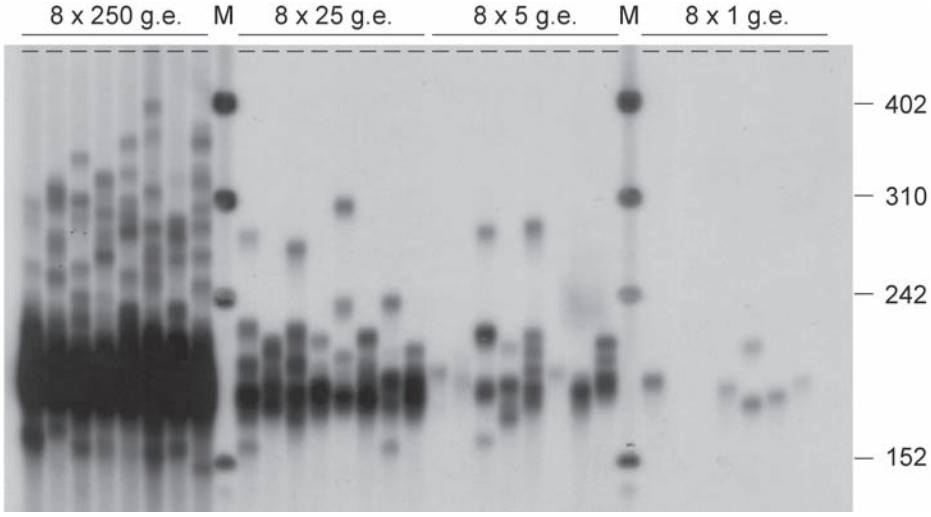

Fig. 2. Trinucleotide repeat instability in tissue samples of a mouse model of unstable DNA. The repeat dynamics in lung cells of a transgenic mouse model, carrying a randomly integrated CAG•CTG repetitive sequence, was analyzed at age 24 mo by SP-PCR techniques. The autoradiographs show the SP-PCR products obtained from the amplification of an average number of 1, 5, 25, and 250 genome equivalents (g.e.). Eight independent reactions were set up for each template DNA concentration. The scale on the right represents the molecular-weight markers (M) converted into repeat numbers. Note how the low concentrations of input DNA reveal the most common variants. Although with higher input DNAs the most common variants can no longer be distinguished, rarer, very large expansions present in only a small subset of cells are revealed.

2. Materials

1. 20-µL, 200-µL, and 1-mL Filter pipet tips.
2. 1.5-mL screw-top Eppendorf tubes.
3. Deionized H_2O.
4. TE: 10 m*M* Tris-HCl, pH 8.0, 1 m*M* EDTA, pH 8.0, in H_2O.
5. Spectrophotometer and cuvets.
6. Selected restriction endonuclease and reaction buffer.
7. *Taq* DNA polymerase (Sigma).
8. Oligonucleotide primers.
9. 1X Polymerase chain reaction buffer (*see* **Note 1**): 45 m*M* Tris-HCl, pH 8.8, 11 m*M* ammonium sulfate, 4.5 m*M* $MgCl_2$, 6.7 m*M* of 2-mercaptoethanol, 4.4 µ*M* EDTA, 1 m*M* dATP, 1 m*M* dCTP, 1m*M* dGTP, 1 m*M* dTTP, and 113 µg/mL bovine serum albumin (BSA) (*see* **Note 2**).
10. Thin-walled polycarbonate PCR tubes.
11. Thermal cycler (PE Applied Biosystems).
12. Mineral oil (Sigma).
13. Agarose (Sigma).
14. 1X TBE: 90 m*M* Trizma base, 90 m*M* orthoboric acid, 2 m*M* EDTA (*see* **Note 3**).

15. Magnetic stirrer and stirrer bar.
16. Ethidium bromide stock solution: 25 m*M*.
17. 5X DNA-loading dye: 0.5% (w/v) sodium dodecyl sulfate (SDS), 0.25% (w/v) xylene cyanol, 0.25% (w/v) bromophenol blue, 1.5% (w/v) Ficoll® 400, in 3X TBE.
18. DNA molecular-weight ladder (New England Biolabs).
19. Agarose gel electrophoresis trays (20 cm wide × 40 cm long), tanks, and power packs (*see* **Note 4**).
20. Ultraviolet (UV) transilluminator.
21. Large trays (>20 cm wide, 30 cm long, and 4 cm deep).
22. Depurinating solution: 0.25 *M* HCl.
23. Denaturing solution: 0.5 *M* NaOH, 1.5 *M* NaCl.
24. Neutralizing solution: 1.5 *M* NaCl, 0.5 *M* Tris-HCl, pH 7.5.
25. Cling film.
26. Whatman filter paper or gel blotting paper.
27. Paper towels.
28. Nylon DNA hybridization membrane.
29. DNA UV crosslinker.
30. Temperature-controlled rotating hybridization oven with hybridization bottles.
31. Hybridization solution: Equal amounts of solution A and B, warmed to 65°C. Solution A: 14% (w/v) SDS, 2 m*M* EDTA; solution B: 1 *M* Na_2HPO_4 and H_3PO_4 to pH 7.2.
32. [α-^{32}P]dCTP (3000 Ci/nmol).
33. 100°C Heated block or boiling water bath.
34. 20X SSC: 3.0 *M* NaCl, 0.3 *M* Na citrate.
35. High-stringency washing solution: 0.2% (w/v) SDS, 0.2X SSC.
36. Autoradiography cassettes.
37. X-ray film (Kodak).

3. Methods

Restriction-digested genomic DNA is serially diluted and multiple aliquots of "small pools" (3–600 pg, or 1–200 haploid genome equivalents) are amplified by PCR in replicate, using primers flanking the repeat. The products are subsequently resolved by agarose gel electrophoresis and detected by Southern blot analysis with an internal radiolabeled double-stranded DNA probe. Separation of SP-PCR products by agarose gel electrophoresis and detection by Southern blot hybridization allows the resolution of the characteristic smears observed by standard genomic Southern blot analysis and bulk PCR amplifications into discrete and sharp bands, which can be easily observed, quantified, and sized ***(5)*** (*see* **Fig. 2**).

3.1. DNA Purification and Quality

Care should be taken to ensure that DNA solutions to be analyzed are of high purity ($OD_{260}/OD_{280} > 1.8$) to minimize the risk of low yields of PCR amplification as a result of the presence of impurities such as proteins and lipid molecules, which may interfere with the activity of DNA polymerase. Good quality genomic DNA can be obtained by standard phenol–chloroform extraction and ethanol precipitation techniques, followed by at least two washes with 70% ethanol ***(10)***. Alternatively, genomic DNA extraction kits are commercially available and they provide high-purity DNA. If

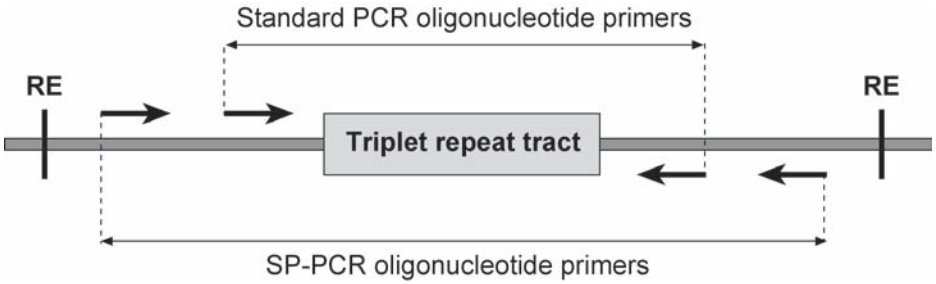

Fig. 3. Schematic representation of the annealing sites of oligonucleotide primers. Given the risk of contamination when working with very low numbers of template molecules, care should be taken when designing primers for SP-PCR analysis. The primers used for SP-PCR amplification should anneal outside the sequence of bulk PCR products, to avoid their amplification and detection in subsequent SP-PCR analyses. To aid in the uniformity of dilutions, the DNA should be digested with restriction enzymes (RE) that cut outside the region to be amplified.

purifying sperm DNA, it is essential that a differential lysis procedure be used to prevent contamination with leukocyte or epithelial cell DNA ***(4)*** (*see* **Note 5**). The concentration and purity of DNA in solution should be estimated using UV spectroscopy. The quality of the DNA preparation can be further assessed by resolving an aliquot of the sample on a 0.8% agarose gel stained with ethidium bromide and a DNA molecular-weight marker. High-molecular-weight DNA should run at the resolving point of the gel (>20 kb). Degraded DNA will present as a smear of smaller fragments. By comparison with the molecular-weight marker, it is also possible to estimate an approximate concentration for the sample.

3.2. Restriction Endonuclease Digestion

To ensure an even suspension of DNA in solution and avoid sampling errors when serially diluting the template to be amplified, genomic DNA should be digested with restriction endonucleases prior to amplification. Restriction enzymes that cut outside of the fragment to be amplified and have high activity should be used (*see* **Fig. 3**).

3.3. PCR Primer Design

One of the most critical parameters for successful PCR is the design of the oligonucleotide primers: A poorly designed primer can result in a PCR that will not work. The general rules for primer design in standard PCR applications apply when designing primer oligonucleotides for SP-PCR analysis. Several variables must be taken into account when designing PCR primers. Among the most critical are specificity, primer length, melting temperature, complementary primer sequences, GC content and polypyrimidine or polypurine stretches, and the nature of the residue at the 3' end.

Because both specificity and the temperature and efficiency of annealing are at least partly dependent on primer length, primers must be designed so that they are complex enough to anneal with a unique sequence within the template DNA that is to

be amplified, but not so long that they can misanneal to related sequences at the relatively low (<72°C) annealing temperatures used in PCR. In general, oligonucleotides between 18 and 24 bases are extremely sequence specific in complex mammalian genomes, provided that the annealing temperature is optimal. Primer length is also proportional to annealing efficiency: Generally, the longer the primer, the more efficient the annealing. The goal should be to design a primer with an annealing temperature of 55–72°C. Both forward and reverse oligonucleotides should be designed such that they have similar melting temperatures.

Primers need to be designed with no intraprimer pairing potential beyond 3 basepairs to avoid the formation of partially double-stranded structures, which will interfere with annealing to the template DNA. The base composition of primers should ideally be between 45 and 55% GC. The primer sequence must be chosen such that there are no polyG or polyC stretches that could promote nonspecific annealing or mispriming. PolyA and polyT stretches should also be avoided, as these may breathe and destabilize the primer–template duplex.

The 3'-end position of a PCR oligonucleotide primer appears to control the possibility of mispriming. The inclusion of a G or a C residue at the 3'-terminal ensures stronger hydrogen-bonding and higher efficiency of priming; it also limits end breathing. Most critically, the 3' end of a primer should not be complementary with itself or partner primer, as otherwise, primer dimers will be synthesized preferentially to any other products.

To increase the sensitivity of the method and to size the products generated by SP-PCR amplification more accurately, oligonucleotide primers should be designed so that they anneal close to the repeat tract. A short sequence flanking the repeat maximizes the possibility of determining small repeat number changes and, therefore, contributes to the sensitivity of the method (however, *see* **Subheading 3.4.** and **Fig. 3** concerning positioning of SP-PCR primers relative to previously used primers).

In summary, the ideal primers should have a near-random mix of nucleotides and an approx 50% GC content, be around 20 bases long, and anneal close to the repetitive sequence of interest. Oligonucleotide primers that have been used successfully in SP-PCR at human disease-associated triplet repeat loci are shown in **Table 1**.

3.4. Contamination

Because SP-PCR consists in the amplification of a very low number of template DNA molecules, extraneous DNA will be readily amplified and originate false-positive mutant alleles. The possibility exists that an observed product might result from contamination by a DNA template derived from a variety of sources, including the individual setting up the reactions, other genomic DNA sequences, previously amplified PCR products, and cloned fragments that contain the target sequence. In practice, contamination with one's own DNA and other sources of genomic DNA usually is not a problem and is easily avoided by careful techniques. However, extra care should be taken to avoid contamination with previously amplified PCR products and cloned material, as these are likely to exist in billions of copies that are easily spread around the laboratory by sloppy techniques. One way to reduce the risk of contamination is to

Table 1
Reagents and Cycling Conditions for SP-PCR Amplification of Trinucleotide Repeat Sequences at Various Human Loci

Locus	Primer oligonucleotide sequences	Reaction conditions	Anneal. temp.	No. of cycles	Ref.
DM1	Forward primer: DM-C 5'-AACGGGGCTCGAAGGGTCCT-3' Reverse primer: DM-BR 5'-CGTGGAGGATGGAACACGGAC-3'	1X Custom PCR buffer (ABgene); 200 n*M* of each primer; 0.175 U *Taq* DNA polymerase	68°C	28	***5***
FRDA	Forward primer: 104-F 5'–GGCTTAAACTTCCCACACGTGTT-3' Reverse primer: 629-R 5'-AGGACCATCATGGCCACACTT-3'	1X Custom PCR buffer (Roche/CLP); 500 n*M* of each primer; 0.5 U *Taq* DNA polymerase	60°C	30	***9***
HD	Forward primer: LK-1 5'-CCCATTCATTGCCCCGGTGCTG-3' Reverse primer: LKH-5 5'-TGGGTTGCTGGGTCACTCTGTC-3'	1X Custom PCR buffer (ABgene); 10% (v/v) DMSO; 200 n*M* of each primer; 0.35 U *Taq* DNA polymerase	68°C	30	***7***
SCA7	Forward primer: SCA7-A 5'-GCGACTCTTTCCCCCTTTTTTTTG-3' Reverse primer: SCA7-BR 5'-CGGAAGCCTCAACCCACAGATTC-3'	1X Custom PCR buffer (ABgene); 8% (v/v) DMSO; 200 n*M* of each primer; 0.175 U *Taq* DNA polymerase	62°C	28	***11***

Abbreviation: DMSO, dimethyl sulfoxide.

design two different sets of oligonucleotide primers: one set for routine PCR amplification, such as genotyping and probe generation, and another set reserved for SP-PCR analyses. SP-PCR primers should be designed so that they do not anneal with PCR products previously generated, probes and/or cloned fragments used routinely in the laboratory (*see* **Fig. 3**). In addition, physical preventative measures such as the use of disposable gloves and a dedicated lab coat, dedicated pipets and filter pipet tips should be employed. If possible, SP-PCR experiments should be set up in a sterile laminar-flow hood in a room separate from the main laboratory or in a dedicated PCR chamber (*see* **Note 6**). All reagents, including oligonucleotide primers and 10X PCR buffer, should be aliquoted into 1.5-mL screw-top Eppendorf tubes (*see* **Note 7**). In all cases, zero DNA (no template) control reactions should be included in the analysis (*see* **Subheading 3.5.**, **steps 1** and **7**). Experiments that yield positive results from zero DNA control reactions should be viewed with caution, if taken into consideration at all.

3.5. DNA Purification, Dilution, and SP-PCR

1. Purify genomic DNA of interest using standard phenol–chloroform extraction and ethanol precipitation methods ***(10)*** or one of many DNA extraction kits commercially available. Resuspend DNA in 1X TE (or sterile H_2O) in a 1.5-mL screw-top Eppendorf tube. Ideally, a zero DNA control purification should also be performed to check for contamination introduced during the extraction procedure.
2. Determine DNA concentration by ultraviolet (UV) spectroscopy, using standard methods ***(10)***.
3. Digest 20 μg of genomic DNA (approx 3×10^6 genome equivalents [g.e.]) with restriction endonuclease of choice, using standard molecular methods ***(10)*** (*see* **Note 8**).
4. Serially dilute digested genomic DNA into 1.5-mL screw-top Eppendorf tubes with 1X TE, containing 0.1 μ*M* of carrier primer (*see* **Note 9**). As a general rule, the carrier primer is usually the forward primer used in subsequent PCR amplifications. Prepare a series of dilutions for each DNA sample, aiming to cover the concentration range approx 1–500 g.e./μL (*see* **Note 10**).
5. To ensure that the DNA dilutions are as uniform as possible, we recommend that serial dilutions are performed no greater than 1/10 at each step and that very small volumes, which are difficult to pipet accurately (<10 μL), are not transferred at any stage. Also make sure that DNA solutions are highly homogenous by vortexing for a few seconds prior to further dilution.
6. Amplify 0.5 μL of each diluted DNA solution in multiple replicate reactions (*see* **Note 11**) in a final volume of 7 μL, with 0.175 U of *Taq* DNA polymerase and 0.2 μ*M* of each primer, in 1X PCR buffer (*see* **Note 12**). To reduce preparation time, increase pipetting accuracy, and reduce the potential for contamination, reactions should be set up via the use of master mixes. Initially, a global master mix should be set up containing all the reagents excluding DNA and including *Taq* polymerase, oligonucleotide primers, PCR buffer, and water. DNA dilutions can be added to submaster mixes, mixed, and aliquoted into the final 200-μL thin-walled reaction tubes (*see* **Note 13**). Given the small final reaction volume, it is recommended to cover each final reaction with 20 μL of mineral oil to avoid evaporation—even in thermal cyclers that have a heated lid. Cycle reactions through 28 rounds (*see* **Note 14**) of 96°C (45 s), annealing temperature (45 s), 70°C (3 min), and a chase of annealing temperature (1 min) and 70°C (10 min) (*see* **Note 15**).

7. To control for contamination, multiple zero DNA control reactions (approx 16% of all reactions) must be set up in parallel. Ideally, these should consist of zero DNA preparations, which have also been endonuclease digested and diluted using the same reagents.

3.6. Agarose Gel Electrophoresis of SP-PCR Products

1. Prepare 20 × 40-cm agarose gels in 0.5X TBE (approx 400 mL) from 0.7 to 3%, depending on the length of the fragments to be resolved. To ensure even cooling of the boiled agarose solution, stir it on a magnetic stirrer for 45–60 min, before adding ethidium bromide to a final concentration of 500 n*M* and pouring the liquid gel into the gel-forming tray.
2. Place and cover the gel in 0.5X TBE (also containing 500 n*M* ethidium bromide) (*see* **Note 16**), precooled to 4°C, in a refrigerated room, as soon as the agarose sets, to avoid the accumulation of dust and other impurities on the top of gel and prevent drying out of the gel surface, which may interfere with the gel blotting and hybridization detection. Let the gel cool and equilibrate with the buffer for at least 30 min before loading the PCR products.
3. Add 3 μL of DNA-loading dye (*see* **Note 17**) to each PCR product and load 5 μL of the final mixture on the gel (*see* **Note 18**). The gel may be loaded at room temperature, as long as care is taken to leave it at room temperature for as short a time as possible. DNA size ladders should be electrophorezed down each side and down the middle of each gel for sizing of mutant alleles.
4. Apply an initial maximal power of 300 V for 30 min to ensure minimal DNA loss by diffusion from the wells into the buffer. Following this initial period, resolve the PCR products at 3–4 V/cm for 16 h at 4°C.
5. Check the progression of DNA migration through the agarose gel by checking how far the DNA molecular-weight markers have run under UV light, on a transilluminator.

3.7. DNA Transfer From Agarose Gels Onto a Nylon Membrane by Southern "Squash" Blotting

1. Once the PCR products have resolved sufficiently, use a scalpel and a ruler to cut off excess gel not required for blotting, including the loading wells and edges of the gel (*see* **Note 19**).
2. Rinse the gel in deionized H_2O and cover completely in depurinating solution in a large tray. Shake gently on a benchtop shaker for 10 min. Repeat the wash with denaturing solution for 30 min and neutralizing solution for 30 min. Rinse the gel in deionized H_2O between washes. Multiple gels may be treated in the same tray, providing care is taken to ensure that each wash solution flows freely between gels and that gels are not muddled up.
3. Cut a piece of Nylon hybridization membrane to the same size as the gel fragment to be blotted and label it in the top right-hand corner with a pen. Wet the membrane by gently laying on the surface of a tray of deionized H_2O and then equilibrate it in neutralizing solution for a few minutes.
4. Place a piece of cling film, somewhat larger than the gel, on the bench. Layer a piece of Whatman or gel-blotting paper, wetted in neutralizing solution, on the cling film and place the gel on top of this. Very carefully lay the Nylon membrane on top of the gel with the labeled side against the gel. Air bubbles trapped under the membrane must be removed by rolling a wet 10-mL pipet over the surface to force them out of the edge of the blot. Layer two sheets of gel-blotting paper, rinsed in neutralizing solution, onto the membrane and check again for air bubbles (*see* **Note 20**).

5. Top the blot with a thick layer of gel-blot paper or paper towels and a glass plate to distribute an approx 500- to 1000-g weight. Allow transfer of the DNA from the gel onto the membrane by capillary action from 3 to 16 h (*see* **Note 21**).
6. Dismantle the blot in reverse order and place the membrane on a piece of dry gel-blotting paper, DNA side up (i.e., label up). Dry the membrane at 80°C and fix the DNA to the membrane by exposure to 1200 J/m^2 of UV light in a DNA crosslinker.
7. Keep the membrane in a dry place at room temperature until hybridization.

3.8. Hybridization of PCR Products Transferred Onto a Nylon Membrane

1. Wet the membrane in deionized H_2O, roll it up, and place it in a hybridization bottle (DNA side facing the inside), taking care to avoid air bubbles. If two membranes are hybridized in the same bottle, they should be placed back to back, with the DNA sides facing out from each other.
2. Add 10 mL of hybridization solution and incubate the bottle at 65°C for 30 min in a temperature-controlled rotating hybridization oven. Repeat the prehybridization step with a fresh aliquot of hybridization buffer for an additional 30 min.
3. Label 10 ng of a double-stranded DNA probe with [α-^{32}P]dCTP (3000 Ci/nmol) using standard methods ***(10)*** (*see* **Note 22**). Include 10–100 pg of the DNA size ladder in the probe-labeling reaction so that the molecular-weight size makers can also be visualized on the final autoradiograph.
4. Denature the probe at 100°C for 5 min, quench on ice for 3 min, and add to the hybridization bottle with the prehybridized membranes containing 5 mL of fresh hybridization solution. Hybridization is performed at 65°C overnight.
5. Following hybridization, discard the hybridization solution and rinse the membrane (still inside the bottle) with approx 50 mL of a high-stringency washing solution (0.2% [w/v] SDS, 0.2X SSC) at room temperature to remove excess probe and free [α-^{32}P]dCTP. Wash the filters twice in 30 mL of the same high-stringency washing solution for 30 min at 65°C in the bottle with rotation.
6. Finally, transfer the membrane into a large flat tray and rinse with gentle shaking at room temperature in another fresh batch of the same washing solution for a further 5 min.
7. Remove the washed filters and place onto a sheet of dry blotting paper (DNA side up). Thoroughly dry the filters in an 80°C oven and expose directly against X-ray film in an autoradiography cassette. Alternatively, damp filters may de sealed in plastic during exposure (*see* **Note 23**). Exposure at –70°C may increase the intensity of the bands if using intensifying screens; however, it also makes the bands more diffuse and thus decreases the accuracy of size estimates.
8. Develop autoradiographs after an exposure time varying from 4 h to 3 d.

3.9. Quantification of Repeat Dynamics

For the degree of variation in a given sample to be quantified accurately, it is necessary to know the effective DNA concentration in each reaction. Although this is theoretically known from the amount of input DNA, inaccuracies in determining the primary DNA concentration and secondary limitations of PCR amplification efficiency mean that, in practice, it is necessary to determine the average number of amplifiable molecules empirically for each sample. This can only be done using very low amounts of input DNA (*see* **Fig. 4**). If the degree of variation in a given sample is very high, then it may prove possible to count directly the number of input molecules in each

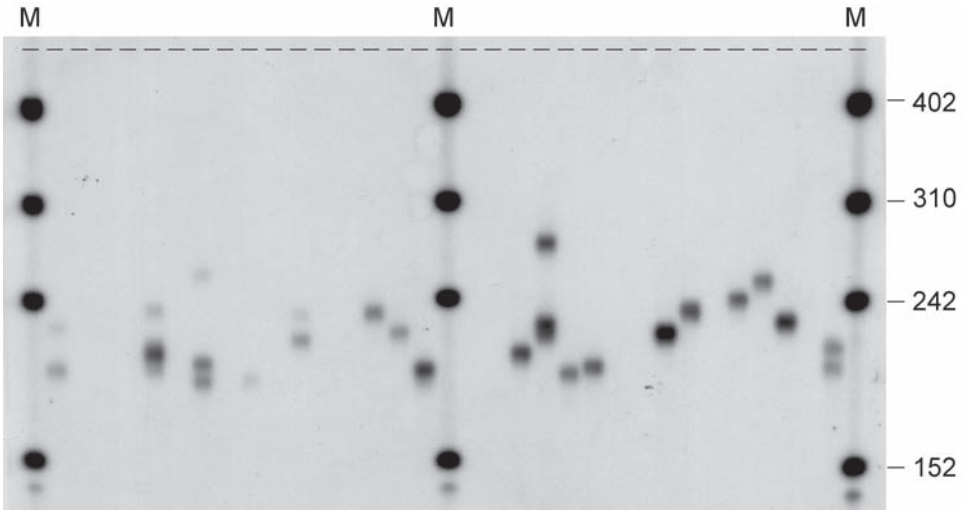

Fig. 4. Single molecule SP-PCR analysis of repeat instability in mouse cells. The trinucleotide repeat mutation profile in a brain sample from a mouse model of unstable DNA was determined by the amplification of an average of 0.8 template molecules per reaction. Such low amounts of input DNA allow the sizing of individual alleles and the empirical determination of the effective concentration of amplifiable DNA. The scale on the right represents the molecular-weight markers (M) converted into repeat numbers.

reaction, assuming that each gives rise to an individual resolvable allele. However, in samples that show less variation, it cannot be assumed that the amplification product of each input molecule can be distinguished within a reaction (because input molecules with the same number of repeats in the same reaction cannot be separated). In these situations, the only frequency measurement that can be counted directly is the number of reactions that failed to yield any signal (i.e., contained zero amplifiable input molecules) and those that were positive (i.e., contained at least one amplifiable input molecule). Using the ratio of positive to negative reactions, it is possible to determine the average number of input molecules using the Poisson distribution: $f(i) = e^{-m}m^i/i!$, where, in this case, $f(i)$ is the frequency of reactions with i input molecules, m is the average number of input molecules per reaction, e is the base of natural logarithms (e approx 2.7), and ! is the factorial symbol [e.g., $3! = 3 \times 2 \times 1 = 6$, and $4! = 4 \times 3 \times 2 \times 1 = 24$]. Usually, it is only possible to count directly $f(0)$; this, nonetheless, enables us to determine the average number of input molecules, $m = -\ln(f(0))$.

1. Perform multiple SP-PCR amplifications at low DNA concentrations (0.5–2 g.e./reaction) and determine the average number of input molecules amplified in each reaction, according to the Poisson distribution (*see* **Note 24**):

$$\text{Frequency of negative amplifications, } f(0) = \frac{\text{(total no. of reactions} - \text{no. of reactions yielding a PCR product)}}{\text{Total number of reactions}}$$

and then

$$\text{Average no. of molecules per reaction, } m = -\ln(f(0))$$

2. From the concentration of amplifiable input DNA determined, it is possible to calculate the effective amount of input DNA at other DNA dilutions and thus estimate the total number of molecules surveyed and derive appropriate mutation frequencies.
3. Multiple reactions using large amounts of input DNA can be used to measure the frequency of rare large length change events, and amplifications at low DNA concentrations can be used to derive detailed distributions of the frequency of common variants. Typically, 100–200 independently amplified single molecules might be sized to derive a detailed quantitative measure of the variation present in a sample (*see* **Note 25**).

4. Notes

1. Prepare a 10X stock of the PCR buffer and store in 100-µL aliquots at –20°C. Aliquots thawed on ice can be refrozen multiple times and are stable for at least 1 yr.
2. Use molecular-biology grade BSA. Do not use the acetylated BSA solution that frequently ships with restriction endonucleases, as this has a strong inhibitory effect on *Taq* DNA polymerase at high concentrations.
3. Make up a 5X stock of TBE. More concentrated stocks can be made, but they tend to precipitate out after relatively short times.
4. Such large agarose gel electrophoresis tanks and trays are not commercially available and have to be custom made. In-house workshops usually have no problems scaling up a design based on the examination of smaller commercially available equipment. Smaller gel tanks (e.g., 20 × 20 cm) can be used, but are of more limited utility, particularly in regard to the resolution of smaller length change variants (<± 20 repeats).
5. Semen often contains a high proportion of nonsperm cells that typically have very different mutational dynamics compared to sperm. Therefore, it is essential that such contaminating epithelial cells and leukocytes are removed. Fortunately, this is simply achieved using differential lysis procedures based on the resistance of sperm heads to lysis by SDS ***(4)***. Semen samples should also be checked microscopically for the presence of sperm, as a significant proportion of men are azoospermic, particularly those with some of the inherited triplet repeat expansion disorders.
6. A dedicated, fully enclosed PCR chamber provides an alternative physical barrier, minimizes air currents, and allows UV-mediated decontamination of potential pre-PCR contaminants. Additionally, all dedicated materials (pipets, etc.) used for pre-PCR manipulations are efficiently segregated from the rest of the lab. Several benchtop designs are commercially available. It is advisable to place the chamber in an area as far away from the areas where post-PCR manipulations are performed, and the doors should be kept shut at all times when the chamber is not being used. A 15- to 20-min UV treatment of the chamber prior to setting up reactions or making dilutions is recommended.
7. The most likely route through which contamination is introduced into PCR experiments is transfer through the inside of Eppendorf tube lids. Flip-top tubes are very difficult to open without touching the inside of the lid and should be avoided. On the other hand, screw-top tubes can be opened easily using a standard aseptic technique with a greatly reduced risk of introducing contamination and, therefore, should be used for storing reagents and DNA and for preparing PCR master mixes.
8. Spermidine (1 m*M*) and/or BSA (0.1 mg/mL) might be added to the endonuclease reac-

tion to increase the extent of digestion, although high concentrations of acetylated BSA should be avoided.

9. Highly diluted genomic DNA is not stable during long-term storage, as DNA molecules are lost by degradation and/or adsorption to the plastic tubes. The presence of a carrier primer in the dilution buffer and the use of siliconized tubes counterbalance these effects, ensuring minimal loss of genomic DNA as it is serially diluted. Nevertheless, highly diluted DNA solutions (<300 pg/μL) should not be kept for later amplification, as the number of amplifiable molecules decreases over time, even in the presence of a carrier primer.
10. As a starting dilution series, we would suggest the following concentrations: 500 g.e./μL, 50 g.e./μL, 10 g.e./μL, and 2 g.e./μL. Assuming that the source DNA is from humans or mice, this equates to concentrations of 1.5 ng/μL, 150 pg/μL, 30 pg/μL, and 6 pg/μL, respectively.
11. If performing SP-PCR on a sample for the first time, we recommend setting up eight reactions with each of the following input DNAs: 250 g.e., 25 g.e., 5 g.e., and 1 g.e. (*see* **Fig. 2**). This range of concentrations should allow a rapid assessment of the overall degree and pattern of repeat-length variation in a given sample and enlighten the choice of concentrations to be used for additional experiments, if needed. The use of a wide range of dilutions also ensures against inaccurate primary DNA concentration determinations.
12. For some loci with very high GC content, it may be necessary to use additional denaturants in the PCR. For example, dimethyl sulfoxide (DMSO), dimethyl formamide (DMF), urea, or formamide might be added to the reaction buffer. These additives are believed to lower the melting temperature of the target DNA and some have been used in SP-PCR protocols ***(7,11)***.
13. If setting up large numbers of SP-PCRs, much time can be saved using semiautomated electronic pipets that are able to take up master mixes and dispense multiple aliquots into separate tubes. The use of 96-well PCR plates is also advantageous when setting up large numbers of reactions.
14. The number of amplification cycles necessary to produce a band visible following hybridization is critical for SP-PCR analysis. Given the low number of template DNA molecules, the number of cycles must be high enough to generate detectable PCR products. However, too many cycles can result in an excess of product, which migrates as a broad band on an agarose gel, difficult to size accurately. More importantly, the use of too many cycles favors the amplification of smaller products and the concomitant loss of larger alleles—the very problem that besets bulk PCR analyses.
15. Touchdown amplification protocols, in which the annealing temperature gradually decreases in successive amplification cycles, might be necessary to increase the SP-PCR yield at some loci ***(7)***.
16. It is essential that ethidium bromide is included in both the gel and gel-running buffer. If it is omitted, then large expanded repeat-containing fragments do not resolve according to their size but, instead, separate out into multiple different bands based on their secondary structure (Gomes-Pereira and Monckton, unpublished observations).
17. To estimate how far the samples have run through the agarose gels, with no need to continuously check the gels under UV light, a more concentrated dye can be used in the loading buffer, accounting for the diffusion that will take place during the approx 16 h electrophoresis.
18. Half of the PCR product usually is enough to give rise to a strong signal from single molecules upon Southern blot hybridization. Store the remaining half of the SP-PCR product at 4°C, as it may be needed to load on a second gel at a later stage.

19. When analyzing a new sample for the first time, care should be taken to include the full range of potential products from 0 to approx 3000 repeats on the gel and transfer these to the Nylon hybridization membrane (alleles greater than 3000 repeats are unlikely to be amplified efficiently using PCR). Subsequently, depending on the range of products produced, it may be possible to resolve the fragments more clearly by running the gel for longer (if smaller alleles are not observed) and/or to reduce the amount of gel blotted by cutting off the top of the gel (if large expansions are not observed).
20. This method works well for 0.7–1.5% agarose gels. For higher-percentage gels (up to 3%), we recommend the following modification to avoid drying of gels leading to poor/uneven transfer. Soak a 5-cm-thick sponge (slightly larger than the size of the gel) in a dish containing 10X SSC buffer. Sequentially layer the following on the wet sponge: two Whatman papers, the treated gel (upside down), Nylon membrane, two Whatman papers, paper towels, and weight as described.
21. The longer the blotting time, the higher the efficiency of DNA transfer. However, longer blotting times result in broader bands in the final autoradiograph, which are more difficult to size accurately.
22. The probe typically consists of a gel-purified PCR product derived using the internal nested primers from an allele with 50–200 repeat units. Such a probe will work equally well on additional loci with the same repeat unit. Double-stranded DNA probes may also be labeled with dioxigenin-11-2'-deoxyuridine-5'-triphosphate (DIG-11-dUTP). Alternatively, end-labeled oligonucleotide repeat probes labeled to high specific activity may also be used. In such cases, the hybridization and detection procedures must be adapted accordingly.
23. Once filters have been dried, it is very difficult to remove the bound probe. Probes can be effectively stripped from filters that have been kept wet throughout by 2X 15-min washes at 65°C in denaturing solution and 2X 5-min washes in neutralizing solution at room temperature.
24. The accuracy of the amplifiable molecule determination is dependent on the number of reactions analyzed (with sampling error less for more reactions) and the actual frequency of negative reactions. Ideally, such concentration estimations should be based on the analysis of at least 100 reactions with an average input of approximately one molecule such that the frequency of negative amplifications is approx 30%.
25. The concentration of DNA that needs to be amplified to derive repeat-length distributions from single-input molecules is dependent on the overall degree of variation present in the sample. For samples in which there are high degrees of variation with widely dispersed repeat-length variants, it may be possible to use input quantities as high as five molecules per reaction. However, for samples in which the frequencies of variation are low and/or length-change variants differ only slightly from the progenitor, it may be necessary to use dilutions averaging 0.5 input molecules per reaction because even for reactions that contain an average of only one input molecule, approx 30% will contain two or more molecules that may not be resolved. In either case, the observed distribution of detectable alleles per reaction should be compared to that predicted from the Poisson equation using the average calculated using the frequency of negative reactions.

Acknowledgment

D. G. Monckton is a Lister Institute Research Fellow. S. I. Bidichandani is supported by a grant from the NIH/NINDS (R01 NS047596).

References

1 Richards, R. I. (2001) Dynamic mutations: a decade of unstable expanded repeats in human genetic disease. *Hum. Mol. Genet.* **10,** 2187–2194.

2 Leeflang, E. P., Zhang, L., Tavaré, S., et al. (1995) Single sperm analysis of the trinucleotide repeats in the Huntington's disease gene: quantification of the mutation frequency and spectrum. *Hum. Mol. Genet.* **4,** 1519–1526.

3 Zhang, L., Leeflang, E. P., Yu, J., et al. (1994) Studying human mutations by sperm typing: instability of CAG trinucleotide repeats in the human androgen receptor gene. *Nature Genet.* **7,** 531–535.

4 Jeffreys, A. J., Tamaki, K., MacLeod, A., et al. (1994) Complex gene conversion events in germline mutation at human minisatellites. *Nature Genet.* **6,** 136–145.

5 Monckton, D. G., Wong, L.-J. C., Ashizawa, T., et al. (1995) Somatic mosaicism, germline expansions, germline reversions and intergenerational reductions in myotonic dystrophy males: small pool PCR analyses. *Hum. Mol. Genet.* **4,** 1–8.

6 Fortune, M. T., Vassilopoulos, C., Coolbaugh, M. I., et al. (2000) Dramatic, expansion-biased, age-dependent, tissue-specific somatic mosaicism in a transgenic mouse model of triplet repeat instability. *Hum. Mol. Genet.* **9,** 439–445.

7 Kennedy, L. and Shelbourne, P. F. (2000) Dramatic mutation instability in HD mouse striatum: does polyglutamine load contribute to cell-specific vulnerability in Huntington's disease? *Hum. Mol. Genet.* **9,** 2539–2544.

8 Zhang, Y., Monckton, D. G., Siciliano, M. J., et al. (2002) Age and insertion site dependence of repeat number instability of a human *DM1* transgene in individual mouse sperm. *Hum. Mol. Genet.* **11,** 791–798.

9 Sharma, R., Bhatti, S., Gomez, M., et al. (2002) The GAA triplet-repeat sequence in Friedreich ataxia shows a high level of somatic instability in vivo, with a significant predilection for large contractions. *Hum. Mol. Genet.* **11,** 2175–2187.

10. Sambrook, J. and Russell, D. (2001) *Molecular Cloning: A Laboratory Manual*, 3rd ed. Cold Spring Harbor Laboratory, Cold Spring Harbor, NY.

11. Monckton, D. G., Cayuela, M. L., Gould, F. K., et al. (1999) Very large $(CAG)_n$ DNA repeat expansions in the sperm of two spinocerebellar ataxia type 7 males. *Hum. Mol. Genet.* **8,** 2473–2478.

6

Real-Time RT-PCR for CTG Repeat-Containing Genes

Maria Eriksson

Summary

Myotonic dystrophy (DM1) is a neuromuscular disorder caused by a CTG_n expansion in the 3'-untranslated region (UTR) of myotonic dystrophy protein kinase (*DMPK*). *SIX5* is a homeodomain gene located just downstream of the repeat, and myotonic dystrophy WD protein (*DMWD*) is located close upstream of *DMPK*. It has been hypothesized that the expansion might influence the expression of the three myotonic dystrophy locus genes (DM1-locus), contributing to the complex and varied phenotype in this disorder. Real-time quantitative reverse transcription–polymerase chain reaction, or TaqMan, is a very sensitive method that enables quantification of expression levels of genes from small amounts of tissue and lowly expressed genes. Because data are collected during the assay, the quantification is possible over a wide range of expression levels. By the use of a standard curve and an endogenous control, we have applied the TaqMan system for absolute quantification of the expression levels of the three genes (*DMPK, DMWD*, and *SIX5*) in the same tissue sample.

Key Words: Real-time quantitative PCR; TaqMan; DM1-locus; gene expression; absolute quantification; DMPK; CTG repeat.

1. Introduction

By the use of TaqMan technology (trademark of PE Applied Biosystems) or real-time quantitative reverse transcription-polymerase chain reaction (RT-PCR), we have developed a high-throughput system to quantify the expression of the myotonic dystrophy 1-locus genes (myotonic dystrophy protein kinase, *DMPK*, myotonic dystrophy WD-repeat protein, *DMWD*, and *SIX5*) in mouse and human tissue samples ***(1,2)***. The protocol outlined in this chapter contains the description for real-time PCR and absolute quantification of the DM1-locus genes, on human tissue samples. This protocol describes a specific assay of the DM1-locus genes, but could serve as a useful

From: *Methods in Molecular Biology, vol. 277: Trinucleotide Repeat Protocols*
Edited by: Y. Kohwi © Humana Press Inc., Totowa, NJ

manual for quantification of transcripts from other repeat-containing genes or gene transcript quantification in general. The TaqMan system is based on the *Taq* polymerase 5' exonucleatic activity on double-stranded DNA ***(3)***. This cleaves a dually labeled nonextendible TaqMan probe designed to hybridize to a sequence between the forward and the reverse primer for every particular amplicon. The probe has a quencher dye on its 3' end and a reporter dye on its 5' end. Fluorescence emission from the reporter dye is quenched by the quencher dye on its 3' end until nuclease degradation during the extension phase of the PCR separates the reporter from the probe and the quencher and enables the detection of the reporter dye's fluorescence emission ***(4,5)***.

2. Materials

1. Human tissue samples.
2. RNase- and DNase-free sterile Eppendorf tubes.
3. RNase- and DNase-free water.
4. Microfast track mRNA isolation kit (Invitrogen).
5. cDNA synthesis cycle kit (Invitrogen).
6. High-performance liquid chromatography (HPLC)-purified oligonucleotide primers.
7. TOPO TA-cloning kit (Invitrogen).
8. Plasmid midi kit (Qiagen).
9. TaqMan probes (PE Applied Biosystems).
10. TaqMan PCR core reagent kit including TaqMan buffer A, dATP, dCTP, dGTP, dUTP, AmpliTaq Gold polymerase, AmpErase uracil-*N*-glycosylase, $MgCl_2$ (PE Applied Biosystems).
11. MicroAmp Optical 96-well plates and caps (PE Applied Biosystems).
12. Agarose and DNA-sequencing gel equipment.
13. Primer and probe design softwares; Primer Express (Applied Biosystems) and Oligo 5 (National Biosciences).
14. ABI 7700 and Sequence detector software 1.6.3 (PE Applied Biosystems).

3. Methods

The methods described in this section outline (a) mRNA extraction and cDNA synthesis from human tissue samples, (b) real-time RT-PCR assay, (c) production of a standard curve for absolute quantification, and (d) data analysis.

3.1. mRNA Extraction and cDNA Synthesis

Percutaneous muscle biopsy samples were taken from either the vastus lateralis or tibialis anterior muscles. The biopsies were immediately snap-frozen in Freon, cooled in liquid nitrogen, and stored at –80°C until processed. Cytoplasmic polyA mRNA was isolated from 25–40 mg of tissue, using the Invitrogen Microfast Track 2.0 kit (*see* **Note 1**). The mRNA was resuspended in 10 µL of elution buffer.

cDNA synthesis was performed on 0.5 µg cytoplasmic polyA mRNA or 70% of the total amount obtained from the mRNA extraction, using random hexamer primers (cDNA synthesis cycle kit, Invitrogen) (*see* **Note 2**). The RT step was repeated once with the addition of reverse transcriptase followed by incubation at 42°C for 60 min. No-reverse transcriptase controls were performed simultaneously on 30% of the

Table 1
Primer and Probe Squences

Target cDNA	Oligonucleotide	5'→3' sequence	Amplicon size
DMPK	DMPK forward	ggtagtgaagatgaagcagacgg	92 basepairs
	DMPK reverse	ggaagcacgacacctcgc	
	DMPK probe	cctcttcagcatgtcccacttgttcatg	
DMWD	DMWD forward	ggagccaacggtccattg	94 basepairs
	DMWD reverse	gcagtgaactggttgaaatcgt	
	DMWD probe	caagcggatctacaagggcacccag	
SIX5	SIX5 forward	ccactgccccaggaaactt	97 basepairs
	SIX5 reverse	gcggtgaggatgatcttgc	
	SIX5 probe	ccaaccctgtgtctggcagccc	

mRNA from the extraction, but without the addition of enzyme. The cDNA reactions were purified by phenol–chloroform extraction and ethanol precipitated; the pellets were resuspended in 65 μL of sterile, nuclease-free water.

3.2. Real-Time Quantitative RT-PCR

The primers and probes for the DM1-locus genes were designed with Primer Express (Perkin-Elmer) and Oligo 5.0 software (National Biosciences) (*see* **Table 1** for primer and probe sequences). Primers were designed to cover at least one exon–exon boundary for every amplicon. Primers and probes aligning in regions with repetitive DNA were avoided (*see* **Note 2**). For *DMPK*, the forward primer was in exon 2 and the reverse primer spanning the junctions of exons 3 and 4. For *DMWD*, the forward primer was spanning the junctions of exons 1 and 2 and the reverse primer was in exon 2. For *SIX5*, the forward primer was spanning the junctions of exons B and C and the reverse primer was in exon C (*see* **Note 3**). Reporter dyes and quencher dyes for all probes were 6-carboxyfluorescein (FAM) and 6-carboxytetramethylrhodamine (TAMRA), respectively. The same batch of primers and probes were used throughout the whole experiment.

The real-time PCR reaction mixes were optimized for each amplicon and the different amplicones were run in singleplex (*see* **Note 4**). A PCR master mix for each amplicon to be amplified was prepared according to the following compositions:

- TaqMan PCR reaction mix for *DMPK*

  1X TaqMan buffer A;
  5 m*M* $MgCl_2$;
  200 μ*M* each of dATP, dCTP, and dGTP;
  400 μ*M* dUTP;
  100 n*M DMPK* probe;
  900 n*M DMPK* forward primer;
  50 n*M DMPK* reverse primer;
  0.625 U AmpliTaq Gold DNA polymerase;
  0.25 U AmpErase uracil-*N*-glycosylase.

- TaqMan PCR reaction mix for *DMWD*

  1X TaqMan buffer A;
  5 m*M* $MgCl_2$;
  200 μ*M* each of dATP, dCTP, and dGTP;
  400 μ*M* dUTP;
  100 n*M DMWD* probe;
  900 n*M DMWD* forward primer;
  300 n*M DMWD* reverse primer;
  0.625 U AmpliTaq Gold DNA polymerase;
  0.25 U AmpErase uracil-*N*-glycosylase.

- TaqMan PCR reaction mix for *SIX5*:

  1X TaqMan buffer A;
  5 m*M* $MgCl_2$;
  200 μ*M* each of dATP, dCTP, and dGTP;
  400 μ*M* dUTP;
  100 n*M SIX5* probe;
  50 n*M SIX5* forward primer;
  900 n*M SIX5* reverse primer;
  0.625 U AmpliTaq Gold DNA polymerase;
  0.25 U AmpErase uracil-*N*-glycosylase.

All real-time PCR reactions were run in a reaction volume of 25 μL, including 5 μL of cDNA from **Subheading 3.1.** Each sample was run in triplicate; that is, for quantification of the expression levels of *DMPK* in cDNA sample X, 16 μL of cDNA sample X was mixed with 64 μL of reaction mix for *DMPK* and 25 μL were transferred to three different wells of a MicroAmp optical plate. The wells were covered with MicroAmp optical caps and centrifuged (1600*g* for 1 min) to collect the sample at the bottom of the well and remove bubbles. For each mix, we included a negative control, which was also run in triplicate. The negative controls contained 20 μL reaction mix and 5 μL nuclease-free sterile water. The plate was loaded on a ABI7700 immediately (*see* **Note 5**).

All reactions were run on a ABI7700 sequencing detector, according to the following PCR thermal cycle conditions:

Cycle	Temperature	Time	Repeat	Ramp
HOLD	50°C	2 min		Auto
HOLD	95°C	10 min		Auto
Cycle	95°C	15 s	45	Auto
	60°C	1 min		Auto

To compare the expression levels of the different genes between different samples, we used β-actin as an endogenous control. By the use of β-actin, we were able to control for differences between samples in mRNA extraction efficiency and reverse transcriptase activity. The primer and probe sequences for β-actin were as described by Kreuzer et al. ***(6)***. All constituents and the cycling conditions for the assessment of

β-actin were as for our DM1-locus amplicons, except for the $MgCl_2$ and primer concentrations, which were according to previously published work *(6)*.

3.3. Generation of Standard Curves

To achieve absolute quantification, it is necessary to include a standard curve. We have used a standard based on plasmids each containing the four individual amplicons (*DMPK*, *DMWD*, *SIX5*, and *β-actin*).

1. The four amplicons were amplified from a skeletal muscle cDNA preparation using standard PCR methodologies (primers were the same as for the real-time PCR; *see* **Table 1**).
2. PCR products were purified to remove primers and buffers.
3. Each amplicon was cloned into the pCR2.1-TOPO vector (TOPO TA-cloning kit, Invitrogen), plated, and, subsequently, individual clones were picked and grown in 3-mL Luria–Bertani medium (LB) containing amphicillin. The following day, the plasmids were purified using the Qiagen plasmid purification kit.
4. Plasmids were sequenced with M13 vector-backbone primers and digested with *Eco*RI to confirm identity and eliminate clones with double inserts.
5. A larger batch of plasmid DNA from the confirmed clones containing the correct amplicon sequence was prepared from 300 mL of overnight culture, using stages 1–4, of the Qiagen plasmid midi kit. The supernatant was precipitated in absolute ethanol, washed in 70% ethanol, resuspended in 1 mL of 10 m*M* Tris-HCl, 1 m*M* EDTA, pH 8, buffer, and further purified by standard CsCl centrifugation and dialysis *(7)*. We chose to use CsCl centrifugation to exclude bacterial DNA contamination and any contaminating agents that could inhibit a PCR reaction. Glycerol stocks (15% glycerol) were prepared from the overnight cultures, preplasmid purification.
6. The concentrations of the plasmids were determined by spectrophotometry and purity was confirmed by agarose gel electrophoresis.
7. The plasmids were diluted into single use aliquots in nuclease-free sterile water of six different concentrations and stored at –20°C.

All standards were run in triplicate and ranged between 1.2×10^6 and 1.2×10^1 estimated copies of plasmids. A standard curve, consisting of at least five different dilutions of plasmids, for the relevant amplicon was included on every plate and for every mix (*see* **Fig. 1C**).

3.4. Data Analysis

During the real-time PCR assay, the linear increase in fluorescence signals from the reporter dye is collected every 7 s by the ABI Prism 7700 instrument (PE Applied Biosystems). The instrument uses optical fibers to direct the fluorescent signals to a spectrograph with a charge-coupled device (CCD) camera. Following the run, the raw data are analyzed using Sequence Detector Software 1.6.3 and the ΔR_n value is calculated based on the equation $\Delta R_n = R_n^+ - R_n^-$. R_n^+, where R_n^+ is the ratio of reporter dye emission and passive reference dye emission at any given point during the PCR reaction (*see* **Fig. 1A**) and R_n^- is the ratio of reporter baseline emission and passive reference dye emission during the cycles before an increase in PCR amplification is detected (*see* **Fig. 1A**). In our assays, the baseline was set between cycles 3 and 13 (*see* **Fig. 1A,B**).

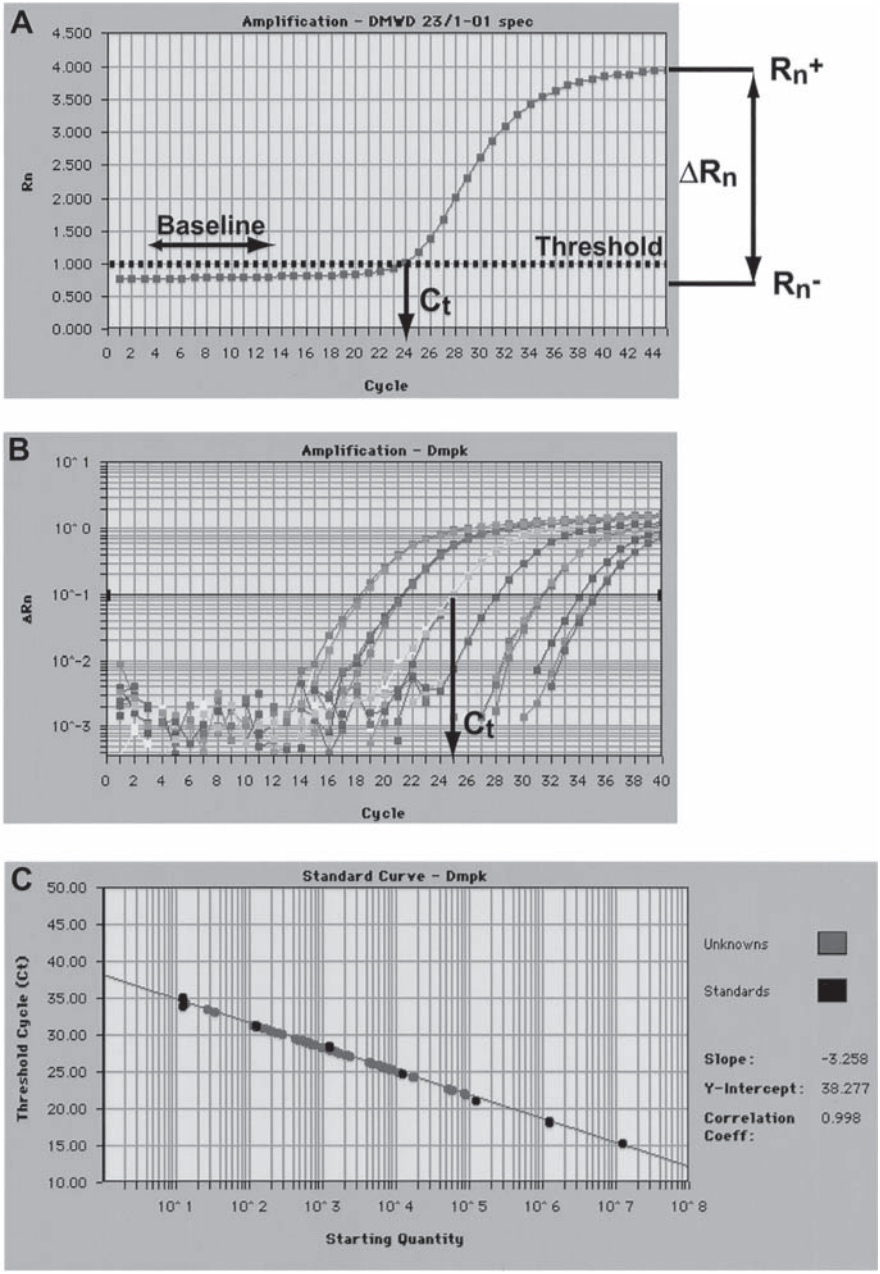

Fig. 1. Amplification plots and a standard curve from real-time PCR experiments with *DMPK* and *DMWD*. **(A)** The software displays the amplification plot of an unknown sample for *DMWD*. On the *Y*-axis is the R_n value and on the *X*-axis are the PCR cycles (1–45). R_n^+ is the ratio of reporter dye (FAM) emission intensity and passive reference dye emission (ROX, which is included in TaqMan buffer A) in a reaction-containing template, and R_n^- is the ratio of reporter baseline emission and passive reference dye emission during cycles 3–13 or in a reaction with no template. (*continued*)

All calculations for the standard curves and the samples were performed using Sequence Detector Software 1.6.3 (PE Applied Biosystems). Data were only considered acceptable if the correlation coefficient for the standard curve exceeded 0.98 (*see* **Fig. 1C**). The copy number of a specific transcript in each TaqMan reaction was determined by reference to the appropriate standard curve. For C_t values < 30, triplicates were not allowed to differ by more than 0.3 units. For C_t values >30, the triplicates were not allowed to differ by more than 0.5 units. Finally, all three DM1-locus genes were normalized to the internal control, β-actin.

4. Notes

1. Initial evaluation of two other extraction methods showed that this protocol gave the best results in terms of mRNA quality and quantity.
2. For the cDNA synthesis, we chose to use random primers instead of oligo-dT primers, as the CTG repeat is located in the 3' UTR of *DMPK (8)* and we wished to avoid stalling of the reverse transcriptase across long repetitive stretches. For the same reason, none of the oligos in the different amplicons aligned to repeat regions.
3. The critical issues that were essential for achieving absolute quantification of gene expression are summarized as follows:
    a. Because there is no gel resolution involved in the TaqMan assay, it is important to establish that only a single PCR product can be amplified under the reaction conditions used. By the use of one primer covering an exon–exon boundary, we have excluded the possibility of amplifying contaminated non-cDNA templates. In addition, all primer pairs were tested to ensure that they did not amplify any product from genomic DNA.
    b. In all our experiments, amplicons are designed to be short (70–150 bp) and as similar in size to each other as possible.
    c. All primers used were HPLC purified.
    d. Primers and probes for the different amplicons were designed with Primer Express and Oligo 5.0 software, and critical parameters were set to avoid excess secondary structure of the formation of primer–dimmers.
    e. The probes were designed to have a T_m between 67 and 70°C and the primers a T_m between 58 and 60°C. A temperature difference between the probe and primer annealing is recommended, as the probe has to be tightly aligned during DNA synthesis.

Fig. 1. *(continued)* Baseline was set between cycles 3 and 13. The fluorescence threshold is set within the linear phase across all samples in a particular run and was set to $1.15R_n$. The C_t (cycle threshold) value is where the threshold crosses the amplification plot, which equals the cycle at which a statistical increase in ΔR_n is first detected. **(B)** Amplification plot of standards in triplicates (ranging between 1.2×10^6 and 1.2×10^1 estimated copies of plasmids) for *DMPK*. On the *Y*-axis is ΔR_n, and on the *X*-axis are the PCR cycles (1–40). The C_t value (24.86) is marked for the standard with 1.2×10^4 estimated copies of plasmids. The threshold was set at $\Delta R_n = 0.096$. Amplification plots from unknown samples have been extracted from the picture for clarity. **(C)** Standard curve for *DMPK*. The standards (based on triplicate samples) are marked in black and the unknown samples are marked in red. On the *Y*-axis is the C_t value, and on the *X*-axis is the starting quantity. The C_t value is linearly related to the log of the initial amount of template (or primary target), in each reaction, allowing estimation of initial number of copies in the unknown samples by comparison with the standard for each amplicon. The calculations were performed with the Sequence Detector Software 1.6.3. (See color insert following p. 84.)

f. A G nucleotide was avoided in the 5' end of the probe because it has been shown to quench the reporter dye (Melin, unpublished results, PE Applied Biosystems).
g. We have used the same reporter and quencher dyes throughout all of the TaqMan experiments, as there are differences in sensitivity between different fluorophores.
h. Useful additional information can be found in the user bulletins supplied on request by PE Applied Biosystems.

4. Polymerase chain reaction conditions were optimized using the cloned constructs before running any samples. Parameters included the following: $MgCl_2$ concentration, as this stabilizes binding of the probe and permits the use of higher annealing/extension temperatures, which increases the PCR amplification efficiency ***(9)***; probe and enzyme concentration; the selection of the primer concentration that gives the lowest C_t with the highest ΔR_n^+.
5. The prepared plates can be stored for short periods, a few hours at 4°C, protected from light.

Acknowledgments

The author thanks Dr. Nessa Carey for critical reading of the text. The author also wishes to thank all of the co-authors who participated in the studies, which are the basis for this chapter ***(1,2)***. This work was supported by grants from the Swedish Medical Research Council (3875), the Swedish Association of Neurologically Disabled (NHR), the Swedish Society for Medical Research, the Karolinska Institute, the Petrus and Augusta Hedbergs Foundation, and the Torsten and Ragnar Söderberg Foundation. The work was approved by the Karolinska Hospital Ethical Committee.

References

1 Eriksson, M., Ansved, T., Edström, L., et al. (2000) Independent regulation of the myotonic dystrophy 1 locus genes postnatally and during adult skeletal muscle regeneration. *J. Biol. Chem.* **275,** 19,964–19,969.
2. Eriksson, M., Hedberg, B., Carey, N., et al. (2001) Decreased DMPK transcript levels in myotonic dystrophy 1 type IIA muscle fibers. *Biochem. Biophys. Res. Commun.* **286,** 1177–1182.
3 Holland, P. M., Abramson, R. D., Watson, R., et al. (1991) Detection of specific polymerase chain reaction product by utilizing the 5'–3' exonuclease activity of Thermus aquaticus DNA polymerase. *Proc. Natl. Acad. Sci. USA* **88,** 7276–7280.
4 Gibson, U. E., Heid, C. A., and Williams, P. M. (1996) A novel method for real time quantitative RT-PCR. *Genome Res.* **6,** 995–1001.
5 Heid, C. A., Stevens, J., Livak, K. J., et al. (1996) Real time quantitative PCR. *Genome Res.* **6,** 986–994.
6 Kreuzer, K. A., Lass, U., Landt, O., et al. (1999) Highly sensitive and specific fluorescence reverse transcription–PCR assay for the pseudogene-free detection of beta-actin transcripts as quantitative reference. *Clin. Chem.* **45,** 297–300.
7. Sambrook, J., Fritsch, E. F., and Maniatis, T. (1989) *Molecular Cloning, A Laboratory Manual*, 2nd ed, Cold Spring Harbor Laboratory, Cold Spring Harbor, NY.
8 Brook, J. D., McCurrach, M. E., Harley, H. G., et al. (1992) Molecular basis of myotonic dystrophy: expansion of a trinucleotide (CTG) repeat at the 3' end of a transcript encoding a protein kinase family member. *Cell* **68,** 799–808.
9. Eckert, K. A. and Kunkel, T. A. (1991) DNA polymerase fidelity and the polymerase chain reaction. *PCR Methods Appl.* **1,** 17–24.

III

Detection and Analysis of Polyglutamine-Containing Proteins and Their Aggregates

7

Antibodies Against Huntingtin

Production and Screening of Monoclonals and Single-Chain Recombinant Forms

Ali Khoshnan, Susan Ou, Jan Ko, and Paul H. Patterson

Summary

Antibodies can be extremely useful tools for the field of triplet repeat diseases. These reagents are important for localizing proteins in tissues, and within cells, they can be used in the isolation and characterization of the components of protein complexes, they can distinguish proteins with normal or an expanded polyglutamine repeat, they may be able to distinguish distinct conformations of a protein, and they can be used to perturb the function of proteins in living cells. Our group has produced monoclonal and recombinant single-chain antibodies that can be used for each of these purposes with huntingtin. This is the protein that, when mutated to contain an expanded polyQ motif, causes Huntington's disease.

Key Words: MAb; scFv; huntingtin.

1. Introduction

What has the field, using antibodies, learned about Huntington's disease (HD)? It is striking that all monoclonal antibodies produced thus far against the polyQ motif show much more binding to the expanded repeat form of huntingtin (Htt) than to the normal form. This could be the result of the availability of more space for antibodies to bind to the longer polyQ region ***(1)*** or to mutant Htt taking on a different conformation from that of normal Htt. It is further interesting that anti-Htt monoclonal antibodies (MAbs) generally do not bind to the nuclear aggregates that characterize HD pathology; rather, they bind to Htt in various regions of the cytoplasm (*see* **ref. *2***). Thus, the MAbs that bind very strongly to mutant Htt on immunoblots do not bind well to sections of brains

From: *Methods in Molecular Biology, vol. 277: Trinucleotide Repeat Protocols*
Edited by: Y. Kohwi © Humana Press Inc., Totowa, NJ

from mouse models of HD with expanded polyQ repeats or to human HD brain sections. These seemingly contradictory findings could be the result of polyQ-binding proteins covering the epitope in mutant Htt-expressing cells. An alternative hypothesis is that mutant Htt has a different conformation than normal Htt, making the polyQ motif unavailable for Ab binding of nuclear aggregates. The altered conformation hypothesis is supported by our finding that the anti-Htt MAb (MW8) preferentially binds Htt in tissue sections when Htt is in aggregates rather than when it is in the cytoplasm ***(2)***. This MAb was, in fact, produced using an aggregated form of Htt, and it binds not the polyQ domain but the C-terminus of exon 1. Consistent with this conformational hypothesis is our recent finding that the anti-polyQ MAbs can indeed bind Htt in nuclear aggregates in histological sections if the tissue is fixed in acetone (instead of the usual paraformaldehdye), which is known to drastically alter protein conformation ***(3)***.

Another interesting MAb that was produced using aggregated Htt as the antigen is MW7, which recognizes the polyP (proline) domains of Htt. This MAb has proven particularly useful in perturbing the function of Htt in living cells ***(4)***. The form of MW7 that was used for such functional experiments was the recombinant single-chain antibody (scFv). This was produced by cloning the genes for MW7 heavy and light chains and then linking just the regions of the molecule that code for the antigen-binding domains, yielding a single-chain Ab of approx 30 kDa that can be transfected into cells. The scFv form of MW7 has the important property of inhibiting the toxicity of mutant Htt in cultured cells ***(4)***, in a *Drosophila* model of HD ***(5,6)***, and in acute brain slices ***(7)***.

The methods that were used for producing and screening anti-Htt MAbs and scFvs are described in the following subsections.

1.1. Monoclonal Antibody Production

For many purposes, MAbs (usually obtained from mice) are preferable to polyclonal antisera (often obtained from rabbits). This is because of their specificity in antigen recognition, the ease in obtaining large quantities of antibody, and the ability to obtain the same antibody indefinitely. Detailed protocols for the generation of MAbs are widely available ***(8)***. Briefly, a mouse is injected with antigen and adjuvant until the titer of antibody in its serum is sufficiently high. At that point, the animal is sacrificed and its spleen taken and dissociated into a single cell suspension. These cells are then fused to a myeloma line, producing hybridoma cells, which are immortal cells, each producing a single antibody. These cells are grown in multiwell plates and their culture supernatants assayed for binding to the antigen of interest. Cells producing suitable antibodies are cloned, larger amounts of antibody produced, and the cells are frozen for future use.

The immunological response to an antigen usually is determined by its chemical structure and whether or not it is in a form that is recognized by the host animal as foreign. Using synthetic peptides as the antigen can generate site-directed Abs that bind specific regions of a protein. This approach can also be useful in generating Abs against a protein that is not immunogenic when the whole protein is presented as an

antigen. The main problem with using synthetic peptide antigens is that only one in three or four of the Abs generated in this way can recognize the native protein ***(9)***.

1.2. MAb Screening

To be successful, it is essential to develop an appropriate screening method before the hybridoma fusion begins. To identify the appropriate hybridoma within the 7–10 d it takes for them to grow to confluency, the preliminary screen needs to be simple and fast. Because enzyme-linked immunosorbent assay (ELISA) and dot-blot binding assays are the fastest screening methods, they are commonly used. However, these two methods require pure or partially pure antigen and do not discriminate between low- and high-affinity antibodies ***(10,11)***. Western immunoblots and immunohistochemical staining provide more specific information about which MAbs to select for cloning. It is highly recommended to choose one of these more specific methods for rescreening hybridoma supernatants. Rescreening can also help eliminate any false-positive clones. The general rule is to choose a screening method based on the eventual use of the MAb; that is, if the MAb will primarily be used for histology, rescreening on histological sections is recommended.

Western blots are critical for determining the protein(s) to which an Ab binds. Normally, this technique involves separating proteins using the highly denaturing conditions of sodium dodecyl sulfate-polyacrylamide gel electrophosesis (SDS-PAGE), followed by transfer of the proteins to a nitrocellulose membrane, where significant renaturation can occur before Ab binding occurs ***(2,12)***. It is striking that two of the anti-polyQ MAbs (MW1 and MW2) displayed detectable binding only to mutant Htt on blots, despite the presence of other polyQ-containing proteins in the cells and tissues used and despite the presence of wild-type Htt. This has also been observed with other anti-polyQ MAbs, such as 1C2 (Chemicon, 2). Recall that Htt was not used as the antigen in generating MW1 and MW2.

We determined the specific epitopes on Htt to which the MW MAbs bind through the use of arrays of dot blots of overlapping 14-mer peptides corresponding to the Htt exon-1 sequence ***(2)***. It is striking that such a method works well, given that many epitopes on proteins have been found to be noncontiguous amino acids that are brought together by protein folding ***(13)***. Such peptide arrays can be commercially obtained for any protein.

Our anti-Htt MAbs were rescreened using immunoblotting and histology using fixed tissue, so all of the MW MAbs display excellent binding to sections. If a nondenatured protein is used as the antigen, it should be surprising that the MAbs obtained would bind well to sections made from tissue fixed in paraformaldehyde. If, in fact, MAbs do not bind well to such sections, it is recommended to use fast-frozen, unfixed sections for histology. However, it was surprising that several of the anti-polyQ MAbs produced quite different binding patterns in neurons ***(2)***. Some stained the Golgi selectively, whereas others stained the neuropil or other cellular membranes. One interpretation of this diversity is that Htt acquires different conformations in various subcellular compartments. However, it must be said that one can never know with certainty what antigen an Ab is binding in a tissue section; that is, even though

immunoblots of a tissue show that a MAb binds Htt selectively, it does not mean that the MAb binds Htt in the cellular context. The usual control showing that binding to sections disappears when the MAb is preincubated with the antigen used to generate the MAb does not, of course, rule out that the MAb is binding to a different protein in the cellular context. Also, as mentioned previously, the method of fixation can drastically alter the pattern of Ab binding (**Fig. 1**).

We have developed an efficient and economical method for production of large quantities of MAbs in tissue culture flasks ***(14)***. This standing-flask method saves labor and costly materials and minimizes contamination risk. Other in vitro techniques include the gas-permeable cell culture flask by Baxter ***(15)***, the Celline Culture System by Integra Bioscience ***(16)***, and the miniPERM Bioreactor, Hollow Fiber Bioreactor, Cellmax Artificial Capillary Cell Culture System, and Cell Pharm systems ***(17)***. The in vivo method involves the use of mice. By suppressing the immune system with Pristane 1–2 wk before the intraperitoneal injection of hybridoma cells, the hybridoma cells can multiply and the ascites fluid that forms has a high concentration of secreted Abs. The advantages of this method are the high yield of Abs (1–20 mg/mL) and the minimal amount of labor involved. However, it is painful for the animals, the individual batches of fluid are of variable quality, and they are contaminated with cytokines ***(18)***. We developed a modified version of the ascites fluid technique that is very useful ***(19)***.

1.3. Single-Chain Antibody Strategy

Recombinant anti-Htt exon-1 (HDx-1) scFvs offer a valuable tool for gaining insight into the molecular mechanism of HD pathology. The scFvs can be used to identify the pathogenic epitopes in mutant Htt in living cells or animals. In addition, scFvs that reduce the toxicity and/or aggregation of HDx-1 can be developed into potential therapeutics ***(4,20,21)***. The technology is based on cDNA cloning of the antigen-binding domain of the antibody, namely the variable heavy and light chains (V_H and V_L), joining the two via a linker sequence to obtain a single-chain antibody, and intracellular expression for binding to the target protein. We have routinely used two approaches to isolate recombinant Abs against mutant HDx-1. We outline these methods and discuss various applications of anti-HDx-1 scFvs for studying the molecular pathogenesis of HD.

2. Materials

2.1. Producing Anti-Htt MAbs

1. Antigens: We used four different types of antigen to generate anti-Htt antibodies. Based on our results, the length of the polyQ repeats in the fusion protein antigen does not make a significant difference in obtaining Abs that bind preferentially to mutant Htt (*see* **Note 1**).

    a. We started immunization by GST–DRPLA–Q19 (construct provided by James R. Burke, the purified fusion protein was generated by the Protein Expression Facility at the California Institute of Technology), which contains the portion of the dentatorubral palliodoluysian atrophy (DRPLA) protein (a protein involved in a different triplet repeat disease) with the polyQ domain (with 19 Q repeats), and we fused it to glu-

tathione-*S*-transferase (GST) as a tag, which also solubilizes the protein. The DRPLA sequence surrounding the polyQ domain was: GST-LVPRGSVSTHHHHH (polyQ) HHGNSGPPEFPGRLERPHRD. This construct was used out of convenience, because it contained the polyQ domain without significant surrounding sequence from the host protein. As described in **Subheading 2.2.1.**, we screened the resulting hybridoma supernatants by ELISA against this antigen and against GST alone. We selected MW1 from this fusion, after confirming the specificity of binding by Western blotting, as described below.

b. The second immunization protocol utilized alternating injections of GST–DRPLA–Q35 and MGGPPSTP(Q35)TSRTYPYDVPDYA fused to thioredoxin (TRX-Q35) (construct provided by Parsa Kazemi-Esfarjani). Alternating these antigens was done so as to maximize the possibility of obtaining anti-polyQ rather than anticarrier MAbs. After seven boosts, we selected MW2 and MW5 from this fusion.
c. The third immunization protocol used a construct containing the expanded polyQ domain (67Q) of Htt exon 1, fused to GST. After four boosts with this soluble protein, we selected MW3, MW4, and MW6 after screening supernatants.
d. Given that all of the previous MAbs bound to the polyQ domain, we used a different strategy to obtain MAbs against other Htt domains. The fourth immunization protocol used two injections of soluble GST–Htt exon 1 (67Q) (construct provided by Peter Thumfort) and nine boosts of the protein in an insoluble, aggregated form made by cleaving off the GST. One can obtain different reagents through Cure HD Initiative Resource Bank (www.hdfoundation.org/chdireagent). We selected MW7 and MW8 from this immunization.

2. HL-1 complete medium (Biowhittaker, Walkersville, MD) with 1% fetal bovine serum (FBS), 1 m*M* Na-pyruvate, 4 m*M* L-glutamine, and 5 IU/mL penicillin and 5 μg/mL streptomycin.
3. RPMI 1640 medium (Gibco-BRL).
4. 3% Acetic acid in water.
5. Phosphate-buffered saline (PBS): 137 m*M* NaCl, 2.7 m*M* KCl, 8.1 m*M* Na_2HPO_4, 1.5 m*M* KH_2PO_4, pH 7.4.
6. 0.2% Trypan blue in PBS.
7. PEG 1500, 50% (w/v) in 75 m*M* HEPES (Roche Diagnostics).
8. AAT: Aminopterin, Adenine, Thymidine (Sigma).
9. HCF: Hybridoma Cloning Factor (Fisher Scientific).
10. HL-1 conditioned medium.
11. Balb/c mice (Jackson Laboratory).
12. MPL + TDM emulsion (RIBI adjuvant system, RIBI; *see* **Note 2**).

2.2. Screening Anti-Htt MAbs

2.2.1. ELISA Assay

1. Nunc-Immuno plate (MaxiSorp F96).
2. Antigen (Ag), as described in **Subheading 2.2.**
3. PBS–Tween-20: Add 1 mL of Tween-20 to 1 L of PBS.
4. Diluent: 2% bovine serum albumin (BSA, fraction V; Sigma-Aldrich), 10% normal goat serum (NGS; Sigma) in PBS.
5. Biotin-conjugated goat anti-mouse IgG + M antibody (Biot-GAM; Chemicon; 130B).
6. Horseradish peroxidase (HRP)-conjugated streptavidin (HRP-Strep; Chemicon; SA202).

7. ABTS substrate kit (Vector Laboratories; SK-4500).
8. Microplate spectrophotometer (Molecular Devices; SPECTRAmax 190).

2.2.2. Immunoblotting Assay

1. HD human lymphoblast cell lysate (*see* **Note 3**).
2. Dissociation buffer: 10 m*M* Tris-HCl, pH 6.8, 20% glycerol, 6% sodium dodecyl sulfate (SDS).
3. 5% SDS-PAGE gel with preparative well (*see* **Note 4**).
4. Nitrocellulose membrane (Schleicher & Schuell; 10402580).
5. Blocking reagent (Boehringer Mannheim; 1 096 176).
6. Mini-incubation trays (Bio-Rad; 170-3902).
7. 4-Chloro-1-naphthol stock solution: 0.5 g of 4-chloro-1-naphthol (Sigma; C8890) dissolved in 50 mL methanol.
8. 30% H_2O_2 (Sigma).

2.2.3. Immunohistochemistry

1. Cryosections of R6/2 and WT brain (*see* **Note 5**).
2. ImmEdge pen (Vector Laboratories).
3. DTAF goat anti-mouse IgG+M (Chemicon), Hi Fluorescence goat anti-mouse IgG (Antibodies, Inc.).
4. Mounting medium (Molecular Probes; *see* **Note 6**).

2.2.4. Producing Large Quantities of MAbs

1. Same as **Subheading 2.1.**, **items 2** and **11**.
2. Pristane (Sigma).

2.3. The scFv Strategy

1. The mouse scFv module (Amersham; 27-9400-01) kit includes primed first-strand reaction mixes, variable heavy-chain primers, variable light-chain primers, *Sfi-Not*I site primers, pUC18 (*Sfi, Not*I digested), Sephacryl S-400 HR, and a step-by-step protocol manual.
2. The expression module (Amersham; 27-9401-01) kit includes phagemid pCANTAB 5E, M13KO7 helper phage, *Escherichia coli* TG1 and HB2151, and a step-by-step protocol manual.
3. Trizol (Invitrogen) for RNA extraction.
4. Oligotex mRNA isolation kit (Qiagen).
5. Ni-NTA superflow resin (Qiagen).
6. 2YXT medium: 16 g trypton, 10 g yeast extract, 5 g/L NaCl, supplemented with 2% glucose for working medium.
7. LB-amp: Luria-Bertani (LB) medium including 10 g Bacto-trypton, 5 g yeast extract, and 10 g NaCl, pH 7.5, with ampicillin (50 mg/L).
8. Agar plate: Bacto-agar 15 g/L medium.
9. Top-agarose plate: 7 g/L agarose medium.
10. GST–Sepharose beads (Pharmacia).

3. Methods

3.1. Producing Anti-Htt MAbs

1. Grow HL-1 cells in HL-1 complete medium until the cell density is over 10^6 cells/mL. Harvest the supernatant to use as HL-1 conditioned medium. A total of 10^8 cells is generally used for fusion with one spleen (*see* **Note 7**).
2. Prepare the AAT selection medium by mixing 40% HL-1 complete medium, 40% HL-1 conditioned medium, 10% HCF, 10% FBS, and AAT.
3. Prepare the AT selection medium by mixing 90% HL-1 complete medium, 10% FBS, and AT.
4. RPMI 1640 medium, AAT selection medium, and PEG 1500 are warmed to 37°C.
5. Harvest the HL-1 cells and wash three times with RPMI 1640. Resuspend cells in 30 mL RPMI 1640 medium. Check viability by taking 10 μL cell suspension and mix it 1:1 with trypan blue solution. The stained cells are dead cells.
6. Remove spleen from the immunized mouse (*see* **Note 8**) and wash three times with RPMI 1640 medium. Dissociate the spleen cells by gently rubbing between two sterile frosted slides. Rinse the cells from the slide with RPMI 1640 medium and centrifuge at 1000 rpm for 10 min.
7. Resuspend the spleen cells in 30 mL RPMI 1640 medium and check the cell number by taking 10 μL cell suspension and mix 1:1 with 3% acetic acid to lyse the red blood cells.
8. Based on the spleen cell number, add the HL-1 myeloma cells to a ratio of 3:1 to 10:1 (spleen/myeloma), then centrifuge the mixture at 1000 rpm for 10 min.
9. Remove the supernatant and loosen the cell pellet by gently tapping the bottom of the centrifuge tube.
10. One milliliter of warmed PEG 1500 is added drop by drop over 1 min to the cells while the tube is constantly shaken gently. Shake the tube gently for another minute.
11. Five milliliters of warmed RPMI 1640 is added drop by drop over the next 5 min.
12. Centrifuge the suspension at 900 rpm for 10 min. Remove the supernatant.
13. The cells are resuspended very gently in a volume necessary to yield 2×10^5 cells/well and 150 μL/well of AAT selection medium. The cell suspensions are plated into a 96-well plate and placed in 5% CO_2 incubator at 37°C.
14. Negative controls should be set up by plating HL-1 cells in the AAT selection medium.
15. After 7 d, replace half of the medium in each well with AT selection medium. Repeat this procedure subsequently every other day.
16. Clones will become visible after 5–7 d and supernatants can be harvested for testing when cells reach 75% confluency.
17. After testing the supernatants of the clones, transfer the positive clones to a 24-well plate by resuspending the cells gently with a sterile Pasteur pipet.
18. The cells can be subcloned at this stage to obtain single clones or frozen for future purpose.

3.2. Screening and Characterization of Anti-Htt MAbs

3.2.1. ELISA Assay

1. Add 100 μL of Ag (diluted in PBS) to wells of the immunoplate and incubate overnight at 4°C in a humid atmosphere (*see* **Note 9**).
2. Remove excess Ag by flicking the plate over a container. Wash the plate three times by adding and removing 100 μL PBS–Tween-20.

3. Incubate the plate with 2% BSA in PBS, 100 μL/well for 1.5 h at 37°C to block the remaining protein-binding sites on the wells.
4. Wash the plate three times with PBS–Tween-20.
5. Identify the hybridoma clones on the plate cover (*see* **Note 10**) and add 100 mL of the test solution (hybridoma supernatant) to each well. Incubate for 2 h at room temperature.
6. Wash the plate three times with PBS–Tween-20, 100 μL/well.
7. Incubate wells with Biot-GAM at 1/1000 in diluent, 100 μL/well for 1 h at room temperature.
8. Wash the plate with PBS–Tween-20 three times, 100 μL/well.
9. Incubate the wells with HRP-Strep at 1/1000, diluted with 2% BSA, 10% NGS, 100 μL/well for 1 h at room temperature.
10. Wash the plate with PBS–Tween-20 three times, 100 μL/well.
11. Wash the plate with H_2O twice, 100 μL/well, and develop using ABTS substrate kit following the instructions from the manufacturer.
12. Read the optical density using a microplate spectrophotometer.

3.2.2. Immunoblotting and Epitope Mapping

1. One milligram (*see* **Note 11**) of HD human lymphoblast cell lysate heated in 70°C for 3 min.
2. Centrifuge at 14,300 rpm (1000*g*) in an Eppendorf centrifuge for 2 min.
3. Resuspend the pellet in 6 *M* urea (*see* **Note 12**) and add dissociation buffer with 2-mecaptoethanol.
4. Boil at 95°C for 10 min, cool, and load the sample in the preparative well.
5. Run the gel at 20 mA for the first 15 min to pack the protein in the stacking gel and increase to 35 mA afterward (*see* **Note 13**).
6. Electrotransfer the gel to the nitrocellulose membrane at 35 mA overnight with cooling (*see* **Note 14**).
7. Preblock the membrane with 1% blocking reagent/PBS for 1 h (*see* **Note 15**).
8. While the blot is wet, lay the blot on a clean glass plate, mark the blot with color ballpoint pen with a horizontal line (*see* **Note 16**), and cut the blot with sharp blade vertically to make 2-mm strips. Label each strip.
9. Incubate individual strips with hybridoma supernatant (*see* **Note 17**) overnight at room temperature.
10. Wash blots with PBS–Tween-20 three times, 10 min each with rocking (*see* **Note 18**).
11. Incubate individual blots with Biot-GAM at 1/1000 dilution in 2% BSA, 10% NGS for 1 h (*see* **Note 19**).
12. Wash with PBS–Tween-20 three times, 10 min each.
13. Incubate blots with HRP-Strep at 1/1000 in 2% BSA, 10% NGS for 1 h.
14. Wash with PBS–Tween-20 three times for 10 min each, and wash further with PBS, two times for 10 min each.
15. Develop the blots in the following solution: 5 mL stock solution of 4-chloro-1-naptol, 95 mL PBS, 0.1 mL of H_2O_2.
16. Stop the color development by washing in H_2O.

3.2.3. Immunohistochemistry

1. Circle the sections with an ImmEdge pen (Vector; H-4000) to create wells.
2. Apply test hybridoma supernatants to the brain sections. Incubate overnight at room temperature in a humid chamber (*see* **Note 20**).

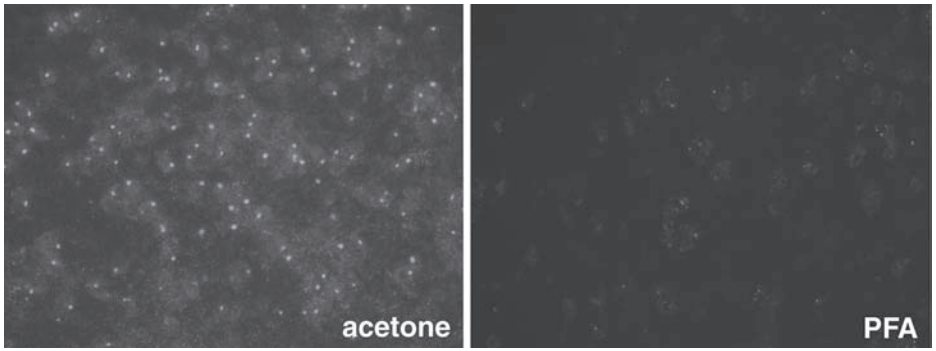

Fig. 1. MW3 staining of nuclear inclusions is dependent on the fixation. An R6/2 Htt mouse brain was fresh frozen and frozen sections made. Sections were fixed for 15 min in paraformaldehyde (4%) or 7 min acetone (100%) at room temperature. Sections were then stained with MW3, an anti-polyQ Htt mAb. As with other anti-polyQ antibodies, staining of nuclear inclusions is weak when paraformaldehyde is used. However, acetone fixation opens up the epitope for strong mAb binding. (See color insert following p. 84.)

3. Remove hybridoma supernatants and wash slides in PBS three times for 10 min each.
4. Dilute DTAF goat anti-mouse IgG+M 1/100, Hi Fluorescence goat anti-mouse IgG 1/100 in diluent. Centrifuge at 14,300 rpm (1000*g*) for 5 min. Collect supernatants and filter through a 20-μm syringe filter.
5. Remove the slides from PBS, apply the freshly prepared secondary antibodies, and incubate on sections for 1 h at room temperature.
6. Repeat washing as in **step 4**.
7. Remove the slides from PBS, dry the slides around the sections, and mount slides with mounting medium.

3.2.4. Producing Large Quantities of Antibody

1. The antibody concentration in culture supernatants ranges from 5 to 60 μg/mL, and ascites fluid is normally 1000-fold more concentrated. Depending on the amount needed, one can use the in vitro or in vivo method for antibody production.
2. The in vitro method involves expanding the hybridoma cells by growing (1:4 dilution) in tissue culture flasks. Harvest the supernatant when cells reach 100% confluency by centrifuging the cell suspension at 400*g* for 10 min and collecting the supernatant.
3. We have developed an efficient and economical method for the production of large quantities of MAbs in tissue culture flasks ***(14)***. Cells are grown in tissue culture flasks until they reach 80–90% confluency. The flasks are then filled with HL-1 complete medium and let stand in the incubator for 3–4 wk until all cells die. The supernatant is then harvested.
4. The in vivo method involves the use of mice. Mice are injected with 0.5 mL pristane intraperitoneal (ip) 1–2 wk before ip injection of hybridoma cells; 10^7 hybridoma cells are injected into each mouse.
5. Mice are checked each day for the development of ascites fluid. It usually becomes apparent by 6–7 d. The ascites fluid is harvested when the mice start to look sick. Then, 3–5 mL ascites fluid can be collected from each mouse.

3.3. scFv Strategy

3.3.1. Specific Cloning scFvs of MAbs (MW1–MW8)

Anti-HDx-1 scFvs were cloned and assembled from existing MAbs (MW1–MW8). First, cDNA libraries were made from each hybridoma cell line secreting a MW MAb.

1. RNA was extracted from 1×10^7 hybridoma cells by Trizol. Cells were lysed in 1 mL of Trizol and vortexed for 20 s, followed by incubation at room temperature for 5 min. Two hundred microliters of chloroform was added and vortexed for additional 20 s. The mixture was centrifuged at full speed in a microfuge for 15 min.
2. The aqueous layer was transferred into a new tube and an equal volume of isopropanol was added, followed by incubation at room temperature for 10 min. RNA was precipitated by centrifugation for 15 min at 4°C in a microfuge at full speed. The pellet was rinsed with 70% ethyl alcohol and air-dried. RNA was resuspended in 500 μL of DEPC-treated H_2O. Yields are between 0.5 and 1 mg.
3. Messenger RNA was extracted from total RNA using oligo-T. We obtained 3–5 μg mRNA.
4. Using the mouse scFv module kit, cDNA libraries from each existing MAb were made by applying the above-purified mRNA.
5. From these libraries, both V_H and V_L chains were amplified by PCR, using primers complementary to the consensus sequences flanking each domain (provided by the kit; *see* **Note 21**).
6. The amplified V_H and V_L of each MAb were assembled by PCR using a linker DNA fragment encoding $(Gly_4Ser)_3$ provided in the kit.
7. These scFv genes were cloned into the M13 phagemid and used to transform *E. coli*, strain TG1, which supports production of recombinant phage on 2YXT agar plate (Expression Module Kit, Amersham).
8. The amplified recombinant phage population was selected for binding to mutant HDx-1 on a nitrocellulose filter, which was prepared by SDS-PAGE separation followed by blotting to nitrocellulose. The HDx-1 region on the membrane was cut by the size of MW of the protein and confirmed by specific antibody binding (Western).
9. The phage that specifically bound mutant Htt was eluted from the nitrocellulose and incubated with log phase *E. coli* TG1. Colonies infected with phage were selected on LB-amp plates and amplified further, followed by further characterization.

3.3.2. Selective Cloning scFvs From Human scFvs Library

Recombinant HDx-1 can be used as a bait to screen existing synthetic human scFv libraries, which were obtained from G. Winter ***(20,22)***.

1. HDx-1 with 103Qs was cloned in frame with C-terminus His tag in PQE-60 plasmid (Qiagen). Plasmids were introduced into competent BL21 Gold (Stratagene). Induction was for 5 h at 37°C. Purification of HDx-1 was accomplished using Ni-NTA superflow resin (Qiagen) according to the manufacturer's instruction. Protein purity was evaluated by SDS-PAGE.
2. A six-well plate was coated with 5 μg of purified protein in 1 mL of PBS overnight at 4°C. The excess was removed and the well rinsed 3X with PBS.
3. The well was preincubated with blocking solution (10% powdered milk in PBS) for 2 h at room temperature, then rinsed with PBS and incubated with 1 mL of phage from the library encoding approx 9×10^{10} clones, and diluted 1:1 with blocking solution and 0.1% triton-X100 at 37°C for 2 h with gentle shaking.

4. The well was washed approx 40 times in PBS to remove unbound phage.
5. One milliliter of log phase *E. coli* TG1 was added to the well and incubated for 1 h at 37°C with gentle shaking.
6. The mixture was removed, bacteria pelleted and resuspended in 10 mL fresh medium, and coinfected with approx 5×10^9 M13 helper phage particles (Expression Module Kit, Amersham). The culture was incubated at 37°C overnight with shaking.
7. The recombinant phage was concentrated by addition of 1/5 vol of PEG/NaCl (20% polyethylene glycol 6000–2.5 *M* NaCl), incubated on ice for 30 min, and centrifuged at 11,000*g* for 15 min. The phage were resuspended in TE (10 m*M* Tris-HCl, 1 m*M* EDTA, pH 8.0). This cycle was repeated four additional times.
8. Five micrograms of GST–HDx1(50Q) were bound to GST–Sepharose beads. After washing, the beads were coincubated with 500 µL concentrated phage clones in PBS–10% glycerol and 5 m*M* dithiothreitol, and rocked for 3 h at room temperature.
9. The beads were washed extensively in PBS and coincubated with log phase *E. coli* TG1 at 37°C for 1 h. Colonies were selected on LB-amp plates.
10. Individual clones were isolated and expressed and recombinant scFvs were tested for binding to His-HDx1 in vitro by dot-blot assay.

3.3.3. Expression and Evaluation of scFvs

It is ultimately desirable to express anti-HDx-1 scFvs in mammalian cells. We subcloned the reading frame for each scFv into the mammalian plasmid pcDNA3.1 in the frame with the Flag epitope for ease of detection. Selected clones were amplified and used to transfect 293 cells by Lipofectamine (Invitrogen). We have thus far succeeded in expressing soluble scFvs for MW1, MW2, and MW7. These scFvs are functional in that they coprecipitate with HDx-1 from cell extracts and they colocalize with HDx-1 in cells when examined by confocal microscopy. This is fortunate, as scFvs can be nonfunctional for various reasons, including denaturation in the pH and redox milieu of the living cell. It also appears that expression of these scFvs alone is innocuous to mammalian cells, as we observed no changes in cell number or morphology in their presence ***(4)***. However, we found that the MW7 scFv, targeted to polyP domains of HDx-1, reduces the toxicity and aggregation of mutant HDx-1. Surprisingly, the anti-polyQ scFvs MW1, and MW2 exacerbate the toxicity of mutant HDx-1 ***(4)***. Thus, one application of anti-HDx-1 scFvs is to determine specific epitopes that contribute to mutant HDx-1 toxic function. Anti-polyQ scFvs can also be useful tools to study other proteins with expanded polyQs. Intracellular expression of MW1 and MW2 scFvs promotes aggregation of the androgen receptor with expanded polyQ (M. Diamond et al., unpublished data).

Expression of soluble anti-HDx-1 can be achieved in many expression systems. For example, we have cloned human anti-HDx-1 downstream of the T-7 promoter and have expressed ^{35}S-methionine-labeled scFvs in rabbit reticulocytes (*see* **Fig. 2A**). An advantage of this approach is that high-throughput screening can be used to evaluate a large number of scFv clones isolated from phage libraries after the initial screening. Individual scFv clones can be expressed and ^{35}S-labeled in rabbit reticulocytes in a 96-well format and then examined for binding to HDx-1 on nitrocellulose blots (Gold TNT T7 express, 96 system, Promega, cat. no. L5600; prepared lysate, just add plasmid). Reactive scFvs can be visualized by autoradiography. ^{35}S-labeled scFvs can also

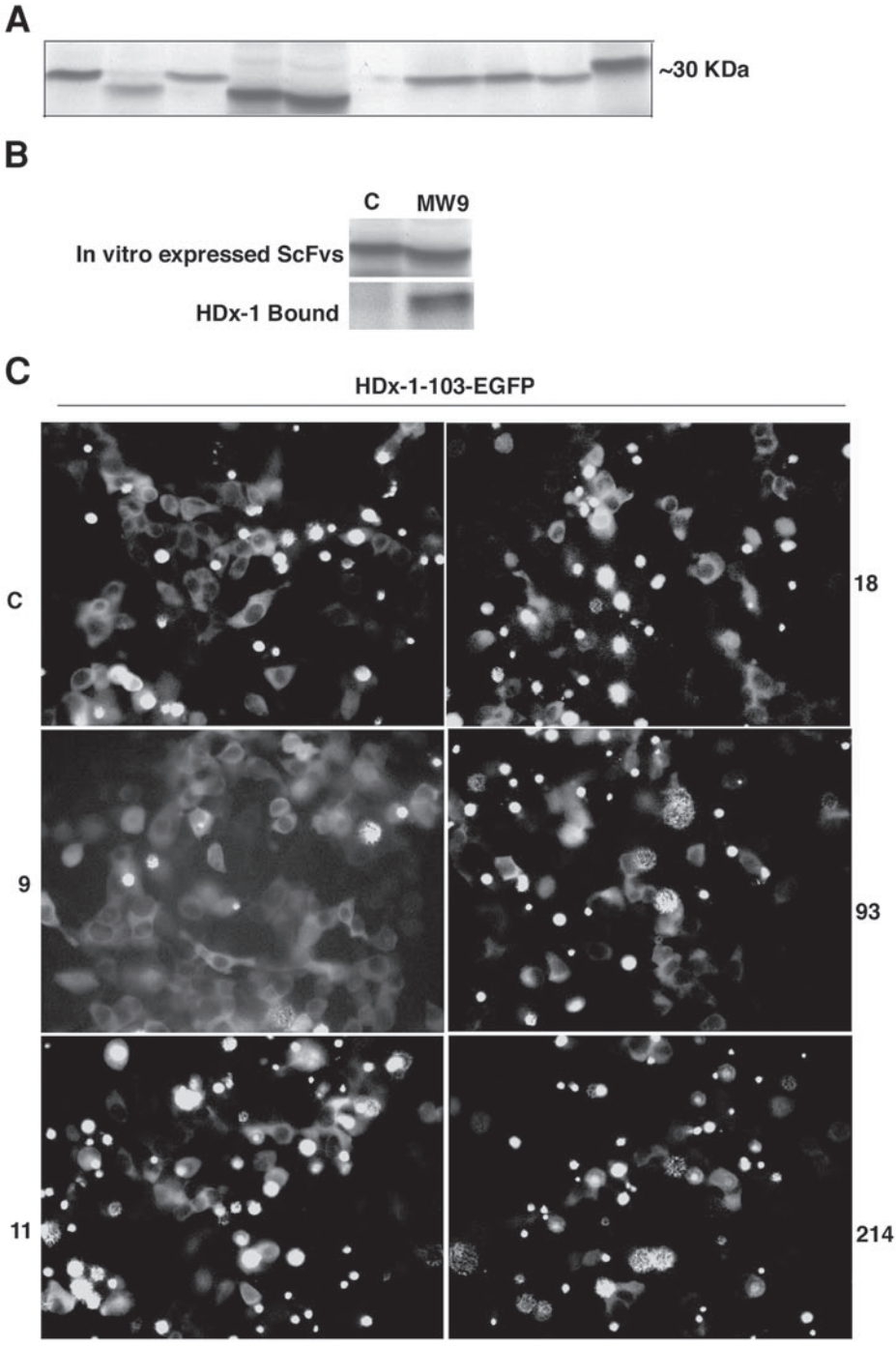

Fig. 2. **(A)** In vitro expression of anti-HDx1 ScFvs. Pooled cDNAs isolated from anti-HDx-1 specific phage clones were subcloned in pcDNA 3.1 (Invitrogen, San Diego, CA) downstream of the T-7 promoter. The library was introduced into *E. coli* and individual colonies

(*continued*)

be tested for binding to recombinant mutant HDx-1 in a solution-based assay. **Figure 2B** shows that an anti-HDx-1 scFv binds specifically to mutant HDx-1 in a GST pull-down assay. The in vitro-generated scFvs method eliminates the need for purification of each scFv and reduces steps in subsequent testing for binding to HDx-1 by ELISA. Using this methodology, we have isolated a large number of HDx-1-specific scFvs that, when coexpressed with mutant HDx-1-EGFP, are either ineffective, promote, or inhibit mutant HDx-1 aggregation and induced cell death in 293 cells (*see* **Fig. 2C**). In vitro-expressed scFvs can also be used to identify mutant HDx-1 epitopes involved in binding to other cellular components. For example, we have demonstrated in solution that the addition of in vitro-generated MW7 scFv interferes with binding of identified proteins to the polyP domain of HDx-1 ***(23)***. In summary, anti-HDx-1 scFvs are excellent molecular reagents that can be of help in understanding the biology of mutant Htt and possibly other proteins with expanded polyQ repeats.

4. Notes

1. It can be difficult to generate MAbs against a particular antigen because the antigen is poorly immunogenic, it is recognized as self, or there is another antigen in the mixture that is highly immunogenic. There are numerous of specialized techniques available to overcome this problem. The most effective approaches we have found involve either cyclophosphamide immunosuppression ***(24)*** or adult tolerization ***(25)***.
2. The RIBI adjuvant system (monophosphoryl lipid A and synthetic trehalose dimycolate) gives a higher titer and fewer granulomatous inflammatory lesions when compared with Freund's adjuvant ***(26)***. We used RIBI adjuvant for the first two injections of antigen. After the animals showed a positive reaction against the antigen, boosts were done with antigen alone until the sera displayed a high antibody titer (positive reaction at > 1:1000 dilution). Various components of micro-organisms have the capacity to stimulate the immune system. When such adjuvants are administered with an antigen, the animal usually generates an immune response to the antigen that is stronger than that elicited by the antigen alone ***(27)***. The combination of an emulsion of mineral oil and killed mycobacte-

Fig. 2. (*continued*) isolated. Plasmid DNA isolated from each colony was added to a coupled transcription–translation rabbit reticulocyte mixture (Promega, Madison, WI).[35] S-labeled methionine was added to label the synthesized scFvs. Aliquots from several reactions were examined by SDS-PAGE, followed by autoradiography. **(B)** An example is shown illustrating an in vitro translated anti-HDx-1 scFv specifically binding GSD-HDx-1 (Q51). Equal amounts of control and anti-HDx-1 scFvs were incubated with 5 μg recombinant GST–HDx-1 bound to glutathione beads in a buffer containing mild detergent and glycerol. Following incubations for 3 h at room temperature, the beads were washed in the same 5X buffer. Bound scFvs were detected by SDS-PAGE and autoradiography. **(C)** Anti-HDx-1 scFvs have variable effects on mutant HDx-1 toxicity and aggregation. Anti-HDx-1 scFvs were tested for their effects on mutant HDx-1 toxicity. Two hundred ninety-three cells were cotransfected with each scFv and mutant HDx-1–Q103–EGFP by lipofectamine (Invitrogen). Two days posttransfection, cells were examined by fluorescence microscopy. Numbers on the sides of the panels refer to individual clones. C is the control. Please note that although cotransfection with clone 9 inhibits the toxicity of mutant HDx-1, others such as 11 and 214 increase the number of apoptotic cells (condensed green bodies). Clones 18 and 93 yield similar results to those of the control plasmid.

rium (Freund's adjuvant) had been used extensively because of its effectiveness as an immunostimulant, but it tends to cause inflammatory and toxic side effects.

3. Huntington's disease human lymphoblast cells were extracted in 300 m*M* NaCl, 1 m*M* EDTA, 0.5% Triton X-100, 50 m*M* Tris-HCl, pH 7.0, and complete protease inhibitor cocktail (Boehringer Mannheim).
4. We prepared discontinuous gels with 3.5% stacking and 5.5% resolving gels and SDS. To create the wells, the 2D/prep well comb (Bio-Rad; 161-0996) was used in casting the gels. Alternatively, ready gel Bio-Rad 161-1212 can be used.
5. We have used 4% paraformaldehyde-perfused or acetone-fixed brain sections from R6/2 and WT mice (Jackson Laboratories, B6CBA-TgN[HDexon1]62Gpb, stock number 002810). To prepare the paraformaldehyde solution, 4 g paraformaldehyde is added to 50 mL H_2O with 100 μL of 10 *N* NaOH. The solution is heated to 65°C until dissolved. Then, 75 μL concentrated HCl (12.7 *N*) is added to the solution. After it is chilled, 10 mL of 10X PBS is added, and the volume is adjusted to 100 mL with H_2O.
6. Mounting medium can be prepared by dissolving 0.1 g *p*-phenylenediamine (Sigma) in 2 mL of 1 *M* Tris-HCl, pH 8.6, plus 8 mL of H_2O. Then, 90 mL glycerol is added to this solution and mixed well. The medium can be aliquoted, wrapped with foil to protect against light, and frozen at –80°C. After mounting the cover slips, excess mounting medium is drained off by standing the slides vertically. The edges of the slide are sealed with nail polish.
7. The cells should be in log phase growth for fusion and the cell viability at the time of collecting should be >95%.
8. Antigen was mixed with 0.2 mL MPL + TDM emulsion and injected into the mouse by intraperitoneal injection. There is a need to wait at least 14 d before the second injection. The mice are bled from the tail vein by cutting off the tips 8–10 d after the second immunization to check the serum titer. Further boost without adjuvant is done every other week until the serum titer is at least 1:1000. Three days before the fusion, a final boost is given intraperitoneally.
9. It is convenient to use a multichannel pipet to deliver protein solutions. The Ag-coated and preblocked plates can be prepared ahead and stored in 4°C. When checking the titers of serum from preimmune and immunized mice, serial dilutions of Ag can be used, and the results are informative for determining the optimal amount of Ag for later screening. We have used 0.2 μg/mL purified fusion proteins as Ags for most of our ELISA screening. We also have included carrier proteins in the ELISA plates to select clones that bind the Ag and not carrier proteins. Including wells for positive and negative controls is also helpful. Omitting the test Abs or using an irrelevant Ab as a negative control is optimal. The positive serum is a positive control here.
10. One can score the positive clones easily on the cover when the assay is complete.
11. Load the wells with sufficient Ag in order to detect clones with weaker staining.
12. The amount used is half of the original lysate. Here, we can reduce the total volume of protein loaded in the well to get a tight band and get rid of the high salt used in the extraction, avoiding distortion of the gel.
13. To separate the bands of mutant and WT Htt, the gel was run until the myosin marker reached the lower third of the gel. The amount of constant current needed should be determined with each individual power supply.
14. The constant current used should be determined with each individual power supply to have complete transfer of Htt.

15. Because many clones need to be screened at one time, it is best to prepare blots ahead of time, wrap them in Saranwrap after blocking (wet), and store at –20°C.
16. The horizontal line is critical for aligning the stripes, especially to determine clones that prefer to bind to mutant Htt. The line can be marked either at the top or bottom of the gel.
17. A positive control Ab should be included with the test hybridoma supernatants to identify mutant and WT Htt for reference. If the amount of supernatants is not sufficient to cover the stripe, PBS can be added. Keep the incubation tray in a humid chamber to avoid high background.
18. The following steps such as washing, incubation, and color developing should be done with rocking.
19. Because there can be many clones to be screened at one time, it is easier to handle color development rather than enhanced chemiluminescence. With amplification using biotin-conjugated secondary antibody, we also can detect weaker binding clones.
20. We have glued serological pipets (broken into appropriate length) to a plastic box as a raised bed to hold slides. A small amount of water is placed in the box to keep the slides from drying.
21. Although the company did not provide the sequence of the oligos (proprietary), there are good sources for oligo information (R. Kontermann and S. Duel [eds.] *Antibody Engineering*, Springer-Verlag, New York, 2001). PCR conditions are as stated in the kit's instruction manual.

Acknowledgment

Work cited from the authors' laboratory was supported by the Hereditary Disease Foundation.

References

1. Bennett, M. J., Huey-Tubman, K. E., Herr, A. B., et al. (2002) A linear lattice model for polyglutamine in CAG-expansion diseases. *Proc. Natl. Acad. Sci. USA* **99,** 11,634–11,639.
2 Ko, J., Ou, S., and Patterson, P. H. (2001) New anti-huntingtin monoclonal antibodies: implications for huntingtin conformation and its binding proteins. *Brain Res. Bull.* **56,** 319–329.
3. Ko, J. and Patterson, P. H. Unpublished data.
4 Khoshnan, A., Ko, J., and Patterson, P. H. (2002) Effects of intracellular expression of anti-huntingtin antibodies of various specificities on mutant huntingtin aggregation and toxicity. *Proc. Natl. Acad. Sci. USA* **99,** 1002–1007.
5 Jackson, J. R., Salecker, I., Dong, X., et al. (1998) Polyglutamine-expanded human huntingtin transgenes induce degeneration of *Drosophila* photoreceptor neurons. *Neuron* **21,** 633–642.
6. Jackson, G., Khoshnan, A., and Patterson, P. H. Unpublished data.
7. Khoshnan, A., Reinhart, P., and Patterson, P. H. Unpublished data.
8. Harlow, E. and Lane, D. (1988) *Antibodies: A Laboratory Manual*, Cold Spring Harbor Laboratory, Cold Spring Harbor, NY, pp. 55–56 and 72–73.
9 Gullick, W. J. (1988) Production of antiserum to synthetic peptides. *Methods Mol. Biol.* **3,** 341–354.
10 Hawkes, R., Niday, E., and Gordan, J. (1982) A dot-immunobinding assay for monoclonal and other antibodies. *Anal. Biochem.* **119,** 142–147.

11 Al Moudallal, Z., Altschuh, D., Briand, J. P., et al. (1984) Comparative sensitivity of different ELISA procedures for detecting monoclonal antibodies. *J. Immunol. Methods* **68,** 35–43.
12 Birk, H.-W. and Koepsell, H. (1987) Reaction of monoclonal antibodies with plasma membrane proteins after binding on nitrocellulose: renaturation of antigenic binding sites and reduction of nonspecific antibody binding. *Anal. Biochem.* **164,** 12–22.
13 Davies, D. R., Padlan, E. A., and Sheriff, S. (1990) Antibody-antigen complexes. *Annu. Rev. Biochem.* **59,** 439–473.
14 Ou, S. K. and Patterson, P. H. (1997) A more efficient and economical approach for monoclonal antibody production. *J. Immunol. Methods* **209,** 105–108.
15. Stang, B. V., Wood, P. A., Reddington, J. J., et al. (1998) Monoclonal antibody production in gas-permeable flexible flasks, using serum-free medium. *Contemp. Topics* **37,** 55–60.
16. Scott, L. E., Aggett, H., and Glencross, D. K. (2001) Manufacture of pure monoclonal antibodies by heterogeneous culture without downstream purification. *Biotechnique* **31,** 666–668.
17. Jackson, L. R., Trudel, L. J., and Lipman, N. S. (1999) Small-scale monoclonal antibody production in vitro: methods and resources. *Lab. Anim.* **28,** 20–30.
18. Marx, U., Embleton, M. J., Fischer, R., et al. (1997) Monoclonal antibody production. The report and recommendations of ECVAM workshop 23. *Altern. Lab. Anim.* **25,** 121–137.
19 Ou, S. K., Hwang, J. M., and Patterson, P. H. (1993) A modified method for obtaining large amounts of high titer polyclonal ascites fluid. *J. Immunol. Methods* **165,** 75–80.
20 Rondon, I. J. and Marasco, W. A. (1997) Intracellular antibodies (intrabodies) for gene therapy of infectious diseases. *Annu. Rev. Microbiol.* **51,** 257–283.
21 Lecerf, J.-M., Shirley, T. L., Zhu, Q., et al. (2001) Human single chain Fv intrabodies counteract *in situ* huntingtin aggregation in cellular models of Huntington's disease. *Proc. Natl. Acad. Sci. USA* **98,** 4764–4769.
22 Winter, G. (1998) Making antibody and peptide ligands by repertoire selection technologies. *J. Mol. Recog.* **11,** 126–127.
23. Khoshnan, A., Ko, J., Paige, L., et al. Submitted.
24 Matthew, W. D. and Sandrock, A. W. (1987) Cyclophosphamide treatment used to manipulate the immune response for the production of monoclonal antibodies. *J. Immunol. Methods* **100,** 73–82.
25 Lebron, J. A., Shen, H., Bjorkman, P. J., et al. (1999) Tolerization of adult mice to immunodominant proteins before monoclonal antibody production. *J. Immunol. Methods* **222,** 59–63.
26 Lipman N. S., Trudel L. J., Murphy J. C., et al. (1992) Comparison of immune response potentiation and in vivo inflammatory effects of Freund's and RIBI adjuvants in mice. *Lab. Anim. Sci.* **42,** 193–197.
27. Rudbach, J. A., Cantrell, J. L., and Ulrich, J. T. (1988) Molecularly engineered microbial immunostimulators, in *Technological Advances in Vaccine Development* (L. Lasky, ed.), Alan R. Liss, New York, pp. 443–454.

8

Using Antibodies to Analyze Polyglutamine Stretches

Elizabeth Brooks, Montserrat Arrasate, Kenneth Cheung, and Steven M. Finkbeiner

Summary

Expansion of a homomeric stretch of glutamine residues beyond a critical threshold can produce neurodegenerative disease. This observation led to the idea that abnormal polyglutamine stretches can alter protein structure in ways that contribute to disease. Because they are prone to aggregation, proteins with abnormal polyglutamine expansions have been difficult to study with conventional biophysical approaches. Some of these proteins are also very large, complicating efforts to generate them in vitro or to purify them for biochemical studies. An alternative approach has been to use antibodies with known binding specificity as probes of protein folding and protein structure. Antibodies can often bind to specific protein epitopes *in situ* and are, therefore, one of the few tools that can be used to probe protein structure in a physiological context and in the presence of that protein's normal binding partners. However, antibodies are complex reagents, and an understanding of their binding properties, methods of use, and limitations is needed to interpret results properly. We have developed monoclonal antibodies that specifically recognize expanded polyglutamine stretches in mutant huntingtin. Here, we describe several methods for using one of these antibodies to explore the structure of abnormal polyglutamine expansions and the proteins that contain them.

Key Words: Polyglutamine; Huntington's disease; CAG repeat; triplet repeat expansion; immunocytochemistry; immunoprecipitation; Western blot; HEK 293 cells; transient transfection; protein conformation; monoclonal antibody.

1. Introduction

1.1. Abnormal Polyglutamine Stretches in Human Disease

Although they are otherwise unrelated, the genes that cause Huntington's disease (HD), X-linked spinal bulbar muscular atrophy (XSBMA), dentatorubropallidoluysian atrophy, and several spinocerebellar ataxias share a common type of mutation—an

From: *Methods in Molecular Biology, vol. 277: Trinucleotide Repeat Protocols*
Edited by: Y. Kohwi © Humana Press Inc., Totowa, NJ

abnormal expansion of the triplet CAG (or CAA) codon ***(1)*** that produces a homomeric stretch of polyglutamines within the mature protein. In each case, the pathogenic versions of the protein exceed a threshold number of glutamines. Although the threshold varies, many of the disorders are associated with polyglutamine expansions greater than 35 residues in length ***(2)***. These expansions appear to confer a toxic function to the protein that contains them ***(3–7)***; however, they could also reduce the normal function ***(8–13)*** in ways that could contribute to disease.

1.2. Models of Polyglutamine Structure and Function

The nature of the toxic function conferred by polyglutamine expansions and the molecular basis for the disease threshold remain unclear; however, several ideas have been proposed. Proteins that contain abnormally long polyglutamine expansions are prone to aggregate with each other ***(14–16)*** and with other selected proteins ***(17–20)***. Based on hypothetical models of protein folding, the tendency to aggregate may be a property of abnormally expanded polyglutamine stretches ***(21,22)***. Whether and how aggregation contributes to pathogenesis remains unclear. The appearance of inclusion bodies—insoluble microscopic protein deposits in cells—has been correlated with disease ***(23,24)***, and inclusion bodies have been proposed to be a major pathogenic feature of proteins that contain abnormal polyglutamine expansions ***(25–29)***. Inclusion bodies might harm neurons by numerous mechanisms, such as disrupting cytoarchitecture ***(30)***, sequestering other essential proteins ***(31–34)***, or abnormally inhibiting or activating specific biological processes ***(35,36)***.

On the other hand, behavioral abnormalities may precede inclusion body formation in mouse models of polyglutamine disorders ***(37–39)***, and inclusion body formation does not necessarily predict neuronal death in Huntington's disease ***(40)***. Several experimental manipulations have evidently dissociated inclusion body formation from neurodegeneration ***(41–44)***, raising the possibility that inclusion body formation is not the major pathogenic mechanism *per se* or that it might represent a beneficial coping response by the neuron to sequester more toxic, soluble forms of proteins that contain polyglutamine expansions ***(45–47)***. In vitro, proteins with polyglutamine expansions aggregate into multimeric assemblies and fibrils, which may represent precursor forms that eventually become incorporated into inclusion bodies in cells ***(15,48)***. In other diseases characterized by protein aggregation, such as Alzheimer's disease and Parkinson's disease, oligomeric or fibrillar forms of the amyloid β (Aβ peptide or α-synuclein appear to be more toxic than more highly aggregated forms ***(49–51)***. However, it remains to be shown that aggregation intermediates of proteins containing polyglutamine expansions are toxic.

In yeast, numerous endogenous prion proteins have been discovered that contain glutamine- or asparagine-rich regions and are prone to aggregate ***(52,53)***. These regions enable the proteins to adopt two or more distinct conformations ***(54,55)*** that may subserve different cellular functions ***(56)***. The glutamine- and asparagine-rich regions of one of these proteins can be substituted by a homomeric polyglutamine stretch ***(52)*** and the propensity of the protein to adopt one conformation or another can be regulated by the length of the glutamine- and asparagine-rich regions ***(55)***. Isolated

polyglutamine peptides may be unable to adopt distinct and stable conformations themselves ***(57)***, but it is unclear how they might function *in situ* in the context of a full-length protein such as huntingtin and its binding partners ***(58,59)***. The parallels with some yeast prion proteins raise the intriguing possibility that homomeric polyglutamine stretches might mediate similar conformational changes in proteins and that abnormal polyglutamine expansions might alter the conformation of protein monomers in ways that are important for human disease ***(60–62)***. The extent to which conformational change regulates protein function independently of aggregation remains to be elucidated ***(63)***.

1.3. Using Antibodies as Probes of Protein Structure

Antibodies are useful for probing protein structure ***(64,65)***. They are often exquisitely specific and can distinguish the subtlest differences in protein structure (even single amino acid changes). Conformation-specific antibodies recognize an epitope on the surface of an antigen that is destroyed when that antigen is denatured ***(66)***. Recognition depends on contacts between the surface of the Fab and a constellation of amino acid side chains of the antigen ***(67–69)***. The amino acids of the antigen that contribute to a conformational epitope usually are separated from each other in the primary amino acid sequence. Folding (or misfolding) brings these distant amino acids together to form a surface of the protein. Antibodies have been used extensively to probe the structure of many proteins ***(65,70–73)***, including ion channels ***(74–76)***, which are also prone to aggregate. Antibodies are also useful structural tools because they can be used to probe protein conformation *in situ*.

However, using antibody binding as an assay for protein structure also has important limitations. Notably, antibodies are multivalent, with 2–10 identical binding sites per molecule, depending on the antibody class ***(77)***. Multivalency can significantly affect the avidity with which an antibody binds to an antigen ***(78)***. For example, if a bivalent antibody can bind to a target antigen through both binding sites simultaneously, its overall avidity for the antigen may be much higher than the individual affinities of each binding site for antigen (and may approach the product of the affinities) ***(79–81)***. Although the structure of expanded polyglutamine stretches remains to be determined, they may contain repeated, multivalent epitopes that bind multivalent antibodies avidly. In principle, some antibodies could bind preferentially to long polyglutamine stretches if those stretches selectively supported high-avidity, bivalent binding ***(82)***. For these reasons, it has been useful to isolate monovalent binding fragments of antibodies as probes of protein structure. Later, we will present a method for proteolytically cleaving a bivalent antibody and biochemically purifying the monovalent binding moieties for general use.

Many additional factors influence antibody binding and must be considered in the interpretation of binding assays. Antibodies themselves are proteins and binding can change the conformation of either or both the antibody and antigen ***(69,70,83,84)***. Thus, failure of antibodies to bind a protein *in situ* (e.g., immunocytochemically) could occur if the antibody binds to a particular protein conformation and that conformation has changed ***(85,86)***. However, the binding site may be unavailable for many reasons,

including the possibility that the binding site has been deleted because of proteolytic cleavage or that the binding site is obscured by dimerization, by the presence of another bound protein, or by the presence or absence of posttranslational modifications ***(87–89)***. Binding may also be unexpectedly regained. It is commonly assumed that subjecting proteins to sodium dodecyl sulfate-polyacrylamide gel electrophoresis (SDS-PAGE) and Western blotting leaves them fully denatured. However, it is clear that some domains of proteins are more resistant to SDS denaturation than others ***(90–92)*** and that proteins can refold and renature on a nitrocellulose membrane after SDS-PAGE, regaining antigenicity and function ***(93–99)***. Therefore, some conformation-specific antibodies may bind proteins transferred to nitrocellulose membranes and recognition of an epitope by Western blotting is not proof by itself that the epitope is unfolded.

2. Materials

2.1. Clinicals, Reagents, and Equipments

1. Mammalian expression plasmid encoding a hemagglutinin (HA) epitope tag (pCMV4-3HA).
2. Mammalian expression plasmids (pCDNA1) encoding N-terminal 171 amino-acid fragments of huntingtin with C-terminal FLAG tags and different-length polyglutamine expansions ***(41)***.
3. Restriction enzymes, DNA polymerase, DNA ligase, calf-intestinal phosphatase (New England Biolabs).
4. Competent *Escherichia coli* strain DH5α cells (Invitrogen).
5. Granulated agar (Gibco) for plates.
6. Petri dishes (100 × 15 mm; Falcon).
7. Gel purification kit (Qiagen).
8. Maxi-prep kit (Qiagen).
9. Human embryonic kidney (HEK) 293 cells (American Type Culture Collection).
10. Dulbeccos's modified Eagle medium (DMEM) (Gibco).
11. Calf serum (calf serum; Gibco).
12. Penicillin/streptomycin (Gibco).
13. L-Glutamine, 200 m*M* (100X stock solution) (Gibco).
14. Poly-D-lysine (Sigma).
15. Six- and 24-well tissue culture dishes (Corning).
16. Complete Protease Inhibitor Cocktail Tablets without EDTA (mini) (Roche).
17. Cell lifter (Costar).
18. Precast 10% Tris-HCl gels (Bio-Rad).
19. BenchMark Prestained protein ladder (from 10 to 200 kDa) (Invitrogen).
20. Whatman 3-mm filter paper.
21. Nitrocellulose membrane Hybond-C Extra 45 Micron (Amersham).
22. Gel electrophoresis apparatus (Mini Protean III Cell; Bio-Rad).
23. Transfer apparatus (Mini Trans-Blot Elecrophoretic Transfer Cell; Bio-Rad).
24. ^{125}I-conjugated anti-mouse secondary antibody (Perkin-Elmer).
25. Phosphorimager plate (Fuji).
26. Phosphorimager scanner and Quant 1 analysis software (Molecular Dynamics).
27. Protein G–Sepharose beads (Sigma).

28. Horseradish peroxidase (HRP)–conjugated anti-mouse secondary antibody (Calbiochem).
29. Photography film (Kodak).
30. Round cover slips, size for 24-well plates (Fisher).
31. Bovine serum albumin (BSA) (Sigma).
32. Blotting-grade blocker nonfat dry milk (Bio-Rad).
33. Rabbit polyclonal antihemagglutinin antibody (Zymed).
34. Mouse monoclonal antihemagglutinin antibody (Babco).
35. Anti-mouse IgG (Fab specific) (Sigma).
36. Goat anti-mouse Cy3-coupled secondary antibody (Jackson Laboratory).
37. Goat anti-rabbit Cy5-coupled secondary antibody (Jackson Laboratory).
38. Glycerol gelatin mounting solution (Sigma).
39. Microscope Slides Precleaned Super frost/Plus (Fisher).
40. Enhanced chemiluminescence reagent (Perkin-Elmer).
41. 1 *M* L-Cysteine, HCl salt (Sigma) stock solution.
42. Papain (Sigma).
43. Slide-A-Lyzer dialysis cassette, 3–15 mL (Pierce).
44. BioLogic LP chromatography system (Model 2110; Bio-Rad).
45. LP Data View 1.0 software (Bio-Rad).
46. HiTrap Q Sepharose FF ion-exchange column (Amersham Pharmacia).
47. HiPrep 26/60 Sephacryl S-200 size-exclusion column (Amersham Pharmacia).
48. Centriprep centrifugal filter device with YM-10 membrane (Amicon).
49. Bradford protein assay reagent (Bio-Rad).

2.2. Buffers and Growth Media

1. LB: Dissolve Luria-Bertani (LB) base (25 g/L) in distilled H_2O. Autoclave at 121°C for 15 min. Store at room temperature.
2. LB with agar for plates: Dissolve LB base (25 g/L) and granulate agar (15 g/L) in distilled H_2O. Autoclave at 121°C for 15 min. Cool to approx 50°C while stirring. Add ampicillin to a final concentration of 20 µg/mL. Pour into 10-cm Petri dishes to cover the bottom. Let solidify. Invert and store at 4°C.
3. 2X Boiling lysis buffer (LSB): 100 m*M* Tris-HCl (pH 6.8), 4% SDS (electrophoresis grade), 0.2% bromophenol blue, 20% glycerol. Store at room temperature. Add 10% β-mercaptoethanol immediately before use.
4. TGEK: 50 m*M* Tris-HCl, pH 7.5, 10% glycerol, 1 m*M* EDTA, 100 m*M* KCl. Store at room temperature. Immediately before use, add one protease inhibitor tablet per 10 mL of lysis buffer and Nonidet P-40 (NP40) to a final concentration of 1%.
5. 2X HEPES-buffered saline (HBS): 274 m*M* NaCl, 10 m*M* KCl, 1.4 m*M* Na_2HPO_4, 15 m*M* dextrose (D-glucose), 42 m*M* HEPES (free acid). Using 5–10 *N* NaOH, adjust the pH dropwise. The pH of this buffer is critical to the formation of calcium phosphate precipitate. We recommend preparing aliquots of 2X HEPES that vary in pH from 6.96 to 7.04 and then determining empirically which aliquots are optimal by the transfection efficiency that they produce with a standard marker gene DNA.
6. SOB medium: Per liter: 20 g Bacto-tryptone, 5 g Bacto-yeast extract, and 0.5 g NaCl. Dissolve the solutes in 950 mL of deionized H_2O. Add 10 mL of a 250-m*M* solution of KCl. Adjust the pH to 7.0 with 5 *N* NaOH. Adjust the volume of the solution to 1 L with deionized H_2O. Sterilize by autoclaving. Just before use, add 5 mL of a sterile solution of 2 *M* $MgCl_2$ ***(100)***.
7. SOC medium: SOB medium with 20 m*M* glucose. Prepare a sterile solution of 1 *M* glu-

cose by filtration through a 0.22-µm filter. Add the glucose to the autoclaved SOB medium once the temperature is 60°C or cooler ***(100)***.

8. Phosphate-buffered saline (PBS): 137 m*M* NaCl, 3 m*M* KCl, 10 m*M* Na_2HPO_4, 2 m*M* KH_2PO_4, adjust the pH to 7.4 ***(100)***.
9. Tris-buffered saline (TBS): 20 m*M* Tris-HCl, pH 7.4, 137 m*M* NaCl, 3 m*M* KCl.
10. TBST: Tris-buffered saline (TBS) and 0.01% Tween-20.
11. Gel-running buffer: 25 m*M* Tris-HCl, 250 m*M* glycine (electrophoresis grade), pH 8.3, 0.1% SDS.
12. Gel-transfer buffer: 48 m*M* Tris-HCl, 39 m*M* glycine, 0.037% SDS, 20% methanol.
13. Growth medium for HEK 293 cells: DMEM, 10% calf serum, 2 m*M* glutamine, 10 U/mL penicillin/streptomycin.
14. Digestion buffer: 0.1 *M* Tris-HCl, pH 8.0, and 2 m*M* EDTA.
15. Binding buffer: 5 m*M* Tris (base), pH 8.25.
16. Elution buffer: 5 m*M* Tris (base), pH 8.25, and 1 *M* NaCl.
17. Coomassie brilliant blue stain: 450 mL of methanol, 450 mL of distilled H_2O, 100 mL of glacial acetic acid, 2.5 g of Coomassie brilliant blue R250.
18. Coomassie brilliant blue destain: 450 mL of methanol, 450 mL of distilled H_2O, 100 mL of glacial acetic acid.
19. Ampicillin (Sigma): Prepare 200 mg/mL of ampicillin in 50% ethanol, 50% deionized H_2O. Store at –20°C.
20. 4% Paraformaldehyde: This solution has to be prepared in a chemical fume hood. Dissolve the paraformaldehyde in PBS by warming. Prevent the boiling of the solution. Adjust the pH to 7.4. Make aliquots and store at –20°C.
21. Hoechst 33258 (Sigma; 2000X stock solution): Prepare the stock solution of Hoechst staining at 5 mg/mL in deionized H_2O. Store in aliquots at –20°C.
22. 0.5 *M* Iodoacetamide (Sigma; stock solution): Prepare the iodoacetamide stock solution at 0.5 *M* in deionized H_2O. Store at room temperature and protected from light (*see* **Note 1**).

3. Methods

3.1. Expression Plasmids

Mammalian expression constructs encoding an N-terminal fragment of huntingtin, 171 amino acids long, with polyglutamine stretches of various lengths, and both an HA epitope tag on the N-terminus and a FLAG epitope tag on the C-terminus are used. Epitope tags are added to both the C- and N-terminus to facilitate detection of the full-length protein. Constructs are named to reflect features of the encoded protein. For example, HA-171-17Q-FLAG encodes a protein with an HA tag fused to the N-terminus of the first 171 amino acids of huntingtin with 17 glutamines and with a FLAG tag fused to the C-terminus of huntingtin. Five constructs are used that contain 17, 40, 68, 89, or 142 glutamines. An N-terminal 171-amino-acid fragment of huntingtin with an expanded polyglutamine stretch (more than 36 glutamines) is sufficient to recapitulate features of HD in cellular and mouse models.

3.1.1. HA Expression Vector

The pCMV4-3HA (*see* **Fig. 1A**) vector is used as a mammalian expression vector.

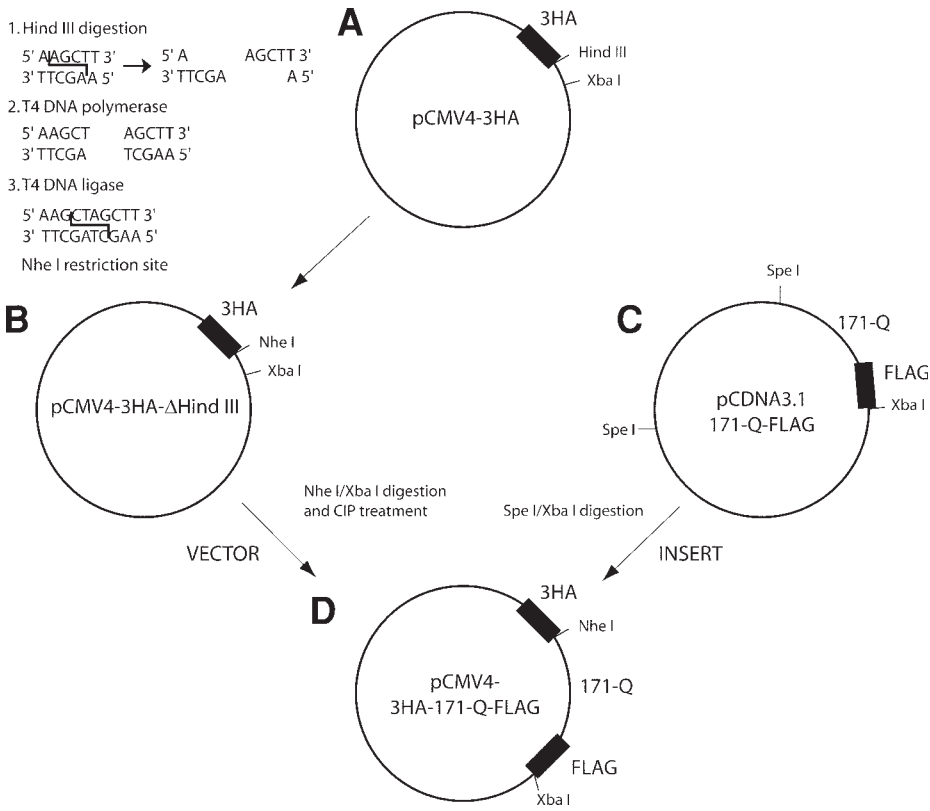

Fig. 1. Strategy for constructing the mammalian expression plasmid pCMV4-3HA-171-polyQ-FLAG. **(A)** Original pCMV4-3HA mammalian expression plasmid. **(B)** Destruction of *Hin*dIII site in pCMV4-3HA results in pCMV4-3HA-Δ*Hin*dIII. **(C)** Original source plasmid for cDNA-encoding N-terminal 171-amino-acid huntingtin fragment with a FLAG epitope fused to the C-terminus. **(D)** Ligation of insert from pCDNA3.1-171-Q-FLAG into pCMV4-3HA-Δ*Hin*dIII generates mammalian expression plasmid pCMV4-3HA-171-Q-FLAG.

3.1.2. Huntingtin Plasmids

The 171-polyQ-FLAG huntingtin constructs are in a pcDNA3.1 expression vector and are subcloned into the pCMV4-3HA vector, in the frame with the HA epitope tag on the N-terminus as depicted in **Fig. 1**.

3.1.3. Cloning

The pCMV4-3HA expression vector (*see* **Fig. 1A**) is digested with the restriction enzyme *Hin*dIII and the 5' end is filled in with T4 DNA polymerase. After gel purification using the Qiaquick Gel Purification Kit, the linearized plasmid is religated with T4 DNA ligase to generate the pCMV4-3HA-Δ*Hin*dIII vector, which contains a new *Nhe*I site, as in **Fig. 1B**. The pCMV4-3HA-Δ*Hin*dIII is doubly digested with the enzymes *Nhe*I and *Xba*I. The major fragment is obtained by gel purification and treated

with calf intestinal phosphatase (CIP) to avoid religation. For insert generation, each of the pcDNA3.1-171-polyQ-FLAG plasmids is doubly digested with *Spe*I and *Xba*I. Each plasmid has two *Spe*I restriction sites, but we can identify the fragment corresponding to the insert of interest by its size, as in **Fig. 1C**. Each fragment containing the 171-polyQ-FLAG insert is obtained by gel purification and is ligated into the *Nhe*I/*Xba*I site of pCMV4-3HA-Δ*Hin*dIII, as in **Fig. 1D**. The newly ligated plasmids are then transformed into chemically competent *Escherichia coli* DH5α cells.

3.1.4. Bacterial Transformation

1. Thaw 50 µL of DH5α cells on ice for each plasmid to be transformed.
2. Add 10 µL of the ligation mixture to a fresh microcentrifuge tube on ice.
3. Add competent cells to DNA solution. Keep on ice for 30 min.
4. Heat shock the cells for 20 s in a 37°C water bath and immediately place on ice for 2 min.
5. Add 950 µL of freshly made SOC medium to the cells and incubate at 37°C for 1 h, with shaking.
6. Plate 200 µL of cell solution onto an LB-ampicillin plate. Incubate the plates overnight at 37°C. Single colonies carrying the plasmid of interest will grow.

3.1.5. Verifying the Cloning

To verify that the cloning worked properly and that the bacteria were transformed successfully, isolate one colony from the plate and culture it overnight at 37°C in fresh LB-ampicillin broth. Isolate the plasmid DNA by standard methods ***(100)***. HA-pCMV4-3HA-171-polyQ-FLAG plasmids are verified by a restriction digest with *Stu*I and by performing DNA sequencing.

3.2. Protein Expression

Human embryonic kidney 293 cells are excellent for heterologous protein production. They are easy to transfect and achieve sufficient levels of expression for subsequent biochemical analysis. Always use sterile procedures under a tissue culture hood.

3.2.1. Passaging HEK 293 Cells

Grow the cells in 10-cm plates until confluent and then split the cells into new plates at 20% confluency.

3.2.2. Transient Transfection

1. Coat each well of a six-well plate with 2 mL of 50 µg/mL poly-D-lysine and incubate at 37°C for 1 h.
2. Aspirate the poly-D-lysine and wash each well with 2 mL of sterile distilled H_2O.
3. Aspirate and repeat the wash twice. Plates can be stored at 4°C until needed.
4. Warm the coated plates in a 37°C incubator for 30 min before plating cells.
5. Plate enough HEK 293 cells in each well so that the culture is approx 50–75% confluent by the next day.
6. Remove the medium from the cells and wash them three times with serum-free DMEM.
7. Place the cells in the incubator and wait 1 h before adding the precipitate.
8. Calculate the total amount of DNA and the total volume required for the transfection (100 µL final volume for each well in six-well plate).

9. Aliquot the volume of 2X HBS to propylene tubes.
10. Aliquot the sterile H_2O to a second set of propylene tubes and add the DNA to the water. Usually, a total of 4 µg of plasmid DNA per well (for a six-well plate) is used.
11. Finally, add 0.1 vol of 2.5 *M* $CaCl_2$ and mix thoroughly by pipetting up and down.
12. Transfer the DNA/$CaCl_2$ mixture to the 2X HBS dropwise with constant mixing.
13. Put the mixture in a dark place and incubate at room temperature for 20 min.
14. Add 100 µL of the precipitate mix to each well.
15. Return the plate to the incubator until fine precipitate appears on the cells. Typically, the appearance of a fine precipitate occurs in 30–90 min.
16. Wash the cells three times with DMEM and then replace the DMEM with growth media.
17. Return the plate to the incubator and wait 48 h to allow time for protein expression.

3.3. Protein Extraction

The method used to extract protein from cells depends on the experiment. Cells can be lysed under denaturing conditions (**Subheading 3.3.1.**) for analysis by SDS-PAGE and Western blotting or under nondenaturing conditions (**Subheading 3.3.2.**) for use in immunoprecipitation experiments. Whichever method is used, it is important to work quickly and keep the cells and protein cold to minimize protein degradation. HEK 293 cells are lysed 48 h after transfection. Typically, two wells of a six-well plate yield enough protein for Western blotting or immunoprecipitation experiments (*see* **Note 2**).

3.3.1. Extraction With Denaturing Boiling Lysis Buffer

Forty-eight hours after transfection, use the following protocol:

1. Place 2X LSB (with β-mercaptoethanol added) in a boiling water bath for 10 min.
2. While the lysis buffer is heating, remove plates of transfected 293 cells from the incubator and place the plates on ice.
3. Aspirate the medium.
4. Wash the cells with PBS.
5. Aspirate the PBS.
6. Repeat the wash and aspirate twice.
7. Remove the final wash and add 200 µL (for one well of a six-well plate) of 2X LSB to each well.
8. Scrape the bottom of the well with a cell lifter.
9. Transfer the lysate to a microcentrifuge tube (lysate will be quite viscous).
10. Boil the lysate for 10 min.
11. Spin the lysate at maximum speed (10,000 *g*) to remove insoluble material.
12. Transfer supernatant to a new microcentrifuge tube.
13. Proceed to Western blot (*see* **Subheading 3.4.**) or store lysate at –80°C.

3.3.2. Extraction With Nondenaturing Lysis Buffer

1. Add one protease inhibitor tablet to 10 mL of TGEK.
2. Add 100 µL of NP40 to TGEK to achieve a final concentration of 1%.
3. Cool TGEK with NP40 on ice.
4. Remove cells from the incubator and place on ice.
5. Aspirate the medium.

6. Wash the cells with cold PBS.
7. Aspirate the PBS.
8. Repeat the wash and aspiration twice more.
9. Remove the final wash and add 200 µL of TGEK/NP40 (for one well of a six-well plate).
10. Scrape the bottom of the well with a cell lifter.
11. Transfer the lysate to a microcentrifuge tube.
12. Spin the lysate at maximum speed (10,000 *g*) to remove insoluble material.
13. Transfer supernatant to a new microcentrifuge tube.
14. Assay protein concentration (*see* **Note 3**) and dilute with lysis buffer to a concentration of 1 mg/mL.
15. Proceed to immunoprecipitation (*see* **Subheading 3.5.**) or store lysate at –80°C.

3.4. Quantitative Western Blot

Quantifying protein by Western blot can be difficult because the chemiluminescent signal generation and photographic film detection are often not linearly related to the amount of primary antibody binding or amount of antigen. To quantify proteins by Western blot, we use ^{125}I-conjugated secondary antibody and phosphorimager detection. Phosphorimager detection of the ^{125}I signal remains linear over a wide range of signal intensities and can be used to accurately measure the amount of primary antibody bound to the blot. This information is valuable in understanding the relation between antibody binding, polyglutamine length, and structure.

3.4.1. SDS-PAGE

1. Lyse transfected HEK 293 cells under denaturing conditions as described in **Subheading 3.3.1.**
2. Set up gel electrophoresis apparatus with 10% polyacrylamide gel.
3. Cover wells with gel-running buffer.
4. Remove plastic comb.
5. Load 10 µL of prestained protein ladder in one well.
6. Load 10–20 µL (10–20 µg) of each lysate to be tested in adjacent wells.
7. Carefully fill gel box with enough buffer to cover the electrodes without disturbing samples loaded in wells of the gel.
8. Plug gel apparatus into a power supply.
9. Run at 100 V for 1–2 h, until the leading edge of dye front is near the bottom of the gel but has not run off.

3.4.2. Transfer to Nitrocellulose

1. Make up 1 L of transfer buffer.
2. Remove the gel from the electrophoresis apparatus.
3. Cut a piece of Whatman filter paper slightly larger than the gel itself and wet it in transfer buffer.
4. Place the gel on the wetted Whatman filter paper, smoothing the paper to remove any trapped air bubbles.
5. Place both the gel and filter paper on a piece of foam pad support from the transfer apparatus.
6. Cut a piece of nitrocellulose membrane to the size of the gel and wet with transfer buffer.
7. With gloves, place the nitrocellulose membrane on top of the gel.

8. Carefully remove any air bubbles between the membrane and the gel.
9. Wet a second piece of Whatman paper in transfer buffer and place it on top of the membrane.
10. Top the gel sandwich with a second piece of foam from the transfer apparatus.
11. Place the sandwich into the transfer apparatus such that the nitrocellulose membrane is closest to the positive electrode of the transfer apparatus.
12. Transfer the protein to the membrane at 100 V for 1 h at 4°C, with stirring.

3.4.3. Detection With Primary and Radiolabeled Secondary Antibodies

The 3B5H10 antibody is one of the monoclonal antibodies that we have developed. It specifically recognizes expanded polyglutamine stretches in mutant huntingtin.

1. After the transfer is complete, disassemble the apparatus and transfer the nitrocellulose membrane to a small tray.
2. Block the membrane with 25 mL of 5% milk–PBS solution for 1 h at room temperature.
3. Remove block solution and replace with fresh block solution containing primary antibody.
4. Incubate with primary antibody overnight, with shaking. For 3B5H10 antibody, use a 1:15,000 dilution in 5% milk–PBS. For α-HA antibody, use a 1:5,000 dilution in 5% BSA–TBST.
5. Remove primary antibody solution.
6. Wash the membrane three times for 5 min each in either PBS or TBST, with shaking.
7. Incubate with 5 μCi of ^{125}I-labeled α-mouse secondary antibody in 20 mL of 5% milk–PBS or 5% BSA–TBST for 2 h at room temperature, with shaking (*see* **Note 4**).
8. Wash three times for 5 min each in either PBS or TBS, with shaking. Dispose of each ^{125}I wash into a liquid waste bottle according to local applicable regulations for ^{125}I waste.
9. Wrap the blot in plastic cellophane.
10. Affix the wrapped blot to a phosphorimager screen and place in a autoradiography cassette overnight.

3.4.4. Analysis

1. Open Quant 1 software.
2. Change settings to match isotope (^{125}I) and phosphorimager screen (Fuji) used.
3. Open the autoradiography cassette and remove the blot from the phosphorimager screen.
4. Scan exposed phosphoimager screen
5. Trace the perimeter of each band using the freehand tool (*see* **Fig. 2**).
6. Measure background signal from a similar-sized area using the traced perimeter of each band as a template (*see* **Fig. 2**).
7. For each band, subtract the corresponding amount of background signal.
8. Normalize the 3B5H10 signal to the HA signal by dividing the background-subtracted 3B5H10 signal measured on one blot by the analogous background-subtracted anti-HA signal measured on a sister blot.

3.5. Immunoprecipitation

Lyse transfected HEK 293 cells in nondenaturing lysis buffer (TGEK/NP40), as described in **Subheading 3.3.2.** Keep protein on ice throughout the protocol.

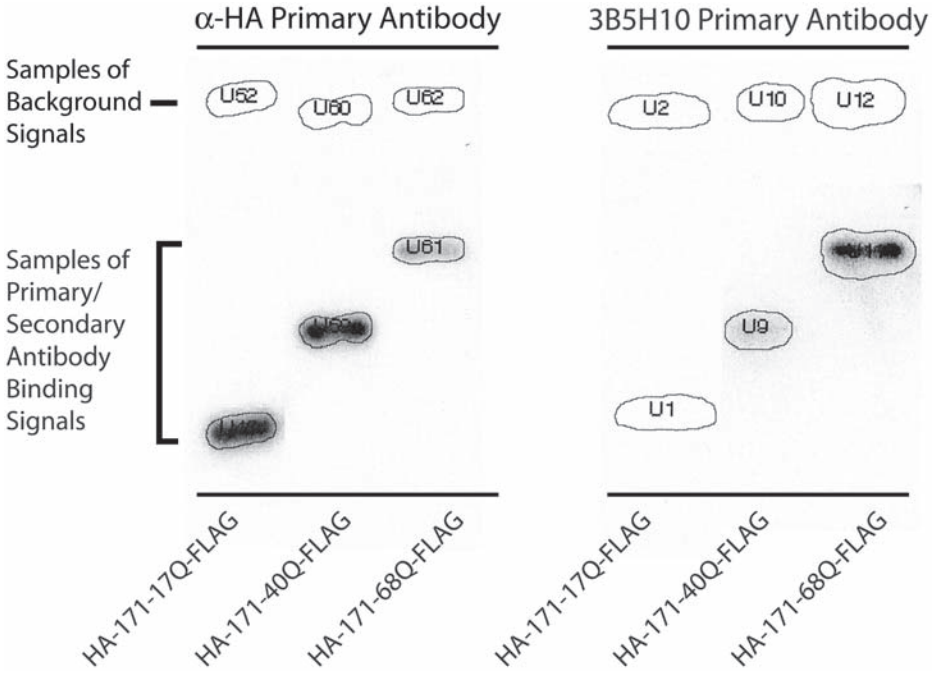

Fig. 2. Quantifying Western blot signals. Extracts from HEK 293 cells that contain either HA-171-17-FLAG, HA-171-40-FLAG, or HA-171-68-FLAG were blotted with either anti-αHA (left blot) or 3B5H10 (right blot) primary antibody and ^{125}I-conjugated anti-mouse secondary antibody. Blots were exposed to a Fuji phosphorimager screen overnight and then scanned with a molecular Dynamics Phosphorimager and Quant 1 software. Primary antibody signals are measured by tracing the perimeter for each band (e.g., U51, U59, U61, U1, U9, or U11). To measure corresponding background signals, an identical perimeter is traced in a section of the blot without identifiable bands (e.g., U52, U60, U62, U2, U10, or U12).

3.5.1. Incubation With Primary Antibody

1. Add 2 µL of 3B5H10 or 5 µL of monoclonal anti-HA antibody to 100 µL of lysate in a 1.7-mL microcentrifuge tube.
2. Dilute antibody–lysate mixture up to 500 µL with lysis buffer.
3. Incubate the mixture by rocking gently at 4°C for 2 h.

3.5.2. Incubation With Protein G–Sepharose Beads

During this incubation time, prepare the Protein G–Sepharose beads. The beads are stored in ethanol, which is removed by washing in lysis buffer.

1. Add 50 µL of beads to a fresh Eppendorf tube.
2. Spin at 3000*g* for 1 min.
3. In order to wash the beads, remove supernatant and add 25 µL of lysis buffer.
4. Repeat wash twice.
5. Add 25 µL of lysis buffer so that a 50% (v/v) bead–lysis buffer slurry remains.

6. Add 50 µL of the bead slurry to the antibody–lysate mixture after the end of the second hour of incubation with the primary antibody.
7. Let tubes rock at 4°C for 2 h.

3.5.3. Harvest

1. Spin the tubes at 3000*g* for 1 min. Save the supernatant.
2. Wash beads with 100 µL of lysis buffer and repeat the spin. Discard supernatant. Repeat wash and spin twice.
3. Add 100 µL of boiling 2X LSB and heat at 100°C for 10 min.
4. Spin at 5000*g* for 2 min and transfer the supernatant to a new tube.
5. Subject the extracts to SDS-PAGE and Western blotting.

3.5.4. Western Blot

1. Subject 10 µL of lysate to SDS-PAGE as described in **Subheading 3.4.1.**
2. Transfer the protein from the acrylamide gel to a nitrocellulose membrane as described in **Subheading 3.4.2.**
3. Block the membrane with 25 mL of 5% milk–PBS solution for 1 h at room temperature.
4. Incubate with primary antibody overnight, with shaking. For 3B5H10 antibody, use 1:15,000 in 5% milk–PBS; for anti-HA antibody, use 1:5,000 in 5% BSA–TBST; for α-FLAG antibody, use 1:1000 in 5% milk–PBS.
5. Wash three times for 5 min each in PBS or TBST, with shaking.
6. Incubate with HRP–labeled anti-mouse secondary antibody diluted 1:20,000 in 25 mL of 5% of milk–PBS or 5% BSA–TBST for 2 h at room temperature with shaking.
7. Wash three times for 5 min each in either PBS or TBS, with shaking.
8. Incubate with 3 mL of oxidizing reagent and 3 mL of enhanced luminol reagent (Perkin-Elmer) for 2 min, with shaking.
9. Expose blots to photographic film (Kodak) and develop by standard methods (*see* **Fig. 3**).

3.6. Immunocytochemistry

An important feature of antibodies as putative probes of protein structure is that they can be used to assess proteins *in situ* by immunocytochemistry.

3.6.1. Plate HEK 293 Cells on Glass Cover Slips

1. In a tissue culture hood, sterilize each cover slip by grasping with tweezers, dipping in 95% ethanol, and passing through a flame.
2. Once the ethanol has burned off, place one cover slip into each well of a sterile 24-well tissue culture dish.
3. Add 0.5 mL of 0.05 mg/mL poly-D-lysine to each well.
4. Incubate the cover slips with the poly-D-lysine solution at 37°C for 16 h.
5. Aspirate the poly-D-lysine and wash each well with 0.5 mL of sterile, distilled water. Aspirate and repeat wash twice. Plates can be stored at 4°C until ready for use.
6. Place HEK 293 medium in a 37°C water bath.
7. Warm the plate with coated cover slips in a 37°C incubator for 30 min before plating cells.
8. Resuspend HEK 293 cells from a standard tissue culture plate into growth media and plate cells onto cover slips at the desired density.

3.6.2. Transient Transfection

Transfect HEK 293 cells with the pCMV4-3HA-171-polyQ-FLAG constructs by the calcium phosphate method described in **Subheading 3.2.2.**

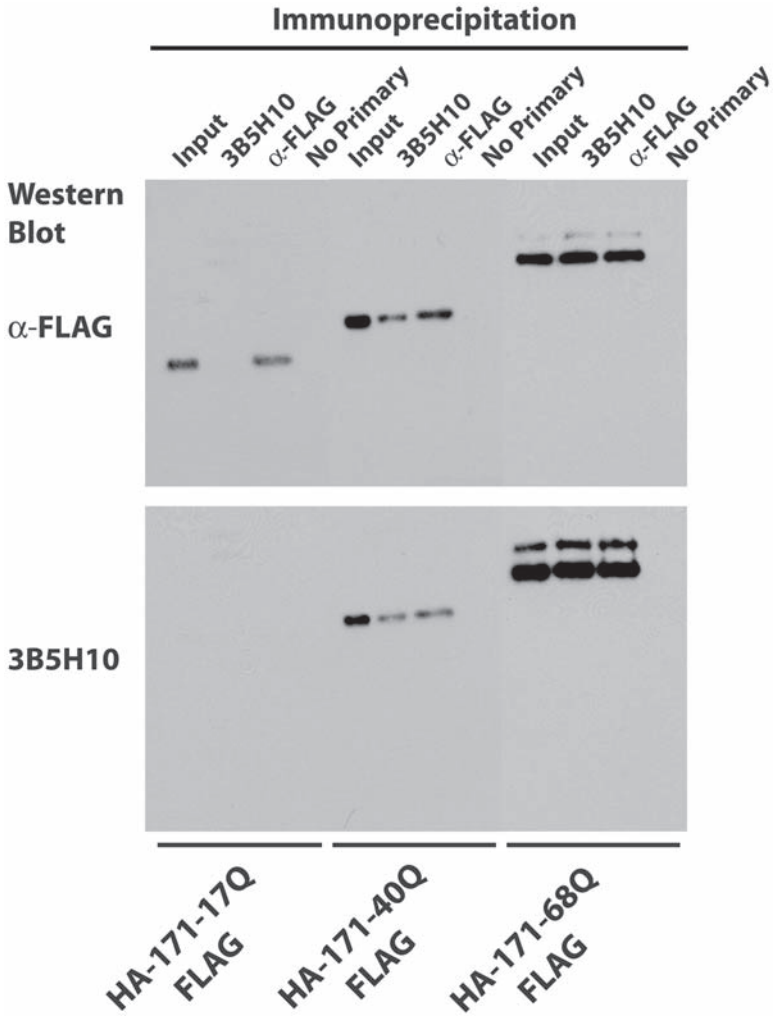

Fig. 3. Immunoprecipitation of huntingtin. Extracts from HEK 293 cells that contain either HA-171-17-FLAG, HA-171-40-FLAG, or HA-171-68-FLAG were mixed together with anti-FLAG, 3B5H10, or no primary antibodies, and then coprecipated with Protein G–Sepharose. Samples of the original extracts (Input) or the coprecipitated proteins were subjected to SDS-PAGE and blotted with either anti-FLAG or 3B5H10 antibodies as indicated.

3.6.3. Fixation and Immunocytochemistry Protocol With Anti-HA and 3B5H10 Antibodies

1. Remove the culture medium from the cells and wash the cells with PBS.
2. Add 4% paraformaldehyde in PBS. Incubate 15 min at room temperature.
3. Wash twice with PBS.
4. To permeabilize the cells, treat them with PBS and 0.1% Triton X-100 for 30 min.

5. Inactivate excess fixative by incubating each cover slip with 1 *M* glycine in PBS for 20 min (prepare fresh before use).
6. Incubate each cover slip with block solution (2% calf serum, 3% BSA in PBS containing 0.1% Triton X-100) for 1–2 h at room temperature
7. For double labeling, dilute both primary antibodies in block solution (mouse monoclonal antibody 3B5H10 diluted to 1:10,000 and rabbit polyclonal anti-HA antibody diluted to 1:500). Incubate each cover slip with this solution of primary antibodies for 90 min.
8. Wash three times for 5 min each with PBS.
9. Dilute the secondary antibody (goat anti-mouse Cy3 and goat anti-rabbit Cy5 1:300) in block solution. Incubate each cover slip with this solution of secondary antibodies for 1 h, protecting from light.
10. Wash five times with PBS for 5 min each.
11. Wash twice for 5 min each with 2.5 µg/mL of Hoechst 33258 in PBS dye to stain the nuclei.
12. Wash twice for 5 min each with PBS.

3.6.4. Mounting the Cover Slips

1. Heat the glycerol gelatin mounting solution to 70°C.
2. Place one drop (approx 4 µL) of mounting solution onto a slide.
3. Aspirate the liquid from the cover slip and place it on the drop of the mounting solution, cell side down.
4. Protect from light and let dry.
5. View cells under a microscope equipped with filter cubes that enable fluorescence detection (*see* **Fig. 4**) (*see* **Note 5**).

3.7. Generation and Purification of Monovalent 3B5H10 Fab

Intact antibodies are multivalent and can bind to antigens through multiple binding sites simultaneously. The resulting increase in avidity that results from multivalent binding can complicate the interpretation of such experiments. It is possible to isolate biochemically monovalent moieties (e.g., Fab) of intact antibodies that may retain their binding properties and can be used themselves as probes of protein structure.

3.7.1. Digestion of Intact IgG (Affinity Purified)

1. Make 1 *M* L-cysteine stock fresh and adjust pH to 7.
2. Add 400 µg of papain (approx 9 U) to 1 mL of digestion buffer and add 10 µL of the 1 *M* L-cysteine stock solution (final concentration, approx 10 m*M*). Incubate at 37°C for 15 min (*see* **Note 6**).
3. Transfer 40 mg of antibody to fresh tube. Supplement the antibody solution with 1 *M* L-cysteine stock solution (*see* **Note 7**).
4. After the 15-min incubation, add the activated papain to the prepared antibody. Papain should be present at a 1:100 mass ratio to antibody.
5. Mix gently, cover with parafilm, and incubate at 37°C for 16–18 h.
6. After the digest, centrifuge tube briefly (600*g*, 30 s) and add 0.54 mL of 0.5 *M* iodoacetamide (1:25 dilution) to terminate the digest. The final iodoacetamide concentration should be 20 m*M*. Incubate at 4°C for at least 30 min (*see* **Note 1**).
7. Subject samples to SDS-PAGE and analyze by Coomassie staining or by Western blotting (*see* **Fig. 5A**). Store digested material at 4°C.

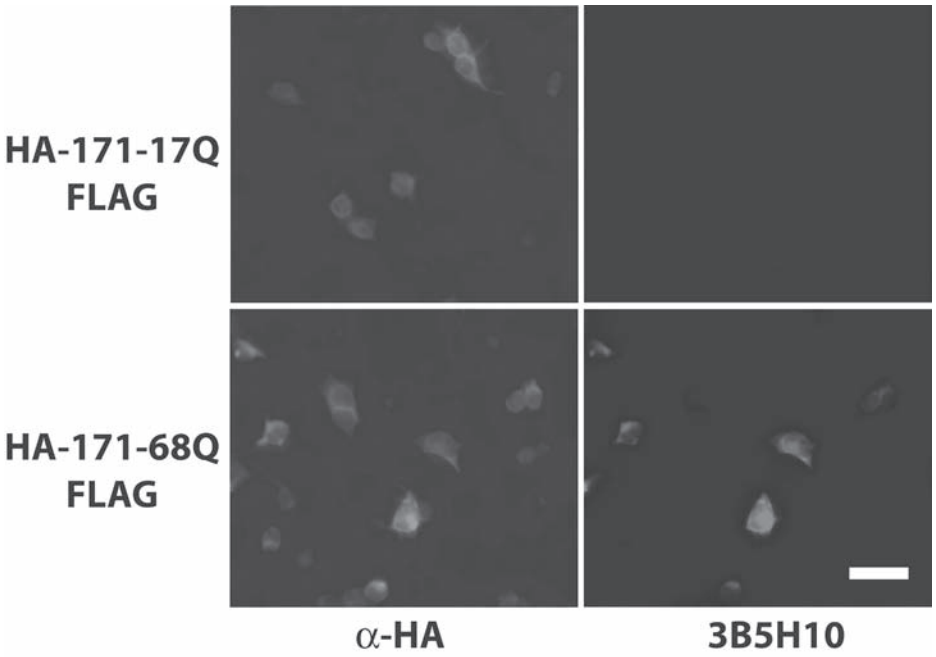

Fig. 4. Immunocytochemistry performed in HEK 293 cells transfected with HA-171-17Q-FLAG and HA-171-68Q-FLAG with rabbit polyclonal anti-HA and mouse monoclonal 3B5H10 simultaneously. Scale bar = 40 μm. (See color insert following p. 84.)

3.7.2. Dialysis Into Ion-Exchange (Q) Column Binding Buffer

1. Transfer digested protein (3–15 mL) to Slide-A-Lyzer cassette via one of the four side ports. Use a syringe (18-ga needle) for the transfer and be sure to remove all air within the cassette. Mark the port that was used for loading.
2. Suspend the cassette in 4 L of binding buffer (5 m*M* Tris-HCl, pH 8.25) by attaching the flotation device (provided by the manufacturer) to the corner of the cassette with the port that was used for loading. Incubate overnight, gently stirring the buffer and exchange buffer at least twice in 24 h.
3. Once dialysis is complete, remove digested material by accessing one of the unused side ports of the cassette with a syringe. Store at 4°C.

3.7.3. Ion-Exchange Column Chromatography

1. Mount a HiTrap Q Sepharose FF ion-exchange column onto the chromatography apparatus.
2. Open the LP Data View application and turn on the ultraviolet (UV) light of the LP Logic fraction collector.
3. Wash column. Place the two input lines of tubing that lead to the mixer into distilled

water. Run pump manually for 5 min at 4 mL/min at a 50% mix from both input lines to flush the mixer and to wash the column (*see* **Note 8**).

4. Transfer one of the input lines (input A) to binding buffer and the other (input B) to elution buffer. Run the following program to equilibrate the column:

   a. 0–40 mL: binding buffer (input A) at 4 mL/min.
   b. 40–80 mL: elution buffer (input B) at 4 mL/min.
   c. Repeat this cycle two additional times (total volume: 240 mL).
   d. End with 40 mL of binding buffer (input A) at 4 mL/min (total volume: 280 mL).

5. Save 5 µL of the digested material, add 5 µL of 2X LSB, and boil for 10 min. Set aside as a sample of the input and evaluate later along with the purified fractions.
6. Load the column by placing input line A into the tube with the digested material and run manually at 1 mL/min. Turn on the recorder and zero the UV reading. Stop the pump when digested material is almost all gone. Be sure not to let air bubbles into the line. Rinse tube with 10 mL of binding buffer to collect residual digest and load rinse via input line A at 1 mL/min. When the 10 mL of rinse is nearly loaded, stop the pump and place input line A back into the binding buffer. Run manually at 1 mL/min until initial UV peak is gone (*see* **Note 9**).
7. Once the sample has been loaded, run the following program:

   a. 0–10 mL: binding buffer (input A) at 0.5 mL/min.
   b. At 0 mL, start collecting 4-mL fractions.
   c. 10–30 mL: gradient from 0–30% of elution buffer (Input B) at 0.5 mL/min.
   d. At 16 mL, start collecting 0.5-mL fractions.
   e. 30–50 mL: elution buffer (input B) at 0.5 mL/min.
   f. At 40 mL, start collecting 1.5-mL fractions.
   g. 50–75 mL: binding buffer (input A) at 4 mL/min.
   h. At 52 mL, divert to waste.

   The total volume will be 75 mL, and the program takes about 2 h to complete.
8. Once complete, save collected fractions at 4°C. Save the LP DataView file.

3.7.4. Coomassie Staining of Ion-Exchange Column Fractions

1. A typical chromatograph should have two main peaks; the first one corresponds to the eluted Fab and should have a considerably larger amplitude than the second peak that corresponds to the Fc. There may also be a smaller third peak occurring later in the chromatograph that corresponds to the intact antibody. Examine the chromatograph and select fractions that correspond to the start of the Fab peak through the maximum of the Fc peak. At a minimum, select the starting Fab fractions, the maximal peak of the Fab fraction, and the fractions that overlap between the Fab and Fc peaks.
2. Remove 5 µL of the selected fractions, add 5 µL of 2X LSB, and boil for 10 min. Load fractions onto a 10% polyacrylamide gel, along with 4 µL of the boiled digested material–LSB mixture removed earlier.
3. Run the gel.
4. Once complete, place gel in Coomassie brilliant blue stain and gently shake for 1 h at room temperature. Rinse gel briefly with water and then place gel in Coomassie destain. Gently shake for 6–8 h, changing solution regularly, until protein bands become clearly visible above the background.

5. Pool collected fractions to run on size-exclusion column; include all fractions that correspond to the Fab peak except for those that also contain portions of Fc. Exclude these Fc-containing fractions stringently. Save fractions with both Fab and Fc to rerun on the ion-exchange column to purify further Fab.

3.7.5. Size-Exclusion Column Chromatography

1. Mount a HiPrep 26/60 Sephacryl S-200 size-exclusion column onto the chromatography apparatus.
2. When changing columns, place both inputs into the binding buffer and manually run at 50% mix at 1 mL/min to wash the lines.
3. Equilibrate the column by running 1600 mL of binding buffer (through just input A) at 1.78 mL/min. This will take approx 15 h to complete.
4. Turn on the UV lamp at least 1 h before loading the sample. Collect pooled fractions into a syringe and inject sample slowly into the line while running the following program:
   a. 0–420 mL of binding buffer (input A) at 0.38 mL/min.
   b. At 50 mL, start collecting 4-mL fractions.
   c. At 90 mL, start collecting 2-mL fractions.
   d. At 130 mL, start collecting 4-mL fractions.
   e. At 320 mL, divert to waste.
5. Once the sample is injected, wash the syringe with buffer in the flow and inject the wash slowly. Zero UV reading after loading sample.
6. Once complete, save fractions at 4°C and save LP DataView file (*see* **Fig. 5B**).

3.7.6. Coomassie Staining of Size-Exclusion Column Fractions

1. The chromatograph should have one major peak corresponding to the Fab, and a considerably smaller peak immediately before it that corresponds to the higher-molecular-weight species. The smaller peak may be difficult to see because of its small size and the overlap between the peaks. Select fractions between the two peaks to separate between the Fab and higher-molecular-weight species, and also fractions at the end of the Fab peak to ensure that all Fab fractions are included.
2. Remove 20 µL of each fraction, add 20 µL of 2X LSB, and boil for 10 min. Subject samples to SDS-PAGE and analyze by Coomassie staining or by Western blotting (*see* **Fig. 5B**).

3.7.7. Concentration of Size-Exclusion Column Fractions and Protein Quantification

1. Pool all fractions with Fab, excluding any fractions that contain the higher-molecular-weight species (*see* **Note 10**).
2. Transfer fractions to Centriprep YM-10 cartridges and concentrate the protein by centrifugation (600*g*) in four successive spins with durations of 40 min, 10 min, 5 min, and 5 min.
3. Quantify Fab with a standard Bradford protein assay reagent according to standard methods ***(100)***.

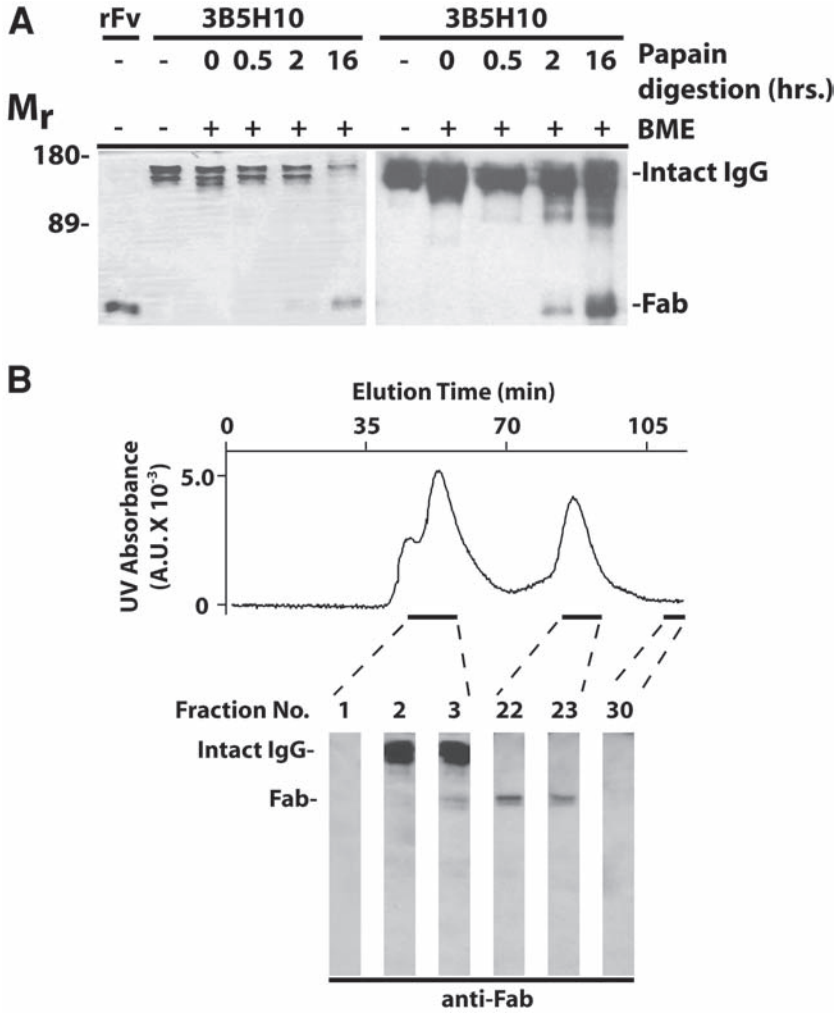

Fig. 5. Generation and purification of monovalent Fab from 3B5H10 antibody. **(A)** 3B5H10 antibody is digested with papain for various times and then analyzed by Coomassie staining (left) or with anti-Fab antibodies by Western blot (right). A sample of an unrelated recombinant single-chain antibody (rFv) is run in the first lane for comparison. **(B)** Digestion products are subjected to ion-exchange chromatography (not shown) and to size-exclusion chromatography and then evaluated with an anti-αFab antibody by Western blotting. Fractions containing pure Fab are pooled and concentrated for general use.

4. Notes

1. Iodoacetamide solution can be kept at room temperature but is light sensitive. If color turns slightly brown, remake a fresh solution.
2. The amount of cells transfected and lysed can be increased to isolate enough protein for several experiments. Pooling lysate from additional wells of a six-well plate or using a larger plate (e.g., 10-cm dish; use 1 mL of lysis buffer) will yield enough protein for several experiments. The lysate should be aliquotted and stored at –80°C. Choose an aliquot size that is appropriate for one experiment in order to avoid repeated freeze–thaw cycles of your sample. There are two advantages to increasing the amount of lysate collected. First, it saves time because the transfection does not need to be repeated. Second, aliquots can be used to reproduce results or to perform additional experiments on a different aliquot of the same lysate.
3. Protein concentration for Western blot can be determined with a standard Bradford assay ***(100)***.
4. Proper precautions should be used whenever working with radioactive material. Be sure to have appropriate shielding, detection equipment, and training for the type of activity in use.
5. Ideally, these cells should be analyzed with confocal microscopy to address questions of colocalization. However, a discussion of fluorescence and confocal microscopy is beyond the scope of this chapter.
6. L-Cysteine functions as a reducing agent to maintain a thiol group in the active site of papain.
7. To keep papain active throughout the digest, the final L-cysteine concentration of the solution that contains the antibody and the activated papain (*see* **Subheading 3.7.1., step 4**) is maintained at 2.5 m*M*. To achieve this concentration, it is necessary to add L-cysteine to the antibody solution; when calculating the appropriate amount of L-cysteine to add, consider the volume of the antibody solution and the volume of the final mixed solution (activated papain and antibody).
8. Make sure all air bubbles have been removed from lines. Air bubbles can severely disrupt the application of the sample and buffers to the column.
9. Loading of the sample through the input line is less than ideal because the sample is spread out as it travels through the tube before it reaches the column. Ideally, the sample should be loaded as close to the column as possible. The volume of the 40-mg digest described in this protocol prohibits this type of loading.
10. Eliminating higher-molecular-weight species is essential to maintain the monovalency of the final purified product. For any experiments where valency is a concern, be sure to exclude this bivalent product.

Acknowledgments

We thank Warner Greene (Gladstone Institutes) for the generous gift of the pCMV4-3HA plasmid. We thank Manar Chaban and members of the Finkbeiner lab for useful discussions, Stephen Ordway and Gary Howard for editorial assistance, and Kelley Nelson for administrative assistance. M. Arrasate is a MECD-Fulbright Fellow. S. Finkbeiner is supported by the National Institute of Neurological Disease and Stroke (R01 NS39074), National Institute of Aging (P01 AG022074), the Hereditary Disease Foundation Cure Huntington's Disease Initiative, the Huntington's Disease Society of America, and the J. David Gladstone Institutes. Some antibody production was carried out at the National Cell Culture Center with the support of the NIH.

References

1 Gusella, J. F. and MacDonald, M. E. (1996) Trinucleotide instability: a repeating theme in human inherited disorders. *Annu. Rev. Med.* **47,** 201–209.
2 Zoghbi, H. Y. and Orr, H. T. (2000) Glutamine repeats and neurodegeneration. *Annu. Rev. Neurosci.* **23,** 217–247.
3 Gusella, J. F. and MacDonald, M. E. (1995) Huntington's disease: CAG genetics expands neurobiology. *Curr. Opin. Neurobiol.* **5,** 656–662.
4 Paulson, H. L. and Fishbeck, K. H. (1996) Trinucleotide repeats in neurogenetics disorders. *Annu. Rev. Neurosci.* **19,** 79–107.
5 Andrew, S. E., Goldberg, Y. P., and Hayden, M. R. (1997) Rethinking genotype and phenotype correlations in polyglutamine expansion disorders. *Hum. Mol. Genet.* **6,** 2005–2010.
6 Zeron, M. M., Hansson, O., Chen, N., et al. (2002) Increased sensitivity to *N*-methyl-D-aspartate receptor-mediated excitotoxicity in a mouse model of Huntington's disease. *Neuron* **33,** 849–860.
7 Ambrose, C., Duyao, M. P., Barnes, G., et al. (1994) Structure and expression of the Huntington's disease gene: evidence against simple inactivation due to an expanded CAG repeat. *Somat. Cell Mol. Genet.* **20,** 27–38.
8 Dragatsis, I., Levine, M. S., and Zeitlin, S. (2000) Inactivation of *Hdh* in the brain and testis results in progressive neurodegeneration and sterility in mice. *Nature Genet.* **26,** 300–306.
9 Chamberlain, N. L., Driver, E. D., and Miesfeld, R. L. (1994) The length and location of CAG trinucleotide repeats in the androgen receptor N-terminal domain affect transactivation function. *Nucleic Acids Res.* **22,** 3181–3186.
10. Mhatre, A. N., Trifiro, M. A., Kaufman, M., et al. (1993) Reduced transcriptional regulatory competence of the androgen receptor in X-linked spinal and bulbar muscular atrophy. *Nature* **5,** 184–187.
11 Rigamonti, D., Bauer, H. J., De-Fraja, C., et al. (2000) Wild-type huntingtin protects from apoptosis upstream of caspase-3. *J. Neurosci.* **20,** 3705–3713.
12 Leavitt, B. R., Guttman, J. A., Hodgson, J. G., et al. (2001) Wild-type huntingtin reduces the cellular toxicity of mutant huntingtin in vivo. *Am. J. Hum. Genet.* **68,** 313–324.
13 Zuccato, C., Ciammola, A., Rigamonti, D., et al. (2001) Loss of huntingtin-mediated BDNF gene transcription in Huntington's disease. *Science* **293,** 493–498.
14 Scherzinger, E., Lurz, R., Turmaine, M., et al. (1997) Huntingtin-encoded polyglutamine expansions form amyloid-like protein aggregates in vitro and in vivo. *Cell* **90,** 549–558.
15 Georalis, Y., Starikov, E. B., Hollenbach, B., et al. (1998) Huntingtin aggregation monitored by dynamic light scattering. *Proc. Natl. Acad. Sci. USA* **95,** 6118–6121.
16 Martindale, D., Hackam, A., Wieczorek, A., et al. (1998) Length of huntingtin and its polyglutamine tract influences localization and frequency of intracellular aggregates. *Nature Genet.* **18,** 150–154.
17 Rajan, R. S., Illing, M. E., Bence, N. F., et al. (2001) Specificity in intracellular protein aggregation and inclusion body formation. *Proc. Natl. Acad. Sci. USA* **98,** 13,060–13,065.
18 Nucifora, F. C., Jr., Sasaki, M., Peters, M. F., et al. (2001) Interference by huntingtin and atrophin-1 with CBP-mediated transcription leading to cellular toxicity. *Science* **291,** 2423–2428.
19 Preisinger, E., Jordan, B. M., Kazantsev, A., et al. (1999) Evidence for a recruitment and sequestration mechanism in Huntington's disease. *Phil. Trans. R. Soc. (Lond.) B: Biol. Sci.* **354,** 1029–1034.

20 Kazantsev, A., Preisinger, E., Dranovsky, A., et al. (1999) Insoluble detergent-resistant aggregates form between pathological and nonpathological lengths of polyglutamine in mammalian cells. *Proc. Natl. Acad. Sci. USA* **96,** 11,404–11,409.
21 Stott, K., Blackburn, J. M., Butler, P. J. G., et al. (1995) Incorporation of glutamine repeats makes protein oligomerize: implications for neurodegenerative disease. *Proc. Natl. Acad. Sci. USA* **92,** 6509–6513.
22 Perutz, M. F. (1995) Glutamine repeats as polar zippers: their role in inherited neurogenerative disease. *Mol. Med.* **1,** 718–721.
23 DiFiglia, M., Sapp, E., Chase, K. O., et al. (1997) Aggregation of huntingtin in neuronal intranuclear inclusions and dystrophic neurites in brain. *Science* **277,** 1990–1993.
24 Davies, S. W., Turmaine, M., Cozens, B. A., et al. (1997) Formation of neuronal intranuclear inclusions underlies the neurological dysfunction in mice transgenic for the HD mutation. *Cell* **90,** 537–548.
25 Ross, C. A. (1997) Intranuclear neuronal inclusions: a common pathogenic mechanism for glutamine-repeat neurodegenerative diseases. *Neuron* **19,** 1147–1150.
26 Becher, M. W., Kotzuk, J. A., Sharp, A. H., et al. (1998) Intranuclear neuronal inclusions in Huntington's disease and dentatorubral and pallidoluysian atrophy—correlation between the density of inclusions and IT-15 CAG triplet repeat length. *Neurobiol. Dis.* **4,** 387–397.
27 Davies, S. W., Beardsall, K., Turmaine, M., et al. (1998) Are neuronal intranuclear inclusions the common neuropathology of triplet-repeat disorders with polyglutamine-repeat expansions? *Lancet* **351,** 131–133.
28 Davies, S. W., Turmaine, M., Cozens, B. A., et al. (1999) From neuronal inclusions to neurodegeneration: neuropathological investigation of a transgenic mouse model of Huntington's disease. *Phil. Trans. R. Soc. (Lond.) B: Biol. Sci.* **354,** 971–979.
29 Perutz, M. F. and Windle, A. H. (2001) Cause of neural death in neurodegenerative disease attributable to expansion of glutamine repeats. *Nature* **412,** 143–144.
30 Li, H., Li, S. H., Yu, Z. X., et al. (2001) Huntingtin aggregate-associated axonal degeneration is an early pathological event in Huntington's disease mice. *J. Neurosci.* **21,** 8473–8481.
31 Chen, S., Berthelier, V., Yang, W., et al. (2001) Polyglutamine aggregation behavior in vitro supports a recruitment mechanism of cytotoxicity. *J. Mol. Biol.* **311,** 173–182.
32 Stenoinen, D. L., Cummings, C. J., Adams, H. P., et al. (1999) Polyglutamine-expanded androgen receptors form aggregates that sequester heat shock proteins, proteasome components and SRC-1, and are suppressed by the HDJ-2 chaperone. *Hum. Mol. Genet.* **8,** 731–741.
33 Suh, S., Senut, M., Whitelegge, J., et al. (2001) Identities of sequestered proteins in aggregates from cells with induced polyglutamine expression. *J. Cell Biol.* **153,** 283–294.
34 La Spada, A. R., Fu, Y.-H., Sopher, B. L., et al. (2001) Polyglutamine-expanded ataxin-7 antagonizes CRX function and induces cone-rod dystrophy in amouse model of SCA7. *Neuron* **31,** 913–927.
35 Kouroku, Y., Fujita, E., Jimbo, A., et al. (2002) Polyglutamine aggregates stimulate ER stress signals and caspase-12 activation. *Hum. Mol. Genet.* **11,** 1505–1515.
36 Bence, N. F., Sampat, R. M., and Kopito, R. R. (2001) Impairment of the ubiquitin–proteasome system by protein aggregation. *Science* **292,** 1552–1555.
37 Hodgson, J. G., Agopyan, N., Gutekunst, C. A., et al. (1999) A YAC mouse model for Huntington's disease with full-length mutant huntingtin, cytoplasmic toxicity, and selective striatal neurodegeneration. *Neuron* **23,** 181–192.

38 Heintz, N. and Zoghbi, H. Y. (2000) Insights from mouse models into the molecular basis of neurodegeneration. *Annu. Rev. Physiol.* **62,** 779–802.
39 Huynh, D. P., Figueroa, K., Hoang, N., et al. (2000) Nuclear localization or inclusion body formation of ataxin-2 are not necessary for SCA2 pathogenesis in mouse or human. *Nature Genet.* **26,** 44–50.
40 Kuemmerle, S., Gutekunst, C. A., Klein, A. M., et al. (1999) Huntingtin aggregates may not predict neuronal death in Huntington's disease. *Ann. Neurol.* **46,** 842–849.
41 Saudou, F., Finkbeiner, S., Devys, D., et al. (1998) Huntingtin acts in the nucleus to induce apoptosis, but death does not correlate with the formation of intranuclear inclusions. *Cell* **95,** 55–66.
42 Kim, M., Lee, H.-S., LaForet, G., et al. (1999) Mutant huntingtin expression in clonal stratial cells: dissociation of inclusion formation and neuronal survival by caspase inhibition. *J. Neurosci.* **19,** 964–973.
43 Cummings, C. J., Reinstein, E., Sun, Y., et al. (1999) Mutation of the E6–AP ubiquitin ligase reduces nuclear inclusion frequency while accelerating polyglutamine–induced pathology in *SCA1* mice. *Neuron* **24,** 879–892.
44 Yu, Z.-X., Li, S.-H., Nguyen, H.-P., et al. (2002) Huntingtin inclusions do not deplete polyglutamine-containing transcription factors in HD mice. *Hum. Mol. Genet.* **11,** 905–914.
45 Sisodia, S. S. (1998) Nuclear inclusions in glutamine repeat disorders: are they pernicious, coincidental or beneficial? *Cell* **95,** 1–4.
46 Rich, T., Assier, E., Skepper, J., et al. (1999) Disassembly of nuclear inclusions in the dividing cell—a novel insight into neurodegeneration. *Hum. Mol. Genet.* **8,** 2451–2459.
47 Floyd, J. A. and Hamilton, B. A. (1999) Intranuclear inclusions and the ubiquitin-proteasome pathway: digestion of a red herring? *Neuron* **24,** 765–766.
48 Scherzinger, E., Sittler, A., Schweiger, K., et al. (1999) Self-assembly of polyglutamine-containing huntingtin fragments into amyloid-like fibrils: implications for Huntington's disease pathology. *Proc. Natl. Acad. Sci. USA* **96,** 4604–4609.
49 Walsh, D. M., Klyubin, I., Fadeeva, J. V., et al. (2002) Naturally secreted oligomers of amyloid b protein potently inhibit hippocampal long-term potentiation in vivo. *Nature* **416,** 535–539.
50 Lambert, M. P., Barlow, A. K., Chromy, B. A., et al. (1998) Diffusible, nonfibrillar ligands derived from Abeta 1–42 are potent central nervous system toxins. *Proc. Natl. Acad. Sci. USA* **95,** 6448–6453.
51 Conway, K. A., Lee, S.-J., Rochet, J.-C., et al. (2000) Acceleration of oligomerization, not fibrillization, is a shared property of both a-synuclein mutations linked to early-onset Parkinson's disease: implications for pathogenesis and therapy. *Proc. Natl. Acad. Sci. USA* **97,** 571–576.
52 DePace, A. H., Santoso, A., Hillner, P., et al. (1998) A critical role for amino-terminal glutamine/asparagine repeats in the formation and propagation of yeast prion. *Cell* **93,** 1241–1252.
53 Osherovich, L. Z. and Weissman, J. S. (2001) Multiple Gln/Asn-rich prion domains confer susceptibility to induction of the yeast [*PSI*$^+$] prion. *Cell* **106,** 183–194.
54 Lindquist, S., Krobitsch, S., Li, L., et al. (2001) Investigating protein conformation-based inheritance and disease in yeast. *Phil. Trans. R. Soc. (Lond.) B: Biol. Sci.* **356,** 169–176.
55 Scheibel, T. and Lindquist, S. L. (2001) The role of conformational flexibility in prion propagation and maintenance for Sup35p. *Nature Struct. Biol.* **8,** 958–962.
56 Serio, T. R., Cashikar, A. G., Kowal, A. S., et al. (2000) Nucleated conformational con-

version and the replication of conformational information by a prion determinant. *Science* **289,** 1317–1321.
57 Altschuler, E. L., Hud, N. V., Mazrimas, J. A., et al. (1997) Random coil conformation for extended polyglutamine stretches in aqueous soluble monomeric peptides. *J. Pept. Res.* **50,** 73–75.
58 Minor, D. L., Jr. and Kim, P. S. (1994) Context is a major determinant of b-sheet propensity. *Nature* **371,** 264–267.
59 Minor, D. L., Jr. and Kim, P. S. (1996) Context-dependent secondary structure formation of a designed protein sequence. *Nature* **380,** 730–734.
60. Lathrop, R. H., Casale, M., Tobias, D. J., et al. (1998) Modeling protein homopolymeric repeats: possible polyglutamine structural motifs for Huntington's Disease. *Proc. Int. Conf. Intell. Syst. Mol. Biol.* **6**, 105–114.
61 Peretz, D., Williamson, R. A., Legname, G., et al. (2002) A change in the conformation of prions accompanies the emergence of a new prion strain. *Neuron* **34,** 921–932.
62 Peretz, D., Williamson, R. A., Kaneko, K., et al. (2001) Antibodies inhibit prion propagation and clear cell cultures of prion infectivity. *Nature* **412,** 739–743.
63 Li, L. and Lindquist, S. (2000) Creating a protein-based element of inheritance. *Science* **287,** 661–664.
64 Laver, W. G., Air, G. M., Webster, R. G., et al. (1990) Epitopes on protein antigens: misconceptions and realities. *Cell* **61,** 553–556.
65 Sachs, D. H., Schechter, A. N., Eastlake, A., et al. (1972) An immunologic approach to the conformational equilibria of polypeptides. *Proc. Natl. Acad. Sci. USA* **69,** 3790–3794.
66 Sela, M. (1969) Antigenicity: some molecular aspects. *Science* **166,** 1365–1374.
67 Chen, G., Dubrawsky, I., Mendez, P., et al. (1999) In vitro scanning saturation mutagenesis of all the specificity determining residues in an antibody binding site. *Protein Eng.* **12,** 349–356.
68 Chothia, C. and Lesk, A. M. (1987) Canonical structures for the hypervariable regions of immunoglobulins. *J. Mol. Biol.* **196,** 901–917.
69 Chothia, C., Lesk, A. M., Tramontano, A., et al. (1989) Conformations of immunoglobulin hypervariable regions. *Nature* **342,** 877–883.
70 Zou, W., Mackenzie, R., Therien, L., et al. (1999) Conformational epitope of the type III group B *Streptococcus* capsular polysaccharide. *J. Immunol.* **163,** 820–825.
71 Bernstein, F. C., Koetzle, T. F., Williams, G. J. B., et al. (1977) The protein data bank: a computer-based archival file for macromolecular structures. *J. Mol. Biol.* **112,** 535–542.
72 Graille, M., Stura, E. A., Corper, A. L., et al. (2000) Crystal structure of a *Staphylococcus aureus* protein. A domain complexed with the Fab fragment of a human IgM antibody: structural basis for recognition of B-cell receptors and superantigen activity. *Proc. Natl. Acad. Sci. USA* **97,** 5399–5404.
73 Kistler, J., Aebi, U., Onorato, L., et al. (1978) Structural changes during the transformation of bacteriophage T4 polyheads: characterization of the initial and final states by freeze-drying and shadowing Fab-fragment-labelled preparations. *J. Mol. Biol.* **126,** 571–589.
74 Fairclough, R. H., Twaddle, G. M., Gudipati, E., et al. (1998) Mapping the mAb 383C epitope to a_2 (187–199) of the *Torpedo* acetylcholine receptor on the three-dimensional model. *J. Mol. Biol.* **282,** 301–315.
75. Sun, W., Barchi, R. L., and Cohen, S. A. (1995) Probing sodium channel cytoplasmic domain structure. Evidence for the interaction of the rSkM1 amino and carboxyl termini. *J. Biol. Chem.* **270,** 22,271–22,276.

76 Tzartos, S. J., Barkas, T., Cung, M. T., et al. (1998) Anatomy of the antigenic structure of a large membrane autoantigen, the muscle-type nicotinic acetylcholine receptor. *Immunol. Rev.* **163,** 89–120.
77. Harlow, E. and Lane, D. (1988) *Antibodies: A Laboratory Manual*. Cold Spring Harbor Laboratory, Cold Spring Harbor, NY.
78. Berzofsky, J. A., Berkower, I. J., and Epstein, S. L. (1999) Antigen antibody interactions and monoclonal antibodies, *Fundamental Immunology*, 4th ed. (W. E. Paul, ed.), Lippincott–Raven, Philadelphia, pp. 75–110.
79 Ways, J. P. and Parham, P. (1983) The binding of monoclonal antibodies to cell-surface molecules. A quantitative analysis with immunoglobulin G against two alloantigenic determinants of the human transplantation antigen HLA-A2. *Biochem. J.* **216,** 423–432.
80. Parham, P. (1984) The binding of monoclonal antibodies to cell surface molecules. Quantitative analysis of the reactions and cross-reactions of an antibody (MB40.3) with four HLA-B molecules. *J. Biol. Chem.* **259,** 13,077–13,083.
81 MacKenzie, R. and To, R. (1998) The role of valency in the selection of anti-carbohydrate single-chain Fvs from phage display libraries. *J. Immunol. Methods* **220,** 39–49.
82 Stevanin, G., Trottier, Y., Cancel, G., et al. (1996) Screening for proteins with polyglutamine expansions in autosomal dominant cerebellar ataxias. *Hum. Mol. Genet.* **5,** 1887–1892.
83 DeLano, W. L., Ultsch, M. H., de Vos, A. M., et al. (2000) Convergent solutions to binding at as protein-protein interface. *Science* **287,** 1279–1283.
84 Lescar, J., Stouracova, R., Riottot, M.-M., et al. (1997) Three-dimensional structure of an Fab–peptide complex: structural basis of HIV-1 protease inhibition by amonoclonal antibody. *J. Mol. Biol.* **267,** 1207–1222.
85 Persichetti, F., Trettel, F., Huang, C. C., et al. (1999) Mutant huntingtin forms in vivo complexes with distinct context–dependent conformations of the polyglutamine segment. *Neurobiol. Dis.* **6,** 364–375.
86 Ko, J., Ou, S., and Patterson, P. H. (2001) New anti-huntingtin monoclonal antibodies: implications for huntingtin conformation and its binding proteins. *Brain Res. Bull.* **56,** 319–329.
87 Mende-Mueller, L. M., Toneff, T., Hwang, S. R., et al. (2001) Tissue-specific proteolysis of huntingtin (htt) in human brain: evidence of enhanced levels of N- and C-terminal htt fragments in Huntinton's disease striatum. *J. Neurosci.* **21,** 1830–1837.
88. Kim, Y. J., Yi, Y., Sapp, E., et al. (2001) Caspase 3-cleaved N-terminal fragments of wild-type and mutant huntingtin are present in normal and Huntington's disease brains, associate with membranes, and undergo calpain-dependent proteolysis. *Proc. Natl. Acad. Sci. USA* **98,** 12,784–12,789.
89 Humbert, S., Bryson, E. A., Cordelières, F. P., et al. (2002) The IGF-1/Akt pathway is neuroprotective in Huntington's disease and involves huntingtin phosphorylation by Akt. *Dev. Cell.* **3,** 1–20.
90 Das, T. K., Mazumdar, S., and Mitra, S. (1998) Characterization of a partially unfolded structure of cytochrome *C* induced by sodium dodecyl sulphate and the kinetics of its refolding. *Eur. J. Biochem.* **254,** 662–670.
91 Mitraki, A., Barge, A., Chroboczek, J., et al. (1999) Unfolding studies of human adenovirus type 2 fibre trimers. *Eur. J. Biochem.* **264,** 599–606.
92 Dunn, S. D. (1986) Effects of the modification of transfer buffer composition and the renaturation of proteins in gels on the recognition of proteins on Western blots by monoclonal antibodies. *Anal. Biochem.* **157,** 144–153.

93. Hubbard, M. J. and Klee, C. B. (1987) Calmodulin binding by calcineurin. Ligand-induced renaturation of protein immoblized on nitrocellulose. *J. Biol. Chem.* **262,** 15,062–15,070.
94 Birk, H. W. and Koepsell, H. (1987) Reaction of monoclonal antibodies with plasmamembrane proteins after binding on nitrocellulose: renaturation of antigenic sites and reduction of nonspecific antibody binding. *Anal. Biochem.* **164,** 12–22.
95 Celenza, J. L. and Carlson, M. (1991) Renaturation of protein kinase activity of protein blots. *Methods Enzymol.* **200,** 423–430.
96 Fischer, R., Wei, Y., and Berchtold, M. (1996) Detection of calmodulin-binding proteins using a ^{32}P-labeled GST-calmodulin fusion protein and a novel renaturation protocol. *Biotechniques* **21,** 292–296.
97 Klinz, F. J. (1994) GTP-blot analysis of small GTP-binding proteins. The C-terminus is involved in renaturation of blotted proteins. *Eur. J. Biochem.* **225,** 99–105.
98 Shackelford, D. A. and Zivin, J. A. (1993) Renaturation of calcium/calmodulin–dependent protein kinase activity after electrophoretic transfer from sodium dodecyl sulfate–polyacrylamide gels to membranes. *Anal. Biochem.* **211,** 131–138.
99 Zeng, F. Y., Oka, J. A., and Weigel, P. H. (1996) Renaturation and ligand blotting of the major subunit of the rat asialoglycoprotein receptor after denaturing polyacrylamide gel electrophoresis. *Glycobiology* **6,** 247–255.
100. Sambrook, J., Fritsch, E. F., and Maniatis, T. (1989) *Molecular Cloning: A Laboratory Manual,* 2nd ed., Cold Spring Harbor Laboratory, Plainview, NY, p. 16.

9

Solubilization of Aggregates Formed by Expanded Polyglutamine Tract Expression in Cultured Cells

Noriko Hazeki and Ichiro Kanazawa

Summary

The expression of expanded polyglutamine in mammalian cells causes the formation of aggregates. For elucidation of the biochemical properties of the aggregates, isolation and solubilization of the aggregates are required. This chapter provides useful protocols for the solubilization of polyglutamine aggregates and further applications of protein analysis.

Key Words: Polyglutamine; aggregate; formic acid; green fluorescent protein (GFP); fluorescence-activated cell sorter (FACS); quantification; Huntington's disease.

1. Introduction

Cells that express recombinant proteins with expanded polyglutamine contain aggregates *(1,2)*. The aggregates cannot be solubilized with heat treatment in buffer containing sodium dodecyl sulfate (SDS), and the purification procedure for insoluble materials is not well established. Therefore, it is difficult to characterize the biochemical properties of the aggregates, including identification of the components of the aggregates, determination of the turnover rates of aggregate components, and analysis of modification of aggregate components.

Here, we describe useful protocols for solubilization of polyglutamine aggregates. Polyglutamine-containing aggregates tagged with green fluorescent protein (GFP) are readily isolated by fractionation with centrifugation followed by fluorescence-activated cell sorting (FACS) and are solubilized by treatment with concentrated formic acid at 37ºC, resulting in dissociation of the components. We also show the application of these methods for the identification and quantitation of components in the aggregates that contain polyglutamine proteins.

From: *Methods in Molecular Biology, vol. 277: Trinucleotide Repeat Protocols*
Edited by: Y. Kohwi © Humana Press Inc., Totowa, NJ

2. Materials

1. Expression vectors (pEGFP-N1 [Clontech]; pQBI-25 [Quantum Biotechnologies]).
2. Template (polyglutamine protein cDNA; BlueScript SK- plasmid and λ phage containing exon 1 of human huntingtin gene were kindly donated by Dr. H. Ishiguro ***[3]***).
3. Mammalian cells (Neuro 2A, ATCC; Cos7, ATCC).
4. Culture medium (α-MEM for Cos7 or Dulbecco's modified Eagle's medium [DMEM] [high glucose] for Neuro2A supplemented with 100 U/mL penicillin, 100 μg/mL streptomycin, and 10% fetal bovine serum [FBS]; all reagents were supplied from Gibco).
5. Transfection reagents (SuperFect transfection reagent [Qiagen]; Calphos Mammalian Transfection Kit [Clontech]).
6. Fluorescence microscope.
7. Anti-GFP monoclonal antibody (Clontech).
8. Water bath.
9. Sonicator (Ultrasonic Disruptor, Model UR-200P, TOMY Seiko; Sonic Dismembrator 550, Fisher Scientific).
10. Protease inhibitor stock solutions: aprotinin (Roche), 1 mg/mL H_2O; Pefabloc SC (Roche), 0.5 *M* in H_2O; EDTA (Sigma), 0.5 *M* in H_2O; leupeptin (Sigma), 5 mg/mL H_2O; *N*-ethylmaleimide (Sigma), 1 *M*/ethanol; and pepstatin A (Roche), 1 mg/mL ethanol.
11. Protease inhibitor working solution: stock solutions are diluted; final concentration: 1 μg/mL aprotinin, 0.5 m*M* Pefabloc SC, 1 m*M* EDTA, 10 μg/mL leupeptin, 1 m*M* N-ethylmaleimide (NEM; Sigma), and 10 μg/mL pepstatin.
12. Formic acid (90%; Wako).
13. Cellulose acetate membrane (Schleicher and Schuell; 0.2-μm pore size).
14. Dotblot equipment (Bio-Rad).
15. Vacuum centrifuge (SpeedVac; Savant).
16. SDS-PAGE (sodium dodecyl sulfate-polyacrylamide gel electrophoresis) equipment (AE-6530P, Atto; DPE-1020, Daiichi; Mini-Protean II Cell, Bio-Rad).
17. SDS–sample buffer: 80 m*M* Tris-HCl, pH 6.8, containing 2% SDS, 10% glycerol, and 10% 2-mercaptoethanol.
18. Fluorescence-activated cell sorter (Epics Elite; Beckman Coulter).
19. Immunoblotting equipment (Marisol and Bio-Rad).
20. PBS: Dulbecco's phosphate-buffered saline (Gibco–Invitrogen).
21. TBSX: Tris-buffered saline with Triton X-100 (50 m*M* Tris-HCl, pH 7.5, containing 150 m*M* NaCl, 0.5% Triton X-100).
22. TBST: Tris-buffered saline with Tween-20 (0.05%).
23. CBB staining solution: Coomassie brilliant blue R250 (Bio-Rad) 2.5 g in 450 mL of methanol, 450 mL of deionized water (dH_2O) and 100 mL of glacial acetic acid. Destaining solution without CBB.

3. Methods

3.1. Expression of Polyglutamine in Mammalian Cells

The DNA manipulations are performed by standard recombinant DNA methods ***(4)*** to construct the expression plasmids and are not described in detail here.

1. HD exon 1 fragments are amplified by polymerase chain reaction (PCR) from BlueScript SK- plasmid and λ phage containing HD exon 1, using the primers 5'-GATGCTAGCATG GCGACCCTGGAAAAG-3' and 5' TCTCTAGACGGTCGGTGCAGCGGCTC-3', and are cloned into the *Nhe*I site of the pQBI-25 expression vector, designated as HD-77-GFP (*see* **Fig. 1**) ***(1)***.

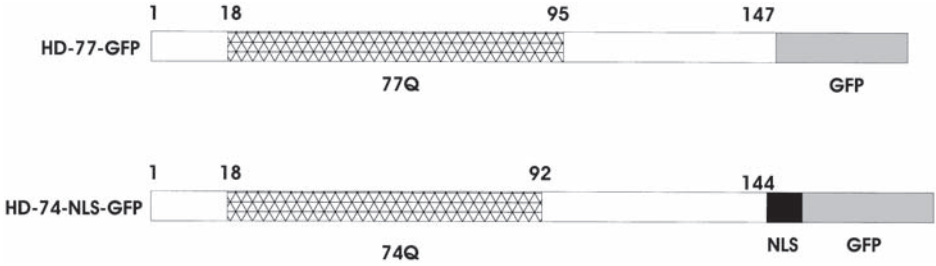

Fig. 1. Schematic structures of the expressed fusion proteins containing expanded polyglutamine. The nuclear localization sequence (NLS) of the SV40 large-T antigen (PKKKRKV) was added at the C-terminus in HD-74-NLS-GFP. The numbers above each box indicate the amino acid position. The regions encoding glutamine repeats (Q), NLS, and GFP are represented by lattice, black, and gray, respectively.

2. To generate a vector containing the nuclear localization signal (NLS) of the SV40 large-T antigen (PKKKRKV) ***(5)***, HD exon 1 fragments from an allele with an expanded polyglutamine sequence [$(CAG)_{77}$] in HD-77-GFP are amplified by the PCR primer with the sequence 5'-GGAATTCTATGGCGACCCTGGAAAAGCT-3' together with the primer containing the NLS, namely 5'-CCGGATCCACCTTTCGCTTCTTCTTCGGT-CGGTGCAGCGG-3'.
3. The PCR reaction mix is prepared with 4 µL of template (HD-77-GFP, 2 ng/µL), 0.5 µL of LA *Taq* (Takara, Japan), 25 µL of 2X GC buffer, 8 µL of dNTP mix (2.5 m*M* each), 1 µL of 50 µ*M* primer, and 10.5 µL of H_2O.
4. The PCR reaction mix is overlaid with mineral oil and was heated for 5 min at 95°C to denature the template.
5. The PCR is carried out in an automated thermal cycler for 30 cycles under the following conditions: denature 1 min at 94°C, hybridize 1 min at 64°C, extend 2 min at 72°C, and then extend an additional 10 min at 72°C in the last cycle to make the products as complete as possible.
6. The PCR products are digested with *Eco*RI and *Bam*HI and subcloned into the pEGFP-N1 expression vector (Clontech) to yield HD-74-NLS-GFP (*see* **Fig. 1**) ***(6)*** (*see* **Note 1**).
7. The nucleotides sequences are confirmed by the dideoxynucleotide chain terminator method of sequencing (ABI).
8. Plasmid DNAs are prepared and purified using Endo-Free Plasmid Maxi Kit (Qiagen). Transfections are performed using SuperFect transfection reagent (Qiagen) or the Calphos Mammalian Transfection Kit (Clontech) according to manufacturer's instructions (*see* **Note 2**). The cells are incubated for 24 h or longer after transfection (*see* **Note 3**).

3.2. Isolation of Aggregates

Aggregates are isolated from cells transfected with HD-77-GFP or HD-74-NLS-GFP as outlined in **Fig. 2**.

1. The cells expressing aggregates are harvested from 10-cm culture dishes with PBS by using a cell scraper and centrifuged at 300*g* at 4°C for 5 min.
2. The cells are washed twice with PBS and the cell pellet is frozen at –80°C.
3. The pellet is suspended in cold TBSX with protease inhibitors and sonicates on ice for 15 s (set to 1 in the Ultrasonic Disruptor).

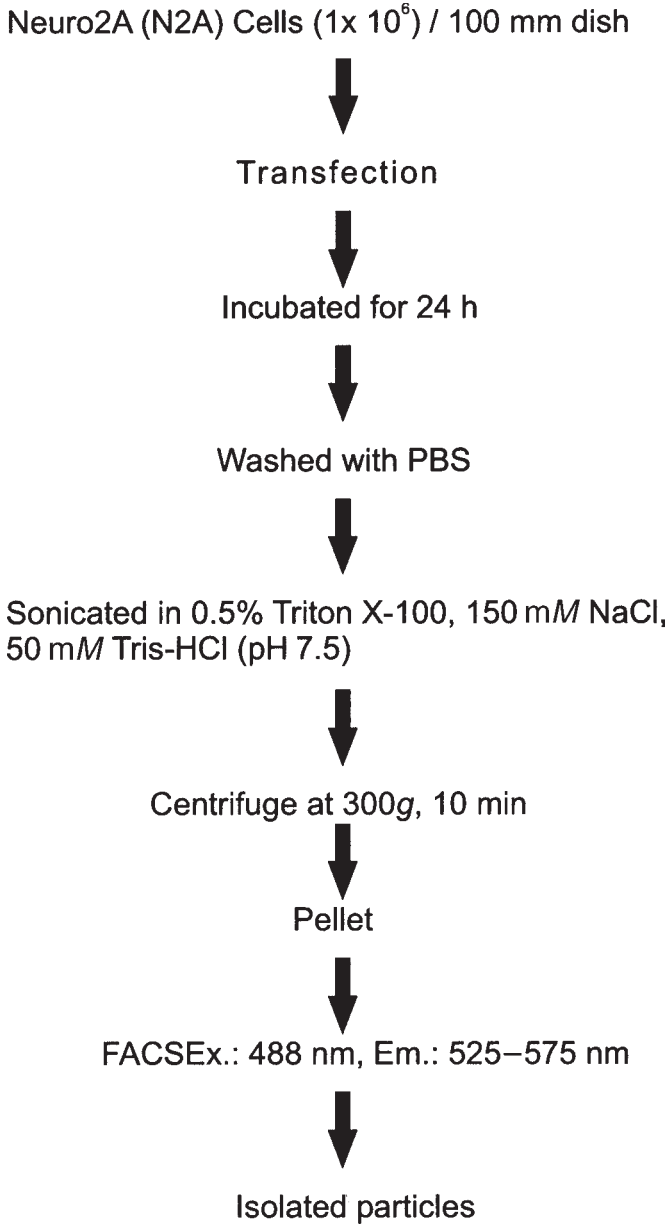

Fig. 2. Protocol of isolation of aggregates from N2A cells. (Reprinted from **ref**. ***6*** with permission from Elsevier.)

4. The suspension is centrifuged at 300*g* at 4°C for 10 min, and the supernatant is removed.
5. The pellet is resuspended in cold TBSX, and the same process repeats twice.
6. Particles from the final pellet are sieved through a 45-μm Nylon mesh (NBC Inc., Tokyo) and applied to a cell sorter ***(7)***. Particles are sorted at a flow rate of 200–500 particles/s using a 76- or 100-μm flow-cell tip nozzle and an argon laser with an excitation maximum set at 488 nm. Emission signals are selected by a 525- to 575-nm bandpass filter followed by a 675-nm long-pass filter.
7. The sorted fraction is centrifuged at 300*g* at 4°C for 10 min. The pellet is resuspended in TBSX and sonicated on ice for 15 s (set to 1 in the Ultrasonic Disruptor). The particles are then filtered and resorted as described in **step 6**.
8. The capture of fluorescent particles is confirmed by fluorescent microscopy.

3.3. Solubilization of Aggregates

The following steps are applied to solubilize not only isolated aggregates but also whole cells, including aggregates.

1. The number of aggregates is counted using a hemocytometer.
2. The sorted fraction is centrifuged at 300*g* at 4°C for 10 min.
3. The aggregates (1×10^6 particles per lane for detecting by protein staining) are suspended and incubated in 500 μL of concentrated formic acid for 1 h at 37°C (*see* **Note 4**).
4. The samples are dried by vacuum centrifugation (*see* **Note 5**).
5. Aggregates treated with formic acid are suspended in SDS–sample buffer and mixed with bromphenol blue (BPB, final 0.001% w/v) and neutralized with 1 *M* Trizma base until the indicator dye turned blue.
6. The suspension is boiled for 5 min.

3.4. Analysis of Components of Aggregates

The efficiency of solubilization of aggregates is confirmed by using a membrane filter assay ***(8,9)*** (*see* **Fig. 3**). The turnover and quantification of components in the aggregates are analyzed by using SDS-PAGE and immunoblotting (*see* **Fig. 4**) or Coomassie staining (*see* **Fig. 5**). Furthermore, the components of aggregates are identified by protein sequencing ***(6)***. SDS-PAGE, immunoblotting, and protein sequencing are performed by standard protein assay methods ***(3,6,9)*** and are not described here.

3.5. Membrane Filter Assay

1. The 200 μL of the sample solution is filtered on a dot-blot filtration unit (9 × 12 cm; Bio-Rad) through a cellulose acetate membrane that is pre-equilibrated with 2% SDS.
2. The membrane is washed twice with 0.1% SDS on a dot-blot filtration unit.
3. The membrane is removed from the filtration unit and is treated with 50 mL of TBST containing 4% skim milk and 1% BSA (Sigma) with rocking for 30 min at room temperature to block nonspecific binding.
4. The membrane is incubated with anti-GFP monoclonal antibody (Clontech, diluted 1:1000 in 15 mL TBST) with rocking at 4ºC overnight.
5. The membrane is washed three times in TBST (10 min each).
6. The membrane is incubated with anti-mouse secondary monoclonal antibody (Amersham; diluted 1:500 in 15 mL TBST) with rocking for 1 h at room temperature.
7. The membrane is washed three times in TBST (10 min each).

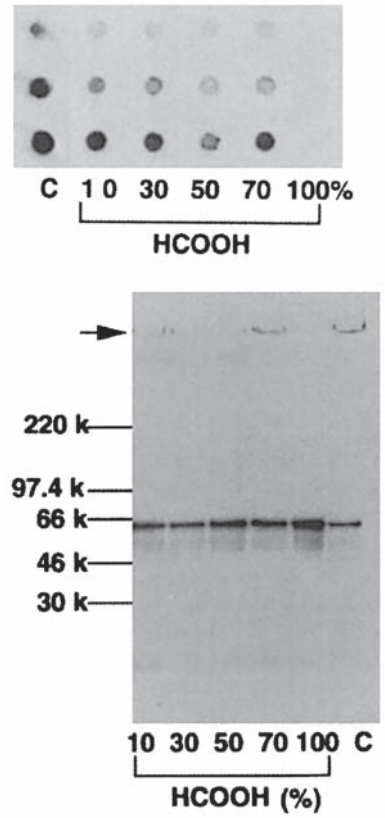

Fig. 3. Detection of solubility of aggregates by using membrane filter assay. (**Upper panel**) Cos7 cells transfected with HD-77-GFP construct were suspended in lysis buffer and lysed on ice for 30 min. Insoluble pellets were prepared by centrifugation at 16,000*g* at 4°C for 5 min. The samples were incubated at 37°C for 1 h in formic acid (10%, 30%, 50%, 70%, or 100%), dried by vacuum centrifuge, and boiled in Tris buffer containing SDS and dithiothreitol (DTT). Untreated pellet was boiled in Tris buffer containing SDS and DTT as a control (C). Suspensions were filtered through a cellulose acetate membrane and aggregates captured on the membrane were detected with anti-GFP antibody. The relative sample volumes were 1:3:9 from the top row to bottom row respectively. (**Bottom panel**) The suspensions used in the membrane filter assay were resolved by SDS-PAGE. Proteins were blotted to polyvinylidene difluoride (PVDF) membrane followed by immunostained with anti-GFP antibody. Arrow indicates the top of the gel. The numbers at the left represent molecular weights of separated proteins. (Reprinted from **ref. *9*** with permission from Elsevier.)

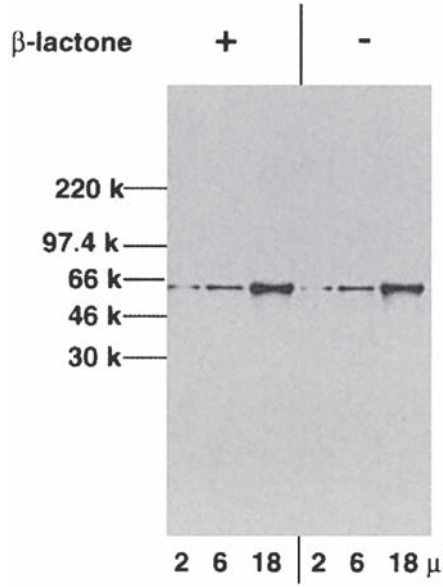

Fig. 4. Effect of proteasome inhibitor (β-lactone) on protein accumulation in Cos7 cells bearing aggregates. The cells transfected with HD-77-GFP construct were treated with β-lactone (10 μ*M*), harvested 48 h after transfection, and then centrifuged. The cell pellets were incubated in 100% formic acid at 37°C for 40 min and then dried and boiled in SDS–sample buffer for 5 min. The 2-, 6-, and 18-μL aliquots were resolved by SDS-PAGE and then the proteins were blotted and immunostained with anti-GFP antibody. (Reprinted from **ref. *9*** with permission from Elsevier.)

8. Immunoreactive spots are visualized using an enhanced chemiluminescence (ECL; Amersham) Western blotting system, according to the manufacturer's instructions.

4. Notes

1. The localization of aggregates could depend on the length of the polyglutamine protein and duration of the cell cycle ***(10,11)***. The localization of aggregates should be confirmed by using fluorescence microscopy before proceeding with the isolation of aggregates.
2. There are various methods for transfection (Calcium phosphate, DEAE–dextran, lipofection, etc.). The selection of the transfection method is dependent on cell type (Cos7, Superfect, Qiagen; Neuro2A, Superfect, Qiagen, or calcium phosphate, Clontech). The cell density (0.5×10^5/35-mm dish for Cos 7; 1×10^6 cells/100-mm dish for Neuro2A), amount of DNA (2 μg/35-mm dish for Cos 7; 10 μg/100-mm dish for Neuro 2A cells) and incubation time with DNA (5 h for Cos7 and Neuro2A when using Superfect, Qiagen; overnight for Neuro2A when using the Calphos Mammalian Transfection Kit, Clontech) can also affect the efficiency of transfection. A small-scale experiment is recommended for choosing the optimal conditions of transfection for the cells you are using.
3. The rate of aggregate formation is dependent on cell type and the constructs you use (e.g., at the HD-74-NLS-GFP construct, aggregates formed in > 50% of transfected Neuro2A cells within 24 h, whereas at the HD-77-GFP construct in Cos7 cells, > 48 h was required).

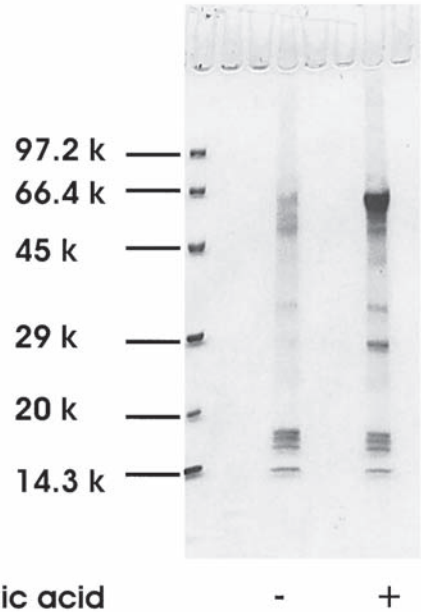

Fig. 5. Protein component of aggregates. Purified aggregates were treated with (+) or without (–) concentrated formic acid and the proteins were resolved in a 10–20% gradient SDS-PAGE gel. Gel was stained with CBB. (Reprinted from **ref. *6*** with permission from Elsevier.)

Analysis of the time-course of aggregate formation by using immunofluorescent microscopy is recommended before proceeding with large-scale experiments.

4. Concentrated formic acid is required to dissociate the aggregates, including polyglutamine protein. The incubation time must be more than 30 min.
5. An alkali trap should be used with the vacuum centrifuge, because of the strength of volatilized formic acid.

Acknowledgments

We thank Dr. H. Ishiguro for providing the BlueScript SK and λ phage containing exon 1 of human HD and Mr. G. M. Corson (Shriners Hospitals for Children) for helpful discussions and critical reading of the manuscript. This study was supported in part by a Grant in Aid for Scientific Research on Priority Areas from the Ministry of Education, Science, Sports and Culture, Japan, and by a grant from CREST, the Japan Science and Technology Corporation.

References

1 Hazeki, N., Nakamura, K., Goto, J., et al. (1999) Rapid aggregate formation of the huntingtin N-terminal fragment carrying an expanded polyglutamine tract. *Biochem. Biophys. Res. Commun.* **256,** 361–366.

2 Paulson, H. L., Perez, M. K., Trottier, Y., et al. (1997) Intranuclear inclusions of expanded polyglutamine protein in spinocerebellar ataxia type 3. *Neuron* **19,** 333–344.

3 Ishiguro, H., Yamada, K., Sawada, H., et al. (2001) Age-dependent and tissue-specific CAG repeat instability occurs in mouse knock-in for a mutant Huntington's disease gene. *J. Neurosci. Res.* **65,** 289–297.
4. Ausubel M. F., Brent, R., Kingston, R. E., et al. (eds.) (2002) *Current Protocols in Molecular Biology*, John Wiley & Sons, New York.
5 Newmeyer, D. D. and Forbes, D. J. (1988) Nuclear import can be separated into distinct steps in vitro: nuclear pore binding and translocation. *Cell* **52,** 641–653.
6 Hazeki, N., Tsukamoto, T. Yazawa, I., et al. (2002) Ultrastructure of nuclear aggregates formed by expressing an expanded polyglutamine. *Biochem. Biophys. Res. Commun.* **294,** 429–440.
7 Iwatsubo, T., Yamaguchi, H., Fujimuro, M., et al. (1996) Purification and characterization of Lewy bodies from the brains of patients with diffuse Lewy body disease. *Am. J. Pathol.* **148,** 1517–1529.
8 Wanker, E. E., Scherzinger, E., Heiser, V., et al. (1999) Membrane filter assay for detection of amyloid-like polyglutamine-containing protein aggregates. *Methods Enzymol.* **309,** 375–386
9 Hazeki, N., Tsukamoto, T., Goto, J., et al. (2000) Formic acid dissolves aggregates of an N-terminal huntingtin fragment containing an expanded polyglutamine tract: applying to quantification of protein components of the aggregates. *Biochem. Biophys. Res. Commun.* **277,** 386–393.
10 Hackam, A. S., Singaraja, R., Wellington, C. L., et al. (1998) The influence of huntingtin protein size on nuclear localization and cellular toxicity. *J. Cell Biol.* **141,** 1097–1105.
11. Martin-Aparicio, E., Avila, J., and Lucas, J. J. (2002) Nuclear localization of N-terminal mutant huntingtin is cell cycle dependent. *Eur. J. Neurosci.* **16,** 355–359.

IV

Establishment of Animal and Cultured Cell Models for Trinucleotide Repeat Diseases

10

Caenorhabditis elegans as a Model System for Triplet Repeat Diseases

Cindy Voisine and Anne C. Hart

Summary

Common features underlie the generation and function of neurons in multicellular animals. It is likely that conserved pathways and genes also are involved in neuronal degeneration and malfunction. To address the molecular mechanisms of complex human neurological disorders, many investigators are choosing to study these diseases in simpler organisms. The nematode *Caenorhabditis elegans* provides an excellent model system to address genetically the mechanisms of triplet repeat diseases. Advantages of using *C. elegans* as a model system include the ease of genetic manipulation, the sequenced genome, and a short life cycle. Furthermore, researchers can precisely identify specific neurons and follow their development or survival throughout the animal's lifetime. This chapter describes the tools and approaches for modeling triplet repeat diseases in *C. elegans* with a specific emphasis on polyglutamine (polyQ) diseases. Although the bulk of the chapter is devoted to generating a polyQ disease model in *C. elegans*, it also addresses potential avenues for assessing the impact of specific candidate genes/pathways on the disease process, including cell death and aging.

Key Words: *Caenorhabditis elegans;* neurodegeneration; triplet repeat diseases; polyglutamine diseases; Huntington's disease.

1. Introduction

When establishing a *Caenorhabditis elegans* model system of a triplet repeat disorder, it is critical to understand the basic mechanism underlying the human disease. Importantly, what effect does the trinucleotide repeat expansion have on the disease gene product? In polyglutamine (polyQ) diseases, a CAG repeat expansion is found in the coding region of the disease allele ***(1–4)***. The mutant form of the protein contains

From: *Methods in Molecular Biology, vol. 277: Trinucleotide Repeat Protocols*
Edited by: Y. Kohwi © Humana Press Inc., Totowa, NJ

an expanded polyQ tract that has been implicated in driving the disease process. Alternatively, the triplet repeat expansion may lie within the noncoding region of the disease gene. In Friedreich's ataxia, the first intron of the frataxin gene contains a GAA repeat expansion, which reduces the level of frataxin mRNA ***(5,6)***. The resulting decrease in the amount of functional frataxin protein contributes to the disease process. These two disorders highlight the likely differences in the molecular mechanisms underlying a triplet repeat disease caused by an expansion in a coding versus an expansion in a noncoding region. At this time, only CAG triplet repeat expansions in the coding region of a disease protein have been modeled successfully in *C. elegans* ***(7–9)***. Therefore, this chapter considers the establishment of a *C. elegans* model for CAG expansion/polyQ disorders.

At least eight neurodegenerative diseases are caused by a polyQ expansion in the corresponding protein ***(1–4)***. However, the mechanism by which these polyQ repeats cause neurodegeneration and cell death is unknown. One current hypothesis is that the glutamine expansion alters the conformation of the disease protein, leading to aberrant protein–protein interactions between polyQ expansions and cellular proteins. The promiscuous nature of polyQ tract interactions results in the formation of large protein aggregates that accumulate within the cytoplasm and nucleus of affected tissues ***(10)***. At this time, the role of aggregates in the pathogenic mechanism of polyQ diseases is unclear.

Although the disease proteins are widely expressed, specific tissues are affected in each polyQ disorder. For example, the primary cellular pathology of Huntington's disease is degeneration of neurons of the striatum and cortex, whereas the Purkinje cells of the cerebellum are primarily affected in spinocerebellar ataxia type 1 ***(11,12)***. The vulnerability of certain neurons to a disease protein may be attributable to specific cellular factors within affected tissues. Alternatively, because expanded glutamine tracts of various disease proteins are embedded within differing full-length proteins, the protein context of the polyQ expansion may account for the sensitivity of certain neural tissues to degeneration. Two areas of intensive investigation are elucidating the toxic nature of the polyQ expansion and understanding the selective vulnerability of specific neurons to a mutant protein.

Typically, the symptoms of human polyQ diseases begin midlife. *C. elegans* only lives 25 d at 20°C; the challenge is to model late-onset neurodegeneration in an animal with a short life-span. Two approaches can be undertaken to accelerate the disease process and induce degeneration in a shorter period of time. One strategy is to express fragments of the disease protein containing expanded polyQ tracts in *C. elegans* neurons. Expression of expanded fragments is more toxic than expression of the full-length mutant protein based on several different polyQ disease models ***(3)***. Furthermore, expanded N-terminal huntingtin fragments containing the polyQ tract are found in patients' tissues ***(10)***. Alternatively, the level and duration of mutant protein expression can be increased. This can be accomplished by judicious choice of the *C. elegans* promoter used to express the polyQ disease protein (details presented in **Subheading 3.1.3.**). Both strategies are used in current models of polyQ toxicity in *C.*

elegans ***(7–9)***. It is important to note that models using only the N-terminal huntingtin fragment that contains the polyQ expansion consequently eliminate the majority of the huntingtin protein. Therefore, the contribution of protein context of the polyQ expansion to tissue specific degeneration is limited in existing *C. elegans* models.

The methods described in this chapter outline the generation of the model system (**Subheading 3.1.**), the analysis of the mutant phenotype (**Subheading 3.2.**), and the evaluation of candidate genetic modifiers (**Subheading 3.3.**).

2. Materials

1. *Caenorhabditis elegans* strains and *Escherichia coli* strains (OP50, HT115) are available from the *Caenorhabditis* Genetics Center (www.biosci.umn.edu/CGC/CGChomepage). There is no charge for educational or nonprofit institutions; commercial organizations pay a fee for each strain. *C. elegans* genomic DNA clones are available from the Wellcome Trust Sanger Institute. As of 2003, requests for *C. elegans* genomic DNA clones should be sent to Audrey Fraser (aef@sanger.ac.uk) and Ratna Shownkeen (rs2@sanger.ac.uk). Please indicate a FedEx/DHL account number to cover shipping costs. *C. elegans* cDNA requests can be made to Dr. Yuji Kohara (ykohara@lab.nig.ac.jp) at the National Institute of Genetics.

   Most *C. elegans* RNAi feeding strains can be obtained from Dr. J. Ahringer (www.hgmp.mrc.ac.uk/geneservice/reagents/products) or from Dr. M. Vidal (worfdb.dfci.harvard.edu). As of 2003, the clone coverage in the Ahringer lab collection is about 80% complete, but the clones may contain polymerase chain reaction (PCR) errors. The Vidal lab clone collection is less complete, but the cDNAs are full-length and in the Gateway cloning system designed by Invitrogen (Carlsbad, CA).

   Antisera for the detection of the huntingtin proteins in transgenic animals can be obtained from individual researchers of the Hereditary Disease Foundation consortium (www.hdfoundation.org/antibody.html).
2. *C. elegans* M9 buffer is composed of 3 g KH_2PO_4, 6 g Na_2HPO_4, 5 g NaCl, and 1 mL of 1 *M* $MgSO_4$ per liter. DiD (1,1'-dioctadecyl-3,3,3',3'-tetramethylindodicarbocynanine perchlorate) for dye filling can be obtained from Molecular Probes (Eugene, OR).
3. A compendium of information on *C. elegans* genes, sequences, and literature can be found at www.wormbase.org/ and www.elegans.swmed.edu.
4. The following books provide comprehensive reviews of *C. elegans* biology and methodologies:

C. elegans: *A Practical Approach* (1999), edited by Ian A. Hope, Oxford University Press, Oxford.

C. elegans *II* (1997), edited by Donald L. Riddle, Thomas Blumenthal, Barbara J. Meyer, and James R. Priess, Cold Spring Harbor Laboratory, Cold Spring Harbor, NY.

Caenorhabditis elegans: *Modern Biological Analysis of an Organism* (1995), edited by Henry F. Epstein and Diane C. Shakes, Academic, New York.

The Nematode Caenorhabditis elegans (1988), edited by William B. Wood and the Community of *C. elegans* Researchers, Cold Spring Harbor Laboratory, Cold Spring Harbor, NY.

3. Methods

3.1. Generation of a C. elegans Model

3.1.1. Selecting the Expression Construct

It is widely accepted that a polyQ expansion creates a deleterious "gain-of-function" mutation within the corresponding protein, which contributes significantly to disease pathology ***(2,3)***. Based on this observation, it is possible to study the toxic effects of polyQ expansions on cellular functions by expressing the polyQ tract independent of the polyQ disease protein in various *C. elegans* tissues. Within the *C. elegans* genome, the longest CAG repeat consists of 14 CAGs. Therefore, it is likely that expression of longer CAG expansions within *C. elegans* will disrupt normal cellular function, which will recapitulate many aspects of human disease pathology. Alternatively, the contribution of the protein context of polyQ diseases could be modeled in *C. elegan*s. If the disease gene has a clear *C. elegans* homolog, then CAG expansions can be inserted into the *C. elegans* homolog and expressed in transgenic animals. If proteins that normally interact with a disease protein are found in the model organism, expression of the human mutant disease protein may be sufficient to reproduce the pathology and allow investigation of this mechanism of action (*see* **Note 1**). In our model system, we have successfully reproduced polyQ-dependent neurotoxicity by expressing the N-terminal polyQ-containing fragment of human huntingtin in *C. elegans* ***(9)***.

3.1.2. Designing Constructs Containing Variable Trinucleotide Repeats

The age of onset of disease symptoms is inversely related to the length of the trinucleotide repeat expansion. Therefore, it is important to establish the minimum expansion in the gene of interest that elicits the disease. For example, 20–25 CAG repeats in the huntingtin gene does not cause Huntington's disease, whereas individuals carrying 37–50 CAG repeats develop symptoms midlife ***(4)***. Therefore, an expansion above 37 glutamines within huntingtin ideally leads to neurodegeneration and cell death in *C. elegans* neurons. However, the short life-span of *C. elegans* may require increasing the size of the trinucleotide repeat expansion to observe a toxic effect (*see* **Note 2**). It is best to design numerous disease gene constructs that contain a wide range of expansion sizes, including both toxic and nontoxic lengths (*see* **Note 3**). Overall, a correlation between the size of the expansion and the severity or onset of toxicity should be observed.

3.1.3. Selecting Specific Promoters for Expression

Despite its relative neuronal simplicity, *C. elegans* has different neuronal classes, including motorneurons, sensory neurons, and interneurons ***(13)***. Furthermore, the *C. elegans* nervous system uses a wide range of classical neurotransmitters also found in vertebrate nervous systems. *C. elegans* neurons also have been classified by neurotransmitter usage (*see* **Table 1**). Additional information regarding the classification of *C. elegans* neurons can be found in the book *C. elegans II* and at the WORMBASE website as described in **Subheading 2.** Some triplet repeat diseases affect specific classes of neurons that also are represented in the *C. elegans* nervous system. By

Table 1
Possible Promoters for PolyQ Expression

Gene	Cellular expression pattern	Associated behavior/phenotype	Ref.
elt-2	Intestinal cells	Viability	***14***
lin-26	Hypodermis	Viability	**15**
myo-2	Pharyngeal muscle	Feeding	***16,17***
unc-54	Body wall muscle	Locomotion	***18,19***
unc-119	Pan-neuronal	Locomotion, feeding, egg laying, etc.	***17–20***
unc-25	GABAergic neurons	Coordinated motion	***21***
glr-1	Interneurons and other neurons	Locomotion	***19,22***
osm-10	ASH and three other classes of neurons	Response to chemosensory and mechanosensory stimuli	***23,24–26***
mec-3	ALM, PLM, and other classes of neurons	Response to body touch	***19,27,28***
cat-4	Catacholaminergic neurons	Serotonergic function, including egg laying and locomotion	***29–32***

Note: Promoters of genes listed in column 1 can be used to drive transgene expression in the cells in column 2. Suggested behaviors/phenotypes to assay for polyQ toxicity are listed in column 3. Additional information on behavioral assays can be found in Chapter 11 of *The Nematode* Caenorhabditis elegans.

selecting the appropriate *C. elegans* promoter, it is possible to express the disease gene in a similar type of neuron in *C. elegans* (*see* **Table 1**). Incorporating targeted expression of the disease gene in the *C. elegans* model system may reveal cellular factors that contribute to the vulnerability of that class of neurons in the human disease.

In many neurodegenerative diseases, neuronal dysfunction often precedes any detectable neurodegeneration, and monitoring neuronal dysfunction can provide insight into the early stages of disease pathology. In *C. elegans*, many behavioral assays have been established that can be used to assess the functional integrity of specific neurons (*see* **Table 1**). Behavioral responses to environmental stimuli are mediated through specific neurons. If the neurons responsible for stimulus detection are defective, the behavioral response is perturbed. Often, it is beneficial to design a *C. elegans* model system with expression of the disease gene in neurons required for a specific behavioral response. Changes in the behavioral response indicate neuronal dysfunction. For example, we expressed N-terminal fragments of human huntingtin using the *osm-10* promoter. *osm-10* is expressed in the ASH sensory neurons and in three other classes of sensory neurons. Mechanosensory and chemosensory behavioral assays revealed that polyQ protein expression perturbs the function of the ASH neurons (*see* **Table 1**) ***(9)***. Neri and colleagues established an alternative *C. elegans* model for polyQ neurotoxicity ***(8)***. PolyQ-containing huntingtin fragments are expressed using the *mec-3* in the mechanosensory neurons of the body that detect light touch. Therefore, polyQ protein expression perturbs response to light touch detected by these neurons (*see* **Table 1**).

The level of the disease protein expression may be critical if the disease mechanism is cumulative. Promoters that drive high levels of expression throughout the lifetime of the animal should maximize the toxicity of the disease protein. To ensure that the *C. elegans* promoter selected does not alter the pathogenic mechanism, the nonexpanded (normal) form of the protein should be expressed using the same promoter and should have no effect. Thus, toxicity can be attributed to the polyQ expansion, not heterologous protein expression.

One limitation of *C. elegans* as a model system is that the only characterized inducible promoter is the heat-shock promoter of the *hsp-16* gene. Heat shock results in the expression of various molecular chaperones, which may protect neurons from polyQ insults ***(3,33)***. Therefore, heat-shock-induced expression of polyQ proteins is problematic.

3.1.4. Generating and Selecting Transgenic Lines

C. elegans transgenic lines can be generated by microinjection of concentrated DNA into the gonad of a hermaphrodite (C. elegans *Methods*, Chap. 19). Through a poorly understood process, an extrachromosomal array that contains multiple copies (often hundreds) of the injected DNAs is generated in the gonad. The extrachromosomal array is transmitted to progeny and subsequent replication and segregation resembles that of "real" chromosomes. Each injected parent can generate multiple progeny, each containing a unique array. These progeny and their offspring constitute independent lines of transgenic animals. Given the variable nature of the biological process underlying extrachromosomal array generation, it is important to identify and analyze multiple transgenic lines expressing the disease protein. To ensure that the expression of the disease protein from the extrachromosomal array is responsible for the toxicity observed, multiple transgenic lines should display a similar phenotype, although this may vary in severity.

Generally, the level of transgene expression from an extrachromosomal array is related to the relative concentration of the transgene in the original injection pool. Therefore, the number of copies of a transgene can be varied dramatically during the generation of transgenic lines (*see* **Note 4**). The neuron-specific promoters discussed earlier can yield dramatically different levels of expression depending on transgene copy number. To ensure that the *C. elegans* transgene copy number does not alter the pathogenic mechanism, multiple transgenic lines expressing similar amounts of the nonexpanded (normal) form of the protein should be examined and should have no effect. Thus, toxicity can be attributed to the polyQ expansion and not gene dosage.

An extrachromosomal array is not as stable as a chromosome. An array has a finite chance of being lost at each cell division, yielding a mosaic animal or nontransgenic progeny. Stability in mitosis and meiosis is usually correlated. Therefore, transgenic lines with a high percentage of transgenic progeny have less cellular mosaicism in each animal and should be retained for analysis. Less cellular mosaicism ensures that the extrachromosomal array will be found more frequently in the cell(s) of interest in a population of animals.

Several approaches can be used to confirm the presence of the transgene array in the cell(s) being assayed. This is critical because the cellular mosaicism of extrachro-

mosomal arrays complicates analysis. One option is to tag the disease protein with GFP (green fluorescent protein), so that cells expressing the disease protein–GFP fusion can be identified by fluorescence microscopy. If expression of the GFP-tagged disease protein results in toxicity in *C. elegans* neurons, then it is important to generate transgenic lines that express the untagged version of the disease protein. These can be used to confirm that the same toxic effects are caused by the untagged polyQ protein and that toxicity is not caused by the addition of GFP. If the presence of the GFP tag alters the toxic effects of the disease protein, it should not be used for detection. The second option for detecting the presence of the transgene array in the cells of interest is to label the cells, not the protein, with GFP (*see* **Fig. 1**). A promoter::GFP construct that drives expression in the cell(s) of interest is added to the DNA injection pool when generating transgenic lines. Cells that carry the transgene array will express both the disease protein and GFP (*see* **Note 5**). Alternatively, immunohistology can be used to detect polyQ transgenes in individual animals, but this approach is prohibitively laborious.

Before embarking on the genetic analyses described next, it is generally advisable to integrate (insert into a chromosome) the extrachromosomal array containing the polyQ transgene. Extrachromosomal arrays must be selected every generation because of meiotic instability. However, arrays that have been integrated into a chromosome are stable in meiosis/mitosis and display Mendelian segregation. Integration dramatically reduces complexity in genetic crosses and screens. Standard techniques (C. elegans *Methods*, Chap. 19) have already been established for inducing double-stranded breaks in chromosomes and selecting for array insertion events. Occasionally, the expression level of an integrated transgene is lower than the original extrachromosomal array, reducing the severity of the polyQ phenotype.

3.2. Examination of Phenotype

Once transgenic lines expressing the disease form of your protein of interest are established, pathological similarities between targeted *C. elegans* neurons and human disease neurons can be evaluated (*see* **Note 6**). In humans, the onset of symptoms begins with the dysfunction of a specific subset of neurons. At the cellular level, axonal and dendritic neuronal processes degenerate and neurons eventually undergo cell death. The function and integrity of *C. elegans* neurons expressing the disease protein can be easily assessed using multiple techniques.

3.2.1. Effect of Trinucleotide Repeat Expansion on Neuronal Function

The toxic effects of a polyQ transgene on neuronal function can be determined by testing behavior as described in **Subheading 3.1.3.** and in **Table 1**. Once a decline in a behavioral response is established, it is important to determine if the loss of neuronal function associated with the loss of behavior is caused by the polyQ expansion. Therefore, behavior must be normal when the disease protein lacking an expansion is expressed. Note that in some cases, expression of the unexpanded polyQ disease protein is toxic ***(34)***.

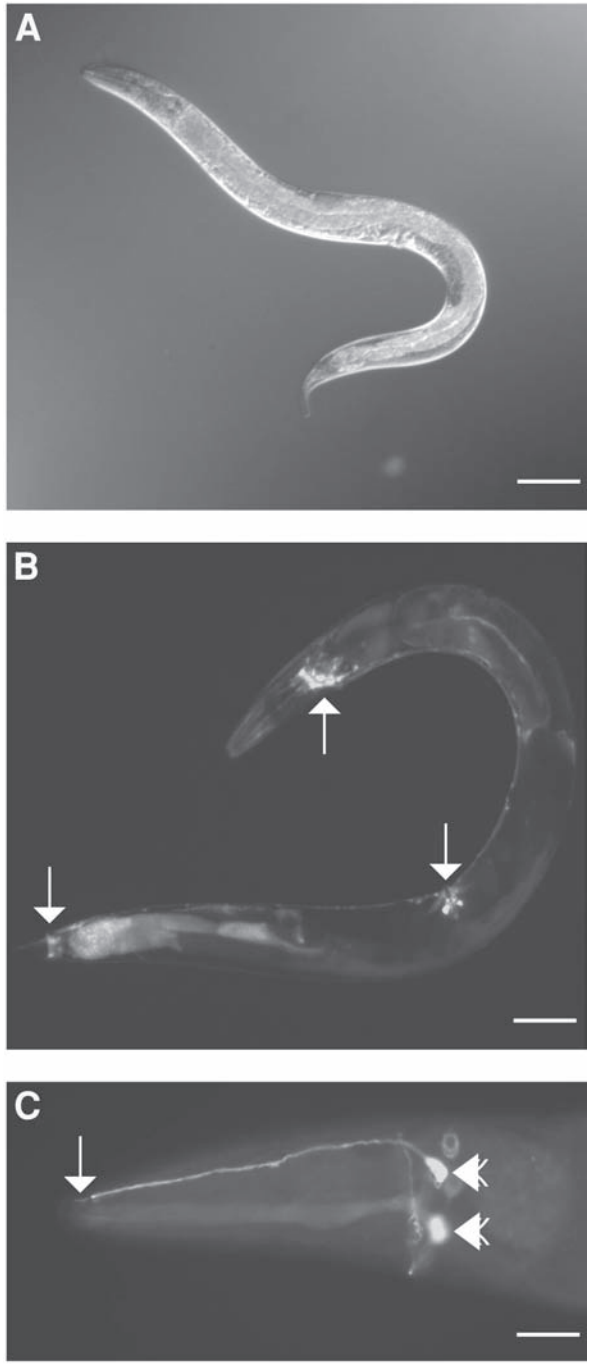

Fig. 1. *Caenorhabditis elegans* and GFP in neurons. **(A)** A Nomarski image of an adult hermaphrodite (bar = 100 μm). **(B)** Using a G protein-coupled receptor kinase (NCBI designation W02B3.2) promoter to drive GFP expression, numerous *C. elegans* neurons can be visualized.

3.2.2. Effect of Trinucleotide Repeat Expansion on Neurodegeneration and Death

Neurodegeneration is an obvious indicator of the toxicity associated with expression of polyQ expansions. To assess degeneration in *C. elegans*, the neuronal morphology can be examined at either the light or electron microscope level to observe changes in size, location, or shape. Recognition and identification of neurons that express the polyQ disease protein can be facilitated by expressing GFP in the neurons of interest from an extrachromosomal array (*see* **Subheading 3.1.4.** for details). Neurons expressing the GFP transgene can be rapidly evaluated for axonal/dendritic process retraction, morphology changes, or cell death.

If the polyQ disease proteins are expressed in the ASH neurons, an alternative technique can be used. Dye filling with the vital dye DiD is a rapid technique for evaluating the morphology of ASH neurons. The distal tip of the ASH neuron sensory process is exposed to the environment. DiD, a lipophilic, fluorescent compound, is taken up by ASH and seven other classes of sensory neurons, which are exposed to the environment at the distal tip of their sensory processes ***(35)***. The fluorescent compound diffuses through the lipid compartments of the neurons allowing visualization of the cell body and axonal process. Because dye filling requires an intact sensory process in contact with the environment, this sensitive technique can be used to assess degeneration of the ASH sensory ending ***(35)***.

If expression of a disease protein leads to degeneration of the sensory process of ASH neurons or if the ASH neurons die, then they will fail to fill with dye. Death can be distinguished from sensory process degeneration by simultaneously monitoring the GFP in the ASH neurons expressed from the polyQ-containing extra chromosomal array. Simultaneous loss of GFP expression and loss of dye filling are usually caused by death of the neuron; ASH neurons that cannot dye fill but do express GFP have defective sensory processes but are not dead. Neurons lacking the polyQ transgene resulting from array mosaicism fill with dye but do not express GFP. To confirm that neurons are dying, the presence of an endogenous protein normally expressed in the neurons of interest should be assayed by immunohistochemical methods. For example, immunohistochemical detection of OSM-10, an endogenous *C. elegans* protein expressed in ASH neurons, can be used to verify the presence or absence of ASH neurons ***(23)***.

3.2.2.1. Dye-Filling Protocol

To assay ASH neurons by dye filling, animals are washed off the culture plate with *C. elegans* M9 buffer and DiD is added at 100 ng/μL. After rocking at 25°C for 2 h,

---

Figure 1 (*continued*) The white arrows point out tail neurons, head neurons, and vulval neurons (from left to right). Transgene expression of GFP often leads to promiscuous intestinal GFP expression located in the posterior region of the animal. The biological significance, if any, of this expression is unclear (bar = 50 μm). **(C)** Two white arrowheads indicate cell bodies of the bilateral ASH sensory neurons located at the head of the animal highlighted by GFP expression from the *osm-10* promoter ***(23)***. Additionally, the single white arrow indicates the ASH sensory process that is visible in this focal plane (bar = 10 μm).

animals are spun down at 400*g* for 2 min and placed onto nematode growth medium (NGM) plates previously spread with OP50 *E. coli*. After 15–30 min, animals are mounted to assay ASH survival based on DiD fluorescence at high-power magnification (*see* **Note 7**).

3.2.3. Recapitulating Additional Disease Aspects: Aggregate Formation

One hallmark of polyQ diseases is the formation of intracellular aggregates containing the expanded disease protein ***(2–4,10,33)***. PolyQ tracts shorter than 36 Qs in disease proteins are not toxic and do not aggregate in patients' tissues. Aggregates are detected first within the cytoplasm and then in the nucleus in affected neurons. The role, if any, of aggregates in polyQ disease toxicity is unclear. The controversy lies in whether the aggregates are neurotoxic, neuroprotective, or simply correlative.

Two different approaches can be used to assess the formation of aggregates in affected *C. elegans* neurons. The disease protein itself can be tagged with GFP and aggregates can be visualized within the live animal using fluorescence microscopy. If aggregation is observed, it is important to determine if the GFP tag has any effect on the aggregation state of the disease protein. Untagged polyQ proteins should be analyzed using antisera that recognize the disease protein itself and confirm that aggregation patterns are similar with and without the GFP tag. Because aggregate formation is dependent on the presence of an expanded polyQ tract in human disease pathology, aggregates should only be observed in animals expressing disease proteins with expanded polyQ tracts. If aggregates are found in animals expressing the normal (nonexpanded) form of the protein, the *C. elegans* model may not accurately replicate the human disease pathology (*see* **Note 8**).

3.2.4. Assaying Age-Dependent Effects of Neurodegeneration

A common feature of human polyQ disorders is their progressive nature; incidence and severity of neuronal dysfunction and degeneration increase with age ***(4)***. This aspect of polyQ diseases can be easily evaluated in the *C. elegans* model system. Typically, it takes 3 d for an animal raised at 25°C to grow from an egg to a young adult and begin to produce progeny. Animals raised at 25°C for longer time periods are considered "aged" animals. Time-points between 8 and 10 d often are selected for analysis of toxic effects in aged animals. Given the progressive nature of polyQ diseases, polyQ disease protein toxicity should be assessed in both young and aged animals. Incidences of neurodegeneration, cell death, behavioral defects, and morphological changes should intensify with increasing age.

Aged animals are often difficult to distinguish from younger adults in a mixed culture, given the short *C. elegans* life cycle. To determine if toxicity increases with age, animals of specific ages must be isolated for assessment. One simple remedy is to passage single worms to a new culture plate each day over the desired time period. Alternatively, populations of aging animals can be sterilized using pharmacological techniques. Specifically, FUDR (5-fluorodeoxyuridine) has been used in laboratories that study aging in *C. elegans,* but the effect of FUDR on polyQ toxicity has not been established.

3.2.4.1. FUDR Protocol

Animals are grown at 25°C on NGM plates that have been spread with OP50 *E. coli.* Once animals have reached the late larval stage, they are transferred to NGM plates containing FUDR at 0.1 mg/mL. Animals can be scored for mutant phenotypes at desired times, 1–5 d after transfer.

3.3. Identifying and Evaluating Genetic Modifiers and Pathways

One of the advantages of *C. elegans* is the rapidity with which previously characterized genes can be examined for their role in the disease process. In addition to the pathways described in **Subheading 3.3.1.**, many other biochemical and signaling pathways are conserved between *C. elegans* and human neurons. The role of candidate modifier genes can be tested if previously characterized mutations in such genes exist or by inhibiting candidate gene function by RNAi/siRNA techniques.

3.3.1. Pre-Established Genetic Pathways

Genes and pathways that control cell death, aging, and synaptic signaling have been intensely studied in *C. elegans*. Thus, *C. elegans* provides the genetic framework for addressing outstanding questions in the polyQ disease field. How and why do neurons die? Does the age of the neuron increase sensitivity to expanded polyQ repeats? Does neuronal or synaptic activity affect age of onset or severity? These and other questions can be addressed in the *C. elegans* model using genetic tests.

3.3.1.1. Apoptosis and Necrosis

Cell death pathways have been well characterized in *C. elegans* ***(36)***. Therefore, the mechanism of cell death at work in *C. elegans* triplet repeat disease models can be readily determined using morphological criteria and pre-existing mutations.

In addition to the differences in the genetic/biochemical pathways activated in apoptosis versus necrosis described here, the morphological characteristics of these processes observed at the light microscope level are distinct. Apoptosis, or programmed cell death, is the normal fate of specific cells during development, but apoptosis can also be activated by degenerative diseases ***(37)***. Under Nomarski illumination, apoptosis is evidenced by the "flattening" of the cell body followed by rapid disappearance of the dying cell, usually within hours ***(36)***. Necrotic cell death is frequently caused by injury, ion channel misregulation, and activated signaling pathways. Necrotic death is a slower process; the dying cell is often dramatically swollen and may not disappear for days ***(38)***.

Mutations have been identified in specific genes that can block apoptosis and/or necrosis. In *C. elegans,* apoptosis can be blocked by mutations in the *cell death defective* (*ced*) genetic pathway. Mutations in genes upstream in the pathway (e.g., *ced-3* and *ced-4*) prevent entry into apoptosis, but mutations in downstream "effector" *ced* genes prevent engulfment and removal of dying cells. *ced-3* encodes a *C. elegans* caspase and *ced-4* encodes a protein similar to mammalian Apaf-1, which activates caspases that effect cell death. Of particular interest is the fact that *ced-3* encodes the

only *C. elegans* caspase that plays a role in cell death, as opposed to the numerous functional caspases found in vertebrates. Apoptosis is completely blocked in animals lacking *ced-3* or *ced-4* gene function, but they are viable and fecund.

Necrotic cell death in *C. elegans* caused by ion channel misregulation or activated G-proteins can be blocked by mutations in *calreticulin-1* (*crt-1*) ***(39)***. Calreticulin normally regulates calcium storage and release from the endoplasmic reticulum; loss of *crt-1* function dramatically decreases necrotic cell death. "Effector" *ced* genes are also required for the removal of necrotic cell corpses ***(38)***.

3.3.1.2. Aging

The symptoms and cell death associated with human polyQ diseases occur late in life, suggesting that age is a factor in disease pathogenesis. The effect of aging in the polyQ disease model can be examined by using mutations that perturb aging. Single gene mutations in *C. elegans* can alter the aging process and these mutant backgrounds can be used to examine the effects of aging on triplet repeat disease pathology. The biochemical mechanisms underlying aging seem to be conserved in all species: insulin signaling, metabolic regulation, and caloric restriction ***(40,41)***. *daf-2* encodes the insulin receptor critical for modulating life-span, and loss of *daf-2* function dramatically increases *C. elegans* life-span. Genes that act downstream of *daf-2* include *age-1, daf-18*, and *daf-16*, which encode a phosphatidylinositol 3 (PI3) kinase, a homolog of the tumor suppressor PTEN (the phosphatase and tension homolog deleted on chromosome 10) and a forkhead class transcription factor, respectively. Genes independent of the insulin signaling pathway that affect aging have also been identified, including *clk-1*, which encodes a homolog of the yeast protein COQ9 and is necessary for the biosynthesis of ubiquinone.

3.3.1.3. Synaptic Signaling

It has been suggested that excessive or prolonged synaptic signaling contributes to neuronal cell death in polyQ diseases ***(42)***. In normal synaptic function, glutamate binds to a variety of excitatory amino acid receptors, which are ligand-gated ion channels. The binding of glutamate activates these receptors, leading to depolarization and excitation. Continuous activation will damage target neurons, leading to cell death. Direct administration of excitatory amino acids into the nervous system replicates a pattern of neuronal death that resembles that of certain polyQ diseases ***(43,44)***.

Many *C. elegans* mutations have been identified that affect neuronal activity by perturbing synaptic release and channel function ***(45)***. As most of the cells in the *C. elegans* nervous system are dispensable for maintenance in the laboratory, the effect of synaptic signaling on neurodegeneration can be assessed readily in *C. elegans*. For example, loss-of-function mutations in two genes that encode proteins critical for synaptic release, *synaptotagmin-1* (*snt-1*) and *synaptobrevin-1* (*snb-1*), result in viable but profoundly uncoordinated animals.

When neuronal activation becomes excessive or prolonged, it can exacerbate polyQ toxicity. In *C. elegans*, dominant mutations in ion channel subunits that increase neu-

ronal activity can be examined. Dominant mutations in the *expulsion defective-2 (exp-2)* gene decrease the function of a potassium channel critical for repolarization in most *C. elegans* neurons ***(46,47)***. This generally results in increased neuronal activity. Increasing sodium influx can also enhance the activity of neurons. Gain-of-function mutations in the *deg-1, mec-4*, or *mec-10* mechanosensory channels cause increased sodium influx, hyperactivity, and, in some cases, cell death ***(45,48)***. These genes are expressed in specific types of sensory neuron, but transgenes containing the leaky channels can be expressed in the cells of interest using alternative promoters.

3.3.2. Assessing Genetic Modifiers Using RNAi

Double-stranded (ds) RNA-mediated inhibition (RNAi) can rapidly decrease the functional expression of a *C. elegans* gene or transgene ***(49)***. RNAi is of widespread utility in multicellular organisms as an experimental technique and takes advantage of endogenous mRNA regulatory mechanisms. Expression of dsRNA identical to a target cellular mRNA results in efficient and long-lasting degradation of the corresponding cellular mRNA. The biochemical pathways underlying this inhibition are under investigation.

The RNAi-based technology permits researchers to test a large number of candidate mutations and to undertake nonrandom reverse genetic screens. There are several techniques for delivery of dsRNA: injection, feeding, soaking, or foldbacks ***(49–52)***. dsRNA corresponding to the gene of interest can be injected into the gonad of the hermaphrodite parent to examine the effect of gene function loss in the progeny. The technique is very effective for inhibition of genes involved in embryogenesis or early larval stages but has little utility in adult stages. Feeding *C. elegans* dsRNA in individual bacterial strains increases the scale and rapidity of the analysis, but careful controls must be done to confirm that the gene of interest is decreased in the tissue of interest. Importantly, feeding dsRNA rarely inhibits genes expressed in the adult nervous system. Similar problems in nervous system sensitivity confound soaking techniques. Although soaking larval stage animals in purified dsRNA can inhibit the expression of some genes, those expressed in the adult nervous system are rarely affected.

The most reproducible, but laborious, approach is to express a dsRNA using a *C. elegans* promoter in transgenic animals. Transgenic animals are generated that express a foldback (inverted repeat) of a cDNA fragment under the control of a *C. elegans* promoter. The self-annealing of the inverted cDNA repeat into dsRNA initiates RNAi in the expressing cells. This is more effective than expressing sense and antisense using the same promotor and dramatically more effective than feeding or soaking for nervous system genes. The use of specialized RNAi sensitive strains (e.g., *rrf-3*) sometimes dramatically increases sensitivity to RNAi, but this is not effective for all neurons ***(53,54)***.

The magnitude of the RNAi inhibition varies with technique, genotype, gene targeted, and neuronal accessibility. Given this possible variation, the RNAi decrease of a specific target gene must be confirmed by independent means (immunohistology or a cellular phenotype) within the cell of interest before conclusions can be drawn from RNAi experiments.

Table 2
Suggested Mutant Alleles in Genetic Pathways of Interest

Gene	Specific allele	Gene	Specific allele
ced-3	*n717*	*clk-1*	*e2519*
ced-4	*n1162*	*exp-2*	*sa26*
crt-1	*bz29* ***(39)***	*snt-1*	*md290*
daf-2	*e1370*	*snb-1*	*md247*
age-1	*hx546*	*deg-1*	*u506*
daf-18	*e1375*	*mec-4*	*u231* ***(39)***
daf-16	*mgDf47*	*mec-10*	*e1515*

Note: Gene names are listed in columns 1 and 3. Specific alleles for analysis are suggested in columns 2 and 4. Ordering information for strains carrying the recommended allele along with the proper references are available at www.biosci.umn.edu/CGC/CGChomepage.

3.3.3. Selecting and Obtaining Mutant Alleles of Candidate Modifier Genes

The choice of the mutant allele of the genetic modifier is just as critical as the choice of which genetic modifier to test. Based on standard genetic principles, a complete loss of function or null allele is preferable. The use of partial-loss-of-function alleles is sometimes necessary when loss of gene function results in sterility or lethality. The use of partial-loss-of-function alleles does have several drawbacks. Primarily, no firm conclusions can be drawn if the partial-loss-of-function allele has no effect. Partial-loss-of-function alleles may affect some tissues or functions more than others. Furthermore, a complete-loss-of-function allele may suppress or enhance, whereas a weak-loss-of-function allele may have no effect. Gain-of-function alleles have similar caveats: The allele may not act in the cell/time of interest or the gain of function may not be severe enough to perturb polyQ toxicity.

Suggested alleles for initial analyses of the pathways described above can be found in **Table 2**. Most can be obtained from the *C. elegans* Genetics Center at no cost to academic laboratories. Individual *C. elegans* laboratories will usually honor reasonable requests for published alleles and reagents.

3.3.4. Assessing Genetic Modifiers Using Mutational Analysis

To test genetic modifiers, it is necessary to introduce them into the polyQ transgene background. Genetic modifiers generally are introduced as mutant alleles of *C. elegans* genes. Recessive and dominant modifier alleles should be assayed as homozygous strains. In both cases, molecular and/or genetic criteria can be used to confirm the genotype of the animals in each experiment.

Crossing arrays and constructing strains is usually straightforward. Males used to initiate genetic crosses can be generated by mating or by heat shock (incubate L4 hermaphrodites, which are too immature to mate, at 30°C for 6 h). Males can be made from either the genetic modifier or the polyQ strain, but transmission of extrachromosomal transgene arrays from males to hermaphrodite progeny is relatively infrequent.

Males tend to segregate extrachromosomal arrays to sperm lacking an X chromosome that accordingly generate male progeny; no such bias exists for integrated arrays.

To control for possible genetic background effects or array instability, it is recommended that the transgene be reisolated with and without the genetic modifier. Alternatively, once the transgene is scored in a genetic modifier background, it can be returned to a wild-type genetic background by an additional mating to confirm transgene stability. This allows the researcher to internally control for genetic background effects and rare array instability.

Proving that the mutant *C. elegans* allele of the genetic modifier being assessed is present and homozygous in the polyQ strain to be analyzed is essential. Null alleles that are generated by the *C. elegans* knockout consortium (http://celegansKO consortium.omrf.org/) contain small deletions and have polymerase chain reaction (PCR)-based genotyping assays that facilitate genotyping. Many mutations in previously characterized alleles cause a single nucleotide polymorphism, which can be assayed as a restriction fragment length polymorphism (RFLP) by PCR and subsequent restriction digest. It may also be convenient to balance a genetic modifier mutation with another closely linked mutation that has a visible phenotype (*see* **Fig. 2**). For example, *ced-4* is located very near *dumpy-17* (*dpy-17*) on chromosome 4 ***(54)***. If *ced-4* males are crossed to *dpy-17* mutant animals carrying an integrated *[polyQ,GFP]* transgene on a different chromosome (*dpy-17;[polyQ,GFP]),* then all cross-progeny that are not Dumpy must have the genotype *dpy-17/ced-4;[polyQ,GFP]* /+ (*see* **Fig. 2**). These animals are allowed to segregate progeny. GFP-expressing animals that are not Dumpy are put on individual plates so that individual broods can be examined. Individual plates with no Dumpy progeny are homozygous for *ced-4*; plates on which all progeny express GFP are homozygous for the polyQ transgene.

3.3.5. Current C. elegans *Models of PolyQ Disease*

The three previously published models of polyQ toxicity in *C. elegans* are described here. In the model established by Neri and colleagues, N-terminal fragments of huntingtin fused to GFP were expressed in ALM and PLM mechanosensory neurons of the body ***(8)***. Expression, using the *mec-3* promoter, of expanded polyQ tracts (Q128), but not unexpanded tracts (Q19), caused behavioral defects and axonal perturbations. However, the aggregation of polyQ fragments did not correlate with polyQ tract length in this model. Strengths of this model include the expression in neurons of huntingtin fragments and behavioral assessment of neuron dysfunction.

In the model established by Hart and colleagues, larger N-terminal fragments of huntingtin were expressed in the ASH sensory neurons using the *osm-10* promoter ***(9)***. Only huntingtin fragments containing the longest expanded polyQ tract (Q150 vs Q23) resulted in sensory process degeneration, aggregation, and perturbed function of the neurons. Neural dysfunction and degeneration, along with aggregate formation, increased with the age of the animal. The progressive nature of polyQ-mediated degeneration demonstrated in this model recapitulates the disease progression in humans. Advantages of this model are the expression of the polyQ transgene in neurons, the differential toxicity of the expanded versus unexpanded huntingtin polyQ tracts, and behavioral assessment of neuron dysfunction.

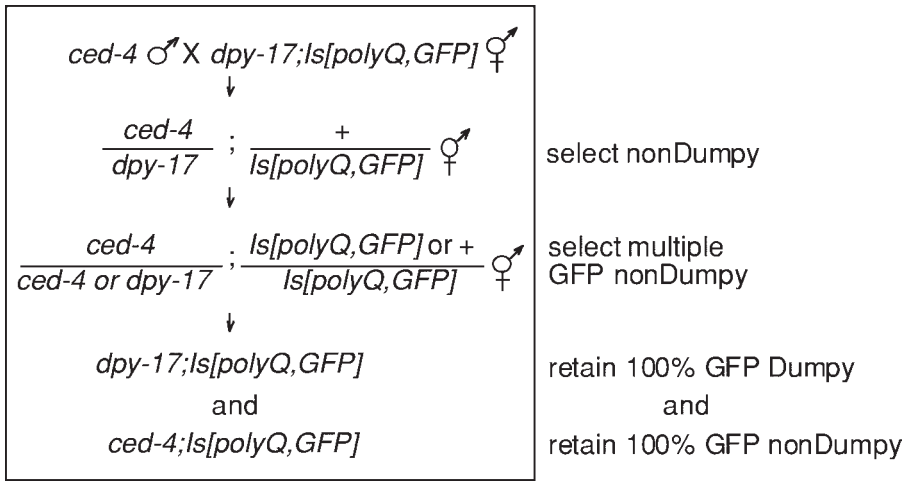

Fig. 2. Introducing candidate modifier genes into polyQ transgene strains. All (trans)genes are recessive and homozygous unless otherwise indicated; GFP expression can be visualized in heterozygous animals. *ced-4* males are crossed (line 1) to *dpy-17;[polyQ,GFP]* hermaphrodites, which are Dumpy because of the homozygous *dpy-17* mutation and express the polyQ transgene and GFP from the same integrated array. In the next generation (line 2), self-progeny are Dumpy and discarded; cross-progeny are not Dumpy and will express GFP. Individual L4 hermaphrodites (which are too immature to mate) are distributed on individual agar plates spread with *E. coli* OP50 and allowed to self-fertilize. In the next generation (line 3), Dumpy animals are disregarded as *dpy-17* homozygous animals. Non-Dumpy animals are either *ced-4* or *ced-4/dpy-17*, but these genotypes cannot be distinguished using a dissecting microscope. Non-Dumpy animals that express GFP must carry one or two copies of the array. So, multiple GFP-expressing non-Dumpy animals are distributed on individual agar plates spread with *E. coli* OP50 culture plates and allowed to self-fertilize. The next generation is examined (lines 4 and 5) on each plate. Plates that contain homozygous populations that are non-Dumpy and express GFP must be of the genotype *ced-4;[polyQ,GFP]*. At least one of these strains is retained for analysis (line 5). Plates that contain one-fourth Dumpy animals and 100% GFP-expressing animals must contain the progeny of a *ced-4/dpy-17;[polyQ,GFP]* animal. A Dumpy animal is selected from at least one of these strains to establish a *dpy-17;[polyQ,GFP]* strain for confirmation of transgene stability and to control for genetic background effects (line 4).

Morimoto and colleagues established a model in which expanded and unexpanded polyQ tracts (Q19 and Q82) tagged with GFP were expressed in pharyngeal and body wall muscles using the *myo-2* and *unc-54* promoters, respectively *(7)*. Aggregation of polyQ fragments along with a delay in development was observed with expression of the expanded polyQ tract but not the unexpanded forms. Furthermore, aggregation and developmental delay increased with age, reminiscent of human disease progression. Advantages of this system include the relatively higher sensitivity of muscles to RNAi by feeding and the possible use of motility/survival assays.

Each of these models has specific advantages and clearly demonstrates the relative ease with which aspects of polyQ toxicity can be modeled in *C. elegans*. All display

polyQ tract length dependence and two display age dependence reminiscent of polyQ diseases in patients. Cytoplasmic polyQ aggregates are observed in each model, although nuclear aggregates have not been documented. Possibly, the short *C. elegans* life cycle does not allow sufficient time for accumulation and detection of nuclear aggregates. Current research efforts in this field are directed toward identification and characterization of genetic modifiers of polyQ toxicity, screening for therapeutic drugs and modeling other diseases. Utilization of these and future models in *C. elegans* should reveal common mechanisms underlying triplet repeat diseases.

4. Notes

1. If the disease gene of interest has a *C. elegans* homolog, the expanded polyQ phenotype may be dramatically affected by the presence of the homologous *C. elegans* protein. Therefore, it may be important to delete the *C. elegans* homolog before establishing the disease model. A deletion of any *C. elegans* gene may be requested at no cost from the *C. elegans* gene knockout consortium (http://elegansKOconsortium.omrf.org). Although technical progress has been made, the time between requesting and obtaining a deletion can be years.
2. In our model, polyQ-induced neurodegeneration was observed in huntingtin fragments containing approx 150 CAG repeats, more than three times the minimum pathological length in human neurons. This may be the result of the relatively short *C. elegans* lifespan.
3. It has been observed that large polyQ tracts can expand or contract during transformation into bacteria. After amplifying polyQ constructs in *E. coli*, the size of the expansion should be confirmed.
4. Researchers should consider the importance of the relative concentration of DNA containing the disease gene in the injection pool when making transgenic strains. Too much can be toxic and too little may have no effect. The disease gene construct should range from a final DNA concentration of 5–500 ng/μL in the DNA injection pool, but the concentration of other DNAs in the injection pool is often a constant determined by previous experiments. Of course, the same concentration must be used for nonexpanded forms of the disease gene to ensure that the toxic effects are the result of the trinucleotide repeat expansion.
5. An alternative approach is the construction of an artificial operon. The *C. elegans* genome normally contains operons. A transgene can be constructed in which the promoter of interest drives GFP expression and the polyQ-containing protein. The coding sequences are placed in tandem behind the promoter separated by an operon intervening sequence (IVS). Details on IVS sequence and operons can be found in Chapter 6 of *C. elegans II*.
6. Phenotypic analyses should be performed on animals raised at 15°C, 20°C, and 25°C. In our model, incidence of polyQ-mediated neurodegeneration and cell death increased with temperature.
7. Typically, 10–15 worms are mounted onto an agarose pad (2% agarose in M9 buffer). Excessive movement of the worms will hinder visualization of the dye-filled neurons. To remedy this problem, sodium azide (final concentration of 15 m*M*) can be added to the 2% agarose mixture. However, because prolonged exposure to sodium azide is toxic to cells, it is best to immediately view the dye-filled neurons after mounting the worms.
8. If aggregates are found in animals expressing the normal (nonexpanded) form of the pro-

tein, reducing the overall expression level of the expanded and nonexpanded form of the protein should be tried. This can be accomplished by lowering the final DNA concentration of the disease gene and normal gene in the DNA injection pool. Alternatively, a promoter that has a lower expression level can be used.

Acknowledgments

The authors thank D. Ferkey, P. Fisette, A. K. Jones, A. E. Pasquinelli, and D. Srinivasan for critically reading the manuscript. We thank A. E. Pasquinelli and H. Fukuto for photos of *C. elegans* and its neurons. This work was supported by a Hereditary Disease Foundation postdoctoral fellowship to C. Voisine and NINDS to A. C. Hart.

References

1 Zoghbi, H. Y. and Orr, H. T. (2000) Glutamine repeats and neurodegeneration. *Annu. Rev. Neurosci.* **23,** 217–247.

2 Ross, C. A. (2000) PolyQ pathogenesis: emergence of unifying mechanisms for Huntington's disease and related disorders. *Neuron* **35 (5),** 819–822.

3 Orr, H. T. (2001) Beyond the Qs in the polyQ diseases. *Genes Dev.* **15,** 925–932.

4 Tobin, A. J. and Signer, E. R. (2000) Huntington's disease: the challenge for cell biologists. *Trends Cell Biol.* **10 (12),** 531–536.

5 Campuzano, V., Montermini, L., Molto, M. D., et al. (1996) Friedreich's ataxia: autosomal recessive disease caused by an intronic GAA triplet repeat expansion. *Science* **271 (5254),** 1423–1427.

6 Campuzano, V., Montermini, L., Lutz, Y., et al. (1997) Frataxin is reduced in Friedreich ataxia patients and is associated with mitochondrial membranes. *Hum. Mol. Genet.* **6 (11),** 1771–1780.

7 Satyal, S. H., Schmidt, E., Kitagawa, K., et al. (2000) PolyQ aggregates alter protein folding homeostasis in *Caenorhabditis elegans. Proc. Natl. Acad. Sci. USA* **97 (11),** 5750–5755.

8 Parker, J. A., Connolly, J. B., Wellington, C., et al. (2001) Expanded polyQs in *Caenorhabditis elegans* cause axonal abnormalities and severe dysfunction of PLM mechanosensory neurons without cell death. *Proc. Natl. Acad. Sci. USA* **98 (23),** 13,318–13,323.

9 Faber, P. W., Alter, J. R., MacDonald, M. E., et al. (1999) PolyQ-mediated dysfunction and apoptotic death of a *Caenorhabditis elegans* sensory neuron. *Proc. Natl. Acad. Sci. USA* **96 (1),** 179–184.

10 DiFiglia, M., Sapp, E., Chase, K. O., et al. (1997) Aggregation of huntingtin in neuronal intranuclear inclusions and dystrophic neurites in brain. *Science* **277 (5334),** 1990–1993.

11 Vonsattel, J. P., Meyers, R. H., Stevens T. J., et al. (1985) Neuropathological classification of Huntington's disease. *J. Neuropathol. Exp. Neurol.* **44 (6),** 559–577.

12 Zoghbi, H. Y. and Orr, H. T. (1995) Spinocerebellar ataxia type 1. *Semin. Cell Biol.* **6 (1),** 29–35.

13. White, J. G., Southgate, E., Thompson, J. N., et al. (1976) The structure of the nervous system of the nematode *Caenorhabditis elegans*. *Phil. Trans. R. Soc. (Lond.)* **B (314),** 1–340.

14 Fukushige, T., Hawkins, M. G., and McGhee, J. D. (1998) The GATA-factor elt-2 is essential for formation of the *Caenorhabditis elegans* intestine. *Dev. Biol.* **198(2),** 286–302.

15 Labouesse, M., Hartwieg, E., and Horvitz, H. R. (1996) The *Caenorhabditis elegans* LIN-26 protein is required to specify and/or maintain all non-neuronal ectodermal cell fates. *Development* **122(9),** 2579–2588.
16 Gaudet, J. and Mango, S. E. (2002) Regulation of organogenesis by the *Caenorhabditis elegans* FoxA protein PHA-4. *Science* **295(5556),** 821–825.
17 Davis, M. W., Somerville, D., Lee, R. Y., et al. (1995) Mutations in the *Caenorhabditis elegans* Na,K-ATPase alpha-subunit gene, eat-6, disrupt excitable cell function. *J. Neurosci.* **15(12),** 8408–8418.
18 Miller, D. M., 3rd, Olson, J. S., Pflugrath, J. W., et al. (1983) Differential localization of two myosins within nematode thick filaments. *Cell* **34(2),** 477–490.
19 Chalfie, M., Sulston, J. E., White, J. G., et al. (1985) The neural circuit for touch sensitivity in *Caenorhabditis elegans*. *J. Neurosci.* **5(4),** 956–964.
20 Maduro, M. and Pilgrim, D. (1995) Identification and cloning of unc-119, a gene expressed in the *Caenorhabditis elegans* nervous system. *Genetics* **141(3),** 977–988.
21 McIntire, S. L., Jorgensen, E., and Horvitz, H. R. (1993) Genes required for GABA function in *Caenorhabditis elegans*. *Nature* **364(6435),** 334–337.
22 Hart, A. C., Sims, S., and Kaplan, J. M. (1995) Synaptic code for sensory modalities revealed by *C. elegans* GLR-1 glutamate receptor. *Nature* **378(6552),** 82–85.
23 Hart, A. C., Kass, J., Shapiro, J. E., et al. (1999) Distinct signaling pathways mediate touch and osmosensory responses in a polymodal sensory neuron. *J. Neurosci.* **19,** 1952–1958.
24 Bargmann, C. (1993) Odorant selective genes and neurons mediate olfaction in *C. elegans*. *Cell* **74,** 515–527.
25 Kaplan, J. M. and Horvitz, H.R. (1993) A dual mechanosensory and chemosensory neuron in *C. elegans*. *Proc. Natl. Acad. Sci. USA* **90,** 2227–2231.
26 Troemel, E. R., Chou, J. H., Dwyer, N. D., et al. Divergent seven transmembrane receptors are candidate chemosensory receptors in *C. elegans*. *Cell* **83,** 207–218.
27 Way, J. C. and Chalfie, M. (1989) The mec-3 gene of *Caenorhabditis elegans* requires its own product for maintained expression and is expressed in three neuronal cell types. *Genes Dev.* **3(12A),** 1823–1833.
28 Chalfie, M. and Sulston, J. (1981) Developmental genetics of the mechanosensory neurons of *Caenorhabditis elegans*. *Dev. Biol.* **82(2),** 358–370.
29 Loer, C. M. and Kenyon, C. J. (1993) Serotonin-deficient mutants and male mating behavior in the nematode *Caenorhabditis elegans*. *J. Neurosci.* **13(12),** 5407–5417.
30 Desai, C., Garriga, G., McIntire, S. L., et al. (1988) A genetic pathway for the development of the *Caenorhabditis elegans* HSN motor neurons. *Nature* **336(6200),** 638–646.
31 Trent, C., Tsuing, N., and Horvitz, H. R. (1983) Egg-laying defective mutants of the nematode *Caenorhabditis elegans*. *Genetics* **104(4),** 619–647.
32 Segalat, L., Elkes, D. A., and Kaplan, J. M. (1995) Modulation of serotonin-controlled behaviors by Go in *Caenorhabditis elegans*. *Science* **267(5204),** 1648–1651.
33 Sakahira, H., Breuer, P., Hayer-Hartl, M. K., et al. (2002) Molecular chaperones as modulators of polyQ protein aggregation and toxicity. *Proc. Natl. Acad. Sci. USA* **99(Suppl. 4),** 16,412–16,418.
34 Fernandez-Funez, P., Nino-Rosales, M. L., de Gouyon, B., et al. (2000) Identification of genes that modify ataxin-1-induced neurodegeneration. *Nature* **408,** 101–106.
35 Perkins, L. A., Hedgecock, E. M., Thomson, J. N., et al. (1986) Mutant sensory cilia in the nematode *Caenorhabditis elegans*. *Dev. Biol.* **117,** 456–487.
36 Liu, Q. A. and Hengartner, M. O. (1999) The molecular mechanism of programmed cell death in *C. elegans*. *Ann. NY Acad. Sci.* **887,** 92–104.

37 Hickey, M. A. and Chesselet, M. F. (2003) Apoptosis in Huntington's disease. *Prog. Neuropsychopharmacol. Biol. Psychiatry* **27,** 255–265.
38. Chung, S., Gurniuenny, T. L., Hengartner, M. O., et al. (2000) A common set of engulfment genes mediates removal of both apoptotic and necrotic cell corpses in *C. elegans*. *Nature Cell Biol.* **2,** 931–937.
39 Xu, K., Tavernarakis, N., and Driscoll, M. (2001) Necrotic cell death in *C. elegans* requires the function of calreticulin and regulators of Ca(2+) release from the endoplasmic reticulum. *Neuron* **31,** 957–971.
40 Hekimi, S. and Guarente, L. (2003) Genetics and the specificity of the aging process. *Science* **299(5611),** 1351–1354.
41 Tatar, M., Bartke, A., and Antebi, A. (2003) The endocrine regulation of aging by insulin-like signals. *Science* **299(5611),** 1346–1351.
42 Tabrizi, S. J., Cleeter, M. W., Xuereb, J., et al. (1999) Biochemical abnormalities and excitotoxicity in Huntington's disease brain. *Ann. Neurol.* **45(1),** 25–32.
43 Brouillet, E. and Hantraye, P. (1995) Effects of chronic MPTP and 3-nitropropionic acid in nonhuman primates. *Curr. Opin. Neurol.* **8(6),** 469–473.
44 Beal, M. F., Brouillet, E., Jenkins, B. G., et al. (1993) Neurochemical and histologic characterization of striatal excitotoxic lesions produced by the mitochondrial toxin 3-nitropropionic acid. *J. Neurosci.* **13(10),** 4181–4192.
45 Bargmann, C. I. (1998) Neurobiology of the *Caenorhabditis elegans* genome. *Science* **282(5396),** 2028–2033.
46 Davis, M. W., Fleischhauer, R., Dent, J. A., et al. (1999) A mutation in the *C. elegans* EXP-2 potassium channel that alters feeding behavior. *Science* **286(5449),** 2501–2504.
47 Thomas, J. H. (1990) Genetic analysis of defecation in *Caenorhabditis elegans*. *Genetics* **124(4),** 855–872.
48 Garcia-Anoveros, J., Ma, C., and Chalfie, M. (1995) Regulation of *Caenorhabditis elegans* degenerin proteins by a putative extracellular domain. *Curr. Biol.* **5(4),** 441–448.
49 Fire, A., Xu, S., Montgomery, M. K., et al. (1998) Potent and specific genetic interference by double-stranded RNA in *Caenorhabditis elegans*. *Nature* **391(6669),** 806–811.
50 Timmons, L. and Fire, A. (1998) Specific interference by ingested dsRNA. *Nature* **395(6705),** 854.
51 Tabara, H., Grishok, A., and Mello, C. C. (1998) RNAi in *C. elegans*: soaking in the genome sequence. *Science* **282(5388),** 430–431.
52 Tavernarakis, N., Wang, S. L., Dorovkov, M., et al. (2000) Heritable and inducible genetic interference by double-stranded RNA encoded by transgenes. *Nature Genet*. **24(2),** 180–183.
53 Simmer, F., Tijsterman, M., Parrish, S., et al. (2002) Loss of the putative RNA-directed RNA polymerase RRF-3 makes *C. elegans* hypersensitive to RNAi. *Curr. Biol.* **12(15),** 1317–1319.
54. Brenner, S. (1974) The genetics of *Caenorhabditis elegans*. *Genetics* **77(1),** 71–94.

11

Monitoring Aggregate Formation in Organotypic Slice Cultures From Transgenic Mice

Donna L. Smith and Gillian P. Bates

Summary

Huntington's disease (HD) is a fatal neurodegenerative disorder caused by a CAG repeat expansion in the first exon of the HD gene. It encodes a protein known as huntingtin, which aggregates in the nuclei of affected neurons. These aggregates are an obvious therapeutic target, thus an organotypic slice culture assay has been designed to screen potential antiaggregation compounds using the R6/2 mouse model of HD. This assay allows the aggregates to be fully quantified using fluorescent confocal microscopy and gives additional information perturbing to drug solubility, delivery, toxicity, concentration, and efficacy of inhibitors. This information is essential to the planning and application of an in vivo drug trial in the R6/2 mice.

Key Words: Aggregate; hippocampus; Huntington's disease (HD); polyQ; R6/2; slice culture; transgenic.

1. Introduction

The misfolding and aggregation pathway is an important therapeutic target in Huntington's disease. PolyQ aggregates can be detected within nuclei of neurons in HD patients and mouse models prior to the onset of symptoms. Aggregates may cause cellular toxicity via the recruitment of factors that are normally important for cell function and viability ***(1,2)***. In keeping with this, certain components of the proteasome ***(3,4)*** transcription factors ***(5–7)*** and chaperones ***(8,9)*** have been identified as aggregate components. Aggregates of polyQ peptides localized to the nuclei have also been shown to cause cell death ***(10)***. In contrast, the analysis of a cell culture model of HD ***(11)*** and a mouse model of spinocerebellar ataxia type 1 (SCA1) ***(12)*** has suggested that aggregates are an epiphenomenon. Although this issue has yet to be resolved, the prevention of aggregation remains an important therapeutic target.

From: *Methods in Molecular Biology, vol. 277: Trinucleotide Repeat Protocols*
Edited by: Y. Kohwi © Humana Press Inc., Totowa, NJ

High-throughput screens of pharmaceutical compound libraries have been developed to identify chemical compounds capable of inhibiting the misfolding and aggregation pathway ***(13,14)***. To better test the efficacy of aggregation inhibitors, we have developed an ex vivo organotypic slice culture system that mimics the aggregation process occurring in the R6/2 mouse brain ***(15)***. The R6/2 mouse model expresses exon 1 of the human HD gene carrying a CAG expansion of greater than 150 repeats ***(16,17)***. The rapid onset and progression of HD in the R6/2 mouse model ***(18,19)*** makes it ideal for screening drugs that may prevent aggregation ***(20–22)***.

Methods used in the organotypic slice culture procedure include genotyping transgenic R6/2 mice, tissue culture and drug delivery, immunohistochemistry, quantification of polyQ aggregation, and statistical analysis. Using the organotypic slice culture assay, we can monitor the effects of compounds on polyQ aggregation and generate information pertaining to compound solubility, toxicity, and efficacy as inhibitors. Knowledge of the dose–response profile of an inhibitor in the slice culture assay will be essential for the design of in vivo drug trials and their interpretation.

2. Materials

2.1. Genotyping

1. Lysis solution: 50 µL Proteinase K solution (10 mg/mL at –20°C), per milliliter of lysis buffer.
2. Lysis buffer: 50 m*M* Tris-HCl, pH 8.0, 100 m*M* EDTA, pH 8.0, and 0.5% sodium dodecyl sulfate (SDS).
3. Saturated NaCl: 65 g NaCl in 200 mL deionized water (dH_2O) warmed at 50°C to dissolve.
4. 1X TE: 10 m*M* Tris-HCl and 0.1 m*M* EDTA, pH 8.0.
5. AM buffer: 670 m*M* Tris base, 166 m*M* ammonium sulfate, 20 m*M* magnesium chloride, 1.7 mg/mL bovine serum albumin (BSA) (using a 5% solution).
6. 5% BSA solution for AM buffer: 50 mg/mL BSA made up to 9 mL with 1X TE; adjust to pH 8.8 with HCl acid. The final volume of 10 mL is made with distilled and deionized water (d_2H_2O) and filter-sterilized.
7. Ultrapure dNTPs: 2'-Deoxynucleoside 5'triphosphate (Pharmacia LKB) diluted with 20 µL of 100 m*M* stock of each dATP, dCTP, dGTP, and dTTP up to 1 mL d_2H_2O, giving a final concentration of 2 m*M*.
8. 50X TAE: 1210 g Trizma-base, 285.5 mL acetic acid, 500 mL of 0.5 *M* EDTA, pH 8.0.
9. Cetus *Taq* DNA polymerase (Promega), 5 U/µL.
10. 50X Electrophoresis buffer stock (1210 g Trizma-base, 285.5 mL acetic acid, and 500 mL of 0.5 *M* EDTA, pH 8.0, with dH_2O up to 5 L. The final electrophoresis buffer used to run and make gels contained 2% 1X TAE electrophoresis buffer and 0.004% ethidium bromide; 10 mg/mL stock to final concentration of 40 ng/mL).
11. Agarose: electrophoresis grade (Amresco).
12. PhiX174-HaeIII (Promega).
13. 10X Loading dye: 50% glycerol, 50 m*M* EDTA pH 8.0, 0.25% xylenol orange, and 20% 1X TAE.

2.2. Organotypic Slice Culture

1. Roth media (Gibco/Scientific Laboratory Supplies): Make fresh as required. 50% modified Eagle's medium (MEM) + Hanks salts with 25 m*M* HEPES, 25% horse serum, 25% Hanks balanced salts, 2 m*M* L-glutamine, 6.4 mg/mL D(+) glucose.
2. Dissecting media (Gibco/Scientific Laboratory Supplies). Make fresh. MEM + Hanks salts with 25 m*M* Hepes, 160 μg/mL penicillin/streptomycin.
3. Sterile cell culture dishes, 60 mm × 15 mm (Nunc).
4. Sterile six-well plates (Nunc).
5. Plastic syringe, 10 mL (Becton Dickinson).
6. Avon Kwill filling tube, 127 mm (CE).
7. Razors (Wilkinson Sword).
8. Permanent marker pen (Texta).
9. Acetone (Sigma): Toxic.
10. Filter paper, circles, 70 mm (Whatman).
11. Millicell-CM Culture Plate Inserts, 0.4 μm (Sigma).
12. Dissection kit including scissors, spring-bow scissors, spatulas, tweezers, hemostat with razor (*see* **Note 1**).

2.3. Immunohistochemistry

1. Paraformaldehyde 4% (TAAB Laboratories).
2. TBS: 0.1 *M* Tris-HCl, pH 7.4, 0.9% NaCl.
3. Blocking solution: TBS with 2% BSA (New England Biolabs) and 0.2% sodium azide (Sigma).
4. S830 (in-house sheep polyclonal antibody for htt exon 1 fusion protein).
5. Alexa Fluor-488 (donkey anti-goat IgG; Molecular Probes): Light sensitive; store at –70°C or at 4°C for current aliquot.
6. Mowiol 4-88: Light sensitive; store at 4°C (Calbiochem).
7. Poly-L-lysine-coated superfrost slides (BDH).

2.4. PCR Primers

Name	Sequence	Function
40063	TGTGGCTGAGGAGCCGCT	Genotyping R6/2 forward primer
40036	TCCCCTCGTGAGAGGACAAGG	Genotyping R6/2 mice reverse primer

3. Methods

The methods described here include (a) genotyping transgenic R6/2 mice, (b) preparation of slice cultures, (c) tissue culture and drug delivery, (d) immunohistochemistry, (e) quantification of polyQ aggregation, and (f) statistical analysis.

3.1. Genotyping Transgenic R6/2 Mice

Transgenic animals are identified by a process of tailing, extraction of DNA using a high-salt method, amplification of the DNA using polymerase chain reaction (PCR), and identification of the transgene fragment using gel electrophoresis.

3.1.1. Tailing

The mice are tailed between 3 and 4 d of age in accordance with the Home Office guidelines. Antithetic cream is applied to the tail tip and the mice left for 5 min, a small (3 mm) piece of tail is then taken. Because of the animals' young age, the mice cannot be earmarked, as their ears have not yet fully developed, and so the mice are marked on their backs and stomachs with a permanent TEXTA marker pen. A series of parallel and antiparallel lines and crosses are used to identify the mice. The mouse pups are returned to their mothers and marking has to be repeated each day until the mice are taken for slice cultures (*see* **Note 2**).

3.1.2. Extraction of Tail Genomic DNA by the High-Salt Method

The tail biopsy is placed in a clean 1.5-µL Eppendorf and lysed in 500 µL of lysis solution at 50°C overnight. Saturated 300 µL NaCl is added to the tube and shaken before centrifuging for 30 min at 13 K. The supernatant is transferred to a tube containing 800 µL of 100% ethanol and spun at 13 K in a centrifuge for 10 min until DNA is pelleted. The supernatant is totally discarded and the pellet washed with 300 µL of 70% ethanol. After letting the pellet dry at room temperature for 10 min, 25 µL of 1X TE is added and the DNA allowed to resuspend overnight. Extracted DNA is diluted 1:10 in d_2H_2O and used for genotyping.

3.1.3. Genotyping by PCR

The reactions are generally performed in a PTC-100 PCR machine with a hot bonnet (MJ Research). A typical reaction contains 200 ng of genomic DNA, 1X AM buffer (2 m*M*), dNTPs (2 m*M*), 1% dimethyl sulfoxide (DMSO), primers 40036 and 40063 (200 ng), and Cetus *Taq* DNA polymerase 0.5 U (0.2 µL) in the reaction. DMSO is added to PCR reactions to eliminate nonspecific products. A total reaction volume of 20 µL is made up using d_2H_2O. Cycling conditions are an initial denaturation at 94°C for 90 s, 35 cycles of 94°C for 30 s, 60°C for 30 s, and extension at 72°C for 90 s, followed by a final 10-min extension at 72°C for 10 min before cooling to 4°C. The products are then checked on a 3% gel (4.5 g electrophoresis-grade agarose with 150 mL of 1X TAE).

3.1.4. Electrophoresis of DNA Fragments

Gels are visualized under short-wave ultraviolet (UV) light after running for the required time in Flowgen electrophoresis tanks (around 30 min for a PCR gel). PCR samples (8 µL) are loaded into the gel with 2 µL of 10X loading dye for accurate positioning. For each lane, 4 µL of PhiX174-HaeIII marker is used to determine the size of the DNA fragment. Positive (previously genotyped positive R6/2 mouse DNA) and negative (water in PCR reaction mix) controls are also run in each gel.

3.2. Organotypic Slice Culture Assay

Hippocampal slice cultures are prepared according to the method of Stoppini et al. ***(23)*** with minor modifications. All procedures are performed using sterile techniques and following Home Office-approved guidelines. R6/2 mice are decapitated and the

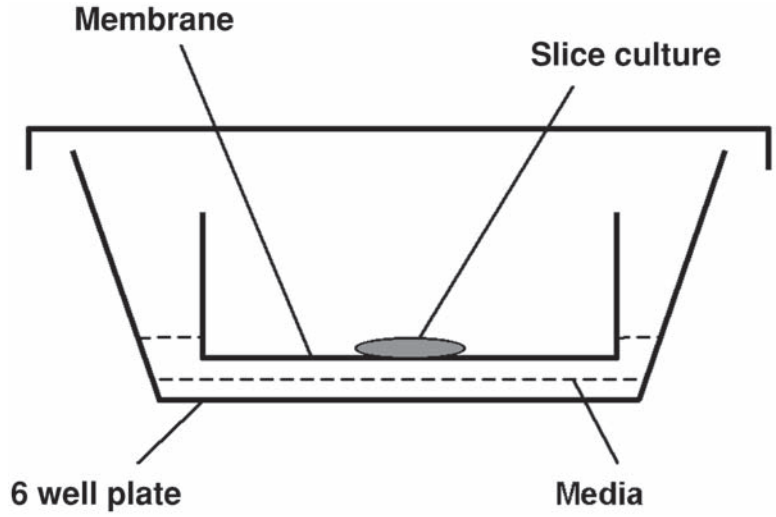

Fig. 1. Diagrammatic representation of the organotypic slice culture setup. Hippocampal slices are placed onto the membrane insert with media in a culture dish below.

brain placed in dissecting media, containing antibiotics (*see* **Subheading 2.**). Hippocampi are dissected from P7–9 mouse pups and 300-μm transverse slices are generated using a McIllwain tissue chopper (Mickle Laboratory Engineering Co., Ltd., Gomshall, Surrey, UK). Slices are transferred to prewarmed growth media (*see* **Note 3**) using a sterile 10-mL syringe and Avon filling tube, filled with media (*see* **Note 4**). Slices are carefully separated using spatulas (*see* **Note 5**) and placed onto prewarmed 30-mm Millicell-CM culture plate inserts (*see* **Fig. 1**). Four to five slices are plated per membrane. Roth growth media (1 mL) is placed below the insert's membrane and excess media on the slices is removed using a p20 Gilson pipet to provide the air interface essential for survival of the slice culture.

3.3. Tissue Culture and Drug Delivery

Slices are maintained in a 5% CO_2 incubator (LEEC) at 37°C and the medium is changed every 2–3 d. Compounds are added to the growth medium from the first day in culture until the termination of the experiment. Drugs with a short half-life have the media changed every day to increase the efficiency of drug delivery to the slice. All compounds are first dissolved in a vehicle before being added to the media. The vehicle used depends on drug solubility and includes d_2H_2O, phosphate buffered saline (PBS), DMSO and hydroxy propyl β-cyclodextrin. Some compounds also have to be heated in a water bath in order to become soluble.

Vehicle stocks are made with 10-fold serial dilutions of compounds (e.g., 1 m*M*, 100 μ*M*, 10 μ*M*, 1 μ*M*, and 0.1 μ*M*). Normally, five drug concentrations are evaluated, with the IC_{50}, if known, being the mid concentration. The highest concentration of

drug is dissolved in the vehicle; then, serial 1:10 dilutions are made for the rest of the stocks. Vehicle stocks are then added to Roth media, with a total volume of 1:100 vehicle to media ratio (100 μL vehicle in 10 mL media). Controls included vehicle alone and untreated Roth media transgenic slices.

Slices are kept in culture for 2, 3, and 4 wk when the drug is given from the outset (d 1). If a positive inhibitory effect is seen for a compound, the experiment is repeated with delayed drug delivery. This mimics an in vivo drug trial when mice are given the drug after weaning, at 4 wk of age. Slices are cultured without drug for 3 wk (which is 4 wk in vivo, as slices are taken at 1 wk of age), and then the drug is added for a further 2 and 3 wk culture.

3.4. Immunohistochemistry

Slice cultures are fixed in 4% paraformaldehyde by pouring the fix directly onto and under the membrane and keeping them overnight at 4°C. For each drug concentration and control, 16 slices (4 membranes containing 4 slices) are fixed to provide sufficient tissue sections for statistical quantification. Where possible, each of the four membranes contained slices that derived from a different animal. Following fixation, slices are coaxed off the membrane using a very thin paintbrush (*see* **Note 6**) and stored in TBS at 4°C until needed. All sections for any one compound being tested, including all drug concentrations and controls for all time-points (2, 3, and 4 wk culture) are immunoprobed together to minimize staining variation between experiments (*see* **Note 7**). When ready for fluorescent immunoprobing, the sections are cryoprotected in 20% sucrose and cut to 20 μm thickness using a freezing microtome (Physitemp) (*see* **Note 8**). Slices are transferred, as free-floating sections, using a paintbrush to modify membranes for easy section transfer (*see* **Note 9**) to TBS. Sections are washed three times in TBS for 5 min each with shaking. Nonspecific sites are blocked by incubation in blocking solution for 30 min (*see* **Subheading 2.**). Slices are incubated in primary antibody diluted in the blocking solution at 4°C overnight. Primary antibody used to detect polyQ aggregation was S830 (1:1000); this is a sheep polyclonal antibody raised against a GST–exon 1 huntingtin fusion protein carrying 53Q ***(24)***.

The next day slices are washed three times in TBS for 5 min each on a shaker, then incubated for 1 h at room temperature in Alexa 488 labeled anti-goat (1:150) fluorescent secondary antibody (Molecular Probes) in blocking solution. The plates are kept in the dark to protect the fluorophores. The last three washes in TBS for 5 min are also in the dark with shaking. Sections are floated using a Petri dish filled with water and TBS onto poly-L-lysine-coated slides and left to dry for 10 min. Mowiol mounting medium is a wet mount for fluorescently stained sections. This is used to cover the slides; they are then left to dry, in the dark, overnight before being stored at 4°C.

3.5. Aggregate Quantification

We aim to quantify 20 sections from different slice cultures for each drug concentration and all analyses are performed blind. Images for quantification are captured using a LSM Confocal microscope (Zeiss) at a 400× magnification. Parameters remain

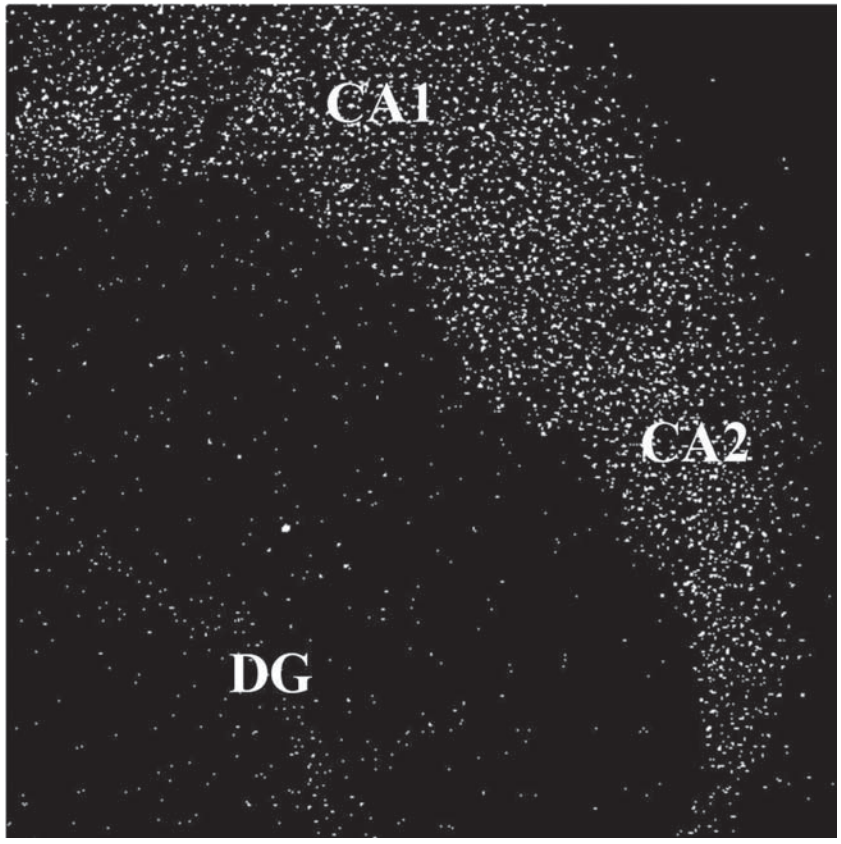

Fig. 2. Hippocampal slice after 3 wk in culture. Pyramidal neurons contain polyQ aggregates stained with S830 and A488 fluorescent secondary antibody in the CA1, CA2, and Dentate Gyrus (DG).

unchanged throughout the analysis of each experiment and are set such that nuclear aggregates are detected at signals below the level of saturation. The CA1 region of the hippocampus is chosen for quantification of aggregation, as it has a very well-defined cell layer that can be easily identified under the microscope (*see* **Fig. 2**).

Images are captured at 1-μm intervals and assembled into a Z-stack. The dimensions of the stack confirm that the sections are of the expected 20 μm thickness. Images are transferred into the KS300 image analysis package (Image Associates Ltd., UK), which included software that has been specially written for this application (Paul Whetton, Image Associates Ltd., UK). The extent of aggregation in the entire stack is calculated by determining the aggregate count (unit = aggregate number), total fluorescent intensity (unit = sum density), and aggregate area (unit = % aggregate area of screen). **Figure 3** presents the results of all measurement parameters over all time-points for doxycycline, an effective inhibitor of aggregation in the slice cultures.

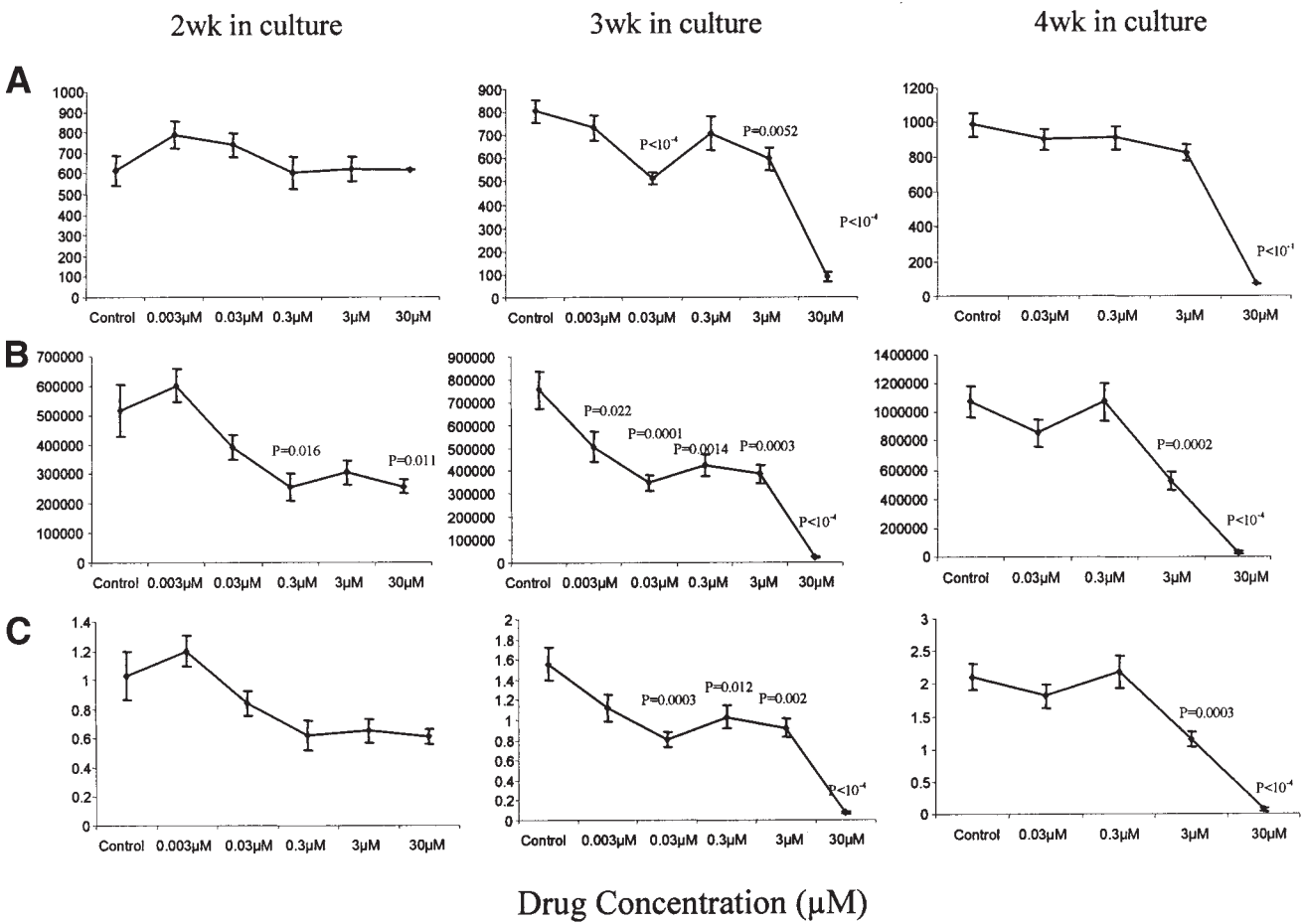

Fig. 3. Reduction of aggregation by doxycycline in hippocampal slice cultures from R6/2 brains after 2, 3, and 4 wk culture. **(A)** Aggregate count (number), **(B)** total fluorescence intensity (sum density), and **(C)** % aggregate area. Inhibition of aggregation at 30 μ*M* concentration of doxycycline over all time-points and all measurement criteria observed with high *p*-values. Drug administered from d 1 in culture.

3.6. Statistical Analysis

Raw data are transferred into Excel and line graphs created with standard deviations and standard error of the mean for each treatment. Statistical analysis is performed using Minitab statistics program. One-way analysis of variance (ANOVA) and two-way sample *t*-tests are performed to give *p* values for each drug concentration against the appropriate control. When a compound is successful at inhibiting aggregation, a very large number of significant *p* values are obtained because, usually, there are five drug concentrations plus two controls for three time-points (2, 3, and 4 wk culture) for each drug tested. To reduce the number of false positive, *p* values within any one experiment, a very stringent false discovery rate (FDR) test ***(25)*** is performed. This test can be used to reduce the expected proportion of false discoveries among positive results to an acceptable level. Conventionally, this is set such that every 1 *p* value in 20 is a false positive. The general linear model of ANOVA can also be applied to the data, as this model involves multiple variables with interacting factors.

4. Notes

1. Small scissors are used to decapitate the mouse; spring-bow scissors are then used to cut the skull along its axis, pulling it apart to expose the brain. The brain is removed using spatulas and cut in half with hemostat and razor. Spatulas are used to dissect out the hippocampus. All instruments are kept in 70% ethanol during procedure for sterility.
2. Ordinarily, mouse pups are left with their mothers until weaning at 4 wk of age. Because slice cultures are performed at P7–9, genotyping has to be completed before this time, thus mice are tailed at 3–4 d of age. After tailing and marking the pups, they are returned to their mothers, who will clean the pups. This disturbs the markings and so they have to be remarked every day until the pups are taken for slice cultures.
3. Roth media is made by filter-sterilizing the constituents, which have first been warmed in a 37°C water bath for 10 min. Glucose is dissolved in the warmed media before filtration.
4. Slices are transferred from media to membranes by a process of suction using an Avon Quill filling tube and a 10-mL syringe. The syringe is attached to the filling tube and suction applied so that only one slice is taken up the tube with media. The slice is then allowed to drop to the bottom of the tube and collect in the droplet of media at the end. The filling tube is then carefully placed onto the surface of the membrane and the droplet of media will dislodge along with the slice. Avon Quill filling tubes are no longer commercially available. However, a sterile plastic Pasteur pipet could be modified by cutting off the tip so that enough space is left for the slice to drop to the end of the pipet without it sticking.
5. Spatulas are modified by filing off the Teflon with a small file so that the end and edges are sharp. One of the two spatulas is bent in the middle using a vice to clamp the spatula and then bending it over 45°. All dissection instruments are kept sterile with ethanol and autoclaving before each procedure.
6. Sections are coaxed off the membrane using a very thin paintbrush with a rolling action. Roll the brush away from the slice using a rotating action until you have the brush under one edge of the slice. It should then come away cleanly from the membrane, with no breakage.
7. As this is a quantitative analysis, all sections are immunoprobed together for any one compound, as subtle variations in staining can occur between experiments.

8. Initially, the hippocampus is cut at a 300-μm thickness. Over time, the sections progressively thin out so that by 2 wk in culture, they are around 100 μm, and by the end of the experiment at 4 wk, they are around 50 μm. At this time, the slices are very fragile, so handle them carefully with a thin paintbrush.
9. When immunoprobing, rather than transferring each section per wash with a paintbrush, a culture plate insert can be modified for quick transfer. This is done by removing the insert from the plastic support. The support is then dried and ladies tights glued (any superglue) to the bottom so that they are taught. When the glue dries, the tights are cut round the circular shape of the support and then placed in the six-well plate for washing and antibody staining.

Acknowledgments

The authors would like to thank Karl Murray (UCL) for transferring the technique to our laboratory. This work was supported by Huntington's Disease Society of America, Wellcome Trust, and Human Frontiers Science Program.

References

1 Kazantsev, A., Preisinger, E., Dranovsky, A., et al. (1999) Insoluble detergent-resistant aggregates form between pathological and nonpathological lengths of polyglutamine in mammalian cells. *Proc. Natl. Acad. Sci. USA* **96,** 11,404–11,409.
2 Perez, M. K., Paulson, H. L., Pendse, S. J., et al. (1998) Recruitment and the role of nuclear localization in polyglutamine-mediated aggregation. *J. Cell Biol.* **143,** 1457–1470.
3 Cummings, C. J., Mancini, M. A., Antalffy, B., et al. (1998) Chaperone suppression of aggregation and altered subcellular proteasome localization imply protein misfolding in SCA1. *Nature Genet.* **19,** 148–154.
4 Waelter, S., Boddrich, A., Lurz, R., et al. (2001) Accumulation of mutant huntingtin fragments in aggresome-like inclusion bodies as a result of insufficient protein degradation. *Mol. Biol. Cell* **12,** 1393–1407.
5 McCampbell, A., Taylor, J. P., Taye, A. A., et al. (2000) CREB-binding protein sequestration by expanded polyglutamine. *Hum. Mol. Genet.* **9,** 2197–2202.
6 Nucifora, F. C., Jr., Sasaki, M., Peters, M. F., et al. (2001). Interference by huntingtin and atrophin-1 with cbp-mediated transcription leading to cellular toxicity. *Science* **291,** 2423–2428.
7 Steffan, J. S., Kazantsev, A., Spasic-Boskovic, O., et al. (2000) The Huntington's disease protein interacts with p53 and CREB-binding protein and represses transcription. *Proc. Natl. Acad. Sci. USA* **97,** 6763–6768.
8 Jana, N. R., Tanaka, M., Wang, G., et al. (2000) Polyglutamine length-dependent interaction of Hsp40 and Hsp70 family chaperones with truncated N-terminal huntingtin: their role in suppression of aggregation and cellular toxicity. *Hum. Mol. Genet.* **9,** 2009–2018.
9 Levine, M. S., Klapstein, G. J., Koppel, A., et al. (1999) Enhanced sensitivity to *N*-methyl-D-aspartate receptor activation in transgenic and knockin mouse models of Huntington's disease. *J. Neurosci. Res.* **58,** 515–532.
10 Yang, W., Dunlap, J. R., Andrews, R. B., et al. (2002) Aggregated polyglutamine peptides delivered to nuclei are toxic to mammalian cells. *Hum. Mol. Genet.* **11,** 2905–2917.
11 Saudou, F., Finkbeiner, S., Devys, D., et al. (1998) Huntingtin acts in the nucleus to induce apoptosis but death does not correlate with the formation of intranuclear inclusions. *Cell* **95,** 55–66.

12 Klement, I. A., Skinner, P. J., Kaytor, M. D., et al. (1998) Ataxin-1 nuclear localization and aggregation: role in polyglutamine-induced disease in SCA1 transgenic mice [see comments]. *Cell* **95,** 41–53.
13 Heiser, V., Engemann, S., Brocker, W., et al. (2002) Identification of benzothiazoles as potential polyglutamine aggregation inhibitors of Huntington's disease by using an automated filter retardation assay. *Proc. Natl. Acad. Sci. USA* **99(Suppl. 4),** 16,400–16,406.
14 Kazantsev, A., Walker, H. A., Slepko, N., et al. (2002) A bivalent Huntingtin binding peptide suppresses polyglutamine aggregation and pathogenesis in Drosophila. *Nature Genet.* **30,** 367–376.
15 Smith, D. L., Portier, R., Woodman, B., et al. (2001) Inhibition of polyglutamine aggregation in R6/2 HD brain slices-complex dose-response profiles. *Neurobiol. Dis.* **8,** 1017–1026.
16 Mangiarini, L., Sathasivam, K., Seller, M., et al. (1996) Exon 1 of the HD gene with an expanded CAG repeat is sufficient to cause a progressive neurological phenotype in transgenic mice. *Cell* **87,** 493–506.
17 Mangiarini, L., Sathasivam, K., Mahal, A., et al. (1997) Instability of highly expanded CAG repeats in mice transgenic for the Huntington's disease mutation [see comments]. *Nature Genet.* **15,** 197–200.
18 Davies, S. W., Turmaine, M., Cozens, B. A., et al. (1997) Formation of neuronal intranuclear inclusions underlies the neurological dysfunction in mice transgenic for the HD mutation. *Cell* **90,** 537–548.
19 Li, Z., Karlovich, C. A., Fish, M. P., et al. (1999) A putative Drosophila homolog of the Huntington's disease gene. *Hum. Mol. Genet.* **8,** 1807–1815.
20 Sanchez, I., Mahlke, C., and Yuan, J. (2003) Pivotal role of oligomerization in expanded polyglutamine neurodegenerative disorders. *Nature* **421,** 373–379.
21 Ferrante, R. J., Andreassen, O. A., Jenkins, B. G., et al. (2000) Neuroprotective effects of creatine in a transgenic mouse model of Huntington's disease [in process citation]. *J. Neurosci.* **20,** 4389–4397.
22 Karpuj, M. V., Becher, M. W., Springer, J. E., etc. (2002) Prolonged survival and decreased abnormal movements in transgenic model of Huntington disease, with administration of the transglutaminase inhibitor cystamine. *Nature Med.* **8,** 143–149.
23 Stoppini, L., Buchs, P. A., and Muller, D. (1991) A simple method for organotypic cultures of nervous tissue. *J. Neurosci. Methods* **37,** 173–182.
24 Sathasivam, K., Hobbs, C., Turmaine, M., et al. (1999) Formation of polyglutamine inclusions in non-CNS tissue. *Hum. Mol. Genet.* **8,** 813–822.
25. Benjamini, Y., Drai, D., Elmer, G., et al. (2001) Controlling the false discovery rate in behavior genetics research. *Behav. Brain Res.* **125,** 279–284.

12

The CGG Repeat and the *FMR1* Gene

Violeta Stoyanova and Ben A. Oostra

Summary

This review intends to provide the different DNA methods for diagnosis of the repeat in the *FMR1* gene. The two DNA methods to determine the CGG repeat size are Southern blot hybridization and the polymerase chain reaction (PCR), including bisulfite treatment.

Key Words: Trinucleotide repeat; DNA diagnostics; *FMR1*; FMRP; CGG repeat; premutation; full mutation; methylation; nonradioactive PCR; bisulfite sequencing.

1. Introduction

Fragile X syndrome is a common X-linked heritable disease characterized by mental retardation, macro-orchidism, and mild facial abnormalities and is always caused by the absence or deficit of the FMR1 protein (FMRP) (for review, *see* **ref. *1***). In the majority of cases, the disease is associated with an expansion of a CGG repeat, located in the 5' UTR (untranslated region) of the *FMR1* gene. In the normal population, this CGG repeat varies from 5 to 50 units, with an average of 30 units ***(2)***. Individuals with the fragile X syndrome are characterized by a CGG repeat with a size above 200 units (full mutation; FM). The expansion of the repeat above 200 units generally results in hypermethylation of both the CpG island and the CGG repeat within the *FMR1* gene (*see* **Fig. 1**). Consequently, the *FMR1* gene is usually transcriptionally silenced and the gene product, FMRP, is absent.

On the basis of the size of the CGG repeat, another group of individuals can be identified as carriers of a premutation (PM), with a size between 50 and 200 units. CGG repeats in the premutation range exhibit transmission instability dependent on the sex of the transmitting parent and the size of the repeat. Premutation alleles are usually unmethylated and FMRP production is normal. Male patients frequently display mosaicism with respect to repeat length, with FM alleles in combination with PM alleles.

From: *Methods in Molecular Biology, vol. 277: Trinucleotide Repeat Protocols*
Edited by: Y. Kohwi © Humana Press Inc., Totowa, NJ

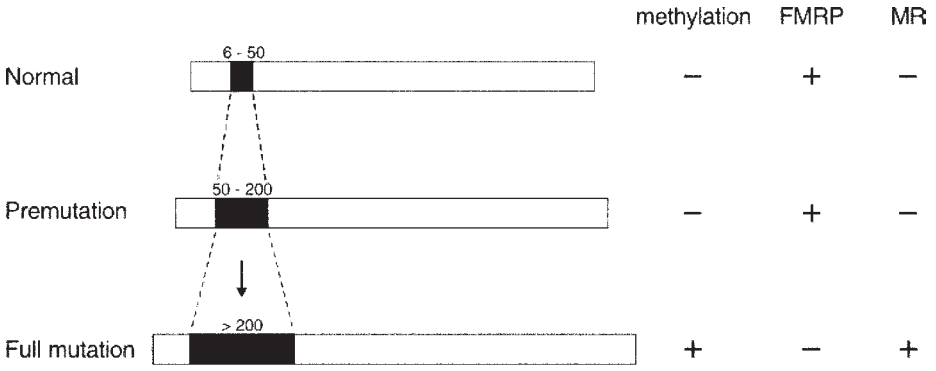

Fig. 1. Schematic representation of the different *FMR1* alleles showing the different size ranges of the CGG repeat. For the different alleles, it is shown whether they are methylated, whether they translated into protein, and whether individuals with such an allele are mentally retarded (MR).

Instability of the CGG repeat is the molecular basis for nearly all mutations (>99%) in the *FMR1* gene, leading to fragile X syndrome. A knockout mouse model has been generated in which exon 5 of the *FMR1* gene was removed and replaced by a neo cassette ***(3)***. This mutation in the mouse leads to a lack of FMRP, in which it resembles the human situation. Recently, a knock-in mouse model has been produced in which the murine CGG repeat has been replaced by a human premutation CGG repeat ***(4)***. Instability has been seen in this mouse model, but up to now, no expansion to a full mutation has been observed.

2. Materials

2.1. Southern Blot Analysis

1. TBE buffer (10X): 900 m*M* Tris, 900 m*M* boric acid, 25 m*M* EDTA, pH 8.0.
2. Ficoll loading buffer (10X): 25% Ficoll, 0.1 *M* Tris-HCl, pH 7.5, 10 m*M* EDTA, 0.25% Oranje G.
3. Denaturation buffer: 0.5 *M* NaOH, 1.5 *M* NaCl.
4. Neutralizing buffer: 3.0 *M* NaCl, 0.5 *M* Tris-HCl, pH 7.0.
5. 20X SSC: 3.0 *M* NaCl; 0.3 *M* sodium citrate; pH 7.0.
6. Orimers for the DIG labeling reaction:

Primer 1: CGC CAA GAG GGC TTC AGG TCT CCT
Primer 2: GAG ACT GTT AAG AAC ATA AAC GCG GG.

2.2. PCR Amplification

1. Polymerase chain reaction (PCR) mix: Prepare PCR reaction (9.75 µL per reaction) in a microcentrifuge tube by combining the following solutions: 6.15 µL H_2O, 1 µL of 10X PCR buffer II (Perkin-Elmer), 0.4 µL of 25 m*M* $MgCl_2$ (Perkin-Elmer), 1 µL dimethyl sulfoxide (DMSO), 0.5 µL dNTPs, 0.2 µL of 10 m*M* primer c, 0.2 µL of 10 m*M* primer f, 0.15 µL α^{32}P-dCTP (10 mCi/mL; 3000 Ci/mmol), 0.15 µL U/µL Ampli Taq Gold.

2. 20X dNTPs: 2000 μ*M* dATP, 2000 μ*M* dCTP, 2000 μ*M* dTTP, 500 μ*M* dGTP, 1500 μ*M* of 7-deaza-2'-dGTP.
3. Primer c: GCT CAG CTC CGT TTC GGT TTC ACT TCC GGT
   Primer f: AGC CCC GCA CTT CCA CCA CCA GCT CCT CCA.
4. Loading buffer: 95% formamide, 20 m*M* EDTA, 0.05% xylene cyanol FF.

2.3. Bisulfite-Based PCR Amplification

1. 2.8 m*M* Sodium bisulfite solution (Sigma S-8890).
2. 40 m*M* Hydroquinone solution (Sigma H-9003).
3. 10 *M* NaOH (Sigma).
4. Isopropanol and 70% ethanol.
5. 1 m*M* Tris-HCl (pH 8.0).
6. Wizard DNA clean-up kit (Promega).
7. Mineral oil (Sigma).
8. 6 *M* Ammonium acetate (pH 7.0).
9. Platinum *Taq* polymerase (Invitrogene).
10. Primer FCDF: 5' CCACTACCAAAAAACATACAAC (10 pmol working solution).
11. Primer FCDR: 5' GTTGGGAGTTTGTTTTTGAGAG (10 pmol working solution).
12. QIAquick PCR Purification Kit (Qiagen): for purification of the PCR band from gel.
13. pcDNA3.1/V5-His TOPO TA Expression Kit (Invitrogen): for cloning of PCR fragment.
14. Luria–Bertani (LB)/ampicillin: 10 g Bacto-tryptone, 5 g Bacto-yeast extract, 10 g NaCl, pH 7.5, with NaOH, supplemented with ampicillin (50 μg/mL).
15. CLONdiscs (Clontech).
16. QIAprep Spin Miniprep Kit (Qiagen): for the extraction of the miniprep DNA.
17. ABI Prism BigDye Terminator Cycle Sequencing Ready Reaction Kit (Applied Biosystems).
18. Primers T7 and BGH (included in the pcDNA3.1/V5-His TOPO TA Expression Kit; Invitrogen).
19. ABI Prism 377 Sequencer and ABI Prism Collection software.

3. Methods

3.1. Southern Blot Analysis

The most common diagnostic method for the detection of the syndrome is Southern blot analysis. Southern blot analysis using a single enzyme (*Hin*dIII or *Eco*RI) allows the detection of full mutations and large premutations and can also be used for the identification of fragile X patients. Combined detection of expansion and methylation can be carried out by digestion with *Hin*dIII and *Eag*I. These combinations offer a good compromise in family studies to determine full-mutation alleles, mosaic patterns, and premutation alleles.

An example of the complexity of the Southern blot patterns is shown in **Fig. 1**.

In normal individuals, a 5.2-kb *Hin*dIII fragment is detected, which can be cut by *Eag*I into a 2.8- and a 2.4-kb fragment (*see* **Fig. 2**). Because of the use of the probe (pP2), only the 2.8-kb fragment is visible on this Southern blot (e.g., seen in individual 7). In affected individuals, an increase of this fragment is found with a length generally above 5.7 kb, and the methylation-sensitive enzyme *Eag*I cannot digest this band. In most cases, a smear is visible as a result of extensive mosaicism (e.g., individual 6

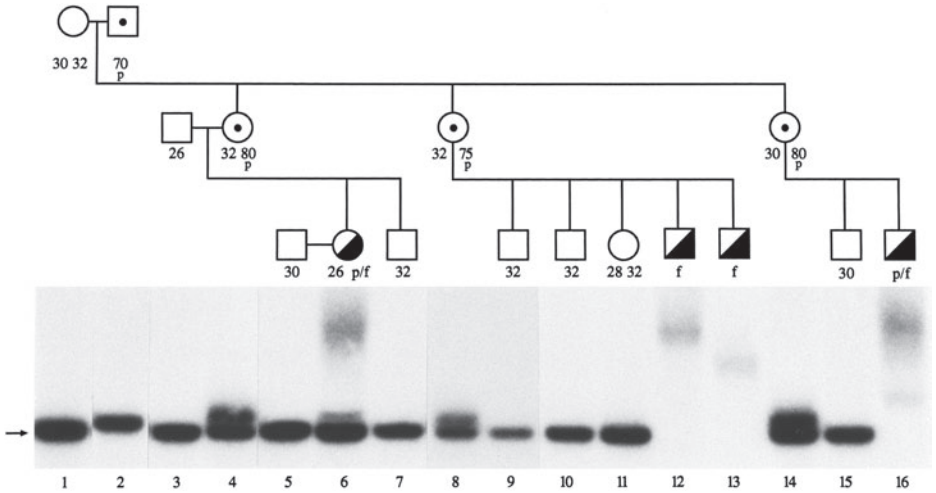

Fig. 2. Detection of the *FMR1* gene in a fragile X family by means of Southern blot analysis. {symbol individual 2} = normal transmitting male; {symbol individual 4} = normal female carrier; {symbol individual 6} = female carrier with cytogenetic expression; {symbol individual 12} = mentally retarded male; number of CGG repeats for the different X chromosomes (determined by PCR) is indicated; p, premutation; f, full mutation. (Example of fragile X DNA diagnosis provided by Dr. D. J. J. Halley and Dr. A. M. W. van der Ouweland.)

and individual 16). In unaffected transmitting male carriers and a portion of female carriers, a premutation allele greater than 2.8 kb is detected (e.g., individuals 2 and 4). For individual 6, a clear mosaic pattern is found of a methylated full mutation together with a premutation band.

3.1.1. Hybridization Probe Preparation

DNA analysis is mostly carried out using radioactive-labeled DNA probes; however, a good alternative is the use of nonradioactive (digoxigenin-labeled) probes followed by chemiluminescent detection ***(5)***. In most instances, the same probe is used, although different names are used, such as pP2, StB12.3, or pfxa3 ***(6)*** (*see* **Note 1**).

3.1.2. Southern Blot

1. In a 1.5-mL microcentrifuge tube digest 7 μg of genomic DNA with 50 units of *Hin*dIII and *Eag*I in a volume of 50 μL, containing 5 μL of 10X SuRE/Cut Buffer H and 3 μL of 50 m*M* spermidine. Incubate overnight (20 h) at 37°C.
2. Optional: 5 μL of the digest can be used to test on an agarose gel whether digestion of the DNA is complete.
3. Prepare a 0.7% agarose gel in TBE buffer plus ethidium bromide (25 μL of a 20-mg/mL solution per liter) for electrophoresis of the digested products.
4. Mix the digested DNA with 5.5 μL of 10X Ficoll loading buffer and load the mix on the agarose gel. Control samples of a control male, control female, and a fragile X patient have to run at the same time for comparison. A molecular-weight marker (e.g., a 1-kb

ladder of InVitroGen) has to be run for sizing of the bands. Electrophorese the samples for 20 h at 45 V to allow optimal separation of the DNA fragments.
5. Following electrophoresis, a photograph of the gel can be taken.
6. The gel is placed for 15 min in 0.25 *M* HCl with gentle shaking. This will introduce breaks in the DNA and will allow a successful transfer of the DNA from the gel to a filter.
7. Place gel 30 min in denaturation buffer with gentle shaking to allow denaturation of the DNA.
8. To neutralize, place the gel for 2X 15 min in neutralization buffer with gentle shaking.
9. Southern transfer of the DNA from the gel to a Nylon filter (Boehringer) is achieved with a blotting buffer of 20X SSC for 18 h.
10. Following the transfer, the filter is washed for a few seconds in 2X SSC. Let the membrane dry on filter paper.
11. The genomic DNA is fixed to the filter by baking the membrane either for 15–30 min at 120°C or for 2 h at 80°C. Alternatively, the DNA can be bound by ultraviolet (UV) crosslinking.
12. Hybridization can be performed with a DNA probe that is generated by labeling 50–100 ng of pP2 DNA with the random primer labeling using radioactive DNA precursors. After the reaction, the nonincorporated precursors have to be removed, which can be achieved by separation on a (Sephudex G50) column.
13. Alternatively, a nonradioactive DIG-labeled DNA probe can be used. The pP2 probe is labeled by PCR amplification, in the presence of DIG-11-dUTP using the labeling kit protocol of Roche.
14. After labeling, the DNA probe has to be denatured by heating the probe for 5 min at 95°C.
15. Prehybridization and hybridization are performed in DIG Easy Hyb solution (Roche, cat. no. 1 603 558). Let it prehybridize for at least 1 h at 42°C. After addition of the labeled probe, the hybridization is carried out for 18–20 h at 42°C.
16. Wash the membrane 2X 5 min with 50 mL of 2X SSC/0.1% SDS at room temperature.
17. Wash the membrane 2X 15 min in 1X SSC/0.1% SDS at 65°C.
18. Incubate membrane for 60 min in 200 mL of 1X blocking solution.
19. Take the membrane out of the 1X blocking solution (Roche) and put it on a piece of SaranWrap. Add 10 µL anti-digoxigenine-AP-conjugate (Roche) to the 1X blocking solution, shake well, and put the membrane back in this solution for 30 min.
20. Discard the antibody solution and wash the membrane in a clean tray filled with 1X washing buffer (Roche) for 15 min.
21. Wash the membrane again for 15 min in 1X washing buffer.
22. Equilibrate the membrane 1–5 min in 1X detection buffer (Roche).
23. Dilute 15 µL CDP star solution (Roche) with 1500 µL of 1X detection buffer.
24. Place the membrane between two sheets of a cut plastic bag. Lift the top sheet and pipet the diluted CDP star solution on top of the membrane. Lower the top sheet of plastic. Remove any bubbles present under the sheet. Incubate the membrane for 5 min.
25. Remove excess liquid from under the plastic by wiping with tissue over the membrane to squeeze out the excess liquid. Close the plastic bag by sealing.
26. Make exposures on X-ray film from 10 and 30 min. In most cases, these exposure times will be OK.

3.2. PCR Amplification Analysis

Detection and sizing of permutations can be done by PCR ***(2)***. Amplification of full mutations is very inefficient because stretches of more than 100–200 CGG repeats are

Fig. 3. Radioactive PCR to determine the repeat length as determined for the CGG repeat mouse. Different mice with different repeat length are shown. Wt = wild-type length of nine CGG repeats. The number of repeats is indicated at the top of the figure.

difficult to amplify, and, therefore, this is not a reliable method. The high CG content requires a specific PCR protocol ***(2,7)***. Initially, radioactivity was used to detect the size of the PCR products. The same PCR method using the same primers can be used for human and mouse repeat analysis. An example for the CGG repeat mouse is shown in **Fig 3**.

Recently, a new nonradioactive method was developed by PE Biosystems. Fluorescent-labeled precursors are used during the PCR amplification and the size of the PCR product can be determined on an automated ABI sequencer (*see* **Fig. 4**). This last method gives a very accurate sizing of the PCR product in both males and females starting from a very small amount of DNA. This diagnostic test can even avoid the necessity of blood sampling (*see* **Note 2**).

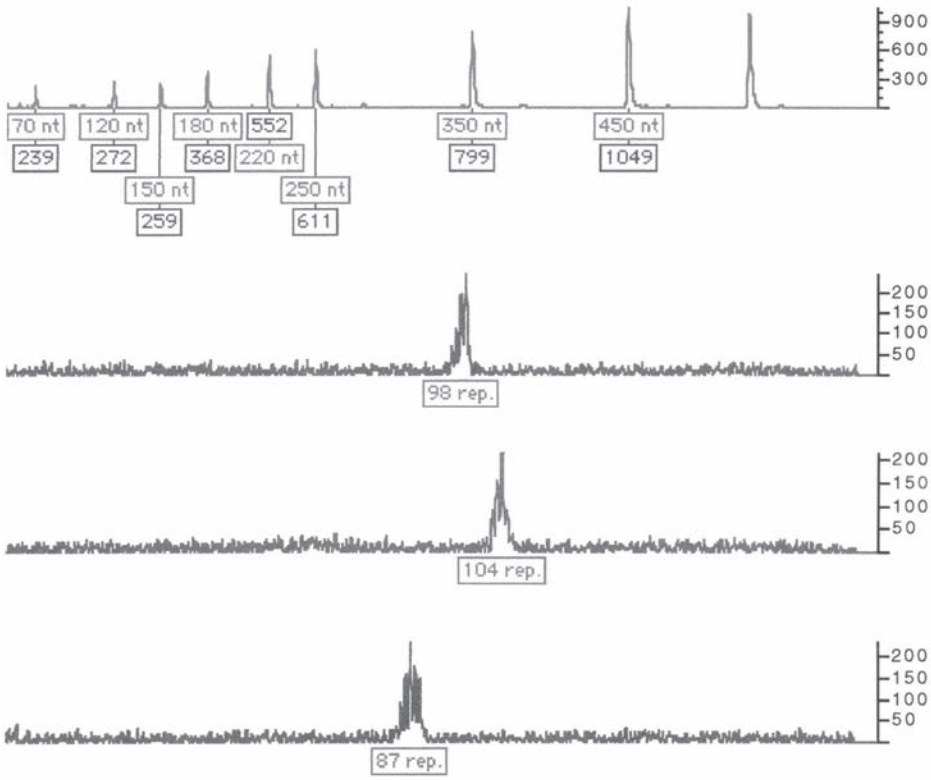

Fig. 4. PCR analysis of *FMR1* genes with premutation alleles with a different repeat length. (Courtesy of Marianne Hoogeveen.)

3.2.1. Radioactive PCR Amplification

1. Dilute the DNA sample to 200 ng/μL, vortex, and add 0.25 μL DNA solution to a PCR tube with 9.75 μL PCR reaction mix.
2. Mix and close the PCR tube.
3. Place the tubes in a thermal cycler and perform the amplification by using the following thermocycler profile: 10 min initial denaturation at 95°C, followed by 30 cycles at 94°C for 45 s, 65°C for 2 min, 30 s. A final extension step at 72°C for 10 min is used to complete the assay. A PCR machine is used with a heated lid; therefore, an oil overlay is not necessary.
4. Prepare a standard denaturating 6% polyacrylamide gel 19:1 (acrylamide/bisacrylamide).
5. Combine 2.5 μL of each PCR product with 2.5 μL loading buffer. Place the samples at 95°C for 5 min, and then on ice. Load samples on gel, including a ^{32}P-labeled sequencing ladder to determine the size of the fragment.
6. Electrophorese the gel at 55 W in TBE buffer until the xylene cyanol dye has run about 30 cm.
7. Fixate the gel for 10 min in 10% acetic acid/10% methanol.

8. Dry gel on a gel dryer and perform autoradiography. Usually, an overnight exposure is enough.
9. Determine the size of each PCR fragment. The most common allele (30 repeats) runs at the length of 308 bases.

3.3. Bisulfite Treatment and Sizing of the CGG Repeat

Recently, an alternative PCR approach was described for the diagnosis of fragile X syndrome based on the methylation-sensitive conversion of C residues to U by sodium bisulfite on single-strand DNA and subsequent amplification of the antisense strand with specific primers. A PCR with primers for methylated C residues will amplify the CpG dinucleotide region upstream to CGG repeats exclusively in affected methylated males. As a result of extensive mismatch between primers and bisulfite-treated DNA, no PCR fragments will be obtained in normal and premutation alleles. However, this method is not as reliable as the Southern blot method to identify FM males and females ***(8–10)***. On the other hand, the bisulfite-based PCR method offers the option of sequencing of the PM CGG repeat and as a result the exact sizing of the CGG repeat ***(10)*** (*see* **Fig. 5**) (*see* **Note 3**).

3.3.1. Bisulfite Treatment and Analysis

The bisulfite conversion of DNA was carried out following the protocol originally developed ***(11)*** with some recent modifications as described in **ref. *12***. After the bisulfite treatment, a PCR has to be performed, followed by cloning of PCR fragments. Subsequently, individual clones have to be sequenced in both directions to determine the length and the composition of the CGG repeat. An example of a CGG repeat of 112 units in the CGG knock-in mouse is shown in **Fig. 5**.

The same method can be used for the detection of the CGG repeat in human and in the CGG repeat mouse ***(4)***.

3.3.1.1. Step 1: Bisulfite Treatment of the DNA

1. Use as start material at least 3 μg DNA. Add to each sample 12 μg tRNA. Prepare the samples to a final volume of 50 μL and add 5.5 μL of 3 *M* NaOH (freshly prepared). Incubate the samples at 37°C for 30 min in a water bath.
2. Denature the samples at 95°C for 3 min and immediately put the samples on ice water.
3. While incubating at 37°C, prepare freshly the solutions. The final solution is 2.8 *M* sodium bisulphite/2.5 m*M* hydroquinone. Check and adjust the pH to 5.0 and filter (0.45 μm) the solution to sterilize.
4. Add to each sample 500 μL of sodium bisulfite/hydroquinone solution. Mix the samples gently.
5. Overlay the samples with 200 μL mineral oil.
6. Incubate the samples at 55°C for 16 h in a water bath at dark.
7. Purify the samples with the Promega Wizard DNA Clean-up system.
8. Desulfonate the DNA eluted in 50 μL buffer by adding 5.5 μL of 3 *M* NaOH.
9. Incubate at 37°C for 20 min.
10. Precipitate the DNA by adding an equal volume of 6 *M* ammonium acetate (pH 7.0) to a final concentration of 3 *M*. Add also 1 μg tRNA and 2 vol (220 μL) absolute ethanol.
11. Store the samples at –20°C for 2 h.

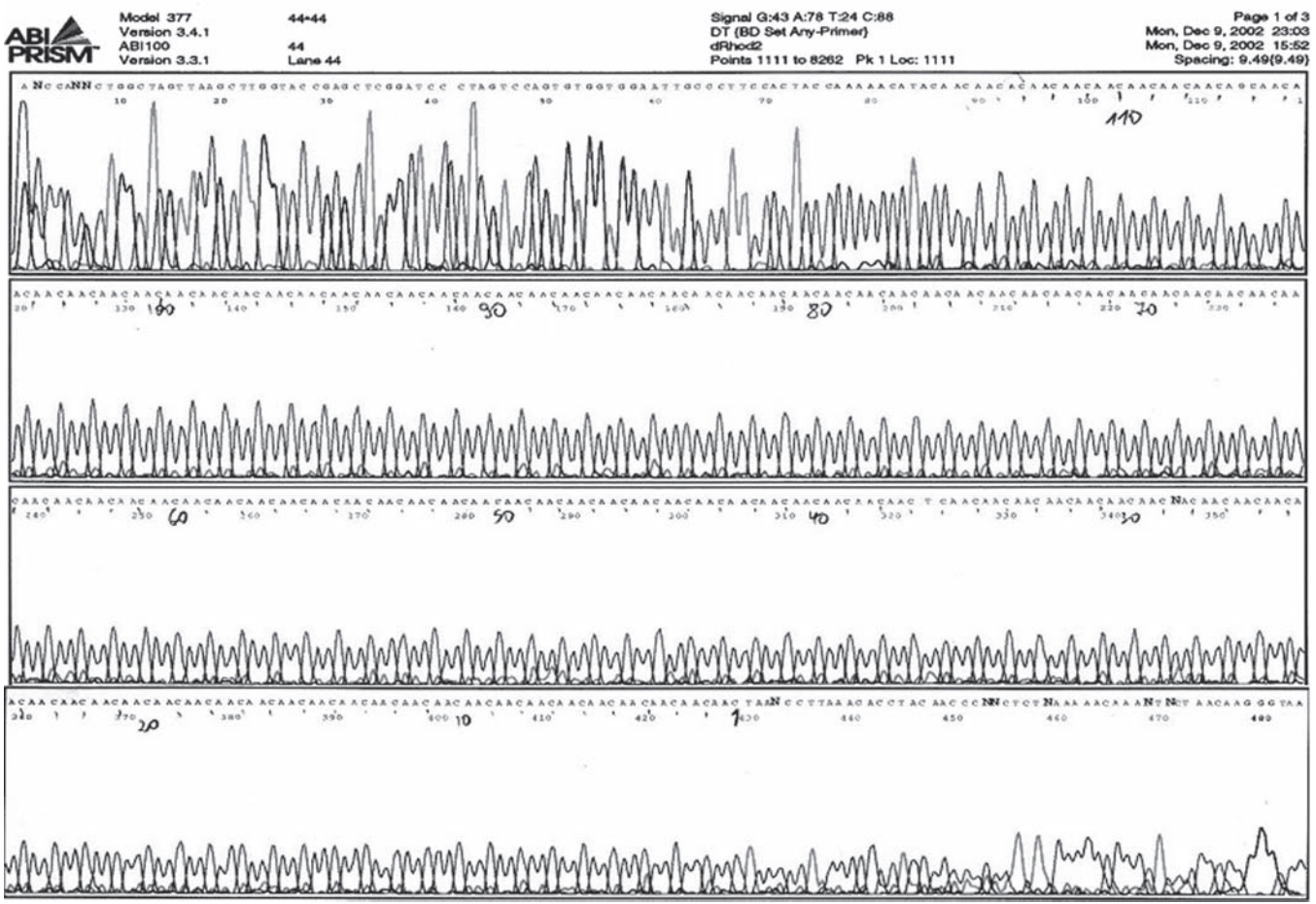

Fig. 5. An example of a CGG repeat of 112 units in the CGG knock-in mouse for which the PCR product is shown in Fig. 3. Because of the bisulfite treatment, the CGG repeat is shown as a CAA repeat.

12. Centrifuge at maximum speed at 4°C for 20 min.
13. Discard the supernatant and wash the pellet with 70% ethanol.
14. Centrifuge at maximum speed at 4°C for 10 min.
15. Discard the ethanol and let the pellet dry at room temperature.
16. Resuspend the DNA in 20 µL sterile 1 m*M* Tris-HCl, pH 8.0.
17. Store the samples at –80°C and avoid frequent thawing and freezing.

3.3.1.2. Step 2: PCR Amplification of the CGG Repeat

1. Use 5 µL of the bisulfite-treated DNA as a template and prepare the PCR samples as follows: 5 µL of 10X buffer, 1 µL $MgCl_2$, 5 µL dimethyl sulfate (DMSO), 2 µL dNTPs, 2 µL of primers FCDF and FCDR, 4 U platinum *Taq* polymerase in a final volume of 50 µL.
2. The PCR conditions are as follows: initial denaturation at 95°C for 10 min, followed by 30 cycles of denaturation at 95°C for 30 s, annealing at 55°C for 30 s and elongation at 72°C for 1 min, and a final elongation step at 72°C for 10 min.
3. The size of the expected band is 74 + 3*n* (*n* = number of CGG repeats).
4. Purify the PCR band from a low-melting 2% agarose gel by using the QIAquick PCR Purification Kit (Qiagen).

3.3.1.3 Step 3: Cloning of the PCR Product

1. Clone the purified PCR product in the pcDNA3.1/V5-His TOPO vector according to the manufacturer's instructions in the following reaction: 4 µL PCR, 1 µL vector, 1 µL salt solution.
2. The TOPO reaction is performed at room temperature for not longer than 15 min; then, 2 µL of the reaction are used for transformation of Top 10 competent cells, following the instructions of the manufacturer.
3. Finally, the transformed bacteria are plated on CLONdisks and incubated at 37°C overnight.

3.3.1.4. Step 4: Miniprep and Isolation of Plasmid DNA

1. Two milliliters of LB/ampicillin is used for inoculation of a miniprep culture. From each transformation, numerous colonies are picked and used for amplification of plasmid DNA.
2. The plasmid DNA is isolated the next day with the QIAprep Spin Miniprep Kit (Qiagen) according to the instructions.

3.3.1.5. Step 5: Sequencing of the Plasmid DNA

1. The sequencing reaction is performed with T7 and BGH primers mapping sequences in the vector, so that the entire insert can be sequenced in both directions. The sequence reaction includes plasmid DNA up to 5 µL, 2 µL BigDye mix, 2 µL of 5X buffer, 1 µL T7 or BGH buffer; final volume = 10 µL.
2. The reactions are performed using a Perkin-Elmer thermocycler 9600 with the following conditions: initial denaturation at 96°C for 45 s, followed by 30 cycles of denaturation at 96°C for 10 s, annealing at 51°C for 5 s, and elongation at 60°C for 4 min. The reactions are stored at –20°C until further processed.
3. The sequence reactions were purified through a 96-well plate with Sephadex G-50 Superfine (Amersham).
4. Prepare the purification plate at least 2 h before use. Add Sephadex G-50 in all 96 wells and add 300 µL water. Let the plate stand for 2 h at room temperature so that the Sephadex is equilibrated.

5. Centrifuge the plate at 910g for 5 min to remove the extra water.
6. Apply the sequence samples on the plate.
7. Centrifuge the plate at 910g for 5 min. The purified samples are now in the collecting plate.
8. Evaporate the water from the samples by placing the plate at 95°C for 10–15 min.
9. Resuspend each sequence reaction in 2 µL loading buffer.
10. Denature the samples at 95°C for 4 min and immediately put on ice water.
11. Load the samples on a sequence gel and run on the ABI Prism 377 Sequencer for 7 h.
12. Analyze the sequence data with the ABI Prism Collection software.

4. Notes

1. For digestion, it is advised to use *Hin*dIII. Alternatively, *Eco*RI can be used, giving similar size bands, but often a background band is visible, making the interpretation of the results more difficult. As a second enzyme for testing methylation, numerous different enzymes can be used: *Eag*I, *Bss*HII, or *Nru*I ***(13)***.
2. With this last method, the whole range of premutations (up to 200 repeat units) can be amplified, whereas with the above-described radioactive method, the amplification in the high premutation range is difficult. However, there are difficulties with the delivery of the FRAX kit by PE Biosystems and the kit cannot be delivered at the moment by PE Biosystems.
3. With this method, it is also possible to determine the number and the position of AGG repeats that often are interrupting the CGG repeat, thereby stabilizing the CGG repeat ***(14)***.

Acknowledgments

The authors wish to thank Wout Deelen for providing information about the nonradioactive Southern blot method—in particular, primer information—and Marianne Hoogeveen for the help with the PCR methodology. Updates on methodologies will be published by Rob Willemsen on the website www.eur.nl/fgg/ch1/fragx/index.html.

References

1 Kooy, R. F., Willemsen, R., and Oostra, B. A. (2000) Fragile X syndrome at the turn of the century. *Mol. Med. Today* **6,** 193–198.
2 Fu, Y. H., Kuhl, D. P., Pizzuti, A., et al. (1991) Variation of the CGG repeat at the fragile X site results in genetic instability: resolution of the Sherman paradox. *Cell* **67,** 1047–1058.
3. Bakker, C. E., Verheij, C., Willemsen, R., et al. (1994) Fmr1 knockout mice: a model to study fragile X mental retardation. *Cell* **78,** 23–33.
4 Bontekoe, C. J., Bakker, C. E., Nieuwenhuizen, I. M., et al. (2001) Instability of a (CGG)(98) repeat in the Fmr1 promoter. *Hum. Mol. Genet.* **10,** 1693–1699.
5 Gold, B., Radu, D., Balanko, A., et al. (2000) Diagnosis of Fragile X syndrome by Southern blot hybridization using a chemiluminescent probe: a laboratory protocol. *Mol. Diagn.* **5,** 169–178.
6 Oostra, B. A., Jacky, P. B., Brown, W. T., et al. (1993) Guidelines for the diagnosis of fragile X syndrome. *J. Med. Genet.* **30,** 410–413.
7 Brown, W. T., Houck, G. E., Jeziorowska, A., et al. (1993) Rapid Fragile-X carrier screening and prenatal diagnosis using a nonradioactive PCR test. *JAMA* **270,** 1569–1575.

8 Das, S., Kubota, T., Song, M., et al. (1997) Methylation analysis of the fragile X syndrome by PCR. *Genet. Test* **1,** 151–155.
9 Panagopoulos, I., Lassen, C., Kristoffersson, U., et al. (1999) A methylation PCR approach for detection of fragile X syndrome. *Hum. Mutat.* **14,** 71–79.
10 Genc, B., Muller-Hartmann, H., Zeschnigk, M., et al. (2000) Methylation mosaicism of 5'-(CGG)(n)-3' repeats in fragile X, premutation and normal individuals. *Nucleic Acids Res.* **28**, 2141–2152.
11 Frommer, M., McDonald, L. E., Millar, D. S., et al. (1992) A genomic sequencing protocol that yields a positive display of 5-methylcytosine residues in individual DNA strands. *Proc. Natl. Acad. Sci. USA* **89,** 1827–1831.
12 Grunau, C., Clark, S. J., and Rosenthal, A. (2001) Bisulfite genomic sequencing: systematic investigation of critical experimental parameters. *Nucleic Acids Res.* **29**, E65.
13 Rousseau, F., Heitz, D., Biancalana, V., et al. (1991) Direct diagnosis by DNA analysis of the fragile X syndrome of mental retardation. *N. Engl. J. Med.* **325,** 1673–1681.
14. Kunst, C. B., Leeflang, E. P., Iber, J. C., et al. (1997) The effect of FMR1 CGG repeat interruptions on mutation frequency as measured by sperm typing. *J. Med. Genet.* **34,** 627–631.

13

Analysis of CTG Repeats Using DM1 Model Mice

Cédric Savouret, Claudine Junien, and Geneviève Gourdon

Summary

This chapter describes how transgenic mice can be made with human genomic DNA fragments cloned from DM1 patients' DNA and how the CTG repeat instability is assessed over generations and in different tissues. Construction of cosmid libraries is fully reported from the extraction of high-molecular-weight DNA from patients' lymphoid cell lines, to the screening and mapping of the positive clones. After establishment of transgenic lines, we explained the methods used to analyze (a) the CTG repeats that are inherited from the transgenic parents, with regard to age, sex, and parental CTG repeat sizes, and (b) the CTG repeat-length variations that can be observed in somatic tissues and in sperm.

Key Words: Myotonic dystrophy; transgenic mice; CTG repeat; cosmid library; small-pool PCR.

1. Introduction

Myotonic dystrophy type 1 (DM1) ***(1)*** results from the expansion of a very unstable CTG repeat located in the 3' untranslated region (UTR) of the DM protein kinase gene (DMPK) ***(2–5)***. The triplet repeat also is located in a large CpG island encompassing the *SIX5* gene. To study the CTG repeat, instability mechanisms over successive generations, in somatic and germinal tissues, transgenic mice have been generated with human genomic DNA fragments of 45 kb of the DM1 region carrying different repeat lengths. In order to reconstitute the accurate human genomic environment in mice, human genomic DNA fragments were cloned from patients' DNA in cosmid libraries ***(6,7)***. To be able to compare the stability of different CTG repeats in the same genomic context, the cosmids carrying either a 20 CTG normal repeat, a moderate expansion of 55 CTG, or a large 350 CTG repeat expansion were carefully mapped and subcloned to be identical except for the CTG repeat length. This chapter describes the making of the transgenic mice and their characterization, followed by the methods for the analysis of CTG repeat instability that is successfully reproduced in tissues and over successive generations, as observed in patients.

From: *Methods in Molecular Biology, vol. 277: Trinucleotide Repeat Protocols*
Edited by: Y. Kohwi © Humana Press Inc., Totowa, NJ

2. Materials

1. Cell lysis buffer: 100 m*M* NaCl, 10 m*M* Tris-HCl, pH 8.0, 25 m*M* EDTA, pH 8.0, 0.5% sodium dodecyl sulfate (SDS), 2% Sarkosyl.
2. Tissue lysis buffer: 100 m*M* Tris-HCl, pH 8.0, 5 m*M* EDTA, pH 8.0, 0.2% SDS, 200 m*M* NaCl, 100 μg/mL proteinase K.
3. Tris-borate EDTA buffer (TBE): (89 m*M* Tri-borate, 89 m*M* boric acid, 8 m*M* EDTA, pH 8.0).
4. PBS: phosphate-buffered saline (10 m*M* phosphate buffer, pH 7.4, 138 m*M* NaCl, 2.7 m*M* KCl).
5. 20X SSC: 175.3 g NaCl, 88.2 g sodium citrate per liter, pH 7.0 with NaOH.
6. Dialysis bag (e.g., Snakeskin Pleated Dialysis tubing; Pierce).
7. LB-amp: Luria–Bertani medium (10 g Bacto-tryptone, 5 g Bacto-yeast extract, 10 g NaCl, pH 7.5 with NaOH) supplemented with ampicillin (50 μg/mL).
8. *Escherichia coli* strain NM554.
9. Cosmid packaging kit (Gigapack packaging extract; Stratagene).
10. SuperCos I cosmid vector (Stratagene).
11. Bacteria agar plates: LB with 15 g/L Bacto-agar, autoclaved, supplemented with ampicilin.
12. Nitrocellulose membranes (Millipore, or Hybond-N+; Amersham).
13. Nylon membranes (Millipore).
14. Oligonucleotide primers and polymerase chain reaction (PCR) equipment as described in the text.
15. Restriction enzymes, T4 DNA ligase and shrimp alkaline phosphatase.
16. Qiagen plasmid kit.
17. Pulse-field gel apparatus.
18. Agarose and electrophoresis equipment for DNA analysis.
19. Acrylamide and sequencing gel equipment.
20. Ultraviolet (UV) lamp for DNA/etidium bromide detection.
21. Radioactivity equipment.
22. Autoradiography equipment.
23. Access to animal facilities.

3. Methods

The methods reported in this chapter describe all of the steps for the making of transgenic mice from the construction of cosmid libraries, the identification of positive clones carrying the CTG repeat, and the preparation of DNA for oocyte injection and establishment of transgenic mice lines to the CTG repeat analysis throughout successive generations in somatic and germinal tissues.

3.1. Cosmid Libraries

Cosmid libraries were constructed using DNA extracted from lymphoblastoid cell line of DM1 patients. DNA from a mildly affected patient with about 55 CTGs was first used to clone the 55 CTG construct. He was the grandfather in a large DM1 family in which the daughter, with a typical adult-onset DM1 and about 500 CTGs, gave birth to a child with the severe congenital form of DM1. DNA from this daughter was used to clone the 20 and the 360 constructs.

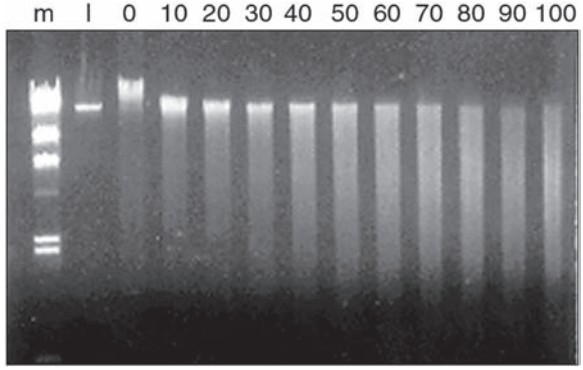

Fig. 1. Control of partial digestion. Samples of DNA digested with MboI for 0, 10, 20, 30, 40, 50, 60, 70, 80, 90, and 100 min were run on 0.8% agarose gel. In this example, 10 min was chosen for the preparative partial digestion time, *t*. m: lambda *Hin*dIII; l: nondigested lambda DNA.

3.1.1. Construction

After trypsinization and centrifugation of the cells according to common protocol ***(8)***, cells pellets were recovered in cell lysis buffer with boiled RNase A (50 µg/mL). After incubation for 1 h at 4°C on a rotating wheel, proteinase K (250 µg/mL final) was added and incubated overnight at 4°C. After addition of 1 vol of cell lysis buffer, DNA was extracted very gently three times with phenol/chloroform and precipitated with 0.3 *M* NaCl final and 3 vol of cold ethanol (*see* **Note 1**). In order to get a maximum of large fragment (around 45 kb), 25 µg of high-molecular-weight DNA was tested for partial digestion with 1 U of *Mbo*I every 10 min up to 100 min (*see* **Fig. 1**). Digestion was checked on 0.8% agarose gel and then the preparative digestion was realized in three independent tubes: (1) at the chosen time *t*, (2) at $t + 5$ min, and (3) at $t - 5$ min. Partially digested DNA was fractionated by pulsed-field gel electrophoresis, and purified fragments, between 40 and 45 kb, were electroeluted from the gel in dialysis bag. After precipitation and resuspension in water and quantification, 200 ng of DNA fragments were ligated in 10 µL with 200 ng of Scossbs vector linearized with *Bam*HI and dephosphorylated with the shrimp alkaline phosphatase. Scossbs derives from SuperCos I vector, modified by insertion of a polylinker containing *Sal*I, *Bam*HI, and *Sal*I restriction sites (*see* **Fig. 2**). Four milliliters of the ligation mix was packaged in NM554 bacteria with the Gigapack II packaging extract according to the manufacturer's instructions and the bacteria were plated on 20 × 20-cm selective (ampicillin) plates.

3.1.2. Screening

Two replica filters were prepared for each plate with nitrocellulose membranes, using classical protocol ***(8)***, and hybridized with the DMHR4/5 probe. This probe was synthesized by PCR using human genomic DNA and primers DMHR4 (GGACGACTTCGAGATTCTG) and DMHR5 (GCATGTCCCACTTGTTCAT),

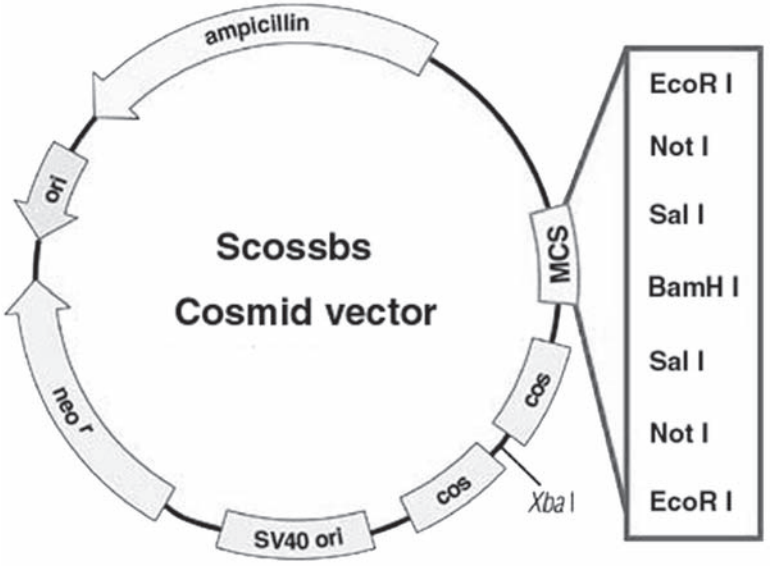

Fig. 2. Schematic drawing of Scossbs used for cosmid libraries. This vector is derived from SuperCos I (Stratagene) modified by the insertion of a polylinker carrying *Sal*I, *Bam*HI, and *Sal*I restriction sites.

respectively, located in exon 2 and exon 3 of the DMPK gene. PCR was performed in a 100-μL reaction containing 100 ng of genomic DNA, 0.2 μ*M* of each primer, 0.2 μ*M* of each dNTP, 1.5 m*M* $MgCl_2$ and 1 U of *Taq* DNA polymerase (denaturing temperature, 94°C; annealing temperature, 54°C; elongating temperature, 72°C. Positive colonies were plated on secondary 10 × 10-cm agar plates and rescreened with the same probe to isolate single positive colonies. Cosmid DNA was extracted from bacteria with Qiagen plasmid extraction kit.

3.1.3. Mapping and Subcloning

Cosmid DNA from the different clones were subjected to single, double, or triple digestion with several enzymes (*Eco*RI, *Eco*RV, *Nde*I, *Bam*HI, *Hin*dIII, *Not*I, *Cla*I) to get a precise map of the 40- to 50-kb genomic human inserts. Lengths of the CTG repeats were determined by sequencing (for the clones carrying 20 and 55 CTG) and by PCR (for the clones with >300 CTG, see PCR conditions and primers in **Subheading 3.3.**). From the two libraries set up with DNA that was extracted from the affected grandfather and with DNA from his affected daughter, three different clones were obtained with 20 (DM20), 55 (DM55), and 360 CTGs (DM300) encompassing a comparable human genomic region, including the *DMPK* gene and the flanking *DMWD* and *SIX5* genes. To obtain fragments identical in all but the size of the repeat, the *Nde*I–*Cla*I fragment, carrying the *DMPK* gene from exon 2 and the *SIX5* gene, was replaced in the DM55 clone by the corresponding fragments recovered from DM300 and DM20 (*see* **Fig. 3**). As there were two *Cla*I sites in DM55 (one in the insert, one in

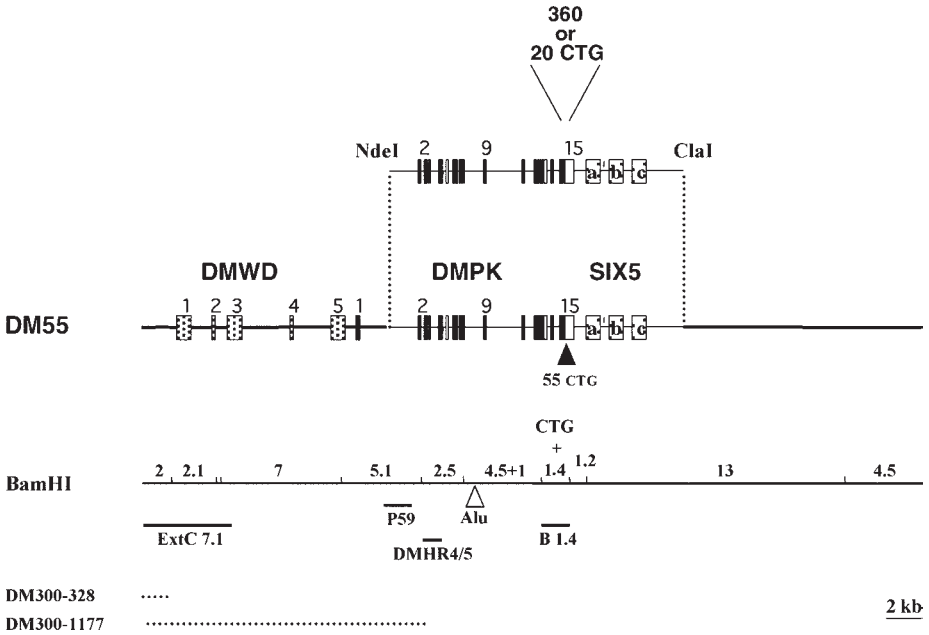

Fig. 3. Structure of the human genomic DNA fragments used to generate transgenic mice. The 45-kb fragments carry the *DMWD*, *DMPK*, and *SIX5* genes. To get DNA fragments with different CTG repeat lengths, the *Nde*I/*Cla*I fragment from DM55 was replaced by *Nde*I/*Cla*I fragments containing 360 or 20 CTGs. Probes used to characterize the transgenic mice are shown below the *Bam*HI restriction map. The Alu insertion carried only by fragments with 55 and 360 CTGs is also indicated on the *Bam*HI restriction map. Dotted lines represent deletions in the integrated fragment in DM300–328 and DM300–1177 lines.

the vector), the DM55 cosmid was prepared by *Nde*I and partial *Cla*I digestion, followed by dephosphorylation with the shrimp alkaline phosphatase. The vector-carrying part of the genomic insert (except for the *Nde*I–*Cla*I fragment) was purified by pulse-field gel electrophoresis and ligated with the *Nde*I–*Cla*I fragments prepared from DM20 and DM300 and packaged as described in **Subheading 3.1.1.** The DM55 and modified DM300 clones were identical except that they carried CTG repeats of different sizes. The *Nde*I–*Cla*I fragment with 20 CTGs originated from a normal allele and did not contain the Alu repeat insertion localized in DMPK intron 8 of the mutated alleles.

3.2. Transgenesis

Described here are the steps that can be used for purification of DNA fragments and establishment of transgenic mice lines.

3.2.1. Preparation of DNA Fragments

Cosmid DNA were digested with *Sal*I and 45-kb inserts were recovered after electroelution from a 0.8% agarose gel (*see* **Note 2**). DNA were purified by passage

through a Sephadex G-50 column, previously equilibrated with injection buffer (10 m*M* Tris-HCl, pH 7.5, 0.1 m*M* EDTA). Transgenic mice were produced by microinjection of the purified insert (0.4 ng/µL; *see* **Note 3**) into pronuclei of fertilized mouse eggs (B6D2/F1), which where subsequently transferred to pseudopregnant females according to classical protocol ***(9)***.

3.2.2. Screening of Transgenic Mice

Tail biopsies, performed at weaning, were incubated overnight at 56°C in tissue lysis buffer. After rapid centrifugation, supernatants were added to 1 vol of isopropyl alcohol. Precipitated DNA was recovered by centrifugation and resuspended in water. Transgenic mice were screened by PCR using DNA from tail biopsies and primers DMHR4/DMHR5 under the conditions described in **Subheading 3.1.2.** Positive founders were confirmed by Southern blotting after digestion with *Bam*HI and hybridization with the *Bam*HI 1.4-kb fragment containing the DMPK CTG repeat (*see* **Fig. 3**) according to standard protocol ***(8)***.

3.2.3. Mapping of the Integrated Fragments

The copy number of the integrated fragments in the different lines was determined by Southern blot hybridization with probe p59 located in the human *DMPK* gene (*see* **Fig. 3**) and with probe EPO, a 1-kb *Pst*I fragment from the murine erythropoietin gene. Densitometric comparison to a fragment from the endogenous single-copy murine gene and to known standards (nontransgenic mouse DNA mixed with known DM55, DM20, or DM320 cosmid copy numbers) allowed one to determine precisely the copy number carried by the founders and their transgenic progeny. The same blots were hybridized with the ExtC 7.1 probe localized at the extremity of the human genomic insert to map the junction fragments. This probe gives information on how the multicopies are inserted (different insertion sites, tandem repeat, etc.). A third hybridization was performed on the blots using the entire DM55 cosmid (digested with *Bam*HI) as a probe, to check the integrity of the integrated fragment in each line. Additional Southern blotting experiments with other enzymes were performed to map carefully deletions of inserts in several lines (*see* **Fig. 3**).

3.2.4. Establishment of Transgenic Lines

The identified founders and the transgenic offspring were crossed with nontransgenic C57BL/6 mice. Some founders carried multiple insertions on different chromosomes, and different sublines were obtained from them. Transgenic mice were reared in an air-conditioned, ventilated animal facility.

3.3. Intergenerational CTG Repeat Instability Analysis

The following methods describe approaches to study CTG repeat variations during transmission of the repeat over successive generations.

3.3.1. Breeding Strategy

Hemizygote mice for the integrated fragment that received it only from one parent are used to study the CTG repeat transmission over generations. Transgenic male or

female of different ages and carrying different CTG repeats are crossed with C57BL/6 nontransgenic mice. These different combinations allow to analyze how sex, age, and CTG repeat length of the transmitting parent affect CTG repeat-length variations in the next generation. Influence of age of the transmitting parent can be also assayed with multiple breedings of the same transgenic mice. Inherited CTG repeat lengths are determined with DNA prepared from tail biopsies obtained at weaning, when somatic instability is limited. To determine genes involved in the CTG repeat instability mechanisms (e.g., repair genes), hemizygous transgenic mice can be crossed with mice knockout for the candidate gene. Then, CTG repeat lengths are studied, as described in the following subsections, in the different genotypes (+/+, +/–, and –/– for the studied gene).

3.3.2. PCR Analysis of the 20 and 55 CTG Repeats

To determine CTG repeat lengths in DM20 and DM55 transgenic mice, PCR analyses are performed in 50-µL reactions containing 16.6 m*M* ammonium sulfate, 67 m*M* Tris-HCl, pH 8.8, 1.5 m*M* $MgCl_2$, 67 µ*M* EDTA, pH 6.8, 10% dimethyl sulfoxide (DMSO), 10 m*M* of 2-mercaptoethanol, 0.2 m*M* dNTPs, 0.2 µ*M* of primers 101 and 102 (101: 5'-CTTCCCAGGCCTGCAGTTTGCCCATC-3'; 102: 5'-GAACGGGGCTCGAAGGGTCTTGTAGC-3'). Cycling parameters are 94°C denaturation, 65°C annealing, 72°C elongation. Two microliters of amplified products are mixed with 2 µL of formamide loading buffer, heated for 5 min at 100°C, separated on 6% denaturing acrylamide gel, blotted onto Nylon membrane, and hybridized with 3'-end-labeled 101 primer. Hybridized bands are detected by autoradiography and their size determined by comparison with M13 sequencing reactions.

3.3.3. PCR Analysis of >300 CTG Repeats

To determine the CTG repeat length in DM300 transgenic mice, 15 ng of tail DNA samples are amplified in 25-µL reactions with 45 m*M* Tris-HCl, pH 8.8, 11 m*M* ammonium sulfate, 4.5 m*M* $MgCl_2$, 6.7 m*M* of 2-mercaptoethanol, 4.4 µ*M* EDTA, pH 6.8, 1 m*M* dNTPs, 113 µg/mL bovine serum albumin ***(10)***, 1.4 µ*M* primer 101, 1.4 µ*M* 102, and 0.2 U of *Taq* polymerase. DNA is denaturated by heating to 95°C for 10 min. Reactions involve 30 cycles of 94°C (45 s), 66°C (45 s), and 70°C (3 min) with a chase of 66°C (1 min) and 70°C (10 min) in a Perkin-Elmer 9600 thermal cycler. Amplified products (2 µL) are mixed with 2 µL of formamide loading buffer, heated for 5 min at 100°C, and subjected to electrophoresis in a 4% denaturing acrylamide gel at 25 W for 16 h. After electrophoresis, the gel is incubated in 1X TBE with ethidium bromide for 10 min (*see* **Note 4**) and UV exposed for 8 min. DNA is blotted onto Nylon membrane and probed with the 3'-end-labeled 101 primer. After autoradiography, the size of PCR products is determined by comparison with a radiolabeled 100-bp DNA ladder (*see* **Note 5**).

3.4. Somatic CTG Repeat Instability Analysis

The study of somatic CTG repeat-length mosaicism in transgenic mice is based on the same methods as for intergenerational instability. However, some technical

changes are necessary along the protocol to obtain further resolution and quality, especially for transgenic mice carrying over 300 CTG repeats.

3.4.1. DNA Extraction From Tissues

1. Kill the mouse by cervical dislocation, in accordance with the country's veterinary laws in application.
2. Perform classical dissection according to the tissues in which the level of instability is to be assayed. First, take between 100 and 150 µL of blood from the thoracic cage or heart. Remove the pancreas quickly, as this tissue suffers fast autolysis after death. A possible sequence for tissue removing is as follows: blood, pancreas, liver, thymus, heart, lungs, stomach, small intestine, kidney, ovaries/testis, quadriceps, soleus and gastrocnemian muscles, and tongue. Turn the mouse with the back upward; then, remove eyes, brain (without olfactive bulbs), and cerebellum. Store the liquid-nitrogen-frozen tissues at –80°C for further extraction.
3. For each tissue (up to 100 mg), add 400 µL of tissue lysis buffer and 100 ng/µL proteinase K in the Eppendorf tube at room temperature.
4. Vortex briefly so that the whole tissue is immerged, and incubate overnight at 56°C in a water bath with moderate agitation.
5. Check the lysis by vortexing the lysis product, which should be homogeneous. If lysis does not appear sufficient, add 1% SDS and leave for 2 more hours at 56°C.
6. After centrifugation for 5 min at 10,000*g* at room temperature, recover 350 µL of supernatant. RNA removal can be performed at this step, if necessary, with 100 µg/mL RNase A for 30 min at 37°C (*see* **Note 6**).
7. DNA is extracted twice with phenol/chloroform, twice with chloroform and precipitated with 3 vol of cold ethanol and 0.5 *M* NaCl, and resuspended in 100 µL up to 400 µL of water or TE (10 m*M* Tris-HCl; 1 m*M* EDTA) according to the size of the DNA pellet.

3.4.2. PCR and Acrylamide Gel

1. Prepare 15-ng/µL dilutions in water for each tissue and perform PCR as described in **Subheading 3.3.3.** It is very important that all PCR products appear homogeneous when loaded onto agarose gel for PCR testing. Do not hesitate to perform PCR once again with adjusted DNA concentrations.
2. Analysis of CTG repeat length in tissues is performed according to **Subheadings 3.3.2.** and **3.3.3.**, with some differences. The acrylamide gel to be used for migration of PCR products from mice with >300 CTG has a 3.5% concentration, to get a better resolution between tissues. Migration is performed for 30 min at 55 W, followed by 13 h, 30 min at 25 W. The size and aspect of the smear obtained for each tissue after hybridization and autoradiography indicates the CTG repeat length mosaicism: Extended smears indicate very unstable tissues, whereas sharper bands correspond to stable tissues. Blood is used as a reference for somatic mosaicism, as this tissue is very stable and is considered to represent the inherited basal CTG repeat length for each mouse. All upper bands in other tissues are considered as expansions, whereas all bands or smears appearing below the level of blood PCR products are considered as contractions.

3.4.3. Small-Pool PCR Analysis of the CTG Repeat

Small-pool PCR (SP-PCR) ***(11)*** is certainly the sharpest and more efficient method to resolve the smears obtained when analyzing somatic instability in tissues. The DNA used

as a matrix for this PCR is diluted so that the amount of DNA used for amplification corresponds to a single diploid genome. Multiplication of these one-cell DNA amplifications is necessary to uncover completely CTG repeat-length mosaicism in the different tissues. This method increases the precision and relevance of results but must be performed with extreme care to avoid contamination with regards to the small amounts of DNA used. In this way, the use of a laminar-flow hood is strongly recommended.

1. Digest 10 μg of tissue DNA in a final volume of 100 μL, with the *Hin*dIII enzyme. Incubate overnight at 37°C and perform phenol–chloroform extraction. After precipitation, resuspend the DNA pellet in 100 μL of water and measure DNA concentration.
2. Prepare dilutions of *Hin*dIII-digested DNA in water with 600 pg/μL (100 theorical diploid genomes), 60 pg/μL (10 theorical diploid genomes), and 6 pg/μL (1 theorical diploid genome), and also 15 ng/μL of blood DNA. Also prepare a 15-ng/μL sample from a positive control DNA (tail DNA from a transgenic mouse, for example).
3. Perform SP-PCR in a 7-μL reaction with 1 μL (6, 60, or 600 pg, 29 times each) of *Hin*dIII-digested DNA, 45 m*M* Tris-HCl, pH 8.8, 11 m*M* ammonium sulfate, 4.5 m*M* $MgCl_2$, 6.7 m*M* of 2-mercaptoethanol, 4.4 μ*M* EDTA, pH 6.8, 1 m*M* dNTPs, 113 μg/mL bovine serum albumin, 1.43 μ*M* of primers 101 and 102 surrounding the CTG repeat, and 1 U of *Taq* DNA polymerase. Also perform this reaction once with 15 ng of positive control DNA, twice with 15 ng of blood DNA, and six times with water instead of DNA to serve as blanks (negative controls). Reactions are performed through 28 cycles of 96°C (45 s), 68°C (30 s), and 72°C (3 min), followed by 68°C (1 min) and 72°C (10 min) to terminate the reaction.
4. Control PCR by loading 4 μL of PCR product and 3 μL of loading buffer on a 1.5% agarose gel with ethidium bromide. This control is only performed on the positive control, a blank, a 600-pg, a 60-pg, and a 6-pg well. Migrate in 1X TBE at 110 mA for 30 min (*see* **Note 7**).
5. The control of SP-PCR products is performed as presented in **Subheading 3.4.2.2.** on a 3.5% acrylamide gel, by loading 2 μL of product mixed with 2 μL of formamide loading buffer. Try to load an equal number of wells for 600, 60, and 6 pg on each gel (e.g., at least 15), preceded by blood as a control and the six blanks at the beginning of the gel. Also, load labeled markers ranging ideally from 100 to 2000 bp (*see* **Note 8**).
6. For results to be of statistical evidence, at least 80 single sharp bands should be obtained from 6-pg wells for each tissue ***(11)***. The results (*see* histograms in **Fig. 4**) represent, with precision, the level of CTG repeat-length mosaicism in tissue.

3.5. Gametic Instability

To get further insight into intergenerational instability, it is important to assay the CTG repeat instability in gametes. The following protocols are devoted to the analysis of CTG repeat-length mosaicism in gametes from transgenic transmitting parents and especially in sperm.

3.5.1. DNA Extraction From Sperm

This protocol is critical for the correct extraction of sperm DNA and avoids the contamination by DNA from epididymis, epithelial cells, or any other nongametic cells ***(12)***. The level of instability observed from this sperm DNA solution, recovered from the vas deferens, reflects the level of mosaicism in spermatozoa that are mature

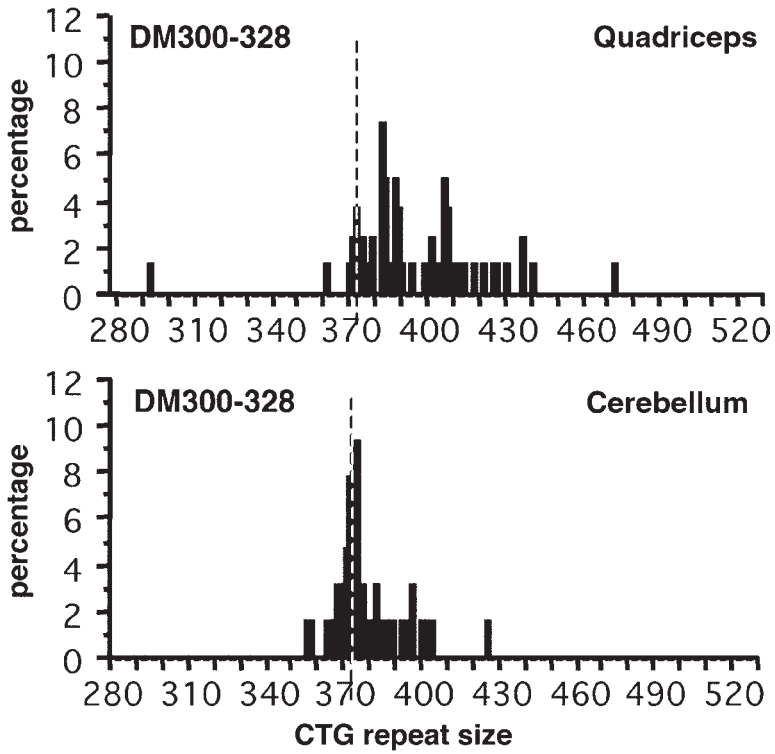

Fig. 4. Histogram showing CTG repeat-length mosaicism in DM300–328 transgenic mouse muscle (quadriceps) and in the cerebellum after small-pool PCR experiments. The *X*-axis represents the CTG repeat size and the *Y*-axis displays the relative percentage for each size among all single molecules analyzed. The dotted line represents the CTG repeat length measured in blood, used as a reference for range and direction of somatic CTG repeat length changes; contractions are displayed on the left of this line, and all lengths higher than blood repeat length are considered as expansions.

and usable for fertilization. From the vas deferens, placed after dissection in a Petri dish with 1X PBS (*see* **Note 9**), proceed as follows:

1. Maintain one extremity of the vas deferens and slide gently from this end with a clean scalpel to remove semen.
2. Carefully pipet the semen with approx 200 µL of 1X PBS into an Eppendorf tube at room temperature.
3. Vortex for about 10 s and centrifuge for 4 min at 12,000 rpm (10,000*g*) at room temperature.
4. Discard the supernatant and resuspend the pellet in 100 µL of 1X SSC, 1% SDS (*see* **Note 10**).
5. Incubate at room temperature for 15 min. This step allows the lysis of epithelial cells and seminal leukocytes.

6. Centrifuge for 4 min at 10,000*g* at room temperature and resuspend the pellet containing spermatozoa heads in 150 µL of 1X SSC, 1% SDS. Repeat this step once.
7. Centrifuge for 4 min at 10,000*g* at room temperature and resuspend the pellet in 150 µL of 1X SSC.
8. Centrifuge for 4 min at 10,000*g* at room temperature and resuspend the pellet in 100 µL of 0.2X SSC, 1% SDS with 1 *M* 2-mercaptoethanol added to lyse spermatozoa heads.
9. Incubate for 1 h at room temperature.
10. Perform phenol–chloroform extraction as described in **Subheading 3.4.1., step 7**. After precipitation with cold ethanol and 0.5 *M* NaCl, resuspend the final DNA pellet in 50 µL of water or TE 10:1 and keep at 4°C before DNA concentration estimation.

3.5.2. PCR and Gel Analysis

The level of CTG repeat size mosaicism in sperm can be first assayed according to **Subheading 3.4.2.** with comparison to blood. Alternatively, SP-PCR can be used to resolve the smears in sperm and increase precision rate. After dissection of males (e.g., at different ages to observe the progression of mosaicisms with age), DNA is extracted from sperm according to **Subheading 3.5.1.** and SP-PCR are performed as described in **Subheading 3.4.3.** The CTG repeat length in blood, relatively stable and representing closely the inherited CTG repeat size, is used as a reference for the expansion/contraction sizes calculation in sperm.

4. Notes

1. Cells were resuspended in 1 mL/10^8 cells. Addition of 1 vol of lysis buffer prevents the solution from becoming viscous and helps to preserve the good quality of high-molecular-weight DNA. During phenol extraction, care must be taken and solution must be mixed very gently.
2. To avoid DNA breakage before injection, agarose gels were run without ethidium bromide (EB). After migration, part of the gel loaded with a control sample was incubated in 1X TBE with EB. A hole was realized in the non-EB-stained gel and in the gel with EB just after the 45-kb band. Bottoms were covered with agarose 1% and holes were filled with 1X TBE. The two parts of the gel were submitted to electrophoresis and the migration of the DNA in the hole followed with an ultraviolet lamp.
3. This low concentration of the injected DNA solution guarantees a low copy number in mice.
4. Although this step may increase the blotting efficiency, we found that incubation of the gel in 1X TBE with EB can be omitted.
5. On the film obtained after autoradiography, draw a line between the highest band of the two markers surrounding the spots. From this line, measure the distance of migration for each band of the marker and for each sample, by considering the center of the band. Proceed with precision to get accurate results. From the migration logarithmic curve of the marker, measure the number of basepairs obtained for each sample from the migration distance. Withdraw 114 bp from this size (part of the PCR 300 amplification product not contained in the CTG repeat) and divide by 3 to get the number of CTGs for each sample. Do not forget to load on the same gel PCR samples from the transmitting parent to analyze precisely the CTG repeat variations over generations.
6. For some tissues, the pellet is not strongly defined or attached at the bottom of the tube. This is often the case for lungs in particular. Supernatant must be carefully removed.

7. Do not attempt to see bands for 60 and 6 pg if dilutions were correct. Only a faint band could be seen for the 600 pg, whereas nothing should appear in the blank. A sharp band should be observed for the positive control and blood.
8. If dilutions used were correct, sharp single bands should be observed in wells with 6-pg DNA amplification products, corresponding to the amplification of DNA contained in a single cell. Ideally, one-third of these wells should be empty (no visible bands after sufficient exposure). If more than one band is observed in 6-pg wells (e.g., 5, 10, 15, . . . or a broad smear), repeat **step 2** of **Subheading 3.4.3.** using corrected dilutions of *Hin*dIII-digested DNA. In contrast, if no bands are observed in 6-pg wells, repeat **step 2** of **Subheading 3.4.3.** with more concentrated dilutions. Wells loaded with 600- and 60-pg DNA amplification products should present smears with respectively 100 and 10 spots. Repeat the SP-PCR experiments and gel loadings until the ideal pattern is observed for 6-pg loadings. From this point, dilutions with 600 and 60 pg can be discarded from the PCR plate and multiple amplifications of 6-pg DNA can be performed on a same plate. Do not forget to load multiple markers and references samples on the same gel to standardize measurement between gels.
9. It is better to extract the sperm DNA just after dissection. However, the vas deferens can be conserved in 1X PBS at 4°C for several hours.
10. Supernatant should be carefully discarded as the spermatozoa heads pellet is not always stuck at the bottom of the tube.

Acknowledgments

The authors thank E. Lodato for attentively caring for the mice. This work was supported by grants from Inserm, the Association Française contre les Myopathies (AFM), and the Université René Descartes. C. Savouret was supported by a grant from the Ministère de la Recherche et de la Technologie.

References

1. Harper, P. S. (2001) *Myotonic Dystrophy,* 3rd ed. Saunders, London.
2. Aslanidis, C., Jansen, G., Amemiya, C., et al. (1992) Cloning of the essential myotonic dystrophy region and mapping of the putative defect. *Nature* **355,** 548–551.
3. Brook, J. D., McCurrach, M. E., Harley, H. G., et al. (1992) Molecular basis of myotonic dystrophy: expansion of a trinucleotide (CTG) repeat at the 3' end of a transcript encoding a protein kinase family member. *Cell* **68,** 799–808.
4. Fu, Y. H., Kuhl, D. P. A., Pizzuti, A., et al. (1992) An unstable triplet repeat in a gene related to myotonic muscular dystrophy. *Science* **255,** 1256–1258.
5. Mahadevan, M., Tsilfidis, C., Sabourin, L., et al. (1992) Myotonic dystrophy mutation: an unstable CTG repeat in the 3' untranslated region of the gene. *Science* **255,** 1253–1255.
6. Gourdon, G., Dessen, P., Lia, A. S., et al. (1997) Intriguing association between disease associated unstable trinucleotide repeat and CpG island. *Ann. Genet.* **40,** 73–77.
7. Seznec, H., Lia-Baldini, A., Duros, C., et al. (2000) Transgenic mice carrying large human genomic sequences with expanded CTG repeat mimic closely the DM CTG repeat intergenerational and somatic instability. *Hum. Mol. Genet.* **9**, 1185–1194.
8. Sambrook, J. and Russell, D. W. (2001) *Molecular Cloning: A Laboratory Manual*, 2nd ed. Cold Spring Harbor Laboratory, Cold Spring Harbor, NY I.126–I.142.
9. Hogan, B., Beddington, R., Costantini, F., et al. (1994) *Manipulating the Mouse Embryo: A Laboratory Manual*, 2nd ed. Cold Spring Harbor Laboratory, Cold Spring Harbor, NY.

10 Jeffreys, A., Neumann, R., and Wilson, V. (1990). Repeat unit sequence variation in minisatellites: a novel source of polymorphism for studying allelic variation and mutation by single molecule analysis. *Cell* **60,** 473–485.

11 Monckton, D. G., Wong, L. J. C., Ashizawa, T., et al. (1995) Somatic mosaicism, germline expansions, germline reversions and intergenerational reductions in myotonic dystrophy males: small pool PCR analyses. *Hum. Mol. Genet.* **4,** 1–8.

12. Jeffreys, A. J., Tamaki, K., MacLeod, A., et al. (1994) Complex gene conversion events in germline mutation at human minisatellites. *Nature Genet.* **6,** 136–145.

14

Lentiviral-Mediated Gene Transfer to Model Triplet Repeat Disorders

Etienne Régulier, Diana Zala, Patrick Aebischer, and Nicole Déglon

Summary

This chapter describes the potential use of viral-mediated gene transfer in the central nervous system as a new strategy in developing animal models of neurodegenerative diseases. To illustrate the approach, procedures for the production of lentiviral vectors encoding polyQ proteins are provided, as well as methods for the determination of viral titers, in vitro infection, and basic protocols for in vivo studies in rodents.

Key Words: Gene transfer; brain; lentiviral vectors; primary cultures; animal models; rodent.

1. Introduction

The identification and cloning of polyglutamine-containing genes and the subsequent development of genetic models for triplet repeat disorders have opened up new opportunities for studying the mechanisms leading to neuronal degeneration. Today, a large panel of in vitro and in vivo genetic models is available ***(1–7)***. Recently, several groups, including ours, have proposed a new strategy for modeling genetic diseases, based on viral-mediated gene transfer. Lentiviral or adeno-associated vectors were injected in the brain of adult rats and primates to create Huntington's or Parkinson's disease models ***(8–13)***. This approach takes advantage of some unique properties of viral vectors and of the recent technical advances that have improved the production of recombinant viruses but also the efficiency of these gene transfer systems ***(14–16)***. Viral vectors are versatile, highly flexible, and relatively easy-to-use tools for performing in vivo studies and modeling central nervous system (CNS) disorders. Multiple genetic models with deletions or mutations in the transgene being expressed can be created in a short period of time. High expression levels can be reached, an important feature, to exacerbate the disease process, obtain functional and behavioral abnormali-

From: *Methods in Molecular Biology, vol. 277: Trinucleotide Repeat Protocols*
Edited by: Y. Kohwi © Humana Press Inc., Totowa, NJ

ties, and induce a strong neuronal degeneration in a time frame compatible with the rodent life-span. Injections in well-defined brain regions can be used to investigate the specificity of the neuropathology. In addition, the local administration of viral vectors eliminates potential side effects associated with a widespread overexpresssion of polyQ proteins ***(17–19)***. Regulated expression systems are available and can be integrated in the vectors to evaluate the reversibility of the pathology and perform gene-dosing experiments ***(20–22)***. Finally, models can be established in different mammalian species, thereby providing an opportunity to conduct studies in nonhuman primates. These primate models will be particularly valuable to assess complex behavioral changes, follow the appearance of the pathology by imaging, and perfom preclinical studies with therapeutic candidates.

1.1. Viral Vectors for CNS Applications

Various techniques have been developed to transfer genes into neurons, organotypic cultures, embryos, or brain of adult animals ***(23)***. Because of their natural propensity to cross the cellular membrane and transfer genetic material into target cells, viral vectors are particularly suitable for these studies. Viral vectors derived from adeno-associated virus (AAV), helper-dependent adenovirus (Ad), lentivirus (LV), or even herpes simplex virus (HSV) hold promise for CNS applications. Each vector is characterized by a unique set of properties, and the choice of the gene transfer system will ultimately depend on the specific aim of the study. In all cases, the viral genomes comprise genes and cis-acting regulatory sequences. In viral vectors, these two functions are separated to avoid recombination and formation of replication-competent viruses ***(24)***. The genes coding for viral proteins (viral particle and enzymes) are expressed from heterologous plasmids (packaging vectors). The *cis*-regulatory elements and a cassette driving the transgene expression are included in the transfer vectors (*see* **Fig. 1B**).

Importantly, multiply attenuated vectors with deletion of some or all pathogenic genes from the natural viruses have been produced (*see* **Fig. 1A,B**). The presence of a packaging signal in the transfer vector ensures the recognition and incorporation of this specific genetic material in the recombinant viral particles (*see* **Fig. 1B**). The transduction of target cells with recombinant viral vectors is therefore an abortive, nonreplicative, or single-round infection procedure (*see* **Fig. 1A**).

1.2. Lentiviral Vectors

Lentiviral vectors were initially derived from HIV-1 ***(25,26)*** and more recently from other members of the lentivirus family (feline immunodeficiency virus [FIV], simian immunodeficiency virus [SIV], equine infections anemia virus [EIAV], and bovine immunodeficiency virus [BIV]) ***(27–29)***. Lentiviral vectors are endowed with specific properties that make them particularly attractive for CNS applications. This includes the ability to infect and integrate into postmitotic cells at high efficiency, the long-term and sustained expression of transgenes, the absence of sequences coding for viral proteins that may evoke an immune response, and a cloning capacity of approx 9 kb, which can accommodate most transgenes. In 1996, Naldini and collaborators demon-

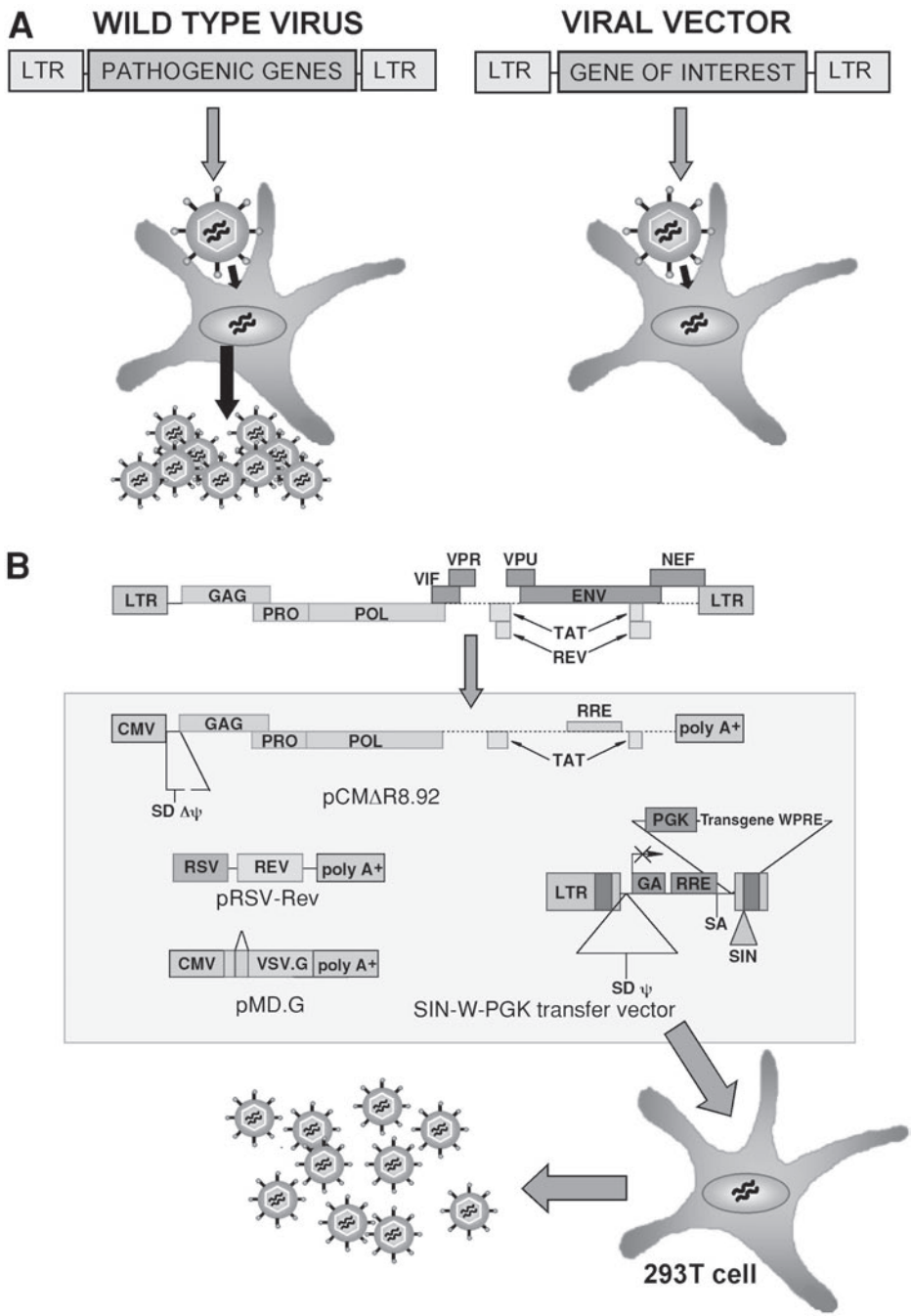

Fig. 1. **(A)** Schematic representation of HIV-1 wild-type and self-inactivating (SIN) lentiviral derived vectors. In contrast to the wild-type virus, which produces multiple particles after infection of permissive cells, SIN vector particles are replication-defective and do not contain genes coding for viral proteins. **(B)** Scheme of multiply-attenuated and SIN HIV-1

(*continued*)

strated that HIV-1-derived lentiviral vectors pseudotyped with the vesicular stomatitis virus G (VSV-G) envelope can efficiently transduce striatal and hippocampal neurons ***(25)***. New generations of lentiviral vectors with improved biosafety properties and incorporating structural elements important for the basic biology of the virus have been designed ***(30–34)***. Third-generation, multiply-attenuated, replication-deficient, and self-inactivating vectors split in four plasmids are now available ***(35)*** (*see* **Fig. 1**). Over the last few years, compelling data have been obtained concerning lentiviral-mediated gene transfer in the brain ***(25,36,37)***.

The present chapter describes the procedures for the production of lentiviral vectors encoding polyQ proteins, determination of viral titers, in vitro infection of cell lines and primary neuronal cultures, and basic protocols for in vivo studies in rodents.

2. Materials

1. 0.5 *M* $CaCl_2$: 73.5 g $CaCl_2 \cdot 2H_2O$; complete to 500 mL with distilled H_2O.
2. Trypsinization medium: Hanks balanced salt solution (HBSS) red phenol, 0.4 g/L KCl, 0.06 g/L KH_2PO_4, 8 g/L NaCl, 0.35 g/L $NaHCO_3$, 0.048 g/L Na_2HPO_4, 1 g/L D-glucose containing 0.05% trypsin and 0.53 m*M* EDTA.
3. 2X HBS: 28 mL of 5 *M* NaCl (final concentration, 280 m*M*), 11.9 g of HEPES (molecular weight [MW] = 238.3; final concentration, 100 m*M*), 750 µL of 1 *M* Na_2HPO_4 (final concentration, 1.5 m*M*). Adjust the pH to 7.1 with NaOH and complete to 500 mL with distilled H_2O. Store at –20°C in 50 mL aliquot (*see* **Note 1**).
4. Dulbecco's modified Eagle's medium (DMEM): 4.5 g/L glucose, 0.5 m*M* L-glutamine, 25 m*M* of HEPES without Na–pyruvate, 10% inactivated FCS (fetal calf serum), 1% penicillin–streptamycin (Pen-Strep: 10,000 U/mL, 10,000 µg/mL).
5. PBS/1% BSA: Add 5 g of bovine serum albumin (BSA) (Fluka, cat. no. 05484) to 500 mL phosphate-buffered saline (PBS), pH 7.4, and pass through a 0.22-µm filter.
6. Dissecting medium (DMX): PBS without Ca^{2+} and Mg^{2+}, 0.6% D-glucose, 1% Pen-Strep (10,000 U/mL, 10,000 µg/mL), 10 m*M* HEPES filtered through a 0.22-µm filter (Invitrogen AG, Basel, Switzerland).
7. Neurobasal media without glutamate containing 1% B27, 1% Pen-Strep (10,000 U/mL, 10,000 µg/mL), 0.5 m*M* L-glutamine, and 15 m*M* KCl (Invitrogen AG, Basel, Switzerland).
8. 120 m*M* Phosphate buffer: 240 m*M* phosphate buffer, pH 7.4, prepared by gently adding a 240 m*M* of NaH_2PO_4 solution (dodecahydrate, MW = 358.14) to a 240-m*M* Na_2HPO_4 solution (monohydrate, MW = 137.99) until pH 7.4. One volume of 249 m*M* phosphate buffer, pH 7.4, is then mixed with 1 vol of sterile H_2O.
9. 4% Paraformladehyde (PAF): Dissolve 40 g of paraformaldehyde (MW = 30.03) in 500 mL of sterile water; then, add 500 mL of 120 m*M* phosphate buffer, pH 7.4 (*see* **Notes 2** and **3**).

Fig. 1. (*continued*) lentiviral vectors based on a four-plasmid system. The packaging construct (pCMVΔR8.92), the pRSV-Rev, the heterologous envelope (e.g., vesicular stomatitis virus G-glycoprotein VSV-G, plasmid pMD.G), and the SIN transfer vector are cotransfected by calcium phosphate in 293T cells. The SIN transfer vector contains an internal promoter (e.g., phosphoglycerate kinase [PGK] and the woodchuck posttranscriptional regulatory element [WPRE]) to increase transgene expression level.

10. 25% Sucrose: Dissolve 25 g of sucrose in 100 mL of 120 m*M* phosphate buffer, pH 7.4.
11. pMD.G plasmid encoding the vesicular stomatitis virus G envelope.
12. pCMVDR8.92 packaging plasmid encoding all the viral genes needed in trans.
13. SIN-W-PGK: Transfer plasmid containing an internal cassette for the cloning of the gene of interest.
14. pRSV-Rev: plasmid encoding the rev protein of HIV-1.
15. Calcium phosphate transfection: polystyrene tubes (ref. no. FA-352054, BD Biosciences, Basel, Switzerland).
16. Ultracentrifugation of viral batches: polyallomer tubes (for SW28 rotor: 25 × 89 mm, ref. no. 358126, for SW60 rotor: 11 × 60, ref. no. 328874; Beckman Coulter, Nyon, Switzerland).
17. Aliquot of lentiviral vectors: 1.7-mL low retention tube (VWR Scientific, Bridgeport, NJ) or silanized tubes.
18. Ultracentrifuge equipment.
19. Culture flask, 6-cm and 10-cm Petri dishes (TPP AG, Trasadingen, Switzerland).
20. 6-, 24-, 48-, and 96-well trays for immunohistochemistry.
21. Filters (Millipore Stericup; Millipore, Volketswil, Switzerland).
22. HIV-1 p24 enzyme-linked immunosorbent assay (ELISA) kit (ref. no. NEK050B five 96-well plates; Perkin-Elmer Life Sciences Inc., USA).
23. Rodents are anesthetized with a mixture of narcoxyl (10 mg/kg) and ketaminol (75 mg/kg) (Veterinaria AG, Zürich, Switzerland).
24. Stereotaxic injection in the brain: Animals are placed on a stereotaxic frame (David Kopf Instruments, Tujunga, CA, USA) and injected with Hamilton syringe type 701 (Hamilton, Reno, NV, USA), using an automatic microinjector (Stoelting Co., Wood Dale, IL).
25. The skin of rodents is sutured with 6-0 Vicryl (Ethicon, Germany).
26. Sliding microtome cryostat.
27. Preservation solution for brain sections: 500 mL of 0.1 *M* phosphate buffer (pH 7.2), 300 gr sucrose, 300 mL ethylene glycol, and adjust to 1 L with double distillated H_2O.
28. Mowiol (Calbiochem, San Diego, CA, USA).
29. Vectastain Elite ABC detection kit (Vector Laboratories, Burlingame, CA, USA).
30. Diaminobenzidine tetrachloride (Immunopure Metal Enhanced DAB substrate kit; Pierce, Rockford, IL, USA).
31. Merkoglas (Merck, Darmstadt, Germany).

3. Methods

3.1. Cell Culture

293T cells (human embryonic kidney cell line immortalized by the adenoviral E1A/E1B protein and expressing the SV40 large T antigen) are split at 1:3 or maximum of 1:5 in HBSS and trypsin twice a week. These cells have a high transfection efficiency and a safe track record for the production of retroviruses ***(38,39)***. The cells are maintained in a 37°C humidified incubator and 5% CO_2 atmosphere.

The viral production yield in 293T cells tend to decrease over time; therefore, it is strongly recommended to produce a cell bank with 293T cells at low passage and regularly thaw new vials. The cells are frozen in 80% FCS and 10% dimethyl sulfoxide (DMSO) and stored in liquid nitrogen.

3.2. Lentiviral Vector Production by Transient Transfection of 293T Cells

293T cells are trypsinized from a confluent 150-cm^2 flask. The cells are centrifuged for 5 min (800*g*) at 4°C to remove trypsin and resuspended in DMEM/10%FCS (10 mL per 10-cm Petri dish). The quality of the serum and the type of flask or dish used for the cell culture greatly influence the adherence and growth of 293T cells as well as the yield of viral vector production (*see* **Note 4**).

The cells are plated at 3×10^6 cells/10-cm Petri dish on the evening prior to transfection. On the day of transfection, the cells should be 50–70% confluent. If the cell density is too low, the virus yield will be significantly decreased.

DNA is prepared for transfection in a 10-cm Petri dish as follows: 13 μg pCMVΔR8.92, 3 μg pRSV-Rev, 3.75 μg pMD.G, and 13 μg SIN-W-PGK are mixed in a 5-mL polystyrene tube with 250 μL of 0.5 *M* $CaCl_2$ and completed with H_2O to a final volume of 500 μL. A second tube is prepared with 500 μL of 2X HBS, pH 7.1. DNA and 2X HBS are mixed dropwise (one drop every other second) while vortexing or shaking. After 15 min, the precipitate solution is added gently to the cells by distributing drops uniformly on the Petri dish medium. Cells are then returned to the incubator and incubated for 8–15 h (*see* **Notes 5** and **6**).

At the end of the incubation, media from 293T cells is aspirated (one plate at a time) and 10 mL of complete DMEM medium is added. The following day, the viral supernatant is harvested. Viral samples are aliquoted in 1.7-mL low-retention tubes (or silanized tubes), stored at –80°C, or further concentrated by ultracentrifugation (*see* **Note 7**).

3.3. VSV-G Pseudotyped Virus Concentration Protocol

Gibbon ape (GALV), MLV-4070A, and MLV-10A1 envelopes as well as baculovirus GP64 and influenza virus H7-HA hemagglutinin have been used to pseudotype lentiviral vectors ***(40–44)***. Whether these envelopes alter the neurotropism of lentiviral particles remains to be established. However, the production of high-titer viral stocks for in vivo studies constitutes a limiting factor, because these envelopes do not increase the mechanical properties and stability of the viral particles—a unique feature of VSV-G, rabies and GP64 proteins that enables the concentration of viruses by ultracentrifugation.

The VSV-G pseudotyped lentiviral vectors (10 mL per 10-cm plate) are collected 48–72 h posttransfection and filtered through a 0.45-μm bottle top membrane. The swinging buckets and rotor caps from an SW28 rotor are prepared by 70% EtOH washing and rinsing with sterile water. This is important for maintaining the sterility during the procedure, as the polyallomer centrifuge tubes are open at the top and splashing of the contents is likely during handing of the rotor. The viral vectors are ultracentrifuged in an SW28 rotor at 50,000*g* (19,000 rpm) at 4°C for 90 min. The supernatant is aspirated and the pellets are resuspended in PBS/1% BSA. Finally, suspensions are left under the hood for 1 h on ice and resuspended before freezing (*see* **note 8**).

Further concentration can be achieved by ultracentrifugation in a SW60 or SW55i rotor (50,000*g*) at +4°C for 90 min. Supernatants are aspirated and resuspended by overlaying in desired volume of PBS/1% BSA. Insoluble material is removed by pulse

spin. The viral batches are split in aliquots of 20 µL, immediately frozen with dry ice and 70% EtOH, and stably stored at –80°C. Lentiviral vectors can be kept for at least 1 yr with no significant loss of viral titer (*see* **Notes 9** and **10**).

3.4. Measurement of the Viral Particle Content and Viral Titer

Particle content measurement is performed by p24 (capsid antigen) ELISA assay, following the manufacturer's recommendations, with serial dilutions of lentiviral vector (1/50 to 1/6,000,000). Values between 150 and 400 ng p24/mL should be obtained for nonconcentrated batches, but the vector design and/or the transgene may affect the viral production (*see* **Note 11**).

DNA, RNA, and marker expression methods can be used to titer lentiviral vectors ***(45,46)***. Usually, functional titers (marker expression) are lower than those obtained from DNA and RNA analysis. Several parameters can affect functional titers of vector stocks, such as the cell line used as the target cells (transduction efficiency varies greatly between cell lines), the volume of medium to which vector particles are added, and the duration of the infection. Cell lines with high transduction rates such as HeLa (ATTC# CCL-2) or 293T cells should be used to determine the viral titers of lentiviral vectors.

293T cells are plated at a density of 2×10^5 cells per well on six-well tissue culture dishes and infected with serial dilutions of the lentiviral vectors (0.1–2 ng p24/well). Low multiplicity of infection (MOI) should be used to obtain single transduction events (<15% infection rate). Forty-eight hours postinfection, the infected cells are fixed with 4% PAF for 15 min at 4°C and the transduced cells are counted by microscopy or by fluorescence-activating cell sorting (FACS) (*see* **Notes 12** and **13**).

The titer *T* is calculated in transducing units per milliliter (TU/mL), according to the formula

$$T = \frac{(\mathrm{NS})(1000)}{V}$$

where NS is the number of stained cells and V is the volume of lentivirus added (µL).

3.5. In Vitro Modeling of PolyQ Disorders With Lentiviral Gene Transfer

Lentiviral vectors encoding mutated polyQ proteins can be used to create in vitro models of triplet repeat disorders in cell lines but also in primary neuronal cultures.

HeLa cells are highly permissive to transduction by lentiviral vectors, adhere strongly, and are easy to maintain. Therefore, these cells are particularly suitable for assessing the functionality of lentiviral vectors, but 293T cells can be used as an alternative cell line. HeLa or 293T cells are plated in a six-well plate at a concentration of 200,000 cells/well and covered with 2 mL of DMEM complete medium. Twenty-four hours later, the cells are infected with 10–20 ng p24 lentivirus per well. The medium is removed 24 h later and replaced by 2 mL of conditioned DMEM/10% FCS. High transduction rates are obtained (80–95%) under these conditions, with no sign of toxicity. Then 48–72 h postinfection, the cells are fixed with 4% PFA and the transgene

expression is revealed by immunohitochemistry or Western blot analysis (*see* **Note 14**).

3.6. Transduction of Primary Striatal Cell Cultures

3.6.1. Embryo Collection and Striatal Dissection

Pregnant Sprague dawley rats (E16) are sacrificed by CO_2 inhalation, the heart is sectioned, and an incision is performed in the abdomen. The placenta containing the embryos is collected in a 10-cm Petri dish and stored on ice. The dissection is performed with a microscope under a laminar-flow hood. The instruments are sterilized with 65% ethanol (*see* **Note 15**).

The placenta is opened with forceps and microscissors, and embryos are isolated from the placenta. The heads are collected in a 6-cm Petri dish containing 5 mL of dissecting medium (DMX). With forceps, the brain is isolated by cutting above the eyes and the back head and then transferred in a new 6-cm Petri dish containing DMX. The two striata are dissociated (LGE: lateral ganglionic eminance) for each brain by opening the lateral cortex with the forceps and then transferred into a new 6-cm Petri dish containing DMX. The striata are cut in small pieces with forceps and collected in a 15-mL Falcon tube. The suspension is left on ice until decanted (*see* **Note 16**).

3.6.2. Cells Dissociation

The supernatant is aspirated and 0.5 mL of DMX with 1% BSA is added to the striata. The striata are carefully flushed three times with a fire-polished Pasteur pipet previously sterilized with 65% ethanol and coated with DMX containing 1% BSA. After decanting on ice, the supernatant is collected in a new 15-mL Falcon tube and stored on ice. Then, 0.5 mL DMX medium is added with 1% BSA to the striata, and the procedure is repeated until all cells are dissociated (*see* **Note 17**).

The DMX with 4% BSA is carefully added at the bottom of the Falcon tube to obtain a final volume of 10 mL. Cells are centrifuged at 4°C for 5 min at 1000*g* and resuspended in 10 mL of Neurobasal (NB) medium. Striatal cells are counted, diluted in NB medium, and plated at a density of 150,000 cells/cm^2 (500,000 cells/mL) in multiwell plates coated with poly-L-lysine (Fluka Holding AG, Buchs, Switzerland) (*see* **Note 18**). The cell cultures are kept in a humid incubator (5% CO_2 and 37°C). Half of the medium is changed once a week. Cultures can be kept up to 8 wk.

3.6.3. Infection of Primary Striatal Cultures With Lentiviral Vectors

The day after plating (1 DIV), the cell cultures are infected with lentiviral vectors (between 1 and 20 ng p24/10^5 cells). At 2 DIV, half of the medium is replaced with fresh medium. Transduction efficiencies of more than 95% are obtained with 10 ng p24/10^5 cells (*see* **Note 19**).

3.7. Lentiviral-Mediated Gene Transfer in Rodents

Multiple brain regions can be targeted with lentiviral vectors ***(36)***. To illustrate the procedures for local delivery of lentiviral vectors encoding polyQ proteins, the protocols for stereotaxic injections in the striatum and substantia nigra are provided.

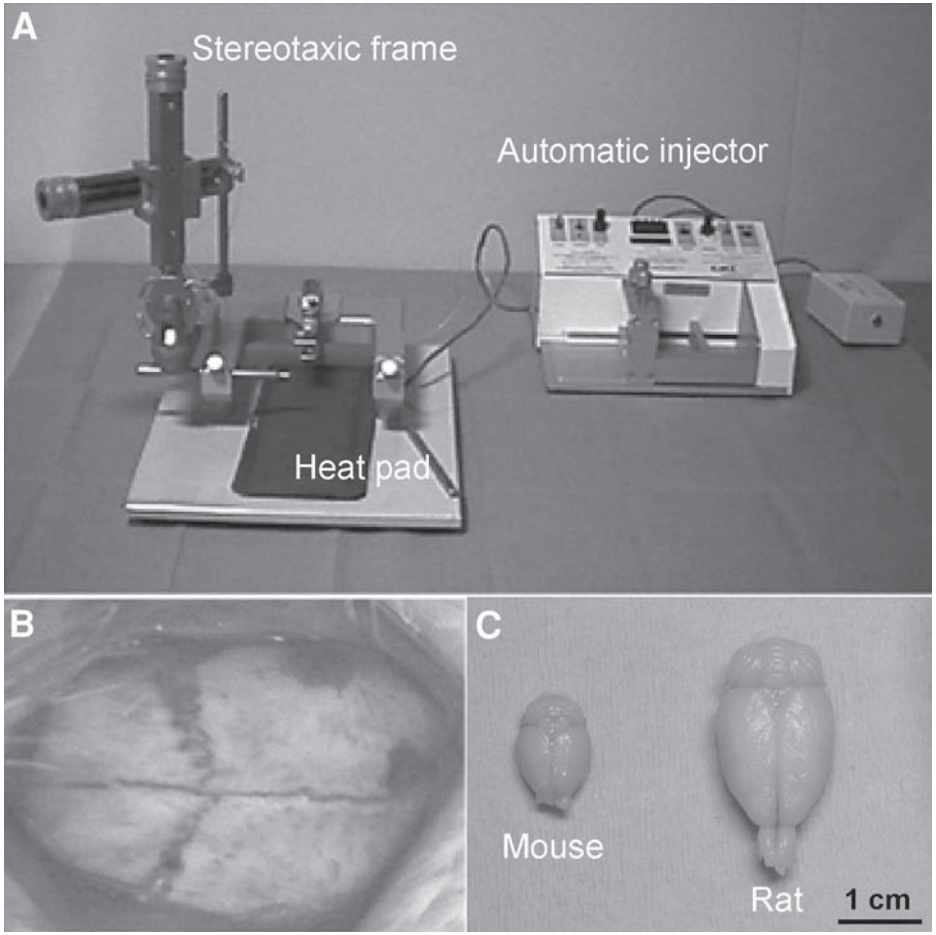

Fig. 2. **(A)** Photograph of the surgical system used for stereotaxic injection of lentiviral vectors in rodents. A heat pad is placed under the animal to prevent a drop in body temperature during anesthesia. A stereotaxic frame with ear bars is used to calculate the coordinates for injection of lentiviruses with an automatic injector. **(B)** Photomicrograph of a rat skull showing the localization of the bregma. **(C)** Top view photomicrograph of mouse and rat brains.

Adult rats weighing 200–250 g or adult mice weighing 20–25 g are anesthetized with a mixture of Narcosyl® (xylasin 10 mg/kg) and Ketaminol® (ketamin 75 mg/kg). Animals are placed in a stereotaxic frame (*see* **Fig. 2A**) with the mouth bar set at 0 mm for striatal injection ***(9)*** or –3.3 mm for substantia nigra pars compacta ***(11,34,47)***. The skin is opened to reveal the skull, and the bregma is localized (*see* **Fig. 2B**). A dental drill is used to make a hole through the skull. The coordinates for the injection are calculated based on the stereotaxic atlas ***(48,49)***. Previous studies have shown that greater accuracy can be achieved with rodents of different weight if the bregma is used

as the reference point for work with rostral structures and the interaural line is used for work with caudal structures ***(49)***. A 10-μL syringe with a 34G blunt tip needle (Hamilton, Reno, NV) is slowly lowered into the brain parenchyma at the following coordinates (*see* **Fig. 2C**):

Rat striatal injection (bregma: +0.5 mm; lateral: ± 3 mm; ventral: 5 mm) ***(9)***
Mouse striatal injection (bregma: +0.4 mm; lateral: ± 1.8 mm; ventral: 3.5 mm) (D. Zala, unpublished data)
Rat nigral injection, two injection sites (first injection: bregma: –4.8 mm; lateral: ± 2 mm; ventral: 7.7 mm. Second injection: bregma: –5.5 mm; lateral: ± 1.7 mm; ventral: 7.75 mm) ***(11)***.
Mouse nigral injection (bregma: –2.9 mm; lateral: ± 1.3 mm; ventral: 4.2 mm) ***(50)***.

Prior to stereotaxic injection, concentrated lentiviral viral stocks are thawed and resuspended by repeated pipetting. In mice, 1–2 μL of 1000X concentrated viruses (100,000 ng/mL) are injected; in rats 2–4 μL of viruses (200,000 ng/mL) are used. The lentiviral preparation is injected at a speed of 0.2 μL/min by means of an automatic injector and the needle is left in place for an additional 5 min. The skin is closed with a running suture using 6–0 Vicryl® (*see* **Note 20**).

3.8. Immunohistochemical Analysis

The animals are given an overdose of sodium pentobarbital and sacrificed by transcardial perfusion for about 1 min with ice cold 120 m*M* phosphate buffer containing 5000 U of heparin (Liquemin, Roche Pharma, Switzerland) followed by 4% PAF, 10% picric acid for 5 min. The brains are removed and postfixed in 4% PAF for approx 12 h, and finally cryoprotected in 25% sucrose/120 m*M* phosphate buffer for 48 h. The brains are frozen in dry ice powder, and coronal sections are cut on a sliding microtome cryostat at a temperature of –20°C and a thickness of 25 μm (rat) or 20 μm (mouse) (*see* **Note 21**).

Sections are collected and stored in 48-well trays as free-floating sections in PBS containing 0.12 μ*M* sodium azide. The trays are stored at 4°C until immunohistochemical processing. A preservation solution can be used for long-term storage of brain sections at –20°C. Preliminary studies are required to set up the staining procedure for each particular antibody used. In general, sections are processed for immunochemistry by incubating slices overnight with a primary antibody at 4°C. Secondary antibodies coupled to fluorescent chromophores (Jackson Immunoresearch Laboratories) or biotin are then incubated for 2 h at room temperature. Fluorescent antibody-stained sections are finally mounted on glass slides with Mowiol or any commercially available antifading reagent and observed under fluorescent light. Sections stained with biotin-coupled secondary antibodies are further processed using the Vectastain Elite ABC detection kit. The avidin and biotinylated horseradish peroxidase macromolecular complex formed is then revealed by diaminobenzidine tetrahydrochloride following the manufacturer's recommendations. The sections are finally mounted, dehydrated by passing twice through ethanol and toluol, and cover-slipped with Merckoglas®.

4. Notes

1. The pH is very important for reaching high transfection efficiency.
2. A better dissolution is obtained by heating the preparation at 60°C and adding a few drops of 1 *N* NaOH.
3. Ten percent of saturated picric acid can be added to the PAF solution to improve the quality of the immunochemistry (crosslinking of epitopes). The impact of picric acid has to be tested before use. In some rare cases, this fixation is not compatible with the staining (e.g., ChAT immunostaining).
4. To avoid clumping of cells after plating, vigorously pipet cells with a 2-mL pipet against the dish two to three times. Do not overtrypsinize, as this will damage cells and also cause clumping.
5. Take care not to add the precipitate directly to cells, as this will disrupt the 293T cells that are loosely adherent.
6. The ratio between the various plasmids, the total amount of DNA, the volume of CaCl2/HBS, and the number of plated cells is very important. In addition, the quality of the DNA greatly influences calcium phosphate transfection efficiency. A double cesium chloride gradient or commercially available columns should be used for large-scale production of DNA. The transfection efficiency should be between 60 and 80% to obtain batches with high viral titers.
7. A VSV-G envelope increases the tropism of HIV-1-based lentiviral vectors. Depending on the generation of lentiviral vectors, the envelope, and the nature of the transgene, specific precautions need to be taken. Biosafety level 2 (BL2) laboratories usually are required to perform these experiments. The local biosafety committee should review the procedures and a biohazard sign should be displayed on the doors of all rooms where viral vectors are handled. All materials and equipment that have been contaminated or in contact with vectors must be neutralized (with specific detergents) before disposal or cleaning for reuse. Disposable materials should be placed in leak-proof, biohazard plastic bags for autoclaving or incineration.
8. Usually, 10–50X concentrated batches (10^6–10^7 transducing units [TU]/mL) are produced for in vitro studies, whereas 1000X concentrated stocks (10^8–10^9 TU/mL) are necessary for in vivo experiments. For concentration of large volumes of supernatant, unconcentrated supernatant can be added to the pellets and the tubes respun.
9. VSV-G pseudotyped lentiviral vectors have a half-life of 24 h at 37°C. Viruses can be stored at 4°C for up to 24 h ***(24,51)***.
10. Other methods of concentration, including filtration and ion-exchange chromatography, have been described ***(52–54)***.
11. One picogram of p24 corresponds to approx 12,000 physical particles ***(55)*** and the ratio between physical particles (nanograms of p24 capsid antigen measured by ELISA) and transducing particles (TU, titrated on 293T or HeLa cells) is on the order of 5×10^4 to 1×10^5 TU/ng p24 ***(56)***. This means that the proportion of defective particles in lentiviral batches is very high (>99% in unconcentrated batches) ***(57)***.
12. Detection of fluorescent protein expression by FACS is more sensitive than by microscopy.
13. Despite the use of third-generation lentiviral system with improved biosafety, assays for the detection of replication-competent retroviruses should be performed. This can be achieved by infecting cultured permissive cells with serial dilutions of the lentiviral preparation. Cultures are scored for the establishment of productive viral replication. Various

assays are have been developed for RCR detection in lentiviral preparation including Tat transactivator activity in HeLa-P4 cells ***(58)***, p24 antigen measurement ***(35)***, quantitative polymerase chain reaction (QPCR) of Gag/Pol, marker rescue, or mobilization assays ***(59)***.

14. Fixed or lyzed materials can be transferred in biosafety level 1 laboratories.
15. On average, 12 embryos are collected per pregnant rat and about 25 million striatal cells are obtained at the end of the dissection.
16. The tissues and the cells should always be kept under ice. All solutions (dissections media and cultured media) are used at 4°C.
17. After three times, the DMX usually is transparent and all cells are dissociated.
18. The wells are coated by adding a solution of 20 µg/mL poly-L-lysine in H_2O for 4–18 h at 37°C. Wells are washed three times with H_2O and dried under the laminar-flow hood.
19. The 10- to 50-fold concentrated viral batches resuspended in PBS/1% BSA (p24 = 1000–10,000 ng/mL) should be used to infect primary cells to minimize the volume added to the cultures.
20. The quality of the viral batch, more specifically the absence of aggregates, the amount of viral particles, the target site, and the injection procedure can greatly influence the inflammatory response. Special care should be taken for the injection of lentiviral vectors in the spinal cord or in the CNS of mice, which seems to be more prone to tissue reaction than rats and primates. The addition of 1% BSA in the freezing solution reduces the clumping of the viral particles and improves the quality of the batches.
21. Addition of Cryomatrix (Thermo Shandon) to the brain allows efficient fixation on the stage and greatly enhances recovery of brain sections.

Acknowledgments

The authors thank Vivianne Padrun, Fabienne Pidoux, Maria Rey, and Christel Sadeghi for expert technical assistance. We are grateful to Romain Zufferey for critical reading of the manuscript.

References

1 Link, C. D. (2001) Transgenic invertebrate models of age-associated neurodegenerative diseases. *Mech. Ageing Dev.* **122,** 1639–1649.
2 Sipione, S. and Cattaneo, E. (2001) Modeling huntington's disease in cells, flies, and mice. *Mol. Neurobiol.* **23,** 21–51.
3 Zoghbi, H. and Botas, J. (2002) Mouse and fly models of neurodegeneration. *Trends Genet.* **18,** 463.
4 Cattaneo, E. and Conti, L. (1998) Generation and characterization of embryonic striatal conditionally immortalized ST14A cells. *J. Neurosci. Res.* **53,** 223–234.
5 Saudou, F., Finkbeiner, S., Devys, D., et al. (1998) Huntingtin acts in the nucleus to induce apoptosis but death does not correlate with the formation of intranuclear inclusions. *Cell* **95,** 55–66.
6 Lunkes, A. and Mandel, J. L. (1998) A cellular model that recapitulates major pathogenic steps of Huntington's disease. *Hum. Mol. Genet.* **7,** 1355–1361.
7 Ho, L. W., Brown, R., Maxwell, M., et al. (2001) Wild type Huntingtin reduces the cellular toxicity of mutant Huntingtin in mammalian cell models of Huntington's disease. *J. Med. Genet.* **38,** 450–452.
8 Senut, M. C., Suhr, S. T., Kaspar, B., et al. (2000) Intraneuronal aggregate formation and cell death after viral expression of expanded polyglutamine tracts in the adult rat brain. *J. Neurosci.* **20**, 219–229.

9 de Almeida, L. P., Ross, C. A., Zala, D., et al. (2002) Lentiviral-mediated delivery of mutant huntingtin in the striatum of rats induces a selective neuropathology modulated by polyglutamine repeat size, huntingtin expression levels, and protein length. *J. Neurosci.* **22,** 3473–3483.
10 Klein, R. L., King, M. A., Hamby, M. E., et al. (2002) Dopaminergic cell loss induced by human A30P alpha-synuclein gene transfer to the rat substantia nigra. *Hum. Gene Ther.* **13,** 605–612.
11 Lo Bianco, C., Ridet, J. L., Schneider, B. L., et al. (2002) Alpha-synucleinopathy and selective dopaminergic neuron loss in a rat lentiviral-based model of Parkinson's disease. *Proc. Natl. Acad. Sci. USA* **99,** 10,813–10,818.
12 Kirik, D., Rosenblad, C., Burger, C., et al. (2002) Parkinson-like neurodegeneration induced by targeted overexpression of alpha-synuclein in the nigrostriatal system. *J. Neurosci.* **22,** 2780–2791.
13 Kirik, D., Annett, L. E., Burger, C., et al. (2003) Nigrostriatal alpha-synucleinopathy induced by viral vector-mediated overexpression of human alpha-synuclein: a new primate model of Parkinson's disease. *Proc. Natl. Acad. Sci. USA* **100,** 2884–2889.
14 Janson, C. G., McPhee, S. W., Leone, P., et al. (2001) Viral-based gene transfer to the mammalian CNS for functional genomic studies. *Trends Neurosci.* **24,** 706–712.
15 Hsich, G., Sena-Esteves, M., and Breakefield, X. O. (2002) Critical issues in gene therapy for neurologic disease. *Hum. Gene Ther.* **13,** 579–604.
16 Kay, M. A., Glorioso, J. C., and Naldini, L. (2001) Viral vectors for gene therapy: the art of turning infectious agents into vehicles of therapeutics. *Nature Med.* **7,** 33–40.
17 Hurlbert, M. S., Zhou, W., Wasmeier, C., et al. (1999) Mice transgenic for an expanded CAG repeat in the Huntington's disease gene develop diabetes. *Diabetes* **48,** 649–651.
18 Mangiarini, L. F.-S., Sathasivam, K. F.-S., Seller, M. F.-C., et al. (1996) Exon 1 of the HD gene with an expanded CAG repeat is sufficient to cause a progressive neurological phenotype in transgenic mice. *Cell* **87(3),** 493–506.
19 Reddy, P. H., Williams, M., and Tagle, D. A. (1999) Recent advances in understanding the pathogenesis of Huntington's disease. *Trends Neurosci.* **22,** 248–255.
20 Kafri, T., van Praag, H., Gage, F. H., et al. (2000) Lentiviral vectors: regulated gene expression. *Mol. Ther.* **1,** 516–521.
21 Mansuy, I. M. F.-B. and Bujard, H. (2000) Tetracycline-regulated gene expression in the brain. *Curr. Opin. Neurobiol.* **10,** 593–596.
22 Regulier, E., Pereira de Almeida, L., Sommer, B., et al. (2002) Dose-dependent neuroprotective effect of ciliary neurotrophic factor delivered via tetracycline-regulated lentiviral vectors in the quinolinic acid rat model of Huntington's disease. *Hum. Gene Ther.* **13,** 1981–1990.
23 Washbourne, P. and McAllister, A. K. (2002) Techniques for gene transfer into neurons. *Curr. Opin. Neurobiol.* **12,** 566–573.
24. Zufferey, R., Nagy, D., Mandel, R. J., et al. (1997) Multiply attenuated lentiviral vector achieves efficient gene delivery in vivo. *Nature* **15,** 871–875.
25 Naldini, L., Blomer, U., Gallay, P., et al. (1996) In vivo gene delivery and stable transduction of nondividing cells by a lentiviral vector. *Science* **272,** 263–267.
26 Naldini, L., Blomer, U., Gage, F. H., et al. (1996) Efficient transfer, integration, and sustained long-term expression of the transgene in adult rat brains injected with a lentiviral vector. *Proc. Natl. Acad. Sci. USA* **93,** 11,382–11,388.
27 Poeschla, E. M., Wong-Staal, F., and Looney, D. J. (1998) Efficient transduction of nondividing human cells by feline immunodeficiency virus lentiviral vectors. *Nature Med.* **4,** 354–357.

28 Rohll, J. B., Mitrophanous, K. A., Martin-Rendon, E., et al. (2002) Design, production, safety, evaluation, and clinical applications of nonprimate lentiviral vectors. *Methods Enzymol.* **346,** 466–500.
29. Negre, D., Duisit, G., Mangeot, P. E., et al. (2002) Lentiviral vectors derived from simian immunodeficiency virus. *Curr. Topics Microbiol. Immunol.* **261,** 53–74.
30 Zufferey, R., Donello, J. E., Trono, D., et al. (1999) Woodchuck hepatitis virus posttranscriptional regulatory element enhances expression of transgenes delivered by retroviral vectors. *J. Virol.* **73,** 2886–2892.
31 Zennou, V., Petit, C., Guetard, D., et al. (2000) HIV-1 genome nuclear import is mediated by a central DNA flap. *Cell* **101,** 173–185.
32 Follenzi, A., Ailles, L. E., Bakovic, S., et al. (2000) Gene transfer by lentiviral vectors is limited by nuclear translocation and rescued by HIV-1 pol sequences. *Nature Genet.* **25,** 217–222.
33 Sirven, A., Pflumio, F., Zennou, V., et al. (2000) The human immunodeficiency virus type-1 central DNA flap is a crucial determinant for lentiviral vector nuclear import and gene transduction of human hematopoietic stem cells. *Blood* **96,** 4103–4110.
34 Deglon, N., Tseng, J. L., Bensadoun, J. C., et al. (2000) Self-inactivating lentiviral vectors with enhanced transgene expression as potential gene transfer system in Parkinson's disease. *Hum. Gene Ther.* **11,** 179–190.
35 Dull, T., Zufferey, R., Kelly, M., et al. (1998) A third-generation lentivirus vector with a conditional packaging system. *J. Virol.* **72,** 8463–8471.
36. Deglon, N. and Aebischer, P. (2002) Lentiviruses as vectors for CNS diseases. *Curr. Topics Microbiol. Immunol.* **261,** 191–209.
37 Blomer, U., Kafri, T., Randolph-Moore, L., et al. (1998) Bcl-xL protects adult septal cholinergic neurons from axotomized cell death. *Proc. Natl. Acad. Sci. USA* **95,** 2603–2608.
38 Farson, D., Witt, R., McGuinness, R., et al. (2001) A new-generation stable inducible packaging cell line for lentiviral vectors. *Hum. Gene Ther.* **12,** 981–997.
39 Yang, S., Delgado, R., King, S. R., et al. (1999) Generation of retroviral vector for clinical studies using transient transfection. *Hum. Gene Ther.* **10,** 123–132.
40 Mitrophanous, K., Yoon, S., Rohll, J., et al. (1999) Stable gene transfer to the nervous system using a non-primate lentiviral vector. *Gene Ther.* **6,** 1808–1818.
41 Negre, D., Mangeot, P. E., Duisit, G., et al. (2000) Characterization of novel safe lentiviral vectors derived from simian immunodeficiency virus (SIVmac251) that efficiently transduce mature human dendritic cells. *Gene Ther.* **7,** 1613–1623.
42 Stitz, J., Buchholz, C. J., Engelstadter, M., et al. (2000) Lentiviral vectors pseudotyped with envelope glycoproteins derived from gibbon ape leukemia virus and murine leukemia virus 10A1. *Virology* **273,** 16–20.
43 Duisit, G., Conrath, H., Saleun, S., et al. (2002) Five recombinant simian immunodeficiency virus pseudotypes lead to exclusive transduction of retinal pigmented epithelium in rat. *Mol. Ther.* **6,** 446–454.
44 Kumar, M., Bradow, B. P., and Zimmerberg, J. (2003) Large-scale production of pseudotyped lentiviral vectors using baculovirus GP64. *Hum. Gene Ther.* **14,** 67–77.
45 Sastry, L., Johnson, T., Hobson, M. J., et al. (2002) Titering lentiviral vectors: comparison of DNA, RNA and marker expression methods. *Gene Ther.* **9,** 1155–1162.
46 Scherr, M., Battmer, K., Blomer, U., et al. (2001) Quantitative determination of lentiviral vector particle numbers by real-time PCR. *Biotechniques* **31,** 520–524.
47 Bensadoun, J. C., Mirochnitchenko, O., Inouye, M., et al. (1998) Attenuation of 6-OHDA-induced neurotoxicity in glutathione peroxidase transgenic mice. *Eur. J. Neurosci.* **10,** 3231–3236.

48 Messier, C., Emond, S., and Ethier, K. (1999) New techniques in stereotaxic surgery and anesthesia in the mouse. *Pharmacol. Biochem. Behav.* **63,** 313–318.
49 Paxinos, G., Watson, C., Pennisi, M., et al. (1985) Bregma, lambda and the interaural midpoint in stereotaxic surgery with rats of different sex, strain and weight. *J. Neurosci. Methods* **13,** 139–143.
50 Bensadoun, J. C., Deglon, N., Tseng, J. L., et al. (2000) Lentiviral vectors as a gene delivery system in the mouse midbrain: cellular and behavioral improvements in a 6-OHDA model of Parkinson's disease using GDNF. *Exp. Neurol.* **164(1),** 15–24.
51 Richardson, J. H., Hofmann, W., Sodroski, J. G., et al. (1998) Intrabody-mediated knockout of the high-affinity IL-2 receptor in primary human T cells using a bicistronic lentivirus vector. *Gene Ther.* **5,** 635–644.
52 Reiser, J. (2000) Production and concentration of pseudotyped HIV-1-based gene transfer vectors. *Gene Ther.* **7,** 910–913.
53 Zhang, B., Xia, H. Q., Cleghorn, G., et al. (2001) A highly efficient and consistent method for harvesting large volumes of high-titre lentiviral vectors. *Gene Ther.* **8,** 1745–1751.
54 Scherr, M., Battmer, K., Eder, M., et al. (2002) Efficient gene transfer into the CNS by lentiviral vectors purified by anion exchange chromatography. *Gene Ther.* **9,** 1708–1714.
55 Connolly, J. B. (2002) Lentiviruses in gene therapy clinical research. *Gene Ther.* **9,** 1730–1734.
56. Follenzi, A. and Naldini, L. (2002) HIV-based vectors. Preparation and use. *Methods Mol. Med.* **69,** 259–274.
57 Higashikawa, F. and Chang, L. (2001) Kinetic analyses of stability of simple and complex retroviral vectors. *Virology* **280,** 124–131.
58 Clavel, F. and Charneau, P. (1994) Fusion from without directed by human immunodeficiency virus particles. *J. Virol.* **68,** 1179–1185.
59. Delenda, C., Audit, M., and Danos, O. (2002) Biosafety issues in lentivector production. *Curr. Topics Microbiol. Immunol.* **261,** 123–141.

15

Mouse Tissue Culture Models of Unstable Triplet Repeats

Mário Gomes-Pereira and Darren G. Monckton

Summary

Once into the expanded disease-associated range, trinucleotide repeat alleles become dramatically unstable in the germline and in somatic cells. The molecular mechanism(s) that underlie this unique form of dynamic mutation are poorly understood. Numerous transgenic mouse models of unstable trinucleotide repeats, which reconstitute the dynamic nature of somatic mosaicism observed in humans, have been generated. Given their easy accessibility, tissues from these mice can be collected to establish homogenous cell culture models of trinucleotide repeat dynamics. This chapter describes how such cultures can be established and maintained. Such in vitro systems may be useful to study relevant biological questions concerning fundamental triplet repeat metabolism. In particular, monitoring of repeat stability in cells growing under controlled conditions could help to clarify the relationship among the accumulation of repeat length variation, cell division rates, and DNA replication.

Key Words: Transgenic mouse; trinucleotide; somatic mosaicism; unstable DNA; triplet repeat; tissue cell culture; primary culture; feeding; subculturing; freezing; thawing; single-cell cloning; immunocytochemistry.

1. Introduction

Understanding of the mechanism of trinucleotide repeat-length mutation in somatic cells has been primarily grounded on the analysis of repeat dynamics in whole-tissue or organ samples comprised of multiple cell types. Different cell types most likely exhibit differing dynamics in terms of both cell turnover and accumulation of repeat-length mutations. The heterogeneous composition of complex tissues and organs has confounded attempts to dissect the molecular mechanism(s) underlying repeat dynamics. However, the analysis of repeat stability in homogenous patient-derived cell lines has, so far, yielded mixed results. Primary dura mater and skeletal cell cultures derived from myotonic dystrophy type 1 (DM1) fetuses have revealed an expansion-biased

From: *Methods in Molecular Biology, vol. 277: Trinucleotide Repeat Protocols*
Edited by: Y. Kohwi © Humana Press Inc., Totowa, NJ

mutation profile ***(1)***. In addition, Epstein–Barr virus (EBV)-transformed lymphoblastoid cell lines established from DM1 patients exhibit complex repeat dynamics, in which a greater frequency of deletions is observed, in clear contrast with the dynamics reported in vivo ***(2,3)***. It appears that EBV transformation may therefore alter DNA metabolism, interfere with repeat dynamics, and reduce the overall utility of these cell lines. Primary cell lines appear as a good alternative to model repeat stability in vitro in a mammalian biological context. Nevertheless, not only is their availability from individuals with rare inherited disorders extremely limited, but also, detailed dissection of the factors affecting instability using patient-derived tissue samples is complicated by confounding influences of patient age, progenitor allele length, tissue type, and genetic background, and so forth on mutation rates and directions.

To create additional model systems in which repeat biology can be assessed in vivo, transgenic mice containing unstable expanded CTG•CAG arrays have been created to resolve the molecular mechanisms that regulate repeat dynamics in a mammalian environment ***(4–12)***. The development of cell culture systems from such animals, which can reproduce in vivo trinucleotide dynamics in vitro, can create new avenues to investigate the multiple factors affecting the metabolism of repetitive sequences under controlled conditions. To this end, cell cultures can be established from various tissue samples harvested from transgenic mice to monitor trinucleotide repeat size variability over extensive periods of time ***(13)***. Levels of repeat-length variability in cultured cells can be accurately assessed by sensitive small-pool polymerase chain reaction (SP-PCR) methods (described in detail in Chapter 5). The establishment of such a system provides a powerful tool to investigate the effect of a large number of cell divisions on trinucleotide repeat stability and the effect of a wide range of environmental agents on the mutation rate of triplet repeats.

Mouse cell systems, derived from transgenic models of unstable DNA, have the advantage of being readily renewable, easily accessible, and relatively inexpensive to maintain. In addition, mouse tissue samples can be collected throughout the animal life-span, hence enabling the analysis of different aspects of repeat biology during different developmental times.

In conclusion, mouse cell culture model systems should provide new insights into the cellular metabolism of the simple tandem repeats associated with human disease. Therefore, this chapter includes a detailed description of techniques used to establish and grow adult and embryonic mouse cell lines in culture derived from transgenic animal models of unstable DNA. It also covers fundamental tissue culture procedures, such as determination of cell viability, single-cell cloning by limiting dilution, freezing and thawing of cultured cells, and immunocytochemistry techniques for cell-type characterization.

2. Materials

1. Dissection kit (small scissors and forceps are kept in 70% ethanol during the procedure for sterility).
2. 6- and 10-cm tissue culture dishes (Falcon).

3. Sterile phosphate-buffered saline (PBS) without Ca^{2+}/Mg^{2+}, pH 7.2: 2.7 m*M* KCl, 1.47 m*M* KH_2PO_4, 136.9 m*M* NaCl, 8.1 m*M* Na_2HPO_4 (Invitrogen).
4. 20-µL, 200-µL, and 1-mL filter pipet tips.
5. 1-mL, 5-mL, 10-mL, and 25-mL graduated sterile plastic pipets.
6. 25-cm^2, 75-cm^2, and 150-cm^2 tissue culture flasks.
7. 6-, 12-, 24-, and 96-well tissue culture clusters.
8. Eight-well chamber slides.
9. 5-mL sterile plastic syringes.
10. 18-gage needles.
11. 15-mL conical tubes.
12. 70% (v/v) Ethanol.
13. Nonessential amino acids (Invitrogen).
14. Penicillin/streptomycin (Invitrogen).
15. Trypsin/EDTA solution: 210 n*M* trypsin, 526.3 µ*M* EDTA•4 Na, 14.5 m*M* NaCl in PBS without Ca^{2+} and Mg^{2+} (10X stock solution from Invitrogen).
16. Dulbecco's modified Eagle medium (DMEM), with GlutaMAX™, 25.0 m*M* D-glucose and sodium pyruvate (Invitrogen).
17. Fetal bovine serum (FBS).
18. Culture medium: 10% (v/v) FBS, 100 U/mL penicillin, and 100 µg/mL streptomycin in DMEM.
19. MEF culture medium: 10% (v/v) FBS, 1X nonessential amino acids (Invitrogen), 0.1 m*M* β-mercaptoethanol, 100 U/mL penicillin, and 100 µg/mL streptomycin.
20. Deionized water (Milli-Q water).
21. Cell scraper (e.g., Disposable Cell Lifter, Fisher).
22. 1.5-mL Eppendorf tubes.
23. 0.4% (w/v) Trypan blue solution in PBS.
24. Common laboratory equipment is required, such as water bath, CO_2 incubator, laminar-flow hood, low-speed centrifuge, inverted-phase-contrast microscope, and hemocytometer.
25. 4% (w/v) Paraformaldehyde solution in PBS, adjust to pH 7.4 with NaOH, freshly prepared.
26. β-Mercaptoethanol, dimethyl sulfoxide (DMSO), Triton X-100, and Tween-20 are purchased from Sigma.
27. Transgenic mouse model of unstable DNA.

3. Methods

3.1. Establishment of Mouse Cell Cultures by Enzymatic Dissociation

The following protocol is recommended for the establishment of cell cultures from large tissue samples, harvested from mouse organs such as the lung, liver, kidney, and heart.

1. Prewarm culture medium and trypsin/EDTA solution to 37°C in a water bath (*see* **Note 1**).
2. Dissect transgenic mouse on a clean bench and collect organs of interest in sterile ice-cold PBS. Keep tissue samples on ice (up to 1 h) until processing. Procedures should be carried out in a laminar-flow hood from this moment on to avoid contamination (*see* **Note 2**).
3. Place tissue sample of interest (approx 25 mm^3) on a 10-cm tissue culture dish with 10 mL ice-cold sterile PBS and wash briefly to remove blood cells.
4. Transfer tissue sample onto a fresh 10-cm tissue culture dish containing 10 mL of ice-cold sterile PBS. Remove any fat tissue. Repeat wash in a fresh dish.

5. Mince organ into approx 1-mm^3 cubes.
6. Transfer minced tissue into a sterile 15-mL conical tube containing 10 mL sterile ice-cold PBS.
7. Allow minced tissue to settle and aspirate PBS.
8. Wash twice with 10 mL sterile PBS.
9. Add 5 mL of prewarmed trypsin/EDTA solution and incubate in a humidified 5% CO_2 incubator at 37°C for 30 min, gently inverting the tube five times every 5 min.
10. Remove plunger from a 5-mL syringe and keep it sterile. Transfer the pieces of tissue and the enzyme solution into the syringe. Put plunger back in syringe and squirt contents of syringe into a 25-cm^2 tissue culture flask, through a sterile 18-gage needle. Place tissue culture flask back in the incubator for an extra 15 min.
11. Transfer the contents of the flask into a 15-mL conical tube. Wash flask with 5 mL of PBS, taking care to collect any cells that may have attached to the bottom of the flask and add to the tube. Allow the pieces of cellular debris to settle down over a period of 2 min.
12. Transfer the supernatant into a fresh 15-mL conical tube and spin at 200*g* for 5 min.
13. Resuspend the pellet in 4 mL of complete culture medium and plate into one well of a six-well cluster and place primary cultures in a 37°C, 5% CO_2 humidified incubator.
14. Add 5 mL of fresh prewarmed trypsin/EDTA solution to the remaining undigested pieces of tissue and repeat incubation at 37°C for 30 min, inverting the tube five times every 5 min. Repeat **steps 11–13**.
15. Repeat procedure until tissue sample is fully digested or until six primary cultures have been independently plated on a six-well tissue culture cluster (*see* **Note 3**).
16. After 24–48 h, wash cells twice with prewarmed PBS to remove debris, nonadherent blood cells, and tissue fragments. Add fresh complete cell culture medium and return to the incubator.
17. Subculture cultures when cells reach 60–80% confluency, pooling all six primary cultures together to establish a single culture maintained in a 25-cm^2 tissue culture flask.
18. Once the cells become 80–90% confluent, subculture them at a 1:5 or 1:10 ratio during the first five passages or so. The split ratio may be increased when the cells start proliferating at higher rates (*see* **Note 4**).

3.2. Establishment of Mouse Cell Cultures by the Explant Technique

The following protocol is recommended for the establishment of primary cell cultures derived from small mouse tissue samples, such as the eye, tail, and ear.

1. Prewarm culture medium and trypsin/EDTA solution to 37°C in a water bath.
2. Transfer the tissue sample into a 10-cm tissue dish containing 10 mL of ice-cold PBS.
3. Rinse the tissue once and, if necessary, remove bones and cartilages (e.g., tail tissue sample). Transfer tissue onto a fresh dish and repeat wash with PBS.
4. Place the tissue cell-side down (*see* **Note 5**) on a 6-cm tissue culture dish. Mince the tissue sample into small fragments (approx 1 mm^3) and disperse them over the dish.
5. Press the tissue firmly in order to attach the tissue to the surface of the dish.
6. Cover tissue with limited amount of medium, taking care to avoid detaching of the tissue fragments.
7. Incubate at 37°C in a humidified 5% CO_2 atmosphere.
8. Fibroblasts will start to grow in 3–6 d. Large pieces of tissue can then be removed.
9. Subculture cells 1:5 or 1:10 when they reach 60–80% confluency for the first few passages. The split ratio may be increased when the cells enter the exponential phase of proliferation.

3.3. Isolation of Primary Mouse Embryonic Fibroblasts

Primary mouse embryonic fibroblast (MEF) cell cultures can be readily isolated from mouse embryos. If subcultured at lower split ratios, MEF cells should exhibit a limited proliferative capacity. These cells may eventually senesce or undergo spontaneous immortalization. Nonetheless, MEF cells may still provide a good model to assess trinucleotide dynamics in genuine primary cultures, prior to immortalization or senescence.

1. Prewarm culture medium and trypsin/EDTA solution to 37°C in the water bath.
2. Sacrifice a pregnant female transgenic mouse 13–14 d after the mating plug is observed.
3. Lay mouse on its back and swab belly with 70% ethanol.
4. Dissect the animal to expose the viscera and the gut.
5. Using sterile forceps and iris scissors, remove the uterus, taking care not to touch the fur or the bench with the uterus or the dissection instruments.
6. Place the uterus into a 10-cm tissue culture dish containing sterile PBS. Swirl around to remove blood. Transfer the uterus to second dish with sterile PBS and repeat the wash. Move dish to a laminar-flow hood.
7. Isolate the embryos and remove the placenta and embryonic sacs.
8. Transfer each embryo onto a 10-cm dish with fresh PBS. Cut off embryo head and dissect out the liver. Keep the head and liver in PBS on ice for genotyping.
9. Transfer the embryo body into a 15-mL conical tube. Add 3 mL prewarmed trypsin/EDTA solution and digest for 10 min in a humidified 5% CO_2 incubator at 37°C, inverting the tube five times every minute.
10. Remove the plunger from a 5-mL syringe and keep it sterile. Drop the embryo bodies inside the syringe. Put the plunger back in the syringe and squirt the contents of syringe into a 25-cm^2 tissue culture flask through a sterile 18-gage needle. Place the flask back in the incubator for an extra 20–30 min.
11. Add 20 mL of fresh prewarmed MEF culture medium, taking care to wash any pieces of tissue off the bottom and walls of the tissue culture flask. Pipet the cell suspension up and down to break any cell aggregates.
12. Transfer the contents of the flask into a 50-mL conical tube and allow the pieces of cellular debris to settle out over a period of 2 min. Transfer the supernatant into a fresh tube and spin at 200*g* for 5 min.
13. Resuspend the pellet in 5 mL of fresh medium and plate on a 25-cm^2 tissue culture flask.
14. Transfer the flask to an incubator at 37°C with 5% CO_2.
15. Add 5 mL of fresh prewarmed trypsin/EDTA solution to the undigested pieces of tissue, transfer into a 25-cm^2 tissue flask, and place in the incubator for 20–30 min.
16. Repeat **steps 11** and **12**.
17. Resuspend the pellet in 5 mL of fresh MEF culture medium and plate the cells on the same 25-cm^2 tissue culture flask, containing the previously dissociated cells.
18. MEFs should attach and begin to divide in 1–3 d. During this time, try not to disturb cultures to allow cells to settle and attach to the substratum. Change the growth medium after 2 d.
19. Split cultures 1:3 or 1:4 when they form a confluent monolayer.

3.4. Feeding Cells

At a minimum, the cells should be fed on a weekly basis. Most likely, the cells will require feeding twice or thrice a week. Ideally, cultures should be examined under the

Table 1
Volume of Culture Medium for Differently Sized Culture Flasks and Clusters

Flask or cluster	Volume of culture medium
25-cm^2 Tissue culture flask	5 mL
75-cm^2 Tissue culture flask	15 mL
150-cm^2 Tissue culture flask	30 mL
96-Well tissue culture cluster	200 µl/well
24-Well tissue culture cluster	0.5 mL/well
12-Well tissue culture cluster	1.5 mL/well
6-Well tissue culture cluster	3 mL/well

microscope on a daily basis, or every other day, to assess whether the cells are growing at their normal rate and to check for bacterial or fungal contaminations.

Handling of cells should be as rapid as possible to minimize fluctuations in their environment. The temperature variation can be reduced during feeding by prewarming the media components to the same temperature at which the cells are being cultured.

1. Prewarm all solutions (cell culture medium, PBS, and trypsin/EDTA) to 37°C in the water bath.
2. Remove the old culture medium carefully, avoiding scratching the surface of the cells.
3. Add fresh culture medium to the cells (*see* **Note 6**). Whenever adding medium, point the tip of the pipet away from the growing surface of the cells, to reduce the chance of scratching or removing the cells from the growth surface.
4. If the purpose of the medium change is to alter the culture conditions (e.g., alter serum concentration, add/remove chemical to/from the medium), the cells should be washed with PBS before adding the fresh medium.
5. The volumes of culture medium vary depending on the surface area of the flask or cluster on which the cells are growing. Suggested volumes of culture medium are shown in **Table 1.**

3.5. Subculture of Adherent Mouse Cells

Once the cells attach to the substratum and spread, they begin to divide, and the cell number will increase. Cells will progress from sparse to subconfluent to confluent. To maintain the proliferative status of a culture and to start the cell expansion process over again, the cells must be removed from their substrata, their number reduced, and an aliquot must be reseeded in a new tissue culture flask (subculturing). Subculturing provides the cells with fresh nutrients and space for continuous growth (*see* **Note 7**). The simplest way to remove the cells is to digest the attachment molecules, leaving the cells intact and free to float in suspension. The continuous subculture of mouse cell cultures results in spontaneous immortalization and generation of cell lines exhibiting unlimited proliferative capacity ***(14,15)***.

Cells collected at every passage can be used to assess repeat size variability by sensitive techniques, such as small-pool PCR analysis, described in detail elsewhere in this book (Chapter 5), thereby enabling continuous monitoring of repeat stability over time and through many cell divisions.

Table 2
Volumes of PBS and Trypsin Solution to Be Used When Subculturing Cells

Flask or cluster	V_{PBS}	$V_{Trypsin}$
96-Well tissue culture cluster	200 µL/well	50 µL/well
24-Well tissue culture cluster	500 µL/well	100 mL/well
12-Well tissue culture cluster	1 mL/well	250 µL/well
6-Well tissue culture cluster	2 mL/well	500 µL/well
25-cm^2 Tissue culture flask	3 mL	2 mL
75-cm^2 Tissue culture flask	9 mL	4 mL
150-cm^2 Tissue culture flask	18 mL	6 mL

Note: In general, the smaller the volume of trypsin solution, the better.

The repeat dynamics in vitro often is disturbed by random population fluctuations, characterized by periods of extremely low repeat-length variability. These selective sweeps are not restricted to any specific stage of the culture, and they continue to occur at any time. Selective sweeps can result in dramatic shifts in repeat-length distributions, which may confound the interpretation of the repeat dynamics in culture ***(3,13)***. Although one cannot predict or avoid the occurrence of such events, care can be taken to minimize their effect on the population dynamics. Dramatic reductions in cell number during passaging will contribute to genetic drift and, therefore, should be avoided. High split ratios (greater than 1:40) should not be used.

1. Prewarm culture medium, PBS, and trypsin/EDTA solution to 37°C in the water bath.
2. Gently wash cells in PBS (*see* **Table 2**).
3. Digest cells with trypsin for 5 min, at 37°C in the CO_2 incubator, to bring them into solution (*see* **Table 2**).
4. Examine the cells under the microscope to check whether the cells have rounded up, lifted off the surface of the culture flask, and are floating in the trypsin solution. When the majority of the cells are rounded and some are floating, stop the digestion (*see* **step 5**). If the majority of the cells are still strongly attached to the growth surface, the incubation at 37°C may be extended for an extra 10 min (*see* **Note 8**). The side and bottom of the flask may be gently tapped to release any remaining attached cells. If necessary, a cell scraper might be used to remove cells from the flask.
5. Neutralize trypsin by adding an equal volume of complete culture medium (containing 10% FBS) at least equivalent to the volume of trypsin solution used. Take a small aliquot (100–200 µL) for cell number and population doubling quantification.
6. Pipet the suspension up and down repeatedly to dissociate cell aggregates and transfer into a conical tube.
7. Collect cells by centrifugation at 200*g* for 5 min (*see* **Note 9**). Remove the supernatant and resuspend cell pellet in fresh medium.
8. Transfer the required number of cells to a new tissue culture flask containing complete cell culture medium.
9. Return cells to the incubator.
10. At every passage, the number of population doublings can be determined based on the cell number (*see* **Subheading 3.6.**).

3.6. Cell Quantification and Viability

It is important to know the number of cells that are in culture at given stages and whether these cells are viable. The use of a hemocytometer and a dye, such as trypan blue, gives a quantitative standard for the viability of the cells. Cells that exclude trypan blue are considered viable, whereas cells that take up the dye are irreversibly dead.

1. Bring cells into suspension using trypsin/EDTA and resuspend in a volume of fresh medium at least equivalent to the volume of trypsin solution used.
2. Remove 100–200 μL of cell suspension to a 1.5-mL Eppendorf tube.
3. Add an equal volume of 0.4% (w/v) trypan blue and mix by gentle pipetting. Remember to take this dilution step into account when working out cell concentration and viability.
4. Count the number of viable cells (seen as bright cells) and nonviable cells (stained blue) in a hemocytometer. Ideally, more than 100 cells should be counted to increase the accuracy of the cell count.
5. Determine the percentage of viable cells as follows:

$$\text{Viability (\%)} = \left(\frac{\text{No. of viable cells}}{\text{Total cell number}} \right) \times 100$$

6. Determine the number of population doublings (PD) as follows:

$$\text{PD} = \log_2 \left[\left(\frac{\text{Cell number at passage } n+1}{\text{Cell number at passage } n} \right) \times \text{split ratio} \right]$$

7. Calculate the population doubling times (PDT) (*see* **Note 10**) by dividing the number of population doublings by the time over which they have occurred: PDT = PD/time.

3.7. Freezing Cells in Liquid Nitrogen

Having a frozen bank of cells provides a backup in case cell cultures are lost for various reasons not always under one's control. Frozen cell stocks are also useful when working with primary cell cultures, given their limited life-span. Some types of primary culture can be prepared in large batches and frozen in a large number of vials. The cells can later be thawed and studied, so that a higher number of experiments can be performed on early passage cells from the same preparation. In addition, frozen cell stocks of immortal lines also provide a permanent record of any changes that might occur with passage number.

1. Digest cells with trypsin, as previously described, to obtain a single-cell suspension. Stop digestion by adding complete culture medium, containing 10% (v/v) FBS.
2. Determine cell viability by the trypan blue exclusion method, described above.
3. Pellet cells by centrifugation at 200*g* for 5 min. Resuspend cell pellet in fresh culture medium, supplemented with 10% (v/v) DMSO, at the desired density. A good standard is to freeze (0.5–1.5) × 10^6 cells/mL.
4. Label each vial individually with the designation of the cell number, passage number, and date (*see* **Note 11**). Transfer cells into the cryovials (*see* **Note 12**) and make absolutely sure that the lid is screwed on tightly.
5. Cells should be frozen slowly to avoid ice crystal formation, which may damage the cells

(*see* **Note 13**). Transfer vials into a freezing container with isopropanol at room temperature, cool down to –70°C for 4 h and then move cryovials to liquid nitrogen (–190°C), where they can be kept until needed (*see* **Note 14**). Alternatively, vials can be placed in a polystyrene rack, kept in the refrigerator for 30 min, then moved to a –80°C freezer, where they should remain for at least 60 min and no longer than overnight (*see* **Note 15**).

3.8. Thawing Cultured Mouse Cells

In contrast to the slow rate of cooling required to freeze cells, cells should be thawed as rapidly as possible to minimize the risk of cell damaging during ice crystal formation. Some cells (10–20%) might die during the freezing/thawing procedure. If the majority of cells are lost, then there is a real possibility that the resultant cell population could differ significantly from the global properties of the prefreezing culture.

1. Remove a vial of cells from the liquid-nitrogen tank. Check the vial for leaks and cracks and ensure that the cap is still tightly screwed.
2. Quickly thaw the cells by immersing the entire vial in a water bath at 37°C and gently shaking (*see* **Note 16**).
3. Transfer cells into a 15-mL conical tube, add 10 mL of prewarmed culture medium to the cells, and mix gently by repeated pipetting.
4. Collect cells by centrifugation at 200*g* for 5 min, and discard the old freezing medium.
5. Resuspend the cell pellet in fresh culture medium and plate suspension in a fresh tissue culture flask. Move the flask to the incubator.
6. When this culture becomes confluent, the cells should be split at low ratio (1:2 to 1:10). After the first passage, most cells are fully recovered from freezing and can be handled normally (*see* **Note 17**).

3.9. Establishment of Single-Cell-Derived Clones

Mouse primary cell cultures are naturally heterogeneous because they are derived from tissue samples comprising multiple different cell types. Such variability may confound attempts to interpret results and to establish simple correlations between repeat instability and environmental and/or cellular conditions. To reduce the genetic variability within a cell culture consisting of a heterogeneous group of cells, clones and subclones might be derived by limiting dilution and subsequent clonal expansion.

1. To derive clonal cell lines, bring cells to suspension by trypsin digestion as previously described (**Subheading 3.5.**), ensuring dissociation of any cell aggregate, either by extending the digestion time up to 20 min, or by extensive pipetting of the suspension.
2. Collect cells by centrifugation at 200*g* for 5 min and resuspend in fresh culture medium, by repetitive pipetting to further ensure single-cell suspension.
3. Determine cell viability using the trypan blue method.
4. Dilute cell suspension to achieve a final cell density of 2.5 cells/mL.
5. Plate 200 μL of diluted cell suspension on each well of a 96-well tissue culture cluster, corresponding to an average of 0.5 cells per well (*see* **Note 18**).
6. Once the culture becomes confluent (usually within 15–30 d), subculture the cells onto a 24-well cluster, and subsequently onto a 6-well cluster or 25-cm^2 tissue culture flask.
7. Determine cell number and calculate the total number of population doublings since cloning as $\log_2$ (total cell number).

3.10. Characterization of Cultured Cell Types

Mouse cells cultures consist of an initial heterogeneous cell population, comprising cells with clearly different morphologies and probable distinct proliferative capacities. The cultures soon become more homogeneous, exhibiting prevalent spindle morphology, typical of fibroblastic cell types ***(13)***. The nature of the cultured cells might be confirmed immunocytochemically by staining with primary antibodies directed against vimentin and cytokeratins ***(16–18)***.

1. Plate cells on eight-well chamber slides and grow them until they are semiconfluent (approx 60–80% confluency).
2. Wash cells once with serum-free DMEM.
3. Mix an equal volume of serum-free DMEM and 4% (w/v) paraformaldehyde solution, for a final concentration of 2% (w/v). Add 200 µL to each chamber and fix cells for 20 min at room temperature.
4. Wash cells once with PBS, add 0.1 *M* glycine (pH 7.2) for 20 min and wash cells twice with PBS.
5. Permeabilize cells in 200 µL of 1% (v/v) Triton X-100 in PBS for 6 min and wash twice with PBS.
6. Dilute primary antibody in 0.01% (v/v) Triton X-100 in PBS and incubate overnight at 4°C with gentle shaking. Add enough antibody solution to cover all of the cells (200 µL of antibody dilution per chamber should be enough). Cells should never be allowed to dry at any stage of this protocol, as this will dramatically increase the background.
7. Wash four times in 0.1% (v/v) Tween-20 in PBS for 5 min each.
8. Dilute secondary antibody in 3% (w/v) BSA in PBS with 0.01% (v/v) Triton X-100 and incubate for 2 h at room temperature with gentle shaking.
9. Wash cells four times in PBS for 5 min each and observe cell staining using fluorescence microscopy.

4. Notes

1. Water baths and incubators could be a source of bacterial and/or fungal contamination. To reduce the risk of contamination, add a biocidal (antibacterial and antifungal) to the water and replace it every 3–4 wk. When collecting tubes and bottles from the water bath, always spray and wipe down their lids with 70% ethanol to avoid any contamination.
2. Contamination in a cell culture will influence virtually any parameter one wishes to study, even if it does not immediately kill the cells. The best solution is to avoid contamination in the first place. Failing this, the next best solution is to carefully discard the contaminated cultures, taking care to avoid spreading the contamination into other cultures. Simple aseptic techniques should be followed to reduce the chances of contamination. Benchtops, hood surfaces, microscopes, and other work surfaces should be wiped down periodically with 70% (v/v) ethanol or another germicide. The inside walls of the laminar-flow hood should be irradiated with ultraviolet (UV) light for at least 20 min prior to the start of the work and then sprayed with 70% (v/v) ethanol. The movement of people and equipment in and out of the room should be minimized. A dedicated lab coat and gloves should be worn at all times. Gloves should be replaced frequently and the hands often disinfected with 70% ethanol.

3. Six primary cultures should be enough. However, if the remaining tissue is still large following trypsin digestion or if a large number of cells is required, extra digestion steps can be performed.
4. The rapid cell growth observed in vitro at later stages is consistent with the spontaneous immortalization of cells, which is known to be a frequent event in mouse cell cultures ***(14,15)***.
5. Skin up, dermis down, in the case of tail and ear tissue samples.
6. Care should be taken to reduce the time cells are without bathing fluid out of the incubator. If there is no fluid on top of the cells, they can become dehydrated and their temperature drops faster. The solution is not to handle too many cultures at a time.
7. If cells are not split frequently enough, the cells may deplete the medium from nutrients and die. If the cells are split too frequently or at very high densities, the cell line may be lost.
8. Do not incubate cells in trypsin for too long. Trypsin can cleave the most accessible proteins, which include membrane proteins, resulting in damage to the cells. The morphology of the cells being trypsinized should be the guide to when to stop incubation.
9. If subculturing involves a high split ratio (e.g., dilution factor greater than 20), it usually is not necessary to remove the residual enzyme by centrifugation. Instead, a small aliquot of cell suspension is mixed with fresh medium and plated in a fresh tissue culture flask. However, if the culture is maintained in serum-free medium, then it is necessary to neutralize the enzyme by the addition of an appropriate protease inhibitor.
10. Following an initial period characterized by low growth rates, mouse cell cultures enter a phase of continuous exponential rate, with population doubling times that may vary among different cell lines ***(13)***. The late rapid cell growth observed in vitro is consistent with the spontaneous immortalization of cells, which is known to occur at a relatively high frequency with mouse cell cultures ***(14,15).***
11. Make sure that the cryovials are labeled with an ink pen that is indelible in organic solvents and liquid nitrogen.
12. Make sure that you use resistant cryovials that will not become brittle when cooled down to liquid-nitrogen temperatures or can shatter or even explode when thawed.
13. A steady decrease of one degree per minute is ideal. It should take 4 h to reach liquid-nitrogen temperature.
14. Cells stored at –180°C will, although very slowly, lose viability. Therefore, valuable lines should be periodically thawed, expanded, and refrozen to ensure a continued supply of cells.
15. Cells will continue to degenerate if kept at –80°C; therefore, they should not be stored at this temperature for more than a few weeks.
16. Be aware that frozen vials can explode on thawing.
17. Allow at least a few days and, ideally, two passages postthaw before using the cells in an experimental protocol.
18. At this stage, cells can be checked under the microscope, and if two cells are observed in one single well of the cluster, the culture resulting from the expansion of these cells should be excluded from the study.

Acknowledgment

D. G. Monckton is a Lister Institute Research Fellow.

References

1. Wörhle, D., Kennerknecht, I., Wolf, M., et al. (1995) Heterogeneity of DM kinase repeat expansion in different fetal tissues and further expansion during cell proliferation in vitro: evidence for a casual involvement of methyl-directed DNA mismatch repair in triplet repeat stability. *Hum. Mol. Genet.* **4,** 1147–1153.
2. Ashizawa, T., Monckton, D. G., Vaishnav, S., et al. (1996) Instability of the expanded $(CTG)_n$ repeats in the myotonin protein kinase gene in cultured lymphoblastoid cell lines from patients with myotonic dystrophy. *Genomics* **36,** 47–53.
3. Khajavi, M., Tari, A. M., Patel, N. B., et al. (2001) "Mitotic drive" of expanded CTG repeats in myotonic dystrophy type 1 (DM1). *Hum. Mol. Genet.* **10,** 855–863.
4. Gourdon, G., Radvanyi, F., Lia, A. S., et al. (1997) Moderate intergenerational and somatic instability of a 55-CTG repeat in transgenic mice. *Nature Genet.* **15,** 190–192.
5. Monckton, D. G., Coolbaugh, M. I., Ashizawa, K. T., et al. (1997) Hypermutable myotonic dystrophy CTG repeats in transgenic mice. *Nature Genet.* **15,** 193–196.
6. Shelbourne, P. F., Killeen, N., Hevner, R. F., et al. (1999) A Huntington's disease CAG expansion at the murine Hdh locus is unstable and associated with behavioural abnormalities in mice. *Hum. Mol. Genet.* **8,** 763–774.
7. Wheeler, V. C., Auerbach, W., White, J. K., et al. (1999) Length-dependent gametic CAG repeat instability in the Huntington's disease knock-in mouse. *Hum. Mol. Genet.* **8,** 115–122.
8. Sato, T., Oyake, M., Nakamura, K., et al. (1999) Transgenic mice harboring a full-length human mutant DRPLA gene exhibit age-dependent intergenerational and somatic instabilities of CAG repeats comparable with those in DRPLA patients. *Hum. Mol. Genet.* **8,** 99–106.
9. Mangiarini, L., Sathasivam, K., Mahal, A., et al. (1997) Instability of highly expanded CAG repeats in mice transgenic for the Huntington's disease mutation. *Nature Genet.* **15,** 197–200.
10. Van Den Broek, W. J., Nelen, M. R., Wansink, D. G., et al. (2002) Somatic expansion behaviour of the (CTG)(n) repeat in myotonic dystrophy knock-in mice is differentially affected by Msh3 and Msh6 mismatch-repair proteins. *Hum. Mol. Genet.* **11,** 191–198.
11. La Spada, A. R., Peterson, K. R., Meadows, S. A., et al. (1998) Androgen receptor YAC transgenic mice carrying CAG 45 alleles show trinucleotide repeat instability. *Hum. Mol. Genet.* **7,** 959–967.
12. Libby, R. T., Monckton, D. G., Fu, Y. H., et al. (2003) Genomic context drives SCA7 CAG repeat instability, while expressed SCA7 cDNAs are intergenerationally and somatically stable in transgenic mice. *Hum. Mol. Genet.* **12,** 41–50.
13. Gomes-Pereira, M., Fortune, M. T., and Monckton, D. G. (2001) Mouse tissue culture models of unstable triplet repeats: in vitro selection for larger alleles, mutational expansion bias and tissue specificity, but no association with cell division rates. *Hum. Mol. Genet.* **10,** 845–854.
14. Meek, R. L., Bowman, P. D., and Daniel, C. W. (1977) Establishment of mouse embryo cells in vitro. Relationship of DNA synthesis, senescence and malignant transformation. *Exp. Cell Res.* **107,** 277–284.
15. Todaro, G. J. and Green, H. (1963) Quantitative studies of the mouse embryo cells in culture and their development into established lines. *J. Cell Biol.* **17,** 299–313.
16. Herrmann, H. and Aebi, U. (2000) Intermediate filaments and their associates: multitalented structural elements specifying cytoarchitecture and cytodynamics. *Curr. Opin. Cell Biol.* **12,** 79–90.

17 Schmid, E., Tapscott, S., Bennett, G. S., et al. (1979) Differential location of different types of intermediate-sized filaments in various tissues of the chicken embryo. *Differentiation* **15,** 27–40.

18. Spector, D. L., Goldman, R. D., and Leinwand, L. A. (1998) Isolation and purification of intermediate filaments, in *Cells: A Laboratory Manual*. Cold Spring Harbor Laboratory, Cold Spring Harbor, New York, Vol. 1, p. 55.1.

V

In Vivo Analysis of Trinucleotide Repeat Diseases

16

Neurotransmitter Receptor Analysis in Transgenic Mouse Models

Caroline L. Benn, Laurie A. Farrell, and Jang-Ho J. Cha

Summary

One of the characteristic findings in human Huntington's disease (HD) is the alteration of neurotransmitter receptors. To a remarkable degree, transgenic HD mouse models recapitulate neurotransmitter receptor alterations. Neurotransmitter receptors can be assessed at the protein level by using receptor-binding autoradiography. One can also measure levels of receptor messenger RNA with *in situ* hybridization (ISH), employing either oligonucleotide or ribonucleotide probes. Both of these techniques—receptor-binding autoradiography and *in situ* hybridization—yield quantitative and regionally specific information regarding neurotransmitter receptors. We describe techniques for performing receptor-binding autoradiography and two types of *in situ* hybridization using oligonucleotide and ribonucleotide probes. With receptor binding and ISH, one can obtain quantitative region-specific assessments of neurotransmitter receptor alteration, a key pathologic event in HD pathogenesis.

Key Words: *In situ* hybridization; ribonucleotide; receptor binding; oligonucleotide; autoradiography; neurotransmitter; glutamate; dopamine; GABA; adenosine; AMPA; NMDA; metabotropic; acetylcholine; brain; mouse; anatomy.

1. Introduction

Neurotransmitter receptors are altered in human Huntington's disease (HD) brains ***(1)***. However, the interpretation of this finding was confounded by the issue of cell loss. The recent development of transgenic mouse HD models has been instructive with regard to the issue of neurotransmitter receptor loss ***(2)***. Transgenic HD mice demonstrate neurotransmitter alteration before frank cell death, arguing that neurotransmitter receptor alteration is an important pathogenic mechanism in HD and other triplet repeat diseases ***(3,4)***.

From: *Methods in Molecular Biology, vol. 277: Trinucleotide Repeat Protocols*
Edited by: Y. Kohwi © Humana Press Inc., Totowa, NJ

For many years, Young and colleagues have pioneered the analysis of neurotransmitter receptors using rodent brain sections ***(5–8)*** (*see* **Fig. 1**). One advantage of the receptor-binding autoradiography technique over traditional homogenate-binding approaches is the ability to obtain regionally precise binding information. In addition, because one performs the binding assays on thin cryostat sections, one can perform multiple receptor-binding assays on a single transgenic mouse brain, thus reducing the number of animals required. *In situ* hybridization (ISH) to visualize particular messenger RNA (mRNA) species offers the same advantages as receptor-binding autoradiography. Here, we describe protocols used routinely in our laboratory. Although there are many steps in each protocol, none of the steps are inherently difficult. A minimal amount of specialized equipment is required to perform these techniques. Used together, these techniques can provide a tremendous amount of information regarding the phenotype of transgenic mouse models ***(3,4,9–14)***.

2. Materials

2.1. Brain Sectioning

1. Superfrost/Plus microscope slides (12-550-15; Fisher).
2. Cryomatrix (Lipshaw).
3. Microscope slide box (22518; Ted Pella Inc.).

2.2. Receptor-Binding Autoradiography

1. Rack and large glass Wheaton jar.
2. Stir plate and stir bars.
3. Beakers.
4. ^{3}H ligand (Perhin Elmer or Amersham).
5. Two hair dryers.
6. Stopwatch.
7. Tritium-sensitive film (Kodak Biomax MS Film, cat. no. 8377616; Kodak intensifying screen, cat. no. 1622034) and film cassette.
8. Two adjustable-volume squirt dispensers.
9. β-Scintillation counter.
10. Glass cutter, double-sided tape, and ruler.
11. Binding buffer (listed in **Table 1**).
12. Glutaraldehyde/acetone solution (2.5% glutaraldehyde in acetone v/v) (*see* **Note 1**).

2.3. In Situ *Hybridization: Oligonucleotide Probes*

1. Wheaton brand borosilicate staining dishes and racks (900203 and 900204; Wheaton Scientific Products).
2. Heating block.
3. Two shaking water baths.
4. RNase-free microcentrifuge tubes.
5. Autoclaved pipet tips for 20-µL to 1-mL pipettors.
6. Shaking table.
7. Oven.
8. Hybridization chamber (e.g., Bioassay trays; Nunc) with plastic sink matting.

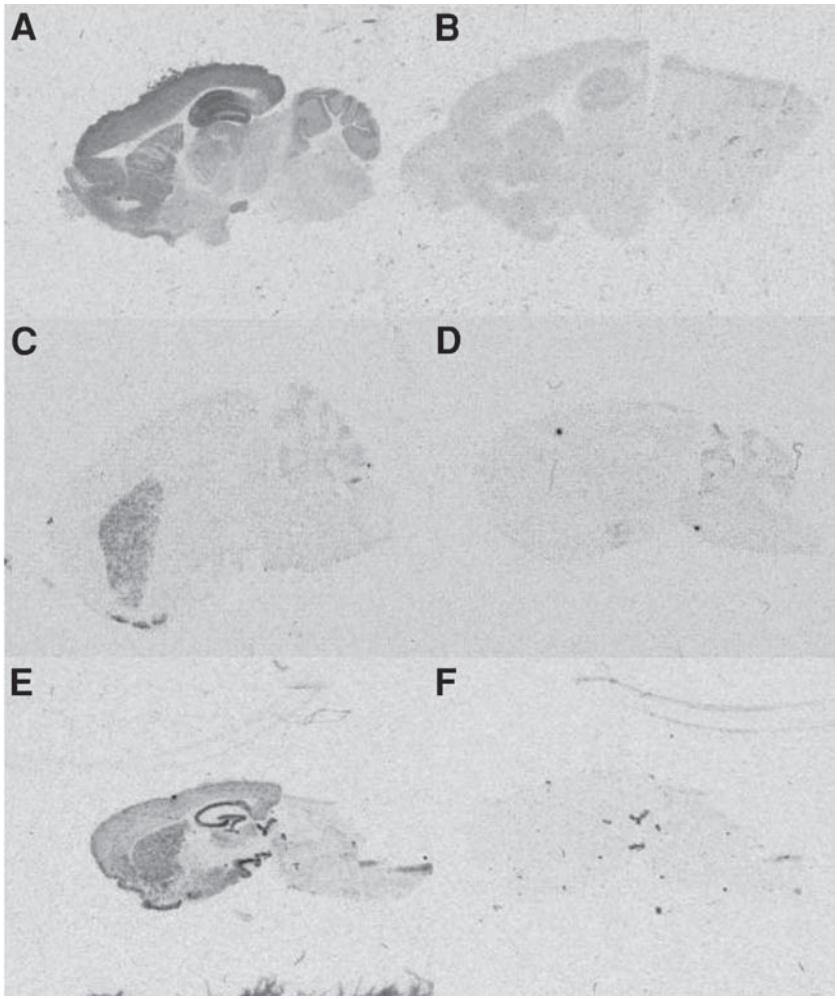

Fig. 1. Neurotransmitter receptor analysis using **(A, B)** receptor-binding autoradiography, **(C, D)** oligonucleotide *in situ* hybridization, and **(E, F)** riboprobe *in situ* hybridization. **(A)** Receptor-binding autoradiography on R6/2 mouse brain for NMDA-type glutamate receptors, "total" condition. **(B)** "Blank" condition for NMDA receptor-binding assay. In the presence of 1 mM NMDA, most specific binding (depicted in **A**) is displaced. **(C)** Oligonucleotide *in situ* hybridization for adenosine A2a receptors demonstrating distinct labeling in the striatum and nucleus accumbens. **(D)** Adenosine A2a receptor *in situ* hybridization in the presence of excess unlabeled oligonucleotide probe ("cold competition"). **(E)** Ribonucleotide probe *in situ* hybridization for metabotropic glutamte receptor mGluR5 using a specific antisense probe. **(F)** mGluR5 riboprobe *in situ* hybridization using a sense probe.

Table 1
Receptor Binding Assays

Receptor subtype	Radioligand and concentration	Prewash buffer	Prewash conditions	Incubation buffer	Incubation time and temperature	Blank condition	Wash buffer	Wash time and temperature	Ref.
Glutamate–NMDA	100 n*M* L-[^{3}H]glutamate	50 m*M* Tris-Ac, pH 7.4	30 min at 4°C	Same as prewash buffer	45 min at 4°C	100 μ*M* NMDA	Same as prewash buffer	Cold squirt[a]	***5***
Glutamate–AMPA	10 n*M* [^{3}H]AMPA	50 m*M* Tris-HCl + 2.5 m*M* $CaCl_2$ + 30 m*M* KSCN, pH 7.2	30 min at 4°C	Same as prewash buffer	45 min at 4°C	1 m*M* glutamate	50 m*M* Tris-HCl + 2.5 m*M* $CaCl_2$, pH 7.2	Cold squirt	***16***
Glutamate–kainate	80 n*M* [^{3}H]kainate	50 m*M* Tris-Ac, pH 7.2	30 min at 4°C	Same as prewash buffer	45 min at 4°C	1 m*M* kainate	Same as prewash buffer	Cold squirt	***5***
Glutamate–metabotropic group I	100 n*M* L-[^{3}H]glutamate	50 m*M* Tris-HCl + 2.5 m*M* $CaCl_2$ + 30 m*M* KSCN, pH 7.2	30 min at 4°C	Same as prewash buffer with 100 μ*M* NMDA and 10 μ*M* AMPA	45 min at 4°C	2.5 μ*M* quisqualate	Same as prewash buffer	Cold squirt	***18***
Glutamate–metabotropic group II	100 n*M* L-[^{3}H]glutamate	50 m*M* Tris-HCl + 2.5 m*M* $CaCl_2$ + 30 m*M* KSCN, pH 7.2	30 min at 4°C	Same as prewash buffer with 100 μ*M* NMDA, 10 μ*M* AMPA, and 2.5 μ*M* quisqualate	45 min at 4°C	1 m*M* glutamate	Same as prewash buffer	Cold squirt	***19***

Table 1 ***(continued)***

Receptor subtype	Radioligand and concentration	Prewash buffer	Prewash conditions	Incubation buffer	Incubation time and temperature	Blank condition	Wash buffer	Wash time and temperature	Ref.
GABA–A	40 n*M* [^{3}H]GABA	50 m*M* Tris-HCl + 2.5 m*M* $CaCl_2$, pH 7.4	30 min at 4˚C	Prewash buffer + 100 μ*M* baclofen	45 min at 4˚C	100 μ*M* isoguvacine	Same as prewash buffer	Cold squirt	***20***
GABA–B	40 n*M* [^{3}H]GABA	50 mM Tris-HCl + 2.5 m*M* $CaCl_2$, pH 7.4	30 min at 4˚C	Prewash buffer + 100 μ*M* isoguvacine	45 min at 4˚C	100 μ*M* baclofen	Same as prewash buffer	Cold squirt	***20***
Dopamine–D1	1.65 n*M* [^{3}H]SCH-23390	None	None	25 m*M* Tris-HCl, pH 7.5, 100 m*M* NaCl, 1 m*M* $MgCl_2$, 1 μ*M* pargyline + 10 mg/L ascorbate	2.5 h at room temp	1 μM cis-flupentixol	Same as prewash buffer	10 min in cold buffer followed by quick dip in H_2O	***21***
Dopamine–D2	180 p*M* [^{3}H]YM-09151–2	None	None	25 m*M* Tris-HCl, pH 7.5, 100 m*M* NaCl, 1 m*M* $MgCl_2$, 1 μ*M* pargyline + 10 mg/L ascorbate	3 h at room temp	50 μ*M* dopamine	Same as prewash buffer	10 min in cold buffer followed by quick dip in H_2O	***22***

Table 1 *(continued)*

Receptor subtype	Radioligand and concentration	Prewash buffer	Prewash conditions	Incubation buffer	Incubation time and temperature	Blank condition	Wash buffer	Wash time and temperature	Ref.
Dopamine uptake sites	6 n*M* [^{3}H]mazindol	50 m*M* Tris-HCl, 5 m*M* KCl, 300 m*M* NaCl, pH 7.9	5 min at 4˚C	Prewash buffer + 300 n*M* desipramine	2.5 h at room temp	10 μ*M* nomifensine	Same as prewash buffer	10 min in cold buffer followed by quick dip in ddH_2O	***23***
Acetylcholine –muscarinic	1 n*M* [^{3}H]QNB	7.75 m*M* Na_2PO_4, 137 m*M* NaCl, 2.6 m*M* KCl	Twice for 5 min at 4˚C	Same as prewash buffer	3 h at room temp	None	Same as prewash buffer	Twice for 5 min in cold buffer, followed by quick rinse in ddH_2O	***24***
Adenosine-A2a	5 n*M* [^{3}H]CGS 21680	50 m*M* Tris-HCl, 10 m*M* $MgCl_2$, pH 7.4 + 2 U/mL adenosine deaminase	30 min at room temp	Same as prewash without adenosine deaminase	90 min at room temp	20 μ*M* 2–chloro-adenosine	Same as prewash buffer without adenosine deaminase	5 min in cold buffer, followed by quick rinse in ddH_2O	***25***

Abbreviations: AMPA: (*RS*)-α-amino-3-hydroxy-5-methylisoxazole-4-propionic acid; ddH_2O: double-distilled water; QNB: quinuclidinyl benzilate. Cold squirt wash is described in **Subheading 3.2.4.1.**

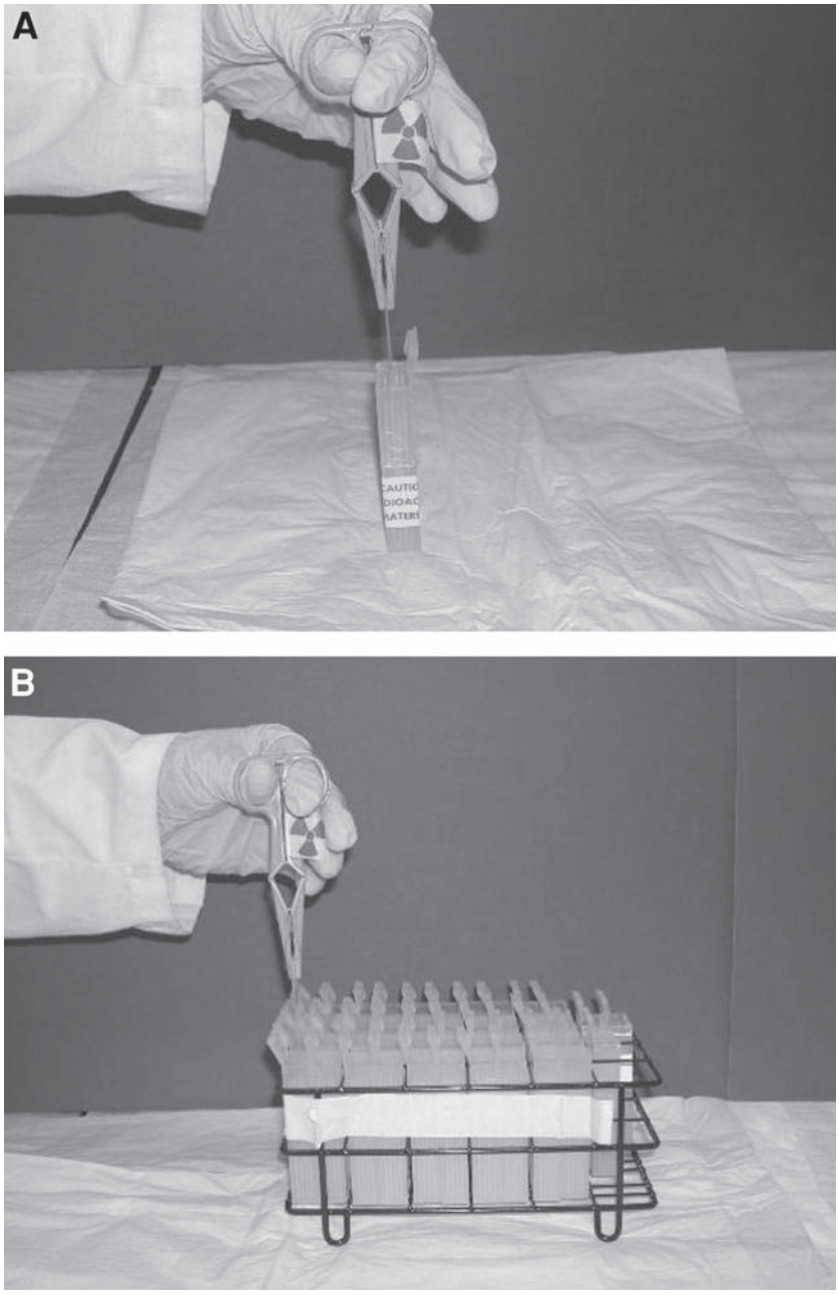

Fig. 2. Cytomailers used in receptor-binding autoradiography. **(A)** Forceps are used to place slides into the slide slots in the cytomailer. **(B)** Typical arrangement of cytomailers in rack, allowing for simultaneous incubation of many slides.

9. Hem-tek slide staining set (Baxter Scientific Products).
10. Oligonucleotide labeling kit (NEP100; Perkin-Elmer Life Sciences).
11. Salmon testes DNA (9.8 mg/mL; Sigma, D-7656).
12. [^{35}S]dATP (NEG-034H; Perkin-Elmer Life Sciences).
13. Mini Quick Spin oligo columns (1 814 397; Roche).
14. Carbon 14 standards [ARC-146(CG); ARC, Inc.].
15. Film (Kodak BioMax MR film) and film cassette.
16. Oligonucleotide primers (listed in **Table 2**).
17. Diethylpyrocarbanate (DEPC)-treated double-distilled water (ddH_2O).
18. 0.1 *M* phosphate-buffered saline (PBS) in DEPC ddH_2O (DEPC-PBS).
19. Hybridization buffer: 50% formamide, 4X saline sodium citrate (SSC; *see* recipe for 20X SSC stock solution in **Subheading 2.4.21.**), 250 μg/mL Salmon testes DNA, 9.8 mg/mL [D-7656], 10% of 50% dextran sulfate (Sigma), 50X Denhardt's solution (D-2532; Sigma).
20. 4% Paraformaldehyde in PBS (*see* **Note 1**).
21. 1 *M* dithiothreitol (DTT).

2.4. In Situ *Hybridization: Riboprobes*

1. Wheaton brand borosilicate staining dishes and racks (Wheaton Scientific Products).
2. Heating block.
3. RNase-free microcentrifuge tubes.
4. Autoclave tips (20 μL to 1 mL).
5. Two shaking water baths.
6. Shaking table.
7. Geigercounter.
8. Hybridization chamber (e.g., Bioassay trays; Nunc) with sink matting.
9. Hem-tek slide staining set (Baxter Scientific Products).
10. Riboprobe labeling kit (Perkin-Elmer Life Sciences).
11. [^{35}S]CTP (NEG-064C; Perkin-Elmer Life Sciences).
12. Reagents for RNA labeling; 5X transcription buffer (P117B; Promega), 100 m*M* dithiothreitol (DTT) (P117B; Promega), 40 U/μL RNasin (N251 A; Promega), 80 U/μL SP6 or T7 polymerase (P407A; Promega), 1 U/μL RQ1 DNase (M610A; Promega), AUG mixture ribonucleotide kit (P1221; Promega).
13. Beta-scintillation counter.
14. Carbon-14 standards [ARC-146(CG); ARC, Inc.].
15. Film (Kodak BioMax MR film; 05-728-24, Fisher) and film cassette.
16. TE (10 m*M* Tris-HCl, pH 7.6, 1 m*M* EDTA buffer) with DEPC water.
17. 3 *M* Na–acetate (pH 5.2) with DEPC water.
18. 70% Ethanol with DEPC, 95% ethanol, and 100% ethanol.
19. Chloroform.
20. TEA/acetic acid anhydride: 0.25% acetic anhydride in 0.1 *M* triethanolamine (TEA), pH 8.0.
21. 20X SSC stock solution: 175.3 g of NaCl, 88.2 g of sodium citrate/L, pH 7.0 with NaOH, for working solution: 2X SSC, 0.1X SSC, and 2X SSC.
22. RNase A (100 μg/mL) (Boehringer Mannheim): Add 5 mL of 10 mg/mL RNase A stock solution in 500 mL buffer of RNAse buffer; store at 4°C.
23. RNase A stock solution: Reconstitute 100 mg of RNase A (Boehringer) in 10 mL of 10 m*M* Tris-HCl, pH 7.5 (100 μL of 1 *M* Tris-HCl stock) and 15 m*M* NaCl (50 μL of 3 *M* NaCl stock), boil for 15 min, let slowly cool to store at room temperature –20°C.
24. RNAse A buffer (Boehringer Mannheim): 0.5 *M* NaCl (29.22 g NaCl per liter of buffer),

Table 2
Oligonucleotide Probes Sequences Used for Study of Neurotransmitter Receptors in Mouse Brain

mRNA target	Oligonucleotide probe sequence (5' to 3')	Ref.
Dopamine D1 receptor	GAC ATC GGT GTC ATA GTC CAA TAT GAC CGA TAA GGC	***3,26***
Dopamine D2 receptor	GGC AGG GTT GGC AAT GAT ACA CTC ATT CTG GTC TGT ATT	***3,27***
Adenosine A2a receptor	CTG TTG ATC CAC ACG GCC CAG CAC ACA AGC ACG TTA CCC AGG ATG	***4***
NMDA receptor NR1 subunit	GCA CAG CGG GCC TGG TTC TGG GTT GCG CGA GCG CGA CCA CCT CGC	***28,29***
NMDA receptor NR2a subunit	CCC TGA AAC ACA TAG TTA CTG AGA CTA TCC TTG TGC CTG TTG GCC	***28,29***
NMDA receptor NR2b subunit	CAC TGT AGC GGT CAC TCT TGA AAG AGA ACT TGC CGT ACA GGT CGC	***28,29***

10 m*M* Tris-HCl, pH 7.2 (10 mL of 1 *M* Tris-HCl per liter of buffer), 1 m*M* EDTA (2 mL of 0.5 M EDTA, pH 8.0, per liter of buffer).

25. DEPC-treated ddH_2O.

3. Methods

3.1. Preparation of Frozen Tissue Sections

Brains should be removed immediately postmortem and snap-frozen in chilled isopentane and stored at –80°C (*see* **Notes 2** and **3**). For cutting, the frozen brains are placed in the cryostat (Shandon) for 40 min to equilibrate to temperature (–20°C). It is important to let the brains warm up from –80°C, because brains will shatter upon sectioning if they are too cold. Brains are divided longitudinally into two hemispheres using a clean razor blade and mounted using cryomatrix. Twelve-micron sections (to achieve approximately one layer of cells per section) are mounted onto glass slides 7 mm from the bottom of the slide (*see* **Note 4**). Slides should be labeled with pencil only, with all relevant information. We typically cut sagittal sections, as this allows for generation of sections that contain cortex, striatum, hippocampus, and cerebellum on a single section. Coronal sections can also be cut and is preferable in some situations, especially when studying either the striatum or the hippocampus. Moisture and frequent freeze–thaw cycles should be avoided to ensure preservation of the mRNA.

3.2. Receptor-Binding Autoradiography

Receptor-binding autoradiography can be used to measure the regional distribution and abundance of neurotransmitter receptors. The methods described below outline (a) preparing the radioligand-binding solution, (b) prewashing the sections, (c) performing the binding assay, (c) separating the bound and unbound ligands, and (e) producing a film autoradiograph and performing densitometric analysis (*see* **Notes 5** and **6**).

3.2.1. Preparation of Ligand

3.2.1.1. Ligand Considerations

Several considerations should be taken into account when selecting a ligand to label receptors, including binding affinity and subtype specificity. Typically, one should select the ligand that is most selective for the receptor subtype that is being targeted. Numerous radiolabeled receptor ligands exist and are available either from Perkin Elmer or Amersham. Most radioligand binding can be carried out in Tris buffers; occasionally, salts will be added to optimize binding parameters. Ionic conditions often influence the level of binding, especially the levels of the anions chloride and thiocyanate and the cations sodium and calcium ***(5,15,16)***. In **Table 1**, we list the binding assays that we perform most commonly, including conditions of binding buffer, concentration of ligand, incubation times, and displacer. More extensive lists of autoradiographic receptor-binding assays can be found in **ref. *17***.

Typically, the radioligand is used at a concentration equivalent to the dissociation constant (K_d) for that ligand. The K_d value is the concentration of ligand at which 50% of the available receptors are bound. Therefore, using the radioligand at the K_d concentration maximizes one's chances of detecting differences in binding between two different conditions (e.g., differences between wild-type and transgenic mice). Ligands with lower K_d values have high affinity for receptors, whereas higher K_d values are indicative of lower affinity. Ligands that bind to receptors for neuromodulators, such as the monoamines or neuropeptides, typically have K_d values in the nanomolar range. In contrast, ligands that bind to receptors for the amino acids glutamate and γ-aminobutyric acid (GABA) have lower affinity, with K_d values in the micromolar range. Differences in ligand affinity have important consequences for performing binding assays. Because the K_d value is determined by a ratio of rates of dissociation and association, the dissociation constant often is indicative of the rate of dissociation, with lower-affinity receptors having faster rates of unbinding than higher-affinity receptors. Thus, for high-affinity receptors, one can use low concentrations of ligand and relative long rinsing times (minutes). However, for low-affinity receptors such as glutamate and GABA receptors, one is required to use higher concentrations of ligand and shorter wash times (*see* **Table 1**).

3.2.1.2. Calculating Concentration of Supplied Radioligand

To calculate how much [^{3}H]ligand to use, one has to know the specific activity of the radioligand. Typically, the specific activity of commercially available radioligand

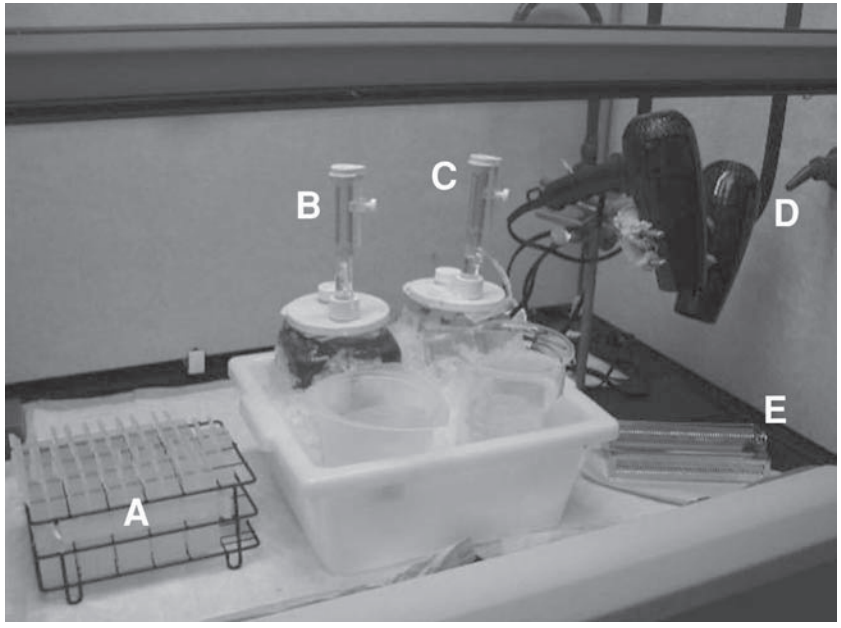

Fig. 3. Setup for performing receptor-binding autoradiography for low-affinity ligands. Because of the glutaraldehyde/acetone mixture, this experiment is performed in a fume hood. Cytomailers for binding incubation (A) are placed next to wash stations, with adjustable volume pipettors containing assay buffer (B) and glutaraldehyde/acetone (C). Following rinsing, slides are rapidly dried under hair dryers (D) and then placed into metal slide racks (E).

ranges from 1 to 100 Ci/mmol. Most commercial suppliers of radioactivity ship radioligands at a concentration of 1 mCi/mL (which is equal to 1 Ci/L). The first step is then to calculate the molar concentration of ligand in the vial of radioligand:

concentration of ligand = 1 Ci/L ÷ s.a. Ci/mmol, where s.a. is the specific activity.

If s.a. is 50 Ci/mmol, then

concentration of ligand = 1/50 mmol/L = 0.02 m*M* = 20 μ*M*

The concentrations of commercially available tritiated ligands are typically in the range 10–50 μ*M*.

3.2.1.3. Calculating the Amount of Ligand to Use

Next, one needs to calculate how much radioligand to add to achieve a final correct concentration in the binding incubation. We prepare a radioligand solution that is slightly higher in concentration than the final desired concentration to account for dilution by displacers. We perform our radioactive incubation in plastic slide holders called cytomailers (*see* **Fig. 2**). Using cytomailers, one can perform binding assays

using incubation volumes of as little as 5 mL; we typically use 10 mL final volume in our binding incubations. Because for each "total" binding condition, there is a corresponding "blank" condition, one has to account for the fact that displacers will be added to some of the cytomailers. Therefore, we typically add 9 mL of ligand solution to each cytomailer. Then, we add an additional 1 mL of either plain buffer or displacer compound, at 10 times the final desired concentration. Because the displacer will de diluted 1:10, the final concentration of displacer will be correct. Because the ligand will be diluted, it needs to be slightly more concentrated than the final desired concentration. Using our example, if the final desired concentration of ligand is 1 n*M*, then one needs to make a ligand solution that is slightly more concentrated:

$$\text{ligand concentration} = \text{Final desired concentration} \times (\text{Final volume} / \text{Predilution volume})$$

$$= 1\ \text{n}M \times (10\ \text{mL} / 9\ \text{mL}) = 1.111\ \text{n}M$$

By making an initial ligand concentration that is slightly more concentrated, the final concentration will be appropriate.

The next step is to calculate how much ligand is needed. Cytomailers can accommodate up to five slides in each container. However, for the purposes of receptor-binding assays, only the middle three slots are suitable for use. One then needs to calculate how many cytomailers will be included. In a typical experiment, we will perform two "total" slides and one "blank" slide for each animal. Always perform binding experiments with comparison groups within the same experiment. Typically, we would use six animals from each group of interest. Thus, if we had six transgenic mice and six wild-type littermate controls, the number of cytomailers required is

$$12\ \text{Animals} \times 3\ \text{Slides per animal (2 Totals and 1 Blank)} = 36\ \text{Slides}$$

$$36\ \text{Slides} \div 3\ \text{Slides per cytomailer} = 12\ \text{Cytomailers required}$$

Recall that each cytomailer will receive 9 mL of concentrated ligand solution:

$$12\ \text{Cytomailers} \times 9\ \text{mL per cytomailer} = 108\ \text{mL of ligand solution required}$$

Although 108 mL of ligand solution is required, it is a good idea to make enough ligand solution to account for pipetting errors. We typically make enough for 2 extra cytomailers. So, in this case, we would make 126 mL of ligand solution.

Now, knowing the concentration of the radioligand in the supplier vial and the total volume of the ligand solution desired, one can calculate the correct amount of ligand (y) to add to the 126 mL of buffer:

$$y(20\ \mu M) = (126\ \text{mL})(1.111\ \text{n}M)$$

$$y = 20 \times 10^{-6}\ \text{mol/L}\ (126 \times 10^{-3}\ \text{L})(1.111 \times 10^{-9}\ \text{mol/L})$$

$$y = 6.999 \times 10^{-6}\ \text{L}$$

$$= 7\ \mu\text{L}$$

So, in this case, add 7 μL of radioligand to 126 mL of ligand buffer.

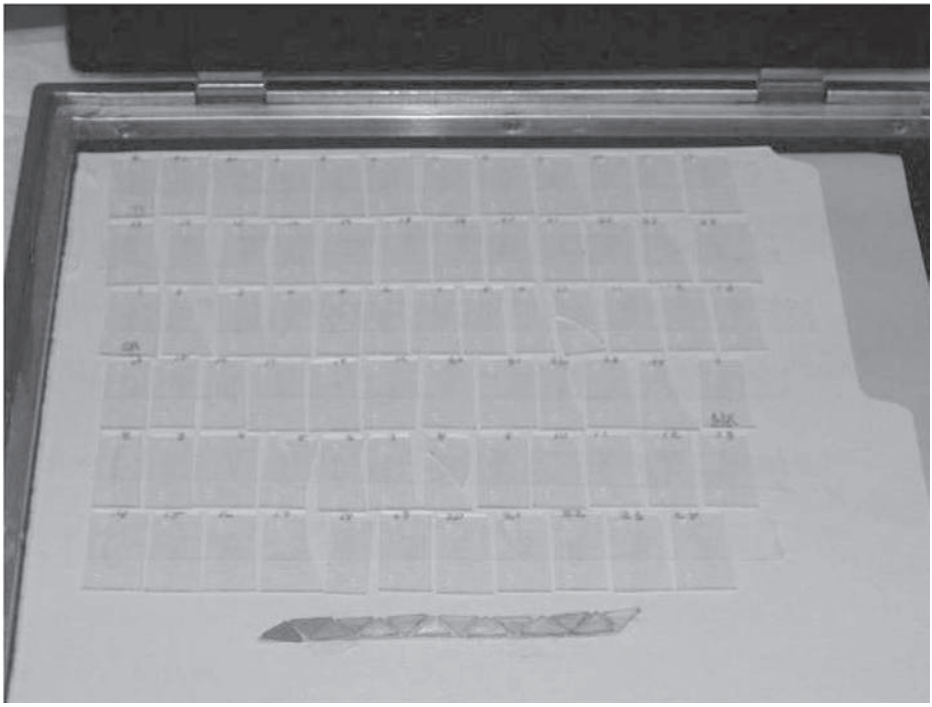

Fig. 4. Arranging receptor binding autoradiography slides for film autoradiography. Using double-sided tape, cut slides are tiled onto a sheet of paper. This sheet of paper is placed within a conventional film cassette. Note the presence of triangular calibrated radioactive standards at the bottom of the figure.

3.2.1.4. Checking Radioactivity

One can then measure the amount of radioactivity to confirm that the ligand is properly made. Because one knows the specific activity (in our example case, s.a. = 50 Ci/mmol), one can calculate the amount of radioactivity that should be present in the ligand solution. One needs to know that 1 Ci = 2.2×10^{12} disintegrations per minute (dpm). To calculate the dpm, use

$$(7\ \mu\text{L of radioligand added})(1\ \text{mL/mCi}) = 7\ \mu\text{Ci added}$$

$$(7 \times 10^{-6}\ \text{Ci})(2.2 \times 10^{12}\ \text{Ci/dpm}) = 15.4 \times 10^{6}\ \text{dpm}$$

Thus, there are 1.54×10^6 dpm in total. We typically sample about 100 µL of the ligand sample. One can then calculate the dpm in this 100-µL sample (= z):

$$z \div 100\ \mu\text{L} = 15.4 \times 10^{6}\ \text{dpm} \div 126\ \text{mL}$$

$$z = 12{,}222\ \text{dpm}$$

Using scintillation counting, one can then predict the counts per minute (cpm) that would result. The cpm–dpm relationship is the *counting efficiency* and it varies among different scintillation counters. If one assumes a counting efficiency of 30%, a 100-µL sample of correctly prepared ligand solution should yield 3667 cpm. The measures results should be within 10% of predicted, otherwise one might suspect error in ligand preparation.

3.2.2. Prewash Incubation

Typically, depending on the type of assay being performed, slides undergo a prewash prior to the actual binding reaction with [^{3}H]ligand. This serves a dual purpose: to equilibrate the tissue to the assay conditions of temperature and ionic environment and to remove endogenous ligands that could potentially interfere with binding of the exogenous ligand. Slides usually are removed from –80°C storage, placed into metal slide rack, and allowed to come to room temperature for 30 min. Thereafter, metal slide racks are transferred for 30 min into large Wheaton dishes filled with sufficient binding buffer to cover the slides. Following this prewash, slides are typically dried under a stream of cool air (we typically use the "low" setting on conventional hair dryers). The slides are now ready for the binding reaction.

3.2.3. Binding Reaction

3.2.3.1. "Total" and "Blank" Conditions

Incubation will occur in two separate conditions: a "total" condition, in which the brain section is exposed to [^{3}H]ligand only, and a corresponding "blank" condition, in which a nonradioactive competitor is also included. Each animal should be subjected to both total and blank conditions; we typically perform duplicate total conditions (*see* **Subheading 3.2.1.3.**). Because the ligand solution was made slightly more concentrated than the final desired concentration, we need to dilute:

Final desired ligand concentration = 1 n*M*;
Concentration of prepared ligand solution = 1.1111 n*M* (from **Subheading 3.2.1.3.**),
for the "total" condition:
  9 mL of prepared ligand solution
  1 mL of binding buffer
for the "blank" condition:
  9 mL of prepared ligand solution
  1 mL of displacer (10X concentrated).

By adding the displacer compound at 10X the final desired concentration, the final concentration of displacer will be correct within the cytomailer. Note that the final concentrations of [^{3}H]ligand will be equivalent in both the "total" and "blank" cytomailers. It is ultimately the difference in binding between the two conditions that is considered "specific" binding to receptors.

The duration of the binding incubation varies according to [^{3}H]ligand. In general, this incubation time is chosen to be long enough to assume that the binding reaction has come to equilibrium. This incubation time can range from 10 min to 3 h.

3.2.3.2. High-Affinity Receptors

Certain ligands have high affinity for their respective receptors. These ligands are typically used in the nanomolar or high picomolar range. Because these ligands have such high binding affinity (and corresponding low K_d values), the dissociation rates are slow. Thus, for these high-affinity receptors, slides can be batch processed. For example, following prewash, the slides can be transferred into cytomailers containing the desired ligand one at a time, without extreme attention to the timing of such a transfer. Binding incubations for high-affinity receptors typically are carried out at room temperature.

3.2.3.3. Low-Affinity Receptors

In contrast to high-affinity receptors, care must be taken with slides when using a low-affinity ligand. For glutamate receptor assays, for example, the incubation time is 45 min, but there is significant dissociation within the first 30 s ***(5)***. Because the rinsing procedure takes several seconds for each slide, to guarantee uniform incubation time, we recommend for low-affinity receptors that the binding incubation be started on a staggered basis. For example, using a stopwatch, we typically start the binding incubation reaction for each individual slide at regular intervals ranging from 15 s to 1 min. We stagger the time at which we drop the slide into the cytomailer. This allows the slides to be rinsed individually 45 min later, guaranteeing that each slide has been exposed to [^{3}H]ligand for the same amount of time. Rinsing each slide requires between 10 and 15 s; if one is using many slides, the rinsing time then becomes significant with respect to the total binding incubation time. To counteract rapid dissociation, binding assays with low-affinity receptors typically are carried out on ice.

3.2.4. Postincubation Washing

Washing slides following the binding incubation is the critical step in receptor-binding autoradiography (*see* **Fig. 3**). It is this step that removes the unbound [^{3}H]ligand, leaving only specifically bound [^{3}H]ligand on the slide. In most cases, washes use the same buffer as used in the binding incubation, without the radioactive ligand.

For high-affinity ligands with slow dissociation times, slides can be transferred into cytomailers containing buffer. Alternatively, slides can be transferred into metal slide racks and batch-washed in large glass trays. It is important to have a sufficient volume of wash buffer to make rebinding of dissociated [^{3}H]buffer unlikely.

3.2.4.1. "Squirt" Washes for Low-Affinity Ligands

Low-affinity ligands require significantly different washing conditions. Here, speed is of the essence (*see* **Note 7**). Because these ligands dissociate from receptors quickly, one needs to rinse nonspecifically bound [^{3}H]ligand and dry the slide quickly to counteract loss of specific binding. For low-affinity receptors, we have employed a rapid-rinse method requiring the use of adjustable-volume liquid dispensers. After the binding incubation, slides are removed from the cytomailers using forceps or a

hemostat. Slides are then rinsed quickly with three rapid squirts of cold binding buffer. Each squirt is dispensed in a volume of 4 mL. A fourth squirt is applied to the back of the slide to remove additional radioactivity. All four buffer squirts should be performed within 5 s, and a large glass beaker should be placed beneath the spout of the liquid dispenser to collect radioactive wash. Immediately thereafter, slides should be squirted twice (once on the front and once on the back) with 2 mL of glutaraldehyde dissolved in acetone (2.5%, v/v). This step allows the tissue to be dried quickly, essentially removing all of the aqueous solution on the slide. Then, the slides should be placed under hair dryers (high heat setting) and then placed into a metal slide rack. Using this method of washing, slides can effectively go from the ligand incubation to being dry within 10–15 s. Such rapid washing is essential to capture specific binding of low-affinity ligands such as GABA and glutamate.

3.2.5. Creating Autoradiographic Images

Once the slides are dried, the radioactive ligand molecules are attached to the tissue. Tritium-sensitive film can be overlaid to develop an image reflective of the amount of binding. Such autoradiographic images yield essentially two types of information: where in the brain the ligand binds and in what amounts. The darkness of the corresponding image reflects the total amount of binding.

Some comment regarding the use of tritium-sensitive film is appropriate. Because tritium is a low-energy radioisotope, uncoated film must be used. Thus, tritium-sensitive film has one face that is uncoated. Therefore, one must handle such film carefully because the uncoated side scratches quite easily. Extreme care must be used in the handling of such film, not only in placing the film on the dried slides but also in handling the film to develop the image. We do not recommend using an automated processor, as this may damage the fragile uncoated emulsion face. Traditional darkroom methods are required to develop these films properly. Alternatively, certain modern phosphorimaging systems have the capacity for handling tritium autoradiography. However, in our experience, the spatial resolution of the screens used for phosphorimagers is inferior to the resolution achieved with tritium-sensitive photographic film.

Once the slides are dried, they are scored with a diamond knife and snapped sharply in order to remove the portion of the slide that does not contain the brain section. The portion of the slide that has the brain tissue is then tiled onto a sheet of paper using double-sided tape. Such cutting and tiling of slides saves on cost, as the tritium-sensitive film is quite expensive, but also offers the advantage of placing all of the slides to be compared on the same piece of film. Alongside this tiling of brain sections, one should also tile-calibrated radioactive standards (*see* **Fig. 4**). The images produced by these standards will ultimately be used in the analysis of the autoradiographic image.

3.3. Oligonucleotide In Situ *Hybridization*

Neurotransmitter receptors can also be analyzed using *in situ* hybridization, which measures mRNA. The methods described outline (a) the design, sequence, and prepa-

ration of the oligonucleotides used for *in situ* hybridization, (b) incorporation of a radiolabel into the oligonucleotide, and (c) the hybridization of the radiolabeled oligonucleotide to the tissue section, washing, and exposure of the labeled tissue section to film (*see* **Notes 8** and **9**).

The time required is as follows:

- Oligonucleotide custom synthesis: between 3 and 8 d (depending on source used)
- Preparation of frozen tissue sections on glass slides: allow 1 h per brain hemisphere
- Labeling of oligonucleotide: 2 h
- Hybridization: 2 d (for both prehybridization and posthybridization)
- Exposure of labeled sections to film: 1 wk
- Densitometry: 1 d (depends on number of sections)
- Overall: approx 2 to 3 wk

3.3.1. Oligonucleotide Probes

3.3.1.1. Design Considerations for Oligonucleotides

Oligonucleotides are ideal for use in ISH experiments, as they are easily synthesized and labeled. The easiest method is to use an oligonucleotide probe that has previously been reported to work in ISH for your target sequence (*see* **Table 2**). If a published sequence is not available, we design our own probes. Typically, we use commercial software such as Oligo (National Biosciences, Inc.) or DNA Strider (CEA, France) to select 45 nucleotide sequences for at least four candidate probes, searching against sequence information obtained from available databases such as GENBANK. Once candidate probes are suggested, a homology search should be run using BLAST or a similar program. Only the target sequence should be returned to guarantee sequence specificity. Using Oligo or similar software, one should then check the candidate probes for internal hairpin formation.

3.3.1.2. Preparation of Oligonucleotides

Oligonucleotides are made by custom synthesis (Gibco-BRL) and shipped in a dried form. Dried oligos are diluted with DEPC-treated water to a concentration of around 1 nmol/μL, and the concentration is checked by measuring the optical density at 250 nm:

$$[\ ] \text{ of undiluted oligo} = (OD_{260})33/\text{m.w.} = \mu\text{mol/mL} = [n]\ \text{pmol/}\mu\text{L},$$

where m.w. is the molecular weight of the oligonucleotide sequence. Some of this stock is diluted to make a working stock of 1.25 pmol/μL:

$$\text{Want final dilution} = 1.25\ \text{pmol/}\mu\text{L}$$

$$\text{Dilution factor (DF)} = [n]/1.25$$

A second stock of oligonucleotide is made at 100 m*M* concentration (1000 times in excess) to use as a competition ("cold" condition). This "cold" (i.e., unlabeled) oligonucleotide is used to ascertain the specificity of the hybridization reaction (*see* **Note 10**).

3.3.2. [^{35}S]-3' Labeling of Oligonucleotide Probes

Oligonucleotide labeling is performed using a 3'-end-labeling kit from NEN (cat. no. NEP100) and the radiochemical [^{35}S]dATP (NEN cat. no. NEG034H). Radioactive polyA is added to the 3' end of the oligonucleotide using terminal deoxynucleotide transferase (TdT). The diluted oligonucleotide concentration is 1.25 pmol/μL and 10 pmoL is labeled in this experiment, so 8 μL of diluted oligonucleotide is needed.

1. The 3'-end-labeling kit is thawed on ice (takes about 1 h).
2. On ice, the following reagents are added in the following order (all are in the labeling kit apart from the radionucleotide):

Diluted oligonucleotide (1.25 pmol/μl)	8.0 μL
TdT buffer	12.5 μL
$CoCl_2$ solution	2.5 μL
^{35}S dATP (1 mCi)	10.0 μL
TdT (35 U)	2.0 μL
Total	35 μL

3. The tube contents are mixed and centrifuged briefly to collect and the reaction is incubated for 30 min at 37°C.
4. The reaction is stopped with the addition of 65 μL of reagent A on ice. Reagent A: 100 m*M* Tris-HCl, pH 7.7, 100 m*M* TEA, 1 m*M* EDTA stored at 4ºC.
5. Oligonucleotide purification is performed with Mini Quick Spin Oligo columns according to the manufacturer's instructions.
6. Five microliters of 1 *M* DTT (stored at –20°C) is added to the purified probe to prevent oxidation.
7. One microliter of probe is counted in duplicate and averaged (for use in calculations of how much to use for probe labeling); 800,000 dpm/μL is required for the experiment. The labeled oligonucleotide can be used immediately or stored at –80°C.

3.3.3. Hybridization of Labeled Oligonucleotides

3.3.3.1. Prehybridization (Day 1)

- Prehybridization is to be performed in the hood with baked Wheatons and only with DEPC-treated solutions.
- All PBS solutions should have autoclaved stir bars.
- 4% Paraformaldehyde is to be disposed of into a designated waste bottle, not down the sink (*see* **Note 8**).

Slides are removed from the –80°C freezer and placed into a baked glass Wheaton rack in a zigzag fashion. (This allows nearly double the number of slides to be put into each rack.) Slides are rapidly dried with a cold airstream until slides are thawed and dry. Use hair dryers on cool settings. The slides are treated as follows with about 200 mL of solution per Wheaton:

Solutions	Time	
4% Paraformaldehyde	10 min	Use stir bars on a stirrer
PBS × 2	5 min each	Use stir bars on a stirrer
70% EtOH with DEPC	2 min	
80% EtOH with DEPC	2 min	

95% EtOH with DEPC	2 min	
100% EtOH	2 min	→ air-dry

The oligonucleotide hybridization buffer stock solution (which can be made prior to experiment and stored at –20°C) is taken from –20°C and kept on ice at all times:

Solution	Final conc.	For 10 mL
Formamide	50%	5 mL
20X SSC	4X	2 mL
50% Dextran sulfate	10%	2 mL
50X Denhardts (Sigma, D-2532)	1X	0.2 mL
Salmon testes DNA (9.8 mg/mL)	250 μg/mL	0.25 mL
Total		9.45 mL

3.3.3.2. Calculation of the Amount of Labeled Probe to Use

The concentration of radioactivity to be used is 3000 cpm/μL of labeled probe in hybridization buffer. Because 80 μL of radioactive hybridization buffer for each slide is used, this means that there is 240,000 cpm/slide (cpm = counts per minute).

Number of slides: [*n*] (overestimate to allow for pipetting errors)

Probe has [*n*] × 80 μL/slide = [*V*] (amount of hybridization/probe mix) × 3000 cpm/μL

= [*C*] (cpm per desired)

Amount of probe in hybridization buffer = [*C*]/[*A*] (average from scintillation count)

A sample calculation for a test hybridization follows. For a test hybridization, six slides of a normal, control brain section are needed for the "hot" (i.e., radioactive) condition and three slides of a normal, control brain for the "cold" competition condition; because separate hybridization solutions will be made for hot and cold conditions, these need to be calculated separately:

Hot condition:

Number of slides = 8(6 + 2 for pipetting errors)

Probe has 8 slides × 80 μL/slide = 640 μL of hybridization/probe mix × 3000 cpm/μL

= 1,920,000 cpm desired

Amount of probe (assume average from scintillation count is 800,000 cpm)

= 1,920,000/800,000

= 2.4 μL

Cold condition:

Number of slides = 4(3 + 1 for pipetting errors)

Probe has 4 slides × 80 μL/slide = 320 μL of hyb/probe mix × 3000 cpm/μL

= 960,000 cpm desired

Amount of probe (assume average from scintillation count is 800,000 cpm)

= 960,000/800,000

= 1.20 μL

3.3.3.3. Hybridization (Using Sample Calculation)

	Hot probe	Cold (competition) probe
Hybridization buffer	640 μL	320 μL
Probe	2.4 μL	1.2 μL
1 *M* DTT (100 μL/mL of hybridization buffer)	64 μL	32 μL
100 m*M* cold oligo (competition)	–	10 μL

1. Tubes are made up with reagents as in the table above vortexed, and left to settle to eliminate excess bubbles. Make sure to keep all reagents on ice.
2. Hybridization trays are set up by lining the bottom with filter paper. Whatman filter paper is wetted with a mixture containing 50% formamide in 4X SSC (final concentration), and air bubbles are removed. A rubber mesh is laid on the moistened filter paper, and the air-dried slides are placed on top of the rubber mesh.
3. Then, 80 μL/slide of hybridization mix per section is added to the section and a cover slip (22 × 30 mm) is placed over the section, and all air bubbles are carefully removed.
4. The tray is covered with a lid and a water-saturated paper towel prior to being placed in a plastic radioactive bag (to minimize liquid evaporation).
5. The sections are incubated overnight at 37°C.

3.3.3.4. Washes (Day 2)

Following overnight incubation with radioactive probe, the slides are washed to remove unbound probe. β-mercaptoethanol (0.001%, 1 μL/100 mL) must be added to all SSC washes. Fresh solutions for each wash must be used if there is more than one rack of slides. The washes are performed as follows:

1. 1X SSC at room temperature, first in a beaker to remove the cover slip, then placed in a glass rack in Wheaton containing 1X SSC. Remove the cover slip by gently waving the slide (held with forceps) in a beaker of 1X SSC.
2. The glass rack is transferred to 1X SSC at 55°C for 30 min. This step is repeated two more times, making a total of three washes at 55ºC.
3. 70% EtOH for 1 min.
4. 95% EtOH for 1 min and subsequently air-dried.

3.3.3.5. Exposure of Sections to Film

Now the slides are ready for exposure to film. The air-dried sections are mounted onto one side of an open paper folder using double-sided sticky tape. Working under safe-light conditions in a darkroom, the emulsion coated side of the Kodak MR1 film is placed face down onto the slides. The sections are exposed for 1 wk.

3.4. *Riboprobe* In Situ *Hybridization*

The methods described outline (a) the design, source, and preparation of the ribonucleotide probes ("riboprobes") used for ISH, (b) incorporation of a radiolabel into the riboprobe, and (c) hybridization of the radiolabeled riboprobe to the tissue section, washing and exposure of the labeled tissue section to film, and (d) analysis of the autoradiographs by densitometry.

The time required is as follows:

- Creation of templates using PCR = 3–4 d
- Generation of probes labeled with ^{35}S-CTP = 6 h
- Hybridization = 1 d
- Exposure to film = 4–14 d

3.4.1. *Riboprobes Used for* In Situ *Hybridization*

3.4.1.1. Design Considerations

The design considerations have been outlined previously ***(30)*** (*see* **Note 9**). Briefly, DNA templates, usually in the form of plasmids, are used to generate runoff transcription of cRNA probes, using an adaptation of the PCR strategy of Sitzman and LeMotte ***(31)***. Using a nested primer approach, one pair of primers ("outer primers") is used to amplify a unique region of the mRNA of interest from a cDNA or a plasmid. Then, a second round of PCR is amplified using a second pair of primers ("inner primers"). Of importance is that the inner primer pairs are 40-mers, with the 20 bases located at the 3' end of the primer specific for the targeted DNA sequence preamplified by the outer primer pair PCR. At the 5' end are 20 bases containing promoter sequences for the RNA polymerases SP6 (5' to 3': GGG ATT TAG GTG ACA CTA TAG AA) or T7 (5' to 3': CTG TAA TAC GAC TCA CTA TAG GG). These polymerases eventually are used to create sense and antisense riboprobes.

3.4.1.2. Preparation of Riboprobes

We use the methods outlined in Kerner et al. ***(30)***. Riboprobes can be generated from plasmid DNA or cDNA. Kerner et al. outline a detailed method for creating linear cDNA templates from brain polyA+ mRNA ***(30)***. Whether derived from a plasmid or linearized cDNA source, the PCR-generated DNA templates should be diluted to a final concentration of approx 0.3 μg/μL. The template should be stored at –20°C until use.

3.4.2. *Riboprobe Labeling of Sense and Antisense Probes*

The next step involves performing a transcription reaction that generates radiolabeled RNA probes. Before doing a riboprobe labeling, ensure that at least 0.3 μg of DNA template is available for labeling.

1. ^{35}S-CTP, sense and antisense DNA templates, and Promega labeling kit are thawed on ice.
2. Label two Eppendorf tubes as AS or S (for antisense and sense, respectively) and add the following sequentially for both tubes:

Transcription buffer (5X)	2 μL
100 m*M* DTT	1 μL
RNasin	0.25 μL
AUG mixture (10 m*M* each)	2 μL
100 μ*M* CTP	2 μL
DNA template (0.1 μg/μL)	3 μL
^{35}S-CTP	2.5 μL
Polymerases (T7 for antisense; SP6 for sense)	1 μL
Total volume	13.75 μL

3. The solutions are incubated for 1 h at 37°C.
4. For the DNase incubation, 1 μL of RQ1 DNase is added prior to incubation at 37°C for 15 min.
5. The probe volume is then increased to a final volume of 25 μL by adding 10.25 μL of 1X TE.
6. The mixture is then ethanol precipitated with the addition of 40 μL of 3 *M* sodium acetate (pH 5.2) to each microfuge tube and 900 μL of ice-cold 100% ethanol at –70°C for 1 h. The mixture is then centrifuged at 15,800*g* for 15 min at 4°C to pellet the DNA, which was subsequently washed with 100 μL of 70% ice-cold ethanol prior to repeating the centrifugation step. Dispose of the supernatant in an appropriate container, as the mixture contains radioactive material.
7. Resuspend the pellet in 35 μL of 1X TE. To dissolve the pellet, it is necessary to vortex for approx 2 min. Incubate at 37°C for 10 min and then vortex for another 2 min. Add DTT (4.0 μL of 100 m*M*) and RNAsin (1 μL).
8. To count the number of disintegrations per minute (dpm) of the labeled riboprobe, 1 μL of each riboprobe is pipetted into a scintillation tube with 4 mL scintillation fluid. Each probe is counted in duplicate and an average of decays per minute per microliter is calculated. This should be between 5 and 12 million. Lower numbers indicate ineffective radiolabeling.
9. The riboprobe can be used immediately or stored at –80°C.

3.4.3. In Situ *Hybridization With Antisense and Sense Riboprobes*

The antisense probe labels the mRNA species of interest. Labeled sense probes are used to demonstrate specificity of the antisense probe. Two brain sections per animal are required for the antisense probe and one section per animal for the sense probe. For a pilot experiment, it is recommended to use 12 sections from a normal control mouse brain for the antisense probe and 6 sections for the sense probe.

3.4.3.1 Prehybridization

The next step is to prepare the tissue sections for the hybridization reaction. Prehybridization requires many steps and is critical in the success of the technique. Again, be sure to use only baked Wheatons and work using RNA precautions (e.g., DEPC-treated solutions and RNA-only pipettors).

The following washes must be performed in the sequence described below:

Solution	Time	Directions
4% Paraformaldehyde	10 min	
DEPC–PBS (first stir plate)	5 min	Stir gently
DEPC–PBS (second stir plate)	5 min	Stir gently
DEPC–PBS (no stir plate)	5 min	
Change after every two slide racks.		
TEA/acetic anhydride (third stir plate)	10 min	Stir, change every rack
Add 0.5 mL acetic anhydride to 200 mL of TEA immediately before placing rack in tray.		
DEPC–PBS (no stir plate)	5 min	
Ethanols:		
70% (DEPC)	2 min	Change every two racks
80% (DEPC)	2 min	
95%	2 min	
100%	2 min	
Chloroform	5 min	
Chloroform	5 min	
Ethanol, 100%	2 min	
Ethanol, 95%	2 min	

Slides are then air-dried.

3.4.3.2. Hybridization Preparation (Can Be Conducted During the Prehybridization)

3.4.3.2.1. Calculation A

First, it is necessary to calculate the total amount of hybridization solution needed:

[*N*] (no. of slides) × 80 μL/slide = Total amount hybridization solution

A hybridization buffer stock is prepared in advance and stored in 840-μL aliquots in RNase-free siliconized Eppendorf tubes at –20°C.

1. Hybridization buffer stock (40 mL):

Solution	Final concentration in calculation D (**Subheading 3.4.3.2.4.**)	mL per 40 mL
Formamide	50%	23.8
1 *M* Tris-HCl	20 m*M*	0.95
0.5 *M* EDTA	5 mM	0.48
5 *M* NaCl	0.3 *M*	2.86
50% Dextran sulfate	10%	9.52
50X Denhardt's solution	1X	0.95
DEPC-H_2O	To volume	1.44

2. Before hybridization, some components need to be added directly to the hybridization buffer Eppendorf (use viscous pipet and special autoclaved viscous tips to pipet the hybridization solution). The mixture should be vortexed.

Solution	Final concentration	μL per 1 mL
Hybridization buffer stock	84%	840
10% sodium thiosulfate	1%	10
10% SDS	1%	10
DTT	10%	100
RNA mix (calculation C)	4%	40

3. Calculation of the amount of radioactive probe that is needed to gain a hybridization solution with 150,000 cpm/μL.

3.4.3.2.2. Calculation B

For antisense,

150,000 cpm/μL × Total amount hybridization solution (from calculation A)

= [V1] μL ^{35}S probe × specific activity of labeled probe (cpm/μL)

For sense,

150,000 cpm/μL × Total amount hybridization solution (from calculation A)

= [V2] μL ^{35}S probe × specific activity of labeled probe (cpm/μL)

4. To prepare the ^{35}S probes, make a RNA mix in advance as follows and store at –20°C:

Solution	Final concentration (after addition of labeled probe)	μL per 1 mL
10 mg/mL Salmon sperm DNA	100 μg/mL	250
20 mg/mL Yeast total RNA, type XI	250 μg/mL	313
25 mg/mL Yeast tRNA	250 μg/mL	250
DEPC-dH_2O	To volume	187

5. Combine the radioactive probe with RNA mix by adding the calculated volume required of the ^{35}S-labeled probe to the RNA mix as follows:

3.4.3.2.3. Calculation C

Component	Antisense probe mix	Sense probe mix
^{35}S-labeled probe	[V1] (from calculation B)	[V2] (from calculation B)
RNA mix	4 μL of RNA mix per each 100 μL of total amount hybridization solution (from calculation A)	4 μL of RNA mix per each 100 μL of total amount hybridization solution (from calculation A)

Mix well using a vortex, centrifuge briefly, then heat for 2 min on a heating block at 99°C (must be 99°C; if 100°C, probe will be denatured) and immediately chill probes

on ice. From this step on, all pipet tips, slides, and cover slips should be disposed of in the radioactive waste and the area checked periodically with a Geiger counter for contamination. All liquid waste containing radioactivity should be disposed of appropriately.

6. Final preparation of hybridization mix which is a mixture of the ^{35}S-labeled probe and the RNA mix (**step 3**) and the hybridization buffer. This is calculated as follows:

3.4.3.2.4. Calculation D

For antisense probe:

Total amount of hybridization solution for antisense = 1120 μL (calculation A)
Amount of hybridization buffer needed (μL) = Calculation A – probe mix (μL)

For sense (using example calculation):

Total amount of hybridization solution for antisense = 640 μL (calculation A)
Amount of hybridization buffer needed (μL) = Calculation A – probe mix (μL)

3.4.3.3 Hybridization Conditions

Hybridization is the process during which the radioactive probe binds to the specific mRNA species within the tissue. In oligonucleotide ISH, the hybridization reaction occurs directly on the tissue section underneath a glass cover slip. In contrast, for riboprobes, hybridization occurs with probe mixture placed directly on the surface of the brain tissue on slides that are kept in a humidified chamber. We use large shallow plastic trays (e.g., Bioassay trays from Nunc) and perform the hybridization reaction in temperature-controlled ovens (*see* **Notes 11** and **12**).

1. A hybridization tray is set up by lining the bottom of the tray with Whatman paper wetted with 4X SSC/50% formamide (no air bubbles) prior to placing a rubber mesh on this. The air-dried slides are placed on the rubber mesh, keeping the slides above the SSC/formamide mixture.
2. The final mixture (calculation D) is mixed using the vortex for 2 min, incubated for 15 min at 37°C, vortexed again for 1 min, and then centrifuged to collect the mixture. The mixture should be left to settle until there were no more air bubbles.
3. The final mixture is pipetted (using a viscous pipettor) onto one to six slides at a time, directly into the sections, taking care not to have any air bubbles. It helps to vortex the buffer before each pipetting set. The hybridization solution should be viscous enough to stay directly on the tissue section.
4. The hybridization tray is covered with a lid and placed in a 50°C oven for 4 h.

3.4.3.4. Posthybridization

1. Ensure that the stock solutions have been made up ahead of time.
2. Preparation for the washes needs to start at least 1 h before the hybridization trays are ready to come out. The water baths are turned on and solutions are prepared to equilibrate to the required temperature.

Solution	Time	Temp.	Notes
2X SSC		Room temp	Remove cover slips into a ^{35}S-labeled beaker (forceps can be used, radioactive waste)

2X SSC	2 min	Room temp	Shaking in radioactive Wheatons (radioactive waste)
2X SSC	2 min	Room temp	Shaking in radioactive Wheatons (radioactive waste)
0.1X SSC	30 min	70°C	Shaking in radioactive Wheatons
RNase A	30 min	37°C	Shaking in radioactive Wheatons
RNase A buffer	15 min	Room temp	Shaking in radioactive Wheatons
0.1X SSC	30 min	70°C	Shaking in radioactive Wheatons
0.1X SSC	30 min	70°C	Shaking in radioactive Wheatons
70% Ethanol	2 min	Room temp	
95% Ethanol	2 min	Room temp	Slides to be air dried (*see* **Note 13**)

3.4.3.5. Autoradiography

1. Put double-sided tape into a manila folder and place the dried slides on the tape alongside calibrated radioactive plastic standards.
2. Place the folder containing the slides into a prelabeled metal case (label when film was put down and when it will be developed). Lay thick card on top of manila folder (pushes film closer to slides)
3. Under safe-light conditions in the darkroom, place film on top of slides inside the manila folder with the emulsion side down.
4. Expose for 1 wk. Note that depending on the probe, exposure time may need to be adjusted from 1 d to 2 wk.

3.5. Image Analysis of the Autoradiographs by Densitometry

For both receptor-binding and *in situ* hybridization, the end result is a autoradiographic film image. There are two main types of information that can be obtained from an autoradiograph: regional distribution and abundance of label. Detailed image analysis protocols have been published, so the current discussion will be limited to some general principles.

Numerous moderately priced image analysis systems are now available. The basic components are common to all systems: a digitizing mechanism that converts optical density readings into numerical information, a microcomputer, and analysis software. The use of radioactive standards is especially useful. Because the optical density of a particular film varies with the exposure time, the images produced by plastic radioactive standards can be used to calibrate the sample image density. Typically, one first reads the densities of the images produced by the radioactive standards, thus creating a standard curve of optical density as a function of known amounts of radioactivity. Once such a standard curve is generated, it is possible to calculate the amount of radioactivity by measuring the optical density of the resultant image. Further, with receptor-binding autoradiography, because one knows the specific activity of the ligand used, one can calculate the actual number of moles of ligand bound in a given tissue sample. Because it is much harder to know specific activity of probes used for ISH, optical density units are used when analyzing these films.

Film exposure times should be optimized to the capacity of the film. Any photographic film will saturate over time. Thus, to make meaningful comparisons, one has to allow the film to be exposed long enough to generate a distinct image, but not so

long that the image is completely saturated. In general, "specific" binding is calculated as the difference between "total" and "blank" conditions.

One final advantage of quantitative image analysis is that numerical comparisons and statistical analyses can be performed. Thus, a great amount of quantitative information can be derived from these essentially anatomical techniques.

4. Notes

1. Care should be taken in removing the brain, as both receptor-binding autoradiography and ISH are essentially anatomical techniques. Good quality sections produce good quality autoradiographs. In particular, one should take care to remove any overlying dura mater before removing the brain from the skull. Prior to freezing, make sure that the surface of the brain is uninjured and remove any adherent hair or pieces of bone, as these materials can damage the cryostat blade during sectioning.
2. We typically freeze the brain for 30 s in a 50-mL conical tube of isopentane placed in a bed of crushed dry ice. Because warm objects tend to freeze when coming in contact with cold objects, one should be careful to touch the frozen brain only with a cooled metal spatula, otherwise sticking will occur. Likewise, warm brains should not be handled with a metal spatula that has been sitting in crushed dry ice or cooled isopentane.
3. We cut brain sections in a manner such that the sections can be used either for receptor binding autoradiography, ISH, or immunohistochemistry. We have found that using SuperFrost slides and 12-µm sections allows for all of these techniques to be run successfully from a single set of mouse brains.
4. Although this chapter has focused on binding assays for neurotransmitter receptors, one can also apply the same techniques for labeling any protein that binds to a small ligand molecule. Thus, using the same principles, one can perform autoradiographic binding assays for neurotransmitter uptake sites, second-messenger systems, mitochondrial enzymes, and ion channels.
5. Note that glutaraldehyde, paraformaldehyde, and acetone may require special disposal conditions, as specified by institutional guidelines.
6. Gloves should be worn for all methods described, especially when dealing with radioactivity.
7. For "squirt" rinses in receptor-binding autoradiography, all equipment must be arranged in order. For example, we typically have the cytomailers for the binding incubation in a tub filled with ice. Next to this, another ice-filled tub contains the squirt rinse dispenser: one for buffer and one for glutaraldehyde/acetone. Finally, next to the rinse dispensers are two hair dryers. To achieve rapid drying, we typically use two hair dryers and focus their hot airstreams to a single point. This is the point where the rinsed slide is placed to be dried. It is important to start the hair dryers for at least 10 min prior to the time when the first slide is to be dried. We have found that the temperature of hair dryers rises significantly during the first 10 min and then stabilizes.
8. When performing ISH experiments, it is important to remember that you are measuring the mRNA expression level. Therefore, you must work with reagents and utensils treated and set aside for RNA work only. For example, all solutions are to be made with DEPC-treated water (DEPC to 0.1%, v/v) and use pipettors that are designated for RNA and radioactive work only.
9. When performing ISH, one has the choice of either oligonucleotide probes or riboprobes. Riboprobes have the advantage of generating a higher signal because the probes are longer

and more radioactivity is incorporated into the riboprobe, compared to the tailing reaction that is employed in generating oligonucleotide probes. Therefore, riboprobes have a distinct advantage in detecting low-abundance mRNA species. However, generating riboprobes necessitates the availability of a suitable DNA template. In contrast, ISH generally is easier when using oligonucleotide probes, as oligonucleotides can be ordered commercially. In addition, oligonucleotides may be more selective, especially when the target molecule has homology to other molecules, as often is the case with receptor subtypes; that is, one can target mRNA sequences that are distinct from other related molecules.

10. We typically include one "cold" competition slide for each brain in oligonucleotide ISH experiments. The major utility of this "cold" slide is to assess the degree of nonspecific hybridization. It is not necessary to have as many "cold" slides as "hot" slides.
11. For hybridization, if there are any air bubbles on the brain section, then the labeled oligonucleotide will not hybridize to the corresponding area of the section.
12. Ensure that slides are completely dry! Damp gloves can make slides wet enough to cause a background on the film (black dots).
13. For ISH using riboprobes, it is important to keep the hybridization chambers level so that hybridization solution does not slide off of the tissue sections and the humidifying SSC/formamide solution does not touch the slide.

Acknowledgments

J.-H. J. Cha is supported by NIH (R01 NS-38106; P01 NS45242), the Coalition for the Cure (Huntington's Disease Society of America), and the Glendorn Foundation.

References

1. Yohrling, G. J. and Cha, J.-H. J. (2002) Neurochemistry of Huntington's disease, in *Huntington's Disease*, 3rd ed. (Bates, G. P., Harper, P. S., and Jones, A. L., eds.), Oxford Medical Publications, London, pp. 276–308.
2. Mangiarini, L., Sathasivam, K., Seller, M., et al. (1996) Exon 1 of the *HD* gene with an expanded CAG repeat is sufficient to cause a progressive neurological phenotype in transgenic mice. *Cell* **87,** 493–506.
3. Cha, J.-H. J., Kosinski, C. M., Kerner, J. A., et al. (1998) Altered brain neurotransmitter receptors in transgenic mice expressing a portion of an abnormal human Huntington disease gene. *Proc. Natl. Acad. Sci. USA* **95,** 6480–6485.
4. Cha, J.-H. J., Frey, A. S., Alsdorf, S. A., et al. (1999) Altered neurotransmitter receptor expression in transgenic mouse models of Huntington's disease. *Phil. Trans. R. Soc. Lond. B: Biol. Sci.* **354,** 981–989.
5. Greenamyre, J. T., Olson, J. M. M., Penney, J. B., et al. (1985) Autoradiographic characterization of *N*-methyl-D-aspartate-, quisqualate-, and kainate-sensitive glutamate binding sites. *J. Pharmacol. Exp. Ther.* **233,** 254–263.
6. Greenamyre, J. T., Penney, J. B., and Young, A. B. (1985) Alterations in L-glutamate binding in Alzheimer's and Huntington's diseases. *Science* **227,** 1496–1499.
7. Young, A. B., Greenamyre, J. T., Hollingsworth, Z., et al. (1988). NMDA receptor losses in putamen from patients with Huntington's disease. *Science* **241,** 981–983.
8. Young, A. B. and Fagg, G. E. (1990) Excitatory amino acid receptors in the brain: membrane binding and receptor autoradiographic approaches. *Trends Pharmacol. Sci.* **11,** 126–133.

9 Ona, V. O., Li, M., Vonsattel, J. P., et al. (1999) Inhibition of caspase-1 slows disease progression in a mouse model of Huntington's disease [see comments]. *Nature* **399,** 263–267.
10 Chen, M., Ona, V. O., Li, M., Ferrante, et al. (2000) Minocycline inhibits caspase-1 and caspase-3 expression and delays mortality in a transgenic mouse model of Huntington disease. *Nature Med.* **6,** 797–801.
11 Cha, J. H., Farrell, L. A., Ahmed, S. F., et al. (2001). Glutamate receptor dysregulation in the hippocampus of transgenic mice carrying mutated human amyloid precursor protein. *Neurobiol. Dis.* **8,** 90–102.
12 Yohrling, G. J., IV, Jiang, G. C.-T., DeJohn, M. M., et al. (2002) Aberrant serotonin systems in a mouse model of Huntington's disease. *J. Neurochem.* **82,** 1416–1423.
13 Chan, E. Y. W., Luthi-Carter, R., Strand, A., et al. (2002) Increased huntingin protein length reduces the severity of polyglutamine-induced gene expression changes in mouse models of huntington disease. *Hum. Mol. Genet.* **11,** 1939–1951.
14 Gomez-Isla, T., Irizarry, M. C., Mariash, A., et al. (2003). Motor dysfunction and gliosis with preserved dopaminergic markers in human α-synuclein A30P transgenic mice. *Neurobiol. Aging*, **24,** 245–248.
15 Cha, J.-H., Greenamyre, J. T., Nielsen, E. Ø., et al. (1988) Properties of quisqualate-sensitive L-[3H]glutamate binding sites in rat brain as determined by quantitative autoradiography. *J. Neurochem.* **51,** 469–478.
16 Cha, J.-H. J., Makowiec, R. L., Penney, J. B., et al. (1992) Multiple states of rat brain (*RS*)-α-amino-3-hydroxy-5-methylisoxazole-4-propionic acid receptors as revealed by quantitative autoradiography. *Mol. Pharmacol.* **41,** 832–838.
17. Sharif, N. A. and Eglen, R. M. (1993) Quantitative autoradiography: a tool to visualize and quantify receptors, enzymes, transporters, and second messenger systems, in *Molecular Imaging in Neuroscience: A Practical Approach* (Sharif, N. A., ed.), IRL Press at Oxford University Press, New York, pp. 71–138.
18 Cha, J. J., Makowiec, R. L., Penney, J. B., et al. (1990). L-[3H]Glutamate labels the metabotropic excitatory amino acid receptor in rodent brain. *Neurosci. Lett.* **113,** 78–83.
19 Catania, M. V., Hollingsworth, Z., Penney, J. B., et al. (1993). Quisqualate resolves two distinct metabotropic [^{3}H]glutamate binding sites. *Neuroreport* **4,** 311–313.
20 Chu, D. C., Albin, R. L., Young, A. B., et al. (1990) Distribution and kinetics of GABAB binding sites in rat central nervous system: a quantitative autoradiographic study. *Neuroscience* **34,** 341–357.
21 Richfield, E. K., Young, A. B., and Penney, J. B. (1986) Properties of D2 dopamine receptor autoradiography: high percentage of high-affinity agonist sites and increased nucleotide sensitivity in tissue sections. *Brain Res.* **383,** 121–128.
22 Cox, R. F. and Waszczak, B. L. (1991) Autoradiography of dopamine D2 receptors using [^{3}H]YM-09151-2. *Eur. J. Pharmacol.* **199,** 103–106.
23 Javitch, J. A., Blaustein, R. D., and Snyder, S. H. (1983) [^{3}H]Mazindol binding associated with neuronal dopamine uptake sites in corpus stratum membranes. *Eur. J. Pharmacol.* **90,** 461–462.
24 Penney, J. B., Jr., and Young, A. B. (1982) Quantitative autoradiography of neurotransmitter receptors in Huntington's disease. *Neurology* **32,** 1391–1395.
25 Jarvis, M. F. and Williams, M. (1989) Direct autoradiographic localization of adenosine A2 receptors in the rat brain using the selective agonist 3H-CGS21680. *Eur. J. Pharmacol.* **168,** 243–246.
26 Qin, Z.-H., Chen, J. F., and Weiss, B. (1994) Lesions of mouse striatum induced by

6-hydroxydopamine differentially alter the density, rate of synthesis, and level of gene expression of D_1 and D_2 dopamine receptors. *J. Neurochem.* **62,** 411–420.

27 Chen, J. F., Qin, Z. H., Szele, G., et al. (1991) Neuronal localization and modulation of the D_2 dopamine receptor mRNA in brain of normal mice and mice lesioned with 6-hydroxydopamine. *Neuropharmacology* **30,** 927–941.

28 Watanabe, M., Inoue, Y., Sakimura, K., et al. (1993) Distinct distributions of five *N*-methyl-D-aspartate receptor channel subunit mRNAs in the forebrain. *J. Comp. Neurol.* **338,** 377–390.

29 Magnusson, K. R. (2000) Declines in mRNA expression of different subunits may account for differential effects of aging on agonist and antagonist binding to the NMDA receptor. *J. Neurosci.* **20,** 1666–1674.

30 Kerner, J. A., Standaert, D. G., Penney, J. B., Jr., et al. (1998) Simultaneous isotopic and nonisotopic in situ hybridization histochemistry with cRNA probes. *Brain Res. Brain Res. Protocols* **3,** 22–32.

31. Sitzmann, J. H. and LeMotte, P. K. (1993) Rapid and efficient generation of PCR-derived riboprobe templates for in situ hybridization histochemistry. *J. Histochem. Cytochem.* **41,** 773–776.

17

Chromatin Immunoprecipitation Technique for Study of Transcriptional Dysregulation in Intact Mouse Brain

Melissa W. Braveman, Alice S. Chen-Plotkin, George J. Yohrling, and Jang-Ho J. Cha

Summary

Transcriptional dysregulation has emerged as an important pathologic mechanism underlying the pathogenesis of Huntington's disease (HD). The control of transcription depends on appropriate binding of transcription factor proteins to specific promoter regions of genes. Chromatin immunoprecipitation (ChIP) is a technique that has been used to study the association of transcription factors with DNA. To address the hypothesis that there is altered transcription factor–DNA association in HD, we have recently adapted the ChIP technique to the study of transgenic mouse brain. Here, we describe our method of performing ChIP in intact mouse brain. We have optimized conditions for formaldehyde crosslinking, antibody immunoprecipitation, and quantitative real-time polymerase chain reaction detection. Using ChIP, one can measure the association of transcription factors with specific genes and determine if this association is altered in transgenic HD mouse models. ChIP applied to whole-mouse brain can thus offer a window into mechanisms of transcriptional dysregulation.

Key Words: Transcription; transcription factor; mRNA; DNA; histone; Sp1; real-time PCR; immunoprecipitation; chromatin.

1. Introduction

Transcriptional dysregulation is likely to be an important pathogenic mechanism in Huntington's disease and other triplet repeat diseases ***(1)***. The most convincing evidence for a problem with transcription in HD has come from the observation that particular messenger RNA (mRNA) species are downregulated in various models of HD ***(2–4)***. Certain transcription factors have been proposed to account for the specificity of the mRNA species that are affected. Recently, we have sought to determine

From: *Methods in Molecular Biology, vol. 277: Trinucleotide Repeat Protocols*
Edited by: Y. Kohwi © Humana Press Inc., Totowa, NJ

whether there is altered association of candidate transcription factors with the chromatin of genes known to be downregulated in HD.

Chromatin immunoprecipitation (ChIP) is a technique that allows assessment of the association of transcriptionally active proteins with the promoter regions of target genes ***(5–9)*** (*see* **Fig. 1**). "ChIP" assays are distinct from the DNA microarray "chips" that are used in mRNA expression-profiling studies ***(10)***. Using ChIP assays, one can assess the relative association of specific proteins with the promoter regions of targeted genes. ChIP has been used most widely to evaluate the association of histone proteins to target chromatin ***(9,11)***. However, ChIP has also been used to evaluate the association of nonhistone transcription factors with promoter regions of target genes ***(5,8,9)***. We have recently adapted ChIP to the study of chromatin–transcription factor interactions in intact transgenic mouse brain.

2. Materials

2.1. Standard PCR Reaction for Verification of Primers

1. 10X Buffer B (final concentration 1X; Fisher Scientific, Pittsburgh, PA, cat. no. FB600060).
2. 25 m*M* $MgCl_2$ (final concentration 1.5 m*M*; Fisher Scientific, FB600055).
3. dNTP mix, 2.5 m*M* each (final concentration 0.1 m*M*; Takara, Japan, 4030).
4. *Taq* DNA polymerase (final concentration 2.5 U per reaction; Fisher Scientific, FB600060).
5. Double process tissue culture water (Sigma, St. Louis, MO, W3500).
6. Custom primers (final concentration 500 n*M*; Invitrogen, Carlsbad, CA, 10336-022).
7. 0.5-mL Thin-walled polymerase chain reaction (PCR) tubes (MJ Research, Waltham, MA, TB1-0501).
8. iCycler thermal cycler (Bio-Rad, Hercules, CA).
9. Agarose gel electrophoresis and fluorescence detection equipment.

2.2. Chromatin Immunoprecipitation

1. ChIP kit (Upstate Biotechnology, Lake Placid, NY, 4309155).
   a. Salmon sperm DNA/protein-A agarose (16-157C).
   b. ChIP dilution buffer (20-153).
   c. Low-salt immune complex wash buffer (20-154).
   d. High-salt immune complex wash buffer (20-155).
   e. LiCl immune complex wash buffer (20-156).
   f. 1X TE buffer (20-157).
   g. 0.5 *M* EDTA (20-158).
   h. 5 *M* NaCl (20-159).
   i. 1 *M* Tris-HCl, pH 6.5 (20-160).
   j. Sodium dodecyl sulfate (SDS) lysis buffer (20-163).
2. 2-mL Microcentrifuge tubes.
3. Vortex.
4. Microcentrifuge that can accommodate 2-mL microcentrifuge tubes at room temperature.
5. Microcentrifuge that can accommodate 2-mL microcentrifuge tubes at 4°C.
6. Centrifuge that can accommodate 15-mL conical tubes at 4°C.
7. Humidified 37°C incubator.

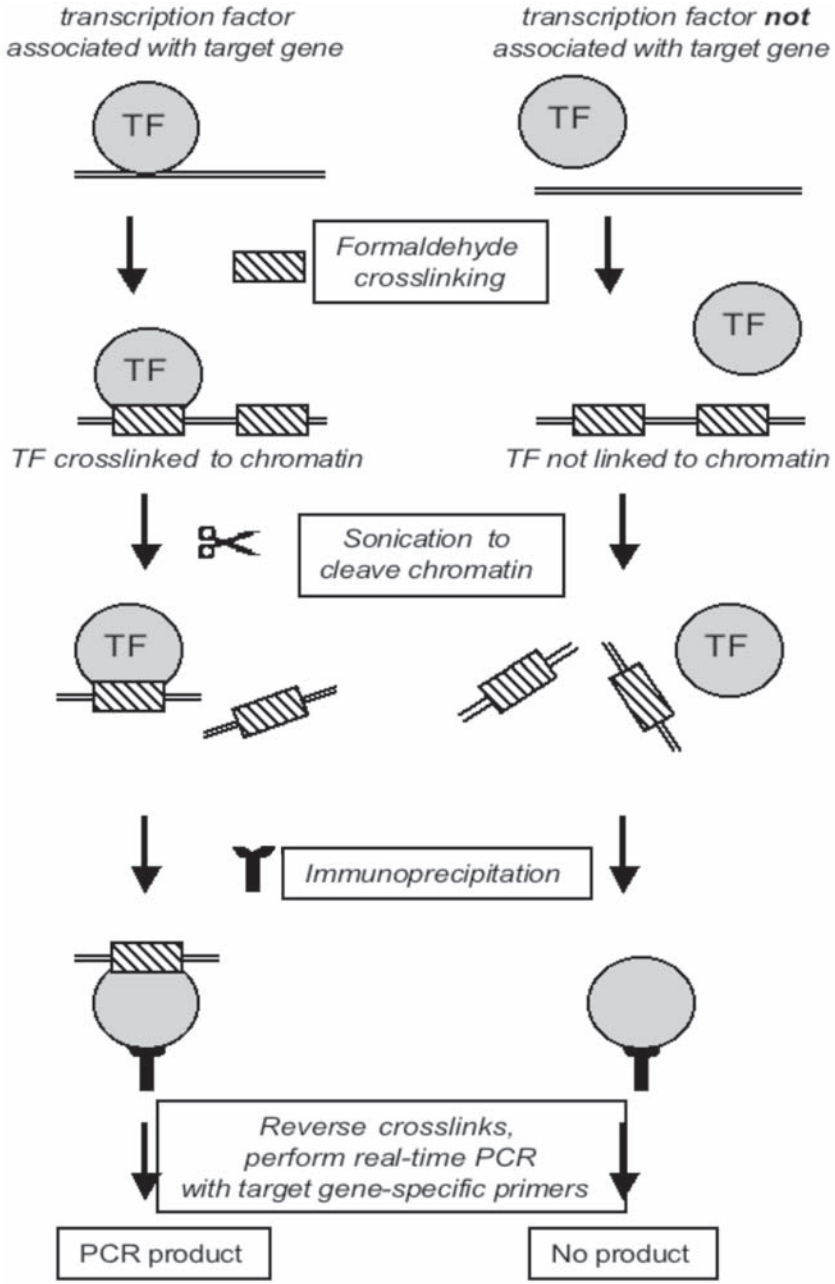

Fig. 1. Schematic of the ChIP method. Two situations are depicted. On the left, a transcription factor protein (TF) is associated with the promoter region of a target gene. On the right, TF is not associated with the gene promoter. In ChIP, associated proteins can be covalently attached to DNA with formaldehyde crosslinking. Next, DNA can be sheared by sonication, creating

(continued)

8. Sonicator (Sonifier Cell Disruptor; Branson Sonic Power Company).
9. Dessicator.
10. Rotating wheel/platform at room temperature.
11. Rotating wheel/platform at 4°C.
12. Variable volume pipettors (5 μL to 10 mL) and tips.
13. 15-mL conical tubes.
14. 50-mL conical tubes.
15. 1X Phosphate-buffered saline (PBS): 8 g NaCl, 0.2 g KCl, 1.44 g Na_2HPO_4, 0.24 g KH_2PO_4, 800 mL nuclease-free H_2O, pH to 7.4 with HCl, bring up to 1 L with nuclease-free H_2O.
16. 10X Protease inhibitor solution (1 Complete Mini Protease Inhibitor Cocktail Tablet; Roche, Mannheim, Germany, 1836153) in 1.5-mL nuclease-free H_2O.
17. Glycogen (ultrapure; Invitrogen, Carlsbad, CA, 10814-010).
18. Precipitating antibody directed against transcription factor or histone protein of interest.
19. 37% Formaldehyde in water (Fisher Scientific, F79-500).
20. 1 cm^3 insulin syringes (Sherwood Medical, St. Louis, MO, 500014).
21. 3 *M* Sodium acetate, pH 5.2: 40.8 g Na–acetate·$3H_2O$, 80 mL nuclease-free H_2O, pH to 5.2 with acetic acid, bring up to 100 mL with H_2O.
22. Phenol/chloroform/isoamyl alcohol (25:24:1; Fisher Scientific, BP1752-400).
23. 100% Ethanol.
24. Proteinase K (molecular-biology grade; Invitrogen, 25530-049).
25. Elution buffer: 1% SDS, 0.1 *M* $NaHCO_3$ in nuclease-free H_2O.

2.3. Western Immunoblot for Confirmation of Immunoprecipitation

Polyacrylamide gel, chemiluminescence reagents, and detection equipment.

2.4. Real-Time PCR and Data Analysis

1. iCycler iQ PCR plates (Bio-Rad, Hercules, CA, 223-9441).
2. iCycler iQ optical quality sealing tape (Bio-Rad, 223-9444).
3. iCycler iQ detection software (Bio-Rad).
4. SYBR Green PCR master mix (Applied Biosystems, Foster City, CA, 4309155).

3. Methods

The methods described outline (a) the chromatin immunoprecipitation technique, as adapted to the study of intact mouse brain, (b) the procedure required to verify successful immunoprecipitation, and (c) real-time PCR quantitation of immunoprecipitated chromatin.

3.1. Chromatin Immunoprecipitation

To perform chromatin immunoprecipitation assays, we have used the Upstate Biotechnology ChIP assay kit, which is designed for use in cultured cells. We describe how we have adapted this technique to the study of intact mouse brain tissue.

Fig. 1. *(continued)* short pieces of DNA (typically, 200–1000 bp), either bound to TF (left) or not bound to TF (right). TF can be immunoprecipitated with an antibody, also bringing down any covalently bound DNA. Following reversal of crosslinks, immunoprecipitated DNA can be detected using quantitative real-time polymerase chain reaction. Thus, by using ChIP, one can compare relative amounts of TF association with target genes of interest.

3.1.1. Mouse Brain Preparation

It is essential that the endogenous proteins and their associations with DNA are maintained postmortem. Mouse brains are quickly removed, flash-frozen for 30 s in isopentane cooled in a bed of dry ice, and stored at –70ºC until use. We typically use one mouse brain hemisphere in each ChIP experiment.

3.1.2. Formaldehyde Crosslinking and Chromatin Shearing

The first step in ChIP is crosslinking. This step allows proteins that are in close proximity to chromatin to be covalently attached to DNA. Following crosslinking, the transcription factor–DNA complexes are sheared by sonication. We have optimized these settings for use with intact mouse brain (*see* **Fig. 2**).

1. Immediately prior to crosslinking, isolate one mouse brain hemisphere over dry ice using a sterile razor blade.
2. Cut each hemisphere into cubes approx 4 mm^3 in size, weigh, and place in a 15-mL conical vial.
3. Covalently crosslink endogenous proteins to DNA by adding 1 mL of 1% formaldehyde per 100 mg tissue to vial.
4. Incubate vial 10 min at 37ºC in humidified bath (*see* **Note 1**).
5. Remove vial from bath, place tissue on ice, and wash twice with 1 mL per wash of cold 1X PBS. Vortex samples and spin down at 100*g* at 4°C for 10 s before and after washes.
6. Add 1 mL SDS lysis buffer per 100 mg tissue.
7. Add 100 µL of 10X protease inhibitor solution (one minitablet in 1.5 mL nuclease-free H_2O) per 1 mL of SDS solution added in **step 6**.
8. Incubate each sample on ice for 10 min.
9. Shear chromatin using a sonicator at 35% power for eight bursts, each 15 s in duration (*see* **Notes 2** and **3**).
10. Divide each sample into microcentrifuge tubes and microcentrifuge sheared material at 15,800*g* for 10 min at 4°C.
11. Following this spin, recombine supernatant fractions of each sample into 15-mL conical tubes.
12. Divide supernatant into 2-mL microcentrifuge tubes, 200 µL per aliquot.
13. Add 1.5 mL of ChIP dilution buffer to each 200-µL aliquot, followed by 200 µL of protease inhibitor solution. At this point, samples can be stored at –70°C for later use.

3.1.3. Immunoprecipitation

The next step is to immunoprecipitate the transcription factor–chromatin complexes using antibodies directed against the transcription factor of interest. This method is basically similar to traditional immunprecipitation protocols.

1. From each sample generated in **Subheading 3.1.2.**, reserve 20 µL and label as "input" for corresponding samples. Save "input" samples at –20°C for later use. We use such "input" samples to account for difference in total amounts of DNA present in different samples. Ultimately, data from immunoprecipitated samples will be normalized to corresponding input samples.
2. Preclear samples. To each remaining sample, add 80 µl of protein A/agarose slurry. Rotate each sample for 30 min at 4°C. This step removes nonspecific debris.

A

DNA concentration (in ng/μL)

Crosslinking Reversal Time:	Sonication Condition (number of repetitions, all at 35% power, 15 sec) 5	6	8	10	12
4 hours	198	142	273	174	210
Overnight	120	199	270	**290**	218

DNA Purity (A260/A280 ratio)

Crosslinking Reversal Time:	Sonication Condition (number of repetitions, all at 35% power, 15 sec) 5	6	8	10	12
4 hours	1.23	1.19	1.23	1.24	1.17
Overnight	1.12	1.16	1.22	**1.37**	1.25

B

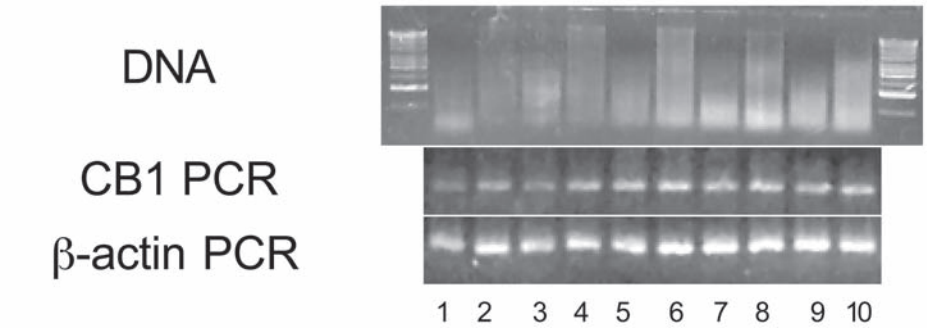

Fig. 2. Optimization of technical parameters for performing ChIP assays in mouse brain. **(A)** Effects of sonication conditions and length of crosslink reversal on DNA yield. Comparison of sonication methods (5–12 repetitions of 35% power sonication, 15-s bursts) and length of crosslinking reversal reaction (4 h vs overnight) on DNA yield and DNA purity, as assessed by spectrophotometry. **(B)** Effect of sonication and crosslink reversal on DNA fragment length and PCR yield. Agarose gel electrophoresis, and PCR products for cannabinoid CB1 receptor or β-actin. Lanes: 1, 5 repetitions (R) + 4 hour (4 h) reversal; 2, 5R + overnight (o/n) reversal; 3, 6R + 4 h; 4, 6R + o/n; 5, 8R + 4 h; 6, 8R + o/n; 7, 10R + 4 h; 8, 10R + o/n; 9, 12R + 4 h; and 10, 12R + o/n. Molecular-weight marker is a 100-bp DNA ladder (Gibco-BRL, 15628-050).

3. Pellet by centrifuging at 100*g* at 4°C for 2 min (*see* **Note 4**).
4. Transfer supernatant to a fresh microcentrifuge tube using a 1-cm^3 insulin needle.
5. Next, add 5 μg of primary antibody directed against target protein to each sample. Add 5 μg of nonspecific IgG antibody to each mock condition for control (*see* **Note 5**).
6. Incubate overnight on a rotating platform at 4°C.
7. Following overnight incubation with antibody, add 80 μL protein A/agarose slurry to collect complex.
8. Incubate samples for 1 h at 4°C on rotating platform.
9. Collect pellet with a 100*g* spin at 4°C for 2 min. Pellet now contains bound target protein–DNA complex.
10. Remove supernatant from each sample and discard using a 1-cm^3 insulin needle.
11. Perform a total of five washes including **step 11**. For each wash, use 700 μL of wash

(listed in order below) and rotate 5 min at room temperature. After each wash, centrifuge at 4°C for 2 min at 1000 rpm and discard supernatant using an insulin needle.
   a. Low-salt immune complex wash buffer.
   b. High-salt immune complex wash buffer.
   c. LiCl immune complex wash buffer.
   d. TE buffer.
12. Perform a second TE wash; this time, prior to removing supernatant, vortex samples and remove 50 µL for later use in Western blots (*see* **Subheading 3.2.**). Then, complete wash as in **step 11**.

The resultant pellet contains the covalently bound DNA–protein complexes and is now ready to undergo elution of precipitating antibodies and reversal of crosslinks.

3.1.4. Elution and Crosslink Reversal

The next step involves eluting antibodies from the DNA–protein complexes and then reversing the crosslinks, thereby removing covalently bound protein from DNA. This step is necessary for efficient PCR amplification. DNA that has not undergone crosslink reversal works poorly in PCR reactions.

1. To each pellet, add 250 µL elution buffer.
2. Vortex samples and rotate for 15 min at room temperature.
3. Spin at 4°C for 2 min at 100*g* to collect pellet. Collect supernatants into new microcentrifuge tubes using a fresh set of insulin needles.
4. Repeat elution with additional 250 µL of elution buffer as in **steps 1–3**, combining the second elution supernatant with the first.
5. At this point, thaw input samples and bring up to volume (approx 500 µL) of eluted samples.
6. Add 20 µL of 5 *M* NaCl to all samples.
7. Reverse crosslinks by incubating samples for 4 h at 65°C in a humidified bath (*see* **Note 6**).
8. Remove samples from bath. Following removal from this bath, samples can be stored overnight at –20°C but should not be stored for longer.
9. To both eluted and input samples, add 10 µL of 0.5 *M* EDTA, 20 µL of 1 *M* Tris-HCl, pH 6.5, and 20 µg proteinase K.
10. Incubate for 1 h at 45°C in a humidified bath.
11. Remove samples from bath.

3.1.5. DNA Isolation

We follow a standard DNA isolation procedure with slight modification. DNA pellets are extremely difficult to visualize and thus require the addition of glycogen and extended times for microcentrifuge steps. Add an equal volume of phenol/chloroform/isoamyl alcohol (pH 8.0) to each sample. Vortex samples 15 s each and centrifuge at room temperature at maximum speed for 15 s to separate. Transfer translucent aqueous phase to fresh microcentrifuge tubes. To each sample, add 1/10 vol of 3 *M* sodium acetate (pH 5.2). Vortex samples. Add 2–2.5X volume of ice-cold 100% ethanol to each tube, followed by 1 µg glycogen (*see* **Note 7**). Vortex samples and place at –80°C for 1 h to precipitate. Remove samples from the freezer and microcentrifuge at 4°C for 30 min. A small, stringy, opaque pellet can be visualized against the tube wall. Remove

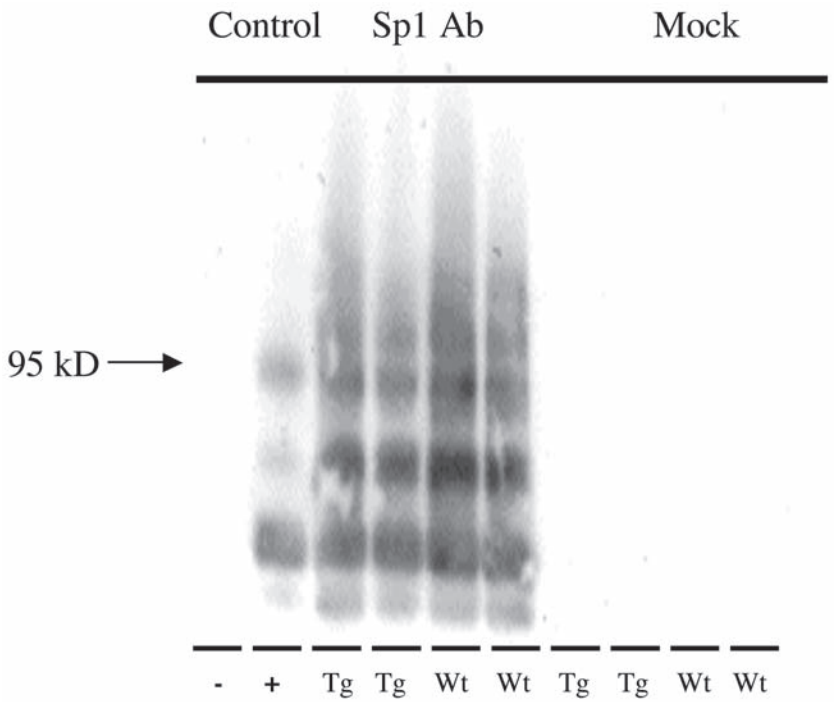

Fig. 3. Western blot (immunoblot) of Sp1, confirming immunoprecipitation of Sp1 target. Target was detected only in lanes corresponding to sample in which Sp1 antibody was utilized. Western blot reveals a 95-kDa protein consistent with Sp1. Negative (–) and positive (+) controls are run alongside mouse brain samples that have been immunoprecipitated with an anti-Sp1 antibody (Sp1 Ab) or samples that have been "mock" immunoprecipitated (i.e., no antibody used). There is no overall difference in the amount of Sp1 immunoprecipitated between the Huntington's disease transgenic mouse brain (Tg) and the wild-type mouse brain (Wt). This blot confirms the specific immunoprecipitation of Sp1.

supernatant with great care. Add 1 mL of 70% ethanol and invert samples four times. Microcentrifuge samples at 4°C for 10 min. Remove supernatant as earlier. Desiccate samples until the pellet is dry and resuspend in 30 µL sterile water.

Following ChIP, DNA concentrations will likely be too low to be measured by conventional spectrophotometry.

3.2. Confirmation of Immunoprecipitation

It is important to confirm immunoprecipitation with antibodies used in ChIP, although this is not routinely performed by most labs. We typically confirm immunoprecipitation in ChIP using traditional Western blotting techniques (*see* **Fig. 3**). Add 50 µL of loading buffer to the 50-µL sample obtained in **Subheading 3.1.4.** Load 30 µL of this total to each lane of a gel. We often use commercial precast gels, choosing polyacrylamide concentration and antibody dilutions appropriate to each protein tar-

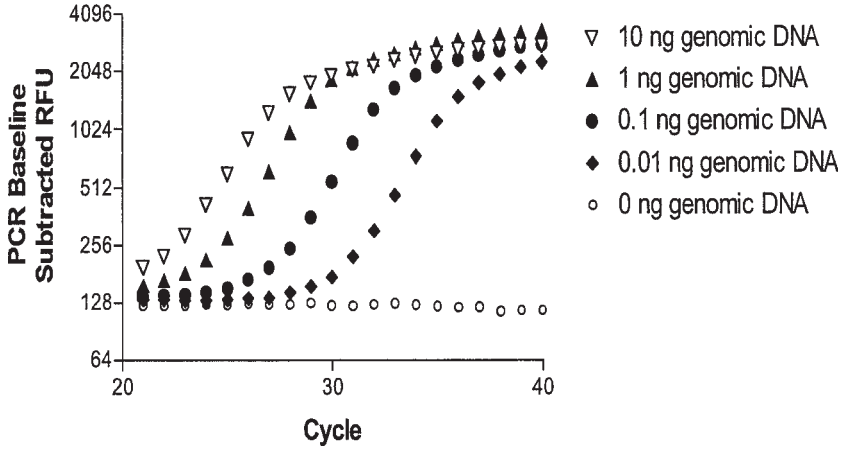

Fig. 4. Example of real-time PCR results. Serial dilutions of mouse genomic DNA (gDNA) were subjected to real-time PCR using primers specific for murine β-actin. SYBR Green fluorescence was used to obtain product formation. The crossing threshold (T_c) is defined as the cycle number at which a fluorescence threshold is reached. Increasing amounts of starting DNA results in lower crossing thresholds.

get and antibody. These specifications follow the antibody manufacturer's protocol, unless experience requires otherwise.

3.3. Quantitative PCR

Once ChIP is complete, real-time PCR and analysis is used to quantitate relative amounts of DNA obtained. The methods described outline (a) the identification of a gene sequence proximal to active transcription factor sites, (b) the selection process for real-time PCR primer pairs, (c) the primer pair screening process, and (d) the quantitation of starting nucleic acid amount by real-time PCR.

3.3.1. Gene Sequence Identification

Gene sequences targeted for priming should be as close as possible to putative transcription-factor-binding sites. Sonication produces a distribution of DNA fragment sizes, with the majority between 200 and 1000 bp in length (*see* **Fig. 2**). As a result, regions of the gene close to transcription-factor-binding sites are preferentially precipitated. Increased proximity of a gene sequence to the promoter region then yields a higher PCR signal following immunoprecipitation for a transcription factor (*see* **Fig. 6**).

3.3.2. Primer Pair Selection

Real-time PCR primer design requirements are stringent. We use SYBR Green to detect PCR product. Because SYBR Green fluoresces linearly with all amplified products, efficient amplification of the product is essential while keeping primer–dimer formation to a minimum. In particular, product length, GC content, melting temperature, secondary structure, polyG and polyC counts, and 3' complementarity are key to

A

Partial list of real-time primers

Target Gene	Primer Set	Accession #
ACE	U42, L156	M55333
ACE	U924, L1043	M61094
Cannabinoid CB-1	U1511, L1631	Y18374
Cannabinoid CB-1	U692, L796	Y18374
Cannabinoid CB-1	**U643, L759**	**Y18374**
β-actin	U252, L346	X03672
Dopamine D2 Receptor	U196, L293	NM010077
Dopamine D2 Receptor	U1724, L1835	NM010077
Preproenkephalin	U342, L484	U20894
Preproenkephalin	U4355, L4456	U20894
Preproenkephalin	U4843, L4990	U20894
Preproenkephalin	U4843, L5059	U20894
Glutamate Receptor NR-1	U1058, L1193	NM008169
Dopamine D1a Receptor	U503, L631	AF171079
Dopamine D1a Receptor	U1056, L1198	AF171079
Dopamine D1a Receptor	U800, L940	AF171079

B

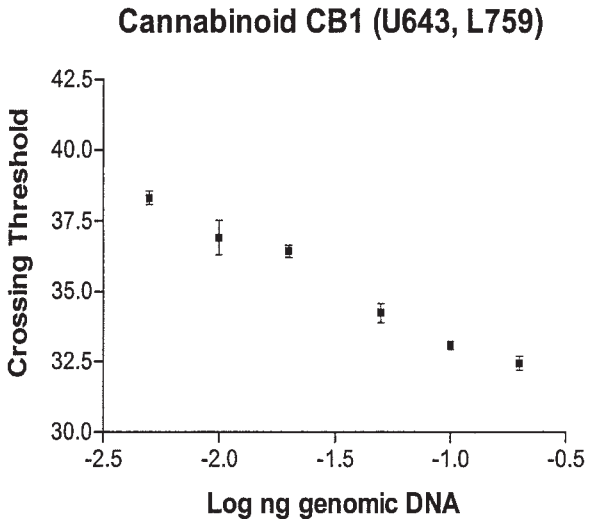

Fig. 5. Screening primers for use in real-time PCR. (**A**) Table of primer pairs suitable for use in real-time PCR at 57°C annealing temperature. Upstream and downstream primers indicated by "U" and "L," respectively. Number following U or L corresponds to numbering given by

effective amplification. Primer pair selection is a three-step process that involves the generation of primer pairs, assessment of secondary structure characteristics, and BLAST query to ensure specificity of primers (*see* **Fig. 5**). These steps follow closely the suggestions in the iCycler (Bio-Rad) manual.

1. Genbank Sequence, nucleotides only, is inserted into Whitehead Institute Primer3 program (www-genome.wi.mit.edu/cgi-bin/primer/primer3_www.cgi). The number assignment of generated primers will correspond exactly to the number of characters inserted into this window. Therefore, it is advisable to insert the entire gene sequence and limit interrogated regions of the gene through the search vehicle.
2. Set sequence length to 80–150 bp. PCR amplicons of this length are optimal for quantitative real-time PCR. "Included Region" function allows target gene region to be isolated. "Included Region" is set to describe the portion of gene to be included in search.
3. Set minimum primer GC content to 50% and maximum to 60%.
4. Set minimum melting temperature to 50ºC, optimal melting temperature to 60ºC, and maximum melting temperature to 65ºC.
5. Set GC clamp to 1.
6. Set Max Complementarity to 5 and Max 3' Complementarity to 1.
7. Set Max Poly-X to 3.
8. Click on the "primer pick" button to start the primer selection program. Several primer pairs and the resultant amplicon will be generated by the program.
9. In order to assess potential secondary structures, enter entire amplicon sequence into Dr. Michael Zuker's Mfold DNA folding website (www.bioinfo.math.rpi.edu/~mfold/dna/form1.cgi).
10. Set Folding temperature to the temperature you will use for PCR. We typically use 57ºC as the annealing temperature.
11. Set Ionic condition Mg^{2+} to 1.5 m*M* and Na^{+} to 50 m*M*.
12. In general, minimization of secondary structures is advisable. A maximum of two hairpin structures at no more than 5°C above annealing temperature is optimal.
13. Use standard nucleotide–nucleotide function of BLAST (www.ncbi.nlm.nih.gov/BLAST) to ensure specificity of primers within organism genome (*see* **Note 8**).

3.3.3. Primer Pair Screening

The first step in screening is to confirm that the correct PCR amplicon is produced. We accomplish this by running a conventional PCR reaction using genomic mouse DNA as starting material and visualizing amplicons on an agarose gel. We use quantitative real-time PCR for subsequent reactions. Our detection method (SYBR Green fluorescence) measures amplified DNA nonspecifically. Therefore, it is essential to eliminate primer pairs that form dimers. Primer dimer formation artificially lowers crossing thresholds (measured in number of cycles), which, in turn, causes artificially high estimates of sample DNA.

Fig. 5. *(continued)* NCBI for listed accession number. All listed primer pairs have been screened against criteria described in **Subheading 3.3.3.** **(B)** Sample primer efficiency curve. Curve generated for cannabinoid CB1 receptor primer pair (U643, L759) listed in **(A)**. Six amounts (between 0.005 ng and 0.2 ng) of mouse genomic DNA were used. The slope of this line is –3.7, indicating nearly 100% efficiency.

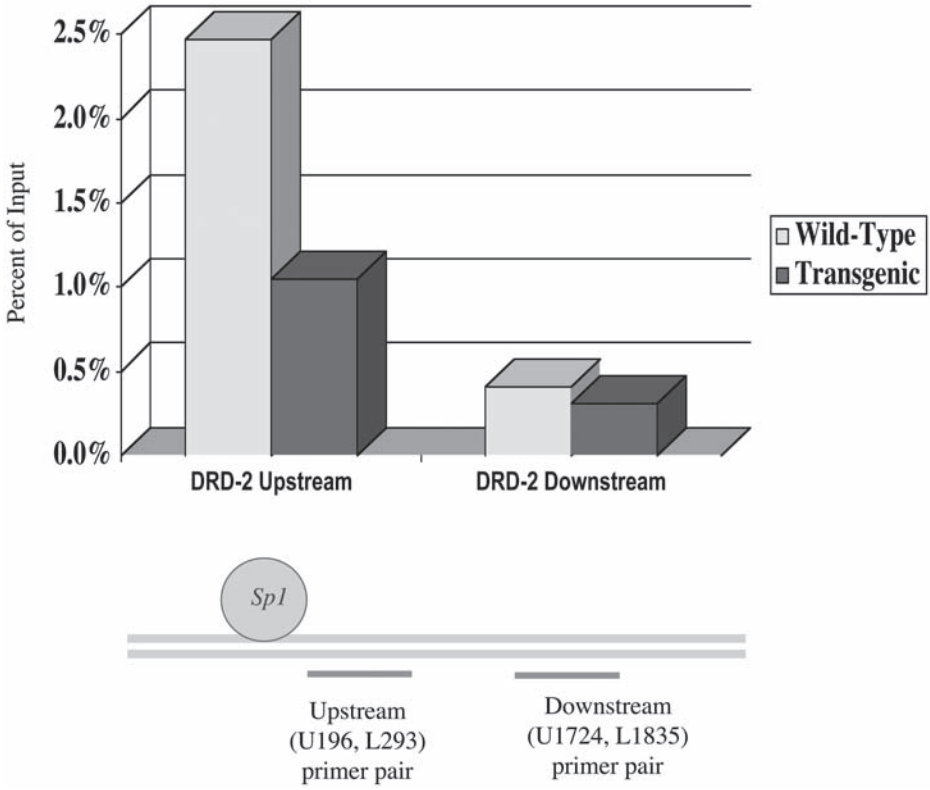

Fig. 6. Demonstrated relationship between signal and primer distance from promoter region of gene. Sp1 association with the DRD2 gene is detected with primer sets targeting both upstream and downstream regions of the gene. PCR signal is amplified closer to promoter because of fragmentation of DNA strands when subjected to ChIP.

Second, the efficiency of amplification of each primer pair needs to be determined to assure reliable and accurate real-time quantitation (*see* **Fig. 5**). To assess specificity and efficiency of a given primer pair, a real-time PCR reaction is run using several concentrations of genomic DNA.

1. Sequence confirmation. Combine 1 ng genomic DNA with 5 µL of 10X buffer B (100 m*M* Tris-HCl, pH 9.0, 500 m*M* KCl) (final concentration, 50 m*M* KCl), 3 µL $MgCl_2$ (final concentration, 1.5 m*M*), 2 µL dNTPs (final concentration, 0.1 m*M* each), 0.5 µL *Taq* DNA polymerase (final concentration, 2.5 U/reaction), 2.5 µL each of 10 µ*M* upstream and downstream primers (final concentration, 500 n*M* each), and double-distilled (H_2O) (Sigma) for a reaction volume of 50 µL. Run conventional PCR with the following reaction parameters: 1 cycle of 95ºC for 5 min, 50 cycles of 95ºC (30 s), 57ºC (30 s), 72ºC (45 s), and a final 10-min 72ºC extension.
2. Visualize PCR products with high-resolution gel (we typically use 5% BioWhittaker Molecular Applications NuSieve 3:1 agarose).

3. We confirm PCR amplicons by conventional DNA sequencing. Proceed to **step 4** only for primer pairs that have been sequence confirmed.
4. Efficiency curve. Serially dilute genomic DNA (0.5 to 0.005 ng). This will allow an efficiency curve to be generated, in addition to providing information about whether primer–dimers are produced. Combine 5 μL DNA with 10 μL of 2X SYBR Green PCR master mix, 1 μL of the upper and lower primers (final concentration, 500 n*M*), and 3 μL of nuclease-free water to create a final reaction volume of 20 μL. Set the reaction parameters as in **step 1**.
5. Primer–dimers typically have a lower melt temperature than legitimate PCR amplicons. Thus, the "melt curve" can detect the presence of primer–dimers. Generate internal melt curve by running melt curve protocol immediately following completion of the PCR reaction. Heat samples from 55 to 95ºC while measuring fluorescence every 10 s at 0.5ºC increments.
6. Adjust the software threshold and baseline settings for data analysis in **steps 7** and **8**. We have been using PCR thresholds set at 50 relative fluorescence units (RFUs) on the software program. This threshold was empirically chosen because it analyzed data at a point when our PCR reactions were doubling with every cycle with a minimum of noise, the principle on which quantitative PCR is based. We keep the baseline setting at 2–10 cycles (the default settings of the software) because this setting adequately subtracts well-specific noise (*see* **Note 9**).
7. Determine the melt temperature for each primer pair. Confirm by agarose gel visualization following **step 5** that product generated is target amplicon. The melt temperature is then determined by the peak whose percentage of total area is above 50, at least twice the area of the next highest peak, and rises above 80°C across all concentrations greater than or equal to 0.01 ng. In our experience, samples that contain at least 10 pg of genomic mouse DNA cross a threshold of 50 RFUs before cycle 40. Therefore, we consider a crossing cycle of greater than 40 cycles to represent negligible product. Proceed to **step 8** only if all concentrations of the template above 0.005 ng produce peaks that fit the above criteria.
8. Generate the primer efficiency curve. This curve tells us whether the primer pair is efficient enough to be used in real-time PCR. Calculate by linear regression the slope of the semilog plot of log of starting material against crossing threshold, measured in cycles. This slope should be close to –3.3. A slope equal to –3.3219 represents 100% efficiency, reflecting doubling of DNA during each cycle in a perfect PCR reaction (*see* **Fig. 5**) (*see* **Note 10**).

3.3.4. Data Analysis

The quantities of ChIP DNA can be assessed by following essentially the same protocol given in **step 2** of **Subheading 3.3.3.**, followed by a set of straightforward calculations. Combine 1 μL of each ChIP DNA sample condition with 10 μL SYBR Green master mix, 1 μL of upper and lower primers for a final concentration of 500 n*M* each, and 7 μL nuclease-free water to create a final reaction volume of 20 μL. Include serial dilution of genomic DNA as in **step 1** of **Subheading 3.3.3.** to serve as standard curve. Include also negative controls, which consist of an additional 1 μL of nuclease water in lieu of DNA template. Set protocol as in **step 2** of **Subheading 3.3.3.**

Target DNA sequence quantities are estimated from threshold amplification cycle numbers (T_c) using the software supplied with the iCycler thermal cycler (Bio-Rad). The T_c value is determined as the cycle at which fluorescence measured in RFUs rises

above a threshold. To achieve uniformity across all experiments, we recommend setting the PCR crossing threshold and baselines based on empirical data. For quantitating DNA isolated from our ChIP experiments, we have been using PCR thresholds set at 50 RFUs. As primer–dimers occasionally form in the absence of sufficient DNA in the sample, melt curve analysis is also performed on the PCR products. Next, samples are normalized for small differences in input amounts. Finally, DNA quantities from antibody-immunoprecipitated samples are compared to those from mock immunoprecipitated samples to assess specificity of immunprecipitation.

1. After running the quantitative PCR reactions, determine T_c values for each sample, defined as the cycle at which fluorescence (measured in RFUs) rises above a baseline threshold, using iCycler software.
2. Differentiate products from primer–dimers using melt curve data. We exclude data points if
   a. PCR samples had < 50% of the product at the correct melting temperature for the target amplicons, or
   b. the amount of target product is not at least twice the amount of the next most abundant peak.
3. Normalize for variation in the amount of starting DNA. For every gene sequence studied, a ΔT_c value was calculated by subtracting the T_c value for the immunoprecipitated sample from the T_c value for the corresponding input DNA (*see* **Fig. 7**). This normalization controls for differences in amounts of starting DNA. DNA quantities were then expressed as percentages of corresponding input using ChIP sample as a percentage of input = $2^{(\Delta Tc)} \times 100$.
4. Compare ChIP samples with mock immunoprecipitated samples. DNA quantities (expressed as percentages of input) are compared for immunoprecipitated versus mock immunoprecipitated samples (expressed as percentages of their own corresponding input samples). Only when immunoprecipitated samples contained > 1.5 times as much DNA as the mock samples are they considered to have sufficient DNA for analysis.

4. Notes

1. We have found that 10 min is an optimal time for formaldehyde crosslinking. Although more protein–DNA complexes are formed following a 1-h treatment with formaldehyde, prolonged treatments make it much more difficult to reverse crosslinks, as is necessary for good quality PCR.
2. Other authors have used micrococcal nuclease instead of sonication to cleave DNA into pieces. We have used sonication because we can control the degree of shearing by adjusting the number of sonication bursts.
3. The optimal amount of sonication time is empirically determined. We have found for intact mouse brain that eight bursts of sonication yield optimal DNA lengths.
4. Maintaining protein A/agarose suspension uniformity across sample conditions is important. However, protein A/agarose slurry tends to come out of suspension. We rotate suspension for 30 min at 4°C before each use. Also, parafilm is required to seal vials between uses.
5. The amount of precipitating antibody to be used needs to be optimized for each antibody. For an anti-Sp1 antibody, for example, we have found that 5 μg of antibody consistently produced higher signal/noise ratio than using 1 μg.

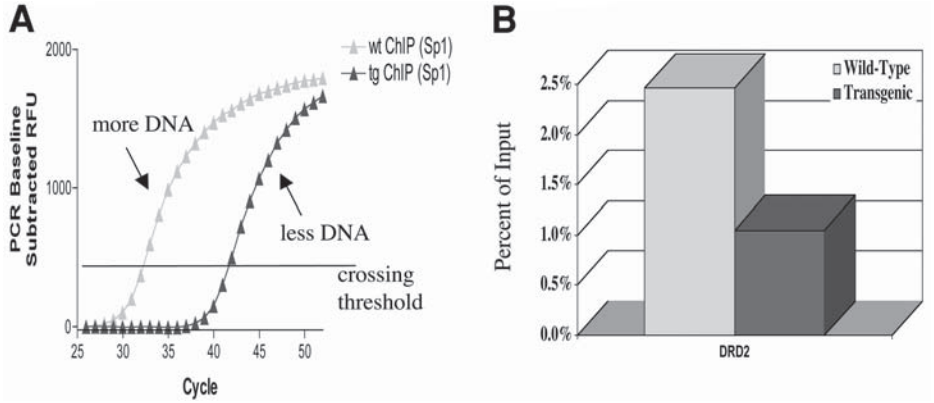

Fig. 7. Example of real-time PCR performed on ChIP DNA samples. Wild-type and Huntington's disease transgenic R6/2 mouse brains were formaldehyde crosslinked, sonicated, and immunoprecipitated with an antibody specific for Sp1. Following chromatin immunoprecipitation, the pelleted DNA was freed from protein crosslinks, and samples were subjected to real-time PCR with sequence-confirmed primer pairs. Fluorescent quantitative real-time PCR was run in the presence of SYBR Green. In all cases, no PCR product is seen with negative (no DNA) control. There is more PCR product generated from ChIP DNA for the R6/2 wildtype than transgenic for the dopamine receptor D2 (DRD2) gene, an Sp1-driven gene with altered mRNAs in HD.

6. For reversal of crosslinks, we have found that incubation at 65°C for 4 h is as effective as 24 h.
7. DNA pellets are extremely difficult to visualize and are easily disturbed during ethanol precipitation steps of isolation. We routinely find we need to return the vials to the microcentrifuge in order to recollect the pellet during extraction of supernatant. Again, the use of glycogen is essential to pellet visualization (*see* **Fig. 2**).
8. Any of the criteria presented in **Subheading 3.3.2.** can be relaxed if necessary; however, more stringent adherence to the requirements promotes better results in the primer screening process.
9. The precise criteria presented in **Subheading 3.3.3.**, **step 6** for eliminating primer–dimer formation are somewhat arbitrary. The important thing is that the product generated is predominantly the correct product, because primer–dimers can also incorporate SYBR Green.
10. For maximally efficient PCR primers, efficiency curves yield a slope of –3.3 cycles per log unit of DNA; that is, a 10-fold difference in amount of starting DNA translates into a difference of about three cycles in quantitative PCR. Although quantitative real-time PCR is undoubtedly more sensitive than conventional agarose gel densitometry, there are practical limits of detection. Because of inherent assay variability, we require a difference (ΔT_c) of at least one cycle to consider samples as being different. A one-cycle difference in quantitative real-time PCR translates into a difference of approx 100% between samples. Simply put, there needs to be a difference of about 100% between samples in order to be able to detect such a difference using ChIP. More subtle alterations, such as a

30% decrease in transcription factor–DNA association, would not be detectable by our methods.

Acknowledgments

J.-H. J. Cha is supported by NIH (R01 NS-38106; P01 NS45242), the Coalition for the Cure (Huntington's Disease Society of America), and the Glendorn Foundation. A. S. Chen-Plotkin is supported by the Howard Hughes Medical Institutes. G. J. Yohrling is supported by the Hereditary Disease Foundation.

References

1 Cha, J.-H. J. (2000) Transcriptional dysregulation in Huntington's disease. *Trends Neurosci.* **23,** 387–392.

2 Cha, J.-H. J., Kosinski, C. M., Kerner, J. A., et al. (1998) Altered brain neurotransmitter receptors in transgenic mice expressing a portion of an abnormal human Huntington disease gene. *Proc. Natl. Acad. Sci. USA* **95,** 6480–6485.

3 Cha, J.-H. J., Frey, A. S., Alsdorf, S. A., et al. (1999) Altered neurotransmitter receptor expression in transgenic mouse models of Huntington's disease. *Phil. Trans. R. Soc. London B: Biol. Sci.* **354,** 981–989.

4 Luthi-Carter, R., Strand, A., Peters, N. L., et al. (2000) Decreased expression of striatal signaling genes in a mouse model of Huntington's disease. *Hum. Mol. Genet.* **9,** 1259–1271.

5 Shang, Y., Hu, X., DiRenzo, J., et al. (2000) Cofactor dynamics and sufficiency in estrogen receptor-regulated transcription. *Cell* **103,** 843–852.

6 Noma, K., Allis, C. D., and Grewal, S. I. (2001) Transitions in distinct histone H3 methylation patterns at the heterochromatin domain boundaries. *Science* **293,** 1150–1155.

7 Lo, W. S., Duggan, L., Tolga, N. C., et al. (2001) Snf1—a histone kinase that works in concert with the histone acetyltransferase Gcn5 to regulate transcription. *Science* **293,** 1142–1146.

8 Breiling, A., Turner, B. M., Bianchi, M. E., et al. (2001) General transcription factors bind promoters repressed by Polycomb group proteins. *Nature* **412,** 651–655.

9 Chen, H., Lin, R. J., Xie, W., et al. (1999) Regulation of hormone-induced histone hyperacetylation and gene activation via acetylation of an acetylase. *Cell* **98,** 675–686.

10 Gerhold, D., Rushmore, T., and Caskey, C. T. (1999) DNA chips: promising toys have become powerful tools. *Trends Biochem. Sci.* **24,** 168–173.

11. Luo, R. X., Postigo, A. A., and Dean, D. C. (1998) Rb interacts with histone deacetylase to repress transcription. *Cell* **92,** 463–473.

18

Techniques for Thick-Section Golgi Impregnation of Formalin-Fixed Brain Tissue

Tracie L. Moss and William O. Whetsell, Jr.

Summary

The histologic staining technique for central nervous system (CNS) tissue known as the Golgi technique was initially developed more than 125 yr ago. It was with this technique that, for the first time, whole nerve cells and their processes were simultaneously observed microscopically. Although the technique was widely used in the early 20th century, its use languished to some extent until the late 1900s when, used in conjunction with ultrastructural studies, it began to provide new insights into microscopic anatomy and pathology of the CNS. Several permutations of the technique have evolved since its early stages. The one represented in this chapter was developed so that Golgi-impregnated CNS tissues could be embedded in polymerized plastic and cut into relatively thick sections for light microscopic study. The advantages are that (a) sections of the clear and almost colorless plastic allow enhanced visualization of the intricate structure and ramification of dendritic elements of CNS neurons, (b) because of the relatively thick microscopic sections (25–30 μm), details of lengths and arborization of dendritic "trees" can be studied and photographed to provide greater detail than in thinner sections, and (c) numbers and morphologic characteristics of synaptic spines can be precisely evaluated.

Key Words: Camillo Golgi; Golgi impregnation techniques; brain tissue; formalin-fixed brain tissue; dendritic spines; light microscopy; thick sections.

1. Introduction

The famous and long-recognized neurohistologic technique known as the Golgi method or the Golgi staining technique carries an interesting history in the annals of neuroscience. Camillo Golgi (1843–1926), working as a young histologist and pathologist in a hospital (hospice) in Aggiategrasso, Italy, invented the original technique in 1873. According to historical records ***(1)***, his procedure was to place blocks of "freshly removed" brain tissue into an aqueous potassium dichromate solution for as

From: *Methods in Molecular Biology, vol. 277: Trinucleotide Repeat Protocols*
Edited by: Y. Kohwi © Humana Press Inc., Totowa, NJ

long as "45 or more days in order to fix and harden the tissue." The blocks were then placed in a silver nitrate solution for various periods and dehydrated and cut, without embedding, into sections as thick as 100 μm or more. The sections were cleared with turpentine, adhered to glass cover slips, and placed over a small opening (an "aperture") in a "hollowed-out wooden slide" so that the tissue could be directly observed with the light microscope. It was with this technique that, for the first time, whole nerve cells and their processes were viewed microscopically. Apparently, Golgi continued to experiment with the technique over the next decade, publishing several reports of his results. However, his most comprehensive descriptions are to be found in his book entitled *Sulla Fina Anatomia Delgi Organi Centrali Del Sistema Nervosa*, published in 1884. In a subsequent publication of the proceedings of a conference in Paris in 1894 ***(2)***, it is stated that "before the appearance of the famous book by Golgi (1884, above), all that was known about the structure of the [cerebral] cortical gray matter was" that cortical pyramidal cells had been recognized and that there was a certain number of cortical layers made up of cells with different characteristics, but that there was "absolute ignorance regarding the disposition of dendritic branches and axonal processes." Golgi's observations using his "black reaction" were hailed in that publication as demonstrating "beyond discussion" the complex arborization of dendritic processes of cortical pyramidal cells, the existence of branched collaterals for descending axons of "almost all cortical pyramids," and "at least two" clearly distinguishable types of neurons.

Even with Golgi's ingenious invention of the method and his continued experimentation with it into the early 20th century, it was Ramon y Cajal who was (and still is) particularly recognized for demonstrating the exquisite capabilities of the technique, in his exhaustive studies of the structure of the central nervous system ***(3)***.

Today, more than 125 yr after its invention, the technique remains an extremely elegant and useful one, which, especially in conjunction with ultrastructural studies ***(4,5)***, continues to provide information on brain structure and brain pathology. Modifications and refinements of the original techniques of Golgi have evolved to procedures that are now known as the Golgi–Cox technique ***(6,7)*** and the rapid-Golgi technique ***(8)***.

This chapter presents a modification of the Golgi method that we have found to be reliable in both tissue culture and intact brain tissue from experimental animals (*see* **Figs. 1** and **2**) and from human postmortem brain specimens. Particularly advantageous features are that the clear plastic sections allow enhanced visualization of the structure and ramifications of dendritic elements, the relatively thick sections (25–30 μm or more) provide greater depth for studying and photographing dendritic lengths and arborization, and the numbers and morphologic characteristics of synaptic spines can be assessed with more precision (*see* **Figs. 1** and **2**). In our studies, these last features have been especially helpful in examining effects of genetic manipulation in portions of the developing central nervous system (CNS). We carried out Golgi impregnation and quantitative histochemical/biochemical studies in Huntington's disease (HD) full-length cDNA transgenic mice that were symptomatic but had not developed to a stage in which neuronal loss could be documented. Golgi staining

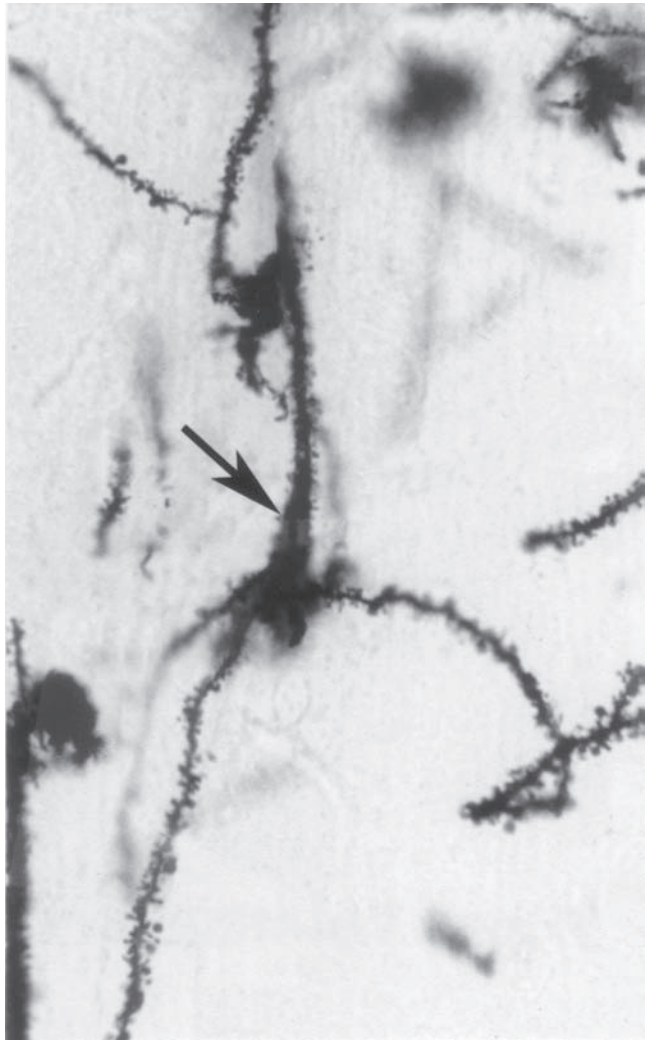

Fig. 1. View of a well-developed cerebral cortical neuron (mouse) stained using the Golgi method described. Note apical dendrite (arrow), several branching basalar dendrites, and rich endowment of dendritic spines (section thickness, 30 μm; original magnification, ×400).

showed morphologic abnormalities that included a significant decrease in the number of dendritic spines and a thickening of proximal dendrites in striatal and cortical neurons ***(5)***.

2. Materials

2.1. Equipment and Preparation

1. 4000-mL Erlenmeyer flask with wide mouth.

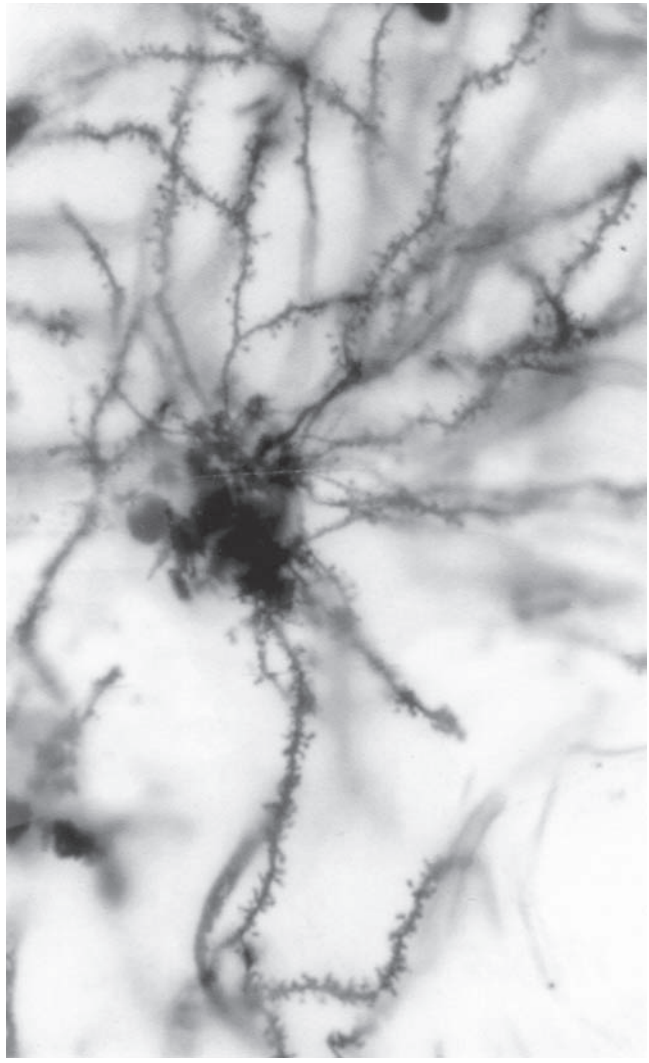

Fig. 2. View of a medium spiney neuron from the striatum (mouse) stained with the Golgi method. Note abundant delicate branched dendrites exhibiting numerous dendritic spines (section thickness, 30 μm; original magnification, ×400).

2. Three 500-mL Erlenmeyer flasks.
3. Four magnetic stir bars.
4. 300-mL Beaker (for normal saline).
5. 500-mL Beaker for boiling water.
6. Numerous standard plastic cassettes sufficient to contain tissue blocks or cover slips bearing tissue cultures.

7. A rubber stopper large enough (used to close the 4000-mL wide-mouth flask).
8. Aluminum foil, string, parafilm, and 4 × 4 gauze pads.
9. An electrical rotating platform.
10. A magnetic stirrer.
11. Acrolein for possible fixation of tissue cultures (Sigma Chemical Co.) (*see* **Note 1**).
12. Spurr's embedding medium kit (two suggested sources: Ted Pella, Inc., Redding, CA, cat. no. 18300; Electron Microscope Sciences, Fort Washington, PA, cat. no. 14300) (*see* **Note 2**).
13. Beem capsules (suggested source: Ted Pella, Inc., Redding, CA).
14. Rotary microtome.
15. Disposable microtome blades (suggested source: Sakura Finetech, USA, Torence, CA) (*see* **Note 3**).
16. 60°C Oven for tissue embedding.

All glassware, plastic cassettes, and magnetic stirbars should be cleaned and prepared as follows: Wash with soapy water in the usual manner, fill flasks and soak stir bars and cassettes for 30 min with 10% HCl solution, rinse for 30 min in tap water, rinse three times in deionized water for 30 min each rinse, and then air-dry and cover until used.

2.2. Solutions

1. Impregnating Solution: The impregnating solution contains a final concentration of 5% potassium dichromate, 4% potassium chromate, and 5% mercuric chloride in distilled water, prepared as described in the following. Each of these components should be prepared as a separate solution of 500 mL. Each of these flasks should be covered with aluminum foil to assure that each is light-tight.

    a. To make the basic potassium dichromate solution, place 25 g of crystallin potassium dichromate (Sigma) into a foil-covered 500-mL flask and pour in approx 450 mL of hot distilled H_2O. Close and cover the flask and keep it light-tight while it cools.
    b. Similarly, for the potassium chromate solution, place 20 g of granular potassium chromate (Sigma) in a foil-covered 500-mL flask, pour in 450 mL of *boiling* water (*see* **Note 4**), cover, and store.
    c. For mercuric chloride, use 25 g of mercuric chloride crystallin (Sigma) in a foil-covered flask, add 450 mL of *boiling* water (*see* **Note 4**), cover, and store.
    d. Using a magnetic stir bar with magnetic stirrer for each flask enhances dissolution of the chemicals. When these flasks have cooled, they can be opened in low light and stirred to assure that the chemicals are dissolved.
    e. The volume of each solution is then brought up to 500 mL With distilled H_2O. All three flasks are again stored in light-tight conditions.
    f. When selected tissues are ready to be placed in the impregnating solution for Golgi staining, the three solutions are poured together into the 4000-mL Erlenmeyer flask. They should be added *in a specific sequence*: 500 mL of potassium dichromate, 500 mL of potassium chromate, then 500 mL of mercuric chloride. Then, 1000 mL of distilled H_2O are added to bring the total volume up to 2500 mL (*see* **Note 5**).
    g. When the final solution has been mixed, the tissue-bearing cassettes are introduced as described below, and the flask is well covered and placed on the rotating platform.

2. Alkalinizing Solution: This solution, to be used at the end of the 10-d impregnation process (*see* **Subheading 3.**), should be made up just prior to use. This solution comprises 0.5 g of lithium hydroxide (Sigma) and 15.0 g of potassium nitrate (Sigma) in 100 mL of distilled water.
3. Glacial Acetic Acid Solution: This solution, to be used following the alkalinization (*see* **Subheading 3.**), is a 0.2% solution (1.0 mL of glacial acetic acid in 500 mL of distilled water).

3. Methods

3.1. Tissue Preparation and Handling

1. Portions of formalin-fixed brain tissue selected for staining should be cut into blocks 2–4 mm thick with a surface area of approx 5 × 5 mm (*see* **Note 6**). Tissue cultures on glass cover slips of an appropriate size to fit into standard embedding cassettes should also be formalin fixed; although acrolein fixation has been recommended for some types of CNS tissue culture ***(7)***, in our experience, formalin fixation for not more than 30 min at room temperature ***(4)*** is adequate.
2. Once secured in the cassettes, the blocks or the culture-bearing cover slips can be stored in 10% formalin until just before beginning the Golgi staining procedure.
3. At that point, the cassettes containing the individual tissue blocks or cover slips are rinsed in normal saline for 15–20 min.
4. Following this rinse, the cassettes (usually no more than 16–18 cassettes) are placed on a square of gauze (spread out from a 4 × 4 pad), and the gauze is gathered around the group of cassettes to form a bag in which they can be suspended in the impregnating solution.
5. One or two acid-cleaned glass stoppers or heavy glass beads are placed in the bag to assure that it is weighted down in the solution during the staining processes, and the bag is tied shut to secure its contents.
6. The weighted bag of cassettes is introduced into the 4000-mL flask containing the impregnating solution. It is completely submerged in the solution and suspended from strings anchored at the top (outside) of the flask in a way that allows the bag of cassettes to move freely in the solution without touching the bottom of the flask.
7. The top of the flask is closed with the rubber stopper covered with parafilm, and a foil hood is secured over the top to assure that the entire flask is *completely light-tight* (very important!).
8. The flask can then be placed and stabilized (with masking tape) on the rotating platform.
9. The platform is set to rotate continuously at a speed of 25–30 rpm for a full 10 d. During that period, the foil covering should be checked periodically for evidence of breakdown because the impregnation solution, if splashed or leaked out, causes the foil to crumble. If any breakdown is noted, the affected area should immediately be covered again with foil.

3.2. Alkalinization Procedures

The process must be done as quickly as possible.

1. On the 11th d from the **Subheading 3.1.**, the gauze bag containing the cassettes is removed from the impregnation solution and rinsed thoroughly in several changes of distilled H_2O for approx 1 h; a continuous slow wash of the bag of cassettes yields best results.
2. Following this wash, the bag is placed in the alkalinizing solution in a beaker in the dark for 6 h, then immediately immersed in the 0.2% glacial acetic acid solution for 18 h.

3. This solution should be changed several times, so that there are at least four fresh washes of glacial acetic acid during this 18-h period.
4. Finally, the bag of cassettes should be washed in several changes of distilled H_2O or a continuous wash over 2 h.
5. The cassettes can be stored in distilled H_2O until time to embed the tissue blocks or to mount the cover slips (*see* **Subheading 3.3.**).

3.3. Embedding Stained Blocks

1. Tissue blocks are removed from the cassettes (**Subheading 3.2.**) and placed individually in clearly labeled polypropylene or glass tubes for dehydration in graded alcohols: 25%, 50%, 70%, 80% (10 min each at room temperature), three times in 95% (10 min each), two times in l00% (10 min each at room temperature), and once more in l00% for 30 min.
2. Next, the blocks are placed in propylene oxide, two times for 10 min each and once for 30 min.
3. Blocks are then embedded in Spurr's medium beginning with a tissue infiltration procedure: Each block is placed in a mixture of equal volumes (1:1) of full-strength Spurr's embedding medium and propylene oxide for 1 h at room temperature.
4. Next, each block is placed in a 3:l mixture (i.e., 3 vol of Spurr's medium to 1 vol of propylene oxide) for 2 h.
5. Finally, blocks are placed in full-strength (100%) Spurr's medium for 2 h.
6. Individual blocks are now ready to be embedded in freshly prepared full-strength Spurr's embedding medium.
7. The blocks are embedded in Beem capsules, each of which has its covering cap snapped on the mouth of the capsule, after which it is inverted and the conical tip is cut off. This forms a small open-ended cylinder that stands upright in the snap-on cap.
8. Each block of tissue is placed in the bottom of a Beem capsule cylinder so that it lies flat, and the cylinder is filled to the brim with the fresh Spurr's medium.
9. Once all blocks have been placed into the cylinders, they are set into the embedding oven at 60°C overnight.

3.4. Cutting Sections for Light Microscopic Study

1. Once polymerization has occurred (**Subheading 3.3.**), blocks are ready to be cut into sections for light microscopy.
2. Sections at least 25–30 μm thick are recommended because thicker sections yield more three-dimensional information with regard to dendritic branching characteristics and ramifications (*see* **Note 7**).
3. The cutting is carried out using a standard rotary microtome of the type used for cutting paraffin sections.
4. The tissue block is placed in the microtome chuck in the usual fashion and cut at the desired thickness (25–30 μm) with a disposable microtome blade.
5. As sections are cut, each is lifted away from the microtome blade with jeweler's forceps and placed on the surface of a large drop of water on a microscope slide.
6. When several sections have been collected onto the water, the slide is placed on a warm hot-plate surface or slide warmer so that as the water evaporates, the sections spread and adhere to the glass.
7. After the slides have dried overnight, each should be cover-slipped with a generous amount of mounting medium to accommodate the thickness of the section.

8. Again, the slides should be allowed to dry overnight before examining at high magnification, to be certain that the mounting medium is dry and that the glass cover slip cannot be compressed or shifted when lowering a high-magnification objective.

3.5. Mounting and Examining Tissue Culture Specimens

1. Tissue culture preparations that have been carried out through this Golgi staining procedure in plastic cassettes (*see* **Subheading 3.2.**) can, upon completion of the last (2 h) wash with distilled H_2O, be dehydrated in graded alcohols from 25 through 50, 70, 85, 95, and 100% for 10 min each at room temperature.
2. At the 100% stage, the tissue cultures should be rinsed in two 10-min washes in xylene to remove the alcohol.
3. After the xylene washes, the culture-bearing cover slips can be inverted and mounted directly onto a glass microscope slide in a pool of mounting medium sufficient to cover the face of the inverted cover slip.
4. Once the mounting medium is set, the stained culture is preserved between the surface of the glass slide and the cover slip itself for excellent viewing by light microscopy; no other embedding *per se* is needed for tissue culture preparations.

4. Notes

1. Acrolein fixation, used in lieu of formalin fixation for tissue culture, should be carried out in a fixing solution of 10% acrolein in normal saline for 30 min at room temperature. Acrolein is extremely toxic and flammable, so appropriate precautions should be taken if this method of fixation is to be used: Use under a chemical hood and rinse glassware and pipets under the hood after use.
2. Spurr's embedding medium is prepared according to specific directions provided with each kit. The individual components and proportions are as follows:
   a. 10 mL Vinylcyclohexene dioxide (VCD).
   b. 6 mL Diglycidyl ether of propylene glycol (DER 736).
   c. 26 mL Nonenyl succiniic anhydride (NSA).
   d. 0.5 mL Dimethyl aminoethanol (DMAE).

   These ingredients are poured together in a glass beaker and stirred vigorously for several minutes to assure complete mixing. The mixture is then used either as full strength or diluted with propylene oxide as described earlier, for 1:l or 1:3 parts.
3. Disposable microtome blades recommended are Accu-Edge 4685 high-profile blades.
4. For preparation of chromate solution and mercuric chloride solution, the water should be boiling as it is poured into the respective flasks.
5. Note that the large Erlenmeyer flask should never be more than two-thirds full, in order to avoid splashing during the prolonged rotation period.
6. For brain tissue from experimental animals, best results are achieved by fixation with cardiac perfusion with 10% formalin. For human postmortem brain tissue, best results are achieved if tissue blocks no larger than about 1 cm^3 are removed from the fresh brain and fixed in 10% formalin for 7–10 d; longer fixation or storage in 10% formalin for 2–3 mo does not seem to impair the staining, but storage in formalin for longer periods definitely reduces the effectiveness of the procedure. After appropriate fixation, these cubes of brain tissue should be cut into smaller flat pieces approx 2–4 mm thick with a surface area approx 5 × 5 mm.
7. However, it is important to note that for sections as thick as 25–30 μm, brittleness and cracking of the sections can be a problem. This can be avoided if the blocks are first faced

with a single-edge razor blade to determine the shape and surface area of the sections to be cut, then soaked overnight in a small water bath or beaker of water at 37–40°C before cutting. This soaking provides just enough softening of the block face to effect smooth cutting of fairly thick sections (25–30 μm or more).

References

1 Pannese, E. (1999) The Golgi stain: invention, diffusion and impact on the neurosciences. *J. Hist. Neurosci.* **8(2),** 132–140.

2. Azoulay, L. (translator) (1894) Section III. Gray cortex of the cerebrum, in *A New Concept of the Histology of the Nerve Centers,* Reinwald, Paris.
3. DeFelipe, J. and Jones, E. G. (1988) In *Cajal on the Cerebral Cortex* (Corsi, P., Jones, E. G., and Shepherd, G. M., eds.), Oxford University Press, New York.
4. Whetsell, W. O., Jr., and Schwarcz, R. (1983) Mechanisms of excitotoxins examined in organotypic cultures of rat central nervous system, in *Excitoxins* (Fuxe, K., Roberts, P., and Schwarcz, R., eds.), MacMillan, London, pp. 207–219.

5 Guidetti, P., Charles, H., Chen, E.Y., et al. (2001) Early degenerative changes in transgenic mice expressing mutant huntingtin involve dendritic abnormalities but no impairment of mitochondrial energy production. *Exp. Neurol.* **169,** 340–350.

6. Ramon-Moliner, E. (1970) The Golgi–Cox technique, in *Contemporary Research Methods in Neuroanatomy* (Nauta, W. J. H. and Ebbesson, S. O. E., eds.), Springer-Verlag, New York, pp. 32–55.

7 Toran-Allerand, D. (1976) Golgi–Cox modifications for the impregnation of whole mount preparations of organotypic culture of CNS. *Brain Res.* **118,** 293–298.

8. Landas, S. and Phillips, M. I. (1982) Staining of human and rat brain vibratome sections in a new Golgi method. *J. Neurosci. Methods* **5,** 147–151.

19

Assessment of Impaired Proteasomal Function in a Cellular Model of Polyglutamine Diseases

Nihar Ranjan Jana and Nobuyuki Nukina

Summary

A protein marked for degradation by the ubiquitin–proteasome pathway (UPP) is attached to multiple molecules of ubiquitin, a 76-amino-acid protein that targets the protein for rapid hydrolysis by 26S proteasome. Impaired function of UPP results in accumulation of misfolded and ubiquitinated proteins and has been implicated in the pathogenesis of various neurodegenerative diseases, including polyglutamine diseases. Impaired function of UPP can be evaluated either by assaying the proteasome's protease activity or the accumulation of ubiquitinated proteins.

Key Words: Polyglutamine diseases; proteasome; ubiquitin; lactacystin; huntingtin.

1. Introduction

The ubiquitin–proteasome pathway (UPP) is the cell's principal mechanism for controlled protein degradation. The pathway has been shown to be involved in the regulation of critical cellular process such as transcription, cell cycle progression, oncogenesis, growth and development, selective elimination of abnormal proteins, and antigen processing ***(1)***.

Dysfunction of the UPP has been implicated in the pathogenesis of numerous diseases, including various neurodegenerative diseases ***(1)***. Recent studies indicate that the proteasome activity is inhibited in the brains of Alzheimer's disease cases ***(2)*** and Parkinson's disease cases ***(3)*** and in the aged brain ***(4)***. In the cellular models of polyglutamine disease, Parkinson's disease, and amyotrophic lateral sclerosis, the expression of mutant protein causes inhibition of proteasome activity over time ***(5–8)***. It seems that impairment of the UPP is a common phenomenon that can be caused by any protein aggregation ***(5)***.

From: *Methods in Molecular Biology, vol. 277: Trinucleotide Repeat Protocols*
Edited by: Y. Kohwi © Humana Press Inc., Totowa, NJ

Degradation of a protein by UPP involves two distinct and successive steps: (1) covalent attachment of multiple ubiquitin molecules to the target protein and (2) degradation of the targeted protein by 26S proteasome. The 26S proteasome is a 2.1-MDa complex of which approx 65 subunits are divided into 3 subcomplexes: 20S, 19S, and 11S. The 20S core catalytic complex is a cylindrical stack of four seven-membered rings and is flanked on both sides by 19S regulatory complexes. Its proteolytic site faces an interior chamber that can be entered only through pores at either end of the cylinder. Because folded proteins cannot enter this chamber, the isolated 20S complex hydrolyzes only small peptides and denatured proteins. Three distinct proteolytic activities have been defined for 20S proteasome: chymotrypsinlike (Tyr or Phe at P1), trypsinlike (Arg or Lys at P1), and postglutamyl peptidyl hydrolyticlike (Glu at P1).

The impairment of the proteasomal function can be assessed either by directly estimating the proteolytic activity of 20S proteasome or by indirectly observing the accumulated ubiquitinated proteins. The most common assessment of 20S proteasome activity is achieved by measuring the hydrolysis of the fluorogenic peptide substrate Suc-Leu-Leu-Val-Tyr-AMC by the proteasome. This substrate is cleaved by the chymotrypsinlike activity of the proteasome, releasing free AMC (7-amino-4-methylcoumarin), which can then be efficiently detected using a fluorimeter (λ_{ex}: 355 nm; λ_{em}: 460 nm). The decrease in proteasome activity will result in an increase in ubiquitinated proteins. Therefore, relative measurement of accumulated ubiquitinated proteins would be another way to measure the impaired proteasome function.

2. Materials

2.1. Equipments

1. Refrigerated centrifuge.
2. CO_2 incubator.
3. Microtiter plate reader or fluorescence spectrophotometer capable of measuring fluorescence at approximate excitation 355 nm and emission 460 nm.
4. Polyacrylamide gel electrophoresis (PAGE) and transfer apparatus with power supply.

2.2. Reagents

1. Dulbecco's modified Eagle's medium (DMEM), heat-inactivated fetal bovine serum (FBS), and penicillin/streptomycin solution (Life Technologies Inc., Gaithesburg, MD).
2. Zeocin, G418, and Ponasterone A (Invitrogen).
3. Proteasome substrate Suc-Leu-Leu-Val-Tyr-AMC and proteasome inhibitor lactacystin (Calbiochem) (*see* **Note 1**).
4. Homogenization buffer for proteasome assay (10 m*M* Tris-HCl, pH 7.4, 1 m*M* EDTA, 5 m*M* dithiothreitol [DTT], 5 m*M* ATP, and 20% glycerol).
5. Proteasome assay buffer (10 m*M* Tris-HCl, pH 7.4, 1 m*M* EDTA, and 50 μ*M* Suc-Leu-Leu-Val-Tyr-AMC (*see* **Note 2**).
6. TN-T buffer (50 m*M* Tris-HCl, pH 7.4, 150 m*M* NaCl, 1% Triton X-100, and complete protease inhibitor cocktail from Roche).
7. Coomassie protein assay reagent (Pierce).
8. TBST (50 m*M* Tris-HCl, pH 7.5, 150 m*M* NaCl, 0.05% Tween-20).
9. Ubiquitin antibody (Dako).
10. Enhanced chemiluminescent (ECL) reagent (Amersham Life Sciences).

3. Methods

3.1. Cell Culture

1. Culture the stable cell lines HD 16Q and HD 150Q (expressing normal and expanded truncated N-terminal huntingtin, respectively, under the control of inducer ponasterone A; *see* **Note 3**) in DMEM supplemented with 10% FBS, 0.4 mg/mL Zeocin, and 0.4 mg/mL G418. Generation of the stable cell lines has been described elsewhere ***(9)***.
2. Plate the cells in six-well tissue culture plates at subconfluent density. On the following day, differentiate (with 5 m*M* dibutyryl cyclic AMP) and induce (with 1 μ*M* of ponasterone A) the HD 16Q and HD 150Q cells for different time periods. Add proteasome inhibitor lactacystin (1–10 μ*M* dose) to the wild-type neuro2a cells or HD 16Q cells for 5 h.
3. Harvest the cells and immediately process for proteasome activity assay or immunoblot analysis. Otherwise, cells can be stored at –20°C for analysis at a later stage.

3.2. Assay of Proteasome Activity

1. Homogenize the cells (by sonication) with ice-cold homogenization buffer and then centrifuge at 15,000*g* for 15 min at 4°C.
2. Measure the protein concentration in the supernatant using Coomassie protein assay reagent.
3. Add 100 μL of proteasome assay buffer in each well of 96-well plate (flat surface) and preincubate at 37°C for 5 min (*see* **Note 4**).
4. Add 25 μL (containing 25 μg protein) of cell supernatant to each well. Mix well and then incubate the plate at 37°C.
5. Monitor the fluorescence reading (λ_{ex}: 355 nm; λ_{em}: 460 nm) in the fluorescence microplate reader every 10-min interval for 1 h.
6. Determine the time-points at which the reaction is linear. Data in the linear range should be used for the analysis of proteasome activity. Proteasome activity can be expressed as change in the fluorescence intensity per minute per milligram of protein or as percent control (considering the proteasome activity in the control sample as 100%) (*see* **Note 5**).

3.3. Western Blot Analysis of Ubiquitinated Proteins

1. After appropriate treatments, wash the cells with cold PBS, scrape with cell scraper, and harvest by centrifugation at 500*g* for 10 min at 4°C.
2. Dissolve the cells on ice for 2 h at 4°C with TN-T buffer. Briefly sonicate the cell lysates and then centrifuge for 15 min at 15,000*g* at 4°C to collect the supernatant.
3. Measure the protein concentration in the supernatant using Coomassie protein assay reagent.
4. Mix the supernatants (10 μL containing 20 μg protein) with sodium dodecyl sulfate (SDS) sample buffer (twice), vortex, and boil for 5 min.
5. Resolve the proteins through SDS–polyacrylamide gel electrophoresis and transfer onto polyvinylidene difluoride (PVDF) membranes.
6. Incubate the membrane in blocking solution (5% skim milk in TBST) for 30 min.
7. Incubate with ubiquitin antibody (1:1000 dilution in TBST) for 4 h to overnight.
8. Wash with TBST three times for 10 min each.
9. Incubate with secondary antibody conjugated with HRP (goat anti-rabbit IgG; 1: 2000 dilution in TBST).

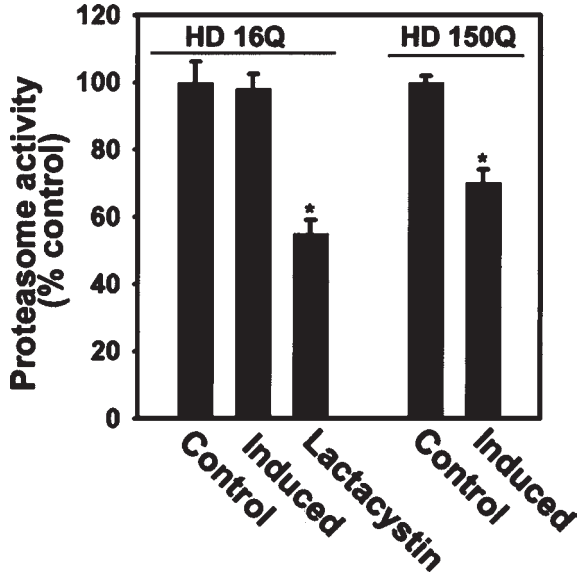

Fig. 1. Assay of proteasome activity in HD 16Q and HD 150Q cells. The cells were left untreated (control) or differentiated with 5 m*M* of dibutyryl cyclic AMP and induced with 1 μ*M* of ponasterone A for 3 d. Cells were then harvested and processed for proeasome activity assay. Lactacystin (5 μ*M*) was added to untreated HD 16Q cell for 5 h. *$p < 0.01$ as compared to untreated cells.

10. Repeat **step 5**.
11. Detect the bands with enhanced chemiluminescence reagent.

3.4. Results

HD 16Q and HD 150Q cells were left untreated or induced for 3 d to express the truncated N-terminal huntingtin containing 16Q (normal) and 150Q (expanded), respectively. The cells were then collected and processed for the proteasome activity assay. As shown in **Fig. 1**, expression of expanded polyglutamine protein causes a significant decrease in proteasome activity, whereas expression of normal glutamine repeats results in no change in proteasome activity. As an experimental control, lactacystin was used to treat untreated HD 16Q cells. Treatment of lactacystin dramatically decreases the proteasome activity (*see* **Fig. 1**). **Figure 2** demonstrates the ubiquitin immunoblotting of the total cell lysate collected from HD 16Q and HD 150Q cells after induction. The expression of expanded polyglutamine protein in HD 150Q cells for 3 d results in a massive accumulation of ubiquitinated proteins. Lactacystin treatment to the HD 16Q cells for 5 h also results in a similar accumulation of ubiquitinated protein. The expression of truncated N-terminal huntingtin containing 16Q does not cause much alteration of the ubiquitinated protein profile.

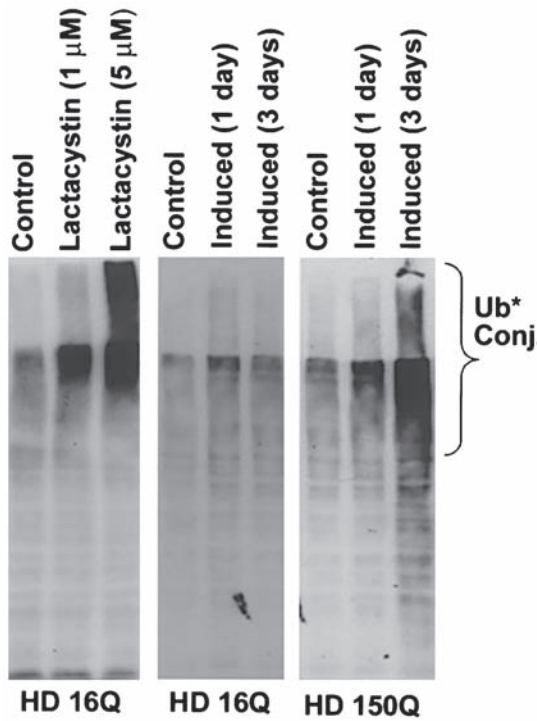

Fig. 2. Immunoblot analysis of ubiquitinated proteins in HD 16Q and HD 150Q cells. The cells were left untreated (control) or differentiated and induced for 1 d and 3 d in a manner similar to that described for **Fig. 1**. Lactacystin (1 and 5 μ*M*) was added to the untreated cells for 5 h. The harvested cells were processed for immunoblotting using antiubiquitin antibody.

4. Notes

1. Dissolve the proteasome substrate in dimethyl sulfoxide (DMSO). Dissolved substrate is stable for 2–3 mo at –30°C. Make fresh proteasome activity assay buffer during assay.
2. 20S proteasome chymotrypsinlike activity is increased by slight denaturation with a low concentration of sodium dodecyl sulfate (SDS) (optimum = 0.03%).
3. The truncated N-terminal huntingtin (tNhtt) expression constructs pIND-tNhtt-enhanced green fluorescence protein (EGFP)-16Q and pIND-tNhtt-EGFP-150Q and the generation of stable and inducible cell lines of these constructs (HD 16Q and HD 150Q, respectively) have been described elsewhere ***(9).*** Each construct contains 1–90 amino acids of tNhtt (predicted molecular weight = 7.8 kDa) with different polyglutamine length fused to the N-terminus of EGFP.
4. For optimum enzymatic activity, assay must be performed at 37°C.
5. For accurate fluorimetric measurements of the precise specific activity of the 20S proteasome, the fluorimeter may be calibrated by generating a standard curve using free AMC ranging from 0 to 100 pmol. Specific activity can be calculated as picomoles of AMC released per minute per milligram of protein.

References

1 Glickman, M. H. and Ciechanover, A. (2001) The ubiquitin–proteasome proteolytic pathway: destruction for the sake of construction. *Physiol. Rev*. **82,** 373–428.

2 Keller J. N., Hanni, K. B., and Markesbery, W. R. (2000) Impaired proteasome function in Alzheimer's disease. *J. Neurochem*. **75,** 436–439.

3 McNaught, K. S. and Jenner, P. (2001) Proteasomal function is impaired in substantia nigra in Parkinson's disease. *Neurosci. Lett*. **297,** 191–194.

4 Keller, J. N., Huang, F. F., and Markesbery, W. R. (2000) Decreased levels of proteasome activity and proteasome expression in ageing spinal cord. *Neuroscience* **98,** 149–156.

5 Bence, N. F., Sampat, R. M., and Kopito, R. (2001) Impairment of the ubiquitin–proteasome system by protein aggregation. *Science* **292,** 1552–1555.

6 Jana, N. R., Zemskov, E. A., Wang, G., et al. (2001) Altered proteasomal function due to the expression of polyglutamine expanded truncated huntingtin induces apoptosis by caspase activation through mitochondrial cytochrome c release. *Hum. Mol. Genet*. **10,** 1049–1059.

7 Tanaka, Y., Engelender, S., Igarashi, S., et al. (2001) Inducible expression of mutant alpha-synuclein decreases proteasome activity and increases sensitivity to mitochondria-dependent apoptosis. *Hum. Mol. Genet*. **10,** 919–926.

8 Urushitani, M., Kurishu, J., Tsukita K., et al. (2002) Proteasomal inhibition by misfolded mutant superoxide dismutase I induces selective motor neuron death in familial amyotrophic lateral sclerosis. *J. Neurochem*. **83,** 1030–1042.

9. Wang, G. H., Mitsui, K., Kotliarova, S., et al. (1999) Caspase activation during apoptotic cell death induced by expanded polyglutamine in N2a cells. *NeuroReport* **10,** 2435–2438.

20

Assessment of In Vitro and In Vivo Mitochondrial Function in Friedreich's Ataxia and Huntington's Disease

Anthony Schapira and Raffaele Lodi

Summary

Huntington's disease (HD) and Friedreich's ataxia (FRDA) are associated with defects of respiratory-chain enzyme activities. In the respective disorders, these can be identified in tissue samples from postmortem brain and also during life from skeletal or cardiac muscle samples. The mitochondrial abnormalities are robust and reproducible. In the case of HD, it is uncertain how these mitochondrial defects fit in the pathogenetic cascade. Studies are ongoing to identify whether the respiratory-chain defect present in the brain is expressed in skeletal muscle at the spectrophotometric level. The presence of a bioenergetic defect as identified by ^{31}P magnetic resonance spectroscopy (MRS) suggests that in HD expression of the mutant protein can exert an influence on mitochondrial function in tissues outside the central nervous system (CNS). It would appear that frataxin deficiency has a direct effect on mitochondrial function, either through iron–sulfur cluster construction or through the generation of free radicals. The identification these bioenergetic abnormalities in these neurodegenerative disorders has opened up the prospect for the development of disease-modifying therapies directed to the biochemical abnormalities demonstrated. ^{31}P-MRS studies have detected a deficit of in vivo oxidative phosphorylation in the skeletal muscle of FRDA and HD patients and in the myocardium of FRDA patients. In both FRDA and HD patients, a relationship between the triplet repeat expansion and the extent of in vivo energy metabolism deficit has been shown. The total safety of MRS scans makes them an ideal tool for repeated assessments to monitor disease progression as well as the effect of new therapies. This chapter describes useful methods for assessment of mitochondrial function in vitro and in vivo.

Key Words: In vivo energy metabolism; ^{31}P-MRS; mitochondrial dysfunction; mitochondria; Huntington's disease; Friedreich's ataxia.

From: *Methods in Molecular Biology, vol. 277: Trinucleotide Repeat Protocols*
Edited by: Y. Kohwi © Humana Press Inc., Totowa, NJ

1. Introduction

1.1. Huntington's Disease

1.1.1. Clinical, Genetic, and Pathophysiological Features of Huntington's Disease

Huntington's disease (HD) has a prevalence of 4–8 per 100,000. Clinically, it is characterized by a decline of cognitive function and the development of motor abnormalities, particularly chorea. Onset is insidious, usually in early middle age, although patients can present at any time from childhood to late adulthood. Death usually occurs within 15–20 yr of onset. Juvenile-onset patients usually progress more rapidly, with death following within 7–10 yr of onset. The cognitive and motor abnormalities are the dominant features throughout the illness, although in the latter stages, there is also significant weight loss and muscle atrophy.

The cause of HD is an expanded CAG repeat within the coding sequence of the gene for huntingtin. The CAG repeat is transcribed and translated and results in a polyglutamine stretch within the protein. In normal subjects, the CAG repeat length is between 9 and 34. Thirty-seven CAG repeats or longer can give rise to HD. The longer the repeat length, the earlier the onset and the more severe the disease ***(1,2)***. HD is inherited as an autosomal dominant disorder with genetic anticipation, a feature common to several other polyglutamine disorders.

The most important pathological feature of HD is neuronal degeneration and astrogliosis in the striatum. There is severe loss of GABA-ergic, medium-size spiny projection neurons with sparing of the medium-sized aspiny neurons. Neuronal intranuclear inclusions are seen in the striatum and cortex of HD patients. Usually, one inclusion is seen per nucleus and approx 1–5% of striatal neurons are affected. Interestingly, interneurons that are spared in HD appear to have the highest frequency of neuronal inclusions. It is not known whether the inclusions, which are aggregates of huntingtin, are protective or toxic. They are not present in presymptomatic patients. They do appear in transgenic mouse models of HD ***(3–5)***. Mutant huntingtin aggregates have also been seen in cultured cells and correlated with toxicity ***(6–8)***, but an alternative culture system has suggested that aggregates can be protective ***(9)***.

The function of huntingtin is not understood. Deletion of the gene results in early embryological death. Features of huntingtin have suggested that it may have an antiapoptotic function and be involved in intracellular trafficking, perhaps including vesicular transport ***(10,11)***.

1.1.2. In Vitro Investigations of Patients With Huntington's Disease

There are no biochemical diagnostic markers of HD. The diagnosis and investigation of patients is dependent on clinical examination, cranial imaging, and examination of DNA for the characteristic CAG repeats. However, several biochemical studies have been undertaken on HD brain and skeletal muscle (*see* below).

In terms of mitochondrial dysfunction, abnormalities were identified in HD postmortem tissue in 1974, when an abnormality of complex II activity was described ***(12)***. Further abnormalities were identified ***(13)***. Defects of mitochondrial membranes

in cerebral cortex and caudate from HD patients were associated with a reduction in cytochrome oxidase activity and in cytochrome-aa_3 in the caudate but not the cortex ***(14)***. The first definitive study of mitochondrial respiratory-chain activity in HD identified a 77% reduction in complex II/III activity ***(15)***. This was confirmed in a larger study that identified a 56% defect of complex II/III activity and a 33% defect of complex IIII activity in HD caudate ***(16)***. Confirmation followed in other studies ***(17)***. There has been a report of complex I deficiency in platelets from HD patients ***(18)***, but this has not been confirmed in another study ***(19)***. A severe defect in aconitase activity was also identified in HD caudate, putamen, and cordex but not cerebellum, the severity of the deficiency paralleled the pathological involvement ***(19)***.

It is of interest that the enzymes predominantly affected in HD include complex II/III and aconitase. All of these are in sulfur-containing enzymes and, as such, may be particularly susceptible to inhibition by peroxynitrite generated from superoxide and nitric oxide ***(20–22)***.

The most accurate determination of mitochondrial respiratory-chain function is achieved by spectrophotometric analysis of isolated mitochondria. This is not possible from frozen postmortem tissue, although if sufficient material is available then it is possible to isolate an enriched sample of mitochondrial membranes. Therefore, it is common practice when studying postmortem brain samples in particular to correct respiratory-chain activities for citrate synthase activity. The latter is a mitochondrial matrix enzyme that is a reflection of total mitochondrial mass. Therefore, correction for citrate synthase activity accommodates for any variation in mitochondrial mass that may result as a consequence of neuronal degeneration.

1.1.3. In Vivo Investigations of Patients With Huntington's Disease

The skeletal muscle energy metabolism was assessed in 12 HD patients, with a CAG repeat expansion ranging from 38 to 57 ***(23)***. Eight subjects were symptomatic and four were presymptomatic. The ATP content, relative to PCr+Pi, in the resting muscle was significantly reduced in both symptomatic (0.24 ± 0.01; $p = 0.0001$) and presymptomatic HDs (0.24 ± 0.02; $p = 0.01$) compared to controls (0.26 ± 0.01). The maximum rate of mitochondrial ATP production (V_{max}), measured after an aerobic exercise, was reduced in both symptomatic (33.1 ± 5 m*M*/min; $p = 0.0007$) and presymptomatic HD (38.0 ± 12; $p = 0.04$) compared to controls (59 ± 17). In HD symptomatic patients, the degree of V_{max} muscle deficit, V_{max}deficit, over age (V_{max}deficit) correlated with the CAG repeat size ($r = 0.71$; $p = 0.04$).

We showed that there is an in vivo mitochondrial dysfunction in skeletal muscle of HD patients that can precede clinical evidence of CNS impairment. The correlation between CAG repeat length and $V_{max_{deficit}}$/age in HD patients suggests that the size of CAG expansion influences the degree of V_{max} defect and supports a cause-and-effect relationship.

Our findings support a role for mitochondrial abnormalities in cell dysfunction and loss in HD. This role is supported by proton magnetic resonance spectroscopy studies (^{1}H-MRS) in which significantly elevated levels of lactate were found in HD occipital cortex ***(24–26)***. Interestingly, increased lactate was not detected in eight pre-

symptomatic individuals in occipital cortex, but a significant elevation was found in the striatum. It is possible that this striatal abnormality reflects early disease and mirrors our findings in the skeletal muscle of presymptomatic HD.

1.2. Friedreich's Ataxia

1.2.1. Clinical, Genetic, and Pathophysiological Features of Friedreich's Ataxia

Friedreich's ataxia (FRDA) is the commonest form of inherited ataxia with a frequency of 1 in 50,000 live births. FRDA is an autosomal recessive degenerative disorder characterized by progressive gait and limb ataxia, loss of limb deep tendon reflexes, spasticity, and extensor plantar responses ***(27,28)***. Neuropathology in FRDA is characterized by early degeneration of large sensory neurons in the dorsal root ganglia, followed by degeneration of sensory posterior columns, spinal–cerebellar tracts, cortical–spinal motor tracts, and atrophy of the large sensory fibers in peripheral nerves. Hypertrophic cardiomyopathy is present in a large proportion of FRDA patients ***(27,28)***.

The causative mutation of FRDA is an abnormally expanded GAA triplet repeat in the first intron of the FRDA gene on chromosome 9q13 ***(29)***. Ninety-seven percent of FRDA patients are homozygous for the GAA expansion, the remainder carrying a repeat expansion in one FRDA allele and a point mutation in the other ***(28,29)***. The size of the GAA expansion in FRDA patients ranges from about 100 repeats to 1700, normal chromosomes having between 8 and 22 repeats ***(28,29)***. The expression of numerous symptoms/signs in FRDA is dependent on the length of the GAA repeat expansion in the smaller allele ***(28)***. In particular, the age at onset correlates negatively ***(28,30)*** and the rate of progression of the disease positively with the number of GAA repeats in the smaller allele ***(28)***. The frequency and severity of hypertrophic cardiomyopathy increases with the size of the GAA expansion in the smaller allele ***(28,31,32)***.

Mutations in the FRDA gene, either GAA expansions or point mutations, result in reduced expression of a protein called frataxin ***(33)***, which has been shown to be localized to mitochondria ***(33–35)***. In normal subjects, the highest level of expression of the FRDA gene has been found in the heart and spinal cord, intermediate levels in the cerebellum, liver, skeletal muscle, and pancreas, and very little in the cerebral cortex ***(29)***. The amount of residual frataxin in lymphoblastoid cell lines from FRDA patients correlates with the GAA expansion size in the smaller allele ***(33)*** and likely represents the molecular basis of the relationship between GAA expansion size and phenotypic expression of the disease ***(28)***.

1.2.2. In Vitro Investigations of Patients With Friedreich's Ataxia

The diagnosis of FRDA, like that of HD, is dependent on clinical evaluation supported by genetic diagnosis of the GAA repeat length. Biochemical investigations remain an experimental development.

Frataxin is a mitochondrially protein ***(36–38)***. Therefore, the main focus for in vitro studies is mitochondrial function. This was first assessed in frataxin knockout mutants

of yeast (YFH1) that developed an abnormality of respiration and loss of mitochondrial DNA. These cells also developed an increase in iron. Therefore, samples from patients with FRDA were assessed to determine whether they reflect the same abnormalities as seen in yeast ***(39,40)***. A consistent abnormality is of a severe deficiency of complexes I and II/III in postmortem heart and a less severe defect of these enzymes in skeletal muscle. These respiratory-chain abnormalities are also associated with severe deficiency of aconitase. All of these proteins, as noted earlier, are iron–sulfur-containing proteins, but are also accessible to damage by free radicals. It is of interest that this exact same pattern of enzyme defect is seen in the manganese superoxide dismutase knockout mouse ***(41)***. It is uncertain at present whether this pattern of mitochondrial defect is a consequence of defective iron–sulfur construction and integration or whether the abnormalities are secondary to free-radical damage. These two hypotheses, of course, are not mutually exclusive. In this respect, it is of interest that the conditional knockout mouse model of FRDA develops respiratory-chain abnormalities prior to iron ***(42)***.

1.2.3. In Vivo Investigations of Patients With Friedreich's Ataxia

Cardiac bioenergetics was assessed in vivo in 18 FRDA patients with and without left-ventricular hypertrophy with a GAA expansion in the smaller allele ranging from 290 to 950 ***(43)***. Cardiac PCr-to-ATP ratios in the FRDA group as a whole were significantly reduced compared to age- and sex-matched controls (FRDA, 1.46 ± 0.53; controls, 2.39 ± 0.13; $p < 0.0001$). The Fisher's test showed significantly reduced PCr/ATP ratios in both groups of FRDA patients with normal (1.44 ± 0.54, $n = 10$) and hypertrophic heart (1.47 ± 0.55, $n = 8$) compared to controls ($p < 0.0001$ for both groups), and similar mean ratios in the two patient groups ($p = 0.85$).

These findings represent the first evidence in humans that cardiac PCr/ATP can be reduced in the absence of either failing contractile function or hypertrophy. In FRDA, the hypertrophic process may be compensatory and caused or contributed to by the bioenergetic deficit, which is also known to stimulate myocyte hypertrophy ***(44)***. This hypothesis is supported by the frequent finding of hypertrophic cardiomyopathy in patients with a deficit of oxidative phosphorylation because of mutations of mitochondrial DNA ***(45)***.

The rate of mitochondrial ATP production was assessed in the skeletal muscle of 12 FRDA patients (GAA expansion in the smaller allele ranging from 290 to 900 repeats) ***(46)***. The skeletal muscle maximum rate of mitochondrial ATP synthesis (V_{max}) was reduced in the patients to one-third of the normal mean. In all 12 patients V_{max} was below the normal control range. This is a typical finding in patients with mitochondrial myopathy as a result of mtDNA mutations ***(47)***. Mitochondrial V_{max} values in FRDA patients were also significantly lower than in a group of disease controls with muscular disorders from different causes and with similar maximal motor ability, indicating that disability *per se* did not account for the reduced mitochondrial function in FRDA patients. We found that mitochondrial V_{max} was strongly dependent on the size of the GAA repeats in the smaller allele ($r = -75$, $p = 0.004$): The higher the number of GAA repeats, the lower the mitochondrial V_{max}. This is clear evidence that

the GAA expansion is the cause of the mitochondrial deficit and suggests a link between degree of mitochondrial respiration deficit and clinical expression of the disease. The length of the GAA expansion has been shown to determine the amount of frataxin expressed ***(33)***, thus suggesting that the residual expression of frataxin probably determines the reduced skeletal muscle mitochondrial ATP production rate we detected in vivo.

We have recently evaluated the effect of antioxidant treatment (coenzyme Q_{10}, 400 mg/d plus vitamin E, 2100 IU/d) on in vivo cardiac and calf muscle energy metabolism a group of FRDA patients ***(48)***. After 6 mo of therapy, the cardiac PCr-to-ATP ratio increased by more than 50% and skeletal muscle mitochondrial V_{max} for ATP production increased by 34% in a group of 10 FRDA patients.

2. Materials

All solutions are prepared in double-distilled water (ddH_2O) unless otherwise specified.

1. Homogenizing buffer (H-buffer): 250 m*M* sucrose, 1 m*M* EDTA, 10 m*M* Tris-HCl, pH 7.4.
2. 25 m*M* Potassium phosphate buffer (pH 7.2): prepare from 25 m*M* KH_2PO_4 and 25 m*M* K_2HPO_4.
3. 1 *M* Sodium citrate (Sigma): stock solution.
4. 20 m*M* NADP (Roche): freshly prepared.
5. 5 m*M* NADH (Roche): freshly prepared.
6. Isocitrate dehydrogenase (Sigma): 100 U/mL in ddH_2O for stock and kept at 4ºC.
7. 1 m*M* Rotenone (Sigma): in ethanol, stored at –20ºC.
8. 10 m*M* Acetyl CoA (Sigma): stored at –20ºC.
9. 10 m*M* of 5,5'-dithiobis-(2-nitrobenzoic acid) (DTNB) (Sigma): pH 8.0, freshly prepared.
10. 10 m*M* Oxaloacetate (Sigma): freshly prepared.
11. 100 m*M* KCN (VWR): freshly prepared.
12. Ubiquinone-1 (Eisai Chemical Co., Japan): The concentration of CoQ_1 must be determined (*see* **Note 1**).
13. 2 m*M* Cytochrome-*c* (Roche): stored at –20ºC.
14. Reduced cytochrome-*c*: A 1% (w/v) solution of cytochrome-*c* (from horse heart; Boehringer Mannheim) is fully reduced (which was monitored at 550 nm to note no further absorbance change) by the addition of an excess of ascorbate (about 12 mg in 100 mL of 10 m*M* potassium phosphate buffer) (*see* **Note 2**).
15. 500 m*M* Succinate (Sigma): stored at –20ºC.
16. 2 m*M* Antimycin A (Sigma): stored at –20ºC.
17. 1 m*M* Potassium ferricyanide (VWR): freshly prepared.
18. 10% (v/v) Triton X-100 (Sigma).
19. Bovine serum albumin (BSA) (Sigma): 50 mg/mL stored at –20ºC.
20. Spectrophotometer: Hitachi U-3210 (Hitachi Scientific Instruments, Workingham, Berks, UK) and Kontron Uvikon 940 (Kontron Instruments, Watford, Herts, UK) split-beam spectrophotometers.
21. Phosphorus MRS (^{31}P-MRS) for in vivo analysis: Magnetic resonance spectroscopy (MRS) is a noninvasive technique that allows, using clinical MR scanners of at least 1.5 T, the measurement of several compounds in vivo without the use of radioactive tracers (*see* **Notes 3** and **4**).

3. Methods

3.1. Preparation of Mitochondrial Homogenates

1. Frozen brain tissues are weighed (about 50 mg) and homogenized in 9 vol of ice-cold H-buffer using a glass–glass homogenizer.
2. Homogenization is carried out by hand for 6–10 strokes or until a uniform color is obtained.
3. The homogenate is used for enzyme assay directly after three cycles of freeze–thawing in liquid nitrogen.
4. The mitochondrial enzymes are immediately analyzed blind and in triplicate at 27ºC.
5. The mitochondria protein is measured by the Lowry method using BSA, fraction V as the standard (*see* **Note 5**). We normally obtain about 10 mg/mL from 50 mg of brain samples.

3.2. Aconitase Activity Measurement

1. Set up 1.0 mL of reaction mixture containing a final concentration of 50 m*M* Tris-HCl, pH 7.4, 0.4 m*M* NADP, 5 m*M* Na–citrate, 0.6 m*M* $MgCl_2$, 1–2 U of isocitrate dehydrogenase, and 10–100 mg of tissue homogenates.
2. Preincubate the reaction mixture for 30 min to activate the enzyme.
3. Monitor the linear absorbance change at 340 nm at 30ºC for 30 min.
4. The linear rates are used for the determinations of aconitase activity and expressed as nanomoles per minute per milligram of protein

3.3. NADH–CoQ_1 Oxidoreductase (Complex I Activity) Measurement

Principle: The assay measures the rotenone-sensitive CoQ_1-dependent oxidation of NADH at 340 nm ***(49)***.

1. Set up two identical cuvets containing 20 m*M* potassium phosphate buffer, pH 8, 150 μ*M* NADH, 1 m*M* KCN, and sample (5–15 mg protein for homogenized brain or 0.5–1.5 mg protein for platelet mitochondrial) on a final volume of 1 mL (*see* **Note 6**).
2. The reaction is initiated by adding CoQ_1 to give a final concentration of 50 μ*M* to the sample cuvet.
3. The rate of NADH oxidation is monitored at 340 nm.
4. Rotenone is added to a final concentration of 10 μ*M* and the rotenone-insensitive rate is measured.
5. Complex I activity is defined as the rate that is sensitive to rotenone. A molar extinction coefficient (ε) for NADH of 6.81×10^3 is used to allow for the contribution of reduced CoQ_1 to the absorbance at 340 nm. Enzyme activity is expressed as nanomoles of NADH oxidized per minute per milligram of protein (nmol/min/mg protein) or a ratio with citrate sythase (CS).

3.4. Succinate Cytochrome-c Oxidoreductase (Complex II+III) Measurement

Principle: The assay determines the activity of complex II+III of the mitochondrial electron transport chain by detecting the succinate dependent reduction of cytochrome-*c* at 550 nm ***(50)***.

1. Set up two identical cuvets, containing 0.1 *M* potassium phosphate buffer, pH 7.4, 0.3 m*M* EDTA potassium salt (K_2-EDTA), 0.1 m*M* cytochrome-*c*, 1 m*M* KCN, 2.5 mg/mL BSA for a final volume of 1 mL.

2. A mixture of sample, 40 μL of 500 m*M* sodium succinate and 10 μL of 100 m*M* KCN is preincubated at 30°C for 5 min to fully activate the enzyme.
3. The complex II+III activity is calculated as the rate that was sensitive to the addition of antimycin A (final concentration 20 μ*M*).
4. The molar extinction coefficient of cytochrome-*c*, $\varepsilon = 19.2 \times 10^3$, is used. Enzyme activity is expressed as nanomoles of cytochrome-*c* reduced per minute per milligram of protein (nmol/min/mg protein) or a ratio with CS.

3.5. Cytochrome-c Oxidase (Complex IV) Measurement

Principle: The assay monitors the oxidation of reduced cytochrome-*c* at 550 nm ***(51)***.

1. Set up identical cuvets, containing 50 m*M* potassium phosphate buffer, pH 7.0, and 50 μ*M* reduced cytochrome-*c*.
2. Potassium ferricyanide (1 m*M*) is added to the reference cuvet to fully oxidize the cytochrome-*c*.
3. The reaction is initiated by the addition of the sample to the test cuvet and monitored at 550 nm.
4. The assay is first order with respect to cytochrome-*c*, so the pseudo-first-order rate constant *k* is calculated as: the extrapolation of the absorbance back to time = 0.96 (the initial absorbance) and the determination of the change in absorbance at various time-points up to 2 min.
5. The nonenzymatic rate of absorbance change is substracted from these value and *k*/min/mL is calculated as *k* = {ln0.288–ln(0.288–change in absorbance at time *t*) × 1000/Sample volume [μL] × Dilution factor}, where 0.288 is the absorbance of cytochrome-*c* fully reduced.
6. Enzyme activity is expressed as *k*/min/mg protein.

3.6. Citrate Synthase Measurement

Principle: The enzyme catalyzes the condensation of acetyl-coA and oxaloacetate to form citrate, producing CoA, whose free thiol group combines with 5–5'-dithiobis-nitrobenzoic acid (DTNB), resulting in an increase in absorbance at 412 nm ***(52)***.

1. Set up identical cuvets, containing 100 m*M* Tris-HCl buffer, pH 8.0, 200 μ*M* DTNB, 0.1% (v/v) Triton X-100, and sample (10–30 μL) in 1 mL.
2. The reaction is initiated by the additon of 100 μ*M* oxaloacetate to the sample cuvet and followed at 412 nm.
3. Enzyme activity is calculated using the molar extinction coefficient of 13.6×10^4 for the DTNB–coA–SH complex and is expressed as nanomoles DTNB reduced per minute per milligram of protein.

3.7. Phosphorus MRS (^{31}P-MRS) Scans

Principle: Magnetic resonance spectroscopy scans are performed in conventional radiological whole-body magnets with patients laying inside the scanner. Spectra are acquired from cardiac or skeletal muscle and then different compounds as described in this subsection. All calculations are done off-line. ^{31}P-MRS quantifies phosphorus-containing compounds and cytosolic pH. The major compounds detectable are ATP, phosphocreatine (PCr), and inorganic phosphate (Pi) (*see* **Figs. 1** and **2**). Free (metabolically active) [ADP], the major regulator of the oxidative phosphorylation, can be

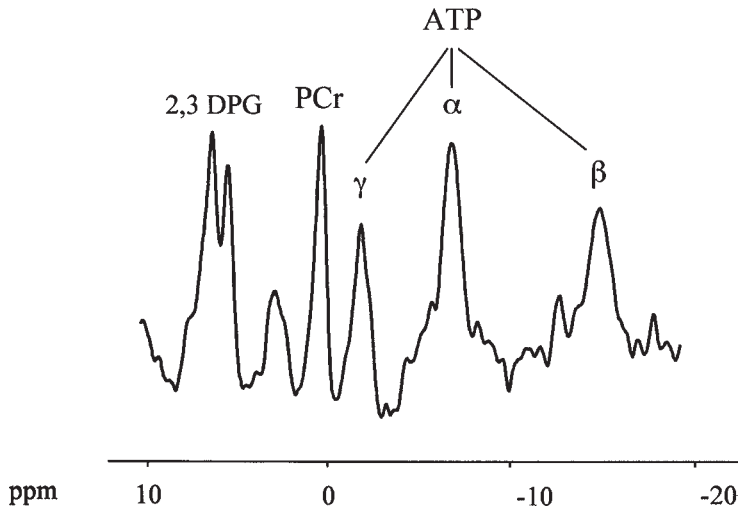

Fig. 1. ^{31}P-MRS cardiac spectrum from a healthy volunteer. 2,3 DPG indicates 2,3 diphosphoglycerate (signal coming from blood contamination), PCr indicates phosphocreatine, and α, β, and γ indicate the three phosphate groups of ATP. The abscissa reports the chemical shift in parts per million (ppm) and the ordinate reports the relative intensity.

calculated from the MRS data using the creatine kinase equilibrium expression ***(53)*** (*see* **Subheading 3.7.2.**).

3.7.1. Cardiac Muscle

Cardiac ^{31}P-MRS enables the in vivo measurement of PCr-to-ATP ratio (*see* **Fig. 1**), which has been shown by ^{31}P-MRS and conventional biochemistry (using freeze-clamped tissues) to be a good measure of the energetic state of cardiac muscle ***(54,55)***.

1. Patients are asked to lie prone in a whole-body magnet.
2. Standard spin-echo magnetic resonance imaging (MRI) is used to position the heart in the center of the magnet.
3. Cardiac ^{31}P spectra are acquired using a 7-cm circular surface coil placed below the chest. Data are acquired using a slice-selective one-dimensional spectroscopic imaging technique that separately localizes the signal from the chest wall and myocardium ***(56)***.
4. Spectra from slices identified as cardiac from their position in the proton images are analyzed using a purpose-written interactive frequency-domain-fitting program incorporating prior knowledge on chemical shifts and *j*-coupling constants and is similar to a method recently described ***(57)***.
5. After fitting, the ATP signal is corrected for blood contamination based on the amplitude of the 2,3-DPG ***(58,59)*** and saturation correction is applied to give the final PCr/ATP ratio.

3.7.2. Skeletal Muscle

Skeletal muscle is an ideal tissue in which to assess in vivo mitochondrial ATP production rate by ^{31}P-MRS, as it can be studied conveniently at rest (*see* **Fig. 2**),

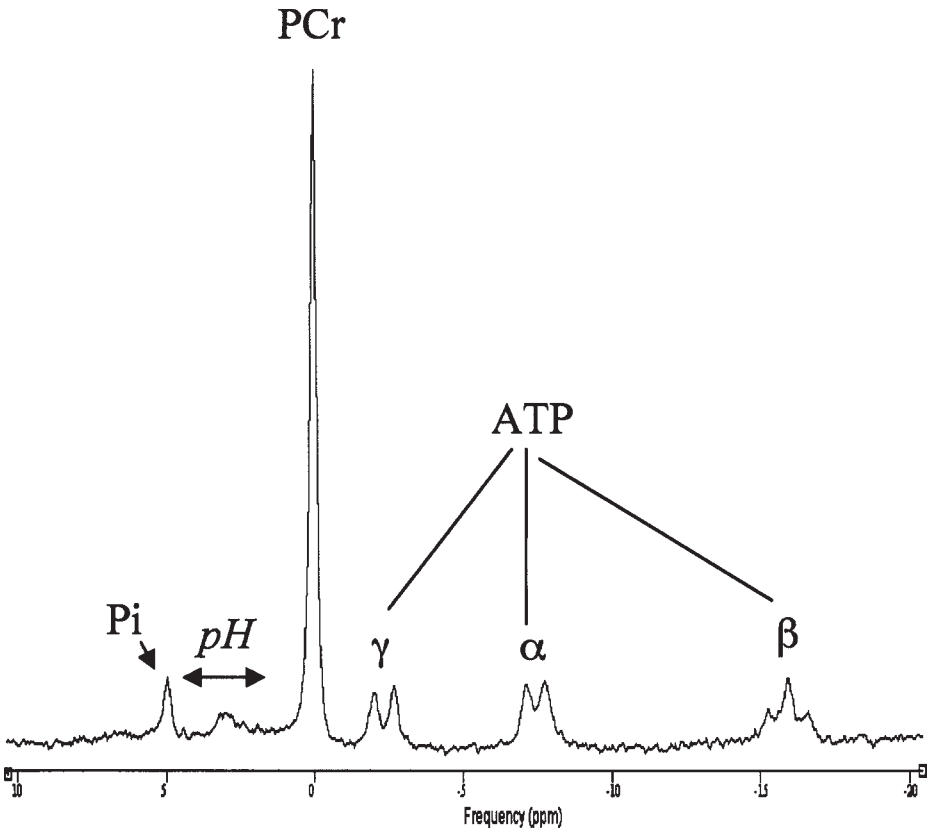

Fig. 2. ^{31}P-MRS calf muscle spectrum from a healthy volunteer at rest. Pi indicates inorganic phosphate, PCr indicates phosphocreatine, and α, β, and γ indicate the three phosphate groups of ATP. The citosolic pH is calculated from the chemical shift of Pi from PCr. The abscissa reports the chemical shift in parts per million (ppm) and the ordinate reports the relative intensity.

during exercise, and in the subsequent recovery phase ***(60)*** (*see* **Note 7**). During incremental exercise, there is a progressive reduction of PCr, hydrolyzed via the creatine kinase reaction to buffer the ATP concentration. As soon as the exercise is stopped, the PCr concentration begins to return to its preexercise values, as PCr is resynthesized from ATP. ATP production during recovery from exercise is entirely the result of oxidative phosphorylation ***(60)***; thus, the PCr resynthesis rate reflects the mitochondrial rate of ATP production.

1. Patients are asked to lie supine in a whole-body magnet.
2. Skeletal muscle ^{31}P-MRS spectra are obtained from the right calf muscle at rest, during an aerobic incremental exercise of plantar flexion, and the following recovery period (*see* **Note 7**).
3. Relative concentrations of inorganic phosphate (Pi), phosphocreatine (PCr), and ATP are

obtained by a time-domain-fitting program (VARPRO/MRUI; www.carbon.uab.es/mrui) and are corrected for magnetic saturation.

4. Absolute concentrations are obtained by assuming that the concentration of ATP in normal muscle is 8.2 m*M* (i.e., mmol/L of intracellular water) ***(61)***.
5. Intracellular pH is calculated from the chemical shift of the Pi peak relative to PCr (δ_{Pi}, measured in ppm) as

$$pH = 6.75 + \log_{10}(\delta_{Pi} - 3.27)/(5.69 - \delta_{Pi}).$$

6. Free cytosolic [ADP] was calculated from pH and [PCr] using a creatine kinase equilibrium constant of 1.66×10^9 M^{-1} ***(62)*** and assuming a normal total creatine content (TCr) of 42.5 m*M* (i.e., mmol/L of intracellular water) ***(61)*** as

$$[ADP] = [ATP][Cr]/[PCr][H^+]K_{eq}$$

where [Cr] is the concentration of creatine calculated as [TCr]–[PCr].

7. The PCr recovery half-times are calculated from the slope of semilogarithmic plots ***(53)*** using the end exercise and the first three recovery spectra.
8. Initial rates of PCr resynthesis after exercise, *V* (m*M*/min), are calculated from the exponential rate constant of PCr recovery ($k = 0.693/t_{1/2}$) and the total fall in [PCr] during exercise (Δ[PCr]) as $V = k\Delta[PCr]$ ***(53)***.
9. Using the hyperbolic ADP control model for mitochondrial respiration ***(63)*** and a normal Km for ADP of 30 μ*M* ***(49)***, the maximum rate of mitochondrial ATP synthesis (V_{max}) is calculated from the initial rate of PCr postexercise resynthesis (*V*) and the end exercise [ADP] ([ADP]end) as

$$V_{max} = V(1 + Km/[ADP]end)$$

4. Notes

1. Briefly, a dilution of CoQ_1 stock was made in ethanol and the absorbance at 275 nm of CoQ_1 was recorded. An excess (1–2 mg) of sodium borohydride (VWR) was added to the reference cuvet to completely reduce the quinone to the quinol and the absorbance change used to calculated the CoQ_1 concentration using a molar extinction coefficient of CoQ_1 of 12.25×10^3 ***(64)***.
2. The reduced cytochrome-*c* solution was transferred to size 1 dialysis tubing (Medicell International Ltd., London, UK) and dialysed against 5 L of 10 m*M* potassium phosphate buffer, pH 7.0, at 4°C for 1–3 h to remove the ascorbate. To check that no excess ascorbate remained, oxidized cytochrome-*c* was added to the dialyzed reduced sample. The assay should show that the excess oxidized cytochrome-*c* could not be further reduced (i.e., no change in absorbance). To check that cytochrome-*c* was fully reduced, the assay should show that the addition of more ascorbate acid failed to reduced the cytochrome-*c* further.
3. Different molecules can be measured in vivo using MRS for different nuclei. This chapter discusses only ^{31}P-MRS. Other metabolites can be measured with other types of MRS (like ^{1}H-MRS, ^{13}C-MRS, etc.), which are not relevant to the present chapter.
4. The spectral peaks are distinguished by their molecular configurations and characteristic spin–spin coupling patterns and are identified based on chemical shift distances in the frequency domain expressed in ppm of the field strength. Peak intensities (or areas) are proportional to the number of nuclei belonging to the corresponding molecule within the sensitive region of the signal-acquiring coil. Both cardiac and skeletal muscle typically

are used circular surface coils that, placed close to the region of interest, receive a signal from an approximate volume that corresponds to a disk with a diameter equal to that of the coil and depth equal to the radius of the coil. The resulting spectrum represents an average of the energy state of all muscle fibers within the sensitive area of the coil.

5. The protein sample (0–80 μg) is diluted to 1 mL with H_2O to which 5 mL of solution I ([2% Na_2CO_3 + 0.4% NaOH]: 1% $CuSO_4$: 2% NaK–tartrate in a ratio of 100:1:1) are added. The mixed samples are incubated for 20 min and then 0.5 mL of 50% (v/v) Follin/Ciocalteus reagent is added to each sample at 15 s intervals. The sample is mixed and incubated for a further 45 min, after which time, sample absorbances are recorded at 750 nm. Protein concentrations are calculated against standard samples of 0, 20, 40, 60, 80, and 100 μg of BSA ***(65)***.
6. To optimize the complex I activity in platelet mitochondrial fractions, modified reagents are used: 20 m*M* potassium phosphate buffer, pH 7.2, including 8 m*M* $MgCl_2$ and 2.5 mg/mL BSA (essentially fatty acid free). The assay is performed as described in **Subheading 3.3.**
7. The muscle is exercised by plantar flexion at 0.5 Hz, lifting a weight of 10% of lean-body mass (calculated from body weight and skin-fold thickness) through a distance of 7 cm. After the first 4 min of exercise, the weight is incremented by 2% of lean-body mass for each subsequent minute of acquisition. Exercise is stopped when the level of PCr is about half of that at rest. Healthy volunteers typically exercise from 8 to 15 min.

References

1 Gusella, J. F. and MacDonald, M. E. (2000) Molecular genetics: unmasking polyglutamine triggers in neurodegenerative disease. *Nature Rev. Neurosci.* **1,** 109–115.

2 Snell, R. G., MacMillan, J. C., Cheadle, J. P., et al. (1993) Relationship between trinucleotide repeat expansion and phenotypic variation in Huntington's disease. *Nature Genet.* **4,** 393–397.

3 Difiglia, M., Sapp, E., Chase, K. O., et al. (1997) Aggregation of huntingtin in neuronal intranuclear inclusions and dystrophic neurites in brain. *Science* **277,** 1990–1993.

4 Davies, S. W., Turmaine, M., Cozens, B. A., et al. (1997) Formation of neuronal intranuclear inclusions underlies the neurological dysfunction in mice transgenic for the HD mutation. *Cell* **90,** 537–548.

5 Hansson, O., Guatteo, E. E., Mercuri, N. B., et al. (2001) Resistance to NMDA toxicity correlates with appearance of nuclear inclusions, behavioural deficits and changes in calcium homeostasis in mice transgenic for exon 1 of the huntington gene. *Eur. J. Neurosci.* **14,** 1492–1504.

6 Cooper, J. K., Schilling, G., Peters, M. F., et al. (1998) Truncated N-terminal fragments of huntingtin with expanded glutamine repeats form nuclear and cytoplasmic aggregates in cell culture. *Hum. Mol.Genet.* **7,** 783–790.

7 Lunkes, A. and Mandel, J. L. (1998) A cellular model that recapitulates major pathogenic steps of Huntington's disease. *Hum. Mol. Genet.* **7,** 1355–1361.

8 Martindale, D., Hackam, A., Wieczorek, A., et al. (1998) Length of huntingtin and its polyglutamine tract influences localization and frequency of intracellular aggregates. *Nature Genet.* **18,** 150–154.

9 Saudou, F., Finkbeiner, S., Devys, D., et al. (1998) Huntingtin acts in the nucleus to induce apoptosis but death does not correlate with the formation of intranuclear inclusions. *Cell* **95,** 55–66.

10 DiFiglia, M., Sapp, E., Chase, K., et al. (1995) Huntingtin is a cytoplasmic protein associated with vesicles in human and rat brain neurons. *Neuron* **14,** 1075–1081.

11 Velier, J., Kim, M., Schwarz, C., et al. (1998) Wild-type and mutant huntingtins function in vesicle trafficking in the secretory and endocytic pathways. *Exp. Neurol*. **152,** 34–40.
12 Stahl, W. L. and Swanson, P. D. (1974) Biochemical abnormalities in Huntington's chorea brains. *Neurology* **24,** 813–819.
13 Butterworth, J., Yates, C. M., and Reynolds, G. P. (1985) Distribution of phosphate-activated glutaminase, succinic dehydrogenase, pyruvate dehydrogenase and gamma-glutamyl transpeptidase in post-mortem brain from Huntington's disease and agonal cases. *J. Neurol. Sci.* **67,** 161–171.
14 Brennan, W. A., Jr., Bird, E. D., and Aprille, J. R. (1985) Regional mitochondrial respiratory activity in Huntington's disease brain. *J. Neurochem.* **44,** 1948–1950.
15 Mann, V. M., Cooper, J. M., Javoy-Agid, F., et al. (1990) Mitochondrial function and parental sex effect in Huntington's disease. *Lancet* **336,** 749.
16 Gu, M., Gash, M. T., Mann, V. M., et al. (1996) Mitochondrial defect in Huntington's disease caudate nucleus. *Ann. Neurol.* **39,** 385–389.
17 Browne, S. E., Bowling, A. C., MacGarvey, U., et al. (1997) Oxidative damage and metabolic dysfunction in Huntington's disease: selective vulnerability of the basal ganglia. *Ann. Neurol.* **41,** 646–653.
18 Parker, W. D., Jr., Boyson, S. J., Luder, A. S., et al. (1990) Evidence for a defect in NADH: ubiquinone oxidoreductase (complex I) in Huntington's disease. *Neurology* **40,** 1231–1234.
19 Tabrizi, S. J., Cleeter, M. W., Xuereb, J., et al. (1999) Biochemical abnormalities and excitotoxicity in Huntington's disease brain. *Ann. Neurol.* **45,** 25–32.
20. Hausladen, A. and Fridovich, I. (1994) Superoxide and peroxynitrite inactivate aconitases, but nitric oxide does not. *J. Biol. Chem.* **269,** 29,405–29,408.
21. Gardner, P. R., Nguyen, D. D., and White, C. W. (1994) Aconitase is a sensitive and critical target of oxygen poisoning in cultured mammalian cells and in rat lungs. *Proc. Natl. Acad. Sci. USA* **91,** 12,248–12,252.
22 Patel, M., Day, B. J., Crapo, J. D., et al. (1996) Requirement for superoxide in excitotoxic cell death. *Neuron* **16,** 345–355.
23 Lodi, R. R., Schapira, A. H., Manners, D., et al. (2000) Abnormal in vivo skeletal muscle energy metabolism in Huntington's disease and dentatorubropallidoluysian atrophy. *Ann. Neurol.* **48,** 72–76.
24 Jenkins, B. G., Koroshetz, W. J., Beal, M. F., et al. (1993) Evidence for impairment of energy metabolism in vivo in Huntington's disease using localized 1H NMR spectroscopy. *Neurology* **43,** 2689–2695.
25 Jenkins, B. G., Rosas, H. D., Chen, Y. C. I., et al. (1998) ^{1}H NMR spectroscopy studies of Huntington's disease. Correlations with CAG repeat numbers. *Neurology* **50,** 1357–1365.
26 Koroshetz, W. J., Jenkins, B. G., Rosen, B. R., et al. (1997) Energy metabolism defects in Huntington's disease and effects of coenzyme Q10. *Ann. Neurol.* **41,** 160–165.
27. Harding, A. H. (1981) Friedreich's ataxia: a clinical and genetic study of 90 families with an analysis of early diagnostic criteria and intrafamilial clustering of clinical features. *Brain* **104,** 598–620.
28 Durr, A., Cossee, M., Agid, Y., et al. (1996) Clinical and genetic abnormalities in patients with Friedreich's ataxia. *N. Engl. J. Med.* **335,** 1169–1175.
29 Campuzano, V., Montermini, L., Molto', M. D., et al. (1996) Friedreich's ataxia: autosomal recessive disease caused by an intronic GAA triplet repeat expansion. *Science* **271,** 1423–1427.
30 Lamont, P. J., Davis, M. B., and Wood, N. W. (1997) Identification and sizing of the GAA

trinucleotide repeat expansion of Friedreich's ataxia in 56 patients. Clinical and genetic correlates. *Brain* **120,** 673–680.

31 Filla, A., DeMichele, G., Cavalcanti, F., et al. (1996) The relationship between trinucleotite (GAA) repeat length and clinical features in Friedreich ataxia. *Am. J. Hum. Genet.* **59,** 554–560.

32 Isnard, R., Kalotka, H., Durr, A., et al. (1997) Correlation between left ventricular hypertrophy and GAA trinucleotide repeat length in Friedreich's ataxia. *Circulation* **95,** 2247–2249.

33 Campuzano, V., Montermini, L., Lutz, Y., et al. (1997) Frataxin is reduced in Friedreich ataxia patients and is associated with mitochondrial membranes. *Hum. Mol. Genet.* **6,** 1771–1780.

34 Babcock, M., DeSilva, D., Oaks, R., et al. (1997) Regulation of mitochondrial iron accumulation by Yfh1p, a putative homolog of frataxin. *Science* **276,** 1709–1712.

35 Koutnikova, H., Campuzano, V., Foury, F., et al. (1997) Studies of human, mouse and yeast homologoues indicate a mitochondrial function for frataxin. *Nature Genet.* **16,** 345–351.

36 Babcock, M., DeSilva, D., Oaks, R., et al. (1997) Regulation of mitochondrial iron accumulation by Yfh1p, a putative homolog of frataxin. *Science* **276,** 1709–1712.

37 Koutnikova, H., Campuzano, V., and Koenig, M. (1998) Maturation of wild-type and mutated frataxin by the mitochondrial processing peptidase. *Hum. Mol Genet.* **7,** 1485–1489.

38 Priller, J., Scherzer, C. R., Faber, P. W., et al. (1997) Frataxin gene of Friedreich's ataxia is targeted to mitochondria. *Ann. Neurol.* **42,** 265–269.

39 Rotig, A., de Lonlay, P., Chretien, D., et al. (1997) Aconitase and mitochondrial iron-sulphur protein deficiency in Friedreich ataxia. *Nature Genet.* **17,** 215–217.

40 Bradley, J. L., Blake, J. C., Chamberlain, S., et al. (2000) Clinical, biochemical and molecular genetic correlations in Friedreich's ataxia. *Hum. Mol. Genet.* **9,** 275–282.

41 Melov, S., Coskun, P., Patel, M., et al. (1999) Mitochondrial disease in superoxide dismutase 2 mutant mice. *Proc Natl Acad Sci USA* **96,** 846–851.

42 Puccio, H., Simon, D., Cossee, M., et al. (2001) Mouse models for Friedreich ataxia exhibit cardiomyopathy, sensory nerve defect and Fe–S enzyme deficiency followed by intramitochondrial iron deposits. *Nature Genet.* **27,** 181–186.

43 Lodi, R., Rajagopalan, B., Blamire, A. M., et al. (2001) Cardiac energetics are abnormal in Friedreich ataxia patients in the absence of cardiac dysfunction and hypertrophy. An in vivo ^{31}P magnetic resonance spectroscopy study. *Cardiovasc. Res.* **52,** 111–119.

44 Rabinowitz, M. (1974) Overview on pathogenesis of cardiac hypertrophy. *Circ. Res.* **35(Suppl. II),** 3–11.

45 Antozzi, C. and Zeviani, M. (1997) Cardiomyopathies in disorders of oxidative metabolism. *Cardiovasc. Res.* **35,** 184–199.

46 Lodi, R., Cooper, J. M., Bradley, J. L., et al. (1999) Deficit of in vivo mitochondrial ATP production in patients with Friedreich ataxia. *Proc. Natl. Acad. Sci. USA* **96,** 11,492–11,495.

47 Lodi, R., Taylor, D. J., Tabrizi, S. J., et al. (1997) In vivo skeletal muscle mitochondrial function in Leber's hereditary optic neuropathy assessed by ^{31}P-MR spectroscopy. *Ann. Neurol.* **42,** 573–579.

48 Lodi, R., Hart, P. E., Rajagopalan, B., et al. (2001) Antioxidant treatment improves in vivo cardiac and skeletal muscle bioenergetics in patients with Friedreich's ataxia. *Ann. Neurol.* **49,** 590–596.

49. Ragan, C. I. (1987) Structure of NADH-ubiquinone reductase (Complex I). *Curr. Topics Bioenergetics* **15,** 1–36.
50 King, T. E. (1967) Preparations of succinate-cytochrome-*c* reductase and the cytochrome b-c1 particle, and reconstitution of succinate-cytochrome-*c* reductase. *Methods Enzymol.* **10,** 275–296.
51 Wharton, D. C. and Tzagoloff, A. (1967) Cytochrome oxidase from beef heart mitochondria. *Methods Enzymol.* **10,** 245–250.
52 Coore, H. G., Denton, R. M., Martin, B. R., et al. (1971) Effects of insulin and adrenaline on rat epididymal-fat-pad pyruvate dehydrogenase. *Biochem. J.* **123,** 38P-39P.
53 Kemp, G. J., Taylor, D. J., and Radda, G. K. (1993) Control of phosphocreatine resynthesis during recovery from exercise in human skeletal muscle. *NMR Biomed.* **6,** 66–72.
54 Ingwall, J. S., Kramer, M. F., and Fifer, M. A. (1985) The creatine kinase system in normal and diseased human myocardium. *N. Engl. J. Med.* **313,** 1050–1054.
55 Radda, G. K. (1986) The use of NMR spectroscopy for the understanding of disease. *Science* **233,** 640–645.
56 Blamire, A. M., Rajagopalan, B., and Radda, G. K. (1999) Measurement of myocardial pH by saturation transfer in man. *Magn. Reson. Med.* **41,** 198–203.
57 Slotboom, J., Boesch, C., and Kreis, R. (1998) Versatile frequency domain fitting using time domain models and prior knowledge. *Magn. Reson. Med.* **39,** 899–911.
58 Conway, M. A., Bottomley, P. A., Ouwerkerk, R., et al. (1998) Mitral regurgitation: impaired systolic function, eccentric hypertrophy, and increased severity are linked to lower phosphocreatine/ATP ratios in humans. *Circulation* **97,** 1716–1723.
59 Hardy, C. J., Weiss, R. G., Bottomley, P. A., et al. (1991) Altered high-energy phosphate metabolites in patients with dilated cardiomyopathy. *Am. Heart J.* **122,** 795–801.
60 Lodi, R., Kemp, G. J., Iotti, S., et al. (1997) Influence of cytosolic pH on in vivo assessment of human muscle mitochondrial respiration by phosphorus magnetic resonance spectroscopy. *Magma* **5,** 165–171.
61 Arnold, D. L., Matthews, P. M., and Radda, G. K. (1984) Metabolic recovery after exercise and the assessment of mitochondrial function in vivo in human skeletal muscle by means of P-31 NMR. *Magn. Reson. Med.* **1,** 307–315.
62 Veech, R. L., Lawson, J. W. R., Cornell, N. W., et al. (1979) Cytosolic phosphorylation potential. *J. Biol. Chem.* **254,** 6538–6547.
63 Chance, B., Leigh, J., Jr., Kent, J., et al. (1986) Multiple controls of oxidative metabolism of living tissues as studied by ^{31}P MRS. *Proc. Natl. Acad. Sci. USA* **83,** 9458–9462.
64 Redfearn, E. R. (1967) Isolation and determination of ubiqinone. *Methods Enzymol.* **10**, 381–384.
65. Lowry, O. H., Rosebrough, N. J., Farr, A. L., et al. (1951) Protein measurement with the folin reagent. *J. Biol. Chem.* **193,** 265–275.

21

Triplet Repeats and DNA Repair

Germ Cell and Somatic Cell Instability in Transgenic Mice

Irina V. Kovtun, Craig Spiro, and Cynthia T. McMurray

Summary

This chapter describes methods for the isolation of specific cell types that reveal how and where expansion can occur. For the hereditary component of expansion, the male germ cell has proved useful in distinguishing processes that can contribute to expansion, as described in our article (*Nature Genetics* **27,** 407, 2001). Mature spermatazoa (SZs) can be isolated directly from the epididymis. Haploid spermatids (STs), diploid spermatagonia (SGs), and tetraploid spermatocytes (SCs) can be removed from the testis and sorted by fluorescence-activity cell sorting (FACS); differences in DNA content and morphology allow resolution by fluorescence and light scattering. Repeat-length measurement can pinpoint the stage at which expansion occurs. Because the timing of meiosis and mitosis with respect to sperm development is known, the analysis can distinguish repair and replication processes. Furthermore, the possible contribution of Y- or X-specific factors can be evaluated by sorting X- and Y-bearing germ cells. To enable analysis of female germ cells, we describe methods for oocyte preparations and a method for the isolation of the eight-cell-stage embryo. Therefore, the methods described here can help to answer such questions as the timing during development of expansion, whether expansion is limited to a single period, whether both replication and repair contribute to instability, and the role of somatic instability in disease. If further expansion of the inherited allele contributes to the phenotype, then intervention in somatic tissue might be therapeutic.

Key Words: R6/1 transgenic mice; testicular cell; oocyte; embryo; cell sorting.

From: *Methods in Molecular Biology, vol. 277: Trinucleotide Repeat Protocols*
Edited by: Y. Kohwi © Humana Press Inc., Totowa, NJ

1. Introduction

Triplet expansion is caused, at least in part, by ineffective action of normal DNA repair proteins ***(1,2)***. Trinucleotide repeat (TNR) expansion does not occur in the context of genomewide instability ***(1,3,4)***. The single disease allele is the only site that is affected, so that properties of the allele but not defective proteins cause expansion. Rather, expansion arises because of aberrant surveillance, processing, or repair at the repetitive DNA of the disease alleles. For example, the formation of a secondary structure at expansion-prone TNRs inhibits the action of the flap endonuclease (FEN-1) ***(5,6)***, which is critical for mutation avoidance as well as for lagging strand DNA synthesis ***(7,8)***.

At least three DNA repair processes have been implicated in the expansion mechanism: mismatch repair (MMR) ***(9–11)***, flap processing by endonuclease FEN-1 ***(5,6,12–14)***, and double-strand break repair requiring MRE11/RAD50 ***(15)***. Strand separation during replication or repair can allow formation of hairpins containing mismatches ***(16,17)***. MMR may not only fail to repair but may also stabilize the structures, thereby interfering with the action of repair proteins such as FEN-1 ***(5,6,9–11,18)***. Strand breaks can arise during DNA synthesis. Polymerase may fail to fully traverse the repeats, resulting in stalling of the replication fork and chromosome breakage ***(19,20)***. In yeast, repair of double-strand breaks induces repeat instability that is dependent on MRE11/Rad50 ***(15)***. In vitro studies have shown that expansion also can arise during repair of abasic sites ***(21)***.

Studies in vitro and in simple organisms—such as yeast and bacteria—have helped elucidate features of repeat expansion and have identified candidate repair proteins that may participate in expansion. However, simple organisms are not sufficient models. Questions about the developmental-stage and tissue specificity of expansion cannot be addressed in unicellular organisms, and instability in yeast and bacteria differs from that in humans. In simple organisms, the changes in long TNR tracts are almost all deletions, but in human disease, expansions predominate.

Therefore, studies in mammals can contribute not only to understanding how disease alleles arise and are transmitted but may also offer a means toward ameliorating disease in affected individuals. Expansion in mammals comprises both somatic and germ cell components, and often these can be recapitulated in transgenic models. For example, the R6/1 mouse model for Huntington's disease (HD) ***(22)*** shows both intergenerational and somatic instability ***(9,10,23)***. An analysis of TNR in a mouse model of HD has shown that TNRs are very unstable in striatum—the region of the brain most susceptible in disease—as compared to other tissues ***(24)***. Similarly, expansion in germ cells of R6/1 mice has revealed that expansion in males occurs during sperm maturation ***(10)***. For both somatic and germ cell expansion, the MMR protein Msh2 has been shown to be essential. In the absence of Msh2, repeats in R6/1 mice are stabilized ***(9,10)***.

Studies in R6/1 mice have, therefore, helped refine models of TNR instability ***(9,10)***. More powerful analysis is possible when mice harboring the disease-length human allele (hHD) are bred with mice specifically altered for DNA repair capability

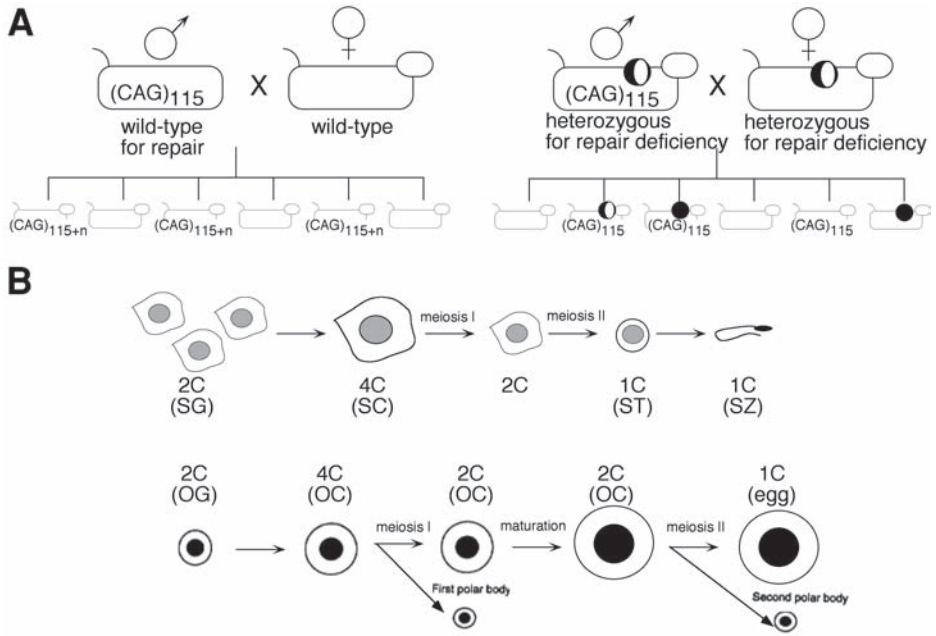

Fig. 1. **(A)** Example of in vivo scheme for testing the role of DNA repair proteins. Mice harboring the disease-length human Huntington's disease allele (hHD) are bred (left) with mice that are heterozygous for repair deficiency (striped). Some of the offspring inherit the hHD allele (indicated by the number of CAG repeats); some are wild type for repair (plain) and some have a single defective repair allele (striped). A heterozygous offspring with hHD allele is then bred with a female heterozygous for repair (right). Among the offspring are mice wild type, heterozygous, and homozygous (filled) for the repair defect. Mice are analyzed for CAG repeat number and repair proteins. **(B)** Schematic of spermatogenesis. The ploidy of cells in each developmental stage is shown. Germ cell precursors, spermatogonia (SGs), are 2C and undergo mitotic replication producing 4C primary spermatocytes (SCs). SC then undergo a rapid first division, producing secondary spermatocytes (2C), which, in turn, generate round spermatids (STs) in the second meiotic division. ST undergo terminal differentiation into spermatozoa (SZs), which travel the epididymis to become mature sperm capable of fertilizing an oocyte. **(C)** Schematic representation of oogenesis. Diploid (2C) oogonia (OG), upon replication, give rise to tetraploid oocytes (OC, 4C) (primary), which undergo first meiotic reduction producing diploid secondary oocytes (OC, 2C). Diploid oocytes that are arrested in the metaphase of meiosis II go through the process of maturation increasing in size. The second meiosis, generating the mature egg, occurs after fertilization.

(25) (*see* **Fig. 1A**). Offspring may harbor the hHD allele in a wild-type repair context or in a deficient repair context. Analysis of repeat length of the hHD allele in tissues of the offspring provides direct evidence on the role of the repair pathway in protecting from or promoting instability in both the parent and offspring. In addition, analysis of DNA repair protein content in different tissues at certain stages of development and differentiation can be useful.

2. Materials

2.1. Animals

The HD transgenic male (line B6CBA-TgN R6/1) was purchased from Jackson Laboratory and bred to B6CBA female partner. Litters were routinely screened for the presence of HD transgene by polymerase chain reaction (PCR) ***(9,10,22)***.

2.2. Reagents

1. Phosphate-buffered saline (PBS) solution, pH 7.4 (without Ca^{2+} and Mg^{2+}).
2. Hoechst 33342 (BisBenzimide H 33342; Calbiochem), 5 mg/mL in water. Store in aliquots at –20°C.
3. Hanks balanced salt solution (HBSS) (Sigma).
4. Collagenase (Worthington).
5. Lysozyme (Sigma).
6. Bovine serum albumin (BSA) (10 mg/mL).
7. Trypan blue (Sigma).
8. TENS buffer: 100 m*M* NaCl, 1% sodium dodecyl sulfate (SDS), 10 m*M* Tris-HCl, pH 8.0, 1 m*M* EDTA.
9. Proteinase K, 20 mg/mL (stored in aliquots at –20°C).
10. TE buffer: 10 m*M* Tris-HCl, pH 8, 1 m*M* EDTA.
11. Acidic Tyrode's solution: embryo culture medium (Sigma).
12. Sodium lactate, 60% (w/w) (Sigma).
13. Sodium pyruvate (Sigma): 100 m*M* for stock.
14. Ultrapure mineral oil.
15. Quantilyse (Hamilton Thorne Research, Inc.) lysis buffer.
16. Spectrum Orange (Imagenetics).
17. Spectrum Green (Imagenetics).

3. Methods

3.1. Preparation of Testicular Single-Cell Suspension

1. Remove testes from a single mouse and place into Petri dish with HBSS, supplemented with 6 m*M* lactate and 3 m*M* pyruvate.
2. Decapsulate each testis, removing tunica albunigea. Place seminiferous tubules into a Petri dish with fresh HBSS containing lactate and pyruvate. Transfer tubules to a 50-mL Falcon tube and wash twice with 30–40 mL of HBSS, allowing them to settle. Aspirate liquid.
3. Dissociate tubules by enzymatic digestion with 1 mg/mL collagenase in 20 mL of HBSS preheated at 37°C. Shake suspension by hand 8–10 times, let tubules settle, aspirate supernatant, and add 20 mL of HBSS.
4. Pour tubules into Petri dish and chop with razor blade.
5. Pour suspension using funnel over five layers of cheesecloth into a 50-mL tube. Centrifuge filtered supernatant at 1000 rpm (400*g*) for 3 min at room temperature.
6. Aspirate supernatant, resuspend cell pellet in 20 mL PBS, vortex, and centrifuge as in **step 5**.
7. Repeat **step 6** twice more to remove all the traces of collagenase.
8. Aspirate supernatant and resuspend pellet in 2–3 mL of PBS.
9. Count cells using trypan blue staining. The expected number of testicular cells from a single animal is $(5–7) \times 10^6$.

10. For sorting, concentration of cells should not exceed 2×10^6 mL^{-1}. Make necessary dilutions.
11. Sort all of the material.

3.2. Cell Sorting

1. Add 3 µL of 5 mg/mL Hoechst solution to 2–3 mL of final testicular cell suspension. Incubate at room temperature for 30–60 min (covered with foil).
2. Prepare three collection tubes with PBS supplemented with BSA (20–30 µg per 500 µL of PBS).
3. Testicular cells are sorted using Becton Dickinson FACStar Plus flow cytometer. A 5-W argon laser is used for fluorescent excitation of the sample. Such sorting parameters as flow pressure and drop delay should be adjusted for each sample (*see* **Note 1**). Fluorescence emission and light scattering are used to discriminate and sort haploid, diploid, and tetraploid subpopulations of testicular cells (*see* **Fig. 2**). The major peak corresponds to haploid spermatids (STs) (at least 75% of total). The two smaller peaks represent diploid spematogonia (SGs) and tetraploid spermatocytes (SCs) (*see* **Figs. 1B** and **2B**). Secondary spermatocytes produced in the first meiotic division comprise a population of diploid cells (along with spermatogonia) (*see* **Fig. 1B**), but they are rarely detected due to their short life-span.
4. Analyze to determine presence and TNR size of disease allele as described below (*see* **Note 2**).
5. Analyze sorted populations for specific repair proteins by immunoblot (*see* **Note 3**).

3.3. DNA Preparation and Amplification

1. To isolate DNA, add 200 µL of TENS buffer and 25 µL of proteinase K to the cell pellet, vortex to mix, and incubate at 50°C until cells are completely lysed (can be left overnight).
2. Add 100 µL of saturated NaCl solution and vortex to mix. Incubate at 55°C for 10 min and microfuge at 5200*g* for 20 min at room temperature.
3. Transfer supernatant to a clean Eppendorf tube, add 2 vol of ice-cold 100% ethanol, and invert to mix.
4. Place at –20°C for 30 min. Microfuge sample at maximum speed for 20 min, then decant supernatant, add 300 µL of 70% ethanol, and invert to mix.
5. Microfuge at maximum speed for 5 min. Remove supernatant and allow pellet to air-dry.
6. Resuspend pellet in 30 µL TE buffer and store at –20°C until needed. For DNA amplification, add 1 µL of each primer (10 µ*M*) to amplification buffer (total reaction volume is 20 µL). Upstream primer: 5' ATGAAGGCCTTCGAGTCCCTCAAGTCCTTC-3' labeled with a fluorescence tag, [(3',6'-dipivaloy fluoresceinyl)-6-carboxamidohexyl]-1-*O*-(2-cyanoethyl)-(*N*,*N*-diisopropyl)-phosphor amidite (6-FAM) (Glen Research); downstream primer: 5'-GCGGCTGAGAGGCGAGGA-3'. Use 10 µL of DNA from total 30-µL volume obtained from sorted cells (*see* **Note 2**) to amplify hHD gene with specific primers (*see* **step 1**). Cycling conditions as described in **ref. *10***. Briefly, 40 cycles: 30 s at 94°C, 30 s at 65°C, 90 s at 72 s, preceded by initial denaturation for 90 s at 94°C, and followed by final extension for 10 min at 72°C.

3.4. Preparation of Spermatozoa Suspension

1. Dissect out epididymis of 7- to 12-wk-old male. Use fine tweezers to clean epididymis from blood vessels. Place epididymis in a Petri dish with PBS and chop with scissors (*see* **Note 4**).

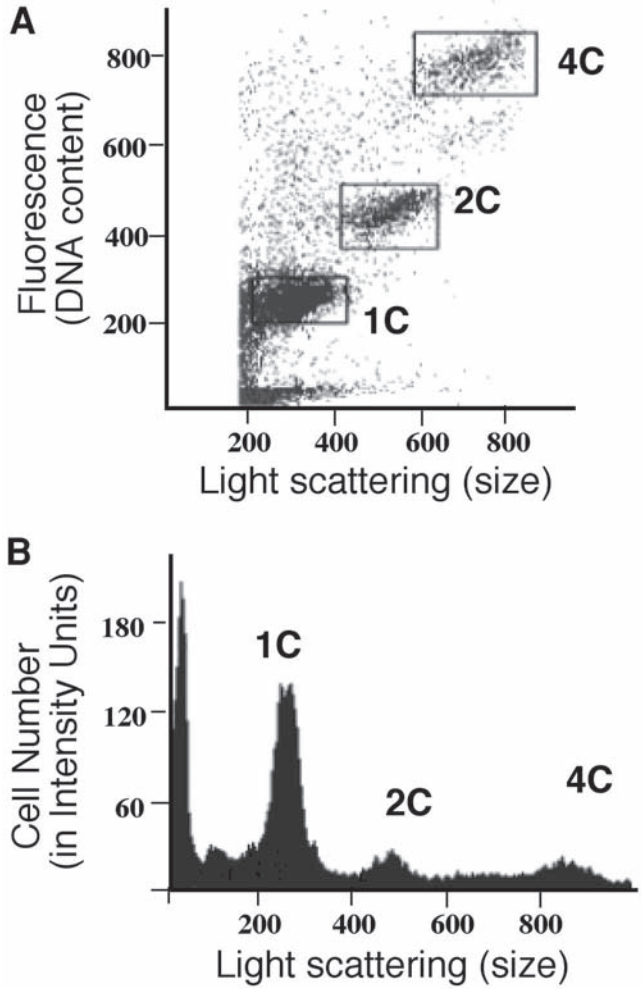

Fig. 2. Flow-sorting data for testicular cells. **(A)** Light scattering on the abscissa and Hoechst staining on the ordinate. Three major populations of sorted testicular cells are indicated. **(B)** Cell distribution showing cell number in arbitrary units (ordinate) after separation using Hoechst staining (abscissa axis).

2. Filter the suspension through five layers of cheesecloth. Centrifuge at 400*g* for 3 min at room temperature.
3. Resuspend the pellet in fresh PBS and repeat **step 2**.
4. Resuspend pellet in 3 mL of PBS and sonicate final suspension to break tails.
5. Count cells using trypan blue staining. The expected number of spermatozoa in suspension is (8–10) × 10^6.

3.5. Sorting for X- and Y-Bearing Spermatozoa

1. Stain sperm suspension with Hoechst dye according to **step 1** of **Subheading 3.2.**

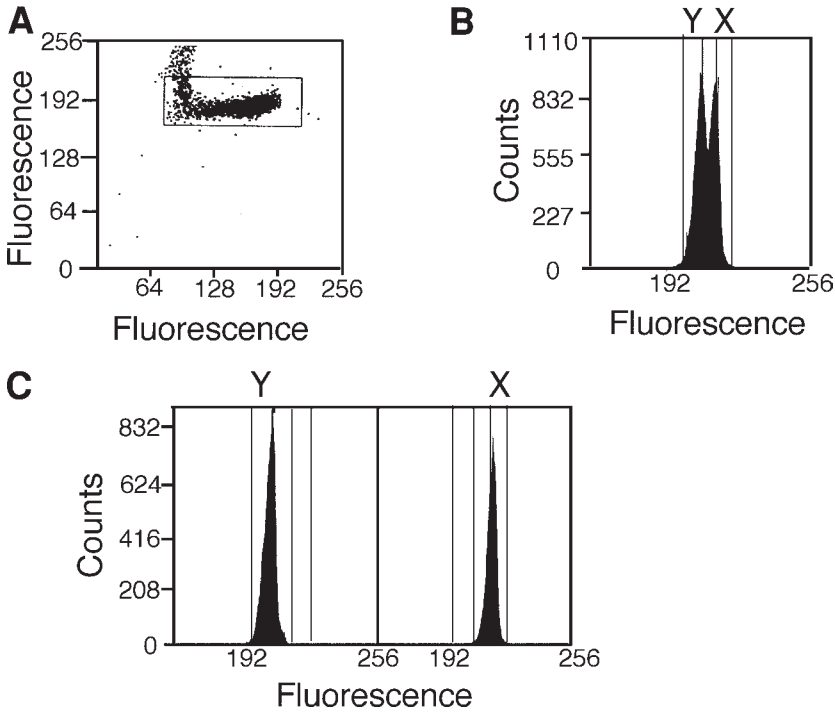

Fig. 3. **(A)** Properly oriented spermatozoa (gated population is shown in the box) were detected by a 90° fluorescence detector. **(B)** The fluorescence profile from a 0° detector. The two peaks are approx 2.8% apart, resulting in overlap. Nonoverlapping areas of the peaks, representing populations enriched in Y and X sperm (left and right peak, respectively), were selected by the electronic sort windows and collected into tubes. **(C)** Aliquots of both sorted populations were reanalyzed to assure the accuracy of sorting.

2. Sperm samples are sorted using a modified FACS Vantage (Becton Dickinson) with an argon laser operating in the ultraviolet spectrum. Modifications for the instrument developed by Johnson and coworkers ***(26–28)*** include sample injection tip (beveled needle) designed to control the orientation of the spermatozoa to the laser beam and additional fluorescence detector positioned at a right angle (90°) to measure the fluorescence from the properly oriented cells. Therefore, fluorescence heterogeneity as a result of high compactness of chromatin in spermatozoa can be diminished by detecting the fluorescence at a 0° angle but from only those cells that are properly oriented (i.e., whose edge is aligned with the 90° detector). The fluorescent signal from spermatozoa stained with Hoechst is proportional to sperm orientation in the laser beam or DNA content depending on the angle of detection. The signal from spermatozoa oriented with their brightest edge toward the 90° detector (highlighted peak) is collected by the 0° detector and represents bimodal distribution (*see* **Fig. 3B**). Thus, the modifications of flow cytometer allow separation of X- and Y-chromosome-bearing spermatozoa based on the 2.8–3% total DNA content difference. Smaller (left) peak contains Y-bearing sperm and larger (right) peak contains

X-bearing sperm (*see* **Fig. 3A,B**). These two populations are electrostatically separated by the flow sorter.
3. Aliquots of both sorted populations are reanalyzed to assure accuracy of sorting (*see* **Fig. 3C**).
4. Identities of sorted spermatozoa are confirmed by double FISH ***(29)*** (fluorescent *in situ* hybridization) analysis using X- and Y-chromosome-specific probes (*see* **Note 5**).

3.6. Preparation of Oocyte Cell Suspension

The method is adapted to isolate mouse oocytes free of somatic tissue ***(30)***.

1. Remove ovaries from adult female (older than 6 wk). Remove as much surrounding connective and fat tissue as possible.
2. Place ovaries into a Petri dish filled with PBS. Tear each ovary into four to five pieces with forceps.
3. Transfer preparation into a 15-mL conical centrifuge tube filled with 10 mL PBS supplemented with 1 mg/mL lysozyme and 0.1% collagenase. Incubate for 30 min at 37°C in shaking water bath.
4. Transfer the preparation to a 100-mm Petri dish and replace enzymatic solution with PBS by sequential dilution.
5. Using a dissecting microscope (15×), pick up individual oocytes with a micropipet.
6. Prepare a 60- or 100-mm dish with several drops of fresh PBS under mineral oil (ultrapure grade). Rinse oocytes several times by transferring them through a series of PBS drops.
7. Transfer oocytes to microfuge tube and pellet by a 5-min spin at maximum speed. Aspirate supernatant carefully. Proceed with DNA isolation or store cells at –70°C until used.
8. Routinely, 50–70 oocytes can be recovered from a single mouse. All oocytes collected from mature female mouse are diploid (have undergone one meiotic reduction) and represent different stages of maturation (judged by difference in size) (*see* **Fig. 1C**).

3.7. Eight-Cell Embryo Isolation

B6CBA females are bred with B6CBA-TgN R6/1 males carrying the hHD transgene. Females are sacrificed at 56–60 h postcoitum (determined by presence of vaginal plug).

1. Open the abdominal cavity. Extract the uterus, oviduct, and ovary with fine forceps. Cut out both oviducts with fine scissors. Transfer oviducts to a 35-mm culture dish with prewarmed cell medium.

All of the following steps are conducted as close to sterile conditions as possible. Use hood when possible to eliminate cross-contamination.

2. Using the dissecting stereomicroscope (Leica Mz12.5, ×40), find the opening to the oviduct (infundibulum) and, holding oviduct with fine forceps, insert needle into the infundibulum. Flush with medium to recover the eight-cell-stage embryos.
3. Prepare a 100-mm dish with drops of acidified Tyrode's solution corresponding to number of embryos and with drops of PBS containing 5 mg/mL polvinylpyrolidine corresponding to the number of embryos ×3, overlayed with mineral oil.
4. To remove the zona pellucida, transfer each embryo to a drop of Tyrode's solution with a flame-polished finely pulled glass capillary using a dissecting stereomicroscope. Wash each embryo by transferring through three drops of PBS.

5. Disaggregate the entire embryo with finely pulled glass capillary under a dissecting stereomicroscope at ×40 magnification to obtain single blastomeres.
6. Wash single blastomeres through three drops of PBS containing 5 mg/mL polvinyl pyrolidine.
7. Transfer individual blastomeres to appropriately labeled microcentrifuge tubes containing 10 μL of Quantilyse overlayed with PCR grade mineral oil.
8. Lyse cells at 50°C for 30 min, followed by a 15-min incubation at 98°C to inactivate the proteinase K.
9. Use aliquots of PBS from the wash drops as contamination controls.
10. Store all samples at –70°C prior to PCR amplification (*see* **Note 6**).

4. Notes

1. Cell-sorting parameters are determined by selection of upper and lower thresholds for both light scatter and fluorescence emission. These settings must be adjusted from sample to sample. They depend on such factors as cell density, clumping, and staining efficiency, which vary. A flow rate as high as 5000 cells/s can be achieved in the system. Intact cells can be easily distinguished according to their right-angle scatter and forward-scatter characteristics. Debris then can be eliminated from the analysis to allow sorting by direct gating on intact cells (*see* **Fig. 2A**). Because of the higher number of STs in the suspension (constitutes 75% of the total), it is easier to obtain sufficient number of STs per each sorting session. Therefore, we recommend starting with the other two groups (SGs and SCs) and using 80% of the sample until 200,000 of each are collected. The remaining 20% is sufficient to obtain 200,000 or more STs.
2. GeneScan analysis is performed as described elsewhere ***(10,22,23)***. Results from PCR analysis are accepted only if genescan traces are reproduced in two to three independent reactions. Two parameters are selected for expansion assessment and compared in sorted germ cells: midpoint (peak with the largest area) of the peak distributions in GeneScan traces and total area comprised of peaks to the right from the midpoint.
3. For protein analysis, several sorting sessions are required in order to collect enough germ cells for each developmental stage (store cell pellet from each sorting at –70°C until used; combine corresponding pellets from different sessions). One to two million cells for each sorted population are recommended for detection by immunoblotting. No protein concentration measurement is necessary if the number of cells in each sorted population are equal.
4. Mature spermatozoa are freely floating inside of epididymis. Crude chopping of the epididymis allows release of SZs, which, upon filtering, are devoid of somatic cell contamination. However, there are a limited number of erythrocytes present (depending on the purity of dissection) in the final suspension. Because these cells do not have nuclei, they can be ignored when DNA analysis is performed. For the protein analysis, these cells, if present in high number, can skew the result. Therefore, we recommend more accurate dissection and cleaning of the blood vessels prior to immunoblot analysis.
5. Aliquots (2×10^4) for each sorted population (X- and Y-chromosome-bearing sperm) in PBS are mounted on glass slides (by centrifugation for 10 min at 400*g*). The supernatant is replaced with cold fixative (75% methanol, 25% acetic acid) for 10 min. Fixative is removed and slides washed three times with 2X SSC. Slides are air-dried and stored at –20°C until used. Dual FISH analysis is used to analyze sperm cells. The sperm cells are decondensed with 10 m*M* dithiothreitol (DTT), denatured using 70% formamide and subsequently hybridized with specific probes for mouse X and Y chromosomes. The probes

are centromere-specific alpha satellite DNA directly labeled with a fluorescent dye. The X chromosome is labeled with Spectrum Orange and the Y chromosome is labeled with Spectrum Green. The spermatozoa are visualized and classified as either X or Y bearing using a Nikon Optiphot-2 microscope equipped with a dual-pass FITC/rhodamine filter.

6. The CAG repeat size in a single blastomere is determined by nested PCR. For the HD allele, outer primers: 5'-TTTTACCTGCGGCCCAGAGC-3'(10 pmol) and 5'-AGCGGCTCCT CAGCCACA-3' (10 pmol) are used in primary amplification reaction. An aliquot of 1 μL of the PCR product is amplified in a secondary PCR round for 40 cycles using primers and conditions described by Sermon et al. ***(31)***. GeneScan analysis was carried out as described.

References

1 McMurray, C. T. (1999) DNA secondary structure: a common and causative factor for expansion in human disease. *Proc. Natl. Acad. Sci. USA* **96,** 1823–1825.

2. Bates, G., Harper, P. S. and Jones, L. (2002) *Huntington's Disease*, 3rd ed. Oxford University Press, Oxford.

3 Goldberg, Y. P., McMurray, C. T., Zeisler, J., et al. (1995) Increased instability of intermediate alleles in families with sporadic Huntington disease compared to similar sized intermediate alleles in the general population. *Hum. Mol. Genet.* **4,** 1911–1918.

4 Goellner, G. M., Tester, D., Thibodeau, S., et al. (1997) Different mechanisms underlie DNA instability in Huntington disease and colorectal cancer. *Am. J. Hum. Genet.* **60,** 879–890.

5 Spiro, C., Pelletier, R., Rolfsmeier, M. L., et al. (1999) Inhibition of FEN–1 processing by DNA secondary structure at trinucleotide repeats. *Mol. Cell* **4,** 1079–1085.

6 Henricksen, L. A., Tom, S., Liu, Y., et al. (2000) Inhibition of flap endonuclease 1 by flap secondary structure and relevance to repeat sequence expansion. *J. Biol. Chem.* **275,** 16,420–16,427.

7 Lieber, M. R. (1997) The FEN-1 family of structure-specific nucleases in eukaryotic DNA replication, recombination and repair. *Bioessays* **19,** 233–240.

8 Tishkoff, D. X., Filosi, N., Gaida, G. M., et al. (1997) A novel mutation avoidance mechanism dependent on *S. cerevisiae* RAD27 is distinct from DNA mismatch repair. *Cell* **88,** 253–263.

9 Manley, K., Shirley, T. L., Flaherty, L., et al. (1999) Msh2 deficiency prevents in vivo somatic instability of the CAG repeat in Huntington disease transgenic mice. *Nature Genet.* **23,** 471–473.

10 Kovtun, I. V. and McMurray, C. T. (2001) Trinucleotide expansion in haploid germ cells by gap repair. *Nature Genet.* **27,** 407–411.

11 van den Broek, W. J., Nelen, M. R., Wansink, D. G., et al. (2002) Somatic expansion behavior of the (CTG)n repeat in myotonic dystrophy knock-in mice is differentially affected by Msh3 and Msh6 mismatch-repair proteins. *Hum. Mol. Genet.* **11,** 191–198.

12 Johnson, R. E., Kovvali, G. K., Prakash, L., et al. (1995) Requirement of the yeast RTH1 5' to 3' exonuclease for the stability of simple repetitive DNA. *Science* **269,** 238–240.

13 Kokoska, R. J., Stefanovic, L., Tran, H. T., et al. (1998) Destabilization of yeast micro- and minisatellite DNA sequences by mutations affecting a nuclease involved in Okazaki fragment processing (rad27) and DNA polymerase delta (pol3-t). *Mol. Cell. Biol.* **18,** 2779–2788.

14 Schweitzer, J. K. and Livingston, D. M. (1998) Expansions of CAG repeat tracts are frequent in a yeast mutant defective in Okazaki fragment maturation. *Hum. Mol. Genet* **7,** 69–74.

15 Richard, G.-F., Goellner, G. M., McMurray, C. T., et al. (2000) Recombination-induced CAG trinucleotide repeat expansions in yeast involve the MRE11/RAD50/XRS2 complex. *EMBO J.* **19,** 2381–2390.
16 Miret, J. J., Pessoa-Brandao L., and Lahue R. S. (1998) Orientation-dependent and sequence specific expansion of CTG/CAG trinucleotide repeats in *Saccharomyces cerevisiae*. *Proc. Natl. Acad. Sci. USA* **95,** 12,438–12,443.
17 Moore, H., Greewell, P. W., Liu, C. -P., et al. (1999) Triplet repeats form secondary structures that escape DNA repair in yeast. *Proc. Natl. Acad. Sci. USA* **96,** 1504–1509.
18 Pearson, C. E. , Ewel, A., Acharya, S., et al. (1997) Human MSH2 binds to trinucleotide repeat DNA structure associated with neurodegenerative diseases. *Hum. Mol. Genet.* **6,** 1117–1123.
19 Samadashwily, G. M., Raca, G., and Mirkin, S. M. (1997) Trinucleotide repeats affect DNA replication in vivo. *Nature Genet.* **17,** 298–304.
20 Freudenreich, C. H., Kantrow, S. M., and Zakian, V. A. (1998) Expansion and length-dependent fragility of CTG repeats in yeast. *Science* **279,** 853–856.
21 Lyons-Darden, T. and Topal, M. D. (1999) Abasic sites induce triplet-repeat expansion during DNA replication in vitro. *J. Biol. Chem.* **274,** 25,975–25,978.
22 Mangiarini, L., Sathasivam, K., Seller, M., et al. (1996) Exon 1 of the HD gene with an expanded CAG repeat is sufficient to cause progressive neurological phenotype in transgenic mice. *Cell* **87,** 493–506.
23 Kovtun, I. V., Therneau, T. M., and McMurray, C. T. (2000) Gender of the embryo contributes to CAG instability in transgenic mice containing a Huntington's disease gene. *Hum. Mol. Genet.* **9,** 2767–2775.
24 Kennedy, L. and Shelbourne, P. F. (2000) Dramatic mutation instability in HD mouse striatum: does polyglutamine load contribute to cell-specific vulnerability in Huntington's disease? *Hum. Mol. Genet.* **9,** 2539–2544.
25 Savouret, C., Brisson, E., Essers, J., et al. (2003) CTG repeat instability and size variation timing in DNA repair-deficient mice. *EMBO J.* **22,** 2264–2273.
26 Johnson, L. A. and Pinkel, D. (1986) Modification of a laser-based flow cytometer for high resolution DNA analysis of mammalian spermatozoa. *Cytometry* **7,** 268–273.
27 Rens, W., Welch, G. R., and Johnson, L. A. (1998) A novel nozzle for more efficient sperm orientation to improve sorting efficiency of X- and Y-chromosome-bearing sperm. *Cytometry* **33,** 476–481.
28 Rens, W., Welch, G. R., and Johnson, L. A. (1999) Improved flow cytometric sorting of X- and Y-chromosome bearing sperm: substantial increase in yield of sexed sperm. *Mol. Reprod. Dev.* **52,** 50–56.
29 Kovtun, I. V., Welch, G., Guthrie, H. D., et al. (2004) CAG repeat lengths in X- and Y-bearing sperm indicate that gender bias during transmission of the Huntington's disease gene is determined in the embryo. *J. Biol. Chem.* **279,** 9389–9391.
30. Hogan, B., Beddington, R., Constantini, F., et al. (1994) *Manipulating the Mouse Embryo*, 2nd ed., Cold Spring Harbor Laboratory, Cold Spring Harbor, NY.
31. Sermon, K., Goossens, V., Seneca, S., et al. (1998). Preimplantation diagnosis for Huntington's disease (HD): clinical application and analysis of the HD expansion in affected embryos. *Prenat. Diagn.* **18,** 1427–1436.

22

Oxidative Damage in Huntington's Disease

José Segovia and Francisca Pérez-Severiano

Summary

Huntington's disease is a hereditary neurodegenerative disorder, characterized by motor, psychiatric, and cognitive symptoms. The genetic defect responsible for the onset of the disease, expansion of CAG repeats in exon 1 of the gene that codes for huntingtin, has been unambiguously identified. On the other hand, the mechanisms by which the mutation causes the disease are not completely understood yet. However, defects in the energy metabolism of affected cells may cause oxidative damage, which has been proposed as one of the underlying molecular mechanism that participates in the etiology of the disease. This chapter describes methods to genotype mice transgenic for the disease, characterizing their progressive neurological phenotype, and biochemical methods that allow determining striatal oxidative damage, and establishing the status of both protective cellular systems, and biochemical pathways that induce the generation of free radicals. The methods described in this chapter permit one to relate the neurological phenotype of the mice with the degree of oxidative damage sustained by the brain.

Key Words: Transgenic mice; genotyping; neurological phenotype; striatal oxidative damage; free radicals; lipid peroxidation; nitric oxide synthase; superoxide dismutase.

1. Introduction

The advent of transgenic animals to model human diseases has been of great relevance in biomedical research, both to unravel the mechanisms underlying the onset of the diseases and for designing therapeutic methods to treat them. Diseases caused by CAG triple repeats are particularly well suited to be studied in transgenic mice because the genetic defect, expansion of polyglutamine tracts in the affected proteins, has been unambiguously identified as the cause of the diseases.

Huntington's disease (HD) is a neurodegenerative disorder clinically characterized by psychiatric, cognitive, and motor symptoms and histopathologically by severe death of caudate–putamen neurons. The disease is caused by a CAG expansion in exon 1 of

From: *Methods in Molecular Biology, vol. 277: Trinucleotide Repeat Protocols*
Edited by: Y. Kohwi © Humana Press Inc., Totowa, NJ

the gene encoding the protein huntingtin (htt). Transgenic mice that overexpress either a mutated exon 1, full-length htt cDNA, the complete human htt mutated gene, or knock-in mice with mutated exon 1 with different CAG expansions have been generated ***(1)***, and these mice have become an essential tool in current HD research because they develop progressive neurological phenotypes and mimic some of the biochemical and morphological traits of HD.

Although the normal function of htt or how the mutation causes the disease is still under intense investigation, defects in the energy metabolism of affected cells may cause oxidative stress, which, in turn, has been proposed as a factor associated with the onset of HD ***(2–5)***.

Oxidative stress occurs when the equilibrium between the formation of free radicals and the protection systems is altered, and cells are not capable of compensating for the formation of reactive oxygen species (ROS) that cause damage. We have previously observed that there is a relationship between the progressive neurological phenotype and striatal oxidative damage in the R6/1 HD transgenic mice that is related to age-dependent changes in the activity of the biochemical machinery responsible for maintaining the cellular redox status. This chapter describes the methods we have used to determine the degree of oxidative damage in the striatum of HD transgenic mice and to study the activity of systems that are related both with the generation of ROS, and cell protection.

2. Materials

1. R6/1 transgenic mice (B6CBA) (Jackson Laboratory, Bar Harbor, ME).
2. DNA lysis buffer: 50 m*M* Tris-HCl, 20 m*M* NaCl, 0.3 % (w/v) sodium dodecyl sulfate (SDS), 1 m*M* EDTA.
3. Proteinase K stock solution (10 mg/mL).
4. Agarose gels: 1% and 3% (w/v).
5. Ethidium bromide (Sigma), 10 mg/mL in purified water for stock.
6. 10X polymerase chain reaction (PCR) buffer: 670 m*M* Tris-base, 166 m*M* NH_4SO_4, 20 m*M* $MgCl_2$, 1.7 mg/mL of bovine serum albumin (BSA), and 10 m*M* of 2-mercaptoethanol, all dissolved in 9 mL of Tris-EDTA. Bring to pH 8.8. Make up the final volume of 10 mL with Tris-EDTA and filter-sterilize.
7. Dimethyl sulfoxide (DMSO) (Sigma).
8. 25 m*M* stock solution of dATP, dCTP, dGTP, dTTP (2'-deoxynucleoside 5'-triphosphates, dNTPs) (Invitrogene).
9. Oligonucleotide primers: 50 pmol per reaction.
10. *Taq* polymerase, diluted 1.5 U/5 μL (Amersham Pharmacia Biotech).
11. Chloroform and methanol, high-performance liquid chromatography (HPLC) grade (Mallinckrodt).
12. Lipid peroxidation calibrating solution, 0.001 mg/mL quinine standard made in 0.05 *M* H_2SO_4 (prepare fresh).
13. Bicinchoninic acid (BCA) reagent (Pierce, Rockford, IL).
14. Nitric oxide synthase (NOS) activity homogenizing buffer: 50 m*M* Tris-HCl, 0.1 m*M* EDTA, 0.1 m*M* EGTA with 0.1% (v/v) β-mercaptoethanol solution, pH 7.5; the solution is kept in the refrigerator (4°C).

15. Protease inhibitors cocktail; add fresh at the following final concentrations in homogenizing buffer: 100 μ*M* leupeptin, 1 m*M* phenylmethylsulfonyl fluoride (PMSF, from a 100-m*M* stock ethanol solution), aprotinin (2 μg/mL), soybean trypsin inhibitor (SBTI; 10 μg/mL), and 0.1% (v/v) Tergitol type NP-40 (Sigma, Saint Louis, MO).
16. Incubation mixture for NOS reaction: Add the following, all final concentrations, in a volume of 100 μL of the buffer described in **item 15**: 10 μ*M* L-arginine, 1 m*M* NADPH, 100 n*M* calmodulin, 30 μ*M* tetrahydrobiopterin (from a 100-m*M* stock solution, prepared fresh), 2.5 m*M* $CaCl_2$, and 0.2 μCi of [^{3}H] L-arginine (approx 66 Ci/mmol; Amersham, Arlington Heights, IL).
17. 1 m*M* EGTA.
18. NOS stop buffer: 2 m*M* EGTA, 2 m*M* EDTA, 20 m*M* HEPES, pH 5.5.
19. Dowex-50W resin (50X8-200; Sigma, St. Louis, MO).
20. 1 *N* NaOH.
21. Preparation of activated Dowex-50W: 100–200 g of resin is added to 300 mL of 1 *N* NaOH to convert the acid form to a salt; the mixture is swirled into a slurry. After the gel settles, the NaOH is removed and the resin is washed several times with abundant water, until the supernatant reaches a pH below 8.0. The equilibrated resin can be stored in stop buffer at 4°C.
22. Aquasol scintillation cocktail (NEN, Boston, MA).
23. Tri-Pure reagent (Roche Diagnostics).
24. Sodium dodecyl sulfate (SDS) (Merck-Schuchardt).
25. Bis-acrylamide and acrilamide (Roche Diagnostics).
26. Ammonium persulfate (Bio-Rad).
27. *N*,*N*,*N*,*N*´-Tetramethylenediamine (TEMED) (Research Organics).
28. 8% SDS–PAGE gel.
29. 2X Western blot sample buffer: 0.125 *M* Tris-HCl, 4% SDS, 20% Glycerol, 10% β-mercaptoethanol, pH 6.8.
30. Nitrocellulose paper (Amersham).
31. Ponceau reagent (Sigma).
32. Western blot blocking solution: 5% skim milk in Tris-buffer solution (TBS; 2.42 g Trisbase, 8.0 g NaCl/L, adjust to pH 7.6), 0.05% Tween-20 (Sigma).
33. Monoclonal antibodies against neuronal NOS (nNOS) and endothelial NOS (eNOS) (Transduction Laboratories. Lexington).
34. Peroxidase-labeled secondary antibody (Zymed Inc., CA).
35. Chemiluminescence Reagent Plus detection system (Perkin-Elmer).
36. XO-Mat film (Kodak).
37. Western blot stripping buffer: 100 m*M* β-mercaptoethanol, 2% SDS, 62.5 m*M* Tris-HCl, pH 6.8.
38. Superoxide dismutase (SOD) homogenizing buffer: 50 m*M* KH_2PO_4 in 1% Triton X-100, pH 7.0.
39. SOD reaction buffer: 0.122 m*M* EDTA, 30.6 μ*M* nitroblue tetrazolium (NBT), 0.122 m*M* xanthine, 0.006% serum albumin bovine, and 49 m*M* sodium carbonate.
40. Xanthine oxidase (168 U/L) in 2 *M* $(NH_4)_2SO_4$; prepare 2 mL and keep at 4°C (Sigma).
41. SOD stop buffer: 0.8 m*M* cupric chloride.
42. 100 m*M* diethydithiocarbamate.
43. SOD dyalizing solution: 5 m*M* PBS, 0.1 m*M* EDTA, pH 7.8.
44. Folin and Ciocalteu's phenol reagent (Sigma).

3. Methods

The methods outlined in this chapter describe (a) the genotyping and analysis of the neurological phenotype displayed by the R6/1 transgenic mice, (b) the determination of striatal oxidative damage, assessed by lipid peroxidation and by the activity and expression of nitric oxide synthase in striatum, as an inducer of the formation of free radicals, and (c) the activity of superoxide dismutase in striatum, as a system protecting cells from the formation of free radicals.

3.1. Genotype and Behavioral Evaluation

The genotyping of R6/1 mice by a PCR method and the behavioral observations assessed to identify the progressive neurological phenotype of the transgenic mice are described in **Subheadings 3.1.1.–3.1.3.** This includes (a) the description of the DNA extraction method, (b) the description of the PCR reaction, and (c) the behavioral observations and tests performed on transgenic and control mice. All animal procedures described in the following subsections are in accordance with the National Institutes of Health Guide for the Care and Use of Laboratory Animals and were approved by the Institutional Review Committee.

3.1.1. DNA Extraction

For the experiments described in this chapter, we use R6/1 males of the CBA × C57BL/6 strain, which carry a human mutated exon 1 with approx 116 CAG repeats ***(6)***. Hemizygous R6/1 male mice, carrying a single copy of the transgene, and nontransgenic CBA females were obtained from the Jackson Laboratory (Bar Harbor, ME), and a colony was maintained in our vivarium (CINVESTAV-IPN), by crossing the hemizygous R6/1 mice with wild-type CBA females and determining the genotype of the offspring by PCR.

To obtain DNA, samples of ear tissue were obtained from mice 4–5 wk old. Each sample, of approx 3-mm diameter, was treated with 20 μL of the DNA lysis buffer plus 2 μL of proteinase K stock solution. Samples are then incubated at 55°C for 15 min, vigorously shaken, and centrifuged at 14,000 rpm (15,000*g*) for 30 s; this procedure was preformed three times. To obtain a final volume of 50 μL, 28 μL of distilled sterile H_2O was added. Samples were then boiled for 7 min, cooled, and stored at –20°C, until PCR assays are performed. We check isolated DNA by running an aliquot of the samples in 1% agarose gels and stain them with ethidium bromide.

3.1.2. PCR Assay

The PCR assays were performed on each mouse to identify the presence of the transgene. The assay was based on the description by Mangiarini et al. ***(6)*** and we have described it elsewhere ***(7)***. Four microliters of the DNA previously obtained was mixed with 5 μL of the 10X PCR reaction buffer, 5 μL of dimethyl sulfoxide (DMSO), 1 μL (50 pmol) of each of the primers, with the sequences forward 3'GCAGCAG CAGCAGCAACAGCCGCCACCGCC and antisense CGGCTGAGGCAGCAG CGGCTGT, 1 μL of stock solution of dNTPs (final concentration 0.5 m*M*), and 5 μL of a *Taq* polymerase solution (1.5 U/5 μL). The volume was brought up to 50 μL with distilled sterile H_2O.

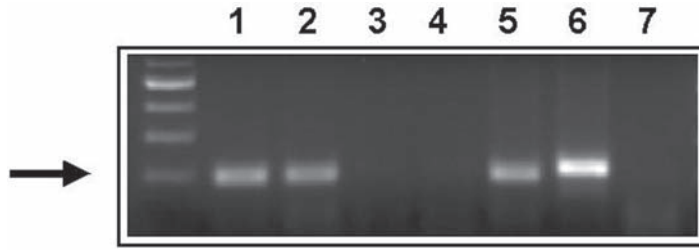

Fig. 1. PCR assay to detect the presence of human htt. PCR products are as follows: Lanes 1 and 2: DNA from R6/1 transgenic mice; lanes 3 and 4: DNA from nontransgenic mice; lane 5: genomic DNA from a patient of HD; lane 6: plasmid; lane 7: negative control (no DNA added). Arrow indicates 100 bp DNA marker.

To amplify transgenic DNA, samples were denaturated at 94°C for 90 s, and then 35 cycles of the following protocol were run: 30 s at 94°C (denature), 30 s at 65°C (annealing), and 90 s at 72°C (extension). A final 10-min extension step was performed at the end of the 35 cycles. Twenty microliters of each sample was run on a 3% (w/v) agarose gel, and the ethidium bromide-stained products were observed with ultraviolet (UV) light. As positive controls for the PCR reaction, we used the pGemHDEL plasmid (a gift from Dr. A. J. Tobin and G. Lawless, University of California, Los Angeles), which contains 4 kb of human genomic DNA, including exon 1 of the htt gene, and human genomic DNA (provided by Dr. M. E. Alonso, Instituto Nacional de Neurología y Neurocirugía) (*see* **Fig. 1**).

3.1.3. Behavioral Testing

It has been our experience that all mice positive for transgene expression develop a progressive neurological phenotype and, thus, that behavioral evaluation is relevant to validate the use of this model. We have tested transgenic mice at various ages starting at 11 wk, when they are undistinguishable from wild-type litter mates by simple visual observation, up to 35 wk of age, when R6/1 mice show a severe neurological phenotype.

Mice of various ages, from 11 to 35 wk of age, were tested for motor behavior in an automated activity system (electronic motility meter 40F; Motron Products, Stockholm, Sweden). Mice were placed in clear plastic boxes, and horizontal and vertical movements (rearing onto their rear legs) were automatically recorded for one single 10-min session for each animal. To determine feet clasping, mice were held by the tail; if a mouse did not clasp its feet within a maximum period of 2 min, we considered it as not presenting the behavior. Mice body weight was recorded every week. We considered that these simple observations permit one to relate the onset of the neurological phenotype with the time-course of striatal oxidative damage and to establish a temporal correlation of the progression of the phenotype with the activity of both the biochemical systems that induce oxidative damage and the cell protection mechanisms.

Transgenic mice started showing feet clasping at 19 wk of age, whereas wild-type mice never presented this behavior ***(7,8)***. R6/1 mice also showed significant body

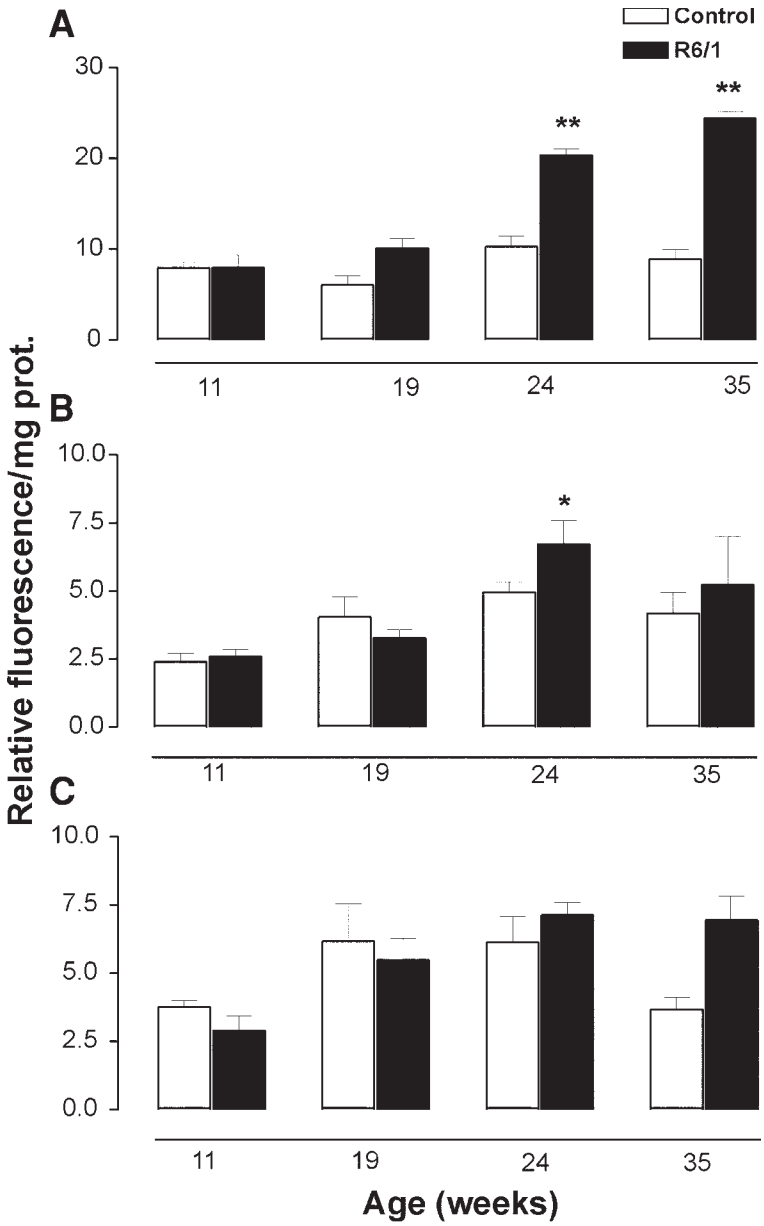

Fig. 2. Lipid peroxidation in different brain areas of transgenic R6/1 and wild-type control mice at different ages. Bars are means and SEM. **(A)** Lipid peroxidation in the striatum, $^{**}p < 0.001$, comparing transgenic mice at 24 and 35 wk with all other groups. **(B)** Lipid peroxidation in the cortex, $^{*}p < 0.05$, comparing transgenic mice at 24 wk with control and transgenic mice 11 wk old. **(C)** Lipid peroxidation in the cerebellum. An analysis of variance (ANOVA) test was performed, followed by a Tukey's multiple comparison test ($n = 3$–4 mice

weight loss, which reaches a 37% loss with respect to nontransgenic litter mates at 35 wk of age ***(8)***. Motor behavior clearly diminishes in transgenic mice, and by 35 wk of age, R6/1 mice showed 81%, and 79% decreases in horizontal and vertical motor activity, respectively, compared with nontransgenic controls ***(8)***.

3.2. Striatal Oxidative Damage

This subsection describes methods that allow us to evaluate the degree of oxidative damage that occurs in the brain, by determining the level of striatal lipid peroxidation and the activity and expression of nitric oxide synthase.

3.2.1. Lipid Peroxidation

One of the most relevant types of cell damage induced by free radicals is lipid peroxidation (LP), which is the oxidative damage to the polyunsaturated membrane lipids, susceptible to oxidation by molecular oxygen through a free-radical chain process ***(9)***. The end result of LP is an alteration in the lipid composition of the cell membrane that changes its physicochemical properties, such as increasing membrane rigidity, which may lead to cell death as a result of energy and structural modifications ***(9,10)***.

R6/1 and nontransgenic littermates of different ages were killed by decapitation, and the striata and other brain regions, cortices and cerebella, rapidly dissected out on an ice-cold surface. To assess LP, we measured the formation of lipid-soluble fluorescence according to an established method ***(11)***, as we have previously described it ***(8)***. Brain tissue (one striatum) was homogenized in 3 mL of distilled H_2O, and 1-mL aliquots were added to 4 mL of chloroform–methanol mixture 2:1 (v/v). Samples were stirred and placed on ice for 30 min in the dark; then, the top phase was carefully removed by aspiration (*see* **Note 1).** Fluorescence of the chloroform phase was determined at 350-nm excitation and 430-nm emission wavelengths (*see* **Note 2**). To calibrate the assay, we adjusted the spectrophotometer to 140 fluorescence units with the calibrating solution. We employed the bicinchoninic acid (BCA) assay (Pierce, Rockford, IL) to determine sample protein content, and the results were expressed as relative fluorescence units per milligram of protein (*see* **Fig. 2**).

3.2.2. Nitric Oxide Synthase Activity

Nitric oxide (NO) is an unstable diatomic radical that plays important roles in several crucial physiological processes, including neuromodulation and synaptic plasticity ***(12,13)***. NO is synthesized by NO synthase (NOS) from L-arginine and producing L-citrulline as a byproduct. Three isoforms of the enzyme exist: neuronal NOS (nNOS), endothelial NOS (eNOS), and inducible NOS (iNOS). The enzymes can be also divided in terms of their dependency on Ca^{2+}: nNOS and eNOS, the activity of which depends on the presence of Ca^{2+}, and iNOS, which is Ca^{2+} independent. Under patho-

Fig. 2. *(continued)* per group). (Reprinted from *Brain Research*, Vol. 862, Pérez-Severiano, F., et al., Striatal oxidative damage parallels the expression of a neurological phenotype in mice transgenic for the mutation of Huntington's disease, pp. 234–237, copyright (2000), with permission from Elsevier Science.)

logical conditions, NO may induce or facilitate oxidative damage, through the formation of the highly reactive metabolite peroxynitrite.

The method we describe to measure NOS activity is based on the stoichiometric conversion of L-arginine to L-citrulline, a stable byproduct of NO synthesis ***(14)***, as we have previously described ***(7,15,16)***. We used one striatum for each assay. Mice were euthanized and the striata from R6/1 and control mice were dissected out on an ice-cold plate and kept at –80°C until assays are performed. Tissue was homogenized in 250 μL of a buffer containing a cocktail of protease inhibitors, which were added fresh to the homogenizing buffer (*see* **Note 3**). The protein content of the samples was determined using the BCA assay. After homogenization, a volume of solution containing 500 μg of protein was used for each reaction and incubated for 30 min at 37°C in the NOS incubation mixture, with moderate shaking. The volume for each reaction was adjusted to 100 μL with homogenizing buffer. Total arginine is 10 μ*M* unlabeled plus 3 pmol labeled per each reaction. To test for iNOS activity, incubations were performed in the presence of 1.0 m*M* EGTA with no added $CaCl_2$. Starting with a 250-μL reaction (one striatum) should be sufficient to run a duplicate both in the presence and in the absence of calcium.

Reactions were stopped by adding 1 mL of ice-cold stop buffer. The reaction mixture was applied to a 2-mL column of activated Dowex-50W resin that had been previously equilibrated with stop buffer (*see* **Note 4**). The cation-exchange resin retained labeled arginine and allowed [^{3}H] L-citrulline to flow through the column. Wash the incubation tube with 1 mL of distilled H_2O, vortex, and pass it over the column to wash through the sample. Samples were measured using a scintillation counter, with 5 mL of scintillation cocktail per 2 mL of eluate (i.e., per sample). To determine background radioactivity, tubes were prepared without tissue, following the procedure just described. The background should not exceed 4% of total counts added, determined counting total counts of a tube containing 0.2 μCi [^{3}H]L-arginine from the master mix. We express NOS activity as nanomoles of [^{3}H] L- citrulline per milligram of protein per 30 min. In Fig. 3, we show results of both Ca^{2+}-dependent and Ca^{2+}-independent NOS activity in striata of R6/1 and control mice, employing the methods we have described in this subsection.

3.2.3. NOS Protein Expression

This subsection describes a Western blot method to determine the expression levels of nNOS and eNOS in the striata of R6/1 and control nontransgenic mice.

Striata from both HD and control mice of different ages were obtained as described in **Subheading 3.2.1.**, and total protein was isolated using the TriPure reagent (Roche Diagnostics) following the manufacturer's instructions. Protein pellets were resuspended in 500 μL of 1% sodium dodecyl sulfate (SDS). The BCA assay was employed to determine protein concentrations and aliquots containing 50 μg of protein (approx 5–15 μL) were used for the following analysis. To those samples, the same volume of sample buffer 2X was added, and run in 8% SDS-PAGE gels. Proteins are transferred from the gel onto nitrocellulose paper using a semidry transfer system (140 mA for 45 min). Membranes were stained with a 2% Ponceau solution to ensure complete protein

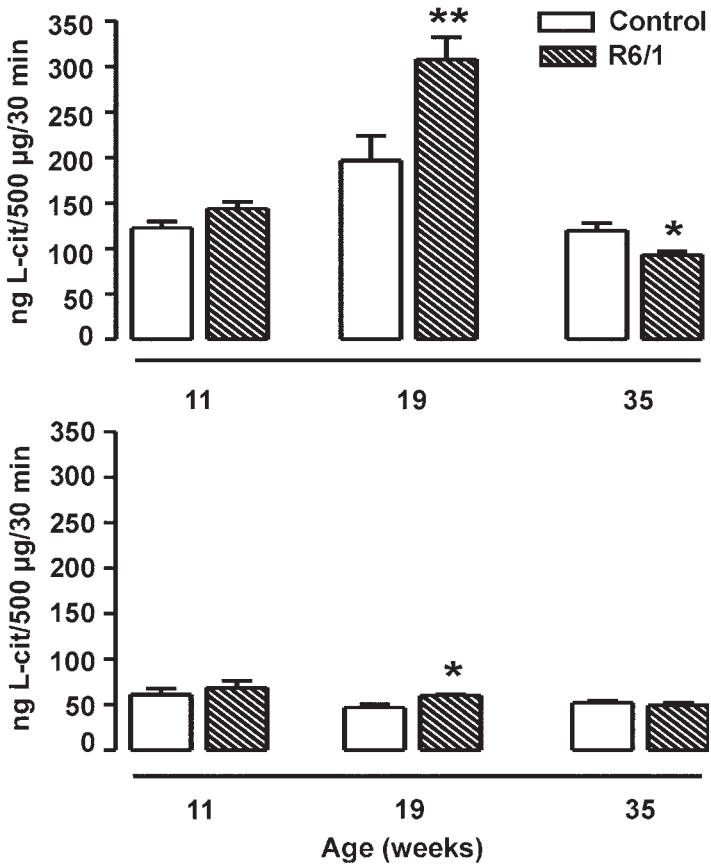

Fig. 3. NOS activity in the striata of R6/1 mice. NOS activity R6/1 and wild-type control mice of different ages. **(A)** Measurements of NOS activity in the presence of Ca^{+2}, and **(B)** in the absence of Ca^{2+} ($n = 6$ for each group). $^{**}p < 0.001$; $^{*}p < 0.05$, Student's *t*-test. (Reprinted from *Brain Research*, Vol. 951, Pérez-Severiano, F. et al., Age-dependent changes in nitric oxide synthase activity and protein expression in striata of mice transgenic for the Huntington's disease mutation, pp. 36–42, copyright (2002), with permission from Elsevier Science.)

transfer. Blots were blocked with 5% skim milk in TBS Tween 0.05% for 1 h at room temperature and incubated with blocking solution overnight at 4°C, in the presence of the monoclonal antibodies against either nNOS or eNOS (Transduction Laboratories) at a final dilution of 1:2500. Membranes were washed three times with TBS solution and incubated with a secondary goat anti-mouse peroxidase-labeled antibody (Zymed) diluted 1:6000 in blocking solution for 1 h at room temperature. Blots were washed three times for 10 min each time with TBS solution and proteins developed using the ECL detection system according with the manufacturer's instructions. Blots were stripped by incubating at 55°C, 30 min, in stripping buffer, then reprobed with a mono-

clonal β-actin antibody at a final dilution of 1:100; a secondary peroxidase-antibody was used to reveal proteins as was described elsewhere ***(16,17)***.

Images from films were digitally acquired with a Bio-DocIt System (UVP) and densitometry analysis performed using the Lab Works™ 4.0 Image Acquisition and Analysis Sofware (UVP) for nNOS, eNOS, and β-actin signals. Densitometry results of nNOS and eNOS were normalized with respect to their β-actin controls, and data were expressed as normalized optical density (OD) arbitrary units (*see* **Fig. 4**).

3.3. Oxidative Protection Systems

3.3.1. Superoxide Dismutase Activity

This subsection describes a method to measure superoxide dismutase (SOD) activity as an indication of the level and functioning of cellular protection systems in the striata of mice transgenic for the HD mutation.

Superoxide dismutase (SOD) functions to protect cells from the presence of the superoxide radical, by generating H_2O_2, and thus to reduce the toxic effects of the superoxide anion, and the subsequent formation of peroxynitrite from $O_2^{\cdot -}$ and NO. Two isoforms of this enzyme exist: Cu/ZnSOD and MnSOD, which are dependent on the presence of Cu and Zn, and Mn, respectively. Furthermore, the two isoforms have different intracellular localization; Cu/ZnSOD is mainly present in the cytosol, whereas MnSOD is a mitochondrial enzyme.

The method we describe allows one to determine total SOD activity and the individual activities of both Cu/ZnSOD and MnSOD. The method is based on a competitive inhibition assay performed using a xanthine/xanthine oxidase system to reduce nitroblue tetrazolium (NBT) ***(18)***. Striata from transgenic and control mice were dissected as previously described and immediately weighed and then homogenized in SOD homogenizing buffer (9 mL/g of tissue). For instance, each striatum weighs approx 0.026 g and it is correspondingly homogenized in 234 μL. For total SOD activity, each homogenized sample was diluted with distilled H_2O (1:50) and 330 μL of the diluted striatal homogenates added to 1.63 mL of the reaction mixture. Then, 33 μL of xanthine oxidase (from the stock solution) was added to the mixture, which was incubated for 30 min at 27°C. Reactions were stopped with 1 mL of 0.8 m*M* cupric chloride, and optical density was recorded at 560 nm. Complete (100%) reduction of NBT was obtained when the tissue sample was replaced with distilled H_2O. The amount of striatal protein that inhibits 50% of maximal NBT reduction was defined as one unit of SOD activity. MnSOD activity was differentiated from Cu/ZnSOD, by inhibiting the former with diethydithiocarbamate (DDC) ***(19)***. Thus, to determine MnSOD activity, samples were incubated with 50 m*M* DDC at 30°C for 60 min and dyalized for 3 h with three changes of 400 vol of dyalizing solution, and determined as described. Cu/ZnSOD activity was obtained by substracting the activity of the DDC-treated samples from those of total SOD activity. Samples for this assay must be dialyzed, as DDC reduces cytochrome-c. Protein concentrations are determined using the Folin and Ciocalteu's phenol reagent ***(20)***. Results are expressed as units of SOD activity per milligram protein ***(21)*** (*see* **Note 5**) (*see* **Fig. 5**).

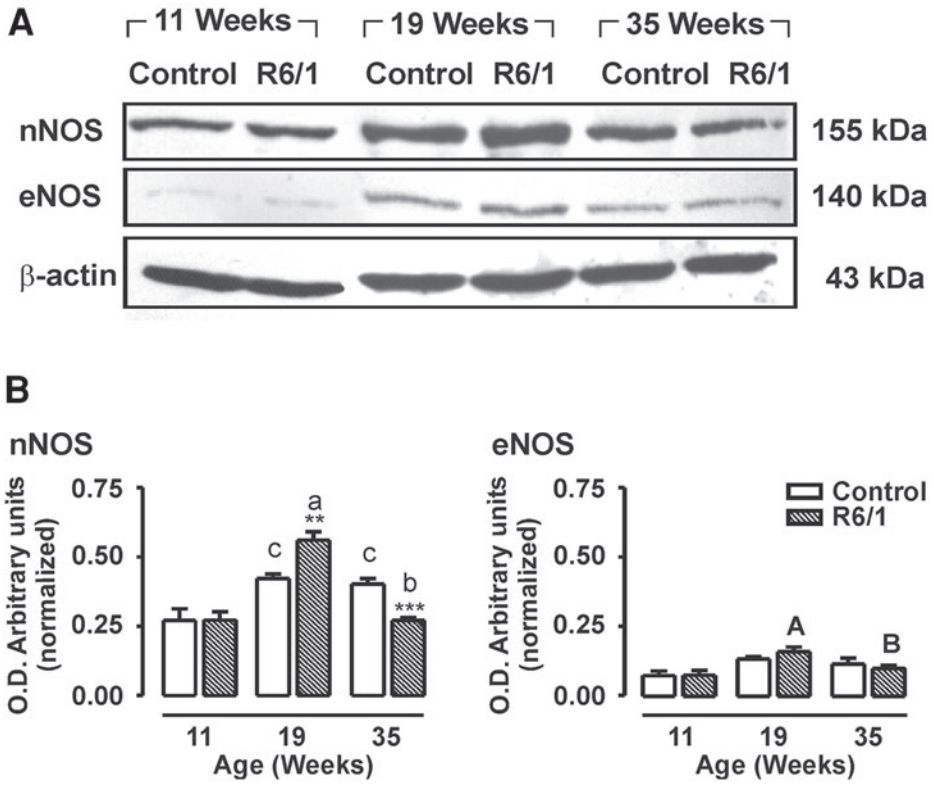

Fig. 4. nNOS and eNOS expression in the striata of R6/1 and wild-type control mice at different ages. **(A)** Representative Western blots of nNOS, eNOS, and β-actin. **(B)** The results of the densitometric analysis of the expression of nNOS and eNOS (n = 3–5 per group), normalized with respect to β-actin. To analyze the data of nNOS expression between control and R6/1 mice at different ages, the Student's t-test was performed. No differences between control and R6/1 mice were observed in 11-wk-old mice; ***$p = 0.0006$, **$p = 0.0071$, when comparing R6/1 mice to same age nontransgenic controls at 35 and 19 wk, respectively. To examine age-dependent nNOS expression, ANOVA followed by Tukey's test was used: **a** is $p < 0.01$ comparing 19-wk-old R6/1 mice to 11-wk-old R6/1 mice; **b** is $p < 0.05$ when comparing 35-wk-old R6/1 mice with 19-wk-old R6/1 mice; **c** is $p < 0.01$ when comparing 19- and 35-wk-old control nontransgenic mice with 11-wk-old nontransgenic mice. No differences were found between control and R6/1 mice at the different ages tested with respect to eNOS expression. With respect to age-dependent changes: **A** is $p < 0.05$ when comparing 19-wk-old R6/1 mice with 11-wk-old R6/1 mice, and **B** is $p < 0.05$ when comparing 35-wk-old R6/1 mice with 19-wk-old R6/1 mice (ANOVA followed by Tukey's test). No differences in eNOS expression were found as a function of age in control mice. (Reprinted from *Brain Research*, Vol. 951, Pérez-Severiano, F. et al., Age-dependent changes in nitric oxide synthase activity and protein expression in striata of mice transgenic for the Huntington's disease mutation, pp. 36–42, copyright (2002), with permission from Elsevier Science.)

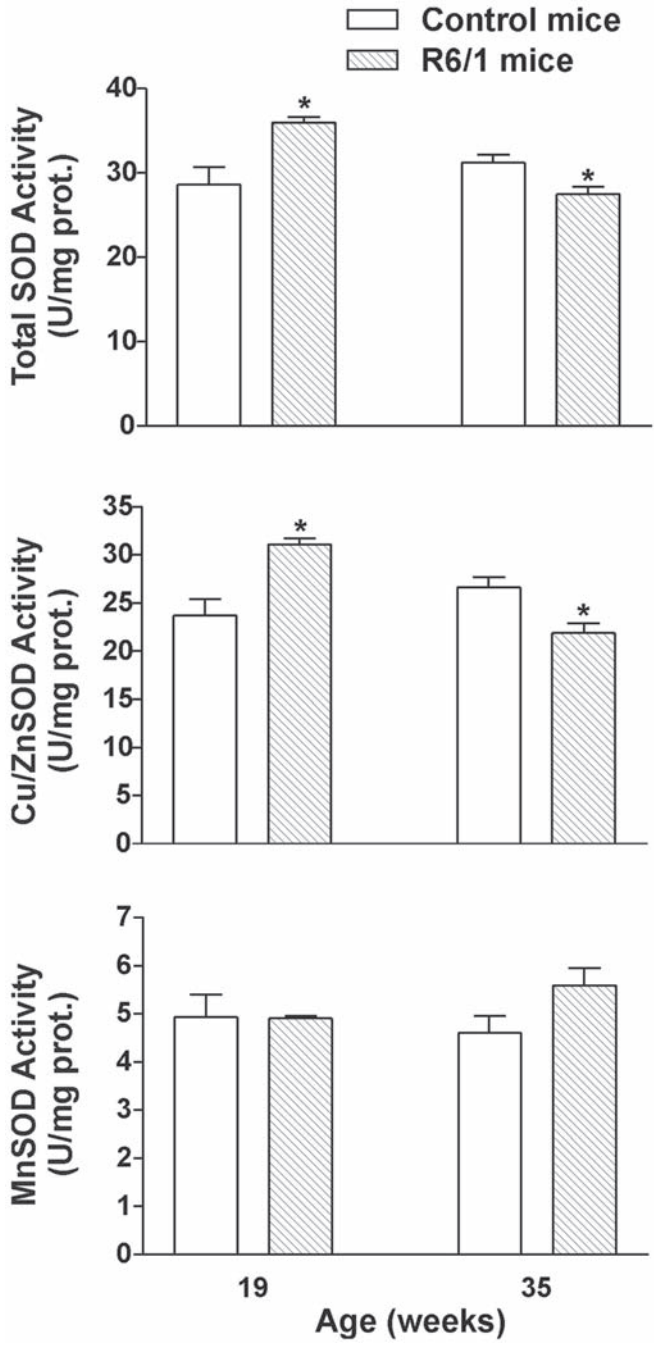

Fig. 5. SOD activity in the striatum of transgenic R6/1 mice and wild-type control mice at different ages. Bars are means and SEM. $^{*}p < 0.05$, $^{**}p < 0.001$ comparing transgenic mice with control mice, Student's *t*-test ($n = 7–10$ mice per group). (Reprinted from *Neurochemical Research*, Vol. 26, Santamaría, A. et al., Comparative analysis of superoxide dismutase activity

4. Notes

1. It is important to completely remove this phase, so it will not interfere with fluorescence determination.
2. We recommend adding 100 μL of methanol (HPLC grade) directly into the quartz cell per milliliter of chloroform phase that you read in the spectrofluorometer. This will enhance and facilitate solution of the mixture.
3. All protease inhibitors are dissolved directly into the homogenizing buffer, except for PMSF, which was previously dissolved in ethanol. After adding PMSF into the protease inhibitor cocktail, the mixture may become cloudy. Make sure to vortex the mixture when you take the volume (250 μL) in which every individual sample is homogenized.
4. We try to keep the pH of the supernatant that is obtained activating the Dowex-50W between 7.5 and 7.9.
5. To calculate SOD activity, we make the following assumptions: Complete reduction of NBT is equal to 100%, and the amount of striatal protein that inhibits 50% of maximal NBT reduction is one unit of SOD activity. To obtain SOD activity in arbitrary units, the absorbance of each individual sample is substracted from total absorbance (100%) and this number is divided by half of total absorbance. Finally, samples are normalized with respect of total protein, and units are defined as units/mg protein.

Acknowledgments

We thank Paula Vergara and Perla D. Maldonado for their assistance and expertise in the development and use of several of the techniques described in this chapter. This work was partially supported by CONACyT grant 33042-N (J. Segovia).

References

1 Sipione, S. and Cattaneo, E. (2001) Modeling Huntington's disease in cells, flies, and mice. *Mol. Neurobiol.* **23,** 21–51.
2 Browne, S. E., Bowling, A. C., MacGarvey, U., et al. (1997) Oxidative damage and metabolic dysfunction in Huntington's disease: selective vulnerability of the basal ganglia. *Ann. Neurol.* **41,** 646–653.
3 Browne, S. E., Ferrante, R. J., and Beal, M. F. (1999) Oxidative stress in Huntington's disease. *Brain Pathol.* **9,** 147–163.
4 Polidori, M. C., Mecocci, P., Browne, S. E., et al. (1999) Oxidative damage to mitochondrial DNA in Huntington's disease parietal cortex. *Neurosci. Lett.* **272,** 53–56.
5 Tabrizi, S. J., Cleeter, M. W., Xuereb, J., et al. (1999) Biochemical abnormalities and excitotoxicity in Huntington's disease brain. *Ann. Neurol.* **45,** 25–32.
6 Mangiarini, L., Sathasivam, K., Seller, M., et al. (1996) Exon 1 of the HD gene with an expanded CAG repeat is sufficient to cause a progressive neurological phenotype in transgenic mice. *Cell* **87,** 493–506.
7 Segovia, J. (2002) Transgenic model for the study of oxidative damage in Huntington's disease. *Methods Enzymol.* **353,** 365–373.

Fig. 5. *(continued)* between acute pharmacological models and a transgenic mouse model of Huntington's disease, pp 419–424, copyright (2001), with permission from Kluwer Academic/Plenum Publishers.)

8. Pérez-Severiano, F., Ríos, C., and Segovia, J. (2000) Striatal oxidative damage parallels the expression of a neurological phenotype in mice transgenic for the mutation of Huntington's disease. *Brain Res.* **862,** 234–237.
9 Gutteridge, J. M. and Halliwell, B. (1990) The measurement and mechanism of lipid peroxidation in biological systems. *Trends Biochem. Sci.* **15,** 129–135.
10 Chan, P. H., Yurko, M., and Fishman, R. A. (1982) Phospholipid degradation and cellular edema induced by free radicals in brain cortical slices. *J. Neurochem.* **38,** 525–531.
11 Triggs, W. P. and Willmore, L. J. (1984) In vivo lipid peroxidation in rat brain following intracortical Fe^{++} injection. *J. Neurochem.* **42,** 976–979.
12 Moncada, S., Palmer, R. M. P., and Higgs, E. A. (1991) Nitric oxide: physiology, pathophysiology and pharmacology. *Pharmacol. Rev.* **43,** 109–143.
13 Schuman, E. M. and Madison, D. V. (1994). Nitric oxide and synaptic function. *Annu. Rev. Neurosci.* **17,** 153–183.
14 Bredt, D. S. and Snyder, S. H. (1990) Isolation of nitric oxide synthetase, a calmodulin-requiring enzyme. *Proc. Natl. Acad. Sci. USA* **87,** 682–685.
15. Pérez-Severiano, F., Escalante, B., and Ríos, C. (1998) Nitric oxide synthase inhibition prevents acute quinolinate-induced striatal neurotoxicity. *Neurochem. Res.* **23,** 1297–1302.
16. Pérez-Severiano, F., Escalante, B., Vergara, P., et al. (2002) Age-dependent changes in nitric oxide synthase activity and protein expression in striata of mice transgenic for the Huntington's Disease mutation. *Brain Res.* **862,** 234–237.
17. Díaz-Barriga, F., Hernández, J. M., Carrizales, L., et al. (1989) Interactions of cadmium with actin microfilaments. *Toxicol. In Vitro* **3,** 277–284.
18 Oberley, L. W. and Spitz, D. R. (1984) Assay of superoxide dismutase activity in tumor tissue. *Method Enzymol.* **105,** 457–464.
19 Iqbal, J. and Whitney, P. (1991) Use of cyanide and diethyldithiocarbamate in the assay of superoxide dismutases. *Free Radic. Biol. Med.* **10,** 69–77.
20 Lowry, O. H., Rosebrougth, N. J., Farr, A. L., et al. (1951) Protein measurement with the folin-phenol reagent. *J. Biol. Chem.* **193,** 265–275.
21. Santamaría, A., Pérez-Severiano, F., Rodríguez-Martínez, E., et al. (2001) Comparative analysis of superoxide dismutase activity between acute pharmacological models and a transgenic mouse model of Huntington's disease. *Neurochem. Res.* **26,** 419–424.

Index